

CHANGES IN QUANTITATIVE EEG AND LOW RESOLUTION TOMOGRAPHY
FOLLOWING CRANIAL ELECTROTHERAPY STIMULATION

Richard C. Kennerly, B.A., M.A.

Dissertation Prepared for the Degree of
DOCTOR OF PHILOSOPHY

UNIVERSITY OF NORTH TEXAS

August 2006

APPROVED:

Eugenia Bodenhamer-Davis, Major Professor
Jerry McGill, Committee Member
Jan Holden, Committee Member
Daniel C. Miller, Committee Member
Joseph Doster, Chair of the Clinical Health
Psychology Program In the Department of
Psychology
Linda Marshal, Chair of the Department of
Psychology
Sandra L. Terrell, Dean of the Robert B. Toulouse
School of Graduate Studies

Kennerly, Richard C., Changes in quantitative EEG and low resolution tomography following cranial electrotherapy stimulation. Doctor of Philosophy (Health Psychology and Behavioral Medicine), August 2006, 425 pp., 81 tables, 233 figures, 171 references.

The effects of cranial electrotherapy stimulation (CES) on human EEG and brain current density were evaluated by quantitative electroencephalography (qEEG) and low resolution brain electromagnetic tomography (LORETA). A total of 72 research subjects were provided with a single session of CES, 38 were provided with 0.5 Hz CES while 34 were provided with 100 Hz CES. The qEEG paired *t*-tests revealed that in both frequencies of CES there was a significant (.05) increase in alpha relative power with concomitant decreases in delta and beta relative power. The 0.5 Hz CES decreased a wider frequency range of delta activity, while the 100 Hz CES decreased a wider frequency range of beta activity; suggesting some difference may exist in the EEG response to different frequencies of CES. The changes found in qEEG relative power were consistent with the affective and cognitive effects of CES reported in the literature, such as increased relaxation and decreased anxiety. Statistically significant changes for qEEG values other than relative power, such as coherence, amplitude asymmetry, phase lag and power ratios were also found. The LORETA paired *t*-tests found statistically significant (.05) increases in cortical and subcortical theta and alpha frequency current density with concomitant decreases in delta and beta current density. The effects of CES on current density varied by frequency, but did not show a differential in response based on proximity to the contacts, or structures within the brain. Statistically significant changes in current density were found in all 2394 gray matter voxels represented by LORETA, indicating a whole brain response to the CES stimulus. The qEEG and LORETA findings revealed that a single 20-minute session of CES does have a significant effect on the cortical and subcortical activity of the human brain resulting in activity consistent with decreased anxiety and increased relaxation.

Copyright 2006

by

Richard C. Kennerly

ACKNOWLEDGEMENTS

This study would not have been possible without the extraordinary support, assistance and patience of Elisabeth Schumacher, Kristie Earnheart-Kennerly and Genie Bodenhamer-Davis. I am very grateful for all they have done to help initiate, sustain and complete this project.

There would not have been a study without the loan of FDA approved CES units from Dr. Daniel Kirsh of Electromedical International. Dr. Kirsh was remarkably generous in loaning equipment and providing expertise to a student researcher. The assistance provided by Dr. Kirsh and Electromedical International was supplied with no conditions or prepublication reviews.

The analysis conducted in this study was made possible with the generous loan of EEG editing and analysis software (NeuroGuide, NeuroBatch, NeuroStat) from Dr. Robert Thatcher of the Bay Pines VA in Bay Pines, Florida and Applied Neuroscience Inc. Dr. Thatcher developed additional features in his software for this study and provided patient support for the many questions of a student researcher. I also wish to thank Leslie Sherlin and Marco Congedo of NovaTech EEG; who donated EEG software and tools for use in this study before later making them available for the free use of any researcher or clinician. The remarkable ability to image subcortical electrical currents was made possible by the free distribution of LORETA software by Robert Pascual-Marqui of the KEY Institute for Brain-Mind Research in Zurich.

Many other individuals at the University of North Texas and the professional community outside of UNT have shown dedication to facilitating student research through freely donating time, expertise, devices and software to this study. I am deeply grateful for all of their substantial contributions.

I would also like to thank the many people who participated in this study as research volunteers. They were people from all walks of life who generously volunteered their time to

help a student researcher. Without their interest, patience, and generosity, this study would never have been possible.

TABLE OF CONTENTS

	Page
ACKNOWLEDGEMENTS	iii
LIST OF TABLES	x
LIST OF FIGURES	xiv
Chapter	
1. INTRODUCTION	1
Literature Review.....	3
Background of Electromedicine	3
The Background of Cranial Electrotherapy Stimulation.	5
Differences Between CES, Electroanesthesia, tDCS and Electroconvulsive Therapy	7
The Use of CES for Inducing Sleep and Treating Sleep Disorders	15
The Use of CES in Alcohol and Drug Treatment	21
Treating Depression with CES.....	26
CES for the Treatment of Movement Disorders	28
CES for the Treatment of Anxiety	29
CES for the Treatment of Pain.....	31
Previous EEG Studies of CES	34
Mechanism of Effect in CES	40
Summary of Research on CES.....	42
Rationale and Conceptual Framework for the Study	45
Proposed Activation/Adaptation Model of CES.....	46
Hypothesis.....	50
Hypothesis 1:	50
Hypothesis 2:	50
Hypothesis 3:	51
Hypothesis 4:	51
Hypothesis 5:	52
Hypothesis 6:	52

	Hypothesis 7:	53
	Hypothesis 8:	53
	Hypothesis 9:	54
	Hypothesis 10:	54
	Hypothesis 11:	55
	Hypothesis 12:	55
	Hypothesis 13:	56
	Hypothesis 14:	56
	Hypothesis 15:	57
	Hypothesis 16:	57
	Hypothesis 17:	58
	Hypothesis 18:	58
	Hypothesis 19:	59
	Hypothesis 20:	59
	Hypothesis 21:	60
	Hypothesis 22:	60
	Hypothesis 23:	61
	Hypothesis 24:	61
2.	METHOD	62
	Participants.....	62
	Apparatus	62
	Design	63
	Design of the Study.....	63
	Procedure	64
	Application of the CES	64
	Acquisition of the EEG.....	64
	Collection of EEG.....	64
	Preprocessing of EEG Data	65
	EEG Analysis.....	65
	Statistics	66
	Methodological Issues	67
	Introduction.....	67

	Design of the Study.....	70
	Placebo/Sham CES Group	72
	Effect of a Repeated Measures Design on Degrees of Freedom	74
	Normality of EEG Data	75
	Multiple Comparisons.....	77
	False Positives Resulting From a Large Number of Statistical Tests	79
	Relative Power/Magnitude vs. Absolute Power/Magnitude.....	86
	Choice of Montage.....	102
	Reference Electrodes	104
	The Linked Ears Reference.....	104
	Common Average Reference.....	106
	Weighted Average Reference Montage	107
	Laplacian Montage.....	108
	Low Resolution Brain Electromagnetic Tomography (LORETA)	111
3.	RESULTS	114
	Changes in Raw Wave EEG	114
	Changes in the Spectral EEG.....	114
	Changes in the qEEG	116
	Introduction.....	116
	Relative Power Results	116
	Relative Power Topographical Maps.....	118
	Coherence Results.....	129
	Findings for Hypothesis 10:.....	133
	Amplitude Asymmetry Results.....	133
	Phase Lag Results	137
	Power Ratio Results.....	142
	LORETA Results	148
	LORETA Summary Tables.....	148
	LORETA Paired <i>t</i> -Test Results for 0.5 Hz CES in 1 Hz Increments	153
	LORETA Paired <i>t</i> -Test Results for 100 Hz CES in 1 Hz	

	Increments.....	215
	Common Changes in qEEG Relative Power and LORETA.....	287
	Findings for Hypothesis 17:.....	287
	Findings for Hypothesis 18:.....	288
	Findings for Hypothesis 19:.....	288
	Findings for Hypothesis 20:.....	288
	Findings for Hypothesis 21:.....	289
	Findings for Hypothesis 22:.....	289
	Findings for Hypothesis 23:.....	290
	Findings for Hypothesis 24:.....	290
4.	DISCUSSION.....	291
	Introduction.....	291
	Summary of the Relative Power Findings	291
	Summary of Coherence Findings.....	292
	Summary of Amplitude Asymmetry Findings.....	293
	Summary of Phase Lag Findings	293
	Summary of Power Ratio Findings.....	294
	Summary of LORETA Findings.....	294
	LORETA Artifact in the 100 Hz CES Group.....	296
	Activation/Adaptation Model of CES.....	298
	Further Implications of the Findings.....	299
	Limitations of the Study.....	302
	Conclusions.....	303
Appendices		
A.	SUPPLEMENTARY INFORMATION FOR THE .5 HZ CES LINKED EARS MONTAGE.....	305
B.	SUPPLEMENTARY INFORMATION FOR THE 100 HZ CES LINKED EARS MONTAGE.....	319
C.	COMMON AVERAGE REFERENCE MONTAGE	333
D.	LAPLACIAN MONTAGE.....	376

REFERENCES 413

LIST OF TABLES

		Page
Table 1.	Summary of Changes in Relative Power	126
Table 2.	Summary of Changes in Coherence.....	144
Table 3.	Summary of Changes in Amplitude Asymmetry	150
Table 4.	Summary of Changes in Phase Lag Electrode Pairs.....	155
Table 5.	Summary of Changes in Power Ratio.....	
Table 6	Summary of Changes in LORETA after 0.5 Hz CES.....	149
Table 7	Summary of Changes in LORETA after 100 Hz CES.....	150
Table 8	Focal Increase in Activity at F4 & F8 of the Laplacian Montage	151
Table 9	Changes in Activation Common to the 0.5 Hz and 100 Hz Group.....	152
Table 10	Summary of Changes in Current Density after 20 Minutes of CES	152
Table 11	Summary of Changes in Relative Power and LORETA.....	287
Table A 1	0-40 Hz bands 0.5 Hz Linked Ears FFT Relative Power Group Paired <i>t</i> -Test.	306
Table A 2	1-5 Hz 0.5 Hz CES Single Hz FFT Relative Power Group Paired <i>t</i> -Test	307
Table A 3	6-10 0.5 Hz CES Single Hz FFT Relative Power Group Paired <i>t</i> -Test	308
Table A 4	11-15 Hz 0.5 Hz CES Single Hz FFT Relative Power Group Paired <i>t</i> -Test	309
Table A 5	16-20 Hz 0.5 Hz CES Single Hz FFT Relative Power Group Paired <i>t</i> -Test	310
Table A 6	21-25 Hz 0.5 Hz CES Single Hz FFT Relative Power Group Paired <i>t</i> -Test	311
Table A 7	26-30 Hz 0.5 Hz CES Single Hz FFT Relative Power Group Paired <i>t</i> -Test	312
Table A 8	31-35 Hz 0.5 Hz CES Single Hz FFT Relative Power Group Paired <i>t</i> -Test	313
Table A 9	36-40 Hz 0.5 Hz CES Single Hz FFT Relative Power Group Paired <i>t</i> -Test	314
Table A 10	0.5 Hz CES Baseline FFT Relative Power Group Means	315
Table A 11	0.5 Hz CES Baseline FFT Relative Power Group Standard Deviation	316
Table A 12	0.5 Hz CES FFT Relative Power Post CES Group Mean.....	317

Table A 13	0.5 Hz CES FFT Relative Power Post CES Group Standard Deviation.....	318
Table B 1	0-40 Hz Bands 100 Hz CES FFT Relative Power Group Paired <i>t</i> -Test	320
Table B 2	1-5 Hz 100 Hz CES FFT Relative Power Group Paired <i>t</i> -Test	321
Table B 3	6-10 Hz 100 Hz CES FFT Relative Power Group Paired <i>t</i> -Test	322
Table B 4	11-15 Hz 100 Hz CES FFT Relative Power Group Paired <i>t</i> -Test	323
Table B 5	16-20 Hz 100 Hz CES FFT Relative Power Group Paired <i>t</i> -Test	324
Table B 6	21-25 Hz 100 Hz CES FFT Relative Power Group Paired <i>t</i> -Test	325
Table B 7	26-30 Hz 100 Hz CES FFT Relative Power Group Paired <i>t</i> -Test	326
Table B 8	31-35 Hz 100 Hz CES FFT Relative Power Group Paired <i>t</i> -Test	327
Table B 9	36-40 Hz 100 Hz CES FFT Relative Power Group Paired <i>t</i> -Test	328
Table B 10	100 Hz CES Baseline Means FFT Relative Power.....	329
Table B 11	100 Hz CES Baseline Standard Deviations FFT Relative Power.....	330
Table B 12	100 Hz Post CES Group Means FFT Relative Power	331
Table B 13	100 Hz Post CES Standard Deviations FFT Relative Power.....	332
Table C 1	0-40 Hz 0.5 Hz CES Av. Ref. FFT Relative Power Group Paired <i>t</i> -Test.....	335
Table C 2	1-5 Hz 0.5 Hz CES Av. Ref. FFT Relative Power Group Paired <i>t</i> -Test.....	336
Table C 3	6-10 Hz 0.5 Hz CES Av. Ref. FFT Relative Power Group Paired <i>t</i> -Test.....	337
Table C 4	11-15 Hz 0.5 Hz CES Av. Ref. FFT Relative Power Group Paired <i>t</i> -Test.....	338
Table C 5	16-20 Hz 0.5 Hz CES Av. Ref. FFT Relative Power Group Paired <i>t</i> -Test.....	339
Table C 6	21-25 Hz 0.5 Hz CES Av. Ref. FFT Relative Power Group Paired <i>t</i> -Test.....	340
Table C 7	26-30 Hz 0.5 Hz CES Av. Ref. FFT Relative Power Group Paired <i>t</i> -Test.....	341
Table C 8	31-35 Hz 0.5 Hz CES Av. Ref. FFT Relative Power Group Paired <i>t</i> -Test.....	342
Table C 9	36-40 Hz 0.5 Hz CES Av. Ref. FFT Relative Power Group Paired <i>t</i> -Test.....	343
Table C 10	0.5 Hz Av. Ref. FFT Relative Power Baseline Group Mean.....	352
Table C 11	0.5 Hz Av. Ref. FFT Relative Power Group Baseline Standard Deviation.....	353

Table C 12	0.5 Hz CES Av. Ref FFT Relative Power Post CES Group Mean.....	354
Table C 13	0.5 Hz CES Av. Ref. FFT Relative Power Group Post CES Standard Deviation	355
Table C 14	0-40 Hz 100 Hz CES Av. Ref FFT Relative Power Group Paired <i>t</i> -Test.....	357
Table C 15	1-5 Hz 100 Hz CES Av. Ref FFT Relative Power Group Paired <i>t</i> -Test.....	358
Table C 16	6-10 Hz 100 Hz CES Av. Ref FFT Relative Power Group Paired <i>t</i> -Test.....	359
Table C 17	11-15 Hz 100 Hz CES Av. Ref FFT Relative Power Group Paired <i>t</i> -Test.....	360
Table C 18	16-20 Hz 100 Hz CES Av. Ref FFT Relative Power Group Paired <i>t</i> -Test.....	361
Table C 19	21-25 Hz 100 Hz CES Av. Ref FFT Relative Power Group Paired <i>t</i> -Test.....	362
Table C 20	26-30 Hz 100 Hz CES Av. Ref FFT Relative Power Group Paired <i>t</i> -Test.....	363
Table C 21	31-35 Hz 100 Hz CES Av. Ref FFT Relative Power Group Paired <i>t</i> -Test.....	364
Table C 22	36-40 Hz 100 Hz CES Av. Ref FFT Relative Power Group Paired <i>t</i> -Test.....	365
Table C 23	100 Hz CES Av. Ref FFT Relative Power Baseline Group Mean	372
Table C 24	100 Hz CES Av. Ref. FFT Relative Power Baseline Group Standard Deviation	373
Table C 25	100 Hz CES Av. Ref. FFT Relative Power Post CES Group Mean.....	374
Table C 26	100 Hz CES Av. Ref. FFT Relative Power Post CES Group Standard Deviation	375
Table D 1	0-40 Hz 0.5 Hz CES Laplacian FFT Relative Power Group Paired <i>t</i> -Test.....	378
Table D 2	1-5 Hz 0.5 Hz CES Laplacian FFT Relative Power Group Paired <i>t</i> -Test.....	379
Table D 3	6-10 Hz 0.5 Hz CES Laplacian FFT Relative Power Group Paired <i>t</i> -Test.....	380
Table D 4	11-15 Hz 0.5 Hz CES Laplacian FFT Relative Power Group Paired <i>t</i> -Test.....	381
Table D 5	16-20 Hz 0.5 Hz CES Laplacian FFT Relative Power Group Paired <i>t</i> -Test.....	382
Table D 6	21-25 Hz 0.5 Hz CES Laplacian FFT Relative Power Group Paired <i>t</i> -Test.....	383
Table D 7	26-30 Hz 0.5 Hz CES Laplacian FFT Relative Power Group Paired <i>t</i> -Test.....	384
Table D 8	31-35 Hz 0.5 Hz CES Laplacian FFT Relative Power Group Paired <i>t</i> -Test.....	385

Table D 9	36-40 Hz 0.5 Hz CES Laplacian FFT Relative Power Group Paired <i>t</i> -Test.....	386
Table D 10	0-40 Hz 100 Hz CES Laplacian FFT Relative Power Group Paired <i>t</i> -Test.....	396
Table D 11	1-5 Hz 100 Hz CES Laplacian FFT Relative Power Group Paired <i>t</i> -Test.....	397
Table D 12	6-10 Hz 100 Hz CES Laplacian FFT Relative Power Group Paired <i>t</i> -Test.....	398
Table D 13	11-15 Hz 100 Hz CES Laplacian FFT Relative Power Group Paired <i>t</i> -Test....	399
Table D 14	16-20 Hz 100 Hz CES Laplacian FFT Relative Power Group Paired <i>t</i> -Test....	400
Table D 15	21-25 Hz 100 Hz CES Laplacian FFT Relative Power Group Paired <i>t</i> -Test....	401
Table D 16	26-30 Hz 100 Hz CES Laplacian FFT Relative Power Group Paired <i>t</i> -Test....	402
Table D 17	31-35 Hz 100 Hz CES Laplacian FFT Relative Power Group Paired <i>t</i> -Test....	403
Table D 18	35-40 Hz 100 Hz CES Laplacian FFT Relative Power Group Paired <i>t</i> -Test....	404

LIST OF FIGURES

	Page
Figure 1.	Spectral display of a 10 Hz. test signal in absolute and relative power..... 88
Figure 2.	Raw wave display of the 10 Hz calibration signal at 10 microvolts..... 90
Figure 3.	A spectral frequency analysis of a 10 Hz calibration signal..... 91
Figure 4.	Absolute and relative power analysis of a 10 Hz calibration signal. 92
Figure 5.	Absolute and relative magnitude analysis of a 10 Hz calibration signal 92
Figure 6.	Absolute power analysis of a 10 Hz calibration signal..... 93
Figure 7.	Relative power analysis of a 10 Hz calibration signal..... 94
Figure 8.	Absolute power analysis of a 10 Hz calibration signal..... 94
Figure 9.	Relative power analysis of a 10 Hz calibration signal..... 95
Figure 10.	A z-score display of the 10 Hz test signal..... 96
Figure 11.	Absolute magnitude display of the 10 Hz test signal..... 97
Figure 12.	Raw wave display of 10 Hz test signal by channel with channel by channel spectral display..... 98
Figure 13.	Absolute power spectral analysis of 10 Hz test signal..... 98
Figure 14.	Relative power spectral analysis of 10 Hz test signal..... 99
Figure 15.	A table of absolute power values for the 10 Hz (alpha) test signal. 100
Figure 16.	A table of relative power values for the 10 Hz (alpha) test signal..... 101
Figure 17.	An 8 Hz test signal in absolute and relative power as displayed by a linked ears montage, an average reference montage, and a Laplacian montage..... 110
Figure 18.	A weighted average montage of the hardware generated 10 Hz signal..... 111
Figure 19.	Relative power EEG spectra before and after 0.5 Hz CES..... 115
Figure 20.	Relative power EEG spectra before and after 100 Hz CES 115
Figure 21.	Changes in relative power activity after 0.5 Hz CES 117
Figure 22.	Changes in relative power activity after 100 Hz CES 118

Figure 23.	Relative power p -value topographical map for 0.5 Hz CES.....	119
Figure 24.	Relative power p -value topographical map for 100 Hz CES.....	120
Figure 25.	Comparison of relative power topographical maps for 0.5 Hz and 100 Hz CES in delta, theta, alpha and beta frequency bands.....	121
Figure 26.	Relative power p -value topographical map for 0.5 Hz CES from 1 to 20 Hz ..	122
Figure 27.	Relative power p -value topographical map for 0.5 Hz CES from 21 to 40 Hz	123
Figure 28.	Relative power p -value topographical map for 100 Hz CES from 1 to 20 Hz.	124
Figure 29.	Relative power p -value topographical map for 100 Hz CES from 21 to 40 Hz.	125
Figure 30.	Coherence changes after 0.5 Hz CES.	130
Figure 31.	Coherence changes after 100 Hz CES	131
Figure 32.	Amplitude asymmetry changes after 0.5 Hz CES.	134
Figure 33.	Amplitude asymmetry changes after 100 Hz CES.	135
Figure 34.	Phase lag changes after 0.5 Hz CES..	139
Figure 35.	Phase lag changes after 100 Hz CES.	140
Figure 36.	Power ratio changes after 0.5 Hz CES.....	143
Figure 37.	Power ratio changes after 100 Hz CES, in a table format.	144
Figure 38.	Power ratio changes after 0.5 Hz CES.....	145
Figure 39.	Power ratio changes after 100 Hz CES.....	146
Figure 40.	Paired t -test for 1 Hz LORETA.	153
Figure 42.	Paired t -test for 2 Hz LORETA.	154
Figure 44.	Paired t -test for 3 Hz LORETA.	155
Figure 46.	Paired t -test for 4 Hz LORETA	156
Figure 47.	Paired t -test for 4 Hz LORETA	157
Figure 48.	Paired t -test for 5 Hz LORETA	158

Figure 49.	Paired <i>t</i> -test for 5 Hz LORETA	158
Figure 50.	Paired <i>t</i> -test for 6 Hz LORETA	159
Figure 51.	Paired <i>t</i> -test for 6 Hz LORETA	160
Figure 52.	Paired <i>t</i> -test for 7 Hz LORETA	162
Figure 53.	Paired <i>t</i> -test for 7 Hz LORETA	162
Figure 54.	Paired <i>t</i> -test for 8 Hz LORETA	165
Figure 55.	Paired <i>t</i> -test for 8 Hz LORETA	165
Figure 56.	Paired <i>t</i> -test for 9 Hz LORETA	167
Figure 57.	Paired <i>t</i> -test for 9 Hz LORETA	168
Figure 58.	Paired <i>t</i> -test for 10 Hz LORETA	170
Figure 59.	Paired <i>t</i> -test for 10 Hz LORETA	170
Figure 60.	Paired <i>t</i> -test for 11 Hz LORETA	171
Figure 61.	Paired <i>t</i> -test for 11 Hz LORETA	172
Figure 62.	Paired <i>t</i> -test for 12 Hz LORETA	172
Figure 63.	Paired <i>t</i> -test for 12 Hz LORETA	173
Figure 64.	Paired <i>t</i> -test for 13 Hz LORETA	173
Figure 65.	Paired <i>t</i> -test for 13 Hz LORETA	174
Figure 66.	Paired <i>t</i> -test for 14 Hz LORETA	175
Figure 67.	Paired <i>t</i> -test for 14 Hz LORETA	175
Figure 68.	Paired <i>t</i> -test for 15 Hz LORETA	176
Figure 69.	Paired <i>t</i> -test for 15 Hz LORETA	176
Figure 70.	Paired <i>t</i> -test for 16 Hz LORETA	177
Figure 71.	Paired <i>t</i> -test for 16 Hz LORETA	177
Figure 72.	Paired <i>t</i> -test for 17 Hz LORETA	178
Figure 73.	Paired <i>t</i> -test for 17 Hz LORETA	178

Figure 74.	Paired <i>t</i> -test for 18 Hz LORETA	179
Figure 75.	Paired <i>t</i> -test for 18 Hz LORETA	179
Figure 77.	Paired <i>t</i> -test for 19 Hz LORETA	181
Figure 78.	Paired <i>t</i> -test for 20 Hz LORETA	182
Figure 79.	Paired <i>t</i> -test for 20 Hz LORETA	182
Figure 80.	Paired <i>t</i> -test for 21 Hz LORETA	183
Figure 81.	Paired <i>t</i> -test for 21 Hz LORETA	183
Figure 82.	Paired <i>t</i> -test for 22 Hz LORETA	184
Figure 83.	Paired <i>t</i> -test for 22 Hz LORETA	184
Figure 84.	Paired <i>t</i> -test for 23 Hz LORETA	185
Figure 86.	Paired <i>t</i> -test for 24 Hz LORETA	186
Figure 87.	Paired <i>t</i> -test for 24 Hz LORETA	186
Figure 88.	Paired <i>t</i> -test for 25 Hz LORETA	188
Figure 90.	Paired <i>t</i> -test for 26 Hz LORETA	190
Figure 92.	Paired <i>t</i> -test for 27 Hz LORETA	192
Figure 94.	Paired <i>t</i> -test for 28 Hz LORETA	194
Figure 95.	Paired <i>t</i> -test for 28 Hz LORETA	194
Figure 96.	Paired <i>t</i> -test for 29 Hz LORETA	196
Figure 97.	Paired <i>t</i> -test for 29 Hz LORETA	196
Figure 98.	Paired <i>t</i> -test for 30 Hz LORETA	198
Figure 99.	Paired <i>t</i> -test for 30 Hz LORETA	198
Figure 100.	Paired <i>t</i> -test for 31 Hz LORETA	200
Figure 101.	Paired <i>t</i> -test for 31 Hz LORETA	200
Figure 102.	Paired <i>t</i> -test for 32 Hz LORETA	201
Figure 103.	Paired <i>t</i> -test for 32 Hz LORETA	202

Figure 104.	Paired <i>t</i> -test for 33 Hz LORETA	203
Figure 105.	Paired <i>t</i> -test for 33 Hz LORETA	203
Figure 106.	Paired <i>t</i> -test for 34 Hz LORETA	205
Figure 107.	Paired <i>t</i> -test for 34 Hz LORETA	205
Figure 108.	Paired <i>t</i> -test for 35 Hz LORETA	207
Figure 109.	Paired <i>t</i> -test for 35 Hz LORETA	207
Figure 110.	Paired <i>t</i> -test for 36 Hz LORETA	208
Figure 111.	Paired <i>t</i> -test for 36 Hz LORETA	209
Figure 112.	Paired <i>t</i> -test for 37 Hz LORETA	210
Figure 113.	Paired <i>t</i> -test for 37 Hz LORETA	210
Figure 114.	Paired <i>t</i> -test for 38 Hz LORETA	211
Figure 115.	Paired <i>t</i> -test for 38 Hz LORETA	212
Figure 116.	Paired <i>t</i> -test for 39 Hz LORETA	213
Figure 117.	Paired <i>t</i> -test for 39 Hz LORETA	213
Figure 118.	Paired <i>t</i> -test for 40 Hz LORETA	214
Figure 119.	Paired <i>t</i> -test for 40 Hz LORETA	215
Figure 120.	Paired <i>t</i> -test for 1 Hz LORETA	216
Figure 121.	Paired <i>t</i> -test for 1 Hz LORETA	216
Figure 122.	Paired <i>t</i> -test for 2 Hz LORETA	218
Figure 123.	Paired <i>t</i> -test for 2 Hz LORETA	218
Figure 124.	Paired <i>t</i> -test for 3 Hz LORETA	219
Figure 125.	Paired <i>t</i> -test for 3 Hz LORETA	220
Figure 126.	Paired <i>t</i> -test for 4 Hz LORETA	221
Figure 127.	Paired <i>t</i> -test for 4 Hz LORETA	221
Figure 128.	Paired <i>t</i> -test for 5 Hz LORETA	223

Figure 129.	Paired <i>t</i> -test for 5 Hz LORETA	223
Figure 130.	Paired <i>t</i> -test for 6 Hz LORETA	225
Figure 131.	Paired <i>t</i> -test for 6 Hz LORETA	225
Figure 132.	Paired <i>t</i> -test for 7 Hz LORETA	227
Figure 133.	Paired <i>t</i> -test for 7 Hz LORETA	228
Figure 134.	Paired <i>t</i> -test for 8 Hz LORETA	230
Figure 135.	Paired <i>t</i> -test for 8 Hz LORETA	230
Figure 136.	Paired <i>t</i> -test for 9 Hz LORETA	232
Figure 137.	Paired <i>t</i> -test for 9 Hz LORETA	233
Figure 138.	Paired <i>t</i> -test for 10 Hz LORETA	235
Figure 139.	Paired <i>t</i> -test for 10 Hz LORETA	235
Figure 140.	Paired <i>t</i> -test for 11 Hz LORETA	237
Figure 141.	Paired <i>t</i> -test for 11 Hz LORETA	238
Figure 142.	Paired <i>t</i> -test for 12 Hz LORETA	238
Figure 143.	Paired <i>t</i> -test for 12 Hz LORETA	239
Figure 144.	Paired <i>t</i> -test for 13 Hz LORETA	239
Figure 145.	Paired <i>t</i> -test for 13 Hz LORETA	240
Figure 146.	Paired <i>t</i> -test for 14 Hz LORETA	240
Figure 147.	Paired <i>t</i> -test for 14 Hz LORETA	241
Figure 148.	Paired <i>t</i> -test for 15 Hz LORETA	242
Figure 149.	Paired <i>t</i> -test for 15 Hz LORETA	243
Figure 150.	Paired <i>t</i> -test for 16 Hz LORETA	244
Figure 151.	Paired <i>t</i> -test for 16 Hz LORETA	245
Figure 152.	Paired <i>t</i> -test for 17 Hz LORETA	247
Figure 153.	Paired <i>t</i> -test for 17 Hz LORETA	247

Figure 154.	Paired <i>t</i> -test for 18 Hz LORETA	249
Figure 155.	Paired <i>t</i> -test for 18 Hz LORETA	249
Figure 156.	Paired <i>t</i> -test for 19 Hz LORETA	251
Figure 157.	Paired <i>t</i> -test for 19 Hz LORETA	251
Figure 158.	Paired <i>t</i> -test for 20 Hz LORETA	253
Figure 159.	Paired <i>t</i> -test for 20 Hz LORETA	253
Figure 160.	Paired <i>t</i> -test for 21 Hz LORETA	255
Figure 161.	Paired <i>t</i> -test for 21 Hz LORETA	255
Figure 162.	Paired <i>t</i> -test for 22 Hz LORETA	257
Figure 163.	Paired <i>t</i> -test for 22 Hz LORETA	257
Figure 164.	Paired <i>t</i> -test for 23 Hz LORETA	259
Figure 165.	Paired <i>t</i> -test for 23 Hz LORETA	259
Figure 166.	Paired <i>t</i> -test for 24 Hz LORETA	261
Figure 167.	Paired <i>t</i> -test for 24 Hz LORETA	261
Figure 168.	Paired <i>t</i> -test for 25 Hz LORETA	262
Figure 169.	Paired <i>t</i> -test for 25 Hz LORETA	263
Figure 170.	Paired <i>t</i> -test for 26 Hz LORETA	264
Figure 171.	Paired <i>t</i> -test for 26 Hz LORETA	265
Figure 172.	Paired <i>t</i> -test for 27 Hz LORETA	266
Figure 173.	Paired <i>t</i> -test for 27 Hz LORETA	267
Figure 174.	Paired <i>t</i> -test for 28 Hz LORETA	268
Figure 175.	Paired <i>t</i> -test for 28 Hz LORETA	268
Figure 176.	Paired <i>t</i> -test for 29 Hz LORETA	270
Figure 177.	Paired <i>t</i> -test for 29 Hz LORETA	270
Figure 178.	Paired <i>t</i> -test for 30 Hz LORETA	271

Figure 179.	Paired <i>t</i> -test for 30 Hz LORETA	272
Figure 180.	Paired <i>t</i> -test for 31 Hz LORETA	273
Figure 181.	Paired <i>t</i> -test for 31 Hz LORETA	273
Figure 182.	Paired <i>t</i> -test for 32 Hz LORETA	274
Figure 183.	Paired <i>t</i> -test for 32 Hz LORETA	275
Figure 184.	Paired <i>t</i> -test for 33 Hz LORETA	275
Figure 185.	Paired <i>t</i> -test for 33 Hz LORETA	276
Figure 186.	Paired <i>t</i> -test for 34 Hz LORETA	277
Figure 187.	Paired <i>t</i> -test for 34 Hz LORETA	277
Figure 188.	Paired <i>t</i> -test for 35 Hz LORETA	278
Figure 189.	Paired <i>t</i> -test for 35 Hz LORETA	279
Figure 190.	Paired <i>t</i> -test for 36 Hz LORETA	279
Figure 191.	Paired <i>t</i> -test for 36 Hz LORETA	280
Figure 192.	Paired <i>t</i> -test for 37 Hz LORETA	281
Figure 193.	Paired <i>t</i> -test for 37 Hz LORETA	281
Figure 194.	Paired <i>t</i> -test for 38 Hz LORETA	282
Figure 195.	Paired <i>t</i> -test for 38 Hz LORETA	283
Figure 196.	Paired <i>t</i> -test for 39 Hz LORETA	284
Figure 197.	Paired <i>t</i> -test for 39 Hz LORETA	284
Figure 198.	Paired <i>t</i> -test for 40 Hz LORETA	286
Figure 199.	Paired <i>t</i> -test for 40 Hz LORETA	286
Figure C 1.	Relative power paired <i>t</i> -test table for the 0.5 Hz average reference montage. .	334
Figure C 2.	Relative power paired <i>t</i> -test map for the 0.5 Hz average reference montage. .	344
Figure C 3.	Relative power paired <i>t</i> -test map for the 0.5 Hz average reference montage. .	345
Figure C 4.	Relative power paired <i>t</i> -test map for the 0.5 Hz average reference montage. .	346

Figure C 5.	Coherence for the 0.5 Hz CES average reference montage.....	347
Figure C 6.	Amplitude asymmetry for 0.5 Hz CES average reference montage.	348
Figure C 7.	Phase lag for the 0.5 Hz CES average reference montage.....	349
Figure C 8.	Power ratios for the 0.5 Hz CES average reference montage.....	350
Figure C 9.	Power ratios for the 0.5 Hz CES average reference montage.....	351
Figure C 10.	Relative power <i>p</i> -value tables for the 100 Hz CES average reference montage.	356
Figure C 11.	Relative power <i>p</i> -value map for the 100 Hz CES average reference montage.	366
Figure C 12.	Coherence tables and maps for the 100 Hz group average reference montage.	367
Figure C 13.	Amplitude asymmetry for the 100 Hz group average reference montage.	368
Figure C 14.	Phase lag for the 100 Hz group average reference montage.....	369
Figure C 15.	Power ratios for the 100 Hz CES average reference montage.....	370
Figure C 16.	Power ratios for the 100 Hz CES average reference montage.....	371
Figure D 1.	Relative power <i>p</i> -value tables for the 0.5 Hz CES Laplacian reference montage.	377
Figure D 2.	Relative power <i>p</i> -value map for the 0.5 Hz CES Laplacian reference montage.	387
Figure D 3.	Relative power <i>p</i> -value map for the 0.5 Hz CES Laplacian reference montage.	388
Figure D 4.	Relative power <i>p</i> -value map for the 0.5 Hz CES Laplacian reference montage.	389
Figure D 5.	Coherence tables and maps for the 0.5 Hz CES Laplacian reference montage.	390
Figure D 6.	Amplitude asymmetry for the 0.5 Hz CES Laplacian reference montage.....	391
Figure D 7.	Phase lag for the 0.5 Hz CES Laplacian reference montage.	392
Figure D 8.	Power ratios for the 0.5 Hz CES Laplacian reference montage.	393
Figure D 9.	Power ratios for the 0.5 Hz CES Laplacian reference montage.	394

Figure D 10.	Relative power table for the 100 Hz CES Laplacian reference montage.	395
Figure D 11.	Relative power map for the 100 Hz CES Laplacian reference montage.	405
Figure D 12.	Relative power map for the 100 Hz CES Laplacian reference montage.	406
Figure D 13.	Relative power map for the 100 Hz CES Laplacian reference montage.	407
Figure D 14.	Coherence for the 100 Hz CES Laplacian reference montage.	408
Figure D 15.	Amplitude asymmetry for the 100 Hz CES Laplacian reference montage.....	409
Figure D 16.	Phase lag for the 100 Hz CES Laplacian reference montage.	410
Figure D 17.	Power ratios for the 100 Hz CES Laplacian reference montage.	411
Figure D 18.	Power ratio maps for the 100 Hz CES Laplacian reference montage.....	412

CHAPTER 1

INTRODUCTION

Cranial electrical stimulation (CES) is the deliberate application of low-level current, usually 1 milliamperere or less, to the head for a therapeutic purpose. Based upon efficacy found in peer-reviewed research, the United States Food and Drug Administration (FDA) has approved CES for the treatment of pain¹, insomnia, anxiety and depression (code of federal regulations, title 21, vol. 8, section 882.5800). The FDA regulates the sale of CES equipment in the United States as a medical device and established the official name for all medical devices that put a low level current across the head as “cranial electrotherapy stimulation” (National Research Council, Division of Medical Science, 1974). The level of current used is significantly less than with the other two applications of current to the entire head, electroanesthesia and electroconvulsive therapy. To date there have been 126 human studies and 29 animal studies of CES published in the English language literature. The human studies have involved 4,541 subjects without any report of significant or lasting negative side effects from the use of CES (Kirsch 2002). Both animal and human studies have reported remarkable and sometimes unexpected improvements in their research subjects. Because it has historically been referred to by a variety of names, a literature search for CES does not immediately return all of the published studies. Before the FDA selected CES as the official name, the technology has been referred to by a variety of names; such as electrosleep, cranial transcutaneous electrical nerve stimulator (cranial TENS), electroanesthesia, electronarcosis, transcranial electrotherapy (TCET), transcranial direct current stimulation (tDCS), neuroelectric therapy (NET), cranial stimulation, cranial electrical

¹ When used to treat pain, a CES device is considered by the FDA to be a transcutaneous electrical nerve stimulator (TENS) and is regulated in this category of medical device (code of federal regulations, title 21, vol. 8, section 882.5890).

stimulation, electrical stimulation, electro-acupuncture, auricular electrical stimulation, and electrotherapy. The FDA requires a prescription by a licensed mental health or health care professional to legally obtain and use CES device in the U.S. In all other countries CES is an over-the-counter medical device that does not require a prescription.

The idea of applying electrical currents of any strength to the head may sound a bit unwise at best. Yet, there is an extensive body of research demonstrating that CES is safe and provides an effective form of treatment rivaling and often exceeding comparable drug therapies. CES has the advantage of providing treatment without the risk of serious side effects that accompany many pharmacotherapies. Even though there have been numerous studies demonstrating safety and efficacy of CES, little is known about what effect it has on brain function and activity. Prior to this dissertation, there have been no published studies using brain imaging to investigate the effect of CES on cortical and subcortical activity.

This dissertation attempts to improve the scientific understanding of the effect of CES on brain activity. It evaluates the response of human beings to CES with the EEG based imaging techniques of quantitative electroencephalography (qEEG) and low-resolution brain electromagnetic tomography (LORETA). These two brain imaging techniques are based on computerized analysis of EEG, and will allow for both confirmation of earlier raw EEG and spectral EEG reports as well as for expansion of those reports to the domain of topographical brain mapping. The qEEG will provide amplitude-based maps of cortical activation and deactivation, while LORETA will provide low-resolution mapping of cortical and subcortical current densities. It is hoped that this research will contribute to the process of identifying the central effects and mechanism of action of CES.

Literature Review

Background of Electromedicine

William Gilbert introduced the concept of electricity into medicine in 1700 (Sances, Larson, 1975), yet the use of it as a form of treatment predated this introduction by several thousand years. Some early civilizations, such as the early Greek and Egyptian civilizations, were aware of the electricity produced by animals, such as the Nile catfish and the electric eel. They used shocks from these animals to treat everything from pain and headaches to gout (Kirsh, Lerner, 1997; Himrich, Thornley, 1995). Hippocrates, Galen, and Pliny all wrote of the therapeutic use of the electric eel, as did Plato in his dialogue *Meno* (Plato, 1983; Stainbrook, 1948). The Romans also used and wrote about the therapeutic use of the electric eel, although they were never able to figure out why the eel was an effective treatment (Himrich, Thornley, 1995). With the end of Roman civilization, the use of electrical currents in medicine appears to have ended for more than a millennia. It was not until 1747 that the therapeutic use of electric currents reappeared in the form of a machine to treat pain (Braverman, et al., 1992). Apparently this machine was effective but primitive. It seems to have had limited use and was forgotten. A second machine to treat pain was developed one hundred years later, in 1850, apparently without any knowledge of the previous device. In terms of how it worked, this new device was a primitive version of a now common medical device, a transcutaneous electrical nerve stimulator (TENS unit). As with its 1747 predecessor, the 1850 pain control device was effective, but unknown and unused by the medical community. Another century passed before the use of electrical currents for pain control was incorporated into Western medicine. In both the 1850 device and in a modern TENS unit, pain relief is obtained by applying an electrical current to the area of the body in pain.

In modern western medicine acceptance for a therapy is often dependent not just on objective evidence for its efficacy, but also on a model that explains the mechanism of action within already accepted context of medical knowledge and principles. The application of electrical currents to a site on the body which was in pain was a practice known to and used by ancient Egyptian and Greek physicians, but was not accepted in modern medical practice until the development of the gate control theory of pain by Melzack and Wall (Melzack, & Wall, 1965). The gate control theory provided a sensible explanation for why electricity could be used to reduce pain. The theory applied existing medical knowledge to produce a clear and reasonable explanation for the observed therapeutic effect. The theory was well received, and thus so was the therapy. The history of the TENS unit is provided as an example of the long gap that can occur between the development of a therapeutic use for electric currents and its acceptance into orthodox medical practice. The same sort of lag has occurred with CES. The technology is not new, but despite many positive studies and FDA approval, it is relatively unknown. The reason CES has not been embraced by the medical community despite clear evidence of its efficacy may be the lack of a model for how it works. To tell a physician that light current is run across a patient's head and that somehow something happens and the patient improves, induces skepticism in CES as a treatment. It is reasonable to suppose that CES is relatively unknown and unused because there is no medical model for how it works. The gate control theory of pain was an effective model to gain acceptance for the TENS unit, but it is not a reasonable model to explain the effects of CES. Cranial electrotherapy stimulation can reduce pain, just as a TENS unit does; but its use does not strictly conform to the gate control theory of pain, since the current is applied at the head rather than the site of pain. Even worse, the gate control theory does not provide any explanation for how CES could provide relief from anxiety, disturbed sleep, or

depression (the three FDA approved uses of CES); in fact no current theory does. However the effect of the Gate control theory on the acceptance of an electrotherapy for pain is instructive. The story shows that in order for an unfamiliar new therapy to be broadly accepted, it not only has to be effective, it has to make sense.

The Background of Cranial Electrotherapy Stimulation.

Cranial electrotherapy stimulation is a form of electromedicine for which acceptance has lagged behind its initial discovery and development. The foundations for CES go as far back as 1836, when the Russian physiologist Ilomafitcky demonstrated that an electrical current could have an inhibitory effect on the human nervous system (Obrosow, 1969). In 1902, two French researchers, Dr. Leduc and Dr. Rouxeau, were the first to experiment specifically with the use of low current for electrical stimulation of the brain (Kirsh, 1996). Apparently independent of the work of Drs. Leduc and Rouxeau, CES also appeared in the 1920's in the theoretical musing of the Russian physiologist Ivan Pavlov (Pavlov, 1928). In his research on conditioned responses with dogs, Dr. Pavlov discovered that, given the proper combination of conflicting conditioned responses, the dogs would promptly fall asleep. He considered the reason for this rather strange behavior to be "internal inhibition." Internal inhibition was a theoretical response to overexcitement that protected the nervous system of the animal from damage. Internal inhibition would suppress activity in any part of the brain that became too physiologically aroused. Pavlov came to the conclusion that sleep and internal inhibition were the same thing, with sleep being a case of internal inhibition that has spread across the entire cortex and then into the subcortical structures. Dr. Pavlov theorized that the cranial application of low-level current would induce internal inhibition, and thus eventually sleep. While Dr. Pavlov never investigated his theory of

inducing internal inhibition with low-level current, in 1953 Giljarowski, a Soviet researcher did. Giljarowski became the first documented investigator of therapeutic CES. He applied Pavlov's theory of inducing internal inhibition with low level current, and attempted to use CES as a treatment for insomnia (Douglas, 1995). Because Pavlov had originally theorized that CES would induce sleep Soviet researchers called the new electrotherapy "electrosleep." The Soviets were the first modern researchers of therapeutic CES and have produced an extensive body of research literature on the subject; research that to this day remains largely unknown in Western countries. In 1966 and 1969, two international conferences were held in which Soviet block scientists shared with the rest of the world their research on CES and the related technology of electroanesthesia (Wageneder, & Schuy, 1967, 1970). Electroanesthesia uses higher levels of current than CES, sufficient to produce reliable and effective anesthesia. While the result of CES for the induction of sleep was mixed, Pavlov's theory of internal inhibition appeared to work in that the higher levels of current produced reliable and safe anesthesia in humans and animals. The results presented by the Soviets were interesting, but somewhat suspect by Western researchers, a reaction likely enhanced by Cold War tensions. Critics of Soviet research noted a frequent lack of control groups, lack of double blind protocols and lack of other methodological standards applied in Western science. However, these two conferences stimulated Western research interest in CES, and researchers in the United States, Europe and India started investigating CES. Western research literature has found CES safe and effective for multiple therapeutic uses. Despite the positive findings of Western researchers, CES did not find fertile ground among Western clinicians. The approval of CES by the FDA has provided official recognition of sufficient good science to apply CES as a safe and effective therapy for depression, anxiety, sleep disorders and pain; yet it remains largely unknown to most western

physicians, psychiatrists and psychologists.

Differences Between CES, Electroanesthesia, tDCS and Electroconvulsive Therapy

Most CES devices utilize a very low level of direct current applied to the head. It is the fact that the therapeutic current is quite small that distinguishes CES from other forms of cranially applied current. CES units typically operate at .1 milliamperes (one millionth of an ampere, or 1 microampere) to 1 milliamperes (one thousandth of an ampere) of current and are usually powered by nine-volt batteries. Nine volts at a maximum of 1 milliamperes (mA) of current produces a maximum of .0054 watts, or 11,000 times less power than what is required to operate a 60-watt light bulb (Kirsch, 1996).

Electroanesthesia is a technology related to CES but which uses stronger cranially applied currents for surgical anesthesia. There appears to be little regular use of electroanesthesia in humans in the US, although the FDA has approved it for that purpose (code of federal regulations, title 21, volume 8, part 868 section 868.5400). Electroanesthesia utilizes currents that are 100 times stronger than those used in CES to provide full surgical anesthesia (Sances & Larson, 1975). Electroanesthesia is remarkable for its consistent effectiveness, quick recovery time and the lack of mortality and morbidity associated with chemical anesthesia. As with CES, electroanesthesia has seen little use in Western countries and remains essentially unknown to mainstream Western medicine.

Transcranial direct current stimulation (tDCS) is the application of a very low level direct current to head with the intention of making lasting changes to cortical excitability. The field of tDCS arose from transcranial magnetic stimulation where electromagnets are used to induce changes in cortical activity. In terms of regulatory definitions used by the FDA there is no

difference between tDCS and CES, the FDA definition of CES includes tDCS. However, there is a significant technical difference between tDCS and CES in that the name tDCS specifies a type of CES in which the current is not reversed. In most CES devices the flow of the current is reversed to prevent potential tissue damage to the brain from electrophoresis. In tDCS the current is never reversed, therefore it is called a “direct” current. The migration of electrically charged particles in a current is well understood in biological science and the application of current that is not reversed exploits this phenomenon to create DNA and protein assays. The researchers utilizing tDCS view tDCS as substantially different from CES and not a subtype or more primitive (less safe) version of CES. For these researchers the risk of using of a current that does not reverse direction is necessary to obtain the benefits they hope to provide. The model utilized by tDCS researchers is derived from transcranial magnetic stimulation where stimulation is provided to increase excitability in a targeted region of cortex. In this model the current flow increases cortical activation under positive electrode, a benefit that would be lost if the current was reversed to prevent electrophoresis. In this model electrophoresis is not the only cost of treatment, but also that if there is an increase in cortical excitability in a region under the positive electrode of a non-reversing current, there is a comparable decrease in excitability in the region under the negative electrode (Trivedi, 2006). However, it has also been found that using the negative electrode to a targeted area of cortex can increase performance (Trivedi, 2006), just as using the positive electrode does. This finding is at odds with the operating theory for tDCS which would hold that the region under the negative electrodes should experience an inhibition of activity from the current, and thus reduce performance. The finding that using either a positive or negative electrode enhances performance suggests that the model for why tDCS works may need revision and that indeed tDCS may not be using a different mechanism from

CES. However, tDCS is interesting in that it involves placing electrodes over targeted areas of the cortex and this is a procedural difference from standard CES that may ultimately prove to be of importance. In most CES applications the electrodes are placed in the same location for all subjects and conditions. It is possible that improvements from CES may occur with targeted electrode placement that does not occur from a uniform electrode placement in all subjects. Future research will be needed to determine if electrode placement can alter the effectiveness of CES in some applications. The current research in tDCS has had success in improving mood, memory, learning, sleep, migraines (Marshall, Mölle, Hallschmid, & Born, 2004; Trivedi, 2006) and other affective and cognitive conditions that also benefit from traditional CES. At this point there have been no published findings, which show substantially different results from tDCS than what have been obtained in over forty years of literature on CES. While tDCS may appear to be a more primitive form of CES, it is possible that future research may show benefits not obtained from CES where the current is reversed. In a personal communication with the author, Dr. Juri Kropotov of the Institute of the Human Brain of Russian Academy of Sciences in St. Petersburg Russia reported benefits from tDCS in stroke victims that far exceed any benefits that have been reported from the standard form of CES. It may be that any form of CES, with the current reversing or with direct current may provide benefit with selected placement of the electrodes, or that the hazards of direct current may come with benefits not found if the current is reversed. If the work Dr Kropotov referred to is published and replicated, in the future it may be found that there is indeed a significant clinical difference between CES and tDCS. However, at this time there does not appear to be any strong evidence that tDCS is substantially different from the safer form of CES which reverses the current to prevent tissue damage from electrophoresis.

The only form of cranially applied current routinely used in Western medicine is

electroconvulsive therapy (ECT). This is a form of treatment that utilizes currents that are 3-5 times greater than those used for electroanesthesia, and 300-500 times greater than CES (Sances & Larson, 1975). ECT is both the most powerful form of cranially applied current and the only form of cranially applied current with a history of having killed patients (Smith, 1995), injured patients, or created harmful side effects (Breggin, 1997). As it was originally used, ECT would routinely result in physical injuries due to the strength of the major motor seizures it induced. A naturally occurring seizure rarely breaks bones or fractures teeth, however these injuries were common with early ECT. In order to reduce these injuries, a modified ECT procedure was introduced. The modified ECT utilizes a muscle relaxant (typically succinylcholine) and general anesthesia to prevent overt injuries due to seizure. Because of the strength of the muscle relaxant used, the patient must be placed on a respirator to remain oxygenated. The use of muscle relaxant makes a patient more resistant to seizures, so the level of current used has to be increased to cross the higher seizure threshold. Since ECT is the only form of cranially applied currents with a history of injury, and it is the strength and duration of the current used in ECT which makes it substantially different from electroanesthesia, it is reasonable to assume that the increased current level used in modified ECT increases the risk of injury to the patient. Likewise the introduction of the use of chemical anesthesia introduces the risk of death or injury as a result of the anesthesia. However, even if the modified procedure would appear to expose the patient to a higher risk for brain injury or death, the overt injuries from the original ECT protocol are eliminated. The modified ECT protocol also reduces some of the effects of ECT on cognitive functioning by applying current only to the right (nonverbal) hemisphere, where any disruption of function has less impact on the use of language. Even though the modified form of ECT has been presented as a safe procedure which effectively eliminates the dangers of ECT (Fink, 1999),

it still poses a real risk of harm to memory and other cognitive functions (Breggin, 1997, Templar, 1992), as well as carrying the risk of any major medical procedure requiring general chemical anesthesia.

Because of the widespread use of ECT in the West, it has been evaluated and debated. Yet, curiously, even though ECT is a procedure for injecting large amounts of electrical current into the human brain, the electrical current used in ECT is not considered to be the actual therapeutic agent. The “electro” aspect is relatively ignored while the “convulsive” part is emphasized. The medical community traditionally has viewed ECT as a safe, controllable method of inducing therapeutic seizures. It is the seizure rather than the electrical current that is considered to be the therapeutic agent. It is a paradoxical treatment in that as a general rule modern medicine views seizures as harmful and potentially life threatening, yet individuals who spontaneously experience seizures are placed on medications with significant side effects to prevent seizures. However, in the case of ECT, normal medical wisdom is inverted and the goal is the induction of seizures for a therapeutic benefit. The reason appears to be the medical history leading to the development of ECT. Before electricity was used to induce seizures, chemical agents were used to induce seizures for therapeutic benefit.

Convulsive therapy was invented in 1933 by Ladislav Meduna (Fink, 1999; Kolb & Whishaw, 2000), a Hungarian neurologist and neuropathologist. Dr Meduna routinely performed autopsies that included a visual examination of the brain. He observed differences in the brains of epileptic and demented patients that led him to believe that epileptics were protected from dementia by their seizures. He concluded that seizures and dementia were physiologically inimical to each other. To turn his observations into a treatment Dr. Meduna induced seizures with intramuscularly injected camphor oil. After inducing a seizure, he saw significant clinical

improvements in many of his patients. When he learned that the drug pentylenetetrazol resulted in immediate seizures in animals he began utilizing pentylenetetrazol as his preferred chemical agent. In 1937 Dr. Meduna reported that he had treated 110 patients, with remission of symptoms in 53 of his patients. Unfortunately, the experience for the patient was so frightening and aversive that many people would not repeat the therapy after the first treatment. Dr. Meduna's convulsive therapy was effective only if a patient could be convinced to go through the experience several times. The aversiveness of the convulsive procedure was a practical and significant barrier to its use. Other chemical agents were used to induce seizures, but to varying degrees were medically dangerous to the patient and suffered from the same problem of being overly aversive. As late as the 1960s deliberate overdose with insulin was being used in the United States to provide convulsive therapy for depression.

To be effective and practical, convulsive therapy required a safe and less fear-inducing method of producing seizures than the drugs at hand. Two Italian doctors, Cerletti and Bini, were searching for a better method of inducing therapeutic seizures and settled upon electricity as a promising agent. They were the first physicians to utilize electricity to induce seizures in a human (Fink, 1999). Electricity is a good candidate for both inducing a seizure and overcoming aversion to a second treatment; strong electric shocks physiologically prevent the processing of an experience into a long-term memory. Their first patient recovered from his mental illness after three weeks of alternate days of electroconvulsive therapy. A new and better-tolerated method of inducing seizures had been found. Patients who received ECT did not remember the ECT procedure, or what happened immediately before, so they are more willing to receive multiple treatments with ECT. The primary practical barrier to the use of convulsive therapy had been overcome. The new electrical method did have drawbacks, namely the physical injuries and

cognitive problems it produced. The modified ECT procedure reduced these complaints and became the standard for convulsive therapy. Even though the current modified form of ECT still has negative effects on cognitive functioning, the improvement in affective functioning has been felt to be worth these often-significant side effects. Many patients who are profoundly depressed do not function in society, or even engage in basic self-care. Suicide is the frequent result of severe depression. In the event that medications are not effective, the medical community has frequently viewed ECT as a life saving treatment of last resort.

While ECT is generally regarded by psychiatrist as a safe procedure (Finch, Sobin, Carmody, et al, 1999) it is believed by some psychiatrists that injuries and deaths from ECT may simply go unreported (Breggin, 1997). There is little data on the actual morbidity or mortality of ECT; however, when Texas introduced a law requiring the reporting of all deaths within fourteen days of ECT treatment (Texas health and safety code. section 5.01, subtitle C, title 7, 1993), 15 months of data revealed 8 deaths in 2500 patients (Reid, Keller, Leatherman, Mason, 1998). The cause of death in these 8 patients were heart attack (three patients), suicide (two patients), auto accident (one patient) and embolism (one patient). Two of the patients died on the day of the ECT treatment, one from a heart attack and the other from an embolism. In terms of medical procedures utilizing anesthesia, the death rate was considered to be within what is expected with any procedure requiring anesthesia. The psychiatrists reporting this data concluded that the Texas data confirmed ECT is generally safe and effective.

Because of the history of the development ECT, the medical community has quite reasonably felt that ECT relieves depression by inducing major motor seizures. This belief has persisted, even though the mechanism by which a series of seizures can relieve depression is unknown. The initial hypothesis of Dr. Meduna in 1933 that seizures and dementia were

physiologically inimical to each other seems in light of more modern medical knowledge rather unlikely; his conclusion that seizures are beneficial and protect the brain seems equally unlikely.

Many modern psychiatrists believe ECT is probably changing the neurochemistry in the brain, and it is this supposition that forms the defacto model for the use of ECT. In this informal model of ECT, the seizure produced by ECT is viewed as the primary agent for treatment and not the actual current that is used to induce the seizure.

Because CES does not induce seizures, Western physicians typically do not view ECT and CES as having a common mechanism of action. However, both are cranially applied electrical currents and both are effective treatments for depression (Fink, 1999; Hearst et al. 1974). CES utilizes a tiny current applied for 20-60 minutes a day for two to three weeks to relieve depression. ECT utilizes brief jolts of very high level current several times a week for two to three weeks to relieve depression. It is rather reasonable to suppose that since they both apply the same agent (electrical current), and effectively treat the same condition (depression), that these two techniques of electromedicine may have a similar mechanism of action. Whether or not they share a common mechanism of action, they are both effective non-pharmacological treatments for depression. The puzzling aspect of considering these therapies together is why ECT would continue to be practiced when there is another non-drug therapy at hand that does not pose the same risks as ECT. There is a morbidity and mortality associated with ECT, which does not exist with CES. The use of CES provides similar affective gains as ECT without the risk to cognitive functioning found with ECT; CES has even been shown to improve some aspects of functioning. While similar in some respects, ECT and CES are quite different in terms of risk.

There is also a significant difference between CES and ECT in terms of the expense of each treatment. The use of ECT is costly. It is a medical procedure requiring anesthesia and all

the attendant medical personnel, costs and risks of any procedure involving general anesthesia. The ECT procedure is repeated several times a week for two to three weeks to treat depression; and requires the patient to be hospitalized for several weeks during the course of therapy. The fact that ECT is costly, and used more frequently in the elderly, has led to accusations that profit motives drive the use of ECT as a means to exploit Medicare funds (Reid, Keller, Leatherman, Mason, 1998). In contrast to ECT, the CES procedure for treating depression is a relatively inexpensive outpatient protocol with no risk to most medically fragile population such as the elderly. Outpatient treatment with CES involves teaching patients to place the ear clips from a small hand-held unit on their ears, and letting the device run for 20-60 minutes a day, for two to three weeks. The patient can independently administer the treatment in his or her own home. Unlike some medication for treating depression, there is no risk of overdose or any other misuse of the treatment for self-injury. The use of CES does not involve hospitalization or expensive medical teams, so the cost of the treatment is confined to the cost of the CES unit (typically under \$1,000 US) and progress monitoring by the physician or psychologist.

While both CES and ECT effectively treat depression through the use of cranially applied currents, the costs, complications and risks to patients from ECT create a wide divide between the two therapies. Despite the risk to patients from ECT, and the safety of CES in treating the same symptoms, at this time electroconvulsive therapy is also the only form of cranially applied current widely known or therapeutically used by Western medicine.

The Use of CES for Inducing Sleep and Treating Sleep Disorders

In the United States, the Federal Drug Administration (FDA) has approved CES for the treatment of insomnia. The original Soviet researchers named CES “electrosleep”; and when the

first study on CES was published in the US, it was an attempt to determine if CES indeed did induce sleep (Forster, Post, & Benton, 1963). The researchers discovered that while some of the study subjects fell asleep with CES, many did not. The results were too inconsistent and mixed to conclude that CES induced sleep. Subsequent studies have found that while CES appears to relax subjects and makes most of them drowsy, for some subjects CES actually enhances alertness and decreases fatigue and sleepiness (Forester, et al., 1967). The response to CES by most individuals is an increased sense of relaxation accompanied by either sleepiness or enhanced alertness. The effect of decreased sleepiness may be a function of the frequency of stimulation used. A Russian study found 100 Hz CES to have a stimulation effect on cognitive functioning and to increase physiological arousal, while 10 Hz was found to have a sedative effect (Giginshvili et al., 1995). It may also be that in any frequency of CES, since it increases relaxation, people who are sleep deprived respond to the increased relaxation by falling asleep.

A year after the first CES study was published in English, a second study compared CES with 100 mg of phenobarbital for the induction of sleep in 34 hospital patients complaining of insomnia (Straus, & Bodian, 1964). Straus and Bodian found that CES was more effective than placebo, and was almost as effective as phenobarbital for inducing sleep. Since all of the patients in this study remained on preexisting medications, it is not clear if the results were affected by interactions between CES and medication.

A year after this second sleep study, a third investigation into the use of CES to induce sleep was published in the *British Journal of Anesthesiology* (Magora, et al., 1965). In this study the authors attempted to determine just what was required to induce sleep with CES. Like Forster et al., Magora and his colleagues had mixed findings when trying to use CES to induce sleep. They discovered that despite varying the amount of current, the type of current, and many other

variables across a broad range of values, CES did not consistently induce sleep in all of their subjects. While many of the subjects did fall asleep, a large number did not. The subjects who didn't fall asleep did respond to the CES by becoming very relaxed and had decreases in EMG readings. Some subjects reported that they were so relaxed they lost track of time, but the researchers noted they didn't fall asleep. While sleep is not reliably induced by the very low level of current used in CES, Dr. Pavlov's hypothesis may not have been wrong. He theorized that cranially applied electric current should produce cortical inhibition and thus induce sleep; but while this is not reliably seen in CES, the higher current levels of electroanesthesia do perform as he predicted and reliably induce unconsciousness.

A review of the CES literature shows continued attempts to induce sleep with CES, with mixed results. Most authors agree that sometimes CES does produce sleep and sometimes it does not. It is possible that the lack of clear findings may be the result of variances in fatigue and sleep debt among research subjects. CES usually induces a feeling of relaxation in most subjects, which likely facilitates sleep in tired or sleep-deprived subjects, but not in well-rested subjects. The findings could also be attributed to the fact that among some people, CES has the effect of increasing alertness and decreasing fatigue. If a significant portion of subjects respond to CES in this manner they will always confound studies evaluating only sleep.

The failure to find a reliable induction of sleep with CES does not mean there is no effect from CES on sleep. Whether or not any single session of CES induces sleep, continued use of CES is generally beneficial for disordered sleep. The published research has shown regular use of CES significantly improves sleep quality, reduces time to sleep onset, increases time in deep sleep and normalizes disordered sleep (Feighner, Brown, & Oliver, 1973; Cox, & Heath, 1975; Empson, 1973; Feighner, Brown, & Oliver, 1973; Gomez, & Mikhail, 1974; Hearst, Cloninger,

Robert, & Cadoret, 1974; Hozumi et al., 1996; Lichtbroun, Raicer, & Smith, 2001; Magora, Beller, Assael, & Askenazi, 1967; Philip, Demontes-Mainard, Bourgeois, & Vincent, 1991; Rosenthal, 1972, Rosenthal, & Wulfsohn, 1970; Weiss, 1973).

A good example of the powerful normalizing effect of CES on disturbed sleep can be found in study utilizing CES with drug and alcohol treatment. When alcoholics go into treatment, it usually takes several weeks for their sleep patterns to become normal after going through withdrawal. Likewise, it takes heroin and amphetamine addicts two months to attain a normal sleep pattern, and barbiturate addicts as long as four months. A seven year study of 186 drug addicts and alcoholics admitted for in-patient treatment found that the application of CES not only prevented withdrawal, but returned sleep patterns to normal between the third and ninth night of CES treatment (Patterson Firth, & Gardiner, 1984). This is an impressive finding that illuminates just how powerful CES can be in normalizing disturbed sleep.

The restoration of sleep patterns to normal is a ubiquitous finding in almost all of the CES sleep research that involved multiple treatments over time. There has been only one study that found no effect from the regular use of CES on sleep. This study failed to find any effect from CES on sleep, depression, anxiety or EEG among a group of 17 chronic insomniacs (Frankel, Buchbinder, & Snyder, 1973). The subjects in the study had an average of 20 years of insomnia and were given 15 forty-five minute CES treatments at either 15 Hz or 100 Hz, and then crossed over for 15 more treatments in the opposite condition. The failure of CES to have any effect at all on sleep onset, EEG, corticosteroid levels, anxiety scale ratings and depression scale rating is remarkable given the outstanding level of response on these dimensions found in all other studies of CES. The findings of this study stand in marked contrast to the rest of the literature on CES, and the FDA finding of efficacy for CES in the treatment of sleep disorders,

depression and anxiety. The anomaly presented by this study suggests that there was some sort of error or confound within the study. Such an error or confound can most likely be ascribed to either equipment failure, or the concurrent use by all the study volunteers of medications that blocked the effect of CES.

In an ongoing study of the use of CES in a locked psychiatric setting, some psychotropic medications have been noted to have an apparent interaction with CES that reduces or eliminates the CES benefit (Reed, 2003). Interaction effects between CES and medication are an established part of the literature on CES. It has been shown to enhance the effects of anesthesia medication fentanyl (Naveau et al., 1992; Stanley Cazalaa, Atinault, Coeytaux, Limoge & Louville, 1982) and N₂O (Stanley Cazalaa, Limoge & Louville, 1982), but its interactions with other classes of medication are not well documented. Since CES has been shown to enhance medications having a CNS depressant effect (anesthetics), it may be that a CNS stimulant medication may degrade or block the effects of CES. The subjects in the Frankel et al. study were long-term insomnia patients during the early 1970s when amphetamine was routinely administered for daytime fatigue. It is possible that the subjects in the study may have been taking stimulant medication for daytime fatigue, which may account for the lack of any effect of CES. While this explanation is a possibility, the most parsimonious explanation of why only this study failed to find any effects at all from CES would be equipment failure of the CES unit used in the study

In 1973 a researcher by the name of Marc Weiss recruited research volunteers who had chronic insomnia and obtained a baseline sleep onset evaluation of each of them in a sleep lab. He then randomly assigned the volunteers into CES and placebo groups and conducted a double blind study on the effect of CES on sleep itself, rather than the induction of sleep. The average amount of time for it took the volunteers in the CES treatment group to fall asleep before using

the CES units was 60.8 minutes. After two weeks of CES, this group averaged 10.6 minutes to fall asleep. The group who received placebo CES treatment took an average of 60.5 minutes to fall asleep before the placebo treatments, and after the placebo treatments this second group took an average of 58.8 minutes to fall asleep. The CES treatment group had a statistically significant and clinically significant improvement in sleep latency, while the placebo group did not. A follow-up study showed that all of the benefits experienced by the treatment group were maintained both at two weeks and two years after the CES treatment (Weiss, M., 1973).

Consistent among all studies examining the impact of CES on sleep, except the one noted previously, were findings that repeated CES use improves sleep latency and sleep quality. Even among people suffering from chronic insomnia, sleep latency was significantly reduced and sleep quality was improved (Cox, & Heath, 1975; Feighner, Brown, & Oliver 1973; Flemenbaum, 1974; Patterson et al., 1984; Philip et al., 1991; Rosenthal, & Wulfson, 1970; Sing et al., 1971; Straus, Bodian, 1964; Rosenthal, 1973; Weiss, 1973). To date there have been 27 published studies evaluating the effects of CES on human sleep (Kirsch, 2002), only one of which failed to show a positive effect (as noted above). CES was even found to increase sleep quality among horses (Kirsh, 2002) and monkeys (Sing et al., 1971). Since there is no placebo effect with horses and monkeys, those animal studies provide strong objective evidence for the effectiveness of CES in improving sleep quality. Unlike many of the medications prescribed for sleep disorders, CES is not addictive. The effects of CES on sleep make it a promising treatment for sleep disorder clinics; it decreases sleep latencies, increases sleep duration, decreases the frequency of awakening from sleep and normalizes disordered EEG (Magora, Beller, Assael, 1967; Cox, & Heath, 1975; Feighner, Brown, & Oliver 1973, Flemenbaum 1974; Patterson et al.,

1984; Philip et al., 1991; Rosenthal, & Wulfson, 1970; Sing et al., 1971; Straus, Bodian, 1964; Rosenthal, 1973; Weiss, 1973).

The Use of CES in Alcohol and Drug Treatment

Cranial electrical stimulation has been found to be an effective intervention in drug and alcohol treatment. As mentioned previously, the seven-year Patterson et al. study found CES to be effective for controlling the symptoms of withdrawal from alcohol and other drugs. Other studies in both human and animal subjects have reported similar findings. Omura reported that CES significantly reduced the symptoms of opiate withdrawal in more than 500 subjects (Omura, 1975). Omura was using CES through acupuncture points on the ears and did not double blind his study or control for confounding variables. But this study is noteworthy because of the large number of subjects whose symptoms of withdrawal were reduced or eliminated by the CES treatments.

In 1982, a double blind study was conducted in which CES was compared to the medication alpha methyl dopa for treating symptoms of opiate withdrawal in an inpatient setting (Gold, Pottash, Sternback, Barbaban, & Annitto, 1982). This was a well-controlled and well-designed study in which neither placebo medication nor placebo CES was found to be effective for controlling withdrawal. However CES treatment and alpha methyl dopa treatment were both effective in controlling the symptoms of acute withdrawal, and CES was found effective for protracted withdrawal. Alpha methyl dopa had a side effect of producing a profound rebound depression, while CES was as effective as alpha methyl dopa for withdrawal, but did not produce any rebound depression.

A more heterogeneous group of subjects was used in 1991 in a study of the effects of

CES on drug withdrawal (Phillip, Demontes-Mainard, Bourgeois, & Vincent, 1991). In this study the research subjects had major depression and were receiving a variety of medications, such as barbiturates, benzodiazepines, neuroleptics and antidepressants. All the subjects were taken off all medication on the first day in the study and were placed in either a CES treatment group or CES placebo group. Two of the placebo group subjects experienced seizures (without prior history of seizure) due to benzodiazepine withdrawal. None of the subjects in the CES treatment group experienced seizures. Anxiety and sleep problems rose significantly in the placebo group during the drug washout period, while anxiety during withdrawal actually decreased and sleep improved in the CES group

These studies illustrate that CES is remarkably effective in the treatment of the symptoms of withdrawal from drugs and alcohol. The fact that the effectiveness of CES is retained in double blind protocols indicates that the mechanism of effect is a biological one rather than a psychological one.

Animal research has replicated the human studies showing that CES is effective in treating withdrawal, providing additional support for a biological rather than psychological mechanism underlying the effectiveness of CES in treating the symptoms of withdrawal.

Abrupt morphine withdrawal induces motor hyperactivity in rats during the withdrawal period; however, when the rats are treated with CES there is a significant reduction in the severity of withdrawal as measured by motor hyperactivity (Dougherty, Dong, Faillace, & Dafny, 1990).

Alcohol withdrawal syndrome (AWS) also creates measurable changes in the behavior and activity levels of rats, which is reduced or eliminated by CES (Krupisky, et al, 1991).

Behaviorally, the rats appeared to benefit significantly from the use of CES to attenuate the effects of alcohol withdrawal. An insight into the mechanism of how CES reduces the symptoms

of withdrawal is suggested in the rat AWS study. Cerebral spinal fluid (CSF) was obtained from the rats before and after CES and was compared on levels of beta-endorphin. Beta-endorphin is an endogenous opioid associated with pain relief (Fries, 2002). Significant increases in beta-endorphin were found after CES (Krupitsky et al., 1991), suggesting direct neurochemical changes induced by CES are a part of how it can attenuate the symptoms of withdrawal. Human studies conducted by spinal tap have found a 219% mean increase in beta-endorphin in the CSF after CES (Shealy, et al., 1998). Human and animal studies have also found other significant changes in neurotransmitters and body chemistry from the use of CES, although at this time such changes are still poorly understood (Pozos, 1971; Briones, Rosenthal, 1973; Frankel, Buchbinder, & Snyder, 1973; Kotter, Henschel, Hogan, & Kalbfleisch, 1975; Krupitsky et al., 1991; Rosenthal, 1973, Shealy, et al., 1989, Shealy, et al., 1998).

Cranial electrical stimulation is useful for more than just the treatment of the physical symptoms of withdrawal. It also improves affective functioning during substance abuse treatment. Alcoholics who received CES as a part of their treatment showed significant reductions in anxiety (Bianco, 1994, Krupitsky et al., 1991; May, May, 1993; Passini, Watson, & Herder, 1976; Smith, & Tyson, 2002; Weingarten, 1981; McKenzie, Costello, & Buck, 1976; Padjen, Dongier, Malec, 1995), tension (Tomsovic, & Edwards, 1973), depression (Bianco, 1994; Krupitsky et al., 1991; May, May, 1993; Smith, & O'Neill, 1975; Smith, & Tyson, 2002; Weingarten, 1981; Padjen, Dongier, & Malec, 1995; Padjen, Dongier, Malec, 1995) and total mood disturbance (Smith, & O'Neill, 1975). A relatively small study of just 14 inpatients found that in addition to improvements in anxiety and depression there were significant declines in hostility, with concomitant increases in scales for self worth, positive emotional expressiveness and intimacy with others. A double blind study of 146 alcoholics found the same significant

decrease in anger and hostility with CES (Smith, & Tyson, 2002). Decreases in hostility or agitation have also been found in severe in-patient psychiatric populations (Reed, 2003) and with the elderly (Hozumi, Hori, Okawa, Hishikawa, & Sato, 1996).

The cognitive ability of alcoholics in treatment with CES improves over controls. A study of 227 alcoholics found that CES significantly improved short-term memory over baseline, while the control subjects' short-term memory deteriorated from baseline (Smith, & Day, 1977). There is case evidence from the treatment of posttraumatic amnesia suggests that CES may have beneficial effects beyond short-term memory (Childs, & Crismon, 1998). A double blind study of 100 alcoholic inpatients using placebo CES and sub-sensation CES found significant improvements in spatial abilities as measured by the mazes and spatial relations subtests of the Revised Beta IQ test (Smith, 1982). A second double blind study of 60 alcoholics found significant improvements on the Revised Beta and the digit span, digit symbol and object assembly subtests of the WAIS IQ test by the CES subjects, but not by the controls (Schmitt, Capo, Frazier, & Boren, 1984). Physiologically, the brain of the alcoholic may function better when treatment includes CES. The P300 component of evoked response potentials in the EEG has been found to be of significantly lower amplitude in alcoholics as compared to non-alcoholic controls (Enoch, et al., 2002). The P300 response increases significantly after CES for alcoholics, but not for non-alcoholic controls (Braverman, Smith, Smayda, & Blum, 1990). For many alcoholics, the latency of the appearance of posterior alpha EEG when an alcoholic closes his eyes is longer than what is found in non-alcoholic controls. Cranial electrotherapy stimulation has been found to decrease the latency of the appearance of posterior alpha in eyes closed condition in the EEG record of alcoholics, but not with normal controls (Krupitsky et al., 1991). These findings suggest physiological differences in the brains of alcoholics that are moved

toward normal by CES. The concept of normalization is further supported by the lack of change Krupitsky et al., found in EEG latency in the non-alcoholic controls.

The existing literature documents CES as a remarkably effective adjunctive therapy to existing drug and alcohol treatment. A meta-analysis of CES in substance abuse treatment conducted in 1991 found an effect size of .94 for CES *plus standard treatment* when compared to CES placebo and standard treatment. Standard drug and alcohol treatment alone was found to have an effect size of only .171 (O'Connor, Bianco, & Nicolson, 1991). It appears that the impressive results shown by a combined CES plus standard addictions treatment approach is a synergistic one. This meta-analysis concluded that there is no adjunctive therapy that can increase the effectiveness of the standard addictions treatment programs to the extent that CES does (O'Connor, Bianco, & Nicolson, 1991). If CES is used without an addictions program the results are not as positive as in a combined approach. In a well-controlled double blind study, CES alone provided affective and functional benefits and a significant decline in the amount of alcohol consumed, but no change was seen in general drinking behaviors (Padjen, Dongier, Malec, 1995). With CES alone, the biology appears to change, but the psychology of the drinking behaviors does not. The focus of most drug and alcohol treatment is psychological and behavioral in nature with very little attention to physiology beyond the initial withdrawal period. Together, CES and traditional drug and alcohol treatment provide interventions for both the physiology and the psychology involved in alcohol and substance abuse. In general, it would appear that the effectiveness of substance abuse treatment is greatly enhanced when CES is combined with traditional treatment methods.

Treating Depression with CES

The FDA has approved CES for the treatment of depression (title 21, code of federal Regulations, Part 882.5800). To date there have been 28 published studies and case summaries reporting CES to be an effective treatment for depression. It has been found effective for depression in chemical dependency treatment (Bianco, 1994; Krupitsky et al., 1991; May, May, 1993; Smith, & O'Neill, 1975; Smith, & Tyson, 2002; Padjen, Dongier, Malec, 1995), with VA inpatients (Passini, Watson, & Herder, 1976), with "executive" MBA graduate students (Matteson, & Ivancevich, 1986), with personality disordered patients (Rosenthal, 1972), with psychotically depressed patients (Rosenthal, & Wulfsohn, 1970), with long standing depression that is unresponsive to medication (Rosenthal, & Wulfsohn, 1970, Shealy, et al., 1989), in attention deficit disorder (Smith, 1999), and with head injured patients (Smith, Tiberi, Marshall, 1994). Despite all of the studies reporting clear success in using CES to treat depression, there are four studies which have found CES resulted in little or no improvement in depression (Hearst, Cloninger, Robert, & Cadoret, 1974; Levitt, James, Flavell, 1975; Moore, Mellor, Standage, & Strong, 1975; Philip, Demontes-Mainard, Bourgeois, & Vincent, 1991). In reviewing these studies to see what may have been different, it is striking to see that one was published in 1974 and two were published in 1975, and that all three of these studies maintained their patients on psychotropic medication during the CES treatment (Hearst, Cloninger, Robert, & Cadoret, 1974; Levitt, James, Flavell, 1975; Moore, Mellor, Standage, & Strong, 1975). There are known interaction effects between CES and some medications, and the psychotropic medications in use during the time had considerably more side effects than current medications. It is not clear why these studies found CES had little or no benefit in the treatment of depression when so many other studies have found CES to be effective, however it is possible that there

may have been an interaction with the psychotropic medications which confounded the results. There has been only one study since 1975 that evaluated depression and failed to find a significant improvement from baseline with CES treatment (Philip, Demontes-Mainard, Bourgeois, & Vincent, 1991). The study, published in 1991, took patients on high levels of psychotropic medication and removed them “cold turkey” from all medications on admission into the study. There was a CES treated group and a non-CES treated group. The non-CES treated group showed a significant increase in depression scores with the abrupt termination of their medication. The CES treated group did not display any significant improvement in their depression scores, and consequently the authors concluded CES was not effective in treating depression. A different interpretation of the findings could be that in this case, the lack of a significant improvement in depression scores may have reflected a successful treatment of depression. The people in the non-CES group developed significantly elevated depression scores during the drug withdrawal period, since they were no longer receiving any effective treatment of their depression. The CES treated group did not have any decrease in their depression scores during the drug withdrawal period, but they also did not have any increase in their depression scores. The CES treated patients in this study may have already been benefiting from anti-depressant medication and the CES was successful in maintaining their gains when the medication was abruptly withdrawn. As a result, the depression scores for these patients did not increase; they simply maintained their gains with CES. Despite these four studies reporting a failure to find that CES is effective in treating depression, there have been sufficient well-designed studies finding CES is an effective treatment for depression that the US FDA has approved it for this use.

CES for the Treatment of Movement Disorders

Although the first English language publication on CES in 1963 by Forester et al., did not find the expected induction of sleep with CES, to their surprise, they did discover a decrease in muscle spasticity in patients with hemiplegia, paraplegia or traumatic muscle injuries (Forester, et al., 1963). The second English language publication on CES likewise failed to find an induction of sleep and made the same unexpected finding that CES improved spasticity (Magora, et al., 1965). Magora and colleagues had two patients with Parkinson's and one with dystonia musculorum in their study. These patients experienced a gradual decrease and eventual elimination of involuntary movements as indicated both by clinical measures such as EMG, and by patient self report.

Subsequent studies, which have looked specifically at treating spasticity with CES, have obtained similar positive results. In 1985 a double blind study was conducted with 20 children who had mild to severe spastic cerebral palsy (Malden, & Charash, 1985). The children were divided into placebo and experimental groups, with two daily CES treatments of ten minutes in length. After six weeks, the group membership was reversed for a second six-week period of treatment. Spasticity in the children was assessed using the Malden Gross Motor Rating Scales and the Advanced Gross Motor Skills Scale. The children who received active treatment followed by placebo showed significant gains in function during the active treatment but no additional gains during the subsequent six weeks of placebo treatment. The group that received placebo treatment first did not show any significant gains in motor functioning during the placebo period but showed significant gains in motor skills during the six weeks of CES treatment. In addition, a case study of severe post anoxic spasticity (Childs, A., 1993) also reported significant improvement.

A second double blind study, conducted with adults, evaluated spasticity in terms of work performance while pedaling a stationary bicycle. This study found that the CES treated subjects were able to increase their workload by an average of 43%, while the placebo subjects declined in performance on retest by an average of 5.5% (Logan, 1988). CES results have also been compared to those obtained by occupational therapy (OT) for effectiveness in treating spasticity (Okoye & Malden, 1986). The subjects were divided into three groups, a CES treatment group, an OT treatment group and a combined CES and OT treatment group. The therapy was administered by group for three weeks. The OT treatment group had a 35% improvement in scores, while the CES treatment group had a 59% improvement in scores. The group that received both CES and OT improved the most with an average 88% increase in motor accuracy.

CES for the Treatment of Anxiety

One of the FDA approved clinical indications for using CES is in the treatment of anxiety. The first study reporting a decrease in anxiety with CES was in 1967 (Magora, Beller, Assael, & Askenazi, 1967). In 1970, Saul Rosenthal and Norman Wulfsohn published two small studies also finding CES reduced anxiety, a pilot study of just ten subjects and a larger study of 18 patients (Rosenthal, & Wulfsohn, 1970; Rosenthal, & Wulfsohn, 1970b). They reported finding significant decreases in anxiety; but due to the small sample size of all three of these studies and the lack of controls for confounding variables, these reports were more suggestive than definitive regarding the potential benefit of CES in treating anxiety. In 1972, Rosenthal and Wulfsohn published a larger study (n=22) utilizing a double blind protocol with psychiatric patients (Rosenthal, & Wulfsohn, 1972). They demonstrated once again significant declines in mean anxiety ratings among the CES treatment group, with no significant decline in mean

anxiety among a placebo group. Subsequent research has addressed the limitations of the earlier studies. The successful treatment of anxiety with CES has been replicated in large well-designed studies. These studies have found significant decreases in anxiety through 28 different psychometric tests (Kirsh, 1996). Physiological changes after CES that are indicative of decreased anxiety have also been noted.

In 1999 Stephen Overcash reported a 6-year study of 197 outpatients treated for anxiety with CES (Overcash, 1999). Muscular tension as measured by EMG decreased from a pretreatment mean of 15.8 μ V to a post treatment mean of 4.5 μ V. Sympathetic system activation as measured by electrodermal response decreased from a pretreatment mean of 14.6 ohms to a post treatment mean of 7.6 ohms. Finger temperature increased from a pretreatment mean of 81.2° F to a post treatment mean of 92.1°F. The researcher found all the changes after treatment with CES were significant at the .05 level in paired *t*-tests. A correlation of .86 was found between the changes in physiological measures of anxiety and the scores on self-ratings of anxiety. When evaluated in six month and eight-month follow-ups, 73% of the subjects reported no return of anxiety symptoms, 18% reported some return of anxiety symptoms, and 9% did not respond to attempts to gather follow-up data. Other researchers have found similar changes in EMG, EDR and finger temp when treating anxiety with CES (Gibson, 1987; Heffernan, 1995; McKenzie, 1976; Taylor, 1991; Marshall 1995; Weingarten, 1981). These studies discovered additional correlative changes in the physiology of anxiety patients treated with CES, such as changes in EEG (Heffernan, 1996; Heffernan, 1997; Krupitsky, 1991; McKenzie, 1976; Magora, 1967), catecholamines & ketosteroids (Briones, 1973), heart rate (Heffernan, 1996), and blood levels of MAO-B, GABA (Krupitsky, 1991).

The effectiveness of CES in the treatment of anxiety does not appear to be limited to any

special populations. Cranial electrotherapy stimulation has been shown to significantly reduce anxiety among alcoholics and drug addicts (Bianco, 1994; Gomez, & Mikhail, 1974; Krupitsky et al., 1991; May, May, 1993; Overcash, & Siebenthal, 1989; Schmitt, Capo, & Boyd, 1986; Smith, 1975; Smith, & Tyson, 2002), psychiatric inpatients (Briones, Rosenthal, 1973, Feighner, Brown, & Oliver, 1973; Levitt, James, Flavell, 1975; Magora, Beller, Assael, & Askenazi, 1967, Passini, Watson, & Herder, 1976; Patterson, Firth & Gardiner, 1984; Philip, Demontes-Mainard, Bourgeois, & Vincent, 1991, Ryan & Souheaver, 1976; Ryan, & Souheaver, 1977, Weingarten, 1981), psychiatric outpatients (Hearst, Cloninger, Robert, & Cadoret, 1974; Heffernan, 1996; Heffernan, 1996; Overcash, 1999; Rosenthal, 1972, Rosenthal, & Wulfsohn, 1970; Smith, 1999; Von Richtofen, Mellor, 1980; Voris, 1995), long term treatment resistant psychiatric patients (Flemenbaum, 1974; Moore, Mellor, Standage, & Strong, 1975; Rosenthal, & Wulfsohn, 1970), probationers (Voris, Good, 1996), prisoners (Jemelka, 1975), volunteers who responded to newspaper ads (Gibson, O’Hair, 1983), “executive” MBA students (Matteson, Ivancevich, 1986), and dental patients (Winick, 1999). A meta-analysis conducted by the Harvard School of Public Health in 1995 concluded that CES is statistically more effective, at the .05 level, in treating anxiety than a placebo (Klawansky, et al., 1995).

CES for the Treatment of Pain

The FDA considers any device that applies electrical current to skin for the purpose of pain relief to be a transcutaneous electrical nerve stimulator (TENS) for pain relief (code of federal regulations, title 21, volume 8, sec. 882.5890). The use of CES to treat pain is regulated as a TENS unit. Utilizing this definition, by code any CES unit in the United States becomes a TENS unit once the purpose of the treatment is to relieve pain. The change in classification of

CES to TENS when the intent is to treat pain could be a source of confusion between the two different technologies. While a CES unit can be safely used as a TENS unit, the reverse is not true. A TENS unit should not be used as a CES unit unless it has been designed and FDA approved to function as a CES unit applying current to the head. The reason for this is that in accordance with the gate control theory of pain, the TENS units are attempting to block pain signals from reaching the brain and to do so they may employ higher levels of electrical current than allowed by law for CES. This higher level of current is not only unpleasant when applied to the head but could result in unexpected or adverse reactions.

With the understanding that when used to treat pain CES by FDA regulation becomes TENS, CES is FDA approved to treat pain as a class II device. Some CES devices are designed to be able to provide current to the body as well as to the head to maximize pain relief through applying current to both the head and the site of pain. A third term can be used in place of CES or TENS: microcurrent stimulator (MET). It encompasses both CES and TENS in one term and can accurately describe devices that are capable of being safely used in both roles. For the purposes of clarity and consistency, this paper will only consider the cranial use of electrical currents for pain relief; therefore, the term CES and will continue to be used.

In a double blind study, CES was found effective for controlling dental pain in lieu of pharmacological analgesia and anesthesia (Clark et al., 1987). The 50 dental patients who participated in the study were assigned to either a CES treatment group or a placebo CES group. The patients underwent a wide variety of procedures such as tooth extractions, pulp extirpation, oral surgery, and root planning, all procedures that normally are conducted with a pharmacological analgesic or anesthesia to control pain. Clark et al. found that 80% of the CES treatment group was able to undergo these procedures without the use of any pharmacological

agent, while only 25% of the placebo control group could do so. When asked to rate their experience using CES for control of pain during a dental procedure, 71.8% of the CES treatment group rated their experience favorably. When the CES placebo control group was asked to rate their experience only 8.5% rated their experience favorably. The primary criticism of the Clark et al. study is its relatively small sample size. That limitation was addressed a year later in 1988 when Richard Hochman published a study in *The Journal of the American Dental Association* reporting on the use of CES in 600 dental procedures (Hochman, 1988). Hochman considered the use of CES for the control of dental pain successful if the patient did not request a pharmacological anesthetic and if the patient reported a 90% or greater reduction in pain. Hochman found that in 600 procedures, CES successfully controlled dental pain for 76% of those procedures. Hochman reported greater (86%) success utilizing CES pain control in minor dental procedures. Shealy et al. found a 44% decrease in pain complaints (Shealy et al. 1989).

CES has also been reported to successfully control pain in other medical applications. Naveau et al. conducted a study that was well designed using a double blind crossover that controlled for age, sex, laser energy delivered, sedation, treatment order, tumor size and body weight. This study found a 31% decrease ($p < .05$) in the amount of Fentanyl required for pain relief in 50 rectal laser surgery patients (Naveau, et al., 1992). In 1982 another study randomly assigned 120 surgical patients to anesthesia (N₂O) or anesthesia plus CES groups (Stanley et al., 1982). These researchers found a significant reduction of reported pain in the combined CES and anesthesia group as compared to the anesthesia only group. They estimated that CES was functionally the equivalent of 35-40% of N₂O in analgesic potency. A placebo controlled study found statistically significant reduction in spinal pain with CES (Tomaszek, & Morehead, 2002). An enhancement of the analgesic effect of CES with L-tryptophan has been documented in rats

(as measured by the tail flick test); when the L-tryptophan was administered as a pretreatment (Malin et al., 1990). The first study to evaluate CES for the treatment of headache was conducted at the University of North Texas (England, 1976). The small (n=18) double blind study evaluated the effectiveness of CES in treating migraine headaches after fifteen days of 45-minute treatments. The study found statistically significant reductions in the duration and intensity of headache in the CES treated group but not in the placebo group. A larger (n=112) double blind study of tension headaches also found statistically significant ($p < .01$) reductions in pain with the use of CES (Solomon, et al., 1989). Fibromyalgia patients with chronic headaches have also been reported decreased pain with CES. A study of 75 fibromyalgia patients with chronic headaches found a 70% improvement on self-ratings of pain after receiving four twenty minute CES sessions a day for one month (Romano, 1993). Even severe chronic pain patients have been reported to benefit from CES. In a study involving 23 chronic pain patients who found no relief from medication, there was a 44% reduction in pain after two weeks of daily CES (Shealy et al., 1989).

Previous EEG Studies of CES

There is some indication from the existing literature that CES may have a normalizing effect on EEG. It has been established within the EEG literature that there are EEG abnormalities in many alcoholic populations. One of those abnormalities can be found in the P300 evoked response potential. Most alcoholics have a significantly lower amplitude P300 waves than what is seen in the non-alcoholic population (Enoch et al., 2002). When both alcoholics and non-alcoholics are stimulated with CES, the CES significantly increased the P300 amplitudes in alcoholics, but not in the non-alcoholics (Braverman, Smith, Smayda, & Blum, 1990). The CES

normalized the P300 amplitudes that were abnormally low in the alcoholics, but did not alter the normal P300 amplitudes in the normal controls.

A normalizing effect from CES on the EEG of alcoholics has also been found in the amplitude and latency of occipital alpha. As discussed previously in the review of CES with addiction and alcohol treatment, CES was found to significantly decrease the latency of alpha in the Berger maneuver with alcoholics, but it did not alter the latency of alpha in the non-alcoholic controls (Krupitsky et al., 1991). Occipital alpha is of particular interest in alcoholics since it has been found that there is a decreased amplitude as well as latency in the alpha of alcoholics (Enoch et al., 2002). An increase in alpha activity was also noted in normal subjects after 30 minutes of CES, which did not induce sleep.

The use of CES has been found to normalize the EEG of pain patients. In a study of 50 pain patients, it was reported in *The Canadian Journal of Clinical Medicine* that the EEG spectrum of pain patients is significantly more irregular than the spectrum of normal controls (Heffernan, 1997). The EEG spectrum analyzed in the study was a two minute average of EEG examined by fast Fourier transformation as root mean square (RMS) of amplitude by frequency (0-30 Hz). All of the EEG was collected frontally from FP1 & FP2 (on the International 10-20 system for electrode placement). In this double blind study, the author reported finding that the EEG spectrum of pain patients was not normally distributed. In healthy individuals the lowest amplitude EEG was found in the highest frequencies and the highest amplitude was found in the slowest frequencies. The normal controls also displayed a smooth increase in amplitude from the highest frequencies to the lowest frequencies (when the EEG averages are displayed as a bar chart with equal width bands). The pain patients did not display the EEG pattern of the normal controls. The mean deviation of RMS amplitude for the no pain control group and the pain group

was compared to an idealized normal curve, to determine how closely each group in the study matched the curve. For the no pain control group the deviation from the normal curve was .2 ($p>.01$), while for the pain patients the deviation from the normal curve was 2.4 ($p<.01$). These values provided empirical and statistical support for the abnormal EEG spectral distribution of the pain patients; and the subsequent normalization of the EEG with CES treatment.

This study also suggests that not all CES may have identical effects. Three types of CES devices were used in this study to provide the active CES and sham (placebo) CES. They were similar in that after a single session of CES, all three devices produced a tenfold increase in RMS amplitudes over baseline. However there were differences found between variable waveform vs. steady waveform CES devices. Two of the devices produced a constant waveform, one at 0.5 Hz and another producing a simultaneous 15 Hz, 500 Hz and 1500 Hz. These two CES devices did not produce a change in the distribution of the spectral curve of EEG. The third 0.5 Hz device, which used a variable waveform, produced significant smoothing of the EEG spectral displays of the pain patients. In this study, it was only the variable frequency CES stimulation that provided significant pain relief. In terms of optimizing CES for pain relief, this study suggests that the waveform used by a CES device has an impact on the effectiveness of the CES. This study suggests habituation can occur with continuous wave forms in CES that does not occur with variable waveforms.

Changes in EEG after CES have also been documented in insomnia patients (Sing et al., 1971). As with alcoholics who have deficit alpha, CES produced an increase in alpha for insomniacs. For this group, the increase in alpha amplitude induced by the CES treatment was followed by the onset of sleep. The same effect of an increase in alpha followed by sleep onset has also been documented in psychiatric in-patients suffering anxiety and depression (McKenzie,

et al., 1976). Cranial electrical stimulation increased both the quality and quantity of posterior alpha in these patients after just five days of 30-minute treatments. McKenzie et al. also noticed an increase in slower frequency frontal and temporal EEG after treatment with CES and a concomitant drop in electrodermal activity. The electrodermal activity dropped by half after treatment with CES, and correlated with the patient self-reports of decreased anxiety. An earlier study also found changes in EEG with inpatients suffering from anxiety and insomnia. In this study it was found that 10-20 CES treatments normalized the EEG sleep rhythm (Magora, Beller, Assael, & Askenazi, 1967). It has also been found that for inpatients with insomnia, CES produces a significant increase in the amount of time spent in stage 4 sleep, and in the production of delta frequency activity while sleeping (Weiss, 1973). This sleep study suggests that CES can improve sleep efficiency as well as the restfulness of sleep.

Changes in EEG after CES have been reported in a study combining biofeedback with CES. In 1999, Mark Schroeder wrote his doctoral dissertation at the University of Texas at Austin on the concurrent use of CES with EEG biofeedback (Schroeder, 1999). His study was small, comprising an evaluation of the response of 12 male subjects seen for three sessions of therapy. The EEG was recorded occipitally from O1 & O2 (in the 10-20 system). The EEG was recorded before, during and after each treatment session. A noise cancellation device was utilized to attempt to remove the CES signal from the two channel recordings during the CES treatment. Five treatment conditions were used in a double blind manner, including or a sham (placebo) CES treatment, an EEG biofeedback (Neurofeedback) treatment, a 0.5 Hz CES treatment, a 100 Hz CES treatment, and a combined 0.5 Hz CES and Neurofeedback treatment. The results of the study showed that 100 Hz and 0.5 Hz CES significantly altered the peak frequency of occipital alpha power by moving it downward as compared to placebo controls. The

100 Hz CES was found to significantly reduce occipital beta frequency in the EEG as compared to placebo controls. This study was small, but it is not the only one suggesting a downward shift in peak alpha frequency after CES. In 1971, there was a study using a 100 Hz sine wave CES device that analyzed the EEG in ten subjects during sham or real CES in a crossover design. Surprisingly, no significant differences were found in EEG before and after CES stimulation. The lack of a change in EEG after CES suggests that there may have been problems with the study. The differences that were found in this study were during a reaction time task in which there was an increase in 5-10 Hz activity and a decrease in high alpha and beta (Itil, Gannon, Akpınar, & Hsu, 1971). The downward shift of peak EEG in alpha after CES would not normally be considered a normalization of EEG. Therefore this aspect of CES merits further research to understand if it is a real effect, if so, if it occurs with all types of CES, and finally if it is associated with any affective or cognitive changes.

A normalizing effect on EEG from CES has also been suggested by an interesting case study. The case study reported on a depressed woman with a notable deficit in alpha frequency EEG. She had severe problems with sleep onset insomnia and was implanted with surface and deep EEG electrodes for a long-term sleep study. Initially she was given a placebo CES treatment and monitored and then was provided with actual CES treatment. The placebo treatment did not have any effect on her EEG, or on her self-report of depression or difficulty getting to sleep. The actual CES treatment increased her alpha significantly. The patient also went to sleep immediately after her first CES treatment. Unfortunately, there is no indication in the case report whether her depression also improved (Cox, & Heath, 1975). The only published EEG study which failed to find a change in EEG after CES was the Frankel et al study noted earlier. This study found no changes in EEG, sleep onset, time asleep, duration and frequency of

awakening (Frankel et al., 1973).

The use of CES can improve not only sleep, but has been reported to improve daytime alertness. The daytime alertness of elderly dementia patients as documented by self-report and objectively by EEG and was found to improve after CES (Hozumi et al., 1996). The improved alertness may have been the result of improved sleep found in other studies, or perhaps a more specific effect of the CES in all populations, or in this unique population.

To date there have been no studies of CES utilizing any EEG imaging techniques such as quantitative EEG (qEEG) or LORETA. While there have been studies of standard EEG of the entire cortex after CES, there has never been a computerized analysis objectively identifying what those whole head changes in the EEG are. There have been a few studies of EEG after CES, which have used a computerized analysis, but these studies have involved analysis of EEG from only small areas of the scalp and do not reveal what changes are occurring across the entire cortex. Some authors refer to the Braverman et al. study of P300 responses in alcoholics as a brain electrical activity mapping (BEAM) study, implying that it involved cortical mapping of EEG activity after CES. While the analysis of P300 involves the computerized averaging of EEG, the Braverman et al. study was not a BEAM study in the sense of creating a topographical map of the distribution of the electrical activity across the cortex.

From the existing EEG research, a basic picture emerges of changes in EEG that occur with the use of CES. Abnormal EEG patterns in insomnia patients, pain patients and alcoholics, trend toward normal when treated with CES. These EEG changes support the contention that CES may be producing more normal brain function of individuals with a disturbance in brain activity (Kirsh, Smith, 2000, Heffernan, 1997).

Mechanism of Effect in CES

There is currently no body of research that identifies the complete mechanism underlying the physiological changes reported with CES. However, there is research that suggests some of the possible mechanisms involved. Two studies, one in humans (Shealy, et al., 1998) and one in animals (Krupitsky et al., 1991), have shown that CES significantly increases beta-endorphin in CSF. In the human study, beta-endorphin in CSF was found to increase by an average 219% (Shealy, et al., 1998) after a single session 20-minute exposure to CES. Blood drawn at the same time as the CSF was drawn revealed that while the CSF level of beta-endorphin increased an average of 219%, the blood levels of beta-endorphin increased an average of 50%. Other studies have found changes in catecholamines, ketosteroids (Briones, Rosenthal, 1973), cholinesterase (Shealy, et al., 1989), dopamine, GABA (Krupitsky et al., 1991) corticosteroids (Frankel, Buchbinder, & Snyder, 1973; Sornson et al., 1989), MAO-B (Kotter, Henschel, Hogan, & Kalbfleisch, 1975; Krupitsky et al., 1991), melatonin (Shealy, et al., 1998), norepinephrine (Shealy, et al., 1989, Shealy, et al., 1998), serotonin (Krupitsky et al., 1991; Shealy, et al., 1989, Shealy, et al., 1998), tryptophan (Sornson, et al., 1989) and stomach acid secretion (Kotter, Henschel, Hogan, & Kalbfleisch, 1975).

The literature on the neurochemical changes involved in CES reveals a picture of significant increases in neurotransmitters and hormones known to be involved in the regulation of sleep, pain, affect and stress responses. The published data suggests that the therapeutic benefit of CES is a consequence of its effects on neurotransmitters. There is the suggestion from one animal study that beyond the immediate effects of CES, it normalizes out-of-balance neurotransmitter systems. In the study, chemically disrupted neurotransmitter levels were returned to normal with the use of CES. (Pozos, Richardson, & Kaplan, 1971).

Pretreatment with serotonin can be used to enhance the pain relief provided by CES, while the pain relieving effect of CES can be reversed through the use of blocking agents for serotonin and opioids (Malin et al., 1990). Because this study found that the pain control provided by CES can be manipulated through opioid and serotonin agonists and antagonist, it suggests that the primary mechanism of the analgesic effect of CES occurs through modification of endogenous opioid and serotonin activity.

In the late 1960s and early 1970s research was conducted with monkeys to determine how much of a cranially applied current reaches the brain, and if there is a difference in the amount of current that reaches the cortex versus what reaches subcortical structures. Platinum electrodes were implanted in the monkeys to measure cortical and subcortical penetration of cranially applied currents from electrodes placed on the nasion and inion (the front and the back of the head). The currents applied were from .01 mA (CES) to 100 mA (electroanesthesia) and in terms of frequency, ranged from 10 Hz to 10,000 Hz. Both rectangular and sinusoidal currents were used. Approximately 40% (Rush & Driscoll 1968, Driscoll and Rush 1971) to 46% (Jarzembki, et al. 1970) of cranially applied current was found to actually enter the brain. The current densities measured in both the motor cortex and in the thalamus were consistent, suggesting no drop in current as a function of distance between cortical and subcortical structures. Once the current entered the brain there was no differential in current level based on distance from the CES contacts. A linear relationship was found at all frequencies between current density measured cortically and subcortically and the current applied at the inion and nasion. As the externally applied current was increased the current at the cortex and thalamus also increased by the same percentage (Lang and Larson 1969; Jarzembki, Sances and Larson, 1972).

As a part of the same monkey research, in vivo measurements were made of vesicle activity before CES, during CES and after CES. An activation of vesicles was noted during CES, with an extraordinarily large number of vesicles found opened up to the synaptic cleft. All vesicle activity returned to normal within 5 minutes after the discontinuation of CES (Jarzembki, Sances and Larson, 1972). The synaptic vesicles are the storage vessels for neurotransmitters. When neurotransmitters need to be released by a neuron, the vesicles are activated to release the neurotransmitter into the synaptic cleft. When large numbers of vesicles are activated, the amount of neurotransmitters that are released is substantial. The finding that CES creates widespread and large-scale activation of vesicles indicates that the use of CES should result in a dramatic increase in neurotransmitter activity. As reported above, it has been found that CES does indeed stimulate a dramatic increase in neurotransmitter activity, and can be enhanced or blocked with neurotransmitter agonists and antagonist. It would appear from the work of Jarzembki, Sances and Larson that in terms of neurochemistry, the therapeutic effects of CES occur as a result of its stimulation of vesicle activity and the subsequent increase of neurotransmitter levels. However, other mechanisms may also contribute to the benefits seen with repeated use of CES. Recently it has been reported that the application of low-level currents can speed healing in tissue by turning on the genetic machinery for cellular repair (Zhao, et al. 2006).

Summary of Research on CES

The above review of the literature on CES shows that the application of a small current to the head can have profound cognitive, affective and motor effects that are beneficial in the treatment of pain, anxiety, depression, sleep disorders, substance abuse treatment and movement

disorders. When the level of current is kept low, negative side effects are rare. It is surprising to see that despite the wide variety of technical differences in the CES devices used in the various studies, the outcomes have remained relatively consistent. Components of CES administration, including the level of current, pulse width, electrode placement, frequency, waveform, the number of treatments, and duration of treatment, have all been varied without causing injury or preventing positive therapeutic results. Such efficacy in the face of altering so many variables may suggest a placebo effect is responsible for benefit seen with CES; however, multiple double blind studies and animal research has shown that the placebo effect is not responsible for the benefits documented.

The current animal and human research can lead to the cautious conclusion that CES has the basic effect of regulating and normalizing the neurochemical and neuroelectrical activity of the brain. It is clear that CES makes significant changes in the electrical and chemical activity of the brain. It is also clear that these changes are the result, at least in part, of the activation by CES of vesicles to release neurotransmitters. The question of what other changes are occurring in the brain from CES, and by what mechanism, remains as yet largely unknown. Why do some therapeutic results occur immediately, such as pain relief, while others require a course of treatment such as depression or addictions? Is the therapeutic effect of CES due solely to the stimulation of the large-scale release of neurotransmitters, or are there other mechanisms involved? Does CES stimulate the release of all neurotransmitters equally, or is it selective? Does the release of neurotransmitters change over a course of treatment with CES? The full answer to these and the other outstanding questions about CES will require the continued cooperative efforts of researchers in neuroimaging, neurophysiology, cell biology, medicine and clinical psychology.

One of the questions that is still unanswered about CES is the global effects of CES on EEG. Since the therapeutic agent used in CES is a low level of electrical current, a particularly cogent question is how CES affects the electrical activity of the brain. The electrical activity of the brain can be evaluated using either MEG- or EEG-based techniques. To date there have been no MEG studies of CES, although there have been some EEG studies. Most of the existing EEG studies of CES have relied upon a visual inspection of standard raw EEG recordings and thus have not been able to provide any objective data for quantitative analysis. This limitation presents a problem in the experimental investigation of the effects of CES on raw EEG. The computerized analysis of EEG provides a method of obtaining more reliable data on the changes in EEG that are generated by CES stimulation. To date there have been three EEG studies that did not have this limitation because they included some form of computer analysis of the EEG (Braverman, Smith, Smayda, & Blum, 1990; Heffernan, 1997; Schroeder, 1999). By utilizing computerized analysis techniques, these studies created a more objective and replicable analysis of the EEG data. Computerized analysis of EEG also provided these studies with information that would not be available in a visual inspection of raw wave activity, such as P300 latencies and spectral distributions. Unfortunately, the data in all three of these studies was collected from just two locations on the head, making it impossible to draw any conclusions about changes in electrical activity from CES across several cortical locations. Computerized data about the effect of CES on EEG across the entire cortex would advance the understanding of CES on cortical EEG.

At this time, two animal studies have looked at subcortical effects of CES on electrical activity (Lang and Larson 1969; Jarzembki, Sances and Larson, 1972), and no human studies have evaluated changes in subcortical electrical activity. A better understanding of the effects of

CES on subcortical electrical activity in humans may further enhance the understanding of CES. Multiple CES parameters have been changed without preventing a beneficial effect on CES. Does this mean that all CES is the same, or is a certain form of CES more effective in specific applications than other forms of CES? It has been reported that low frequency CES has a sedating effect while high frequency CES has an activating effect (Gigineshvili et al., 1995), suggesting that not all frequencies of CES have the same effects.

Additional research involving computerized analysis of EEG from the entire cortex; such as quantitative electroencephalography (qEEG), would objectively quantify the effects of CES on cortical EEG. The use of MEG or current density estimation, such as LORETA, would allow for observation of the effect of CES on subcortical electrical currents. A study, which compares CES in two different frequencies using these techniques, would contribute to an exploration of the differential effects of different frequencies of CES on cortical and subcortical electrical activity. The goal of this investigation was to perform such a study in the hope it would help expand the current knowledge about the effects of CES on the electrical activity of the brain.

Rationale and Conceptual Framework for the Study

The function of the human body is as much electrical as it is chemical. Yet most therapies have relied only on the chemical half of the electrochemical functioning of the body to treat disease and promote wellness. Cranial electrotherapy stimulation is an intervention that utilizes the electrical half of the electrochemical functions of the body to do the same. In many respects, the effects of CES appear to be similar those of a drug; and it has documented interactions with some drug therapies. The use of CES as a therapy is as effective as many pharmacological treatments and in some instances provides a therapy not available by medication. Yet as noted in

the Introduction, despite the proven efficacy of CES, it is rarely used in modern medicine, and no model has been put forward to explain its mechanism of effect. The lack of a model for CES may be a significant barrier to its acceptance and use. With a model of efficacy, it is possible to do more than explain how CES works; it becomes possible to predict its action. A model makes it possible to understand what kinds of conditions enhance or limit the treatment effects of CES if there are new uses for which CES may show promise. Finally, a model may lead to modifications of CES that could enhance its therapeutic benefit in specific applications.

Proposed Activation/Adaptation Model of CES

The author of this study is suggesting a two-stage “activation/adaptation” model for the mechanism behind the therapeutic benefits of CES. In this model, stage one is the activation stage. In the activation stage there is an immediate activating effect on the brain from the use of CES that is responsible for the affective, cognitive and physiological changes seen at the time a treatment is administered. In the proposed model, the immediate physiological effects of CES such as the activation of vesicles by the electrical current, the increase in neurotransmitter levels and the increase in alpha production are all activation stage effects of CES. The evidence for the activation stage was described in the literature review in finding such as animal studies that indicating activation of the vesicles with CES and higher-level electrical currents. It is likely that the activation of the vesicles is the primary mechanism for activation stage of CES. Evidence for this supposition can be found in studies showing an increase in neurotransmitter levels with CES and the ability to both enhance and reverse the analgesic effects of CES through opioid and serotonin agonist and antagonists. These findings reveal that the analgesic effect of CES is mediated by changes in endogenous opioid and serotonin activity, and supports the increase of

neurotransmitter levels at the synaptic cleft as one of the primary mechanisms of action in the activation stage.

The second stage of the proposed model is the adaptation stage. The adaptation stage is a persisting change in the function of the brain (presumably occurring primarily in the neurotransmitter system) from a course of treatment with CES. The adaptation stage may start after a single treatment with CES, but is most evident in the treatment effects that occur with repeated use. In the proposed model, the persisting therapeutic effects of CES that occur after a course of treatment are the result of neurotransmitter and receptor changes induced by the CES. The treatment of depression is an example of the adaptation stage effects of CES. A single CES treatment is not effective for depression, but a two or three-week course of treatment is effective for depression. The evidence suggesting that CES has a normalizing effect on the neurochemistry and the electrical activity of the brain is proposed to be a result of the adaptation stage. The adaptation stage is a physiological response where the brain has altered its self-regulation in response to CES. It may be that the adaptation stage involves changes in the number and sensitivity of synaptic receptors, or how and when the synaptic vesicles release neurotransmitters, which in turn has effects on mood, motor abilities and cognitive/behavioral functioning. As adaptation occurs, systemic changes are also expected to be occurring in some individuals. For example an individual who has been experiencing chronic stress may have elevated blood pressure, elevated corticosteroids, and elevated muscle tension, all of which decrease to more normal levels as the adaptation to CES occurs.

This model implies that for some applications, such as pain, the continued use of CES is required to maintain the therapeutic effect. However, for some other applications of CES, a course of treatment may be all that is required to obtain and maintain therapeutic gains.

Depression may be an application of CES where continued use of CES is not required to maintain the therapeutic benefits. There is a third possibility wherein some individuals or for some disorders, occasional use of CES will be required to maintain the benefits. The reason for the latter is that since the adaptation stage is in response to the repeated administration of CES, the discontinuation of CES removes the ongoing stimulus that initiated and in some cases is maintaining the adaptation. An analogy would be the therapeutic use of weight lifting. Weight lifting can stimulate and maintain bone and muscle development that increases mobility and reduces fractures in the elderly. However, the gains and benefits of the weight lifting slowly dissipate if the stimulus provided to the body by weight lifting is discontinued; the removal of the stimulus of weight lifting ends the adaptation of the body and the benefits slowly fade. The proposed activation/adaptation model of CES suggests that in some cases the removal of CES may result in a slow decline in adaptation and with it a decrease in the therapeutic benefits of CES. However, this model does not preclude permanent changes from CES. If prior to CES an individual was in a dysregulated state, and CES returned that individual to a state of balance, then the removal of CES should leave that individual functioning in a state of neurochemical balance. The individual in this situation should remain in a good state of functioning as long as the conditions that caused the original dysregulation do not reoccur.

Based on the proposed activation/adaptation model of CES, there should be distinct changes in the electrical activity of the brain after even a single session of CES. These changes would be the result of the electrical current's stimulation of the vesicles to engage in the large-scale release of neurotransmitters, which in turn results in changes in neuronal firing and subsequently the electrical activity of the brain. The change in the activity of the neurons is responsible for the changes that have been observed on EEG.

It has been noted in the CES literature that some waveforms of CES appear to be more effective in producing an effect. In all frequencies, square waves, and variations of square waves, seem to be more potent than other waveforms. It has also been reported that in some applications different frequencies of CES seem to have different immediate effects. This observation suggests that not all CES waveforms and frequencies evoke the same activation of vesicles. In terms of waveforms it appears that across the board, CES is more effective with square waves, or variations of square waves; and therefore it is likely that square waves are more effective at activating vesicles. It would seem that a square wave, or variation of a square wave would be the best choice for all applications of CES. However, there does not appear to be a single frequency that would be best for all CES applications. Some frequencies of CES have been reported to have unique effects, or enhanced effectiveness in some applications. In the model just proposed, such differences in the response to different frequencies of CES suggest a differential activation of vesicles by different frequencies. Given the literature, it is likely that CES does not activate the release of neurotransmitters from all the vesicles equally. It is probable that CES differentially activates the vesicles for some neurotransmitters to a greater extent than others. An increase in some neurotransmitters may result in a unique increase (or decrease) in the activity of circuits in some locations and frequencies, while an increase in other neurotransmitters may result in other patterns of increased and decreased activity. It may be possible that the frequency of CES can be altered to enhance a pattern of changes in activity that will maximize the effectiveness of CES for the particular condition it is being used to treat.

As adaptation to CES occurs, there should be more persistent changes from baseline in the electrical activity of the brain; changes that for the most part are a re-regulation of any dysregulated neurotransmitter system. The proposed model predicts that the response for most

individuals to a single session of CES of a particular frequency should be fairly uniform, but the adaptation response to repeated CES should be more individualized. Thus, it is theorized that changes in the electrical activity of the brain will be fairly uniform for most individuals after a single session of CES, but more individualized as adaptation occurs.

Hypothesis

The research hypotheses in this study are formulated in the tradition of psychological research, assuming no treatment effect. The following are the research null hypotheses for this study:

Hypothesis 1:

Immediately after a single 20 minute session of 0.5 Hz CES there will be no statistically significant change in mean relative power alpha band activity for any electrodes in the eyes closed qEEG brain map. Stated formally: where $\mu_{.5\alpha B}$ = mean alpha activity in all 19 electrodes at 0.5 Hz baseline and $\mu_{.5\alpha E}$ = mean alpha activity in all 19 electrodes after the experimental stimulus of 0.5 Hz CES; and where the null hypothesis 1 ($H1_0$) = the mean of each 0.5 Hz relative power group is equal, and the alternate hypothesis ($H1_A$) = the mean of each 0.5 Hz relative power group is not equal, hypothesis 1 is:

$$H1_0: \mu_{.5\alpha B} = \mu_{.5\alpha E}$$

$$H1_A: \mu_{.5\alpha B} \neq \mu_{.5\alpha E}$$

Hypothesis 2:

Immediately after a single 20 minute session of 100 Hz CES there will be no

statistically significant change in mean relative power alpha band activity for any electrodes in the eyes closed qEEG brain map. Stated formally: where $\mu_{100\alpha B}$ = mean alpha activity in all 19 electrodes at 100 Hz baseline and $\mu_{100\alpha E}$ = mean alpha activity in all 19 electrodes after the experimental stimulus of 100 Hz CES; and where the null hypothesis 2 (H_{2_0}) = the mean of each 100 Hz relative power group is equal, and the alternate hypothesis 2 (H_{2_A}) = the mean of each 100 Hz relative power group is not equal, the hypothesis is:

$$H_{2_0}: \mu_{.5\alpha B} = \mu_{.5\alpha E}$$

$$H_{2_A}: \mu_{.5\alpha B} \neq \mu_{.5\alpha E}$$

Hypothesis 3:

Immediately after a single 20 minute session of 0.5 Hz CES there will be no statistically significant change in mean relative power delta band activity for any electrodes in the eyes closed qEEG brain map. Stated formally: where $\mu_{.5\Delta B}$ = mean delta activity in all 19 electrodes at 0.5 Hz baseline and $\mu_{.5\Delta E}$ = mean delta activity in all 19 electrodes after the experimental stimulus of 0.5 Hz CES; and where the null hypothesis 3 (H_{3_0}) = the mean of each 0.5 Hz relative power group is equal, and the alternate hypothesis (H_{3_A}) = the mean of each 0.5 Hz relative power group is not equal, hypothesis 3 is:

$$H_{3_0}: \mu_{.5\Delta B} = \mu_{.5\Delta E}$$

$$H_{3_A}: \mu_{.5\Delta B} \neq \mu_{.5\Delta E}$$

Hypothesis 4:

Immediately after a single 20-minute session of 100 Hz CES there will be no statistically significant change in mean relative power delta band activity for any electrodes in

the eyes closed qEEG brain map. Stated formally: where $\mu_{100\Delta B}$ = mean delta activity in all 19 electrodes at 100 Hz baseline and $\mu_{100\Delta E}$ = mean delta activity in all 19 electrodes after the experimental stimulus of 100 Hz CES; and where the null hypothesis 4 (H_{4_0}) = the mean of each 100 Hz relative power group is equal, and the alternate hypothesis (H_{4_A}) = the mean of each 100 Hz relative power group is not equal, hypothesis 4 is:

$$H_{4_0}: \mu_{100\Delta B} = \mu_{100\Delta E}$$

$$H_{4_A}: \mu_{100\Delta B} \neq \mu_{100\Delta E}$$

Hypothesis 5:

Immediately after a single 20 minute session of 0.5 Hz CES there will be no statistically significant change in mean relative power theta band activity for any electrodes in the eyes closed qEEG brain map. Stated formally: where $\mu_{.5\Theta B}$ = mean theta activity in all 19 electrodes at 0.5 Hz baseline and $\mu_{.5\Theta E}$ = mean delta activity in all 19 electrodes after the experimental stimulus of 0.5 Hz CES; and where the null hypothesis 5 (H_{5_0}) = the mean of each 0.5 Hz relative power group is equal, and the alternate hypothesis (H_{5_A}) = the mean of each 0.5 Hz relative power group is not equal, hypothesis 5 is:

$$H_{5_0}: \mu_{.5\Theta B} = \mu_{.5\Theta E}$$

$$H_{5_A}: \mu_{.5\Theta B} \neq \mu_{.5\Theta E}$$

Hypothesis 6:

Immediately after a single 20 minute session of 100 Hz CES there will be no statistically significant change in mean relative power theta band activity for any electrodes in the eyes closed qEEG brain map. Stated formally: where $\mu_{100\Theta B}$ = mean delta activity in all 19

electrodes at 100 Hz baseline and $\mu_{100\Theta E}$ = mean theta activity in all 19 electrodes after the experimental stimulus of 100 Hz CES; and where the null hypothesis 6 (H_{6_0}) = the mean of each 100 Hz relative power group is equal, and the alternate hypothesis (H_{6_A}) = the mean of each 100 Hz relative power group is not equal, hypothesis 6 is:

$$H_{6_0}: \mu_{100\Theta B} = \mu_{100\Theta E}$$

$$H_{6_A}: \mu_{100\Theta B} \neq \mu_{100\Theta E}$$

Hypothesis 7:

Immediately after a single 20 minute session of 0.5 Hz CES there will be no statistically significant change in mean relative power beta band activity for any electrodes in the eyes closed qEEG brain map. Stated formally: where $\mu_{.5\beta B}$ = mean beta activity in all 19 electrodes at 0.5 Hz baseline and $\mu_{.5\beta E}$ = mean beta activity in all 19 electrodes after the experimental stimulus of 0.5 Hz CES; and where the null hypothesis 7 (H_{7_0}) = the mean of each 0.5 Hz relative power group is equal, and the alternate hypothesis (H_{7_A}) = the mean of each 0.5 Hz relative power group is not equal, hypothesis 7 is:

$$H_{7_0}: \mu_{.5\beta B} = \mu_{.5\beta E}$$

$$H_{7_A}: \mu_{.5\beta B} \neq \mu_{.5\beta E}$$

Hypothesis 8:

Immediately after a single 20 minute session of 100 Hz CES there will be no statistically significant change in mean relative power beta band activity for any electrodes in the eyes closed qEEG brain map. Stated formally: where $\mu_{100\beta B}$ = mean beta activity in all 19 electrodes at 100 Hz baseline and $\mu_{100\beta E}$ = mean beta activity in all 19 electrodes after the

experimental stimulus of 100 Hz CES; and where the null hypothesis 8 (H_{8_0}) = the mean of each 100 Hz relative power group is equal, and the alternate hypothesis (H_{8_A}) = the mean of each 100 Hz relative power group is not equal, hypothesis 8 is:

$$H_{8_0}: \mu_{100\beta B} = \mu_{100\beta E}$$

$$H_{8_A}: \mu_{100\beta B} \neq \mu_{100\beta E}$$

Hypothesis 9:

Immediately after a single 20 minute session of 0.5 Hz CES there will be no statistically significant change in mean coherence for any electrode pairs in the eyes closed qEEG brain map. Stated formally: where $\mu_{.5CohB}$ = mean coherence in all 19 electrodes at 0.5 Hz baseline and $\mu_{.5CohE}$ = mean coherence in all 19 electrodes after the experimental stimulus of 0.5 Hz CES; and where the null hypothesis 9 (H_{9_0}) = the mean of each 0.5 Hz coherence group is equal, and the alternate hypothesis (H_{9_A}) = the mean of each 0.5 Hz coherence group is not equal, hypothesis 9 is:

$$H_{9_0}: \mu_{.5CohB} = \mu_{.5CohE}$$

$$H_{9_A}: \mu_{.5CohB} \neq \mu_{.5CohE}$$

Hypothesis 10:

Immediately after a single 20 minute session of 100 Hz CES there will be no statistically significant change in mean coherence for any electrode pairs in the eyes closed qEEG brain map. Stated formally: where $\mu_{100CohB}$ = mean coherence in all 19 electrodes at 100 Hz baseline and $\mu_{100CohE}$ = mean coherence in all 19 electrodes after the experimental stimulus of 100 Hz CES; and where the null hypothesis 10 (H_{10_0}) = the mean of each 100 Hz coherence

group is equal, and the alternate hypothesis ($H10_A$) = the mean of each 100 Hz coherence group is not equal, hypothesis 10 is:

$$H10_0: \mu_{100CohB} = \mu_{100CohE}$$

$$H10_A: \mu_{100CohB} \neq \mu_{100CohE}$$

Hypothesis 11:

Immediately after a single 20 minute session of 0.5 Hz CES there will be no statistically significant change in mean amplitude asymmetry for any electrode pairs in the eyes closed qEEG brain map. Stated formally: where $\mu_{.5AsyB}$ = mean amplitude asymmetry in all 19 electrodes at 0.5 Hz baseline and $\mu_{.5AsyE}$ = mean amplitude asymmetry in all 19 electrodes after the experimental stimulus of 0.5 Hz CES; and where the null hypothesis 11 ($H11_0$) = the mean of each 0.5 Hz amplitude asymmetry group is equal, and the alternate hypothesis ($H11_A$) = the mean of each 0.5 Hz amplitude asymmetry group is not equal, hypothesis 11 is:

$$H11_0: \mu_{.5AsyB} = \mu_{.5AsyE}$$

$$H11_A: \mu_{.5AsyB} \neq \mu_{.5AsyE}$$

Hypothesis 12:

Immediately after a single 20 minute session of 100 Hz CES there will be no statistically significant change in mean amplitude asymmetry for any electrode pairs in the eyes closed qEEG brain map. Stated formally: where $\mu_{100AsyB}$ = mean amplitude asymmetry in all 19 electrodes at 100 Hz baseline and $\mu_{100AsyE}$ = mean amplitude asymmetry in all 19 electrodes after the experimental stimulus of 100 Hz CES; and where the null hypothesis 12 ($H12_0$) = the mean of each 100 Hz amplitude asymmetry group is equal, and the alternate hypothesis ($H12_A$) = the

mean of each 100 Hz amplitude asymmetry group is not equal, hypothesis 12 is:

$$H12_0: \mu_{100AsyB} = \mu_{100AsyE}$$

$$H12_A: \mu_{100AsyB} \neq \mu_{100AsyE}$$

Hypothesis 13:

Immediately after a single 20 minute session of 0.5 Hz CES there will be no statistically significant change in mean phase for any electrode pairs in the eyes closed qEEG brain map. Stated formally: where $\mu_{.5PhB}$ = mean phase in all 19 electrodes at 0.5 Hz baseline and $\mu_{.5PhE}$ = mean phase in all 19 electrodes after the experimental stimulus of 0.5 Hz CES; and where the null hypothesis 13 ($H13_0$) = the mean of each 0.5 Hz phase group is equal, and the alternate hypothesis ($H13_A$) = the mean of each 0.5 Hz phase group is not equal, hypothesis 13 is:

$$H13_0: \mu_{.5PhB} = \mu_{.5PhE}$$

$$H13_A: \mu_{.5PhB} \neq \mu_{.5PhE}$$

Hypothesis 14:

Immediately after a single 20 minute session of 100 Hz CES there will be no statistically significant change in mean phase for any electrodes in the eyes closed qEEG brain map. Stated formally: where μ_{100PhB} = mean phase in all 19 electrode pairs at 100 Hz baseline and μ_{100PhE} = mean phase in all 19 electrodes after the experimental stimulus of 100 Hz CES; and where the null hypothesis 14 ($H14_0$) = the mean of each 100 Hz phase group is equal, and the alternate hypothesis ($H14_A$) = the mean of each 100 Hz phase group is not equal, hypothesis 14 is:

$$H14_0: \mu_{100PhB} = \mu_{100PhE}$$

$$H14_A: \mu_{100PhB} \neq \mu_{100PhE}$$

Hypothesis 15:

Immediately after a single 20 minute session of 0.5 Hz CES there will be no statistically significant change in mean power ratio for any electrodes in the eyes closed qEEG brain map. Stated formally: where $\mu_{.5PRB}$ = mean power ratio in all 19 electrodes at 0.5 Hz baseline and $\mu_{.5PRE}$ = mean power ratio in all 19 electrodes after the experimental stimulus of 0.5 Hz CES; and where the null hypothesis 15 ($H15_0$) = the mean of each 0.5 Hz phase group is equal, and the alternate hypothesis ($H15_A$) = the mean of each 0.5 Hz power ratio group is not equal, hypothesis 15 is:

$$H15_0: \mu_{.5PRB} = \mu_{.5PRE}$$

$$H15_A: \mu_{.5APRB} \neq \mu_{.5PRE}$$

Hypothesis 16:

Immediately after a single 20 minute session of 100 Hz CES there will be no statistically significant change in mean power ratio for any electrodes in the eyes closed qEEG brain map. Stated formally: where μ_{100PRB} = mean power ratio in all 19 electrodes at 100 Hz baseline and μ_{100PRE} = mean power ratio in all 19 electrodes after the experimental stimulus of 100 Hz CES; and where the null hypothesis 16 ($H16_0$) = the mean of each 100 Hz power ratio group is equal, and the alternate hypothesis ($H16_A$) = the mean of each 100 Hz power ratio group is not equal, hypothesis 16 is:

$$H16_0: \mu_{100PRB} = \mu_{100PRE}$$

$$H16_A: \mu_{100PRB} \neq \mu_{100PRE}$$

Hypothesis 17:

Immediately after a single 20-minute session of 0.5 Hz CES there will be no statistically significant change in mean current density of voxels in the alpha band, as calculated by LORETA. Stated formally: where $\mu_{.5\alpha CDB}$ = mean current density at 0.5 Hz baseline and $\mu_{.5\alpha CDE}$ = mean current density after the experimental stimulus of 0.5 Hz CES; and where the null hypothesis 17 ($H17_0$) = the mean of each 0.5 Hz current density group is equal, and the alternate hypothesis ($H17_A$) = the mean of each 0.5 Hz current density group is not equal, hypothesis 17 is:

$$H17_0: \mu_{.5\alpha CDB} = \mu_{.5\alpha CDE}$$

$$H17_A: \mu_{.5\alpha CDB} \neq \mu_{.5\alpha CDE}$$

Hypothesis 18:

Immediately after a single 20-minute session of 100 Hz CES there will be no statistically significant change in mean current density of voxels in the alpha band, as calculated by LORETA. Stated formally: where $\mu_{100\alpha CDB}$ = mean current density at 100 Hz baseline and $\mu_{100\alpha CDE}$ = mean current density after the experimental stimulus of 100 Hz CES; and where the null hypothesis 18 ($H18_0$) = the mean of each 100 Hz current density group is equal, and the alternate hypothesis ($H18_A$) = the mean of each 100 Hz current density group is not equal, hypothesis 18 is:

$$H18_0: \mu_{100\alpha CDB} = \mu_{100\alpha CDE}$$

$$H18_A: \mu_{100\alpha CDB} \neq \mu_{100\alpha CDE}$$

Hypothesis 19:

Immediately after a single 20-minute session of 0.5 Hz CES there will be no statistically significant change in mean current density of voxels in the delta band, as calculated by LORETA. Stated formally: where $\mu_{.5\Delta CDB}$ = mean current density at 0.5 Hz baseline and $\mu_{.5\Delta CDE}$ = mean current density after the experimental stimulus of 0.5 Hz CES; and where the null hypothesis 19 ($H19_0$) = the mean of each 0.5 Hz current density group is equal, and the alternate hypothesis ($H19_A$) = the mean of each 0.5 Hz current density group is not equal, hypothesis 19 is:

$$H19_0: \mu_{.5\Delta CDB} = \mu_{.5\Delta CDE}$$

$$H19_A: \mu_{.5\Delta CDB} \neq \mu_{.5\Delta CDE}$$

Hypothesis 20:

Immediately after a single 20-minute session of 100 Hz CES there will be no statistically significant change in mean current density of voxels in the delta band, as calculated by LORETA. Stated formally: where $\mu_{100\Delta CDB}$ = mean current density at 100 Hz baseline and $\mu_{100\Delta CDE}$ = mean current density after the experimental stimulus of 100 Hz CES; and where the null hypothesis 20 ($H20_0$) = the mean of each 100 Hz current density group is equal, and the alternate hypothesis ($H20_A$) = the mean of each 100 Hz current density group is not equal, hypothesis 20 is:

$$H20_0: \mu_{100\Delta CDB} = \mu_{100\Delta CDE}$$

$$H20_A: \mu_{100\Delta CDB} \neq \mu_{100\Delta CDE}$$

Hypothesis 21:

Immediately after a single 20-minute session of 0.5 Hz CES there will be no statistically significant change in mean current density of voxels in the theta band, as calculated by LORETA. Stated formally: where $\mu_{.5\Theta\text{CDB}}$ = mean current density at 0.5 Hz baseline and $\mu_{.5\Theta\text{CDE}}$ = mean current density after the experimental stimulus of 0.5 Hz CES; and where the null hypothesis 21 ($H21_0$) = the mean of each 0.5 Hz current density group is equal, and the alternate hypothesis ($H21_A$) = the mean of each 0.5 Hz current density group is not equal, hypothesis 21 is:

$$H21_0: \mu_{.5\Theta\text{CDB}} = \mu_{.5\Theta\text{CDE}}$$

$$H21_A: \mu_{.5\Theta\text{CDB}} \neq \mu_{.5\Theta\text{CDE}}$$

Hypothesis 22:

Immediately after a single 20-minute session of 100 Hz CES there will be no statistically significant change in mean current density of voxels in the theta band, as calculated by LORETA. Stated formally: where $\mu_{100\Theta\text{CDB}}$ = mean current density at 100 Hz baseline and $\mu_{100\Theta\text{CDE}}$ = mean current density after the experimental stimulus of 100 Hz CES; and where the null hypothesis 22 ($H22_0$) = the mean of each 100 Hz current density group is equal, and the alternate hypothesis ($H22_A$) = the mean of each 100 Hz current density group is not equal, hypothesis 22 is:

$$H22_0: \mu_{100\Theta\text{CDB}} = \mu_{100\Theta\text{CDE}}$$

$$H22_A: \mu_{100\Theta\text{CDB}} \neq \mu_{100\Theta\text{CDE}}$$

Hypothesis 23:

Immediately after a single 20-minute session of 0.5 Hz CES there will be no statistically significant change in mean current density of voxels in the beta band, as calculated by LORETA. Stated formally: where $\mu_{.5\beta\text{CDB}}$ = mean current density at 0.5 Hz baseline and $\mu_{.5\beta\text{CDE}}$ = mean current density after the experimental stimulus of 0.5 Hz CES; and where the null hypothesis 23 (H23₀) = the mean of each 0.5 Hz current density group is equal, and the alternate hypothesis (H23_A) = the mean of each 0.5 Hz current density group is not equal, hypothesis 23 is:

$$\text{H23}_0: \mu_{.5\beta\text{CDB}} = \mu_{.5\beta\text{CDE}}$$

$$\text{H23}_A: \mu_{.5\beta\text{CDB}} \neq \mu_{.5\beta\text{CDE}}$$

Hypothesis 24:

Immediately after a single 20-minute session of 100 Hz CES there will be no statistically significant change in mean current density of voxels in the beta band, as calculated by LORETA. Stated formally: where $\mu_{100\beta\text{CDB}}$ = mean current density at 100 Hz baseline and $\mu_{100\beta\text{CDE}}$ = mean current density after the experimental stimulus of 0.5 Hz CES; and where the null hypothesis 24 (H24₀) = the mean of each 0.5 Hz current density group is equal, and the alternate hypothesis (H24_A) = the mean of each 0.5 Hz current density group is not equal, hypothesis 24 is:

$$\text{H24}_0: \mu_{100\beta\text{CDB}} = \mu_{100\beta\text{CDE}}$$

$$\text{H24}_A: \mu_{100\beta\text{CDB}} \neq \mu_{100\beta\text{CDE}}$$

CHAPTER 2

METHOD

Participants

Participants for the study were recruited from undergraduate psychology classes, from the UNT community in general by poster, and from the local community by word of mouth. All participants signed an informed consent form approved by the University of North Texas Institutional Review Board. All subjects were at least 18 years old, and no participants were selected from protected populations, including mentally impaired or pregnant individuals. The participants ranged from 18 to 78 years of age. Data was collected from a total of 96 participants, however only the data from 72 of those participants met artifacting and reliability standards to be included in the study. Of those participants, 38 were presented with a 0.5 Hz CES stimulus, while 34 were presented with a 100 Hz stimulus.

Apparatus

Digital EEG data was collected at the University of North Texas Neurotherapy Lab utilizing a Neurosearch-24 amplifier, manufactured by Lexicor Medical Technology Inc., Boulder, Colorado. The Neurosearch-24 is an FDA approved medical device for the collection of digital EEG. Online monitoring of EEG was provided by the NeuroLex (Lexicor v151) software. Offline evaluation and processing of EEG was conducted with the following software, Lexicor v151, Lexicor v70 (Lexicor Inc., 1991), NxLink (Johns, 1999), EureKa!, NTE Mapinsight, (Congedo, 2005), NeuroRep (Hudspeth, 2003), NeuroGuide 2.2.6 (Thatcher, 2006), and LORETA-KEY (Pascual-Marqui, 2003). Hardware calibration signals were produced with the Neurosearch-24, while software generated calibration signals were produced with Wave

Generator (Congedo, 2005). An electrode cap from Electrocap International Inc. was used to provide standardized electrode placement (Blom and Anneveldt, 1982). The CES stimulation was provided by the Alpha-Stim 100, an FDA approved CES device manufactured by Electromedical Products International, Mineral Wells, Texas. Batch processing of the artifacted data was conducted with NeuroBatch 2.2.6 (Applied Neuroscience, Inc.). Identification of Brodmann areas was made possible with the Montreal Neurological Institute brain atlas (Collins, D., Zijdenbos, A., Kollokian, V., Sled, J., Kabani, N., Holmes, C., and Evans, A., 1998; Collins L., Holmes C., Peters T., Evans A., 1995; Evans, A., Collins, D., Mills, S., Brown, E., Kelly, R., and Peters, T., 1993; Evans, A., Collins, D., and Milner, B., 1992) Statistical analysis was conducted with NeuroStat 2.2.6 (Thatcher, 2006), S-PLUS® 6.2 (Insightful Corporation) and JMP 5.1 (SAS Institute Inc.).

Design

Design of the Study

The study used a repeated measures design (within subjects design). Baseline digital EEG data was collected from each research participant for 10-minutes in the eyes closed condition. After the collection of the baseline data, each participant was then provided with 20-minutes of CES stimulation as the experimental stimulus. Immediately after receiving CES the EEG of each subject was recorded again for 10-minutes in the eyes closed condition. Participants were tested in two groups, an initial group who were presented with a 0.5 Hz CES stimulus, and a second group that was presented with a 100 Hz CES stimulus.

Procedure

Application of the CES

The CES was applied through the use of ear clip electrodes attached to each ear. Because of the large variability between subjects for what constituted a comfortable level of current and an uncomfortable level of current, each subject was instructed to adjust the level of CES current to what was comfortable for them.

Acquisition of the EEG

Digital EEG data was collecting from 19 locations using the international 10-20 system of electrode placement. A reference electrode was placed on each earlobe to provide a linked ears montage for the physical reference of the scalp recordings. The impedance of the respective earlobe reference electrodes was maintained within 1 ohm of each other. All other electrode impedances were maintained at 5 ohms or less relative to amplifier input impedance with no more than 3 ohms of variance between any of the electrode contacts.

An electrode was placed on the cheek bone and a second electrode was placed above the orbit; these electrodes provided a reference channel (electrooculogram channel) for recording eye movements. The electrooculogram (EOG) channel was recorded to assist in editing the EEG data for removal of eye movement artifact. The reference channel was not included in any mapping or statistical analysis of the EEG data.

Collection of EEG

The amplifiers used to acquire the EEG were calibrated with sine waves before the acquisition of EEG for each research subject. The EEG equipment was checked at the start of the study for aliasing, and none was found. The EEG data was digitized at a rate of 128 samples per

second without a hardware filter. The acquisition epoch length was 2 seconds per epoch. The EEG was visually inspected online during acquisition to monitor for artifact. When necessary, data collection was stopped to identify and remove persistent sources of artifact such as muscle tension.

Preprocessing of EEG Data

Each digital EEG record was visually examined and the author, using the NeuroGuide EEG editing software, and all artifacts were manually removed. Individual record lengths, after artifacting, ranged from 64 seconds to 450 seconds. Windowing was performed using the Kaiser and Stermann method of a sliding 75% overlap (Kaiser, D., and Stermann, B., 2001). A fast Fourier transform (FFT) was used to convert the raw EEG into the time/frequency/amplitude domains required for computerized analysis. The FFT power spectral density produced frequency values from 0 – 40 Hz in 0.5 Hz increments. Aliasing artifact was avoided by limiting analysis to frequencies from 0-40 Hz, which is below the Nyquist frequency of the study (64 Hz) and by use of a low pass filter to block frequencies above 40 Hz. A split half reliability analysis was conducted on each EEG record after the artifact was removed. Only edited records with split half reliability greater than 95% were included in the group analysis. A \log_{10} transform was used to normalize data for the LORETA analysis. No transformation was used for the other EEG metrics.

EEG Analysis

Analysis of the EEG was conducted through two methodologies, the quantitative EEG (qEEG) and the low resolution brain electromagnetic tomography of Pascual-Marqui.

Quantitative EEG Brain Mapping

The qEEG brain mapping was conducted in a linked ears montage and an average montage for relative power, with additional processing of the data to yield values for coherence, amplitude, asymmetry, phase lag, and power ratios. A spherical harmonic Fourier transformation of scalp potentials was computed to create a surface Laplacian (current source density) transform of EEG. The Laplacian montage was also computed for relative power, coherence, amplitude asymmetry, phase lag and power ratio.

Low Resolution Brain Electromagnetic Tomography

The EEG tomography was conducted with LORETA (Pascual-Marqui, 2003). Each LORETA file was computed from the time frequency domain EEG cross spectra corresponding to the current density of group data in each condition. The LORETA files consisted an x, y and z-axis computation of the current density field for 2394 voxels per epoch. The LORETA voxels exclusively represent grey matter, including portions of the hippocampus and amygdala. The LORETA voxels correspond to an anatomical resolution of 7 mm.

Statistics

A repeated measures design was used in this study. Data was collected in a baseline condition and then compared with data from the same individual after exposure to twenty minutes of CES stimulation. There were two groups of subjects, one receiving 0.5 Hz CES and a second receiving 100 Hz CES. The use of two independent experimental groups provided the ability to compare responses to the CES stimulus.

Group analysis was conducted with a paired *t*-test for the relative power qEEG,

Laplacian, and the LORETA analysis. Because EEG data is highly correlated it is inappropriate to use blind statistical controls for type I error, consequently methodological controls appropriate for EEG data were used. Multiple testing of the group data was avoided through the use of a different montage for each analysis; this approach ensured that paired *t*-tests were conducted only once for each set of group means.

Methodological Issues

Introduction

In recording analogue EEG, an amplifier is used to magnify the signals sufficiently to drive the pens tracing the EEG on paper. Each amplifier has two inputs, and it is common practice to connect each input to the leads from adjacent electrodes, such as FP1 and F7. This arrangement is referred to as a bipolar montage or differential recording. The output of the differential amplifier is the difference in potential between the two electrodes plugged into it. The electrodes in a differential recording are usually connected in a chain, such as FP2 + F8 + T4 + T6 + O2 where intermediate electrodes will contribute to two amplifiers. For example T4 will contribute to the same amplifier as F8, but will also contribute to the same amplifier as T6. If a spike occurs at T4, then the raw wave EEG from both the F8-T4 amplifier and the EEG from the T4-T6 amplifier will have spikes on the EEG tracing. Because the output of each amplifier is the difference in potentials, the effect of a spike at T4 is to produce a spike in the output of both amplifiers with peaks that face each other. This type of an EEG tracing is called a phase reversal. This is a visually striking and easy-to-identify effect when the location of the spike is between the two peaks in the electrode common to both amplifiers. The phase reversal is the principle used to identify the location of focal activity in a bipolar paper recording.

There is another method of recording EEG where the two inputs of the amplifier are connected, not to adjacent scalp electrodes, but where one is connected to an active scalp electrode and the second to a reference electrode². This arrangement is referred to as a referential recording. The output of the amplifier is the difference between the active electrode on the scalp and the reference electrode. The referential recording does not link adjacent electrodes or chains of electrodes; the EEG tracing represents amplitude of EEG activity at the site relative to a reference presumed to contain no EEG activity, not the difference in activity between adjacent active electrodes. In a referential recording, a spike at T4 will be represented as an increase in the amplitude of activity at T4. The electrodes that are adjacent to T4 will also show an increase in amplitude, but to a lesser extent since the strength of the spike decreases as it travels away from the source of the spike. The principle used to localize EEG activity in a referential montage is amplitude, not phase reversals.

If a patient was simultaneously connected to amplifiers for a differential recording and a second set of amplifiers for a referential recording, and the patient experienced a spike at T4, a strange situation could occur where the bipolar montage may not show any spike activity at T4. The referential montage would show spike activity at T4 and in this example also at F8 and T6, but the bipolar montage records spike activity only FP2 + F8 and T6 + O2 with no spike activity at the sites involving F4. Why does the bipolar montage incorrectly display spike activity from the amplifiers connected to F4, the very sensor under which the spike occurs? The bipolar montage is inaccurate in this situation because if the voltage from the spike has not yet declined by the time it reaches the electrodes adjacent to F4 in the bipolar chain, the activity of the spike is canceled out for the amplifiers connected to F4. If the spike was 100 μV in strength at both F8

²Theoretically there should be no EEG signal in the reference electrode.

+ T4 and T4 + T6 then there would be no difference in input to the amplifier from the electrodes due to the spike; only the other (background) EEG activity would be represented. By comparison, the referential montage would correctly display the spike as an equal increase in amplitude at F8, T4 and T6. In most situations the bipolar montage is accurate and useful for raw EEG, however in this particular example it is incorrect in how it represents the EEG activity.

This example illustrates a relatively simple case of a major issue in EEG analysis, namely that the output or display of EEG may appear valid when in fact it is incorrect. There are many cases in which the methods used to collect, process or display EEG can result in an inaccurate display. In the example above, any well trained researcher or clinician would look at the EEG record and recognize that the bipolar montage was not properly displaying the spike activity, even without the referential montage to refer to. They are able to detect the inaccuracy in the display of the EEG because the EEG tracing contains a hint that it is incorrect, which tells the trained eye that there is something wrong (in this situation) with the bipolar montage. The lack of any spike activity between the peaks of a phase reversals is contrary to the very method of localization of spike activity by phase reversals. The physics involved in EEG would make the representation of activity in this example physiologically impossible for real EEG. In this example only the clinician or researcher in training would fail to recognize that the bipolar recording was inaccurate. However, in digital EEG there are many analogous situations that do not contain any hint that the representation of EEG is inaccurate.

Recording digital EEG requires different procedures from analogue EEG to ensure that no artifact has occurred that can't be detected on review. In some instances there is artifact at the time a digital EEG is recorded which makes it inaccurate, and a few of these artifacts are impossible to detect once the EEG has been recorded. Additionally, techniques for processing

digital EEG, such as how artifact is removed, can create what appears to be an EEG signal when in fact it is not. The inappropriate use of statistics can hide patterns in digital EEG data, or create false patterns that do not actually exist. Finally, artifact can occur from how EEG is displayed, such as the use of different scales with the same colors, or inappropriate EEG metrics. Even well trained researchers and clinicians can easily be led astray when viewing digital EEG, primarily because there is rarely a hint in the display when the EEG is inaccurate. Because there are many factors that can result in the inaccurate display of EEG activity without a hint that there is any artifact, digital EEG researchers, and clinicians, are vigilant in using procedures to prevent artifacts. Such consideration is extraordinarily important to ensure that research and clinical conclusions are based on actual EEG activity and not artifact.

There is no globally correct approach or technique that can be used in every clinical or research situation to ensure the accurate display of EEG. Each application requires a thoughtful review of what is appropriate, and why, to ensure that the approach for data collection, data analysis and data display results in an accurate reflection of the EEG activity that is actually present. It is common for EEG researchers and clinicians to ask for the details of the procedures used to record and process digital EEG to consider whether or not the record is accurate or may contain artifact. In the rest of this section we shall consider some of the relevant methodological issues facing the researcher of the current EEG study and what choices were made to ensure that the EEG results displayed in the study are accurate.

Design of the Study

To a significant degree, the moment-to-moment state of the brain is reflected in the EEG. Anxiety, sleepiness and many other transient states have an effect on the EEG and differ from

individual to individual, or even in the same individual across time. Variations in EEG also occur due to differences in the time of day, gender, age, medical conditions, medication and many other factors. The degree to which EEG varies between individuals is statistically significant; and it presents a difficult and an urgent issue to be addressed when attempting to examine EEG in an experimental setting.

If enough EEG records are collected, the principle of regression to the mean makes it possible to ignore individual differences. This approach has a price in terms of loss of statistical power, however it is a solid method for non-experimental EEG applications such as constructing reference databases. Unfortunately in experimental applications, a significant loss in statistical power can occur from relying on regression to the mean. A loss in statistical power may mean that an effect from the experiment is difficult to find even if it is significant, resulting in a false negative finding (type II error). In this situation, there is so much statistical noise that the signal of interest (the treatment effect) is lost in the noise. In general, if individual differences in physiological research are small, then the loss in power may not be of much concern, because the statistical noise is low. However, the error variance due to individual differences in EEG can be quite large; for example a 10% difference in the thickness of the skull between two individuals (common due to gender) can result in an 800% difference in EEG amplitude at all frequencies (Thatcher, Walker, & Biver, 2003). Due to the larger error variance introduced by individual differences in EEG data, clinically and statistically significant treatment effects can be washed out when addressing individual difference through regression to the mean.

Fortunately there is another method of addressing the problem of individual differences in EEG data without sacrificing statistical sensitivity: a repeated measures design. In a repeated measures design each research participant in a study functions as his or her own control. Each

participant is measured at baseline, after which the experimental protocol is conducted and then the participant is measured again. The advantage of this approach is that it controls for individual differences without sacrificing statistical power. The individual differences are eliminated in a manner that reduces overall error variance (statistical noise), forming an attractive solution to the problem of how to deal with individual differences in EEG research. Because of the advantage of using a repeated measures design it was the approach chosen for this study.

A second feature of the design of the study is the repeated testing of CES with a group of subjects who were provided with a 0.5 Hz stimulus, and a second independent group provided with a 100 Hz stimulus. There were no subjects who were members of both groups. It is expected that there may be differences in the response of these two groups to CES, but both of these frequencies of CES have been reported in the literature to be substantially similar in their affective and cognitive effects; therefore, it was expected that they would also share substantial common effects on EEG. To the extent that the EEG effects are in agreement between the two frequency groups, the use of two CES groups provides a methodological mechanism for validating any findings that are in agreement in both groups. To a limited extent, the use of two experimental groups provides a replication of the results of the study within the study. This feature of the design methodologically addresses the possibility of false positive results (type I error). The reason this approach can be used to control for type I error is the low probability that patterns of random false positive results would occur identically in the two independent CES groups (Duffy et al., 1994).

Placebo/Sham CES Group

A placebo group, or sham treatment group, provides a comparison group (control group)

in which the null hypothesis should be true. The placebo group receives a substitute treatment designed to ensure that there is no treatment effect (the placebo). The treatment group and placebo control group are treated identically in terms of every other aspect of the experiment. When properly executed, the only difference between the two groups is whether or not they have received an actual treatment or a placebo treatment. The isolation of the independent variable through the use of a placebo control group allows researchers to make a strong case that they have found or not found a treatment effect. Because a systematic bias can be introduced into the data if the researchers or their subjects know who is in the experimental or placebo control group, it is important for both the researchers and the subjects to be unaware of which participants are in which group. The use of a double blind placebo control group is the gold standard for designing a medical research project and it is the approach of choice for evaluating the effects of medications and medical devices. Previous research with CES has included double blind placebo controlled protocols and found a treatment effect from CES. These studies used sham devices in a double blind manner to provide a placebo control group.

The current study was originally designed to mimic drug research and include a placebo control group. Unfortunately it quickly became clear in the pilot study that due to the striking immediate effect of CES on raw EEG, it was not possible to blind the researcher to the group status of the research participants. Previous double blind placebo controlled research with CES had not used EEG or and had not faced the problem of how to blind the researcher and obtain valid EEG recordings and analysis. Given the resource limitations of student research it was not possible to overcome the problem of blinding the researcher to group status and still obtain valid EEG data. Furthermore, the research subjects spontaneously commented on whether or not they felt they had a sham or working CES unit and for the most part were correct in their perception

of group status. Because it was not possible to hide the group status from the researcher, and it was apparent that most subjects were aware of whether or not they were in a sham group, it was clear that given the current experiment there would be no integrity to a double blind or single blind placebo control group protocol. Consequently, no placebo control group was used in the current study. The use of a repeated measures design isolates the independent variable as much as it is possible to do so when a double blind placebo control group cannot be properly implemented.

Effect of a Repeated Measures Design on Degrees of Freedom

The use of a repeated measures design has been criticized for having the net effect of reducing the degrees of freedom in a t -test, but this is not necessarily the case. The loss of degrees of freedom is not intrinsic to the use of a repeated measures design, but rather the incorrect implementation of it. In a between subjects design there is an independent experimental group and a control group. A minimum number of subjects must be present in each group to have statistically significant results. In a repeated measures design each subject in the experimental group functions as their own control, so there is no need for a second group of subject to serve as the control group. In the repeated measures design each member of the experimental group is also a member of the control group. Thus if a researcher needs a minimum of 20 subjects per group for a between subjects design (40 subjects total), the temptation with a repeated measures design is to keep the same minimum number of subjects per group, resulting in 20 subjects total. This is the incorrect implementation of a repeated measures design. The greater statistical power of a repeated measures design is often used to justify a lower number of subjects used in a study; however, reducing the number of subjects creates a loss in degrees of freedom which in turn

requires a higher t value to reach significance. Such an approach reduces the accuracy of the statistical comparison and makes it more difficult to find significant results. Specifically, in a between groups t -test, the degrees of freedom (df) are greater ($df = n_1 + n_2 - 2$) than in a repeated design ($df = n - 1$) if the group sizes are equal. If an experimenter used 20 subjects per group in a between subject design, the experimenter would have a df of 38 ($df = 20 + 20$). If the same experimenter ran the study with a between subject design then the df would be 19 ($df = 20 - 1$). However, if the same total number of subjects is used in the two types of studies (in this example 40 for the between subjects design and 40 for the within design) there is no loss in the degrees of freedom with a repeated measures design. In a study with 40 subjects, the degrees of freedom for a between groups design with two groups would be 38 ($df = 20 + 20 - 2$) while for the between groups design it would be 39 ($df = 40 - 1$). The current study used a repeated measures design, but maintained the same total number of subject as would be needed for a between subjects design; therefore, the study benefited from the greater statistical power of a paired t -test without suffering a penalty in a loss of degrees of freedom.

Normality of EEG Data

Parametric methods of statistical analysis assume a normal distribution; therefore, consideration must be given to the normality, or non-normality, of the EEG data in when planning a statistical approach. Depending on the metric use, EEG data can be normally distributed, or not. The EEG data for statistical analysis is not unitary; it is a derivative of the raw wave EEG signal. The raw wave EEG signal is not a form of data that can be evaluated statistically. The EEG signal has to be converted in some manner that will quantify the time series; usually this is done with a computer using a fast Fourier transform (FFT). The data is then

further transformed to create an EEG metric such as coherence or relative power. The relevancy to the normality of the data is simply that some metrics produce datasets with normal distributions, while others do not.

Most EEG metrics are normally distributed, with the notable exception of total power, absolute power and phase (Thatcher, Walker, & Biver, 2003). When EEG data is not normal, a simple transformation (such as a \log_{10} transform) will normalize the distribution of the data. This approach is a common solution to non-normal EEG data and yields accurate results in a parametric analysis (Kaiser, 2000; Thatcher, Walker, & Biver, 2003). Additionally, while parametric methods do assume a normal distribution for the data, they are relatively robust to violations of normality and have been found to be appropriate for most standard EEG metrics without any transform (Kiebel, Tallon-Baudry, Friston, 2005).

Nonparametric methods can also be used to address the issue of normality, since nonparametric methods do not assume a normal distribution. However, nonparametric methods are not as statistically sensitive as a parametric approaches (Thatcher, Walker, & Biver, 2003; Kiebel, Tallon-Baudry, Friston, 2005) and therefore decrease the ability of a study to find significant effects when they are present (type II error). In a study which compared parametric (with a \log_{10} transformation) and non-parametric methods for analyzing LORETA data, it was found that both parametric and nonparametric analyses were valid; however the parametric analysis had a lower type II error rate (Thatcher & Biver 2005), making it the more attractive approach.

In the present study, it was deemed most appropriate to use parametric statistics in the analysis of both the qEEG and LORETA. A log transform was used with all EEG metrics to ensure a normal distribution for the parametric analysis.

Serial Correlation

In classical statistical analysis there is an assumption that data that is recorded in a serial fashion is not temporally related (serially correlated). In other words when an observation is recorded the value is not related to the observation that was recorded before or after it. This is an assumption that is violated in the recording of most if not all moment-by-moment physiological data. In the case of EEG the moment-by-moment recording of EEG data (each epoch) is related to the values recorded before and after. The serial correlation in EEG is due to the fact that EEG data is not random, but highly related. Because epoch-by-epoch EEG data is highly correlated in time, a classic statistical analysis is not appropriate to analyze epoch-by-epoch EEG data. In the current study the mean values of the FFT for each electrode site for each EEG record was used for analysis, rather than the epoch-by-epoch data. The mean values of each record are not temporally correlated; therefore a classical statistical analysis (paired t -test) can be used since there is no serial correlation of the data. It should be noted that the mean data for each EEG record at baseline and after the treatment is highly correlated, but the correlation is not serial.

Multiple Comparisons

A significant issue for the analysis of qEEG data is the statistical effect of multiple comparisons of group means. For example, if a set of relative power and coherence means from an EEG record is compared against a database in an exploratory manner for head injury, alcoholism, and ADHD, multiple comparisons of group means has occurred. The relative power and coherence means of the patient has been compared to the database relative power and coherence means three times, once for each possible condition. The result of this type of multiple comparisons of group means is a statistical inflation in the data, which can result in false positive

results (type I error). The issue of multiple comparisons occurs when any of a set of two, or more, group means are compared more than once. If multiple comparisons are being used in a study, or clinical setting, a statistical adjustment is applied to guard against a type I error.

The paired t -test in a qEEG consists of testing the mean differences between the baseline and treatment conditions for each electrode site, a result which is adjusted for the variances and total number of FFT windows (a function of accepted epochs of EEG data). A large number of t -tests are conducted in a qEEG-paired t -test, however no statistical adjustment is required for multiple comparisons because there have been no multiple group comparisons (Hayes, 1973).

In the current study there is no multiple comparison of group means. There are unique data sets created for each EEG metric and each referential montage. The group means are different for all the EEG metrics used in this study, such as relative power and coherence; therefore, t -tests on more than one metric do not involve multiple comparisons of group means. A change in referential montage will also result in different group means for each metric. The values at each site are the result of a comparison of the activity at the site with the value of the reference. When the data is remontaged the value of the reference changes and thus the value for the EEG at each electrode site is different in the new FFT calculations used to create the new montage. The result is that the group means for each metric are different from montage to montage. For example, a paired t -test could be conducted in relative power for a linked ears montage, and a Laplacian montage on the same EEG record. The calculation of two sets of relative power metrics (one for each montage) is not a case of multiple comparisons of means because different data sets are used to create the means that each relative power montage is calculated from. As long as the group means for a particular metric in a particular montage are not tested more than once, no multiple comparisons has occurred. In the current study all

duplicated metrics, such as multiple instances of relative power values were derived from different montages. Care was taken in the current study to ensure that there was no multiple testing of group means.

False Positives Resulting From a Large Number of Statistical Tests

In the qEEG analysis used in this study a paired *t*-test is conducted for each 0.5 Hz frequency of 41 frequencies (0-40 Hz) at 19 electrode sites, producing 1539 paired *t*-tests (41 x 2 x 19) per subject. In each of these paired *t*-tests the differences between the baseline and treatment conditions is compared. A decision is applied to identify whether or not the difference between the means is sufficiently large that it is unlikely to have occurred as the result of random chance. The null hypothesis states that there is no statistically significant difference in the means. Rejecting the null hypothesis is a statement of finding that there has been an effect from the treatment. A type I error occurs when the null hypothesis has been rejected (stating that there is a treatment effect) when in actuality the null hypothesis is true and there is no significant difference between the groups. The probability of making a type I error (false positive finding) is called alpha. The probability level selected for alpha sets the standard for how stringently the difference in the means are tested to determine if there is a statistically significant difference in the means. If the alpha level is too stringent then the probability of a type II error is increased (failing to reject the null hypothesis when the null hypothesis is not true) and thus it is more likely that significant results are not found even if the treatment was successful.

The standard level of alpha for most research is set at a probability level of .05, which in practical terms means that the researcher is willing to gamble that every one out of 20 times a statistical test is performed it has a false positive. The number of statistical false positives in an

experiment can be roughly estimated by multiplying the number of t -tests performed by the alpha level used. In a single t -test, a researcher has to rely on the element of chance to favor the research, and hope that there is no false positive. In this situation an independent replication of the experiment will confirm or cast doubt on the findings, thus the emphasis in science on replicating findings. The situation is even more problematic if a large number of t -tests are performed. Statistical tests will generate random false positive results in uncorrelated trials. Random probability randomly generates random false positive results. In one qEEG metric, such as relative power, the 1539 t -tests performed would be expected to generate approximately 77 false positive results (assuming uncorrelated trials), Statistically these type I errors are traditionally controlled for by any of a number of adjustments, such as a Bonferroni, Tukey or Scheffe, etc. correction. Like the alpha level itself, these statistical adjustments are more or less restrictive depending on the choices of the experimenter. The statistical adjustments are chosen and applied with the intent of controlling for false positives, but also with the hope they are not so stringent that real treatment results are hidden (type II error). Due to the large number of statistical tests involved in the analysis of EEG data, the use of blind statistical correction produces an extraordinary inflation of type II error rates. Since the point of an experiment is to determine if the independent variable has an effect, an approach to controlling type I error that dramatically inflates false negatives is problematic.

Fortunately for EEG researchers, the activity inside the human skull is not random. If the data recorded from the EEG were random, then the use of statistical controls for type I error would be unavoidable. With blind statistical controls for 1539 t -tests it would be difficult to avoid large-scale type II error. However, it is the good fortune of EEG researchers that the activity of the EEG is highly related; therefore, the actual changes in EEG produce patterns

spanning adjacent electrodes and adjacent frequencies. In 1994 the March meeting of the American Medical EEG association formed a committee to study the issues involved in qEEG and report on the current state of qEEG. Dr. Frank Duffy from Harvard University chaired the committee and the findings were reported in the journal *Clinical Electroencephalography* (Duffy et al., 1994). Dr. Duffy and his colleagues discussed the issue created by the use of a large number of *t*-tests in qEEG and pointed out that the related nature of EEG eliminates the concern with type I error that thousands of comparisons would create in classical statistics (Duffy et al., 1994). They made two significant observations about the difference of qEEG statistical tests from classical statistical testing.

Their first point is that the EEG data is correlated, it is not random; thus any data that is in a pattern of activity can be placed under a single factor. Groups of uncorrelated activity form different factors. When the EEG data set is reduced in this manner only a small number of factors are revealed (Duffy et al., 1994), which represent the true number to be considered when estimating type I error rates. These patterns (factors) can be identified visually in a topographical map and also can be evaluated statistically with a principle components analysis.

The second important observation Duffy et al. made is that since random events are random, by definition they do not repeat. Thus, type I errors in qEEG can be eliminated through the use of replication of the EEG data (Duffy et al., 1994). If the results are replicated then they are not the product of type I error, but are true results. With EEG data there are two types of replication that can be performed, remontaging the data (to create a new data set in which the results can be compared to the original data set) and the use of a second (independent) experimental group. In this paper the author used the methodological approach that Duffy and his colleagues advocate to eliminate concern with performing large numbers of statistical

comparisons in the analysis of EEG data. The author used three methodological approaches to control type I error derived from the concepts of Duffy and his colleagues.

Pattern Principle

The first methodological approach to control type I error is the pattern principle. Simply stated, any data that is not part of a pattern should be ignored. A random false positive from statistical error will stand alone in EEG data; it will be a data point in a single electrode and at a single frequency and not part of a larger pattern of significant results (a spatial or frequency cluster). Because of the related nature of EEG activity it would be exceedingly rare to find any real EEG activity that is not visible in adjoining electrodes or frequencies. As noted, by definition random events do not occur in a pattern therefore any activity in a pattern is a factor and not random type I error. The exception to this rule would occur with the use of data interpolation methods capable of converting a point of false positive data into a pattern of activity in terms of location or frequency. This problem would occur primarily with models manipulating estimated data and would not occur in methods (such as standard qEEG) involving comparison of actual EEG data. If interpolation is used then the pattern principle should not be used unless one of the comparison groups does not use interpolation. The pattern principle (in terms of location or frequency clusters) is a simple but practical method of identifying false positives in EEG data. With this method it is possible to control for false positives without the use of a blind statistical control that would significantly reduce the sensitivity of the test. Since each pattern represents a factor, a principle components analysis (PCA) would be a valid statistical method of implementing the pattern principle (Duffy et al., 1994).

Remontaging the EEG Data

Remontaging the EEG with a different referential montage is a second methodological approach available to EEG researchers to control for type I error. This approach is a method of replication of the EEG data with one treatment group. Each referential montage is constructed from comparing the values of the electrode site and the values for the reference. Since each type of referential montage produces a different reference value, the results in the montage for each electrode are different for each type of referential montage. Even though the same EEG records are used to create the group data, the FFT data for each referential montage is different. Consequently, each EEG metric is constructed from a different data set than the same metric in another referential montage. Because of this, it is possible to remontage the EEG, and to compare the results of the same metric without having performed a multiple comparison of group means (the values for the group means are different). As noted above, by definition random events do not occur in a repeating pattern; therefore the statistical results for two different montages can be compared to eliminate false positives.

If statistical false positives have occurred, they would not occur identically in different referential montages. To the extent that the different montages are in agreement, the statistical results can be trusted. Because each type of referential montage is different in its ability to represent EEG activity, there may be true EEG activity that is not represented in both montages simply because the montages differ in their ability to display activity. Therefore, it is possible that the use of remontaging alone will result in the discarding of real treatment effects as type I error. This possibility makes remontaging a conservative approach to controlling type I error. Real results may be rejected because of the way the montages display the data; remontaging does not provide an opportunity to see the activity in an identical presentation. The comparison of

several referential montages, or combining the use of remontaging with another methodological control may help to eliminate problem of replicating results in montages that display the data differently.

Independent Replication

Replication of the results in two independent groups provides a third methodological control for false positives. Using the group replication approach a study conducts the experiment twice, with independent groups, allowing it to replicate its own results. Because random events do not repeat in an identical fashion, the results from the two independent experimental groups can be compared as a control for random type I errors. The results that are in agreement in both experimental groups can be accepted as actual treatment results that are not the product of type I error. This type of an approach does not suffer from the problem of montages displaying the data differently, and thus is a more sensitive approach than remontaging.

The current study uses group replication in that it independently tested two groups with CES. However, it is not a pure example of this type of control since the two groups did not receive identical stimuli, but one of two different frequencies of CES. To the extent that frequency has an effect on CES these two groups are different in their response; however to the extent that CES has effects that occur with both stimulus frequencies, the groups are the same in response. Because the clinical responses to CES are quite similar for both 0.5 Hz and 100 Hz CES, it is assumed that the EEG data for the two groups are more similar than dissimilar. To the extent that the obtained results are in agreement, those results are validated as actual changes and not false positive results.

In this study the large number of statistical tests performed on the qEEG raises the issue

of how the study will control for false positive results. The use of overly restrictive blind statistical control for type I error was rejected in favor of multiple methodological controls. Each methodological method of controlling for type I error in the EEG data is valid; however, the experimenter chose a conservative approach and required the data to be validated by at least two of the three methodological controls to maximize statistical power while minimizing the possibility of a type I error. In the current study, the statistical results were accepted only if they passed at least two of these three methods of control for possible false positives.

Methodological Control with LORETA

The LORETA method involves even more statistical comparisons than the qEEG. There are 2394 gray matter voxels compared in the LORETA *t*-tests, therefore if the data were uncorrelated approximately 120 false positives would be expected. However, since it too is based on EEG data, the LORETA data is correlated and the false positives can be controlled for through the same three methodological approaches used with the qEEG. The caveat with LORETA is that it is not possible to produce a full remontage of the data. Because of the way the LORETA is calculated, a change in the referential montage of the data upon which it is based does not change the results. The LORETA is a reference free method that disregards the physical EEG reference information. Since the LORETA itself cannot be subjected to a remontage, it is reasonable to suppose that the cortical activity displayed in LORETA can be compared to a qEEG; however this is not the case. It is not valid to compare the cortical activity found on a qEEG with the LORETA because the current density activity estimated by LORETA is not visible to an EEG. However, it is possible to obtain a valid cortical map for comparison with the cortical data for LORETA using a qEEG Laplacian montage. The LORETA and Laplacian

montages are both based on estimates of current density, not the amplitude of EEG; therefore they can be compared. The Laplacian is a 2-D calculation of cortical activation based on estimated current density, while the LORETA is a 3-D calculation of cortical and subcortical activation based on estimated current density. Because it was not possible to directly remontage LORETA, a Laplacian montage qEEG was used for comparison of cortical results with the LORETA.

Relative Power/Magnitude vs. Absolute Power/Magnitude

The multitude of options for the digital display and analysis of EEG provides a wealth of information not available in analogue EEG. The added opportunities for data analysis in digital EEG add considerably to the utility of EEG, but it also can add confusion for both authors and readers. A comparison could be made to the choice of statistics in the analysis of the EEG data; while it may be possible to run a large number of statistical comparisons of a data set it is not always advisable to do so. The issue in digital EEG is twofold, one of the methodological appropriateness of the given EEG metric (in a given application is the EEG value appropriate, does it accurately reflect actual activity), and two, whether or not the metric clarifies or obfuscates the data. A shotgun approach of producing every kind of EEG value available to a researcher can be confusing and may even lead lay readers to incorrect conclusions about the data. Like the choice of statistics to analyzed data, ultimately the choice of metric used to present digital EEG is driven by the question the clinician or researcher is attempting to answer, and the type of data being evaluated.

In the present study, group EEG data is being presented by qEEG, and LORETA. Because LORETA is a technique of source localization based on the estimation of current source

density, it does not use any other EEG metrics. However, qEEG does use a variety of EEG values and a researcher or clinician must choose which are the most appropriate to answer the question at hand.

In the qEEG literature, when combining the EEG data of multiple individuals for a group analysis, the historical EEG metric of choice has been relative power (Kaiser, 2000). Relative power and relative magnitude EEG are percentage measures; they reflect the proportion of activity in a frequency at a particular location rather than the signal itself (amplitude). Relative power is a logical choice for use in experimental EEG since it is insensitive to individual differences that affect EEG, such as skull thickness, which can otherwise skew group data. The use of relative power is accepted convention when presenting group data. However, at the time of the conceptualization of this study, the researcher was challenged by a few colleagues to think about whether or not relative power was an appropriate metric to use in the study. The researcher's colleagues contended that due to the proportional nature of relative power, it might not produce qEEG topographical maps that are as accurate as an absolute value map (such as absolute power or absolute magnitude), and therefore may not be the best metric for the current study.

The question arises because in EEG power spectra (compressed spectral arrays) the use of relative power reduces the ease with which group differences can be visually identified in the power spectrum (Davidson, Jackson & Larson, 2000). In terms of compressed spectral arrays relative power can be visually misleading, while absolute measures are not. Relative power has been called "pie chart EEG" where each frequency band (beta, alpha, etc.) can be compared to a slice of the pie. Since relative power is a proportional display, if there is a dominant frequency, it will take up more of the pie (its "slice" will be larger). When this occurs, the dominant frequency

leaves less room for the other frequencies, in effect squeezing them in the display. For example, if alpha were 50% of the total EEG power in a particular person's map, then the activity of the other frequencies would have to be represented within pie slices contained in the remaining 50% of the "pie." The effect of this proportionality on a spectral display of EEG is a suppression of the height of the peaks for non-dominant frequencies (see figure 1). When visually inspecting a spectral display in relative power it becomes more difficult to evaluate non-dominant activity, as compared to an absolute power display. Since the proportional nature of relative power makes it a less accurate metric for EEG spectral arrays, the question naturally arises, doesn't the same effect also render relative measure qEEG maps less accurately than in an absolute measure? It was for this reason that the question arose that perhaps the convention of using relative power with qEEG maps should be reconsidered.

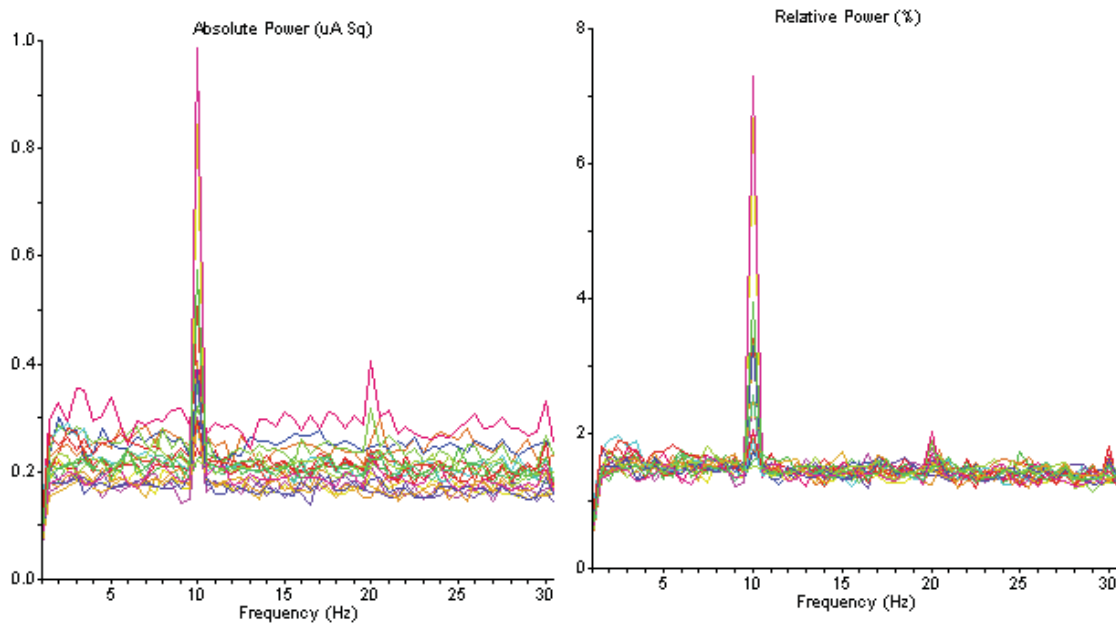


Figure 1. Comparison of the spectral display of a 10 Hz. test signal in absolute and relative power. Note the appearance of a decrease of activity in the non-dominant activity of the relative power display.

In addition, with qEEG a new concern arises in that the proportional nature of relative measures

could also create confusion about whether a particular frequency band has actually increased or decreased activity. If there is an increase in one band in a relative power/magnitude map there is no way to determine visually if the increase is the result of an actual increase in activity, or a decrease in the activity other frequency bands (Duffy et al., 1994). Happily this question is moot for most clinical applications, since the effect or *clinical meaning* of any such change in a qEEG would be the same. In this instance the proportionality of relative measures are actually a strength and make them clinically superior to absolute measures.

For example, if there were an actual increase in theta band activity, or a reduction in activity in other bands that increased the proportion of EEG power in theta, the clinical effect of an increased dominance of theta would be the same. The absolute measures would be clinically inferior since they would not reflect the clinical significance of the change, however the relative measures would. The confusing conclusion of considering this second issue is that because of the proportional nature of relative power it should convey the correct clinical significance of any change in qEEG more accurately than an absolute measure, but it would not always be most accurate a reflection of what change had actually occurred.

In terms of clinical work with qEEG relative measures appear to be the metric of choice, they provide the correct clinical significance of any change that has occurred. However, in terms of research it is still not clear if relative measures are the most appropriate. Are relative measures the most accurate for research as well as clinical work? The original question is still unanswered, since absolute measures produces more useful spectral displays of spectral EEG, do they also produce the most useful (accurate) qEEG topographical maps? The question is not a trivial one, since it directly impacts the conclusions that can be drawn from much of the published qEEG literature as well as the choice of appropriate EEG values for the current study.

I tested the question for the current study through the use of known EEG test signals. The test signals made it possible to conduct a direct comparison of absolute and relative displays of known qEEG data. The comparison was conducted with software generated test signals and with hardware generate test signals processed through the EEG amplifiers and acquisition software used to collect the digital EEG used in the present study.

The EEG signal that is picked up by the scalp electrodes is a small field effect and requires amplification by a factor of one million to be recorded (one microvolt = one millionth of a volt). The degree of amplification in EEG requires careful checks of the amplifiers. If one or more of the amplifiers are not being properly calibrated this would skew the EEG results. The amplifier system used in this study (Neurosearch-24) was capable of providing hardware test signals for calibration and verification of each amplifier output. A 10-hertz hardware test signal was generated for 19 scalp electrode sites and 4 auxiliary sites (see Figure 2.). The signal was visually inspected with the manufacturer's software (NeuroLex) and found to be a uniform sinusoidal 10 Hz signal in all channels. Offline inspection of the recorded signal with an independent software package (EureKa!) independently confirmed the uniform sinusoidal 10 Hz signal in eall EEG channls (Figure 12).



Figure 2. Raw wave display of the 10 Hz calibration signal at 10 microvolts (NeuroLex).

A spectral analysis of the signal processed through a FFT shows that, as expected, the test signal is centered at 10 Hz (see Figure 3, Figure 12 and Figure 18).

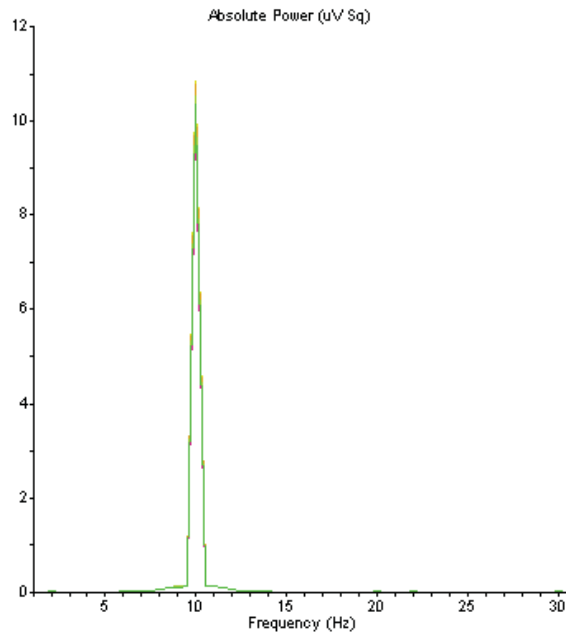


Figure 3. A spectral frequency analysis of the hardware generated 10 Hz calibration signal at 10 microvolts (NeuroGuide).

Since the test signal is known to be at 10 Hz and uniform on all channels, we know that an accurate topographic map should show activity at all sites on the head for the frequency band containing 10 Hz (alpha); and no activity at any site in any other frequency band.

When evaluated with the software package used to digitize EEG in the study (NeuroLex), a relative power topographic map of the signal accurately displays the 10 Hz test signal as present at all electrode sites within the 8-12 Hz (alpha) band, and correctly displays no activity at any site in the other frequency bands (bottom row of Figure 4). However, the absolute power map (top row of Figure 4) incorrectly represents the signal as having significant variation in strength at different sites on the head and as being present in all frequency bands.

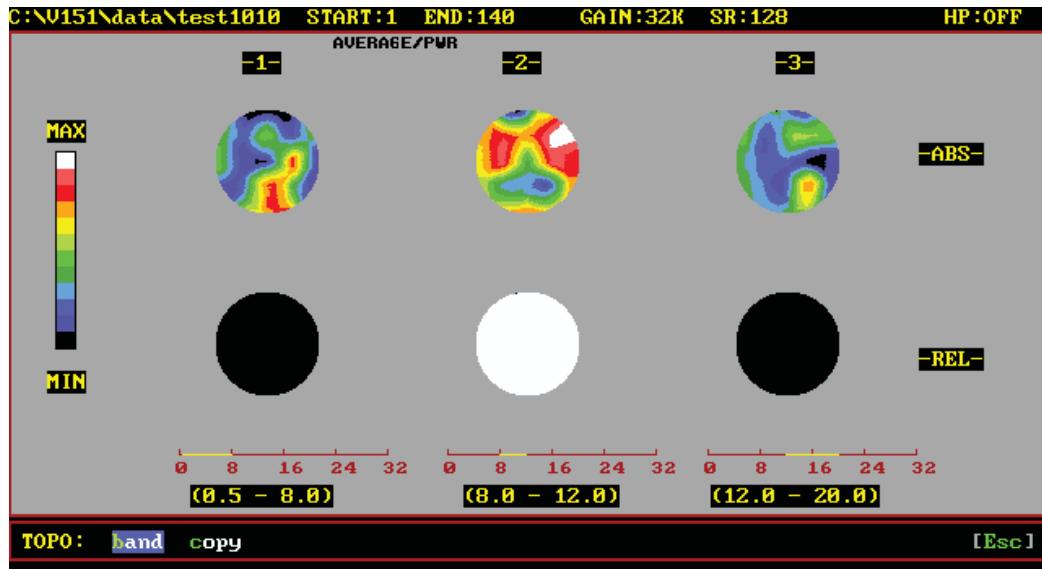


Figure 4. Absolute power (top row) and relative power (bottom row) topographical analysis of the amplifier generated 10 Hz calibration signal (Neurosearch24). Relative power correctly displays the test signal, however the absolute power does not (NeuroLex).

The activity displayed by the absolute power map does not accurately represent the known activity of the test signal. The same phenomena can be seen when comparing absolute magnitude and relative magnitude (figure 5).

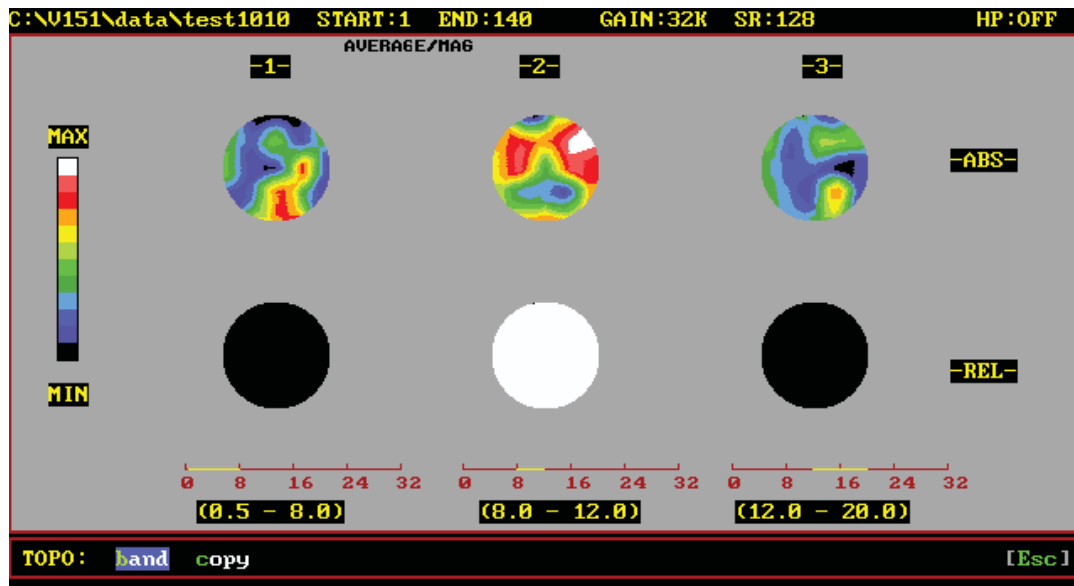


Figure 5. Absolute magnitude (top row) and relative magnitude (bottom row) topographical analysis of the amplifier generated 10 Hz calibration signal (Neurosearch24). Relative magnitude (bottom row) correctly displays the test signal, however the absolute magnitude (top row) does not (NeuroLex).

To address the possibility of a defect in the software being responsible for the less accurate display found with absolute power and absolute magnitude, the same signal was processed with two other software packages, NxLink, and NeuroGuide. When processed by NxLink (Figures 6 & 7) and NeuroGuide (Figures 8 and 9) differences were again found between absolute power and relative power, but the differences were not as dramatic.

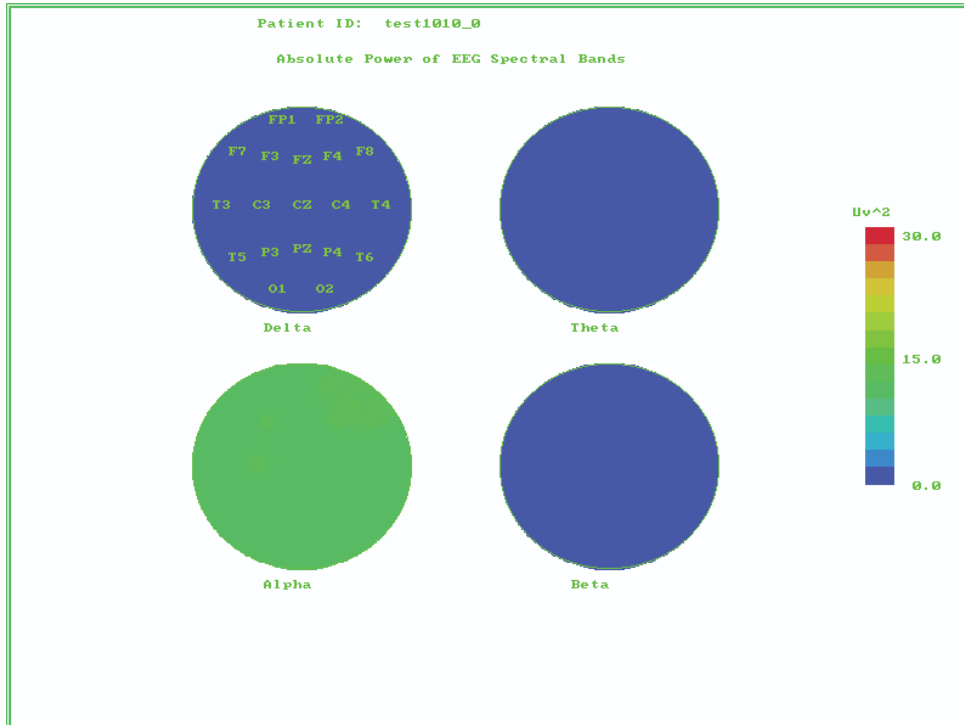


Figure 6. Absolute power topographical analysis of the amplifier generated 10 Hz (alpha) calibration signal. The absolute power display is more accurate than NeuroLex, but still contains errors in that it shows variations in the uniform test signal (NxLink).

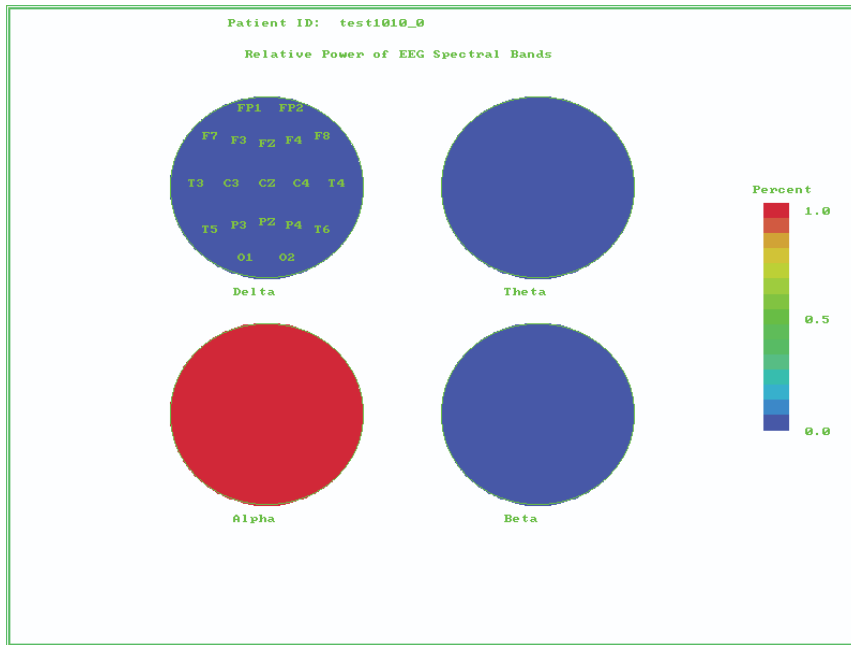


Figure 7. Relative power topographical analysis of the amplifier generated 10 Hz (alpha) calibration signal (NxLink). The relative power display is accurate in representing the test signal.

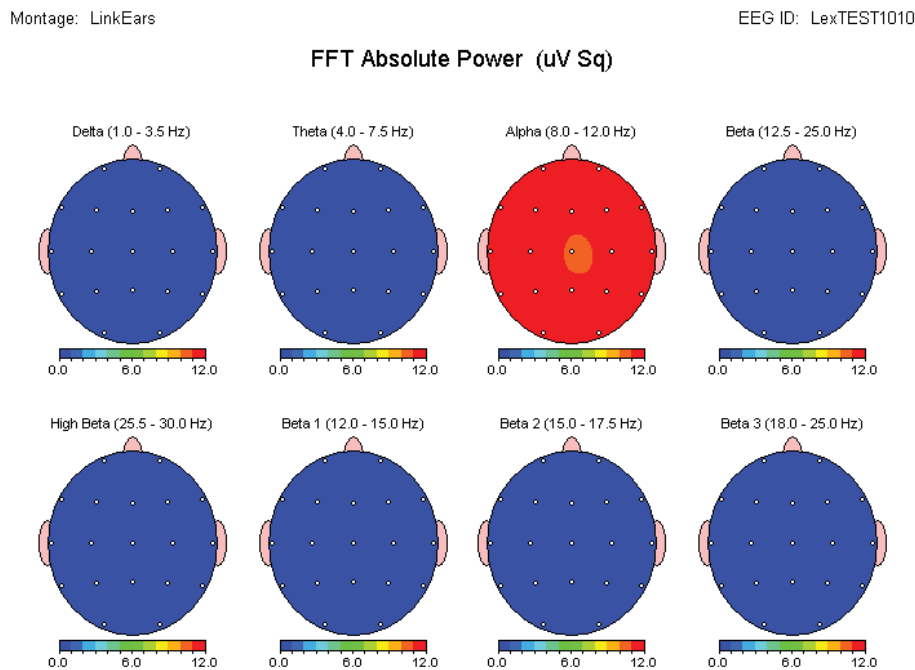


Figure 8. Absolute power topographical analysis of the amplifier generated 10 Hz (alpha) calibration signal. The absolute power display is more accurate than NeuroLex, but still contains errors in that it inaccurately shows variations in the uniform test signal indicating a “hot spot” at CZ (NeuroGuide).

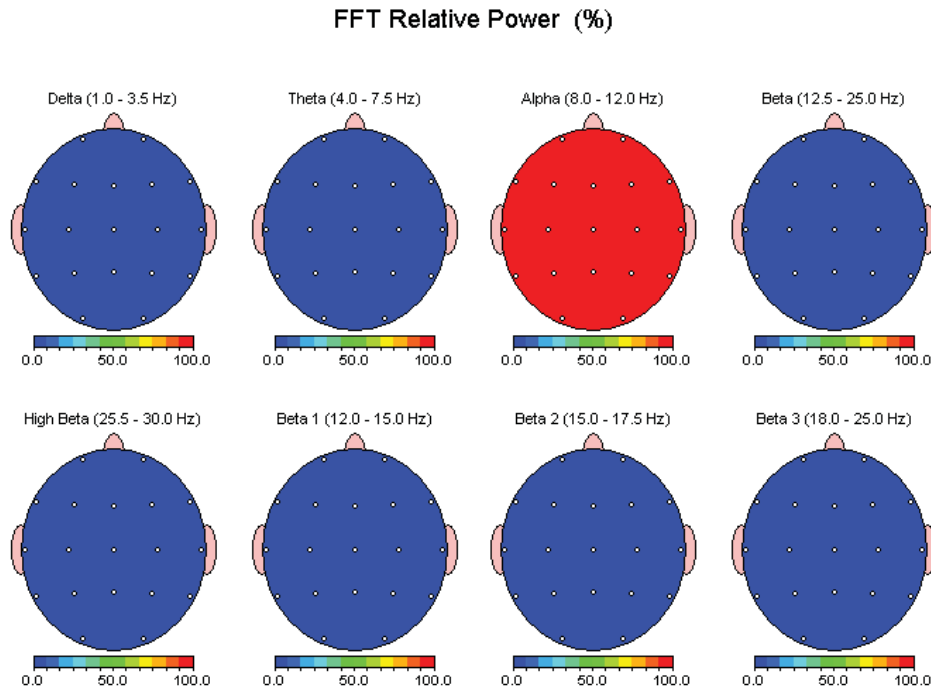


Figure 9. Relative power topographical analysis of the amplifier generated 10 Hz (alpha) calibration signal (NeuroGuide). The relative power display accurately represents the test signal.

Relative power correctly represented the activity in both of the other software packages, however there were minor inaccuracies in the display of absolute power. Absolute power was not accurate in these packages for the topographical distribution of activity, however they were more accurate than NeuroLex since they correctly displayed activity as occurring only in the Alpha band.

Within the NxLink software, a z-score database comparison was also run with the dummy value of 25 for age. Methodologically, this is a useful procedure to see how absolute and relative displays handle z-score data. The test signal was accurately represented by the relative power z-score values in NxLink (Figure 10), but not by the absolute power z-scores.

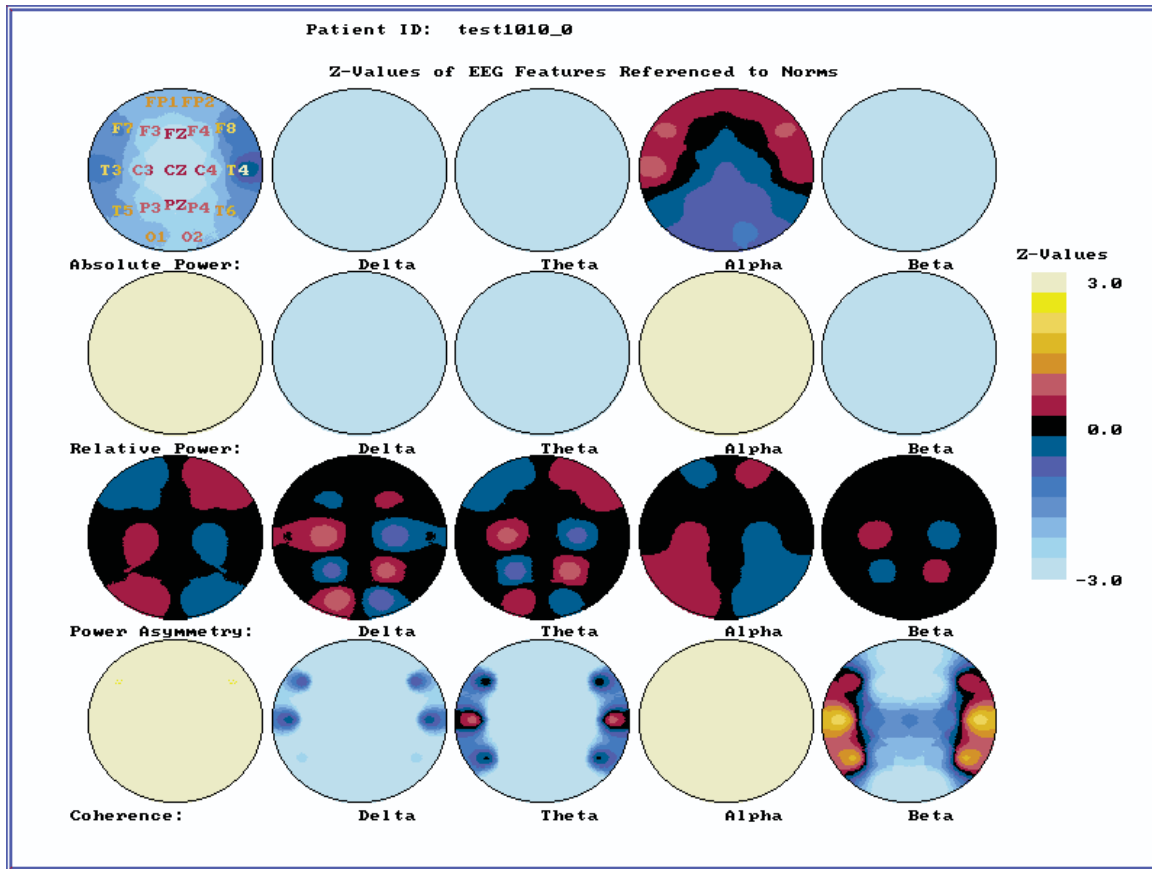


Figure 10. A z-score display of the 10 Hz test signal. The first column represents total power for all bands. The first row is absolute power, while the second row is relative power (NxLink).

In looking at these test signals it is easy to see why early researchers would prefer a relative power display, even when they are not looking at group data. In terms of topographical mapping the relative power (and magnitude) display of the data appears to be more accurate. Why is it that absolute magnitude and absolute power do not accurately represent the test signal? Since they are representations of microvolts and microvolts squared respectively it would seem logical that the absolute measures would provide a more accurate picture of EEG activity than a percentage measure, yet that does not seem to be the case. It may be that part of the answer is the effect of artifact on topographical maps and tables.

An inspection of the signal in absolute magnitude over all epochs reveals the presence of amplifier noise (see the bottom row of activity in figure 11 below and in figure 1). This noise is

similar to the hiss that can be heard on a stereo if the volume is turned up but no audio source is selected. It is an artifact of the high level of amplification required to record EEG.

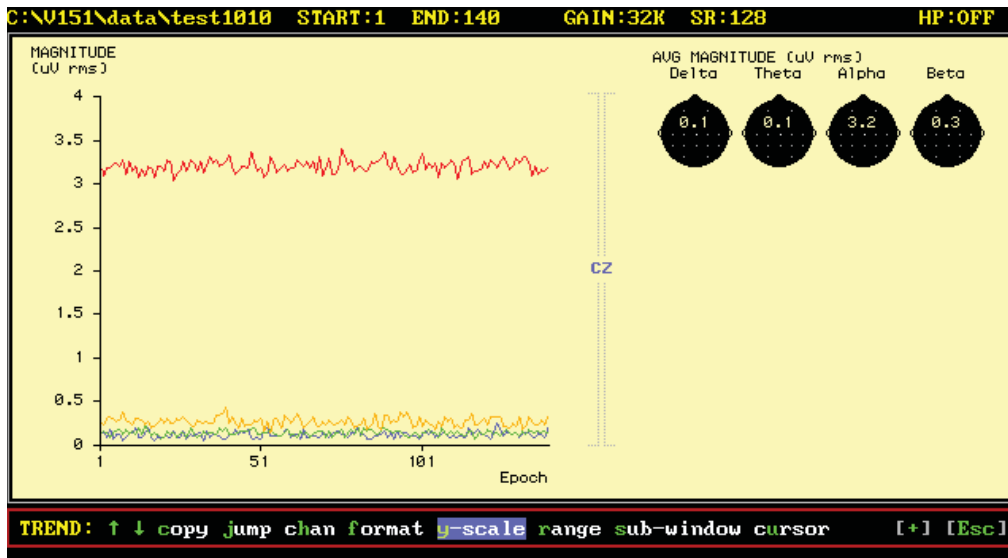


Figure 11. Absolute magnitude display of test signal.

The underlying amplifier noise may be responsible for some of the difference in the absolute power and relative power displays. A visual evaluation of the test signal with a different software package (EureKa!) confirms the signal is indeed a uniform sinusoidal 10 Hz wave (figure 12).

The same software provides a simultaneous spectral display of activity at each channel, which confirms the visual impression of the uniformity of the 10 Hz signal in all channels with no other signal of interest (figure 12).

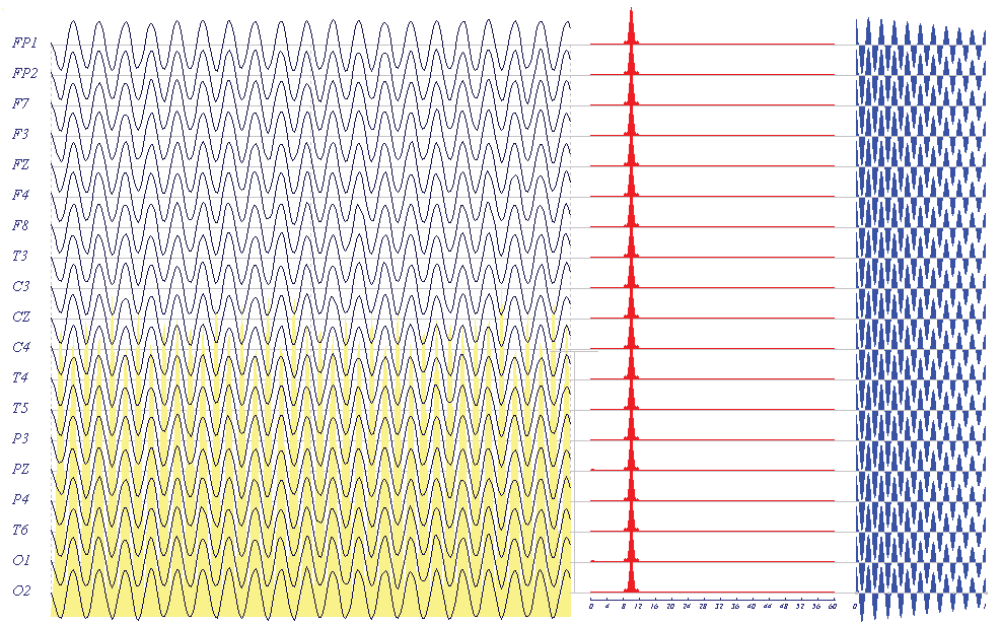


Figure 12. Raw wave display of 10 Hz test signal by channel with channel by channel spectral analysis confirming the uniformity of the test signal in all channels (Eureka!)

An absolute power graph by frequency with the NTE MapInsight software, reveals the same low-level signal noise found in Neurosearch and NeuroGuide, although in this case it is not represented as being present in all frequencies (Figure 1), but only in Delta (figure 13).

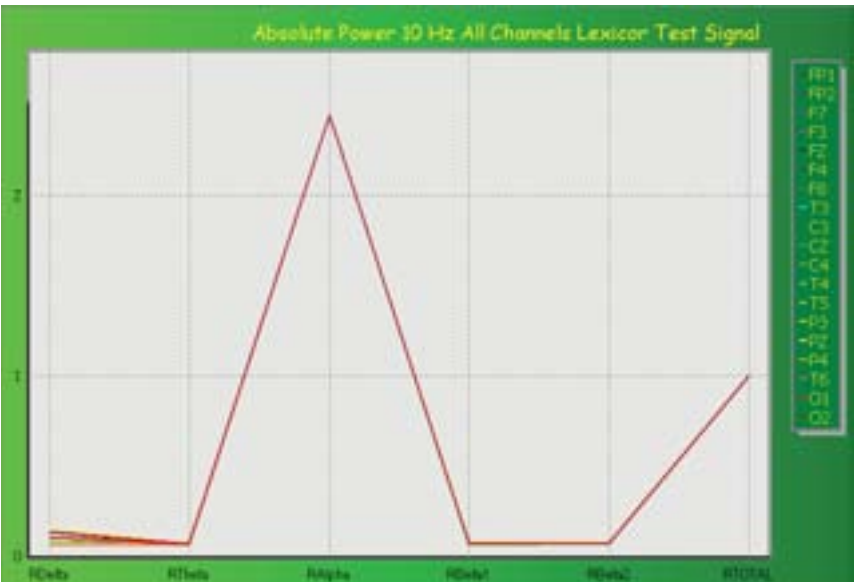


Figure 13. Absolute Power spectral analysis of 10 Hz test signal. The activity in Delta (left side of the figure) is amplifier noise (NTE MapInsight).

A relative power display of the same signal by the NTE MapInsight software shows only the expected test signal (Figure 14).

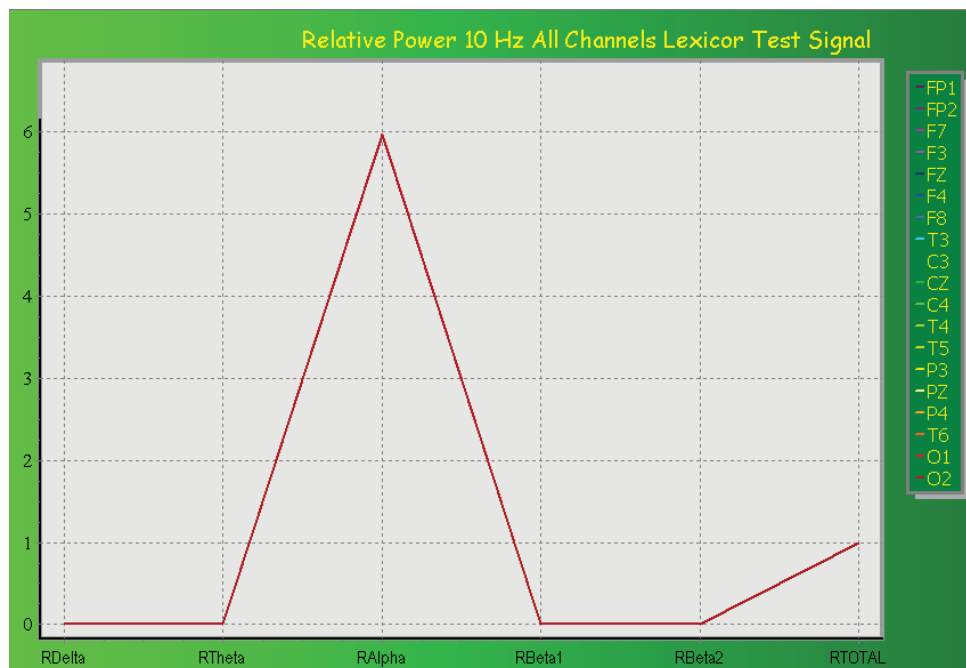


Figure 14. Relative Power spectral analysis of 10 Hz test signal; note the lack of noise in the relative power spectral display (NTE MapInsight).

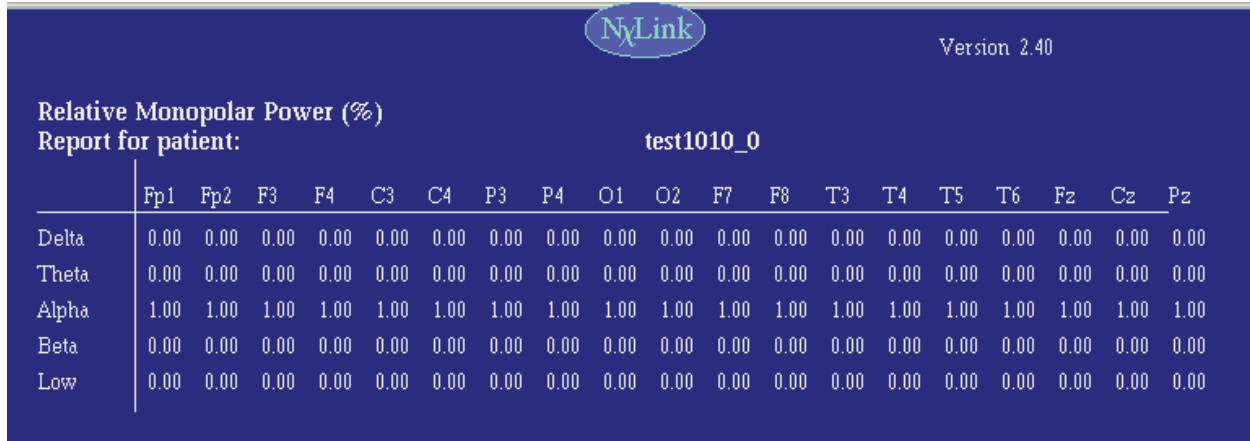
The displays of the test signal in absolute and relative measures by different software packages suggests that in a practical sense, the difference between absolute and relative measures is that the relative measures show just the EEG signal, while the absolute measures also show the much smaller background noise as if it were an EEG signal. In a sense, this may mean that the absolute displays are too accurate for topographical maps. It appears that the absolute measures show noise in a manner that confounds it with EEG signal on a topographical display of EEG, while the relative measures display just the signal.

It is possible to explore this issue further by comparing a table of absolute power values (Figure 15) and relative power values (Figure 16) for the test signal. It can be seen that on the

absolute power table EEG values are registered in frequencies that had no test signal, whereas in the relative power table values are present only where the test signal was presented. The absolute power table is quite interesting since it shows how small the values are for the amplifier noise when compared to the relatively modest strength of the test signal. In this table format the absolute power values would not be mistaken for anything significant, yet in a topographical display it would be easy to mistake these tiny differences as significant variations in the distribution of the EEG signal across the scalp (Figures 4, 5, 6, 8 and 10). When looking at the data of an individual person, clinicians may wish to view the absolute power/amplitude data in table as well as topographically to help get a sense for what is real EEG signal.

Monopolar Power (μV^2)		test1010_0																		
Report for patient:		Fp1	Fp2	F3	F4	C3	C4	P3	P4	O1	O2	F7	F8	T3	T4	T5	T6	Fz	Cz	Pz
Total		11.52	11.70	11.66	11.69	11.88	11.51	11.41	11.31	11.53	11.38	11.38	11.81	11.40	11.48	11.31	11.53	11.53	11.08	11.34
Delta		0.00	0.00	0.00	0.00	0.01	0.00	0.00	0.01	0.01	0.00	0.00	0.00	0.01	0.00	0.00	0.00	0.00	0.00	0.00
Theta		0.01	0.01	0.01	0.01	0.01	0.01	0.01	0.01	0.01	0.01	0.01	0.01	0.01	0.01	0.01	0.01	0.01	0.01	0.01
Alpha		11.47	11.65	11.61	11.64	11.83	11.47	11.37	11.26	11.49	11.33	11.33	11.77	11.35	11.44	11.26	11.48	11.48	11.03	11.29
Beta		0.03	0.03	0.03	0.03	0.03	0.03	0.03	0.04	0.03	0.03	0.03	0.03	0.03	0.03	0.03	0.03	0.03	0.03	0.03

Figure 15. A table of absolute power values for the 10 Hz (alpha) test signal (NxLink). The signal is incorrectly displayed as present in all bands, but the values cue the reader that most of the signal is in alpha and the other activity should be ignored.



NxLink Version 2.40

Relative Monopolar Power (%)
Report for patient: test1010_0

	Fp1	Fp2	F3	F4	C3	C4	P3	P4	O1	O2	F7	F8	T3	T4	T5	T6	Fz	Cz	Pz	
Delta	0.00	0.00	0.00	0.00	0.00	0.00	0.00	0.00	0.00	0.00	0.00	0.00	0.00	0.00	0.00	0.00	0.00	0.00	0.00	0.00
Theta	0.00	0.00	0.00	0.00	0.00	0.00	0.00	0.00	0.00	0.00	0.00	0.00	0.00	0.00	0.00	0.00	0.00	0.00	0.00	0.00
Alpha	1.00	1.00	1.00	1.00	1.00	1.00	1.00	1.00	1.00	1.00	1.00	1.00	1.00	1.00	1.00	1.00	1.00	1.00	1.00	1.00
Beta	0.00	0.00	0.00	0.00	0.00	0.00	0.00	0.00	0.00	0.00	0.00	0.00	0.00	0.00	0.00	0.00	0.00	0.00	0.00	0.00
Low	0.00	0.00	0.00	0.00	0.00	0.00	0.00	0.00	0.00	0.00	0.00	0.00	0.00	0.00	0.00	0.00	0.00	0.00	0.00	0.00

Figure 16. A table of relative power values for the 10 Hz (alpha) test signal (NxLink). The signal is correctly displayed as present only in the alpha band.

Absolute power does indeed appear to be more accurate in a technical sense, and indeed would be more sensitive for spectral displays and summary tables. However, when viewing EEG activity in the form of topographical maps, relative power displays were found to be more accurate than absolute power. While the more modern software packages were better behaved in displaying activity with absolute values, they were still inaccurate and could easily lead to confusion and incorrect conclusions. It is interesting to note that none of the absolute value representations of the test signal by the different software packages were in agreement, although each package was consistent in what it displayed for each time it ran the test signal data file. The difference suggests that whatever the underlying reasons are for the failure of absolute measures to accurately represent the EEG test signal, they cannot be relied upon to consistently produce the same results across software packages (and by implication different researchers). In using absolute values researchers with different software will likely report different results for the same data. Conversely the relative value results were accurate representations of the known signal in all of the software packages and thus can likely be relied up to present the same results regardless of the software package involved. Relative power appears to be the best choice for

experimental work since it provides topographical maps that do not confuse EEG signal with noise and it also give researchers consistent results that can be compared regardless of the software used.

Choice of Montage

In analogue EEG the sequence in which electrode activity is displayed (the montage), is set at the time of recording and cannot be changed; however in digital EEG it is possible to change the montage after recording the EEG³. Digitally changing the montage makes it possible to change not only the sequence in which the channels are displayed, but also the reference for each electrode. Consequently the term montage has expanded in digital EEG to include the sequence in which the EEG channels are displayed as raw waves, and also the type of reference that has been used for the display.

The flexibility to remontage EEG data after it has been collected has opened the door to new methods for the analysis of EEG. The digital remontaging of the raw wave EEG allows for inspection of spikes and other transient activity from several different spatial orientations,, making it visually easier to identify the source of focal activity. In the qEEG analysis of EEG, there is typically no epoch-by-epoch presentation or inspection of topographical maps. Software such as the NeuroLex makes such an inspection of the EEG possible, but it is rarely done. Usually the spikes and other transient activity that are of interest in raw EEG are not included in the epochs of data used to produce a qEEG. The removal of these transients is a part of the artifacting of the EEG to remove anything that is not periodic EEG activity. The reason is that the primary utility of qEEG has been found in collapsing the time domain of EEG into a single

³ Please note that all digital EEG is recorded with a physical reference channel.

average of activity to create a topographical map of periodic EEG activity. Because a qEEG topographical map uses a fixed location for each electrode and is not used for displaying transient activity, remontaging, as done in remontaging raw wave EEG, does not occur. However, many clinicians routinely remontage qEEG data in the sense that they change the reference when examining individual records. In this case they are not digitally altering the sequence of the electrodes to improve visualization of the record, but rather they are changing the type of reference to assist in localizing activity. The reason is usually the same as in raw wave EEG, to help identify possible sources of focal activity; although in case of qEEG it is distributed periodic focal activity rather than transient focal activity. The qEEG provides information about distributed periodic activity; however at times there is focal periodic activity, such as a head injury, which can be identified with a qEEG. Changing the montage in qEEG changes the reference in a way that can help the clinician to better localize and understand any suspected periodic focal activity in a patient.

Changing the montage of a qEEG can have a dramatic effect on the distribution of EEG activity represented on a topographical map. As changing the reference in raw EEG can alter an EEG tracing, changing the montage of a qEEG alters how the signal is displayed. The value for each electrode site is obtained by subtracting the value of the reference. If the reference is changed the value of the reference is changed and thus the value of the EEG at each electrode site. The issue this raises is a methodological one relating to how a researcher, or clinician, will address the artifact produced by different types of referential montages. The choice of montage in qEEG research is important, since like the question of using absolute or relative power, it affects the accuracy of qEEG topographical maps and tables.

Reference Electrodes

A reference electrode is used in a referential recording, and it allows for the recording of activity from a site that does not theoretically contain EEG, such as an ear, a chin or a nose. The activity at a scalp electrode site is compared with the reference to determine how much of the activity at the scalp site probably represents EEG. In reality there are no sites on the body that are electrically neutral. The choice of location for a physical reference electrode is a matter of choosing the best from a list of bad choices. If a reference electrode is too distant then there is excessive 60 Hz artifact introduced to the channel (the lead functions as an antenna). If the reference electrode is placed on the head it is contaminated by EEG due to volume conduction, even if it is placed in a spot with no EEG such as the nose. If the reference is placed below the head it is contaminated with EKG artifact (Rowan & Tolunsky, 2003).

The Linked Ears Reference

A method of compensating for some of these problems is to use two reference electrodes that are linked together in the amplifier to provide one reference signal. With the linked reference, electrode activity that is common to both electrodes is subtracted out. The advantage of this approach is substantial, since it eliminates most environmental artifact that may otherwise contaminate the reference signal, such as electrical activity from appliances or other electrical devices. Because of the advantage of the linked reference, a standard linked ears approach was used in this study for the physical reference.

The linked ears approach also has the advantage that it minimizes the theoretical possibility of artificial inflation of activity in one hemisphere by a single reference, or unequal impedance in lateralized references such as non-linked ears or mastoid references (Miller,

Lutzenberger and Elbert, 1991). A theoretical criticism of the linked ears reference has been raised (Nunez et al., 1997), which concerns the possibility of “shunting,” a situation where unequal impedances at the ears would result in the effective reference drifting away from the midline (Katznelson, 1981). The potential for shunting is generally considered minimal if electrode impedances are low relative to the amplifier input impedance, generally 5-10 ohms. However, in an attempt to determine the actual level of difference at which shunting may occur, a study was conducted to experimentally observe shunting. The study found that there was no evidence of shunting under any conditions, *even if one ear reference was not connected at all* (Senulis & Davidson, 1989; Miller, 1991). Nevertheless, in order to address the possibility of shunting in the present study, the impedances of the respective earlobe reference electrodes were maintained within 1 ohm of each other. All other electrode impedances were maintained at 5 ohms or less relative to amplifier input impedance with no more than 3 ohms of variance between any of the electrode contacts. The current study also utilized a repeated measures design, which methodologically eliminates the effects of shunting, should it occur.

In addition to the problem of shunting, a linked ears (earlobe) reference also suffers from the leakage of EEG into the presumably EEG free area of the earlobe. The result of such leakage is a distortion of the topographical data with an artificial attenuation of activity in sites near the reference electrodes (T3 and T4). This is not a theoretical effect, but one that can be observed when a test EEG signal (uniform at all sites) is compared with normative data collected with a linked ears reference. A negative image of the attenuation of lateral activity due to the leakage of EEG into the ears can be seen in the absolute total power z-score map shown in Figure 10 (the map on the first row and in the first column). The z-score of the 10 Hz test signal shows greater activity near the T3 and T4 sites (the electrode sites closest to the ears). The test signal was

actually uniform across the head, but in actual EEG of the database it was compared to, the EEG is diminished at T3 and T4 due to the proximity of those sites to the common EEG contaminated reference electrodes on the ears. When the uniform activity of the test signal was compared to the average EEG of in the database it was higher than expected, so it is displayed as more activity than expected. In actual EEG, the signal may be as strong at T3 and T4 as at a central location, but it is incorrectly displayed due to the subtraction of common EEG in these electrodes and the adjacent reference electrodes. Clinicians and researchers are aware of this effect, and if there is any question about actual temporal EEG activity, they will change the montage to one which does not attenuate lateral activity to get a more accurate representation of the activity.

Common Average Reference

A reference free montage such as a common average reference montage eliminates the under-representation of activity near the reference electrodes (Duffy, 1986) due to contamination of EEG at the reference site. In a common average reference montage the activity from all electrodes is summated to produce a virtual reference electrode. If the EEG activity at each electrode were unrelated, the common average reference electrode would produce an ideal reference for topographical maps. However, the EEG at neighboring electrodes is often highly related, which suppresses the input of these electrodes just as proximity suppresses display of lateral activity in a linked ears montage. Consequently, the activity at distant electrodes often contributes excessively to the average reference used for the montage. The rather non-intuitive result is that the common average reference montage provides accurate representation of the local activity around each electrode (Pfurtscheller 1988), but does not produce accurate topographical maps for the cortex as a whole (Duffy and Maurer, 1989). The common average

reference montage is inferior to the linked ears montage for producing whole head topographical maps, but clinically it is a valuable adjunct to a linked ears montage. The common average reference can be used to provide an accurate view of the temporal activity that may be attenuated in a standard linked ears montage.

Weighted Average Reference Montage

A variation on the average common reference montage is a local common reference, also known as a weighted average reference or weighted common reference montage. The weighted reference montage computes a unique virtual reference for each electrode from a selection of surrounding electrodes, or all other electrodes, using weights based on the distance from the active electrode and the electrodes being used to create the virtual reference. This approach eliminates the problem of dispersed distant activity overly contributing to the reference and distorting a global representation of activity. While solving the problem of the common average reference montage, the weighted average montage suffers from the problem that not all electrodes are surrounded by other electrodes (10 of the 19 electrodes in the 10-20 placement used in this study are not surrounded by other sensors), therefore the data is incomplete for the construction of a valid virtual references for 10 of the 19 electrodes. The result of the missing reference information is a distortion of activity around the edges of the electrode array (Gordon & Rzempoluck, 2004). The distortion with the weighted average montage decreases as the number of electrodes used increases. However in the present study a high density EEG array was not used, therefore a weighted average montage would be less representative of distributed cortical activity than linked ears montage.

Laplacian Montage

The Laplacian montage is a variation of the weighted average montage that is based on current density. Comparing the voltage of the active electrode with the voltage of the surrounding electrodes and dividing it by the electrode distance calculates the current density at a given electrode. This calculation yields a rate of change, which is the voltage gradient field around the electrode of interest (also known as the first derivative). The field gradient surrounding the electrode changes over time. The rate of this change is referred to as the second spatial derivative (the rate of change of the rate of change), or the Laplacian operator. The second spatial derivative is proportional to the flow of current through the skull perpendicular to the scalp electrode, therefore it can be used to estimate current density and direction at the electrode site (Koles, Kasmia, Paranjape, & McLean, 1989). A Laplacian montage theoretically does not measure the same activity as other EEG montages because it is an estimate of current density, and is not based on amplitude measures. In reality the amplitude measures are used as a proxy to estimate current density, so the Laplacian montage is derived from amplitude measures. Actual current density is not visible on EEG and can only be detected non-invasively with MEG. The advantage of the Laplacian montage over a standard weighted average montage is that it increases the spatial resolution of the topographical maps (Yao, D. et al., 2004). In a practical sense the Laplacian montage is the montage of choice for identifying rhythmic focal activity. Unfortunately, the Laplacian montage is also a type of weighted average montage, so it also suffers from the same distortions at the periphery of the EEG array due to the lack of a complete set of surrounding reference electrodes. Thus the display of distributed activity, or activity which terminates near the edges of the electrode array will be distorted by both weighted average reference and the Laplacian montages such that it will appear that the activity is centered near the

edge (Gordon & Rzempoluck, 2004). The use of a Laplacian montage is therefore best suited as a tool to explore for focal activity not seen in the raw EEG (e.g. transient spikes). Many clinicians search the raw EEG for transients, use a linked ears montage for evaluating distributed activity, and complete the evaluation with a Laplacian montage to identify any focal rhythmic activity (which may not be evident in the raw waves or linked ears montage).

An example of some of the distortion of distributed activity that occurs with an average reference and a Laplacian montage can be seen in Figure 17. In this example software (Wave Generator) was used to generate an EEG test signal with no amplifier noise. An EEG test signal without amplifier noise eliminates any possible artifact in the test signal due to amplifier noise. An 8 Hz signal was generated in all channels and displayed with a linked ears montage, an average reference montage, and a Laplacian montage. Only the relative power linked ears montage correctly displayed the signal. Of the three montages, the Laplacian montage created the worst distortion of the distributed test signal. Both the weighted average and Laplacian montages have also been reported to distort or attenuate all lateral and posterior activity (Nuwer, 1988; Duffy, 1986; Gevins, 1984). An example of this sort of a distortion in a weighted average montage can be seen in Figure 18, where a weighted average montage incorrectly represents a uniform 10 Hz test signal. The spectral analysis by the same software package (NeuroRep) correctly displays the test signal as present in all channels at 10 Hz, but the weighted average montage incorrectly displays the signal as centered occipitally. A comparison of the weighted average and Laplacian montages with the spectral display, or relative power maps would help identify artifacts due to the display characteristics distributed activity in these montages.

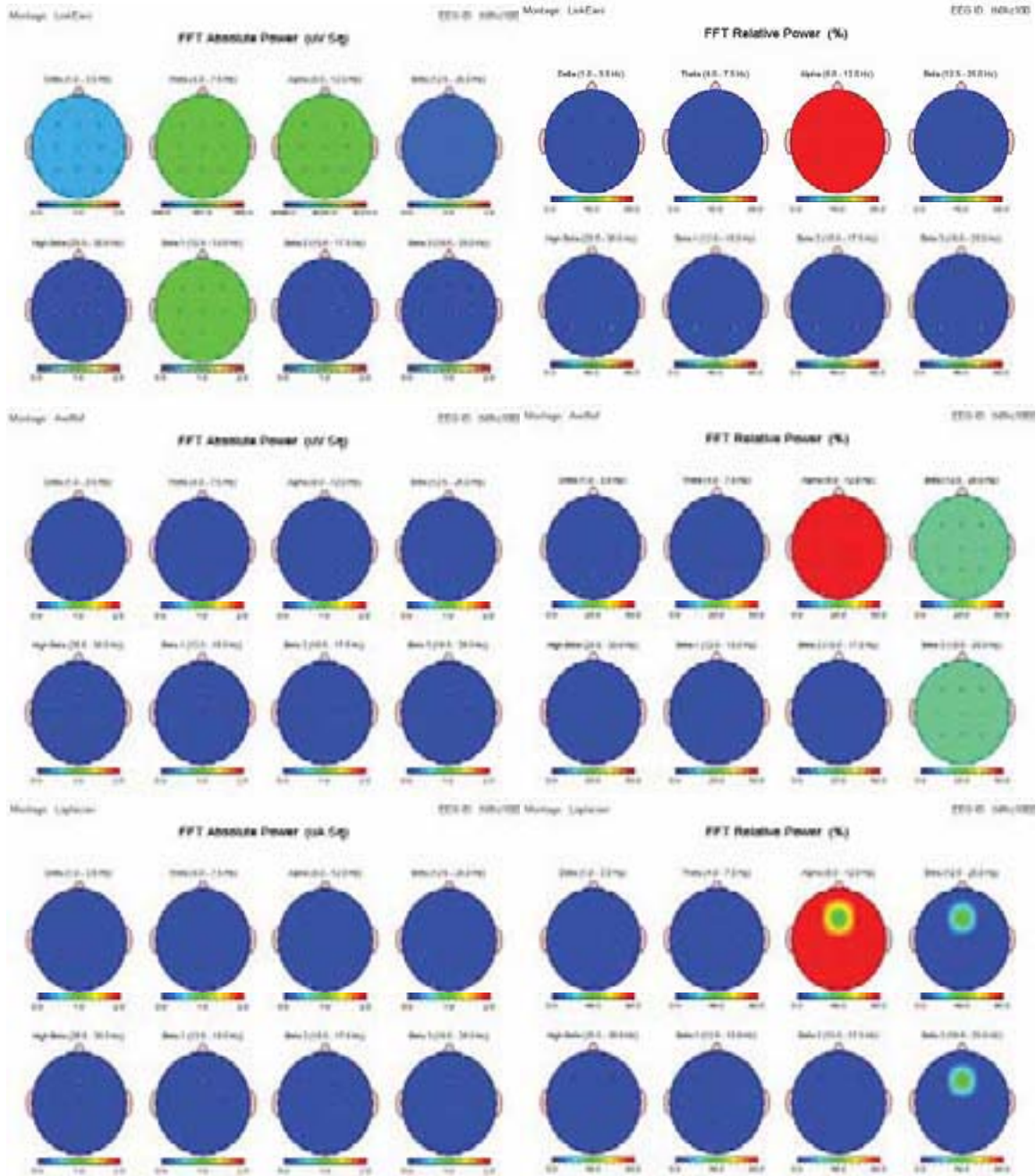


Figure 17. An 8 Hz test signal in absolute (left column) and relative power (right column) as displayed by a linked ears montage (top row), an average reference montage (middle row), and a Laplacian montage (bottom row). Only the relative power linked ears montage (top right) correctly displays the signal. The signal was software generated by Wave Generator with no noise; the topographical maps were generated with NeuroGuide.

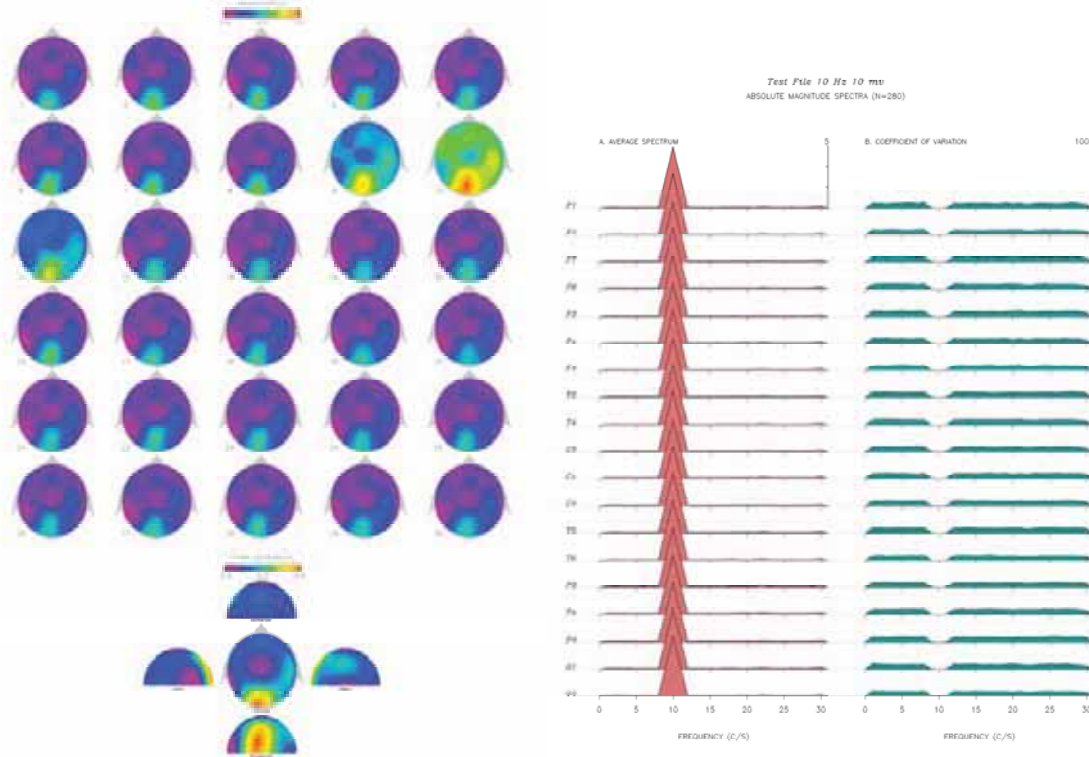


Figure 18. A weighted average montage (on left) of the hardware generated 10 Hz signal. The weighted average map correctly displays the activity as occurring primarily in 10 Hz; but incorrectly represents it as present in all frequencies, and with a posterior focus. The spectral display of the signal (on right) from the same software correctly shows the signal to be uniformly present at all sites on the head at 10 Hz (NeuroRep).

In summary, all common alternatives to the linked ears montage perform poorly in representing distributed EEG activity, however each can be useful in evaluating focal activity. The choice of which type of montage is appropriate is dependent upon the needs of the individual clinician or researcher. Out of the commonly utilized montages, the linked ears montage presents the least distortion of activity on a qEEG topographical map, therefore it was the montage chosen for the current study. An average reference and Laplacian montage was also created in a follow-up analysis to compare statistical outcomes, in the current study, with the qEEG and LORETA respectively.

Low Resolution Brain Electromagnetic Tomography (LORETA)

The formidable task of using scalp recordings to estimate subcortical activity is known as the “inverse problem.” In 1994 the LORETA method was introduced as a 3D discrete linear solution to the inverse problem. The technique LORETA uses to estimate subcortical activity is similar to a Laplacian montage in that it uses estimates of current density calculated from scalp potentials. The dataset created by LORETA is different than the current density data generated by a Laplacian montage because it uses an anatomical model in its algorithms and it creates 3-dimensional rather than 2-dimensional estimates of current density. The method uses a three-shell model of activity that is mapped onto the Talairach-Tournoux human brain atlas database provided by the Montreal Neurological Institute.

LORETA has been validated by a multitude of case studies involving ERP, PET, MRI and fMRI (Anderer, Saletu, & Pascual-Marqui, 2000; Dierks et al., 2000; Frei et al., 2001; Gomez & Thatcher, 2001; Pizzagalli et al., 2001; Vittaco, et al., 2002). In general these studies have found that LORETA produced results that were consistent with expected activations in regions of interest. They found that as a low-resolution method, the results from LORETA were consistent with other methods of functional imaging. LORETA has limitations in that it is a low-resolution method and produces false distributed activity from any point source activity. The creators of LORETA warn that it is a violation of the mathematics of LORETA to use software-generated models of subcortical activity to attempt to validate LORETA; therefore it is not possible to use software tools such as Brain Electrical Source Analysis (Scherg & Berg, 1996) to validate LORETA. However, it is not a violation of the mathematics to use test signals for LORETA from physical head models.

A study using recordings of test signals from a phantom head model (EEG sources placed

inside a real human skull with materials modeling effects of the brain and other tissues on the signal) had mixed results in attempting to validate LORETA (Bailet, et al., 2001). The study found correct localization of dual point source activity within the resolution claimed for LORETA, but also found LORETA was reporting additional activity for which there was no source. The study attributed the localization error to over fitting the data by LORETA. In over fitting the data, the LORETA method registered noise as signal, and/or interpreted sharp changes in activity as a distributed source of activity. The limitation in LORETA discovered by Bailet et al., is congruent with the recommended use of, and limitations of, LORETA. The creators of LORETA describe the method as the tool of choice for identifying distributed EEG/MEG activity; however, they note that it is of limited utility with point source activity. Because of the errors it can produce in the event of point source activity, they recommend a dipole method for identification of point source activity (Pascual-Marqui, 1999; Pascual-Marqui, Esslen, Kochi, & Lehmann, 2002; Pascual-Marqui, 2002).

The literature citing the LORETA method has been expanding rapidly since the introduction of the technique. The software for LORETA is available at no cost; and researchers who are collecting EEG data, or MEG data, can use it to explore subcortical hypotheses that were previously beyond cortical EEG/MEG methods. The method is still new and its full capabilities and limitations are not known. It should also be noted that while there are many small studies verifying LORETA, to date no study with a good sample size has validated the LORETA with a comparison to fMRI or PET results. The LORETA method presents an interesting and exciting opportunity for EEG researchers to obtain low-resolution estimates of subcortical activity; however because of the above noted limitations, at this time any results from the LORETA method should still be interpreted cautiously.

CHAPTER 3

RESULTS

Changes in Raw Wave EEG

The record of each research volunteer was visually inspected for changes in raw wave EEG after the 20 minutes of CES stimulus. In general, it was noted that with both the 0.5 Hz and 100 Hz groups there was an increase in the amplitude of alpha with a decrease in the presence of beta activity. It was also observed that in many records, the raw EEG waves were notably more symmetrical. No attempt was made to objectively rate the raw wave EEG recordings, since the qEEG can provide a more objective quantitative analysis.

Changes in the Spectral EEG

The EEG editing software used in the study provided a spectral analysis of the accepted epochs of EEG for each record. Visual comparison of the relative power spectral display at baseline and after the stimulus revealed a consistent pattern of an increase in alpha activity with concomitant decreases in delta and beta activity. These changes were noted in both the 0.5 Hz group and in the 100 Hz group. The degree to which these changes occurred varied, but the pattern was consistent through all the records. In some records a bimodal distribution appeared in the post CES spectral display that was not present in the baseline condition. The bimodal distribution was found in both the 0.5 Hz CES group and in the 100 Hz CES group (see Figure 19 for an example). No statistical analysis was conducted of the group relative power spectral EEG since a group relative power analysis was conducted with the qEEG.

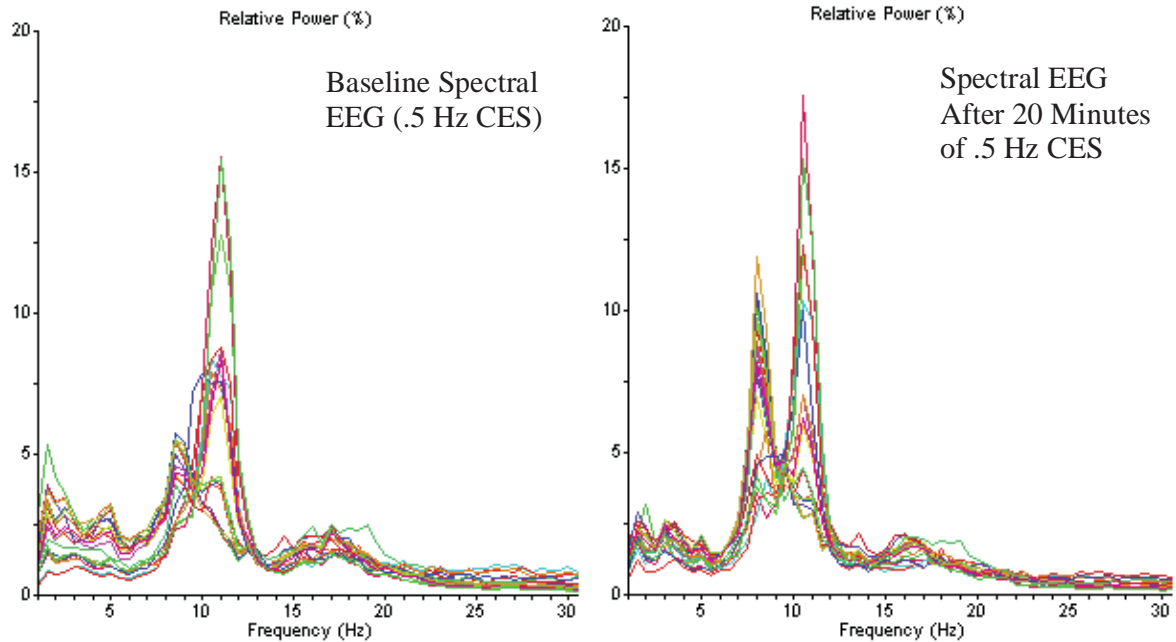


Figure 19 .Relative power EEG spectra of a single individual before 0.5 Hz CES (left column) and after CES (right column). There was an increase in alpha power with decreases in delta and beta Power. The bimodal distribution of the spectral EEG after CES was a response variant found in some individuals within both CES groups.

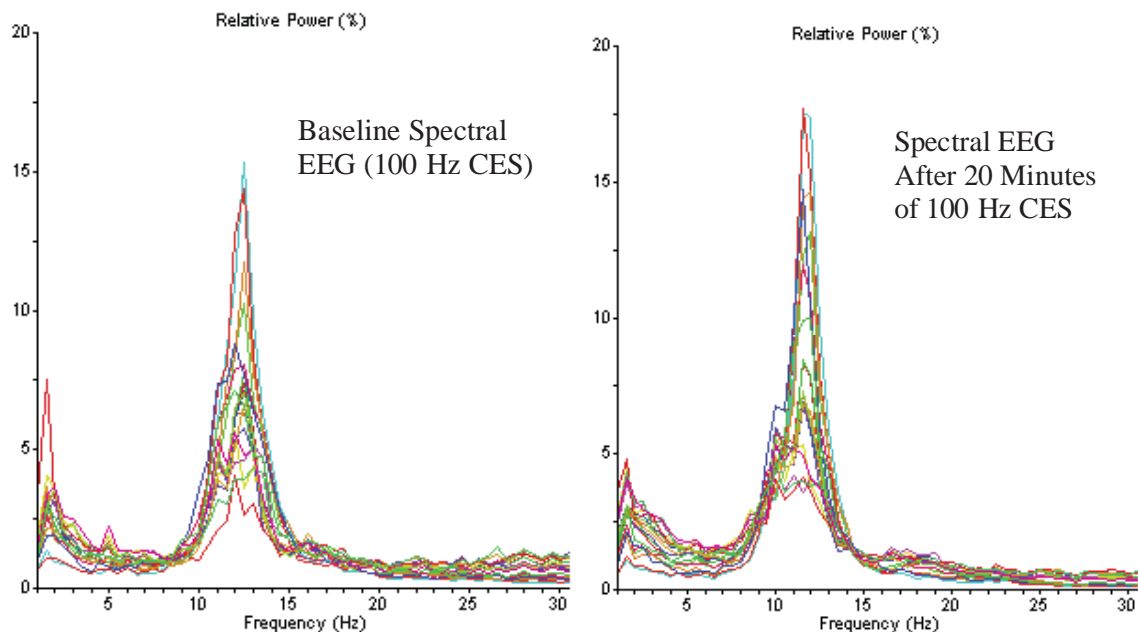


Figure 20 .Relative power EEG spectra of a single individual before 100 Hz CES (left column), and after 100 Hz CES (right column). There was an increase in Alpha Power with a decrease in Delta and Beta Power. The unimodal distribution after CES was characteristic of most individuals within both CES groups.

Changes in the qEEG

Introduction

A paired *t*-test was conducted comparing EEG activity in relative power, coherence, amplitude asymmetry, phase lag and power ratio at baseline, and with activity in the same metrics after 20 minutes of CES. An alpha level of .05 was used for all *t*-tests. The paired *t*-tests found statistically significant changes in relative power, coherence, amplitude asymmetry, and power ratio for both the 0.5 Hz and 100 Hz groups. The EEG data was remontaged into a common average reference montage. The paired *t*-test results of the average reference montage were compared with the results of the main analysis (a linked ears montage). To control for type I error, all statistically significant results in each EEG metric had to meet at least two of the following three criteria: the results had to be part of a pattern of activity, occur in both CES groups, occur in two different montages. Any statistically significant findings that did not meet these criteria were disregarded as potential type I error.

Relative Power Results

The relative power *t*-test revealed that after both 100 Hz and 0.5 Hz CES there was an increase in alpha activity with a decrease in delta and beta activity. These changes were also found in the average reference montage and passed all three methodological controls for false positive results. The specifics of the analysis are presented below in tables and topographical maps.

Relative Power Tables

A table of *p*-values for the 0.5 Hz group are presented in Figure 19, while a table of *p*-

values for the 100 Hz group is presented in Figure 20. The group means, standard deviations and plain text *p*-value tables for frequency bands and single Hz frequencies for the 0.5 Hz group are presented in Appendix A. The group means, standard deviations and plain text *p*-value tables for frequency bands and single Hz frequencies for the 100 Hz group are presented in Appendix B. The average reference relative power *p*-value tables and topographical maps are presented in Appendix C.

FFT Relative Power Group Paired t-Test (P-Value)

Intrahemispheric: LEFT

	DELTA	THETA	ALPHA	BETA	HIGH BETA	BETA 1	BETA 2	BETA 3
FP1 - LE	0.001	0.692	0.003	0.324	0.026	0.839	0.781	0.140
F3 - LE	0.000	0.898	0.002	0.206	0.003	0.524	0.543	0.082
C3 - LE	0.000	0.854	0.011	0.172	0.009	0.672	0.269	0.060
P3 - LE	0.001	0.977	0.043	0.042	0.004	0.086	0.219	0.012
O1 - LE	0.045	0.563	0.222	0.008	0.000	0.008	0.351	0.001
F7 - LE	0.000	0.464	0.001	0.231	0.026	0.370	0.632	0.180
T3 - LE	0.004	0.427	0.000	0.216	0.028	0.813	0.232	0.216
T5 - LE	0.015	0.561	0.118	0.037	0.002	0.055	0.329	0.008

Intrahemispheric: RIGHT

	DELTA	THETA	ALPHA	BETA	HIGH BETA	BETA 1	BETA 2	BETA 3
FP2 - LE	0.000	0.950	0.002	0.339	0.142	0.929	0.716	0.137
F4 - LE	0.000	0.990	0.003	0.150	0.025	0.373	0.404	0.049
C4 - LE	0.000	0.704	0.016	0.087	0.037	0.207	0.168	0.039
P4 - LE	0.004	0.797	0.057	0.031	0.016	0.035	0.209	0.023
O2 - LE	0.036	0.950	0.223	0.012	0.003	0.028	0.223	0.009
F8 - LE	0.001	0.984	0.002	0.280	0.046	0.878	0.421	0.102
T4 - LE	0.033	0.120	0.016	0.106	0.234	0.560	0.104	0.103
T6 - LE	0.073	0.335	0.192	0.053	0.033	0.237	0.076	0.033

Intrahemispheric: CENTER

	DELTA	THETA	ALPHA	BETA	HIGH BETA	BETA 1	BETA 2	BETA 3
Fz - LE	0.000	0.897	0.004	0.226	0.007	0.555	0.667	0.051
Cz - LE	0.000	0.958	0.029	0.148	0.012	0.210	0.269	0.068
Pz - LE	0.001	0.959	0.026	0.031	0.003	0.038	0.252	0.009

Figure 21. Changes in relative power activity after 0.5 Hz CES, as represented by a *p*-value table. Statistically significant (.05 or better) decreases in activation after 0.5 Hz CES are indicated in blue. Statistically significant increases in activation are indicated in red. Decreases were seen in delta and beta with increases in alpha (NeuroGuide).

FFT Relative Power Group Paired t-Test (P-Value)

Intrahemispheric: LEFT

	DELTA	THETA	ALPHA	BETA	HIGH BETA	BETA 1	BETA 2	BETA 3
FP1 - LE	0.001	0.771	0.000	0.121	0.004	0.030	0.999	0.167
F3 - LE	0.001	0.399	0.006	0.433	0.094	0.085	0.850	0.801
C3 - LE	0.026	0.703	0.007	0.262	0.046	0.003	0.802	0.726
P3 - LE	0.029	0.361	0.004	0.000	0.000	0.000	0.219	0.015
O1 - LE	0.024	0.121	0.002	0.000	0.000	0.001	0.034	0.009
F7 - LE	0.011	0.762	0.002	0.163	0.015	0.014	0.668	0.266
T3 - LE	0.053	0.491	0.001	0.011	0.029	0.001	0.587	0.095
T5 - LE	0.010	0.388	0.001	0.002	0.000	0.000	0.345	0.037

Intrahemispheric: RIGHT

	DELTA	THETA	ALPHA	BETA	HIGH BETA	BETA 1	BETA 2	BETA 3
FP2 - LE	0.001	0.968	0.001	0.228	0.005	0.092	0.753	0.221
F4 - LE	0.002	0.469	0.019	0.630	0.022	0.192	0.518	0.813
C4 - LE	0.056	0.776	0.007	0.215	0.004	0.008	0.317	0.319
P4 - LE	0.006	0.560	0.000	0.000	0.000	0.000	0.199	0.013
O2 - LE	0.043	0.231	0.001	0.000	0.000	0.000	0.108	0.002
F8 - LE	0.008	0.541	0.016	0.340	0.016	0.321	0.574	0.111
T4 - LE	0.194	0.231	0.002	0.135	0.076	0.008	0.866	0.211
T6 - LE	0.061	0.738	0.003	0.001	0.001	0.000	0.432	0.010

Intrahemispheric: CENTER

	DELTA	THETA	ALPHA	BETA	HIGH BETA	BETA 1	BETA 2	BETA 3
Fz - LE	0.001	0.450	0.008	0.579	0.039	0.136	0.872	0.968
Cz - LE	0.070	0.664	0.010	0.262	0.096	0.014	0.962	0.667
Pz - LE	0.012	0.307	0.001	0.001	0.001	0.000	0.146	0.011

Figure 22. Changes in relative power activity after 100 Hz CES, as represented by a *p*-value table. Statistically significant (.05 or better) decreases in activation after 0.5 Hz CES are indicated in blue. Statistically significant increases in activation are indicated in red. Decreases were seen in delta and beta with increases in alpha (NeuroGuide).

Relative Power Topographical Maps

The *p*-value tables clearly convey the pattern of change by frequency, but do not always clearly convey changes by location. A topographical map of activity can represent the same information in a graphical manner that more clearly conveys the pattern of change by location.

The topographical maps in Figures 23 and 24 convey the same information presented in Figures 21 and 22. In Figures 21 and 22, white represents no statistically significant change from baseline, while colors indicate statistically significant changes ranging from a p -value of 0.00 to 0.05. To minimize any confusion about the direction of change in a given frequency band, the author has added arrows to the computer graphic to indicate the direction of statistically significant change.

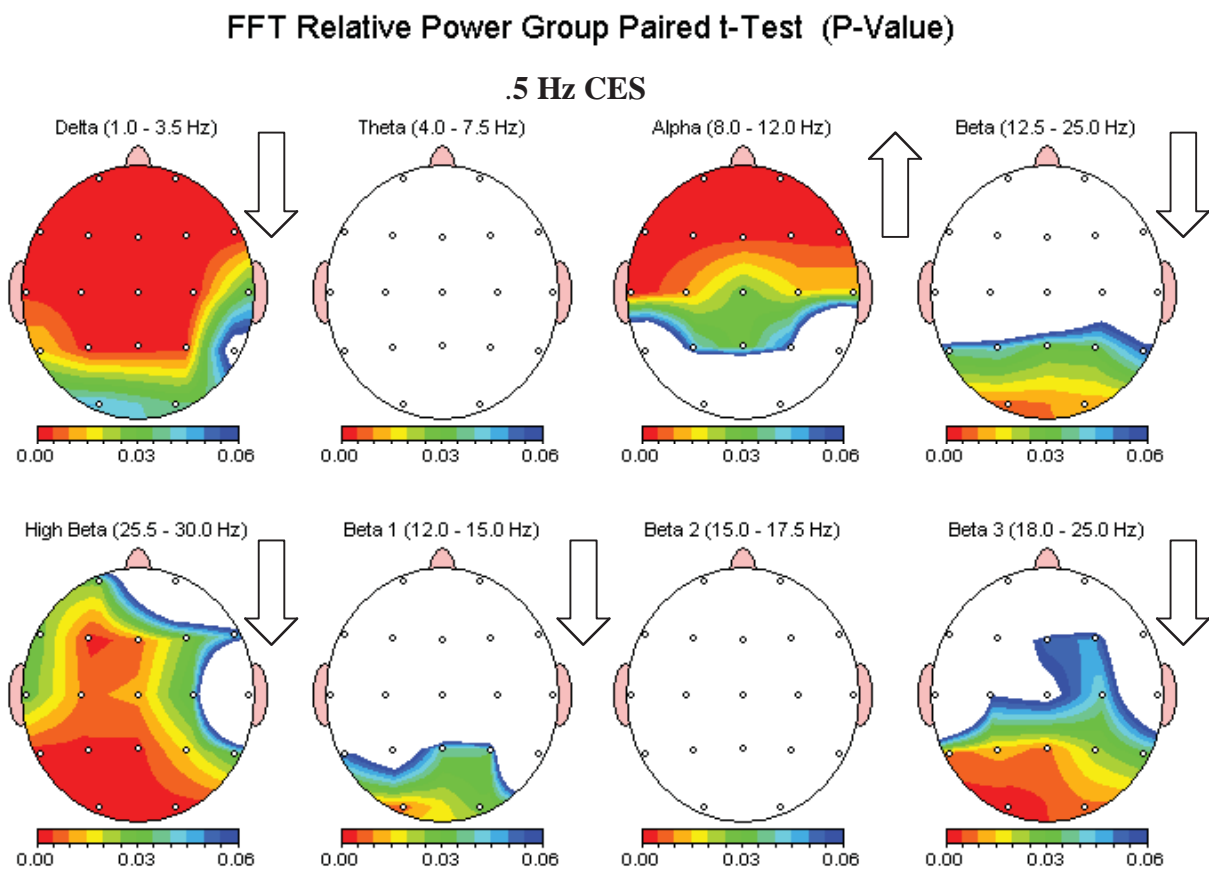


Figure 23. Relative power p -value topographical map for 0.5 Hz CES. Statistically significant changes (.05 or better) after 0.5 Hz CES are indicated by color; white indicates no significant change. The arrows indicate the direction of change. Statistically significant decreases were seen in delta and beta with statistically significant increases in alpha (NeuroGuide).

FFT Relative Power Group Paired t-Test (P-Value)

100 Hz CES

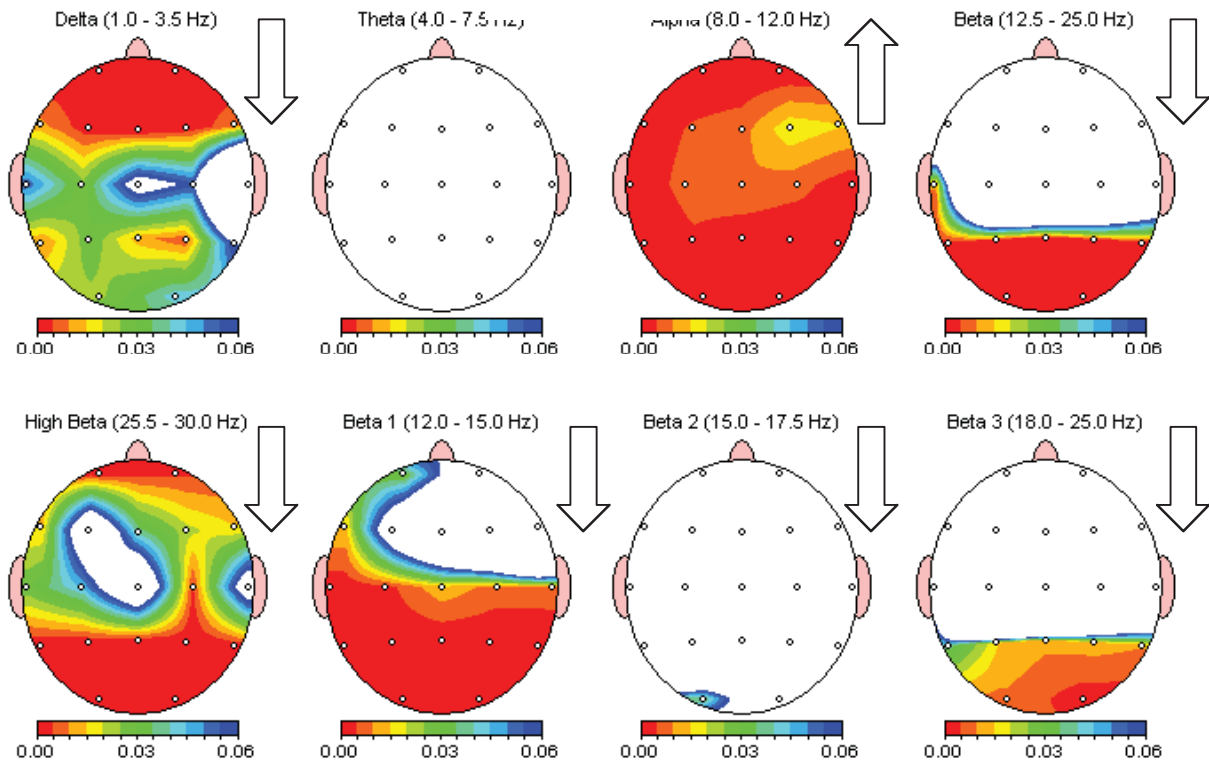


Figure 24. Relative power p -value topographical map for 100 Hz CES. Statistically significant changes (.05 or better) after 100 Hz CES are indicated by color; white indicates no significant change. The arrows indicate the direction of change. Statistically significant decreases were seen in delta and beta with statistically significant increases in alpha.

Both the 0.5 Hz CES and 100 Hz CES had similar effects on EEG activity in the major EEG frequency bands, however there were some differences in the location within each band. To better compare the effects of the two different frequencies of CES on EEG, Figure 23 displays the statistically significant changes in for both groups one graphic.

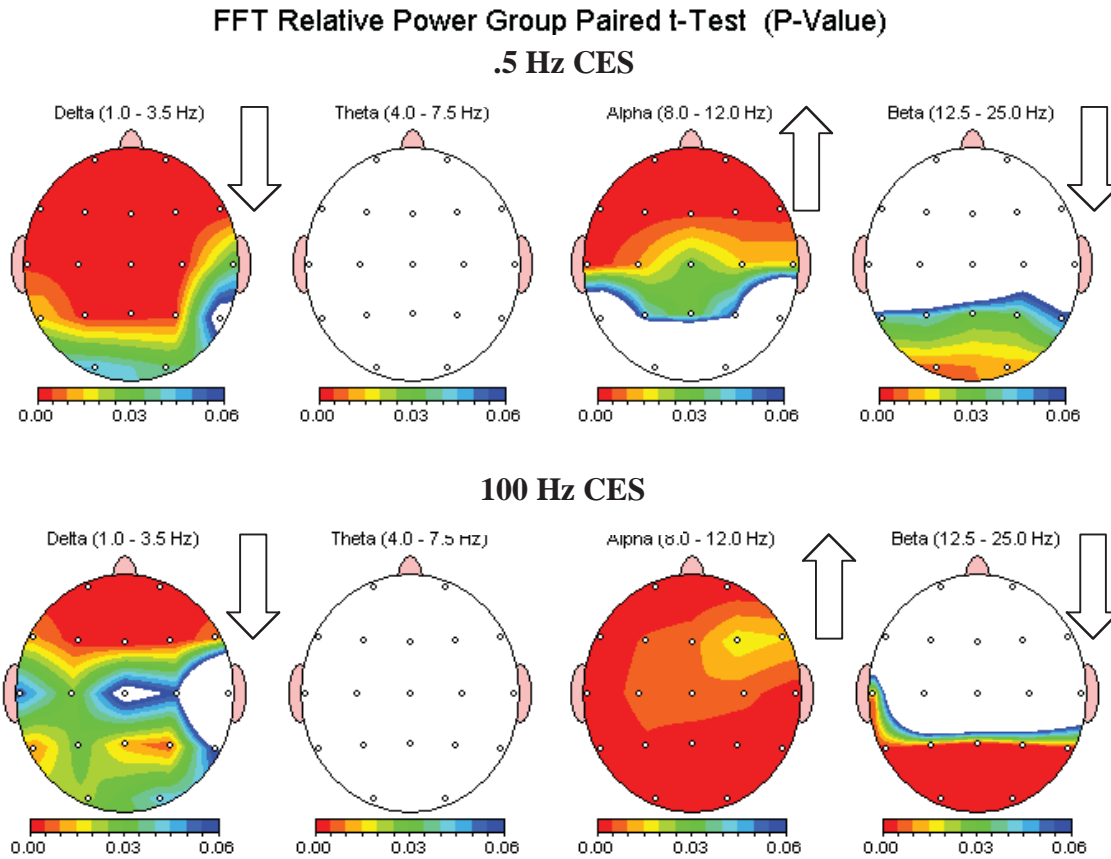


Figure 25. Comparison of relative power topographical maps for 0.5 Hz and 100 Hz CES in delta, theta, alpha and beta frequency bands.

Changes in relative power activity can be presented in 1 Hz increments as well as by traditional EEG bands. The single Hz maps of activity do not display information as succinctly as maps by EEG band, but can show important differences in individual frequency that are not apparent in the traditional EEG bands.

Single Hz Relative Power Topographical Maps for 0.5 Hz CES

The following are topographical maps of the statistically significant changes after 20 minutes of 0.5 Hz CES. These maps graphically represent statistically significant changes ranging from a p -value of 0.00 to 0.05 with colors ranging from red to blue. White indicates no

statistically significant change at the .05 level from baseline. The 0.5 Hz group means, standard deviations and single Hz p -value tables for the single Hz topographical maps are presented in Appendix A.

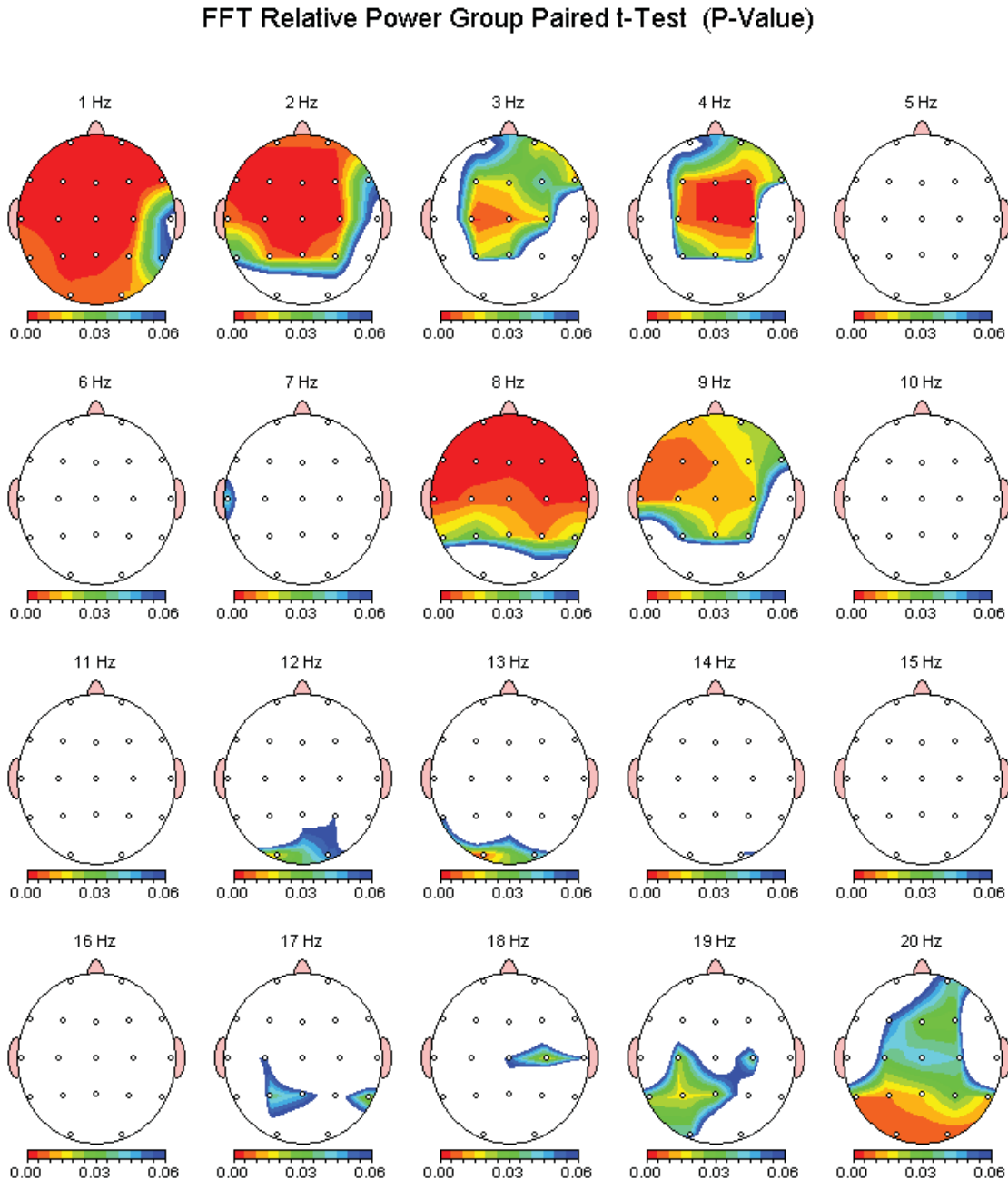


Figure 26. Relative power p -value topographical map for 0.5 Hz CES from 1 to 20 Hz. There was an increase in 8 & 9 Hz activity, all other activity decreased. Statistically significant changes (.05 or better) after 0.5 Hz CES are indicated by color; white indicates no significant change.

FFT Relative Power Group Paired t-Test (P-Value)

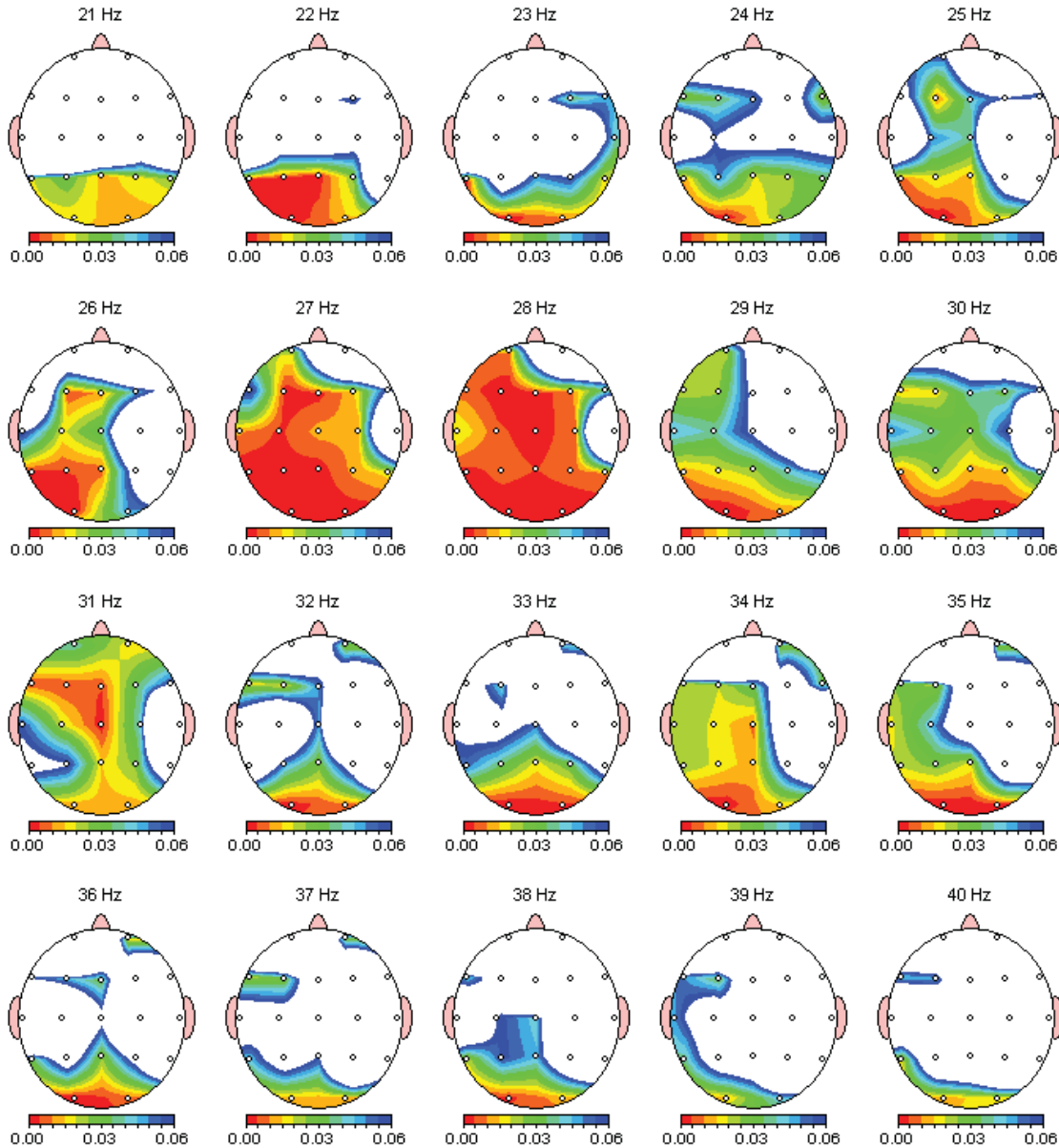


Figure 27. Relative power p -value topographical map for 0.5 Hz CES from 21 to 40 Hz. There was a decrease in all activity from 21-40 Hz. Statistically significant changes (.05 or better) after 0.5 Hz CES is indicated by color; white indicates no significant change.

Single Hz Relative Power Topographical Maps for 100 Hz CES

The following are topographical maps of the statistically significant changes after 20

minutes of 100 Hz CES. These maps graphically represent statistically significant changes ranging from a p -value of 0.00 to 0.05 with colors ranging from red to blue. White indicates no statistically significant change at the .05 level from baseline. The 100 Hz group means, standard deviations and single Hz p -value tables for the single Hz topographical maps are presented in Appendix B.

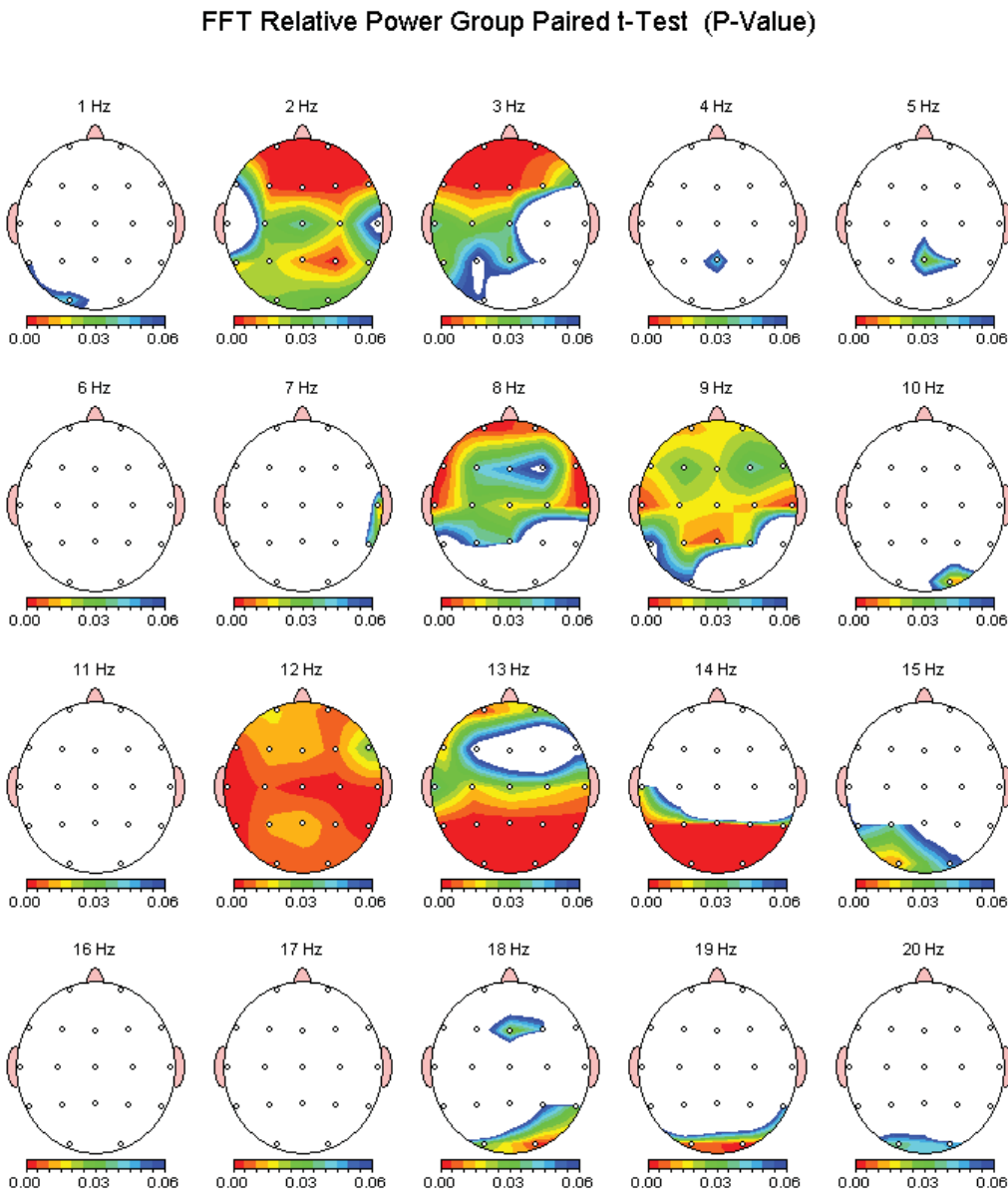


Figure 28. Relative power p -value topographical map for 100 Hz CES from 1 to 20 Hz. There was an increase in 8, 9 and 10 Hz activity, all other activity decreased. Statistically significant changes (.05 or better) after 0.5 Hz CES are indicated by color.

FFT Relative Power Group Paired t-Test (P-Value)

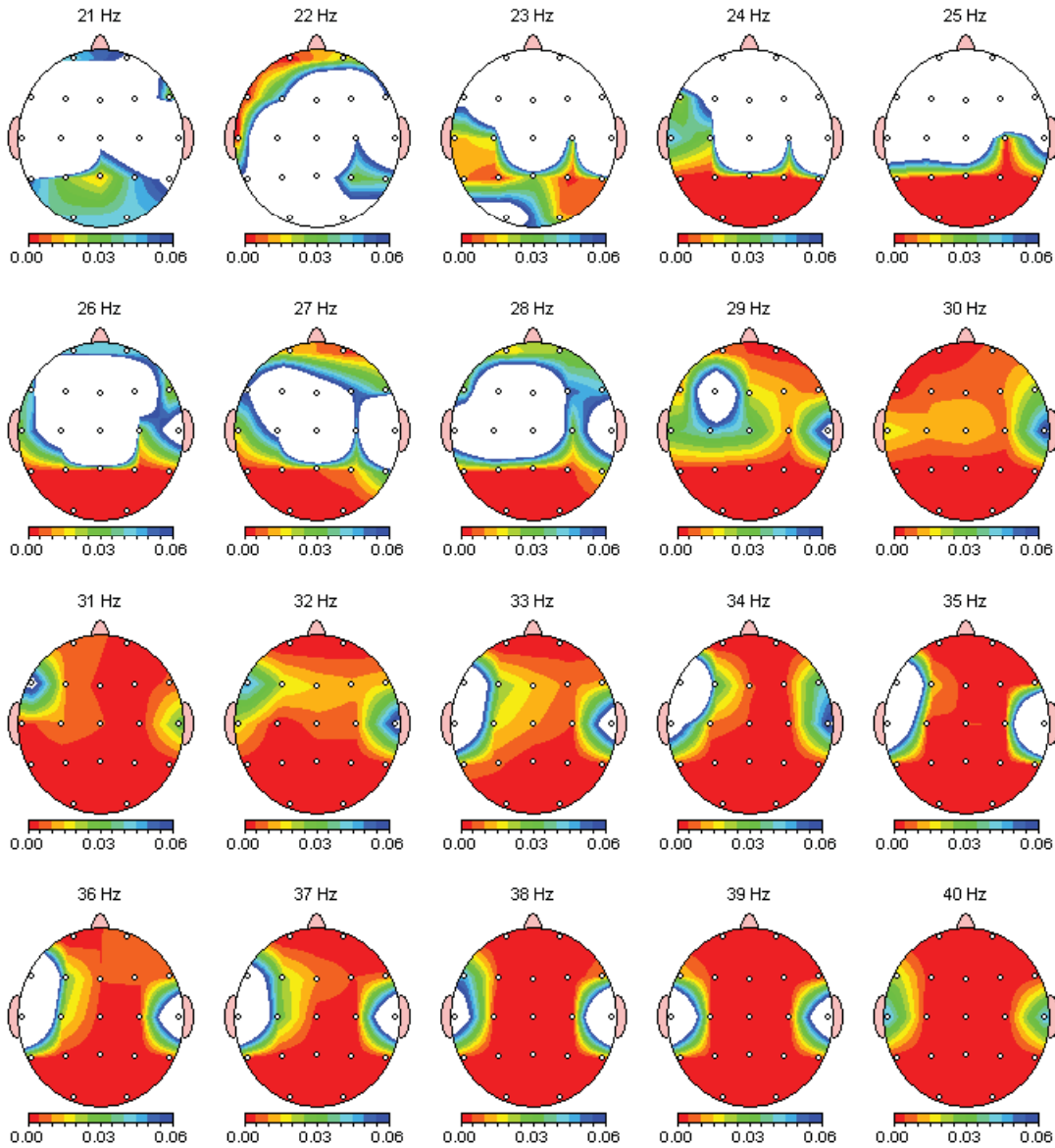


Figure 29. Relative power p -value topographical map for 100 Hz CES from 21 to 40 Hz. There was a decrease in all activity from 21-40 Hz. Statistically significant changes (.05 or better) after 0.5 Hz CES are indicated by color; white indicates no significant change.

Changes in the single Hz activity common to both the 0.5 Hz CES and 100 Hz CES

groups are summarized in Table 1.

Comparison with Average Reference Montage Relative Power

The relative power results of the common average reference montage were substantially in agreement with the results of linked ears reference, revealing a decrease in delta and beta activity with an increase in alpha activity. The analysis of the EEG in an average reference montage was conducted as a control for type I error. For the sake of clarity and brevity, the specifics of the average reference analysis are not presented with the main results. Please see Appendix C for tables of *p*-values, group means, standard deviations, *z*-scores and the topographical maps.

Common Changes in Relative Power in the Linked Ears and Average Reference

The paired *t*-tests revealed that in both frequencies of CES, in both the linked ears and average reference montage, there was an increase in alpha activity with a decrease in delta and beta activity. A summary of the changes found in relative power is presented in table 1.

Table 1

Summary of Changes in Relative Power after 20 Minutes of CES

	5 Hz CES Relative Power	100 Hz CES Relative Power
Linked Ears Reference	Delta, <i>Alpha</i> , Beta	Delta, <i>Alpha</i> , Beta
Average Reference	Delta, <i>Alpha</i> , Beta	Delta, <i>Alpha</i> , Beta
Changes Common to Both Montages	Delta, <i>Alpha</i> , Beta	Delta, <i>Alpha</i> , Beta

Note: Italics indicates an increase.

Findings for Hypothesis 1:

Given the discovery of a significant difference in the mean relative power alpha band activity between the baseline and treatment groups, the null hypothesis 1 was rejected ($H1_0: \mu_{.5\alpha B} = \mu_{.5\alpha E}$) in favor of the alternate hypothesis 1 ($H1_A: \mu_{.5\alpha B} \neq \mu_{.5\alpha E}$). It was found that immediately after a single 20-minute session of 0.5 Hz CES, there was a statistically significant change in mean relative power alpha band activity at one or more electrode sites.

Findings for Hypothesis 2:

Given the discovery of a significant difference in the mean relative power alpha band activity between the baseline and treatment groups, the null hypothesis 2 was rejected ($H2_0: \mu_{.5\alpha B} = \mu_{.5\alpha E}$) in favor of the alternate hypothesis 2 ($H2_A: \mu_{.5\alpha B} \neq \mu_{.5\alpha E}$). It was found that immediately after a single 20-minute session of 100 Hz CES, there was a statistically significant change in mean relative power alpha band activity at one or more electrode sites.

Finding for Hypothesis 3:

Given the discovery of a significant difference in the mean relative power delta band activity between the baseline and treatment groups, the null hypothesis 3 was rejected ($H3_0: \mu_{.5\Delta B} = \mu_{.5\Delta E}$) in favor of the alternate hypothesis 3 ($H3_A: \mu_{.5\Delta B} \neq \mu_{.5\Delta E}$). It was found that immediately after a single 20-minute session of 0.5 Hz CES, there was a statistically significant change in mean relative power delta band activity at one or more electrode sites.

Findings for Hypothesis 4:

Given the discovery of a significant difference in the mean relative power delta band

activity between the baseline and treatment groups, the null hypothesis 4 was rejected ($H_{4_0}: \mu_{100\Delta B} = \mu_{100\Delta E}$) in favor of the alternate hypothesis 4 ($H_{4_A}: \mu_{100\Delta B} \neq \mu_{100\Delta E}$). It was found that immediately after a single 20-minute session of 100 Hz CES, there was a statistically significant change in mean relative power delta band activity at one or more electrode sites.

Findings for Hypothesis 5:

Given the discovery of no significant difference in the mean relative power theta band activity between the baseline and treatment groups, the null hypothesis 5 was supported ($H_{5_0}: \mu_{.5\Theta B} = \mu_{.5\Theta E}$) thus the alternate hypothesis 5 ($H_{5_A}: \mu_{.5\Theta B} \neq \mu_{.5\Theta E}$) was rejected. It was found that immediately after a single 20-minute session of 0.5 Hz CES, there was no statistically significant change in mean relative power theta band activity at one or more electrode sites.

Findings for Hypothesis 6:

Given the discovery of no significant difference in the mean relative power theta band activity between the baseline and treatment groups, the null hypothesis 6 was supported ($H_{6_0}: \mu_{100\Theta B} = \mu_{100\Theta E}$) thus the alternate hypothesis 6 ($H_{6_A}: \mu_{100\Theta B} \neq \mu_{100\Theta E}$) was rejected. It was found that immediately after a single 20-minute session of 100 Hz CES, there was no statistically significant change in mean relative power theta band activity at one or more electrode sites.

Findings for Hypothesis 7:

Given the discovery of a significant difference in the mean relative power beta band activity between the baseline and treatment groups, the null hypothesis 7 was rejected ($H_{7_0}: \mu_{.5\beta B} = \mu_{.5\beta E}$) in favor of the alternate hypothesis 7 ($H_{7_A}: \mu_{.5\beta B} \neq \mu_{.5\beta E}$). It was found that immediately

after a single 20-minute session of 100 Hz CES, there was a statistically significant change in mean relative power beta band activity at one or more electrode sites.

Findings for Hypothesis 8:

Given the discovery of a significant difference in the mean relative power beta band activity between the baseline and treatment groups, the null hypothesis 8 was rejected ($H_{8_0}: \mu_{100\beta B} = \mu_{100\beta E}$) in favor of the alternate hypothesis 8 ($H_{8_A}: \mu_{100\beta B} \neq \mu_{100\beta E}$). It was found that immediately after a single 20-minute session of 0.5 Hz CES, there was a statistically significant change in mean relative power beta band activity at one or more electrode sites.

Coherence Results

The paired *t*-test for coherence revealed that the CES stimulus increased theta and alpha coherence for both the 0.5 Hz and 100 Hz groups. The 0.5 Hz CES lowered delta coherence while increasing theta and alpha coherence in both the linked ears and average reference montages. The 100 Hz CES increased theta and alpha coherence in both montages.

Coherence Maps and Tables

The specifics of the coherence analysis are presented below in tables and topographical maps. The following figures (30 & 31) present changes in coherence after 0.5 Hz and 100 Hz CES. Statistically significant increases at the .05 level are highlighted in the figures with red, while statistically significant decreases are highlighted in blue, text versions of these tables are in appendices A and B. Tables for coherence group means and standard deviations are presented in Appendix A for 0.5 Hz, and Appendix B for 100 Hz.

FFT Coherence Group Paired t-Test (P-Value)

Intrahemispheric: LEFT

	DELTA	THETA	ALPHA	BETA
FP1 F3	0.527	0.083	0.172	0.421
FP1 C3	0.390	0.041	0.464	0.908
FP1 P3	0.245	0.406	0.583	0.433
FP1 O1	0.600	0.463	0.042	0.133
FP1 F7	0.452	0.265	0.334	0.925
FP1 T3	0.355	0.551	0.912	0.406
FP1 T5	0.099	0.393	0.151	0.557
F3 C3	0.440	0.084	0.607	0.464
F3 P3	0.099	0.947	0.581	0.505
F3 O1	0.141	0.805	0.504	0.803
F3 F7	0.657	0.153	0.015	0.179
F3 T3	0.933	0.511	0.797	0.574
F3 T5	0.011	0.188	0.344	0.164
C3 P3	0.113	0.191	0.425	0.638
C3 O1	0.154	0.344	0.827	0.852
C3 F7	0.713	0.072	0.238	0.387
C3 T3	0.500	0.381	0.330	0.172
C3 T5	0.009	0.069	0.170	0.585
P3 O1	0.806	0.841	0.808	0.602
P3 F7	0.180	0.618	0.880	0.779
P3 T3	0.506	0.478	0.615	0.236
P3 T5	0.892	0.486	0.718	0.237
O1 F7	0.312	0.413	0.074	0.995
O1 T3	0.867	0.915	0.883	0.597
O1 T5	0.864	0.369	0.184	0.149
F7 T3	0.653	0.765	0.924	0.668
F7 T5	0.021	0.409	0.486	0.210
T3 T5	0.693	0.191	0.256	0.875

Intrahemispheric: RIGHT

	DELTA	THETA	ALPHA	BETA
FP2 F4	0.352	0.068	0.019	0.166
FP2 C4	0.410	0.034	0.246	0.293
FP2 P4	0.344	0.024	0.468	0.642
FP2 O2	0.393	0.639	0.009	0.795
FP2 F8	0.509	0.018	0.005	0.108
FP2 T4	0.373	0.035	0.089	0.099
FP2 T6	0.011	0.885	0.036	0.883
F4 C4	0.385	0.071	0.540	0.497
F4 P4	0.285	0.167	0.833	0.978
F4 O2	0.357	0.809	0.528	0.248
F4 F8	0.842	0.124	0.005	0.430
F4 T4	0.618	0.328	0.157	0.345
F4 T6	0.012	0.249	0.899	0.230
C4 P4	0.803	0.598	0.554	0.945
C4 O2	0.575	0.481	0.650	0.128
C4 F8	0.888	0.066	0.118	0.318
C4 T4	0.348	0.394	0.549	0.400
C4 T6	0.571	0.135	0.177	0.193
P4 O2	0.516	0.810	0.986	0.327
P4 F8	0.833	0.059	0.594	0.952
P4 T4	0.089	0.188	0.688	0.982
P4 T6	0.774	0.345	0.137	0.441
O2 F8	0.981	0.599	0.131	0.587
O2 T4	0.009	0.892	0.476	0.244
O2 T6	0.321	0.386	0.609	0.078
F8 T4	0.892	0.043	0.263	0.400
F8 T6	0.126	0.677	0.548	0.237
T4 T6	0.355	0.470	0.170	0.548

Interhemispheric: HOMOLOGOUS PAIRS

	DELTA	THETA	ALPHA	BETA
FP1 FP2	0.672	0.033	0.169	0.810
C3 C4	0.635	0.077	0.274	0.181
O1 O2	0.850	0.428	0.018	0.511
T3 T4	0.847	0.296	0.045	0.828

	DELTA	THETA	ALPHA	BETA
F3 F4	0.575	0.019	0.016	0.107
P3 P4	0.212	0.761	0.001	0.147
F7 F8	0.239	0.245	0.001	0.247
T5 T6	0.418	0.755	0.089	0.856

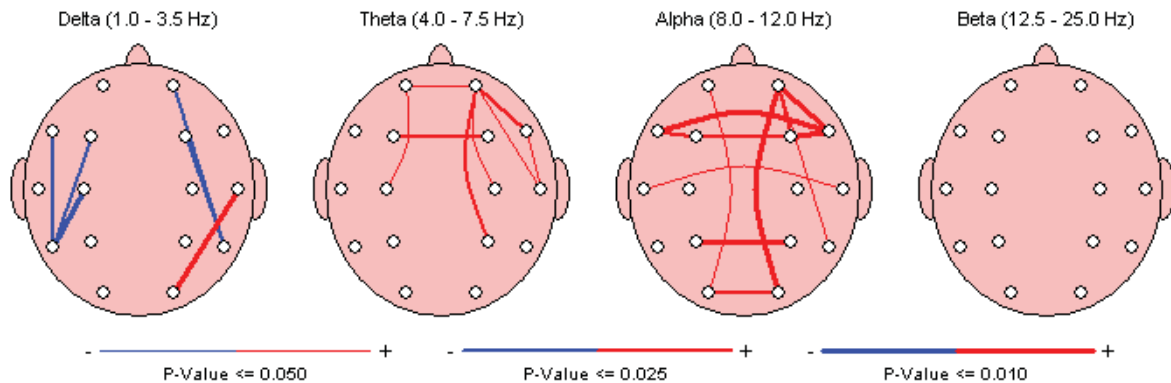


Figure 30. Coherence changes after 0.5 Hz CES. Statistically significant increases are highlighted in red, significant decreases are highlighted in blue.

FFT Coherence Group Paired t-Test (P-Value)

Intrahemispheric: LEFT

	DELTA	THETA	ALPHA	BETA
FP1 F3	0.009	0.002	0.025	0.005
FP1 C3	0.007	0.043	0.275	0.214
FP1 P3	0.003	0.093	0.205	0.529
FP1 O1	0.024	0.049	0.115	0.792
FP1 F7	0.123	0.179	0.187	0.049
FP1 T3	0.002	0.255	0.221	0.096
FP1 T5	0.029	0.002	0.533	0.218
F3 C3	0.021	0.252	0.013	0.490
F3 P3	0.040	0.677	0.124	0.837
F3 O1	0.010	0.518	0.277	0.715
F3 F7	0.019	0.019	0.004	0.058
F3 T3	0.012	0.264	0.191	0.087
F3 T5	0.050	0.654	0.616	0.754
C3 P3	0.108	0.307	0.348	0.708
C3 O1	0.665	0.755	0.490	0.242
C3 F7	0.001	0.002	0.881	0.157
C3 T3	0.448	0.051	0.142	0.091
C3 T5	0.300	0.603	0.373	0.754
P3 O1	0.636	0.363	0.295	0.087
P3 F7	0.000	0.006	0.327	0.530
P3 T3	0.751	0.228	0.839	0.068
P3 T5	0.028	0.394	0.409	0.670
O1 F7	0.032	0.009	0.243	0.624
O1 T3	0.501	0.199	0.353	0.026
O1 T5	0.970	0.254	0.096	0.621
F7 T3	0.007	0.028	0.496	0.128
F7 T5	0.006	0.005	0.564	0.647
T3 T5	0.627	0.544	0.850	0.039

Intrahemispheric: RIGHT

	DELTA	THETA	ALPHA	BETA
FP2 F4	0.010	0.000	0.119	0.125
FP2 C4	0.033	0.060	0.407	0.367
FP2 P4	0.523	0.321	0.506	0.055
FP2 O2	0.231	0.498	0.659	0.460
FP2 F8	0.005	0.001	0.107	0.818
FP2 T4	0.542	0.905	0.423	0.806
FP2 T6	0.495	0.486	0.191	0.096
F4 C4	0.282	0.271	0.227	0.718
F4 P4	0.705	0.616	0.226	0.847
F4 O2	0.400	0.999	0.957	0.306
F4 F8	0.004	0.004	0.009	0.495
F4 T4	0.620	0.855	0.633	0.727
F4 T6	0.504	0.684	0.457	0.360
C4 P4	0.174	0.817	0.025	0.947
C4 O2	0.652	0.762	0.487	0.613
C4 F8	0.140	0.080	0.975	0.616
C4 T4	0.324	0.603	0.212	0.680
C4 T6	0.114	0.357	0.895	0.990
P4 O2	0.953	0.900	0.523	0.411
P4 F8	0.834	0.247	0.702	0.574
P4 T4	0.708	0.197	0.641	0.701
P4 T6	0.241	0.327	0.817	0.999
O2 F8	0.699	0.440	0.752	0.132
O2 T4	0.222	0.396	0.486	0.659
O2 T6	0.571	0.338	0.247	0.223
F8 T4	0.852	0.690	0.587	0.827
F8 T6	0.745	0.696	0.369	0.261
T4 T6	0.714	0.657	0.402	0.660

Interhemispheric: HOMOLOGOUS PAIRS

	DELTA	THETA	ALPHA	BETA
FP1 FP2	0.132	0.002	0.001	0.034
C3 C4	0.333	0.417	0.228	0.596
O1 O2	0.603	0.804	0.259	0.995
T3 T4	0.418	0.320	0.384	0.907

	DELTA	THETA	ALPHA	BETA
F3 F4	0.186	0.073	0.152	0.174
P3 P4	0.006	0.060	0.567	0.223
F7 F8	0.256	0.026	0.012	0.113
T5 T6	0.009	0.256	0.588	0.224

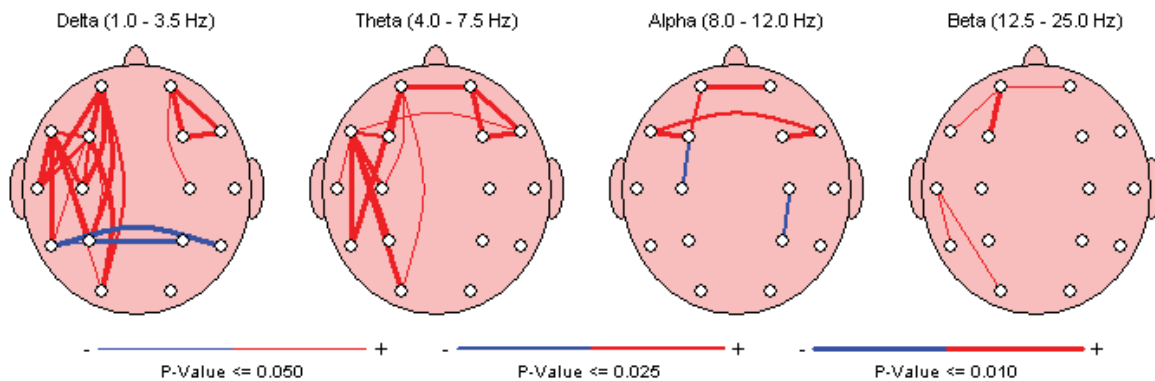


Figure 31. Coherence changes after 100 Hz CES. Statistically significant increases are highlighted in red, significant decreases are highlighted in blue.

Comparison with Average Reference Montage Coherence

In general, the changes found in coherence for the linked ears montage were also found in the average reference montage (Appendix C) and passed methodological controls for false positive results. A summary of the coherence data from the average reference montage is presented with the main analysis in Table 2.

Common Changes in Coherence

The paired *t*-tests revealed that in both frequencies of CES, in both a linked ears and average reference montage, there was an increase in theta and alpha coherence. A summary of the changes in coherence for each group is presented in table 2.

Table 2

Summary of Changes in Coherence After 20 Minutes of CES

	5 Hz CES Coherence	100 Hz CES Coherence
Linked Ears Reference	Delta, <i>Theta, Alpha</i>	<i>Delta, Theta, Alpha, Beta</i>
Average Reference	Delta, <i>Theta, Alpha, Beta</i>	Delta, <i>Theta, Alpha</i>
Changes Common to Both Montages	Delta, <i>Theta, Alpha</i>	<i>Theta, Alpha</i>

Note: Italics indicates an increase.

Findings for Hypothesis 9:

Given the discovery of a significant difference in the mean coherence between the baseline and treatment groups, the null hypothesis 9 was rejected ($H_0: \mu_{.5CohB} = \mu_{.5CohE}$) in favor

of the alternate hypothesis 9 ($H9_A: \mu_{.5CohB} \neq \mu_{.5CohE}$). It was found that immediately after a single 20-minute session of 0.5 Hz CES, there was a statistically significant change in mean coherence at one or more electrode sites.

Findings for Hypothesis 10:

Given the discovery of a significant difference in the mean coherence between the baseline and treatment groups, the null hypothesis 10 was rejected ($H10_0: \mu_{100CohB} = \mu_{100CohE}$) in favor of the alternate hypothesis 10 ($H10_A: \mu_{100CohB} \neq \mu_{100CohE}$). It was found that immediately after a single 20-minute session of 100 Hz CES, there was a statistically significant change in mean coherence at one or more electrode sites.

Amplitude Asymmetry Results

The paired *t*-test for amplitude asymmetry revealed that the 100 Hz CES stimulus decreased intrahemispheric amplitude asymmetry in delta and theta frequencies with possibly an increase in some right hemisphere delta asymmetry and some left hemisphere beta asymmetry. The 100 Hz CES also appeared to increase some central interhemispheric amplitude asymmetry in delta. The 0.5 Hz CES stimulus did not appear to increase delta or theta asymmetry, but it did bilaterally increase alpha amplitude asymmetry. The increase in asymmetry involving just a single site, even if it connected to several sites, was ignored as possible statistical artifact. Tables for amplitude asymmetry group means and standard deviations are presented in Appendix A for 0.5 Hz, Appendix B for 100 Hz and Appendix C for the average reference montage. The specifics of the analysis are presented below in tables and topographical maps. The following figures (32 & 33) present the changes in coherence after 0.5 Hz and 100 Hz CES. Statistically

significant increases at the .05 level are highlighted in the figure with red, while statistically significant decreases are highlighted in blue. The information is also presented in a plain text format in Appendix A for the 0.5 Hz group and Appendix B for the 100 Hz group.

FFT Amplitude Asymmetry Group Paired t-Test (P-Value)

Intrahemispheric: LEFT

	DELTA	THETA	ALPHA	BETA
FP1 F3	0.314	1.000	0.858	0.735
FP1 C3	0.309	0.893	0.244	0.673
FP1 P3	0.264	0.997	0.174	0.843
FP1 O1	0.146	0.260	0.268	0.816
FP1 F7	0.770	0.584	0.260	0.554
FP1 T3	0.874	0.219	0.011	0.389
FP1 T5	0.287	0.910	0.117	0.716
F3 C3	0.551	0.836	0.171	0.655
F3 P3	0.361	0.913	0.190	0.947
F3 O1	0.180	0.192	0.315	0.637
F3 F7	0.517	0.516	0.090	0.257
F3 T3	0.488	0.203	0.006	0.208
F3 T5	0.420	0.924	0.133	0.469
C3 P3	0.346	0.958	0.769	0.662
C3 O1	0.145	0.228	0.749	0.492
C3 F7	0.286	0.448	0.527	0.226
C3 T3	0.362	0.165	0.082	0.151
C3 T5	0.490	0.877	0.426	0.294
P3 O1	0.153	0.163	0.759	0.476
P3 F7	0.239	0.600	0.346	0.451
P3 T3	0.226	0.207	0.380	0.220
P3 T5	0.828	0.829	0.222	0.328
O1 F7	0.112	0.084	0.445	0.968
O1 T3	0.082	0.069	0.812	0.463
O1 T5	0.195	0.128	0.549	0.797
F7 T3	0.655	0.236	0.016	0.467
F7 T5	0.225	0.677	0.239	0.953
T3 T5	0.113	0.162	0.944	0.408

Intrahemispheric: RIGHT

	DELTA	THETA	ALPHA	BETA
FP2 F4	0.055	0.499	0.980	0.884
FP2 C4	0.046	0.643	0.421	0.776
FP2 P4	0.058	0.788	0.035	0.644
FP2 O2	0.118	0.559	0.273	0.599
FP2 F8	0.101	0.900	0.919	0.924
FP2 T4	0.086	0.828	0.014	0.454
FP2 T6	0.226	0.763	0.077	0.489
F4 C4	0.168	0.993	0.391	0.632
F4 P4	0.199	0.953	0.078	0.668
F4 O2	0.367	0.920	0.313	0.800
F4 F8	0.798	0.587	0.902	0.955
F4 T4	0.379	0.856	0.027	0.267
F4 T6	0.563	0.961	0.129	0.610
C4 P4	0.445	0.746	0.082	0.135
C4 O2	0.782	0.900	0.425	0.297
C4 F8	0.514	0.631	0.525	0.701
C4 T4	0.905	0.906	0.012	0.219
C4 T6	0.920	0.962	0.165	0.194
P4 O2	0.838	0.791	0.978	0.764
P4 F8	0.426	0.722	0.066	0.758
P4 T4	0.756	0.934	0.518	0.450
P4 T6	0.847	0.900	0.650	0.541
O2 F8	0.522	0.548	0.349	0.721
O2 T4	0.886	0.743	0.983	0.626
O2 T6	0.988	0.930	0.734	0.689
F8 T4	0.422	0.627	0.010	0.405
F8 T6	0.601	0.658	0.107	0.501
T4 T6	0.911	0.873	0.829	0.631

Interhemispheric: HOMOLOGOUS PAIRS

	DELTA	THETA	ALPHA	BETA
FP1 FP2	0.529	0.886	0.087	0.332
C3 C4	0.030	0.586	0.143	0.506
O1 O2	0.884	0.273	0.833	0.942
T3 T4	0.078	0.189	0.486	0.662

	DELTA	THETA	ALPHA	BETA
F3 F4	0.530	0.411	0.247	0.945
P3 P4	0.060	0.676	0.860	0.393
F7 F8	0.423	0.726	0.248	0.311
T5 T6	0.720	0.697	0.684	0.843

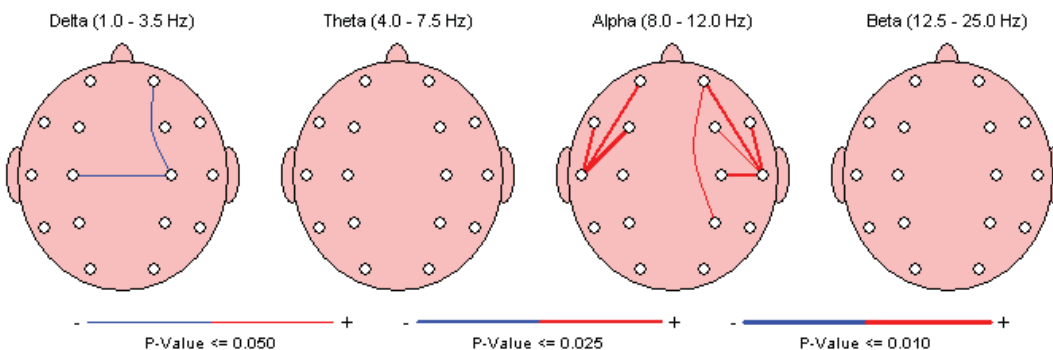


Figure 32. Amplitude asymmetry changes after 0.5 Hz CES. Statistically significant increases are highlighted in red, decreases are highlighted in blue.

FFT Amplitude Asymmetry Group Paired t-Test (P-Value)

Intrahemispheric: LEFT

	DELTA	THETA	ALPHA	BETA
FP1 F3	0.127	0.647	0.869	0.047
FP1 C3	0.007	0.340	0.100	0.159
FP1 P3	0.002	0.039	0.110	0.730
FP1 O1	0.256	0.828	0.284	0.079
FP1 F7	0.057	0.926	0.530	0.774
FP1 T3	0.000	0.004	0.165	0.894
FP1 T5	0.009	0.131	0.094	0.876
F3 C3	0.281	0.633	0.345	0.579
F3 P3	0.120	0.044	0.211	0.170
F3 O1	0.950	0.748	0.317	0.016
F3 F7	0.913	0.684	0.685	0.100
F3 T3	0.113	0.046	0.462	0.379
F3 T5	0.453	0.130	0.152	0.218
C3 P3	0.081	0.010	0.033	0.243
C3 O1	0.187	0.304	0.235	0.028
C3 F7	0.294	0.377	0.390	0.108
C3 T3	0.255	0.046	0.040	0.331
C3 T5	0.793	0.125	0.027	0.204
P3 O1	0.011	0.013	0.976	0.007
P3 F7	0.090	0.036	0.139	0.710
P3 T3	0.682	0.629	0.857	0.699
P3 T5	0.081	0.425	0.722	0.470
O1 F7	0.954	0.791	0.253	0.240
O1 T3	0.086	0.034	0.785	0.532
O1 T5	0.220	0.018	0.752	0.194
F7 T3	0.008	0.001	0.123	0.957
F7 T5	0.291	0.102	0.084	0.987
T3 T5	0.143	0.496	0.675	0.908

Intrahemispheric: RIGHT

	DELTA	THETA	ALPHA	BETA
FP2 F4	0.139	0.087	0.094	0.102
FP2 C4	0.021	0.640	0.217	0.979
FP2 P4	0.001	0.121	0.434	0.706
FP2 O2	0.008	0.733	0.316	0.304
FP2 F8	0.537	0.646	0.219	0.244
FP2 T4	0.290	0.613	0.392	0.263
FP2 T6	0.033	0.030	0.722	0.526
F4 C4	0.070	0.097	0.736	0.168
F4 P4	0.009	0.031	0.212	0.196
F4 O2	0.061	0.357	0.189	0.163
F4 F8	0.043	0.296	0.869	0.026
F4 T4	0.800	0.203	0.965	0.080
F4 T6	0.105	0.011	0.327	0.226
C4 P4	0.037	0.039	0.112	0.534
C4 O2	0.156	0.873	0.099	0.303
C4 F8	0.004	0.551	0.539	0.404
C4 T4	0.411	0.753	0.929	0.220
C4 T6	0.255	0.034	0.248	0.455
P4 O2	0.864	0.233	0.546	0.279
P4 F8	0.001	0.130	0.258	0.755
P4 T4	0.083	0.522	0.267	0.424
P4 T6	0.932	0.137	0.736	0.501
O2 F8	0.011	0.700	0.226	0.575
O2 T4	0.155	0.926	0.301	0.955
O2 T6	0.797	0.058	0.571	0.597
F8 T4	0.075	0.366	0.892	0.516
F8 T6	0.025	0.028	0.488	0.952
T4 T6	0.148	0.067	0.560	0.769

Interhemispheric: HOMOLOGOUS PAIRS

	DELTA	THETA	ALPHA	BETA
FP1 FP2	0.750	0.231	0.993	0.355
C3 C4	0.421	0.993	0.745	0.233
O1 O2	0.029	0.082	0.952	0.553
T3 T4	0.035	0.183	0.163	0.517

	DELTA	THETA	ALPHA	BETA
F3 F4	0.463	0.355	0.175	0.484
P3 P4	0.953	0.849	0.700	0.482
F7 F8	0.036	0.709	0.602	0.684
T5 T6	0.425	0.197	0.356	0.752

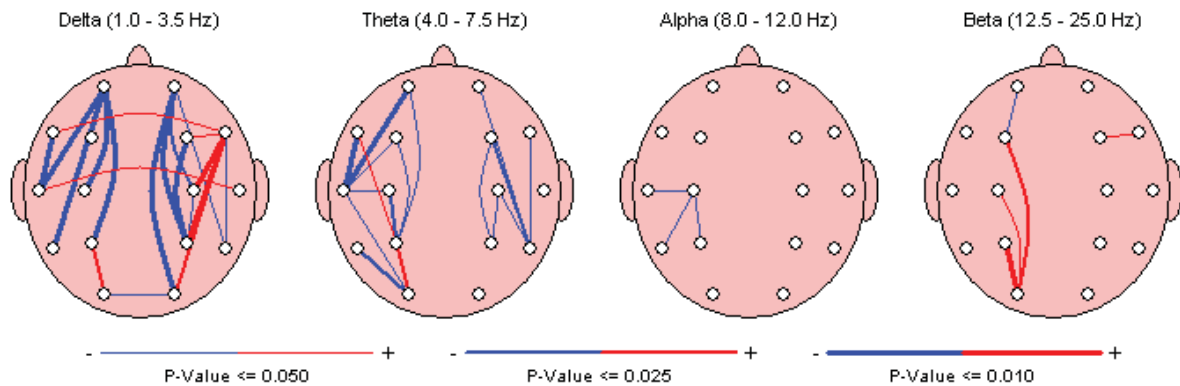


Figure 33. Amplitude asymmetry changes after 100 Hz CES. Statistically significant increases are highlighted in red, decreases are highlighted in blue.

Comparison with Average Reference Montage Amplitude Asymmetry

In the 0.5 Hz CES group the average reference montage confirmed the increase in alpha asymmetry seen in the linked ears montage, but also showed a decrease in delta asymmetry not seen in the linked ears montage. In the 100 Hz CES group the average reference montage confirmed a decrease in theta, with both an increase and decrease in delta. For the 100 Hz group the average reference failed to confirm an increase in beta, finding instead a decrease in beta with an increase in theta. A comparison of the changes in asymmetry by montage is presented in table 3.

Common Changes in Amplitude Asymmetry

The paired *t*-tests revealed that in 0.5 Hz CES, in both a linked ears and average reference montage, there was an increase in alpha amplitude asymmetry. In the 100 Hz CES group, in both the linked ears and average reference montage, there was both an increase and decrease in delta, and a decrease in theta amplitude asymmetry. There were no changes in amplitude asymmetry that were common to both the 0.5 Hz and 100 Hz CES groups. A summary of the changes in asymmetry for each group by montage is presented in table 3.

Table 3

Summary of Changes in Amplitude Asymmetry after 20 Minutes of CES

	0.5 Hz CES Asymmetry	100 Hz CES Asymmetry
Linked Ears Reference	<i>Alpha</i>	Delta, <i>Delta</i> , Theta, <i>Beta</i>
Average Reference	<i>Theta, Alpha</i>	Delta, <i>Delta</i> , Theta, <i>Theta</i> , Beta
Changes Common to Both Montages	<i>Alpha</i>	Delta, <i>Delta</i> , Theta

Note: Italics indicates an increase.

Findings for Hypothesis 11:

Given the discovery of a significant difference in the mean amplitude asymmetry between the baseline and treatment groups, the null hypothesis 11 was rejected ($H11_0: \mu_{.5AsyB} = \mu_{.5AsyE}$) in favor of the alternate hypothesis 11 ($H11_A: \mu_{.5AsyB} \neq \mu_{.5AsyE}$). It was found that immediately after a single 20-minute session of 0.5 Hz CES, there was a statistically significant change in mean amplitude asymmetry at one or more electrode sites.

Findings for Hypothesis 12:

Given the discovery of a significant difference in the mean amplitude asymmetry between the baseline and treatment groups, the null hypothesis 12 was rejected ($H12_0: \mu_{100AsyB} = \mu_{100AsyE}$) in favor of the alternate hypothesis 12 ($H12_A: \mu_{100AsyB} \neq \mu_{100AsyE}$). It was found that immediately after a single 20-minute session of 100 Hz CES, there was a statistically significant change in mean amplitude asymmetry at one or more electrode sites.

Phase Lag Results

There were no changes in phase lag between any pair of electrodes that was common to both the 0.5 Hz and 100 Hz CES groups. There were some changes in phase lag for each CES group that was found in both the linked ears and average reference montages.

The paired *t*-test for phase lag revealed that the 100 Hz CES stimulus increased some left hemisphere phase lag in delta, with the possibility of some increase in left hemisphere phase lag in theta and alpha. There was also some indication of a possible decrease in intrahemispheric phase lag in alpha for the 100 Hz group. When compared with the average reference montage it was found that there were increases in phase lag at C3-T3 and P3-T5 that common to both

montages of the 100 Hz group.

In the 0.5 Hz CES group there was a pattern of increased posterior phase lag in alpha with a possible increase in phase lag in beta. None of the other statistically significant changes appeared to be part of a pattern of changes. When compared with the average reference montage it was found that there was an increase in phase lag at O1-O2 common to both montages of the 0.5 Hz group.

Tables for phase group means and standard deviations are presented in Appendix A for 0.5 Hz, Appendix B for 100 Hz and Appendix C for the average reference montage. Figures 34 and 35 present changes in phase lag after 0.5 Hz CES and 100 Hz CES. Statistically significant increases at the .05 level are highlighted in the figures with red while statistically significant decreases are highlighted in blue.

Comparison with Average Reference Montage Phase Lag

The paired *t*-test results for the average reference montage revealed statistically significant results in common with the linked ears montage for both the 100 Hz and 0.5 Hz CES groups. For the 100 Hz group there were common increases in both montages in left hemisphere phase lag at C3-T3 delta and P3-T5 alpha. For the 0.5 Hz group there was a common increase in both montages in phase lag between O1-O2 alpha. The comparison with the average reference montage validated the increase in phase lag in the linked ears montage for these electrode pairs. All other statistically significant changes were not found in both montages (or groups), and thus are being disregarded as possible type I error.

FFT Phase Lag Group Paired t-Test (P-Value)

Intrahemispheric: LEFT

	DELTA	THETA	ALPHA	BETA
FP1 F3	0.445	0.574	0.702	0.220
FP1 C3	0.749	0.879	0.491	0.147
FP1 P3	0.964	0.916	0.944	0.477
FP1 O1	0.943	0.229	0.765	0.034
FP1 F7	0.949	0.221	0.759	0.126
FP1 T3	0.948	0.506	0.946	0.351
FP1 T5	0.023	0.817	0.875	0.043
F3 C3	0.460	0.471	0.375	0.364
F3 P3	0.603	0.611	0.324	0.553
F3 O1	0.805	0.974	0.536	0.099
F3 F7	0.438	0.437	0.341	0.735
F3 T3	0.771	0.154	0.612	0.325
F3 T5	0.930	0.211	0.151	0.342
C3 P3	0.738	0.233	0.989	0.297
C3 O1	0.229	0.298	0.841	0.324
C3 F7	0.633	0.862	0.378	0.572
C3 T3	0.567	0.399	0.978	0.211
C3 T5	0.263	0.105	0.797	0.238
P3 O1	0.170	0.837	0.925	0.849
P3 F7	0.969	0.643	0.602	0.972
P3 T3	0.606	0.865	0.153	0.442
P3 T5	0.221	0.473	0.219	0.856
O1 F7	0.329	0.341	0.849	0.746
O1 T3	0.852	0.963	0.023	0.214
O1 T5	0.486	0.935	0.065	0.569
F7 T3	0.582	0.448	0.569	0.411
F7 T5	0.909	0.215	0.080	0.331
T3 T5	0.762	0.231	0.189	0.128

Intrahemispheric: RIGHT

	DELTA	THETA	ALPHA	BETA
FP2 F4	0.292	0.814	0.358	0.333
FP2 C4	0.494	0.871	0.250	0.482
FP2 P4	0.838	0.536	0.108	0.417
FP2 O2	0.480	0.258	0.553	0.721
FP2 F8	0.133	0.382	0.430	0.393
FP2 T4	0.116	0.491	0.362	0.789
FP2 T6	0.471	0.692	0.130	0.608
F4 C4	0.184	0.899	0.470	0.190
F4 P4	0.281	0.813	0.696	0.782
F4 O2	0.720	0.761	0.313	0.685
F4 F8	0.949	0.912	0.613	0.095
F4 T4	0.006	0.282	0.550	0.524
F4 T6	0.461	0.769	0.956	0.139
C4 P4	0.659	0.936	0.814	0.738
C4 O2	0.670	0.769	0.089	0.790
C4 F8	0.741	0.982	0.862	0.035
C4 T4	0.009	0.395	0.738	0.531
C4 T6	0.555	0.892	0.053	0.867
P4 O2	0.690	0.667	0.929	0.480
P4 F8	0.297	0.606	0.080	0.108
P4 T4	0.559	0.876	0.582	0.610
P4 T6	0.684	0.820	0.598	0.948
O2 F8	1.000	0.207	0.864	0.055
O2 T4	0.489	0.760	0.153	0.923
O2 T6	0.701	0.663	0.921	0.266
F8 T4	0.077	0.154	0.740	0.913
F8 T6	0.156	0.538	0.967	0.014
T4 T6	0.982	0.692	0.151	0.737

Interhemispheric: HOMOLOGOUS PAIRS

	DELTA	THETA	ALPHA	BETA
FP1 FP2	0.736	0.975	0.949	0.567
C3 C4	0.898	0.760	0.275	0.293
O1 O2	0.208	0.528	0.003	0.073
T3 T4	0.846	0.774	0.825	0.190

	DELTA	THETA	ALPHA	BETA
F3 F4	0.455	0.628	0.427	0.343
P3 P4	0.568	0.878	0.014	0.383
F7 F8	0.447	0.451	0.458	0.757
T5 T6	0.350	0.413	0.203	0.921

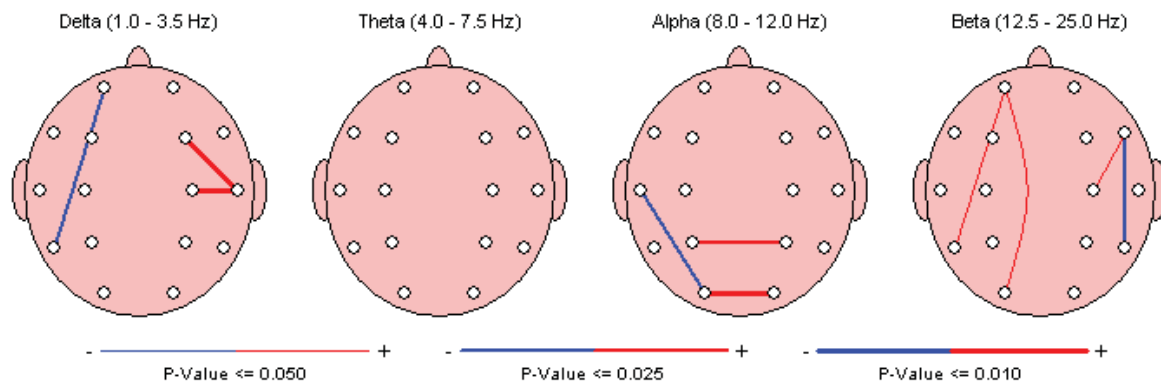


Figure 34. Phase lag changes after 0.5 Hz CES. Statistically significant increases are highlighted in red, decreases are highlighted in blue.

FFT Phase Lag Group Paired t-Test (P-Value)

Intrahemispheric: LEFT

	DELTA	THETA	ALPHA	BETA
FP1 F3	0.197	0.319	0.127	0.072
FP1 C3	0.776	0.848	0.030	0.456
FP1 P3	0.992	0.397	0.099	0.084
FP1 O1	0.422	0.897	0.006	0.433
FP1 F7	0.073	0.117	0.528	0.281
FP1 T3	0.170	0.961	0.945	0.378
FP1 T5	0.669	0.020	0.217	0.755
F3 C3	0.785	0.902	0.161	0.595
F3 P3	0.133	0.633	0.119	0.573
F3 O1	0.523	0.706	0.813	0.125
F3 F7	0.178	0.596	0.390	0.418
F3 T3	0.275	0.951	0.922	0.639
F3 T5	0.547	0.424	0.797	0.655
C3 P3	0.049	0.255	0.947	0.635
C3 O1	0.068	0.479	0.464	0.372
C3 F7	0.024	0.614	0.130	0.569
C3 T3	0.004	0.736	0.700	0.280
C3 T5	0.340	0.864	0.519	0.817
P3 O1	0.274	0.310	0.082	0.063
P3 F7	0.011	0.265	0.160	0.695
P3 T3	0.000	0.463	0.462	0.864
P3 T5	0.494	0.989	0.005	0.569
O1 F7	0.459	0.785	0.030	0.482
O1 T3	0.024	0.310	0.322	0.603
O1 T5	0.645	0.479	0.391	0.036
F7 T3	0.040	0.951	0.915	0.487
F7 T5	0.883	0.664	0.941	0.271
T3 T5	0.037	0.727	0.437	0.811

Intrahemispheric: RIGHT

	DELTA	THETA	ALPHA	BETA
FP2 F4	0.580	0.152	0.161	0.158
FP2 C4	0.652	0.294	0.722	0.261
FP2 P4	0.419	0.469	0.227	0.678
FP2 O2	0.523	0.628	0.386	0.793
FP2 F8	0.664	0.732	0.459	0.809
FP2 T4	0.739	0.914	0.413	0.688
FP2 T6	0.927	0.868	0.518	0.123
F4 C4	0.941	0.382	0.775	0.586
F4 P4	0.192	0.853	0.307	0.305
F4 O2	0.099	0.262	0.321	0.341
F4 F8	0.488	0.106	0.138	0.715
F4 T4	0.380	0.833	0.364	0.888
F4 T6	0.756	0.285	0.806	0.529
C4 P4	0.057	0.528	0.302	0.716
C4 O2	0.112	0.429	0.549	0.787
C4 F8	0.520	0.079	0.151	0.619
C4 T4	0.728	0.583	0.260	0.125
C4 T6	0.241	0.265	0.581	0.655
P4 O2	0.100	0.569	0.123	0.279
P4 F8	0.169	0.632	0.305	0.307
P4 T4	0.636	0.648	0.011	0.035
P4 T6	0.146	0.208	0.282	0.720
O2 F8	0.857	0.767	0.590	0.683
O2 T4	0.229	0.801	0.036	0.064
O2 T6	0.625	0.443	0.388	0.345
F8 T4	0.824	0.229	0.672	0.837
F8 T6	0.673	0.292	0.731	0.640
T4 T6	0.583	0.166	0.068	0.307

Interhemispheric: HOMOLOGOUS PAIRS

	DELTA	THETA	ALPHA	BETA
FP1 FP2	0.698	0.414	0.587	0.673
C3 C4	0.580	0.168	0.058	0.098
O1 O2	0.985	0.525	0.980	0.767
T3 T4	0.716	0.015	0.079	0.880

	DELTA	THETA	ALPHA	BETA
F3 F4	0.266	0.168	0.663	0.944
P3 P4	0.837	0.202	0.069	0.595
F7 F8	0.704	0.717	0.180	0.266
T5 T6	0.507	0.266	0.416	0.081

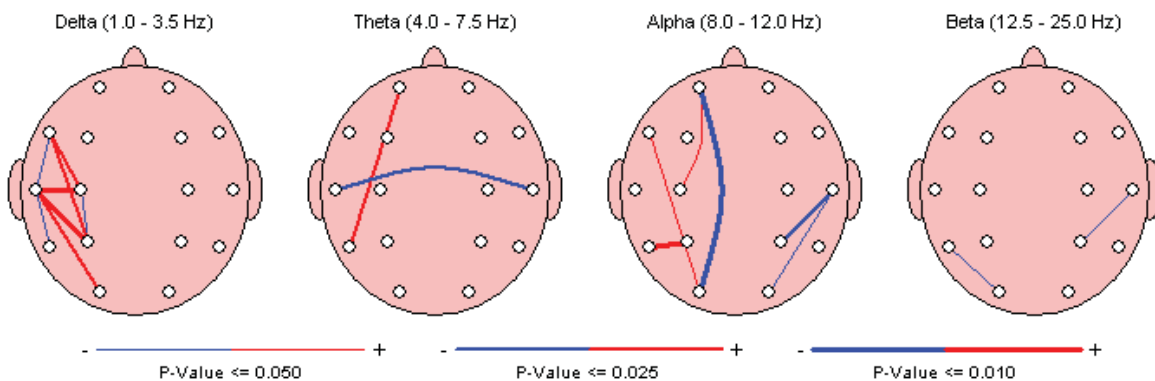


Figure 35. Phase lag changes after 100 Hz CES. Statistically significant increases are highlighted in red, decreases are highlighted in blue.

Common Changes in Phase Lag

No common changes were found in phase lag between the same electrode pairs for the 0.5 Hz and 100 Hz CES groups in the linked ears montage. In the average reference montage there was a common decrease in theta phase lag between F7 and F8.

Table 4

Summary of Changes in Phase Lag after 20 Minutes of CES

	5 Hz CES Phase Lag	100 Hz CES Phase Lag	Common Pairs in Both CES groups
Linked Ears Reference	<i>Alpha, Beta</i>	<i>Delta, Alpha, Alpha, Beta</i>	<i>Alpha</i>
Average Reference	<i>Theta, Alpha, Alpha</i>	<i>Delta, Theta, Alpha, Beta</i>	<i>Theta (F7-F8)</i>
Changes Common to Electrode Pairs of Both Montages	<i>Alpha</i>	<i>Delta, Alpha</i>	

Note: Italics indicates an increase. Results confined to a single electrode pair, or one common electrode, but not replicated in another group/montage are not included in the table.

Findings for Hypothesis 13:

Given the discovery of significant difference in the mean phase lag between the baseline and treatment groups in several electrode pairs, the null hypothesis 13 was rejected ($H_{13_0}: \mu_{.5PhB} = \mu_{.5PhE}$) in favor of the alternate hypothesis 13 ($H_{13_A}: \mu_{.5PhB} \neq \mu_{.5PhE}$). It was found that immediately after a single 20-minute session of 0.5 Hz CES, there was a statistically significant change in mean phase lag at one or more electrode pairs.

Findings for Hypothesis 14:

Given the discovery of significant difference in the mean phase lag between the baseline

and treatment groups in several electrode pairs, the null hypothesis 14 was rejected ($H_{14_0}: \mu_{100PhB} = \mu_{100PhE}$) in favor of the alternate hypothesis 14 ($H_{14_A}: \mu_{100PhB} \neq \mu_{100PhE}$). It was found that immediately after a single 20-minute session of 100 Hz CES, there was a statistically significant change in mean phase lag at one or more electrode pairs.

Power Ratio Results

The paired *t*-test for power ratio revealed that there was an increase in theta/gamma, alpha/beta, alpha/gamma and beta/gamma ratios. These changes were also found in the average reference montage and passed methodological controls for type I errors. Isolated changes such as the increase in theta/beta at T6 should be considered false positives at this time, since they are not part of a larger pattern of significant changes and do not occur identically in both groups. The specifics of the analysis are presented below in tables and topographical maps. Plain text tables for power ratio *p*-values and the group means and standard deviations are presented in Appendix A for 0.5 Hz, Appendix B for 100 Hz and Appendix C for the average reference montage.

Power Ratio Tables

A table of *p*-values for the 0.5 Hz group are presented in Figure 36, while a table of *p*-values for the 100 Hz group is presented in Figure 37. The group means, standard deviations and *z*-scores for the 0.5 Hz group are presented in Appendix A. The group means, standard deviations and *z*-scores for the 100 Hz group are presented in Appendix B. The average reference power ratio *p*-value tables and topographical maps are presented in Appendix C. Statistically significant increases in power ratios (at the .05 level) are highlighted in red, while significant decreases are highlighted in blue.

FFT Power Ratio Group Paired t-Test (P-Value)

Intrahemispheric: LEFT

	D/T	D/A	D/B	D/G	T/A	T/B	T/G	A/B	A/G	B/G
FP1 - LE	0.001	0.000	0.146	0.862	0.028	0.308	0.028	0.012	0.003	0.004
F3 - LE	0.000	0.000	0.135	0.937	0.034	0.314	0.010	0.004	0.000	0.000
C3 - LE	0.000	0.000	0.061	0.766	0.178	0.236	0.022	0.004	0.000	0.001
P3 - LE	0.000	0.004	0.091	0.894	0.285	0.136	0.017	0.006	0.000	0.004
O1 - LE	0.001	0.073	0.481	0.724	0.772	0.045	0.011	0.033	0.003	0.012
F7 - LE	0.000	0.000	0.126	0.835	0.023	0.208	0.036	0.003	0.001	0.012
T3 - LE	0.000	0.000	0.174	0.771	0.076	0.249	0.052	0.000	0.001	0.013
T5 - LE	0.002	0.029	0.289	0.404	0.569	0.069	0.009	0.033	0.002	0.002

Intrahemispheric: RIGHT

	D/T	D/A	D/B	D/G	T/A	T/B	T/G	A/B	A/G	B/G
FP2 - LE	0.001	0.000	0.075	0.404	0.011	0.389	0.183	0.009	0.013	0.112
F4 - LE	0.001	0.000	0.222	0.911	0.039	0.191	0.034	0.007	0.003	0.006
C4 - LE	0.000	0.001	0.125	0.658	0.098	0.289	0.111	0.003	0.002	0.057
P4 - LE	0.001	0.011	0.323	0.910	0.381	0.069	0.030	0.010	0.003	0.064
O2 - LE	0.001	0.062	0.414	0.644	0.577	0.075	0.009	0.042	0.009	0.033
F8 - LE	0.003	0.000	0.191	0.829	0.009	0.336	0.062	0.013	0.005	0.016
T4 - LE	0.001	0.002	0.787	0.995	0.289	0.054	0.126	0.016	0.042	0.654
T6 - LE	0.010	0.110	0.529	0.957	0.622	0.066	0.037	0.029	0.015	0.152

Intrahemispheric: CENTER

	D/T	D/A	D/B	D/G	T/A	T/B	T/G	A/B	A/G	B/G
Fz - LE	0.001	0.000	0.082	0.509	0.041	0.385	0.020	0.005	0.000	0.000
Cz - LE	0.001	0.001	0.095	0.615	0.196	0.233	0.034	0.014	0.001	0.004
Pz - LE	0.000	0.002	0.118	0.892	0.237	0.118	0.016	0.004	0.000	0.012

Figure 36. Power ratio changes after 0.5 Hz CES. Statistically significant increases are highlighted in red, decreases are highlighted in blue.

FFT Power Ratio Group Paired t-Test (P-Value)

Intrahemispheric: LEFT

	D/T	D/A	D/B	D/G	T/A	T/B	T/G	A/B	A/G	B/G
FP1 - LE	0.003	0.000	0.088	0.975	0.016	0.474	0.037	0.004	0.001	0.023
F3 - LE	0.012	0.000	0.068	0.501	0.034	0.979	0.360	0.051	0.028	0.152
C3 - LE	0.090	0.003	0.339	0.850	0.053	0.658	0.147	0.028	0.018	0.180
P3 - LE	0.059	0.005	0.951	0.091	0.027	0.054	0.000	0.000	0.000	0.021
O1 - LE	0.113	0.004	0.991	0.120	0.012	0.179	0.001	0.000	0.000	0.004
F7 - LE	0.036	0.000	0.440	0.496	0.017	0.404	0.052	0.015	0.005	0.016
T3 - LE	0.069	0.000	0.521	0.200	0.014	0.077	0.056	0.001	0.004	0.214
T5 - LE	0.023	0.001	0.869	0.056	0.014	0.167	0.001	0.000	0.000	0.008

Intrahemispheric: RIGHT

	D/T	D/A	D/B	D/G	T/A	T/B	T/G	A/B	A/G	B/G
FP2 - LE	0.002	0.000	0.065	0.830	0.032	0.440	0.019	0.011	0.001	0.022
F4 - LE	0.013	0.000	0.053	0.944	0.062	0.887	0.109	0.120	0.016	0.024
C4 - LE	0.034	0.007	0.442	0.244	0.180	0.299	0.009	0.024	0.003	0.020
P4 - LE	0.078	0.000	0.748	0.095	0.030	0.077	0.003	0.000	0.000	0.044
O2 - LE	0.202	0.003	0.556	0.068	0.019	0.186	0.005	0.000	0.000	0.035
F8 - LE	0.002	0.001	0.128	0.974	0.146	0.240	0.032	0.060	0.010	0.039
T4 - LE	0.028	0.001	0.837	0.639	0.162	0.121	0.083	0.006	0.011	0.240
T6 - LE	0.037	0.009	0.614	0.136	0.309	0.038	0.002	0.001	0.001	0.121

Intrahemispheric: CENTER

	D/T	D/A	D/B	D/G	T/A	T/B	T/G	A/B	A/G	B/G
Fz - LE	0.005	0.000	0.023	0.445	0.047	0.898	0.191	0.072	0.015	0.053
Cz - LE	0.161	0.013	0.479	0.983	0.096	0.608	0.192	0.043	0.032	0.365
Pz - LE	0.096	0.001	0.836	0.193	0.023	0.145	0.003	0.000	0.000	0.033

Figure 37. Power ratio changes after 100 Hz CES, in a table format. Statistically significant increases are highlighted in red, decreases are highlighted in blue.

FFT Power Ratio Group Paired t-Test (P-Value)

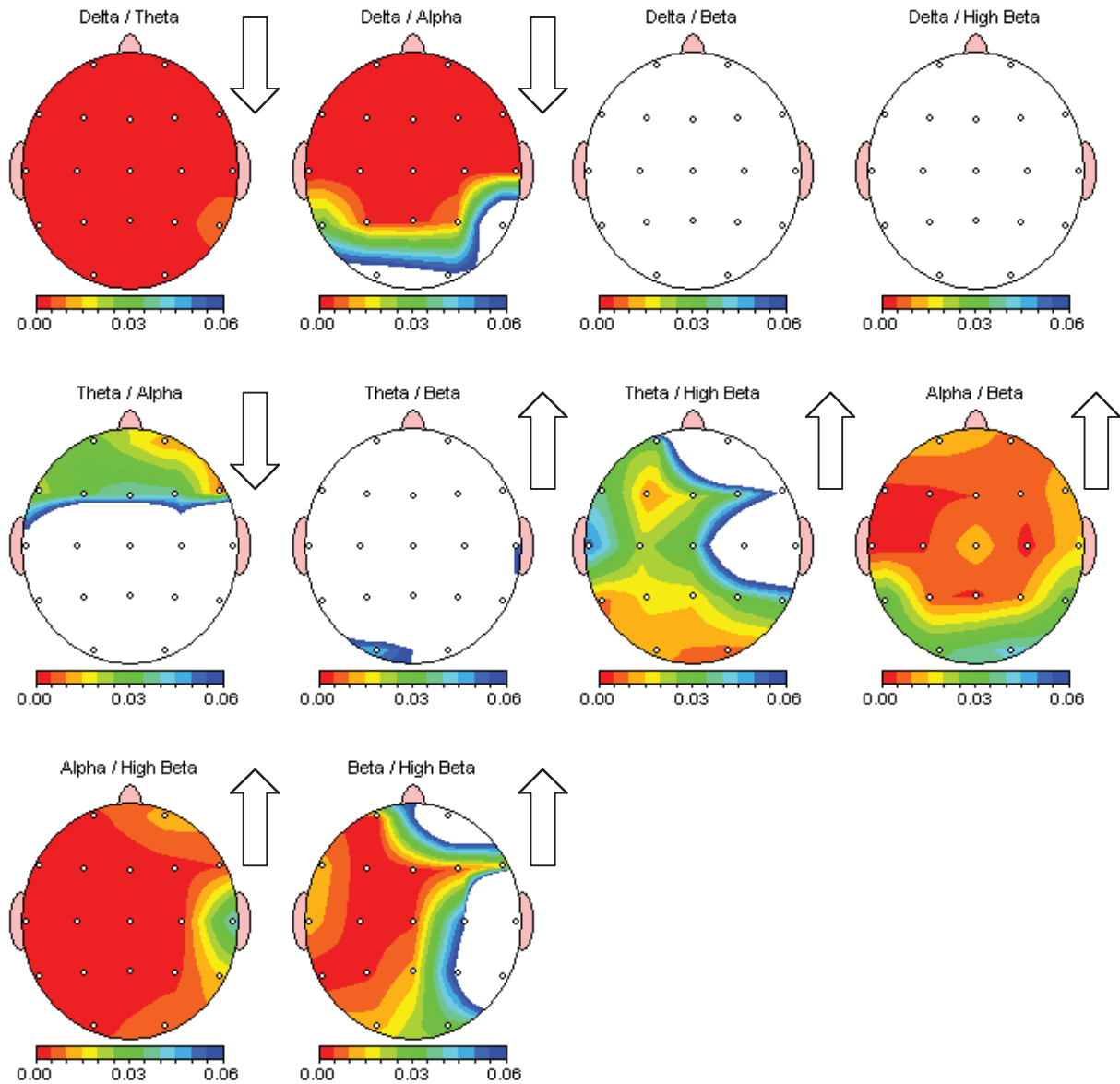


Figure 38. Power ratio changes after 0.5 Hz CES. Statistically significant changes (.05 or better) after 0.5 Hz CES are indicated by color; white indicates no significant change. The arrows indicate the direction of change as an increase or decrease in mean activity.

FFT Power Ratio Group Paired t-Test (P-Value)

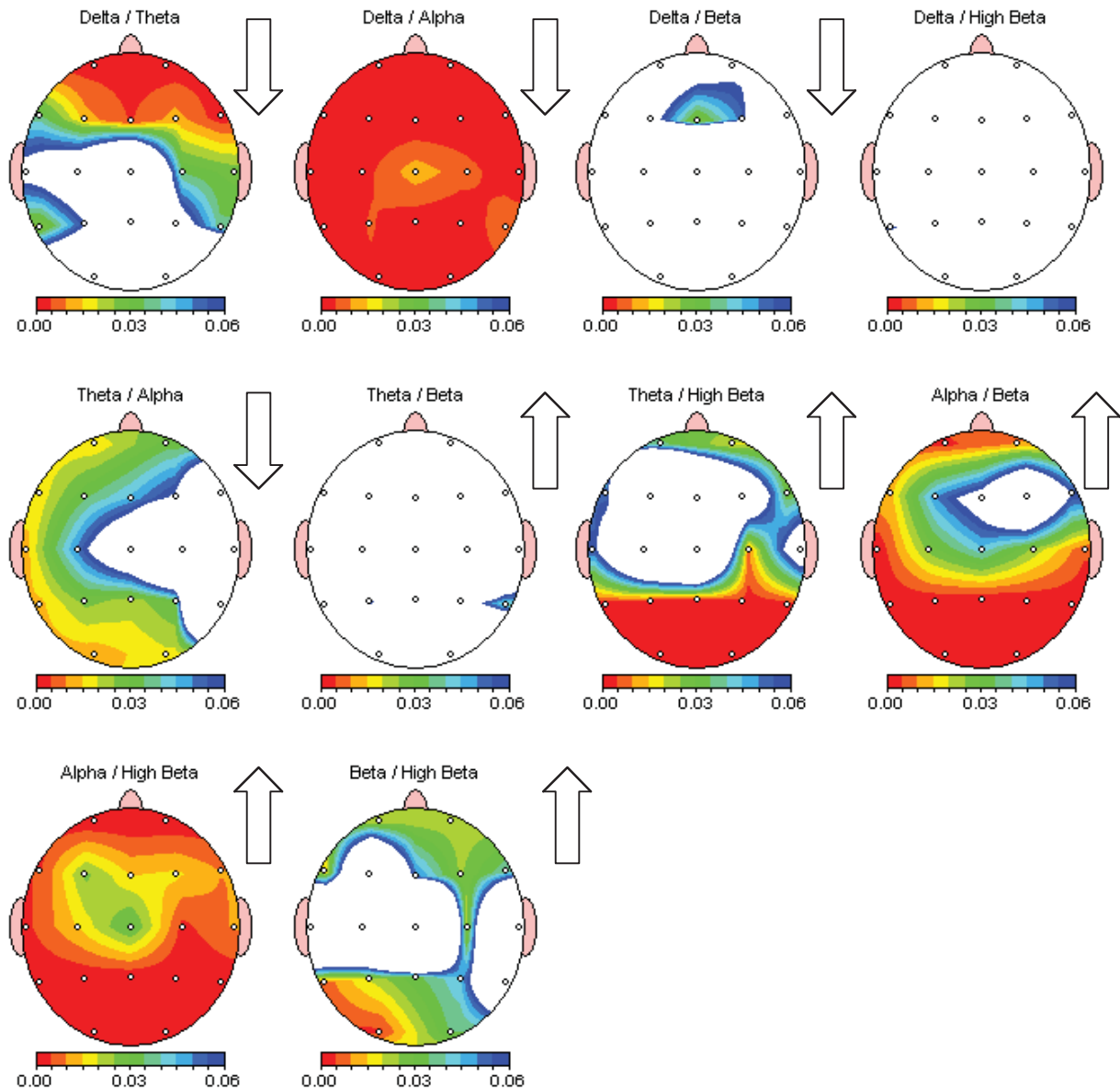


Figure 39. Power ratio changes after 100 Hz CES. Statistically significant changes (.05 or better) after 0.5 Hz CES are indicated by color; white indicates no significant change. The arrows indicate the direction of change as an increase or decrease in mean activity.

Comparison with Average Reference Montage Power Ratio

In both the 0.5 Hz and 100 Hz CES groups the changes in power ratio found with the average reference montage was the same (in terms of frequency band) as was found in the linked

ears montage. There were instances of isolated changes which were unique to the frequency of CES stimulation, but which appeared in both the linked ears and average reference montages. In the 0.5 Hz group the Theta/Beta ratio increased at O1 in both montages. In the 100 Hz CES group Theta/Beta increased at T6, while Delta/Beta decreased at FZ.

Common Changes in Power Ratio

The paired *t*-tests revealed a remarkably uniform set of change in power ratios after CES. In both the 0.5 Hz CES and 100 Hz groups, in both a linked ears and average reference montage, there was a decrease in delta/theta, delta/alpha and theta/alpha with an increase in theta/beta, theta/gamma (high beta), alpha/beta, alpha/gamma and beta/gamma power ratios. A decrease in the delta/beta ratio was seen in the 100 Hz CES group which did not occur in the 0.5 Hz group. This change occurs in both the linked ears and average reference montages so it appears to be a real change which is specific to the 100 Hz CES stimulus. A summary of the changes in power ratio for each CES group is presented in table 5.

Table 5
Summary of Changes in Power Ratio After 20 Minutes of CES

	5 Hz CES Power Ratio	100 Hz CES Power Ratio	Both Frequencies
Linked Ears Reference	D/T, D/A, T/A	D/T, D/A, D/B, T/A	D/T, D/A, T/A
	<i>T/B, T/G, A/B, A/G, B/G</i>	<i>T/B, T/G, A/B, A/G, B/G</i>	<i>T/B, T/G, A/B, A/G, B/G</i>
Average Reference	D/T, D/A, T/A	D/T, D/A, D/B, T/A	D/T, D/A, T/A
	<i>T/B, T/G, A/B, A/G, B/G</i>	<i>T/B, T/G, A/B, A/G</i>	<i>T/B, T/G, A/B, A/G</i>
Changes Common to Both Montages	D/T, D/A, T/A	D/T, D/A, D/B, T/A	
	<i>T/B, T/G, A/B, A/G, B/G</i>	<i>T/B, T/G, A/B, A/G</i>	

Note: Italics indicates an increase.

Findings for Hypothesis 15:

Given the discovery of a significant difference in the mean power ratio between the baseline and treatment groups, the null hypothesis 15 was rejected ($H15_0: \mu_{.5PRB} = \mu_{.5PRE}$) in favor of the alternate hypothesis 15 ($H15_A: \mu_{.5APRB} \neq \mu_{.5PRE}$). It was found that immediately after a single 20-minute session of 0.5 Hz CES, there was a statistically significant change in mean power ratio at one or more electrode sites.

Findings for Hypothesis 16:

Given the discovery of a significant difference in the mean amplitude asymmetry between the baseline and treatment groups, the null hypothesis 16 was rejected ($H16_0: \mu_{100PRB} = \mu_{100PRE}$) in favor of the alternate hypothesis 16 ($H16_A: \mu_{100PRB} \neq \mu_{100PRE}$). It was found that immediately after a single 20-minute session of 100 Hz CES, there was a statistically significant change in mean power ratio at one or more electrode sites.

LORETA Results

The LORETA paired *t*-test revealed that after both 100 Hz and 0.5 Hz CES there was an increase in theta and alpha activity with a decrease in delta and beta activity. For the 100 Hz CES group increases were seen in delta and beta activity which do not pass controls for false positive results and appear to be the consequence of focal activity artifact. The specifics of the analysis are presented below in summary tables and topographical maps.

LORETA Summary Tables

The LORETA tomography presented in this paper makes a within groups paired *t*-test

comparison of activity in 2394 gray matter voxels per half frequency from 0-40 Hz. While only one comparison is made for each pair of means, the list of resulting *p*-values is too extensive to make a comprehensible table (2,394 x 81 = 193, 914 cells). Consequently, the significant *p*-value results for the LORETA have been summarized by location and by frequency in the following summary tables (see the methods section for a discussion of controlling for false positives). Statistically significant increases in current density (at the .05 level) are highlighted in red, while significant decreases are highlighted in blue.

Table 6

Summary of Changes in activation as measured by LORETA after 0.5 Hz CES

Location	Increased Activation	Decreased Activation
Frontal Lobe	<i>Theta, Alpha</i>	L-Beta 1, L-Beta 3, Gamma
Temporal Lobe	<i>Theta, Alpha</i>	R-Delta, Beta 1, L-Beta 3, L-Gamma
Limbic Lobe	<i>Theta, Alpha</i>	Beta 1, Beta 2, L-Beta 3, Gamma
Parietal Lobe	<i>Theta, Alpha</i>	Beta 1, L-Beta 3, Gamma
Occipital Lobe	<i>Theta, Alpha</i>	L-Beta 1, Gamma
Sub-Lobar	<i>Theta, Alpha</i>	Alpha

Note: Italics indicates an increase.

Table 7

Summary of Changes in activation as measured by LORETA after 100 Hz CES

Location	Increased Activation	Decreased Activation
Frontal Lobe	<i>Delta, Theta, Alpha, R-Beta 1, Beta 2, Beta 3, Gamma</i>	Delta, Theta, Gamma
Temporal Lobe	<i>Delta, Theta, Alpha, R-Beta 1, Beta 2, Beta 3, Gamma</i>	Gamma
Limbic Lobe	<i>Delta, Theta, Alpha, Beta 1, Beta 2</i>	Delta, Gamma
Parietal Lobe	<i>L-Delta, Theta, Alpha, Beta 1, Beta 2</i>	Gamma
Occipital Lobe	<i>Theta, Alpha, R-Beta 1, Beta 2</i>	Gamma
Sub-Lobar	<i>L-Delta, Theta, Alpha, R-Beta 1, Beta 2</i>	

Note: Italics indicates an increase.

Comparison with the Laplacian Reference Montage

In both the 0.5 Hz and 100 Hz CES groups, the changes in LORETA current density were compared with the cortical current density estimation of qEEG, the Laplacian montage. In the Laplacian montage the 0.5 Hz CES was found to increase alpha activity while decreasing beta activity. The 100 Hz CES Laplacian map revealed a decrease delta and beta activity with an increase in alpha. The Laplacian montage and the LORETA were in agreement for these

changes. The Laplacian montage did not find the increase in theta activity revealed in LORETA for both groups of CES.

LORETA Artifact

A focal increase in activity was found on the single Hz Laplacian montage for the 100 Hz CES group which is not evident in changes by frequency band. The focal activity occurred at F4 and T4. The activity found in the single Hz Laplacian *p*-value tables (Appendix D) was present at the following frequencies:

Table 8

Focal Increase in Activity at F4 & F8 of the Laplacian Montage Relative Power p-Value Table (Appendix D)

Location	Frequency
F4:	<i>2 Hz, 3 Hz, 4 Hz, 5 Hz, 16 Hz, 17 Hz 18 Hz, 19 Hz, 23 Hz</i>
F8	<i>1 Hz, 2 Hz, 7 Hz, 10 Hz, 12 Hz, 15 Hz, 16 Hz</i>

The focal activity in the 100 Hz CES Laplacian montage is present in the delta and beta frequencies, the same frequencies the 100 Hz LORETA analysis found activity not seen in the 0.5 Hz LORETA or 100 Hz qEEG. Because LORETA is known to represent focal activity incorrectly, at times as false diffuse activity, the focal activity in F4 and F8 suggests that the LORETA results for the 100 Hz CES group not in agreement with the Laplacian montage, or 0.5 Hz CES LORETA are probably artifact. Consequently any LORETA results for the 100 Hz CES group not found in the Laplacian montage or the 0.5 Hz LORETA results should be considered cautiously.

Common Changes in LORETA

The paired *t*-tests revealed that in both the 0.5 Hz CES and 100 Hz groups, there was an increase in theta and alpha activity with a decrease in beta activity. A summary table of the changes found with both frequencies of CES is presented in table 8. For both groups of CES in both the LORETA and the Laplacian montage, there was an increase in alpha activity with a decrease in beta activity. A summary of the changes common to each CES group in both types of current density analysis is presented in table 9.

Table 9

Changes in Activation Common to the 0.5 Hz and 100 Hz Groups after 20 Minutes of CES, as Measured by LORETA

Location	Increased Current Density	Decreased Current Density
Frontal Lobe	<i>Theta, Alpha</i>	Gamma (High Beta)
Temporal Lobe	<i>Theta, Alpha</i>	Gamma (High Beta)
Limbic Lobe	<i>Theta, Alpha</i>	Gamma (High Beta)
Parietal Lobe	<i>Theta, Alpha</i>	Gamma (High Beta)
Occipital Lobe	<i>Theta, Alpha</i>	Gamma (High Beta)
Sub-Lobar	<i>Theta, Alpha</i>	

Table 10

Summary of Changes in Current Density After 20 Minutes of CES

	0.5 Hz CES CD	100 Hz CES CD	Both .5 and 100 Hz
LORETA	<i>Theta, Alpha</i> Delta, Alpha, Beta	<i>Delta, Theta, Alpha, Beta</i> Delta, Theta, Beta	<i>Theta, Alpha</i> Delta, Beta
Laplacian Montage	<i>Alpha</i> Beta	<i>Alpha</i> Delta, Beta	<i>Alpha</i> Beta
Changes Common to Both LORETA and Laplacian	<i>Alpha</i> Beta	<i>Alpha</i> Delta, Beta	<i>Alpha</i> Beta

Note: Italics indicates an increase in activity; no italics indicates decrease in activity.

LORETA Paired *t*-Test Results for 0.5 Hz CES in 1 Hz Increments

The following figures present the results of the LORETA paired *t*-test for the 0.5 Hz CES group. These images represent statistically significant changes at the .05 level after 20 minutes of 0.5 Hz CES. Red indicates a statistically significant increase in activity after CES while blue indicates a statistically significant decrease in activity after CES.

Summary of 1 Hz Changes in Current Density

Decreased Activity in the Temporal Lobe

- Right Superior Temporal Gyrus (Brodmann Area 38)
- Right Middle Temporal Gyrus (Brodmann Area 21)

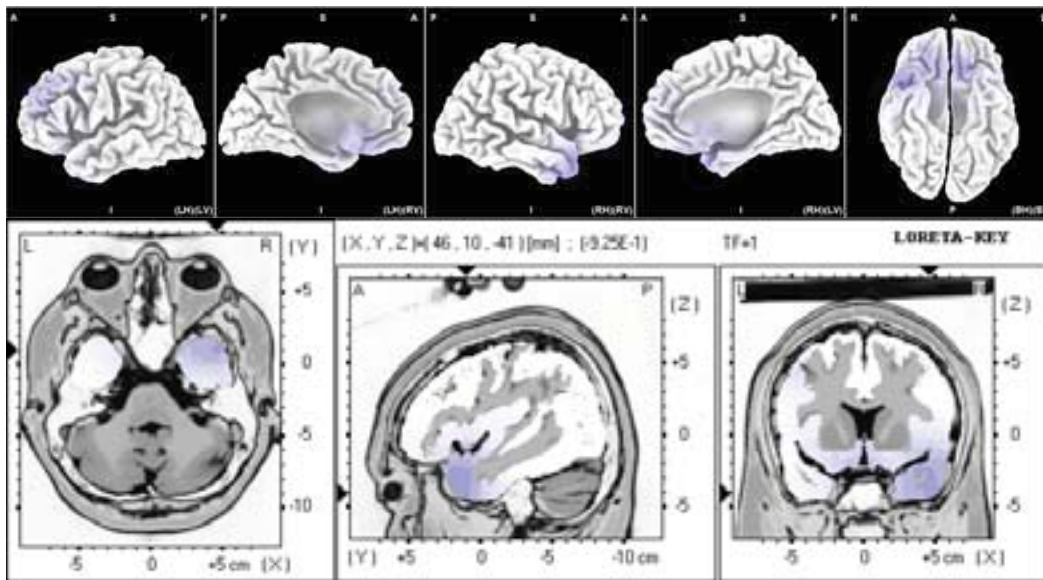


Figure 40. Paired *t*-test for 1 Hz LORETA; significant differences after 20 minutes of 0.5 Hz CES.

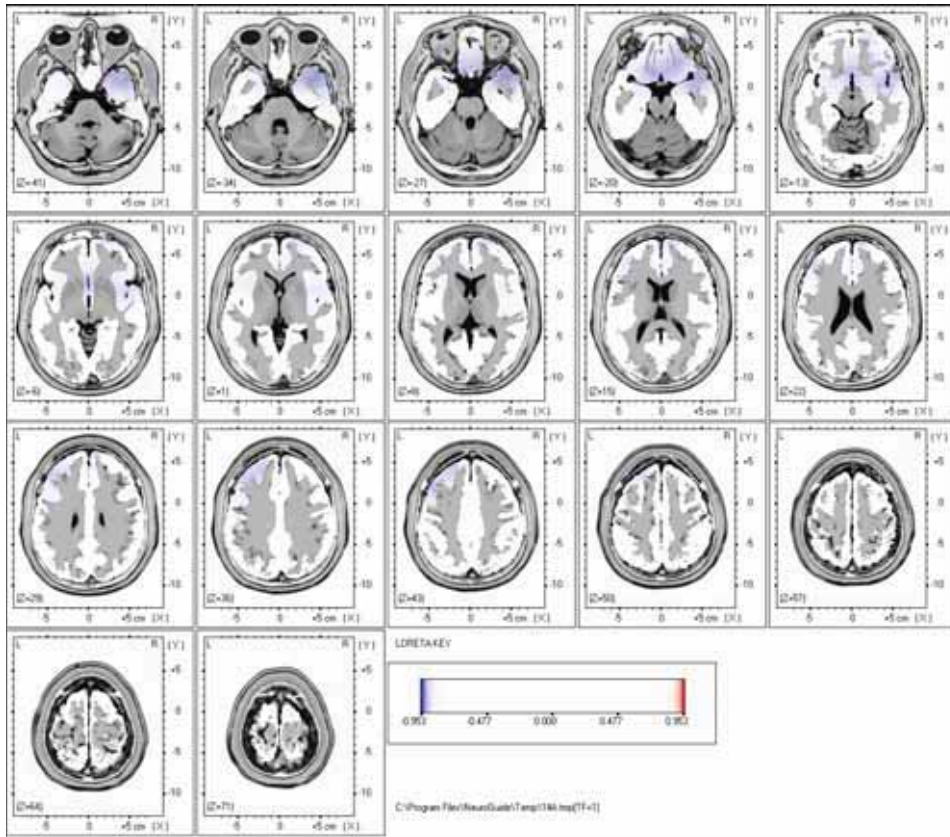


Figure 41. Paired t -test for 1 Hz LORETA; Significant differences after 20 minutes of 0.5 Hz CES.

Summary of 2 Hz Changes in Current Density

There were no statistically significant changes in 2 Hz current density from baseline.

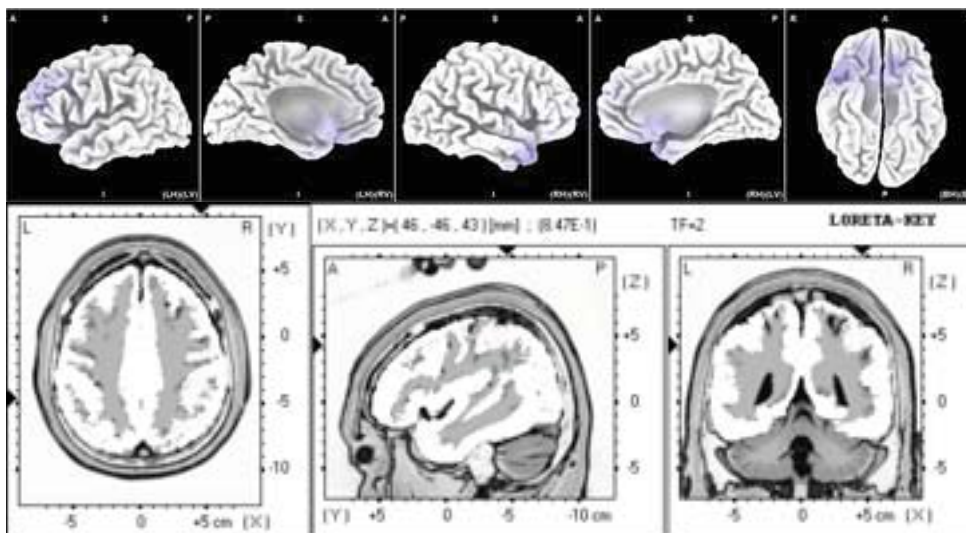


Figure 42. Paired t -test for 2 Hz LORETA; No significant differences after 20 minutes of 0.5 Hz CES.

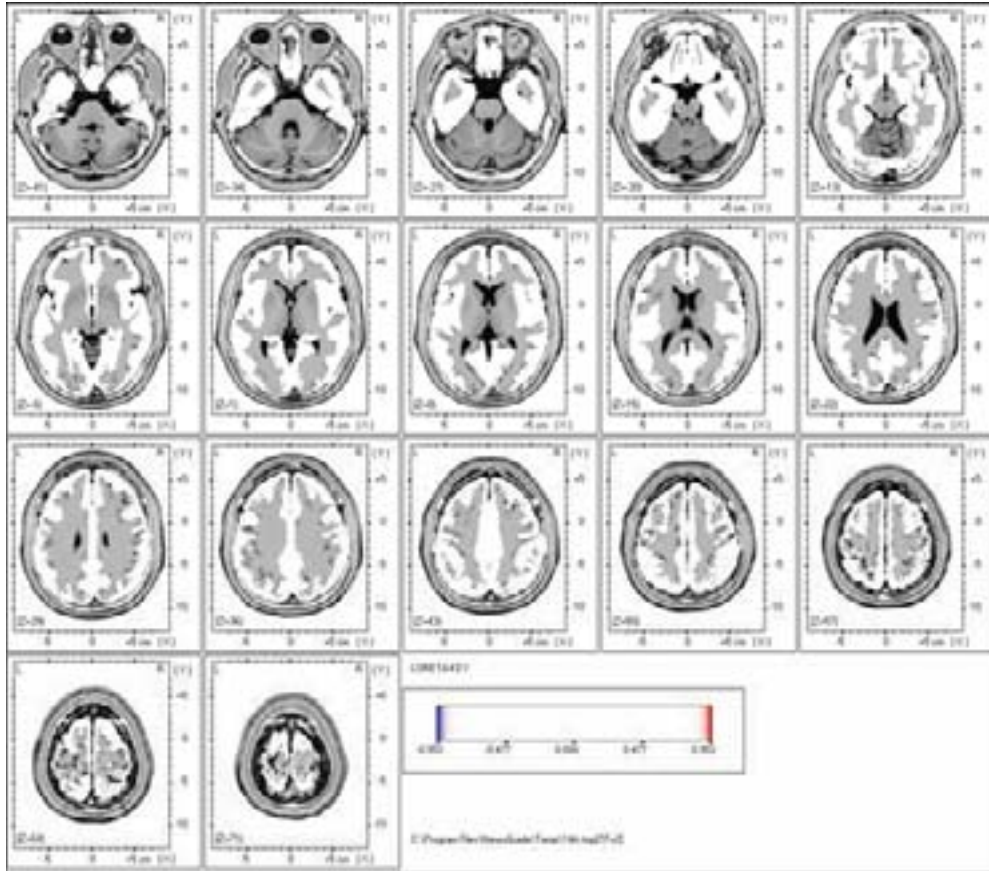


Figure 43. Paired *t*-test for 2 Hz LORETA; No significant differences after 20 minutes of 0.5 Hz CES.

Summary of 3 Hz Changes in Current Density

There were no statistically significant changes in 3 Hz current density from baseline.

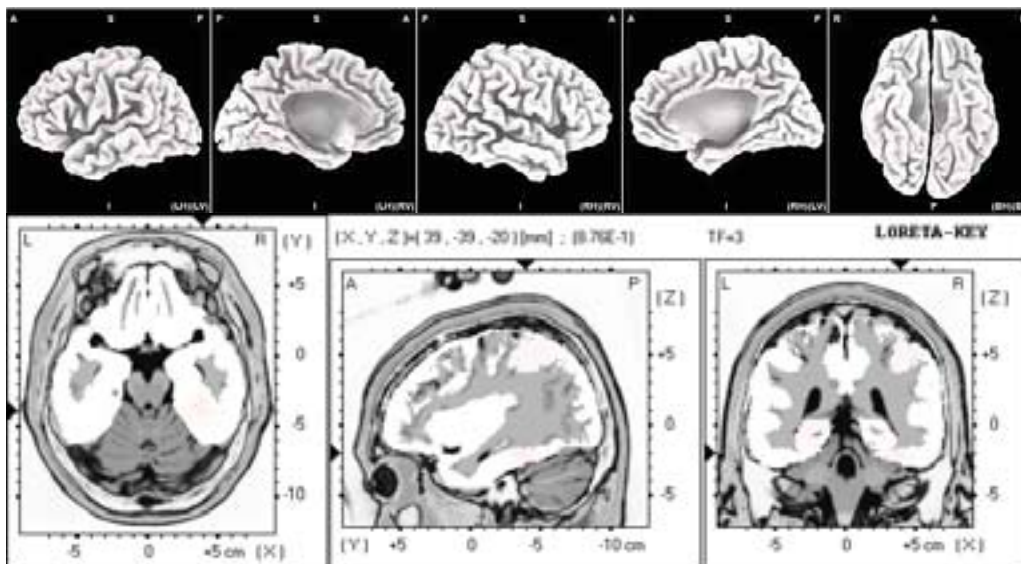


Figure 44. Paired *t*-test for 3 Hz LORETA; Significant differences after 20 minutes of 0.5 Hz CES.

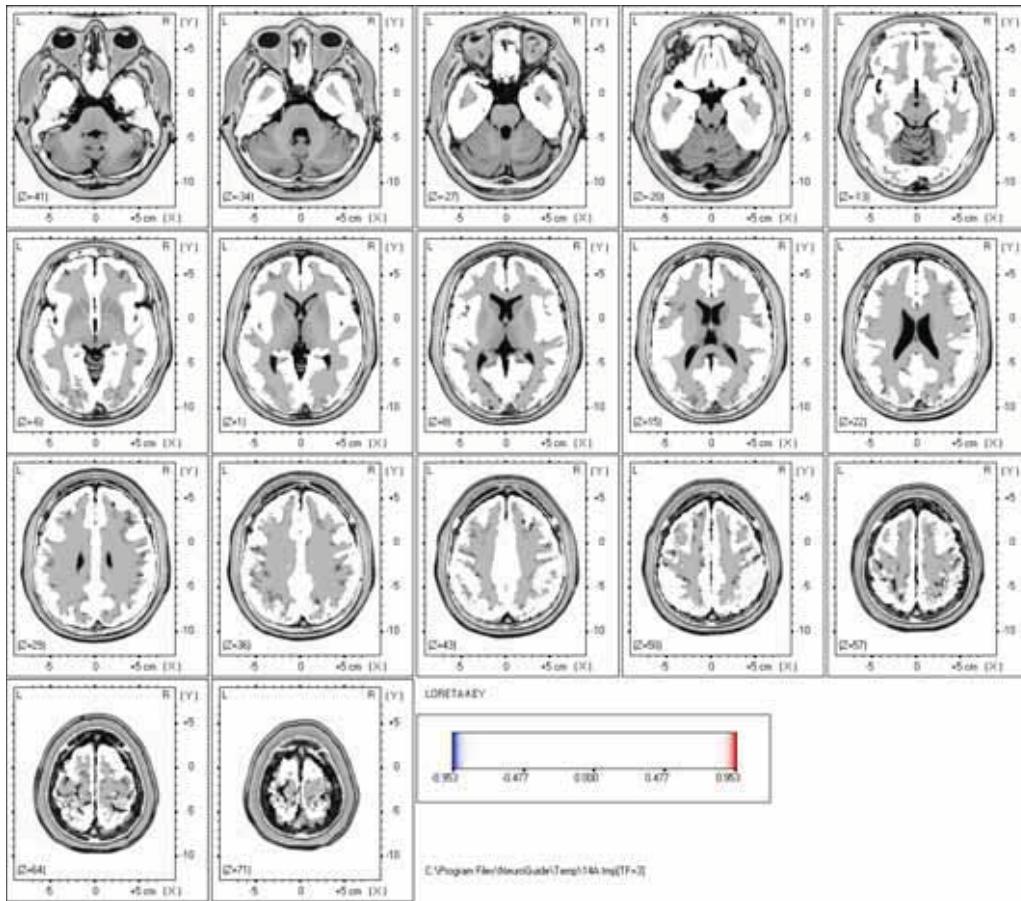


Figure 45. Paired t -test for 3 Hz LORETA; Significant differences after 20 minutes of 0.5 Hz CES.

Summary of 4 Hz Changes in Current Density

There were no statistically significant changes in 4 Hz current density from baseline.

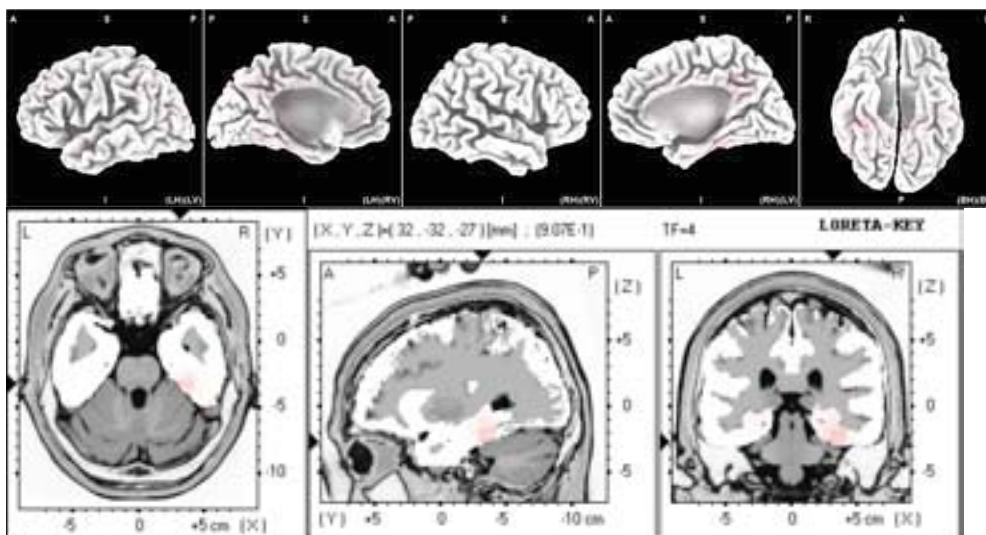


Figure 46. Paired t -test for 4 Hz LORETA; Significant Differences after 20 minutes of 0.5 Hz CES.

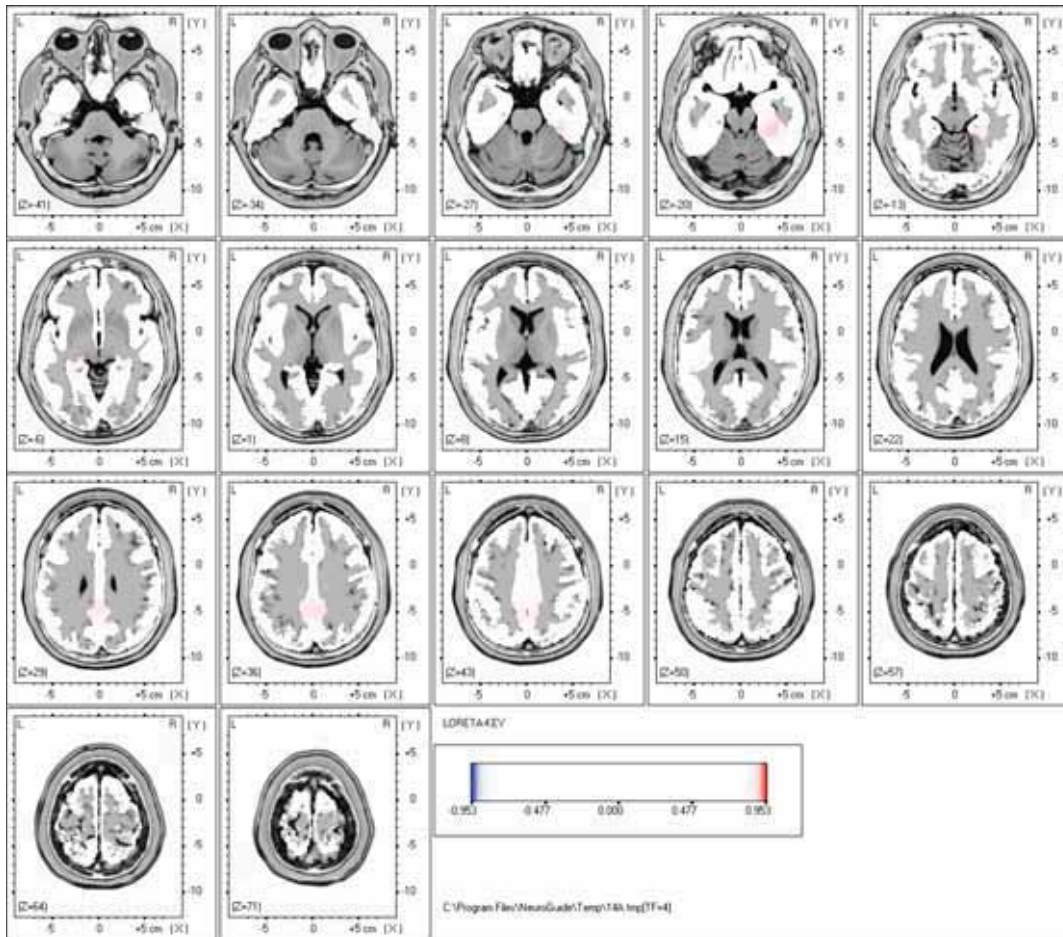


Figure 47. Paired t -test for 4 Hz LORETA; Significant differences after 20 minutes of 0.5 Hz CES.

Summary of 5 Hz Changes in Current Density

Increased Temporal Lobe Activation

- Right Fusiform Gyrus (Brodmann Area 20)

Increased Limbic Lobe Activation

- Right and Left Parahippocampal Gyrus (Brodmann Area 36)
- Right and Left Hippocampus Sub-Gyral
- Left Amygdala
- Left Uncus (Brodmann Area 28)

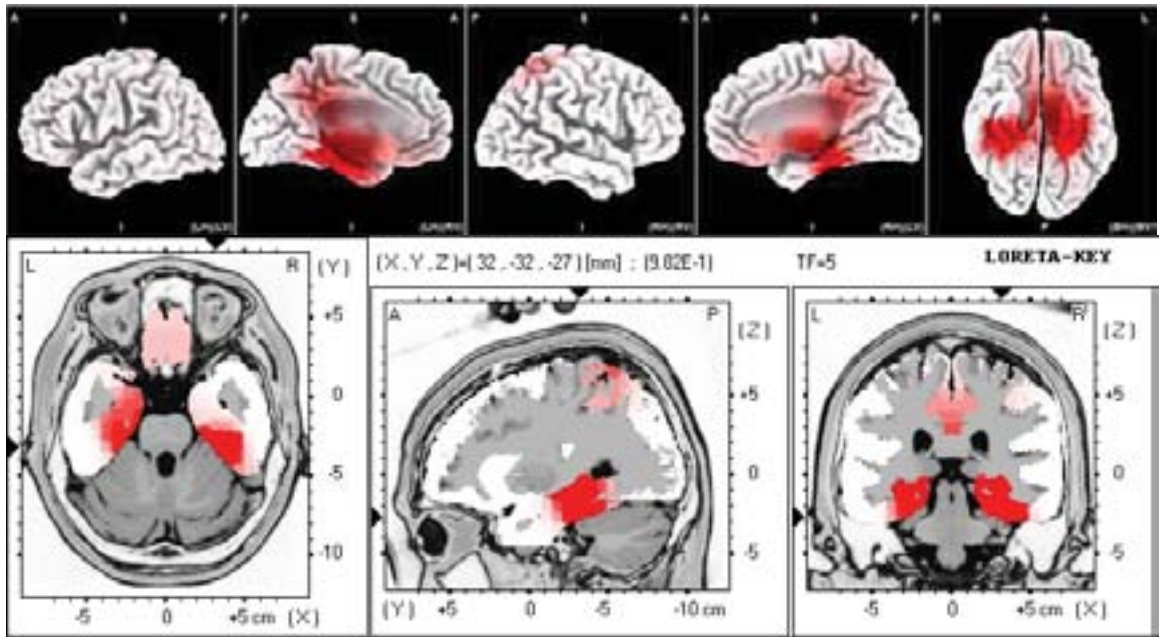


Figure 48. Paired *t*-test for 5 Hz LORETA; Significant differences after 20 minutes of 0.5 Hz CES.

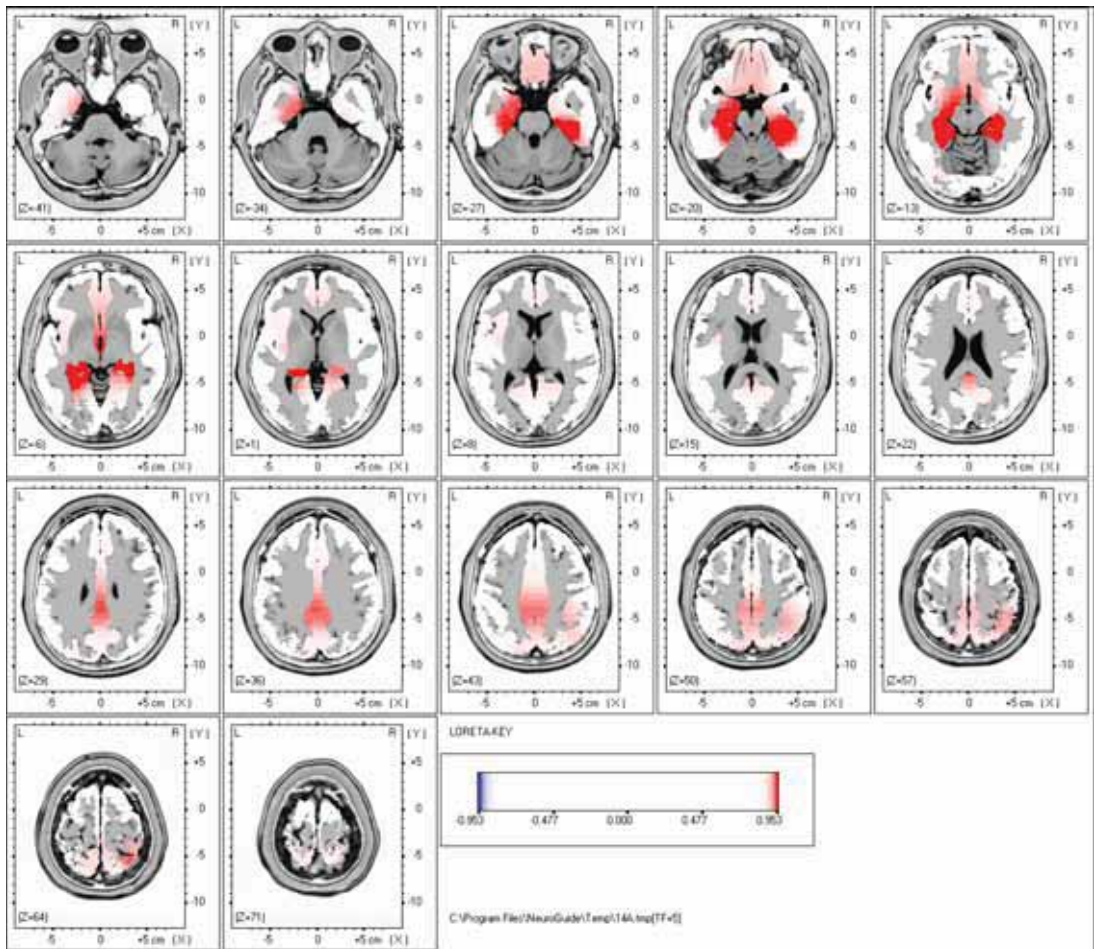


Figure 49. Paired *t*-test for 5 Hz LORETA; Significant differences after 20 minutes of 0.5 Hz CES

Summary of 6 Hz Changes in Current Density

Increased Frontal Lobe Activation

- Right and Left Rectal Gyrus (Brodmann Area 11)
- Right and Left Orbital Gyrus (Brodmann Area 47)
- Right and Left Medial Frontal Gyrus (Brodmann Area 25)

Increased Temporal Lobe Activation

- Right and Left Fusiform Gyrus (Brodmann Area 20)
- Left and Right Inferior Temporal Gyrus (Brodmann Area 37)
- Left and Right Middle Temporal Gyrus (Brodmann Area 37)

Increased Limbic Lobe Activation

- Right and Left Parahippocampal Gyrus (Brodmann Area 36)
- Right and Left Hippocampus Sub-Gyral
- Right and Left Amygdala
- Right and Left Uncus (Brodmann Area 28)
- Right and Left Cingulate Gyrus (Brodmann Area 24)

Increased Parietal Lobe Activation

- Right and Left Precuneus (Brodmann Area 7)
- Right and Left Postcentral Gyrus (Brodmann Area 7)

Right and Left Superior Parietal Lobule (Brodmann Area 7)

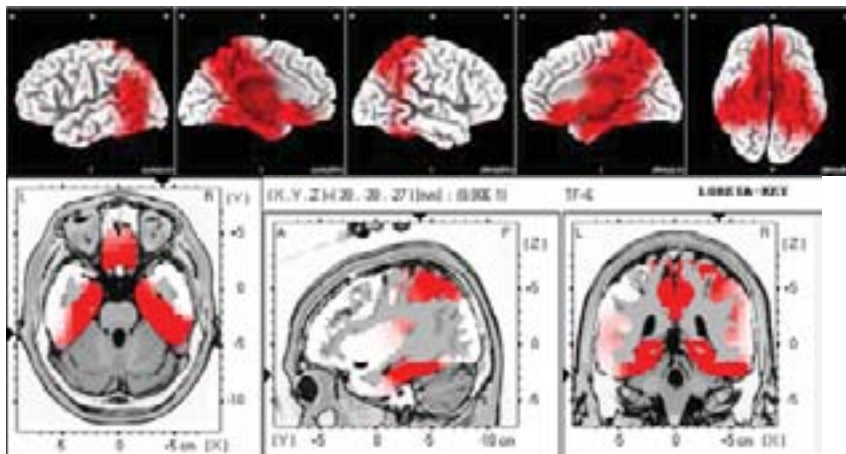


Figure 50. Paired *t*-test for 6 Hz LORETA; Significant differences after 20 minutes of 0.5 Hz CES.

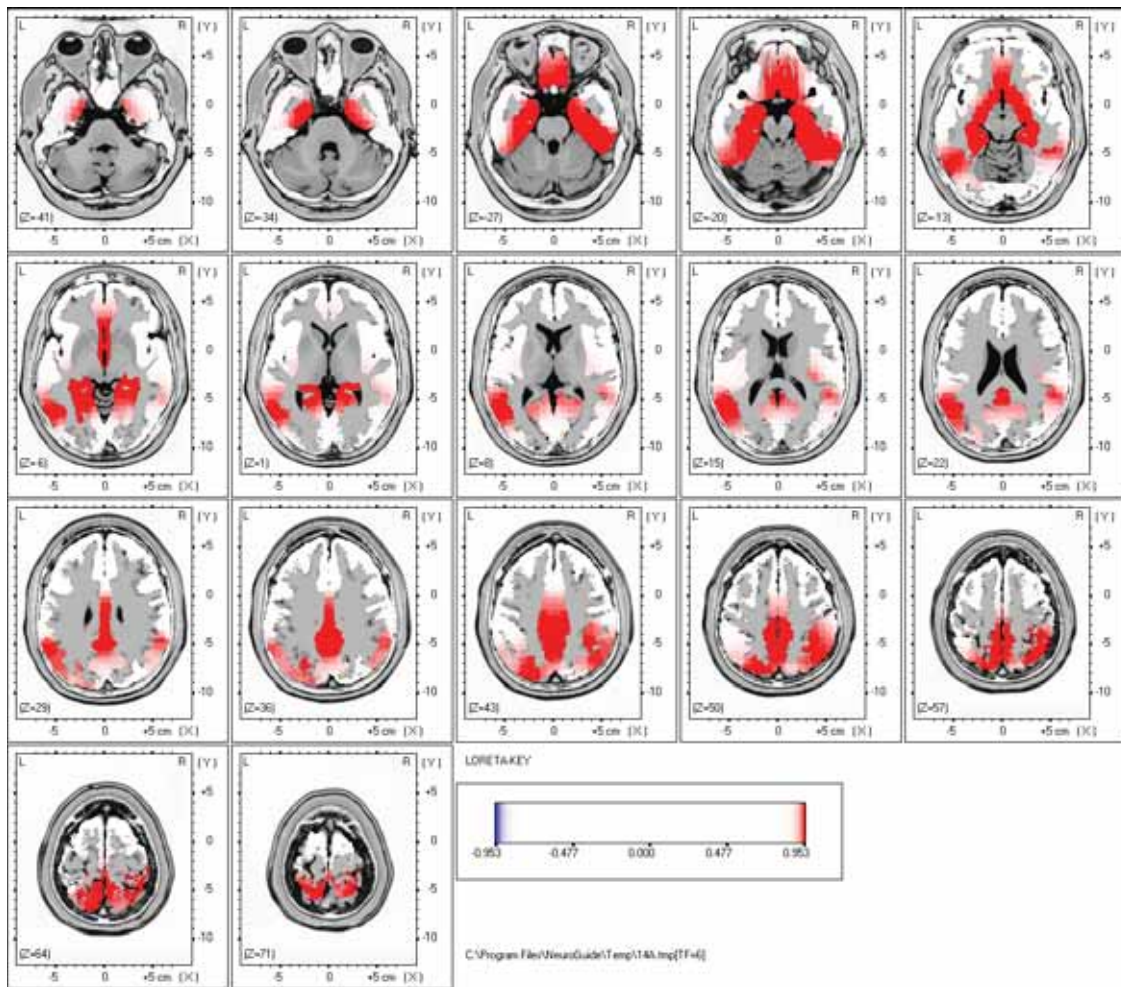


Figure 51. Paired t -test for 6 Hz LORETA; Significant differences after 20 minutes of 0.5 Hz CES

Summary of 7 Hz Changes in Current Density

Increased Frontal Lobe Activation

- Right and Left Rectal Gyrus (Brodmann Area 11)
- Right and Left Orbital Gyrus (Brodmann Area 47)
- Right and Left Superior Frontal Gyrus (Brodmann Area 11)
- Right and Left Inferior Frontal Gyrus (Brodmann Area 11)
- Right and Left Medial Frontal Gyrus (Brodmann Area 10)

Increased Temporal Lobe Activation

- Right and Left Fusiform Gyrus (Brodmann Area 20)
- Left and Right Inferior Temporal Gyrus (Brodmann Area 37)
- Right and Left Superior Temporal Gyrus (Brodmann Area 22)
- Right and Left Transverse Temporal Gyrus (Brodmann Area 41)

Increased Limbic Lobe Activation

- Right and Left Parahippocampal Gyrus (Brodmann Area 36)
- Right and Left Anterior Cingulate (Brodmann Area 32)
- Right and Left Posterior Cingulate (Brodmann Area 30)
- Right and Left Hippocampus Sub-Gyral
- Right and Left Amygdala
- Right and Left Uncus (Brodmann Area 28)
- Right and Left Cingulate Gyrus (Brodmann Area 24)

Increased Parietal Lobe Activation

- Right and Left Precuneus (Brodmann Area 7)
- Right and Left Postcentral Gyrus (Brodmann Area 7)
- Right and Left Superior Parietal Lobule (Brodmann Area 7)
- Right and Left Supramarginal Gyrus (Brodmann Area 40)

Increased Occipital Lobe Activation

- Right and Left Lingual Gyrus (Brodmann Area 30)
- Right and Left Middle Occipital Gyrus (Brodmann Area 19)

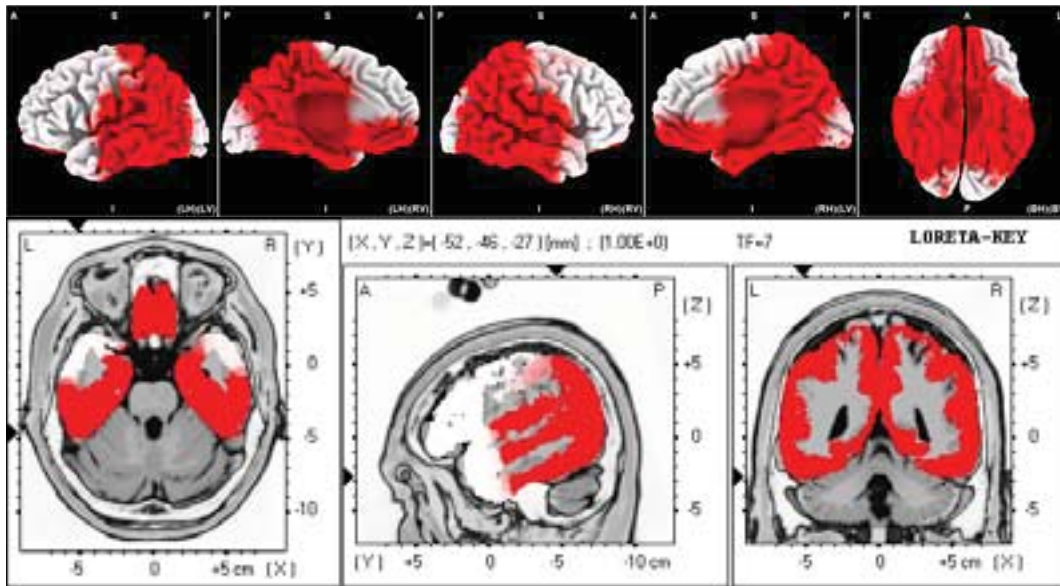


Figure 52. Paired t -test for 7 Hz LORETA; Significant differences after 20 minutes of 0.5 Hz CES.

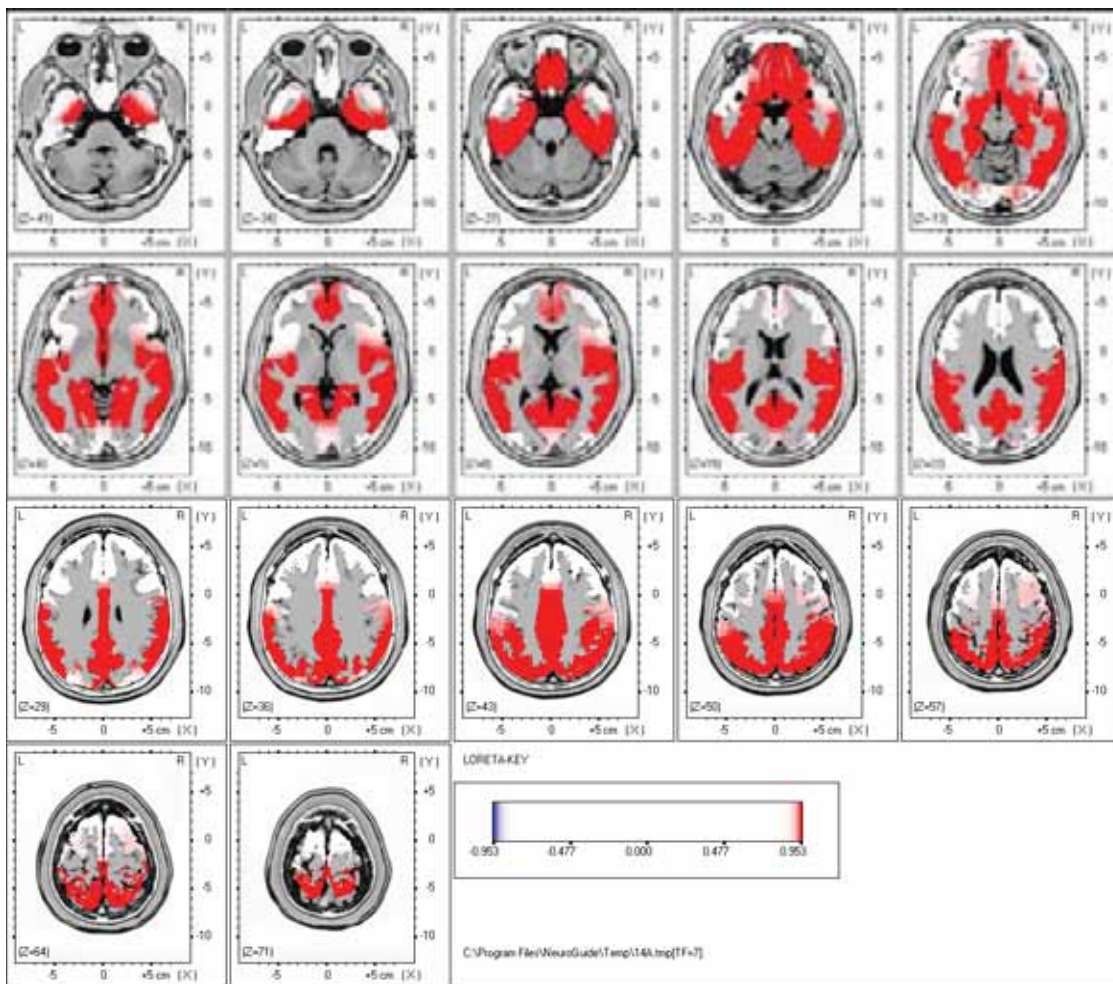


Figure 53. Paired t -test for 7 Hz LORETA: Significant differences after 20 minutes of 0.5 Hz CES.

Summary of 8 Hz Changes in Current Density

Increased Frontal Lobe Activation

- Right and Left Rectal Gyrus (Brodmann Area 11)
- Right and Left Medial Frontal Gyrus (Brodmann Area 11)
- Right and Left Orbital Gyrus (Brodmann Area 47)
- Right and Left Subcallosal Gyrus
- Right and Left Precentral Gyrus (Brodmann Area 6)
- Right Superior Frontal Gyrus (Brodmann Area 11)
- Right Middle Frontal Gyrus (Brodmann Area 9)
- Right Inferior Frontal Gyrus (Brodmann Area 11)
- Right and Left Medial Frontal Gyrus (Brodmann Area 10)

Increased Sub-lobar Activity

- Insula (Brodmann Area 13)
- Extra-Nuclear (Brodmann Area 47)

Increased Temporal Lobe Activation

- Left and Right Inferior Temporal Gyrus (Brodmann Area 37)
- Left and Right Middle Temporal Gyrus (Brodmann Area 37)
- Left and Right Superior Temporal Gyrus (Brodmann Area 22)
- Right and Left Transverse Temporal Gyrus (Area 42)
- Right and Left Sub-Gyral

Increased Limbic Lobe Activation

- Right and Left Parahippocampal Gyrus (Brodmann Area 36)
- Right and Left Anterior Cingulate (Brodmann Area 32)

- Right and Left Posterior Cingulate (Brodmann Area 30)
- Right and Left Hippocampus Sub-Gyral
- Right and Left Amygdala
- Right and Left Uncus (Brodmann Area 28)
- Right and Left Cingulate Gyrus (Brodmann Area 24)

Increased Parietal Lobe Activation

- Right Precuneus (Brodmann Area 7)
- Right Postcentral Gyrus (Brodmann Area 7)
- Right and Left Superior Parietal Lobule (Brodmann Area 7)
- Right and Left Inferior Parietal Lobule (Brodmann Area 40)
- Right and Left Angular Gyrus
- Right and Left Supramarginal Gyrus (Brodmann Area 40)

Increased Occipital Lobe Activation

- Right Cuneus (Brodmann Area 19)
- Right and Left Lingual Gyrus (Brodmann Area 30)
- Right and Left Middle Occipital Gyrus (Brodmann Area 19)
- Right Inferior Occipital Gyrus (Brodmann Area 18)

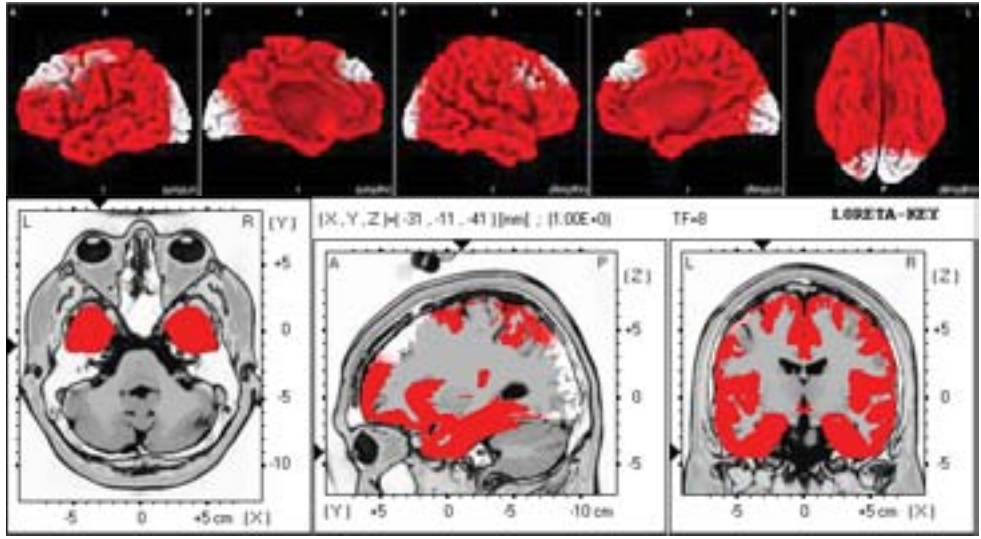


Figure 54. Paired t -test for 8 Hz LORETA: Significant differences after 20 minutes of 0.5 Hz CES.

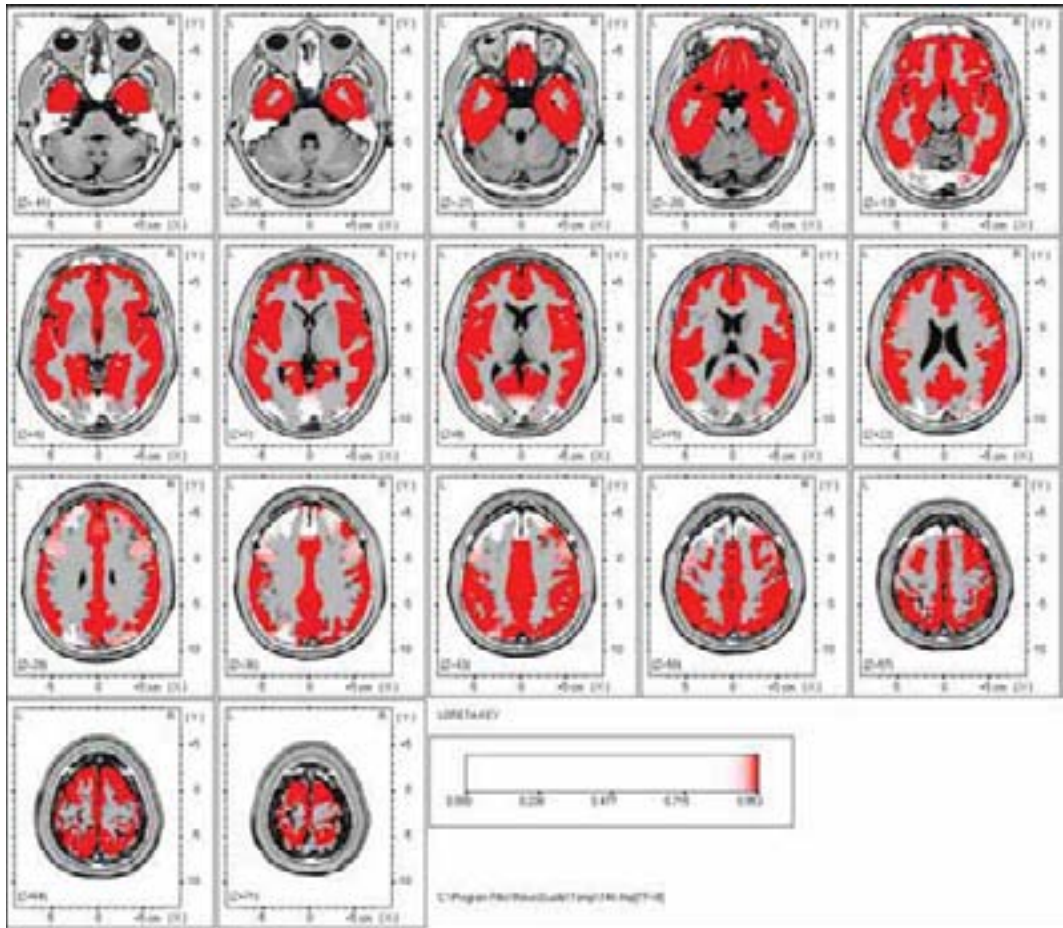


Figure 55. Paired t -test for 8 Hz LORETA: Significant differences after 20 minutes of 0.5 Hz CES.

Summary of 9 Hz Changes in Current Density

Increased Frontal Lobe Activation

- Right and Left Rectal Gyrus (Brodmann Area 11)
- Right and Left Medial Frontal Gyrus (Brodmann Area 11)
- Right and Left Orbital Gyrus (Brodmann Area 47)
- Right and Left Subcallosal Gyrus
- Right Precentral Gyrus (Brodmann Area 6)
- Right Superior Frontal Gyrus (Brodmann Area 11)
- Right Middle Frontal Gyrus (Brodmann Area 9)
- Right Inferior Frontal Gyrus (Brodmann Area 11)
- Right and Left Medial Frontal Gyrus (Brodmann Area 10)

Increased Sub-lobar Activity

- Insula (Brodmann Area 13)
- Extra-Nuclear (Brodmann Area 47)

Increased Temporal Lobe Activation

- Left and Right Inferior Temporal Gyrus (Brodmann Area 37)
- Right Middle Temporal Gyrus (Brodmann Area 37)
- Right Superior Temporal Gyrus (Brodmann Area 22)
- Right and Left Transverse Temporal Gyrus (Area 42)
- Right and Left Sub-Gyral

Increased Limbic Lobe Activation

- Right and Left Parahippocampal Gyrus (Brodmann Area 36)
- Right and Left Anterior Cingulate (Brodmann Area 32)
- Right and Left Posterior Cingulate (Brodmann Area 30)
- Right and Left Hippocampus Sub-Gyral
- Right and Left Amygdala

- Right and Left Uncus (Brodmann Area 28)
- Right and Left Cingulate Gyrus (Brodmann Area 24)

Increased Parietal Lobe Activation

- Right and Left Precuneus (Brodmann Area 7)
- Right Postcentral Gyrus (Brodmann Area 7)
- Right and Left Superior Parietal Lobule (Brodmann Area 7)
- Right and Left Inferior Parietal Lobule (Brodmann Area 40)
- Right and Left Angular Gyrus
- Right and Left Supramarginal Gyrus (Brodmann Area 40)

Increased Occipital Lobe Activation

- Left Cuneus (Brodmann Area 19)
- Right and Left Lingual Gyrus (Brodmann Area 30)
- Right Inferior Occipital Gyrus (Brodmann Area 18)

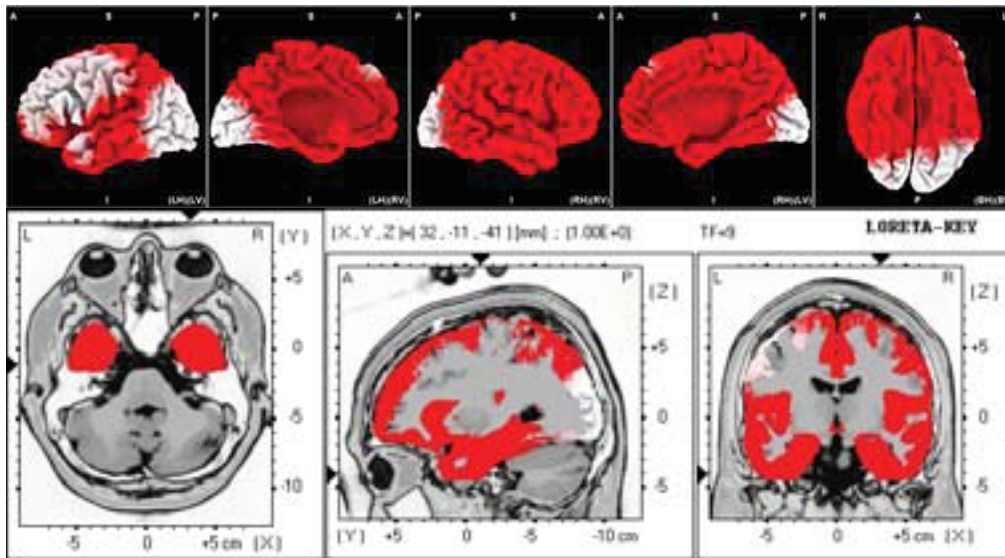


Figure 56. Paired *t*-test for 9 Hz LORETA: Significant differences after 20 minutes of 0.5 Hz CES.

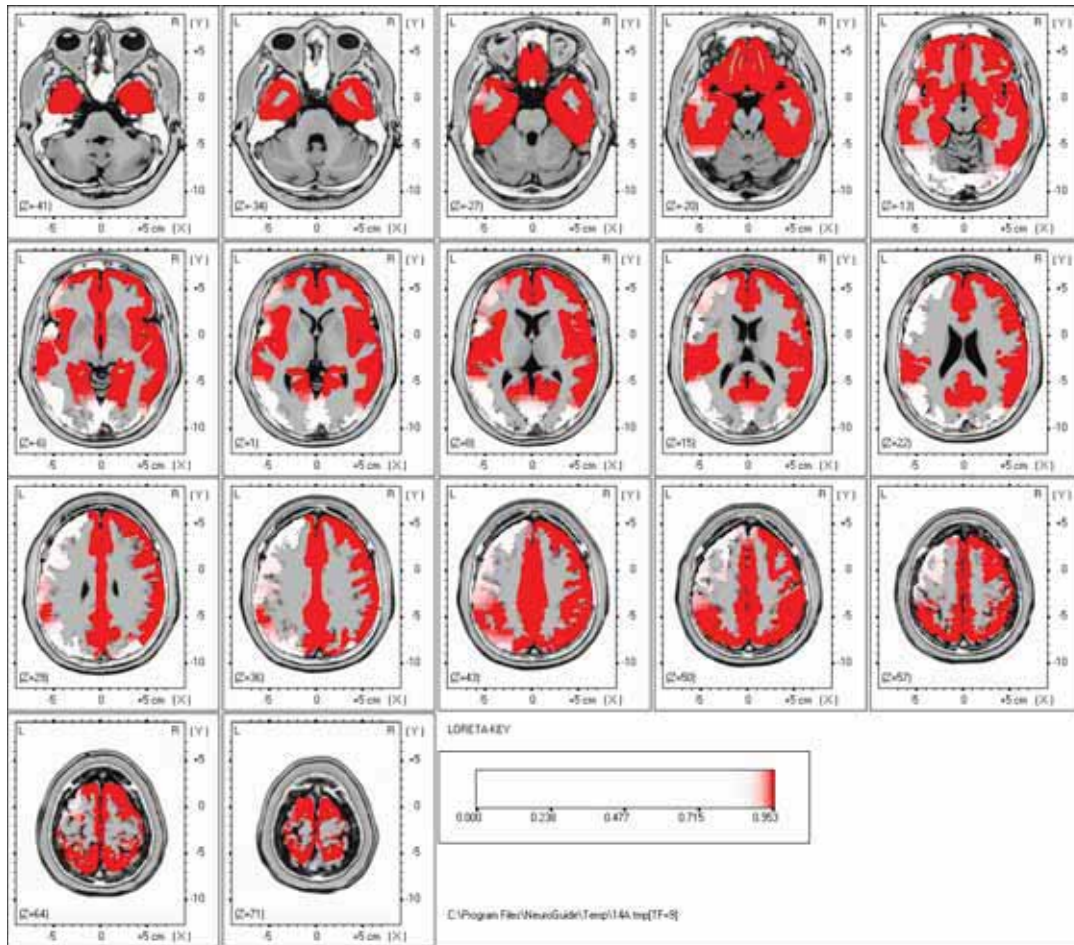


Figure 57. Paired t -test for 9 Hz LORETA: Significant differences after 20 minutes of 0.5 Hz CES.

Summary of 10 Hz Changes in Current Density

Increased Frontal Lobe Activation

- Right and Left Rectal Gyrus (Brodmann Area 11)
- Right and Left Medial Frontal Gyrus (Brodmann Area 11)
- Right and Left Orbital Gyrus (Brodmann Area 47)
- Right and Left Subcallosal Gyrus
- Right Precentral Gyrus (Brodmann Area 6)
- Right and Left Inferior Frontal Gyrus (Brodmann Area 47)
- Right and Left Medial Frontal Gyrus (Brodmann Area 10)

- Right Superior Frontal Gyrus (Brodmann Area 10)

Increased Sub-lobar Activity

- Right Insula (Brodmann Area 13)

Increased Temporal Lobe Activation

- Right Inferior Temporal Gyrus (Brodmann Area 37)
- Right Middle Temporal Gyrus (Brodmann Area 37)
- Right Superior Temporal Gyrus (Brodmann Area 22)
- Right and Left Transverse Temporal Gyrus (Area 42)
- Right and Left Sub-Gyral

Increased Limbic Lobe Activation

- Right and Left Anterior Cingulate (Brodmann Area 32)
- Right and Left Posterior Cingulate (Brodmann Area 30)
- Right Fusiform Gyrus (Brodmann Area 37)
- Right Hippocampus Sub-Gyral
- Right Amygdala
- Right Uncus (Brodmann Area 28)

Increased Parietal Lobe Activation

- Right and Left Precuneus (Brodmann Area 7)
- Right Postcentral Gyrus (Brodmann Area 7)
- Right and Left Superior Parietal Lobule (Brodmann Area 7)
- Right and Left Inferior Parietal Lobule (Brodmann Area 40)
- Right and Left Angular Gyrus
- Right and Left Supramarginal Gyrus (Brodmann Area 40)

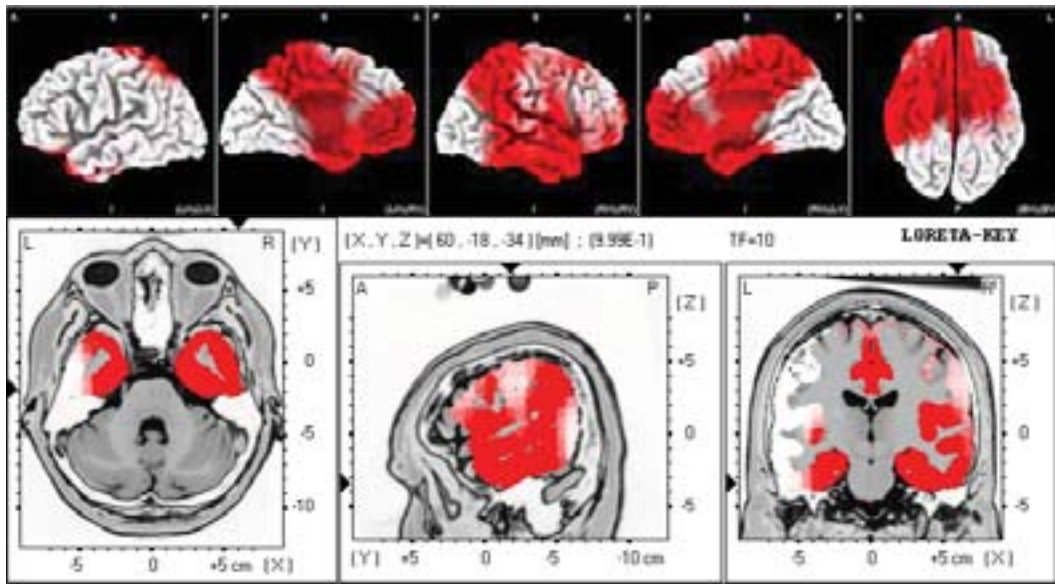


Figure 58. Paired t -test for 10 Hz LORETA: Significant differences after 20 minutes of 0.5 Hz CES.

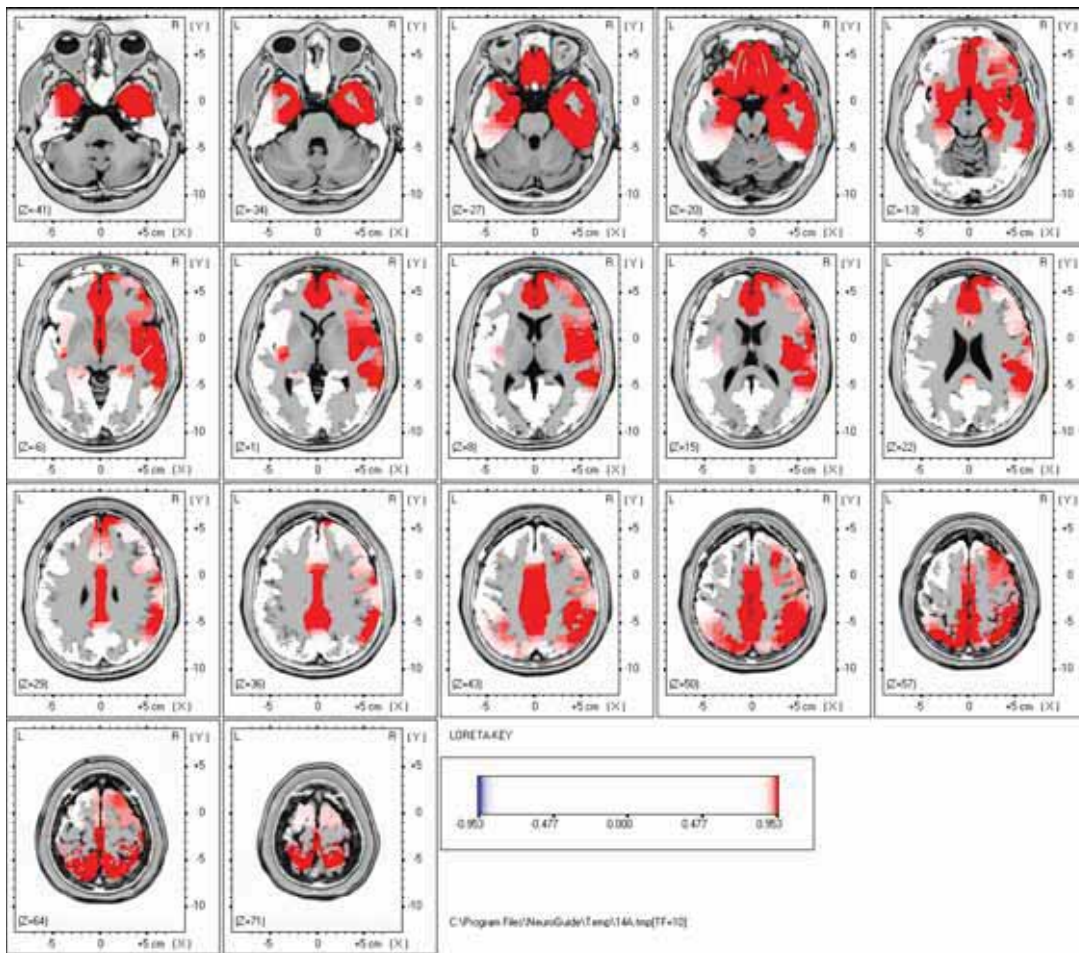


Figure 59. Paired t -test for 10 Hz LORETA: Significant differences after 20 minutes of 0.5 Hz CES.

Summary of 11 Hz Changes in Current Density

Increased Frontal Lobe Activation

- Right Precentral Gyrus (Brodmann Area 6)

Increased Sub-lobar Activity

- Right Insula (Brodmann Area 13)

Increased Temporal Lobe Activation

- Right Inferior Temporal Gyrus (Brodmann Area 37)
- Right Middle Temporal Gyrus (Brodmann Area 37)
- Right Superior Temporal Gyrus (Brodmann Area 22)

Increased Parietal Lobe Activation

- Right Postcentral Gyrus (Brodmann Area 7)
- Right Inferior Parietal Lobule (Brodmann Area 40)

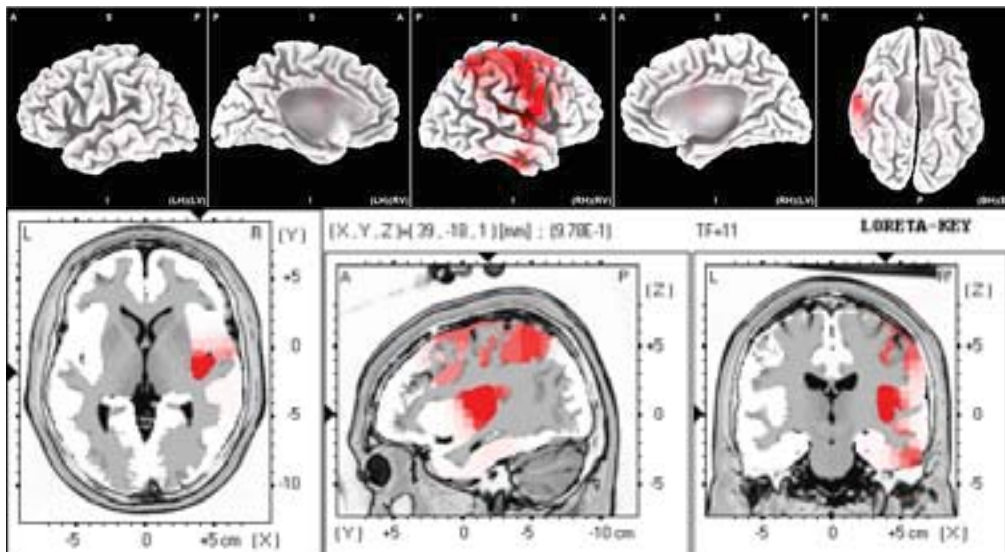


Figure 60. Paired *t*-test for 11 Hz LORETA: Significant differences after 20 minutes of 0.5 Hz CES.

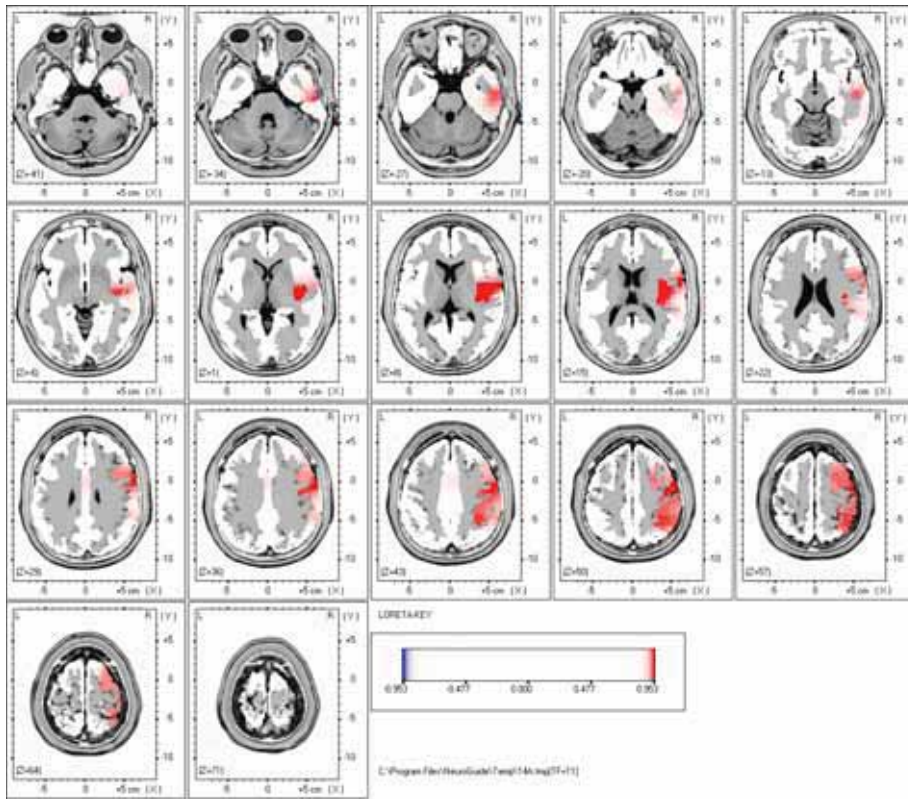


Figure 61. Paired t -test for 11 Hz LORETA: Significant differences after 20 minutes of 0.5 Hz CES.

Summary of 12 Hz Changes in Current Density

Increased Limbic Lobe Activation

- Right Parahippocampal Gyrus (Brodmann Area 36)
- Right and Left Cingulate Gyrus (Brodmann Area 24)

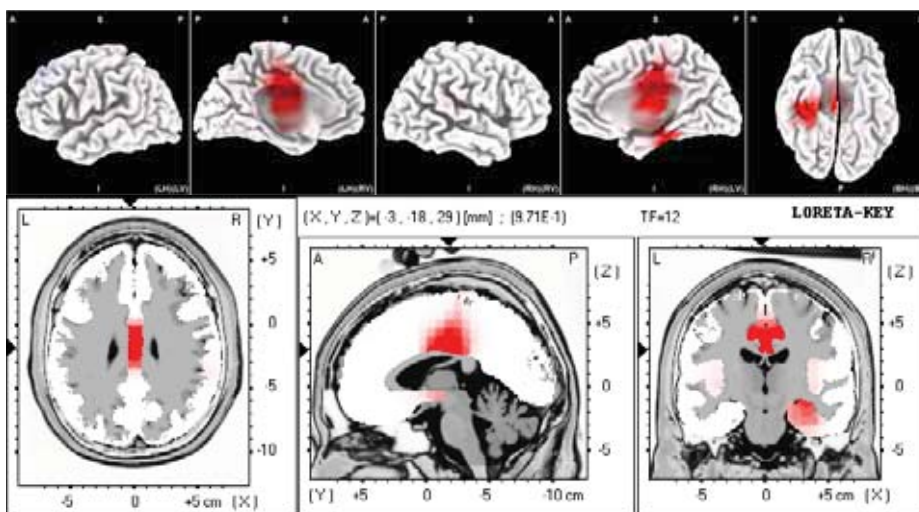


Figure 62. Paired t -test for 12 Hz LORETA: Significant differences after 20 minutes of 0.5 Hz CES.

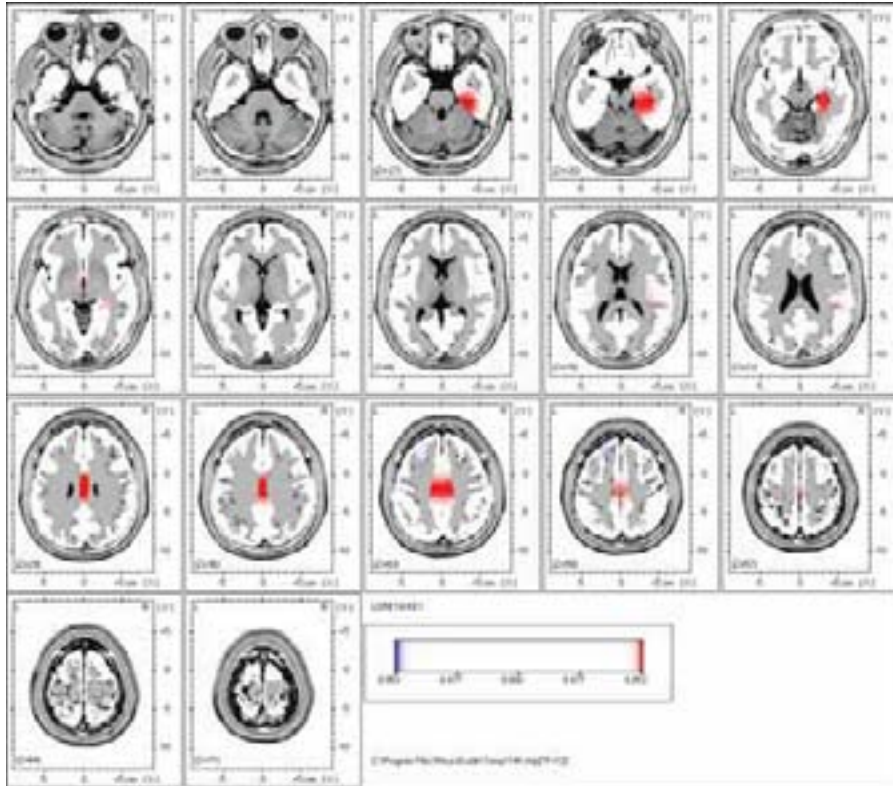


Figure 63. Paired t -test for 12 Hz LORETA: Significant differences after 20 minutes of 0.5 Hz CES.

Summary of 13 Hz Changes in Current Density

Increased Limbic Lobe Activation

- Right Parahippocampal Gyrus (Brodmann Area 36)
- Right Fusiform Gyrus (Brodmann Area 37)
- Right Uncus (Brodmann Area 28)

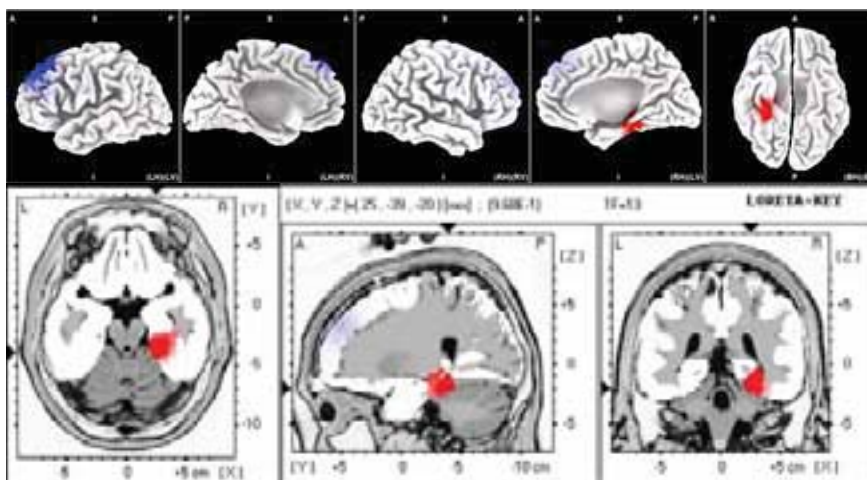


Figure 64. Paired t -test for 13 Hz LORETA: Significant differences after 20 minutes of 0.5 Hz CES.

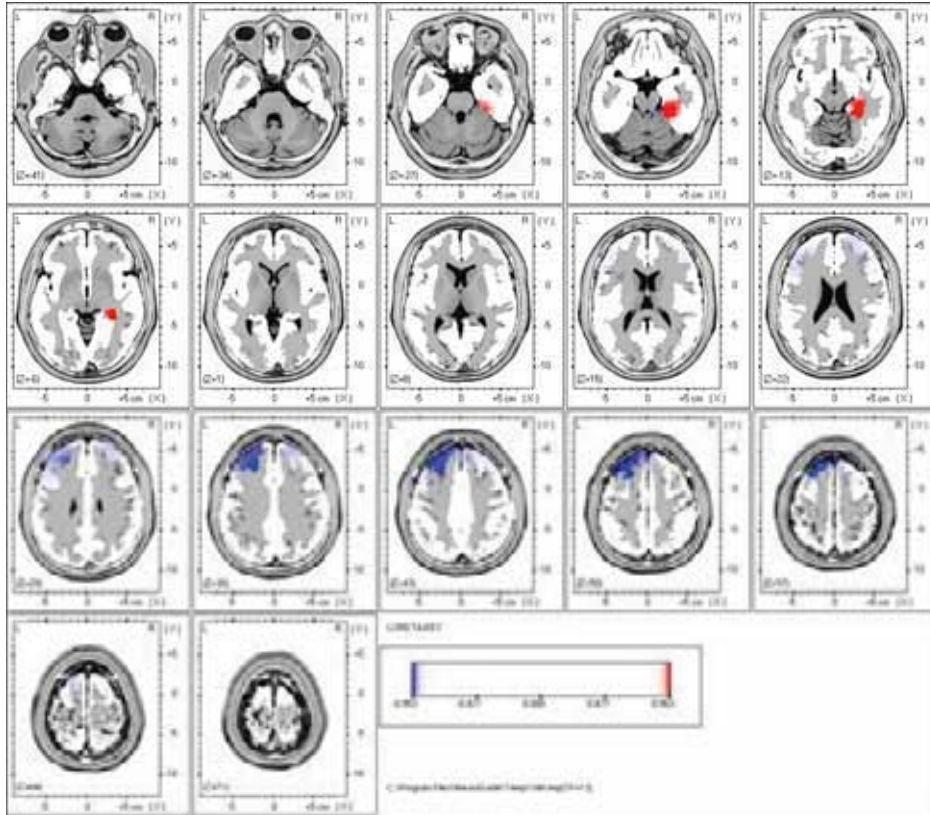


Figure 65. Paired t -test for 13 Hz LORETA: Significant differences after 20 minutes of 0.5 Hz CES.

Summary of 14 Hz Changes in Current Density

Increased Limbic Lobe Activation

- Right and Left Cingulate (Brodmann Area 23)
- Posterior Cingulate (Brodmann Area 29)
- Right and Left Parahippocampal Gyrus (Brodmann Area 36)
- Left Fusiform Gyrus (Brodmann Area 37)

Increased Temporal Lobe Activation

- Hippocampus Sub-Gyral

Increased Parietal Lobe Activation

- Right and Left Precuneus (Brodmann Area 31)

Decreased Frontal Lobe Activation

- Superior Frontal Gyrus (Brodmann Area 9)
- Middle Frontal Gyrus (Brodmann Area 9)

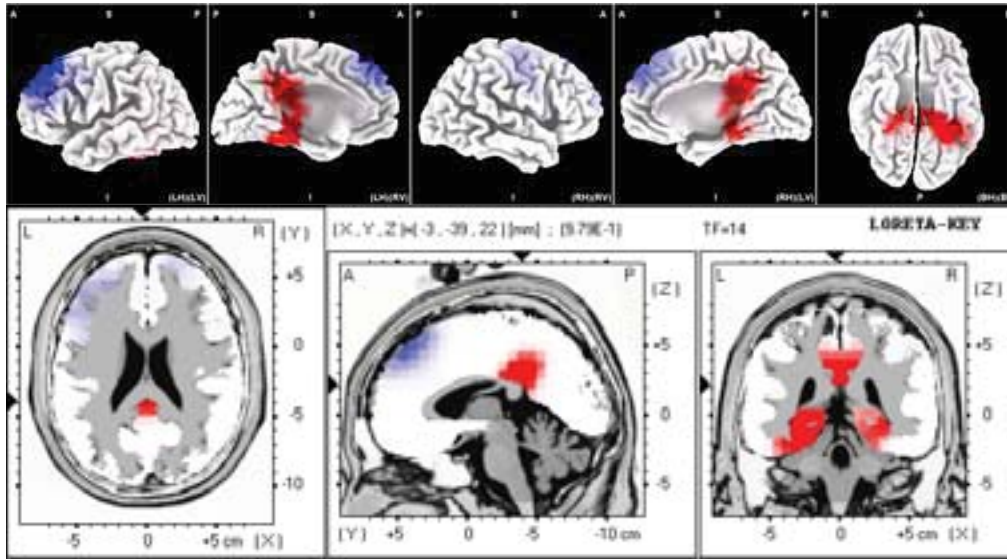


Figure 66. Paired t -test for 14 Hz LORETA: Significant differences after 20 minutes of 0.5 Hz CES.

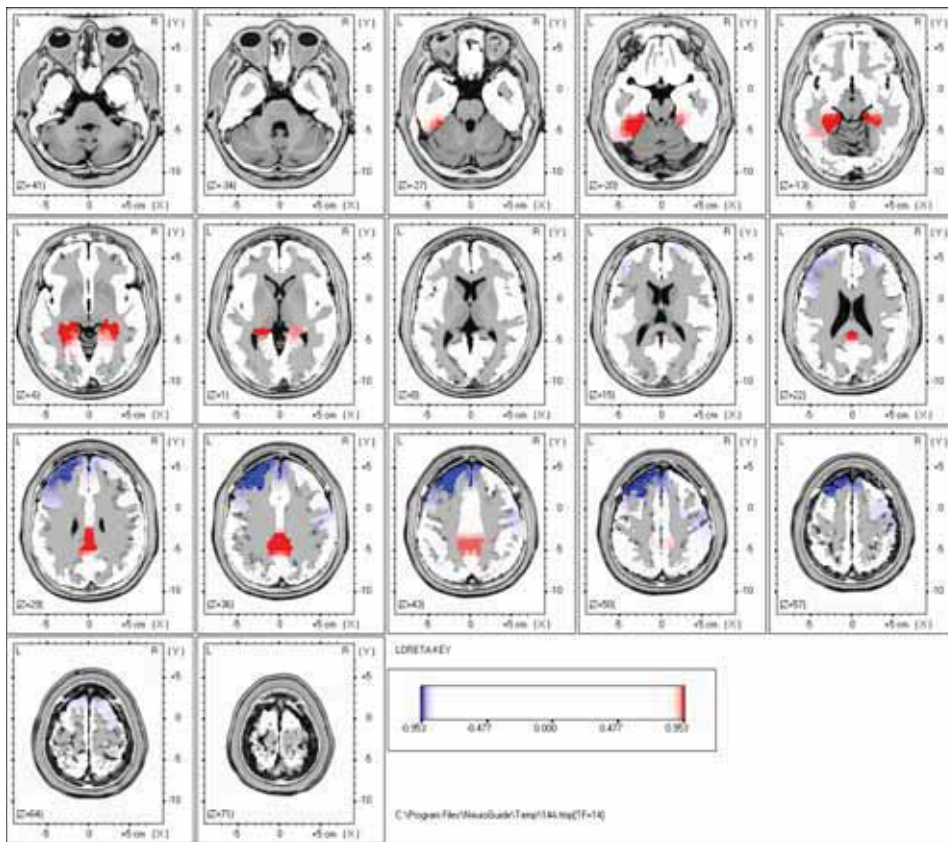


Figure 67. Paired t -test for 14 Hz LORETA: Significant differences after 20 minutes of 0.5 Hz CES.

Summary of 15 Hz Changes in Current Density

Increased Limbic Lobe Activation

- Right and Left Parahippocampal Gyrus (Brodmann Area 36)
- Right and Left Hippocampus (Sub-Gyral)
- Left and Right Cingulate Gyrus (Brodmann Area 31)

Increased Occipital Lobe Activation

- Left Lingual Gyrus (Brodmann Area 19)

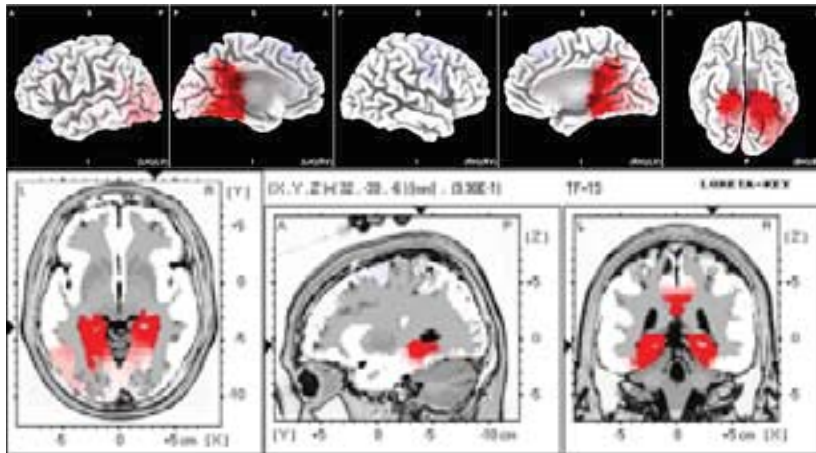


Figure 68. Paired t -test for 15 Hz LORETA: Significant differences after 20 minutes of 0.5 Hz CES.

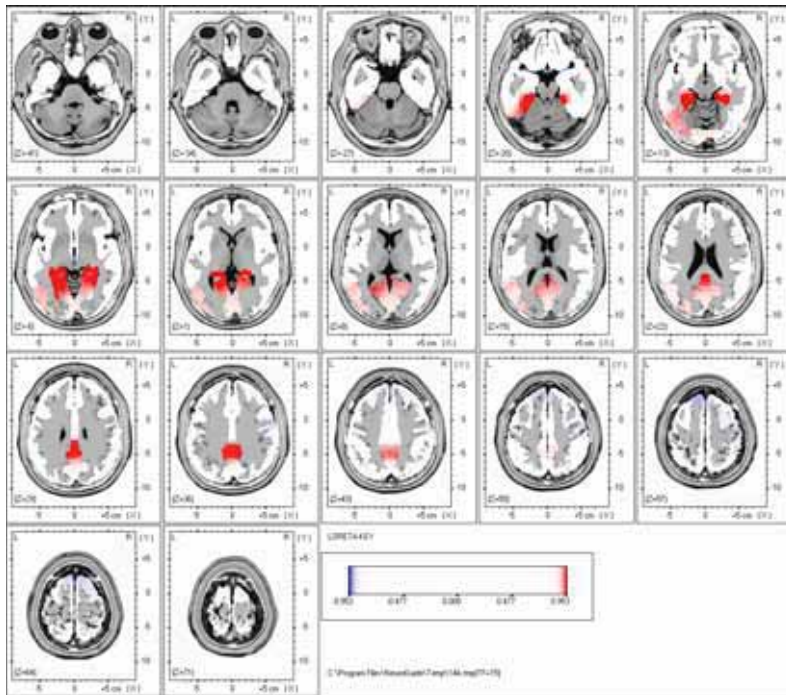


Figure 69. Paired t -test for 15 Hz LORETA: Significant differences after 20 minutes of 0.5 Hz CES.

Summary of 16 Hz Changes in Current Density

Increased Limbic Lobe Activation

- Right and Left Parahippocampal Gyrus (Brodmann Area 36)
- Right and Left Hippocampus (Sub-Gyral)

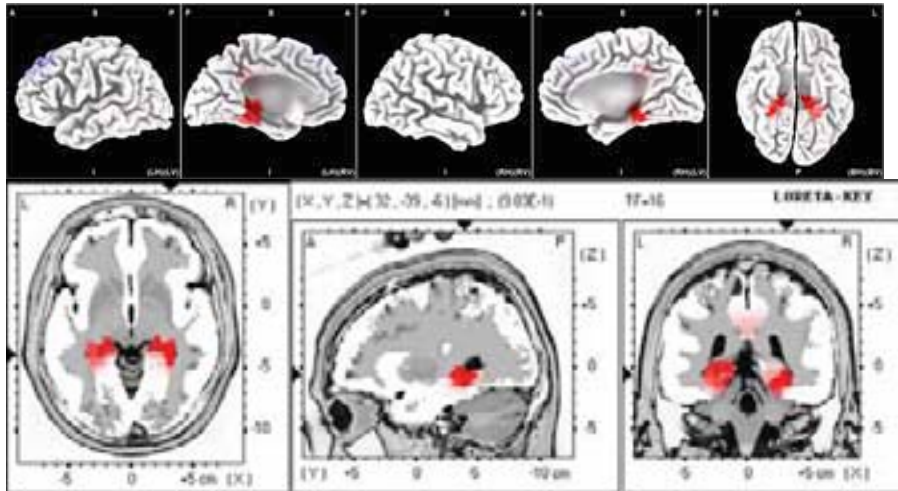


Figure 70. Paired t -test for 16 Hz LORETA: Significant differences after 20 minutes of 0.5 Hz CES.

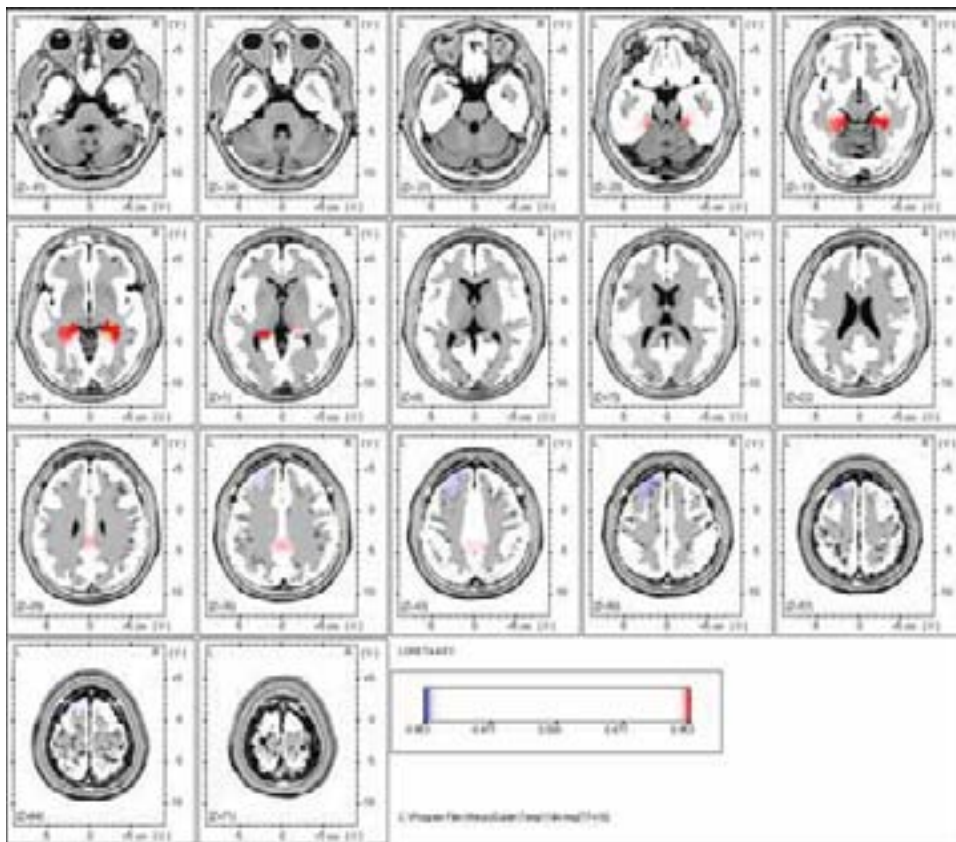


Figure 71. Paired t -test for 16 Hz LORETA: Significant differences after 20 minutes of 0.5 Hz CES.

Summary of 17 Hz Changes in Current Density

Increased Limbic Lobe Activation

- Right Parahippocampal Gyrus (Brodmann Area 36)
- Right Hippocampus (Sub-Gyral)

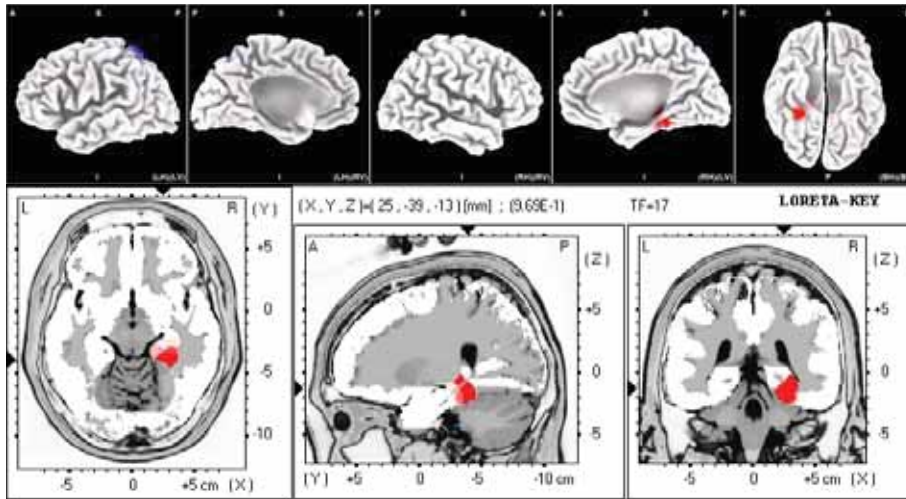


Figure 72. Paired *t*-test for 17 Hz LORETA: Significant differences after 20 minutes of 0.5 Hz CES.

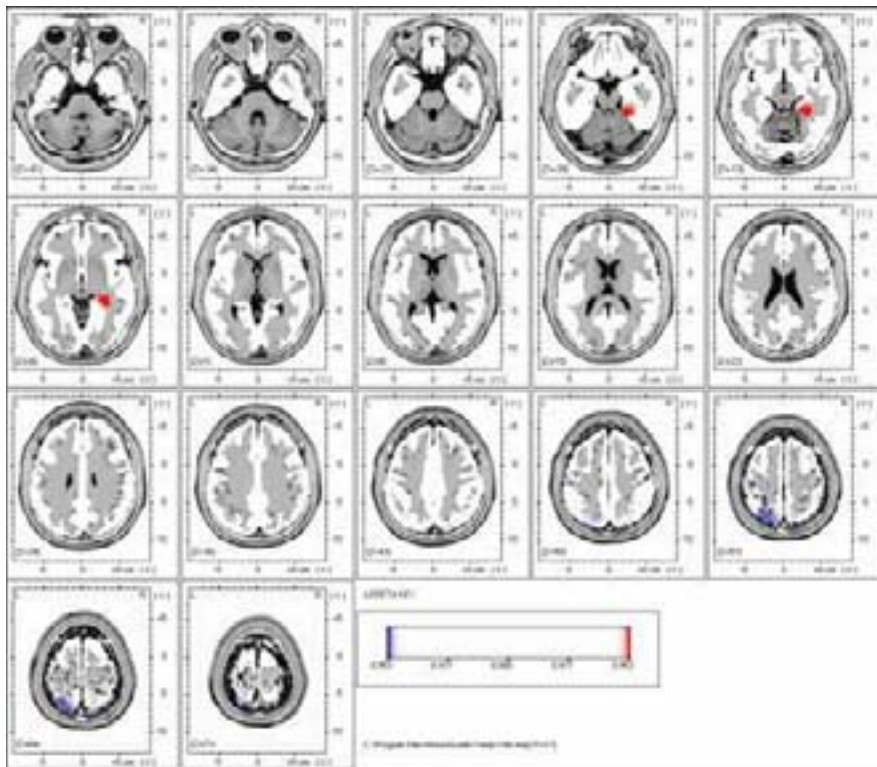


Figure 73. Paired *t*-test for 17 Hz LORETA: Significant differences after 20 minutes of 0.5 Hz CES.

Summary of 18 Hz Changes in Current Density

Increased Limbic Lobe Activation

- Right Parahippocampal Gyrus (Brodmann Area 36)
- Right Hippocampus (Sub-Gyral)

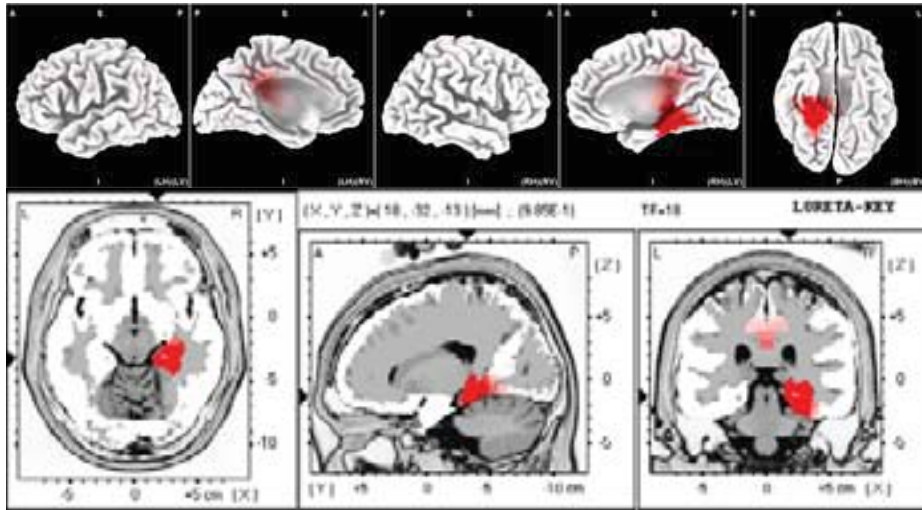


Figure 74. Paired t -test for 18 Hz LORETA: Significant differences after 20 minutes of 0.5 Hz CES.

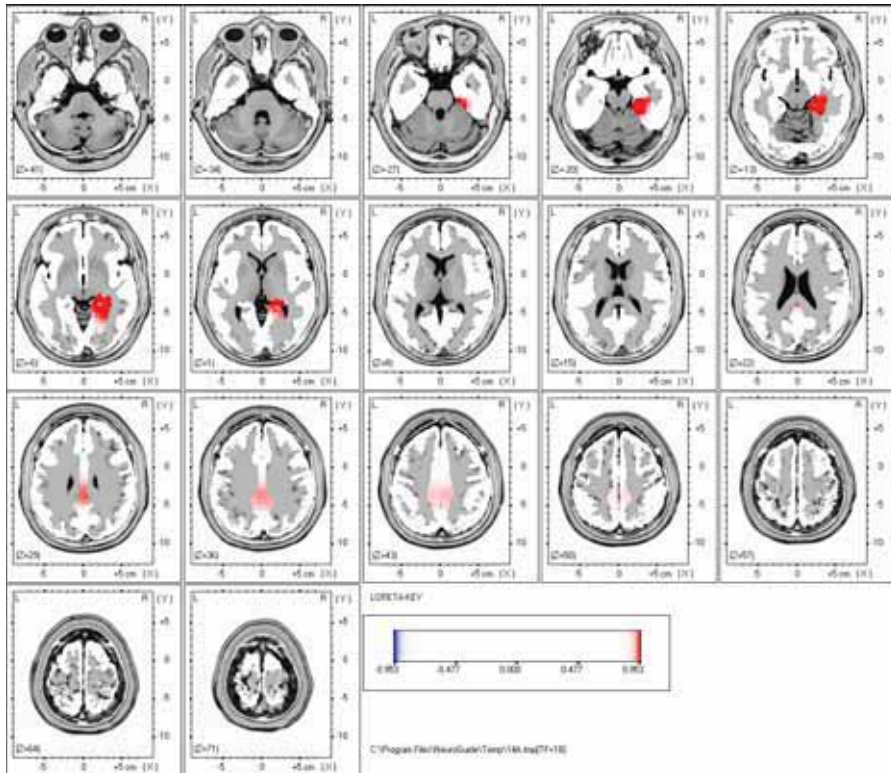


Figure 75. Paired t -test for 18 Hz LORETA: Significant differences after 20 minutes of 0.5 Hz CES.

Summary of 19 Hz Changes in Current Density

Increased Temporal Lobe Activation

- Fusiform Gyrus (Brodmann Area 20)
- Hippocampus (Sub-Gyral)

Increased Limbic Lobe Activation

- Parahippocampal Gyrus (Brodmann Area 36)

Decreased Parietal Lobe Activation

- Left Superior Parietal Lobule (Brodmann Area 7)
- Left Inferior Parietal Lobule (Brodmann Area 39)
- Left Precuneus (Brodmann Area 19)

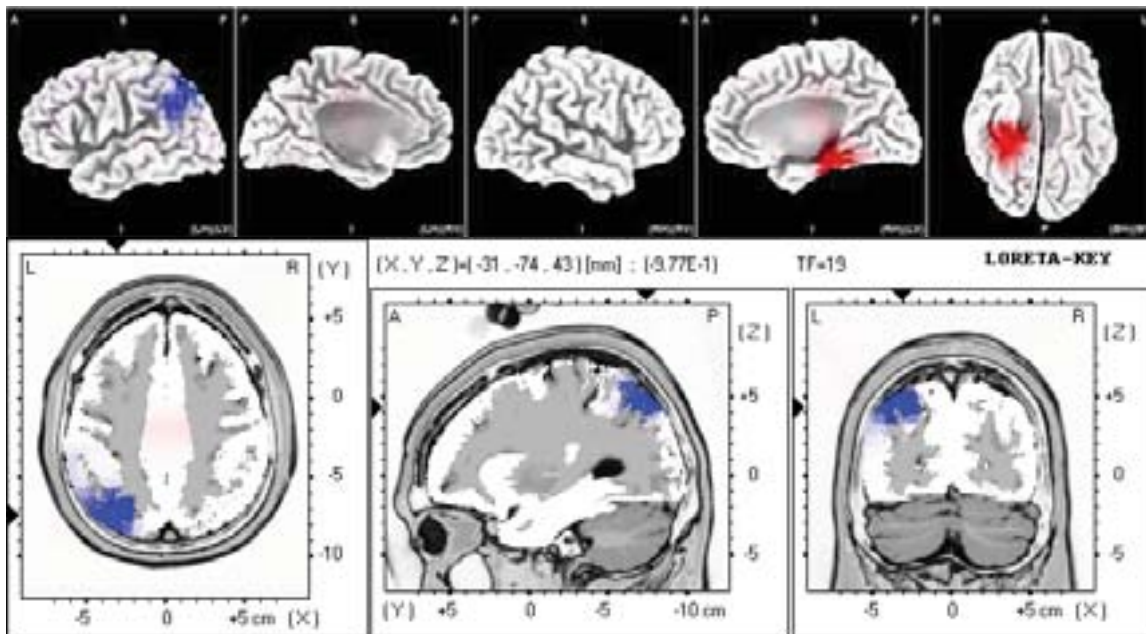


Figure 76. Paired *t*-test for 19 Hz LORETA: Significant differences after 20 minutes of 0.5 Hz CES.

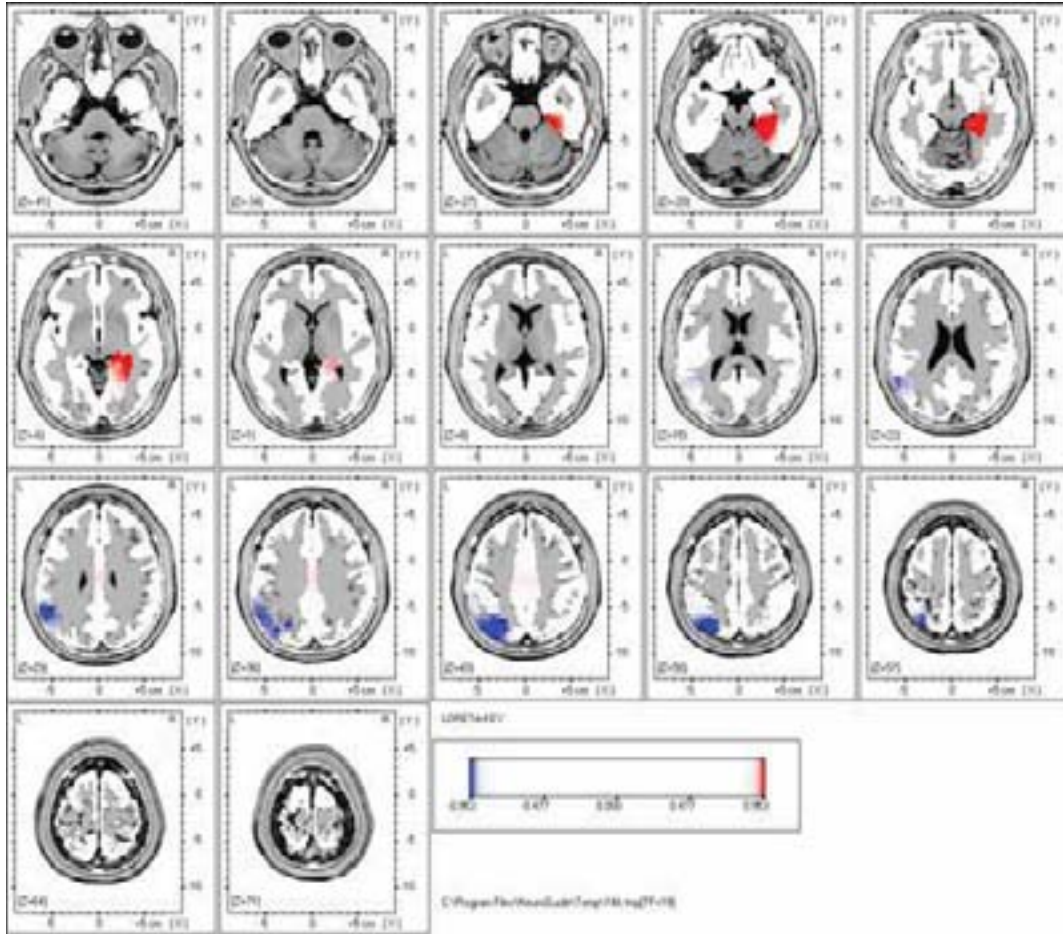


Figure 77. Paired t -test for 19 Hz LORETA: Significant differences after 20 minutes of 0.5 Hz CES.

Summary of 20 Hz Changes in Current Density

Decreased Parietal Lobe Activation

- Supramarginal Gyrus (Brodmann Area 40)
- Left Superior Parietal Lobule (Brodmann Area 7)
- Left Inferior Parietal Lobule (Brodmann Area 39)
- Left Angular Gyrus (Brodmann Area 39)
- Left Precuneus (Brodmann Area 19)

Decreased Temporal Lobe Activation

- Left Middle Temporal Gyrus

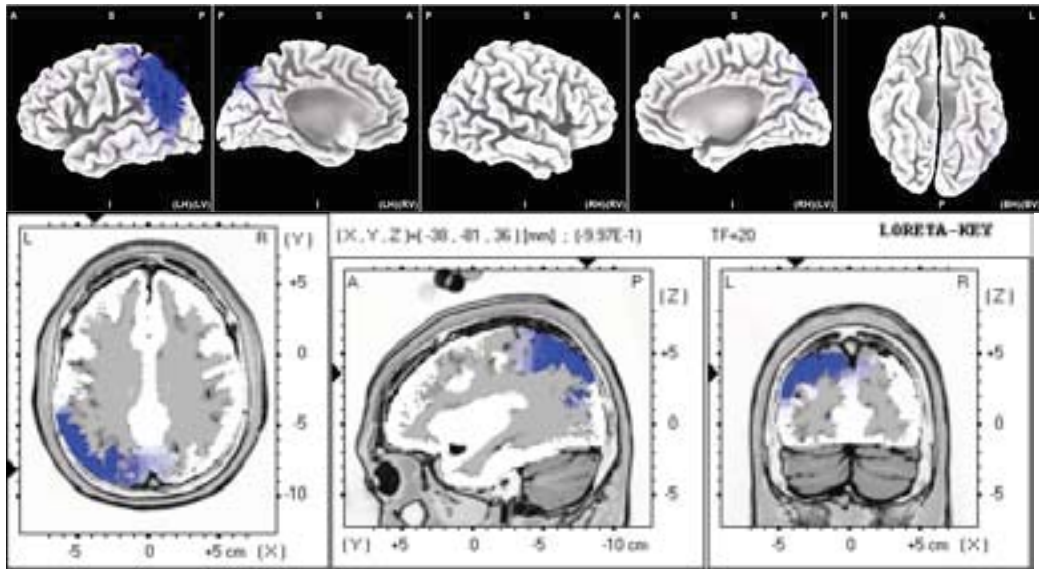


Figure 78. Paired t -test for 20 Hz LORETA: Significant differences after 20 minutes of 0.5 Hz CES.

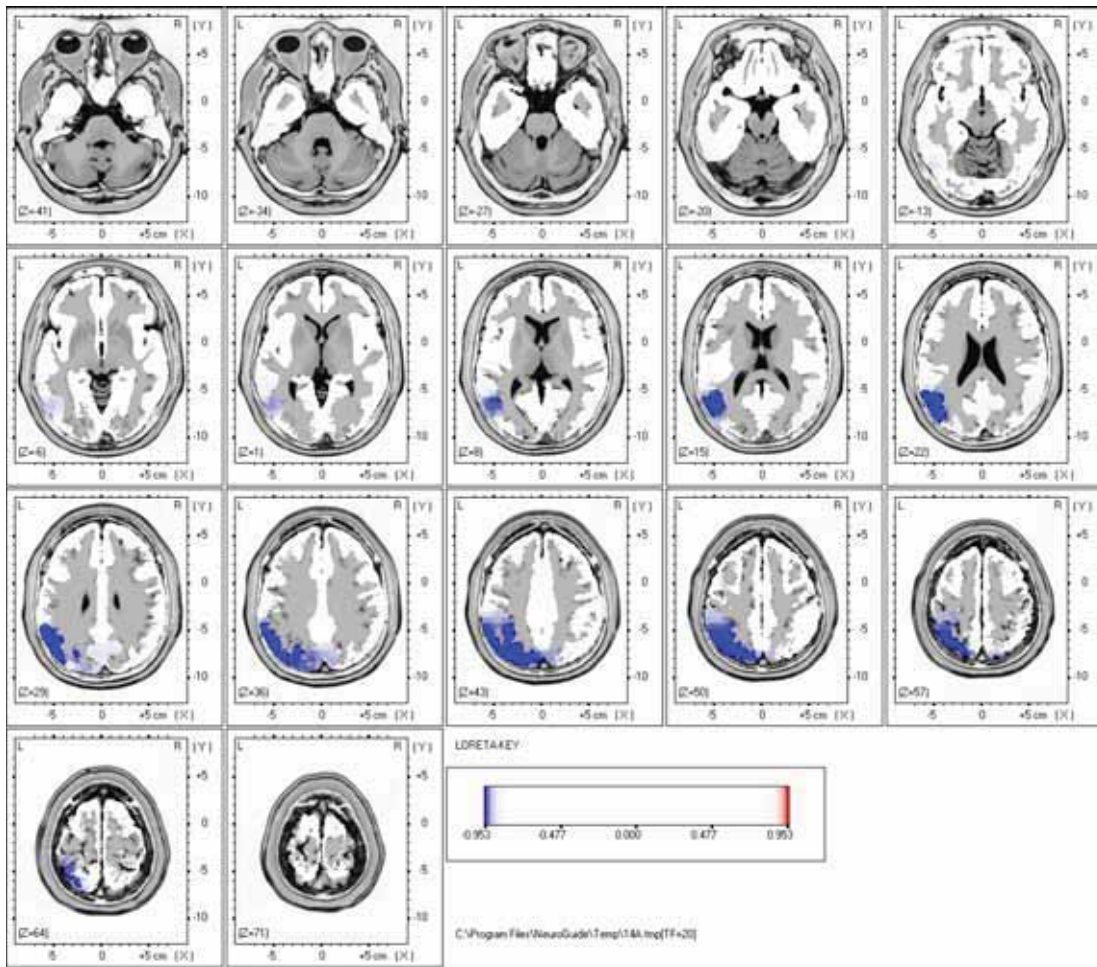


Figure 79. Paired t -test for 20 Hz LORETA: Significant differences after 20 minutes of 0.5 Hz CES.

Summary of 22 Hz Changes in Current Density

Decreased Parietal Lobe Activation

- Supramarginal Gyrus (Brodmann Area 40)
- Left Superior Parietal Lobule (Brodmann Area 7)
- Left Inferior Parietal Lobule (Brodmann Area 39)
- Left Precuneus (Brodmann Area 19)

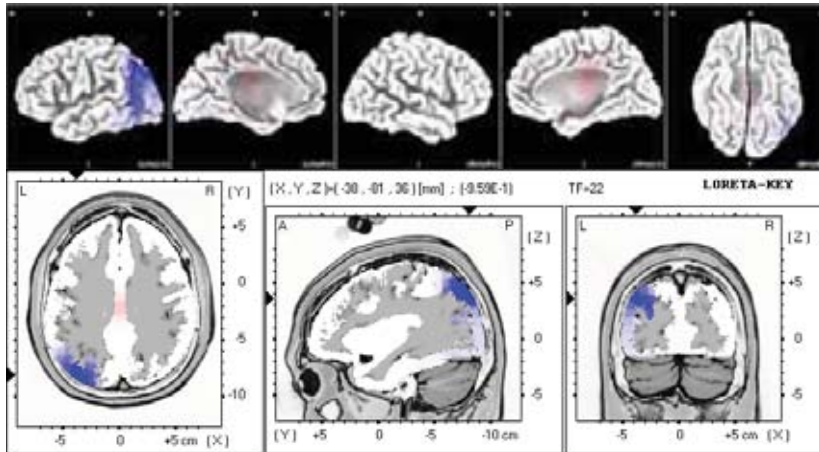


Figure 82. Paired *t*-test for 22 Hz LORETA: Significant differences after 20 minutes of 0.5 Hz CES.

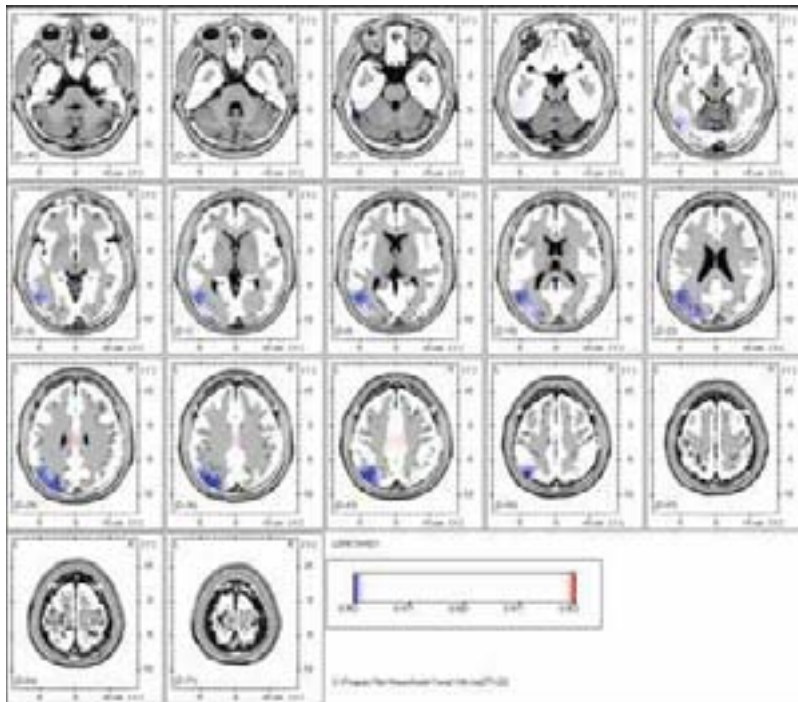


Figure 83. Paired *t*-test for 22 Hz LORETA: Significant differences after 20 minutes of 0.5 Hz CES.

Summary of 23 Hz Changes in Current Density

Decreased Parietal Lobe Activation

- Supramarginal Gyrus (Brodmann Area 40)
- Left Superior Parietal Lobule (Brodmann Area 7)
- Left Inferior Parietal Lobule (Brodmann Area 39)
- Left Precuneus (Brodmann Area 19)

Decreased Temporal Lobe Activation

- Left Middle Temporal Gyrus

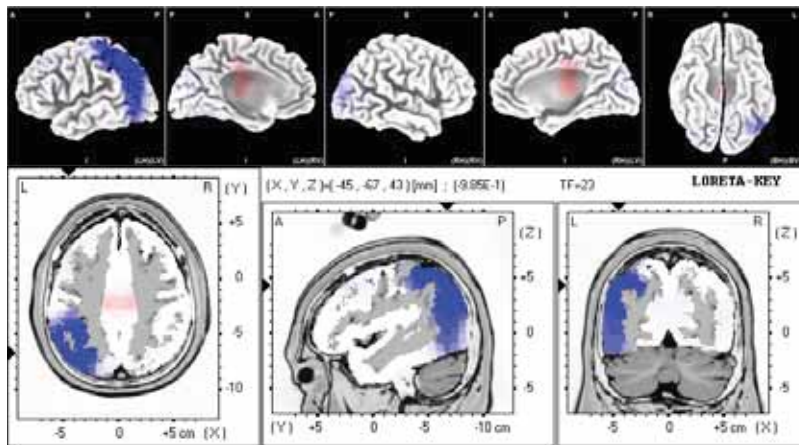


Figure 84. Paired *t*-test for 23 Hz LORETA: Significant differences after 20 minutes of 0.5 Hz CES.

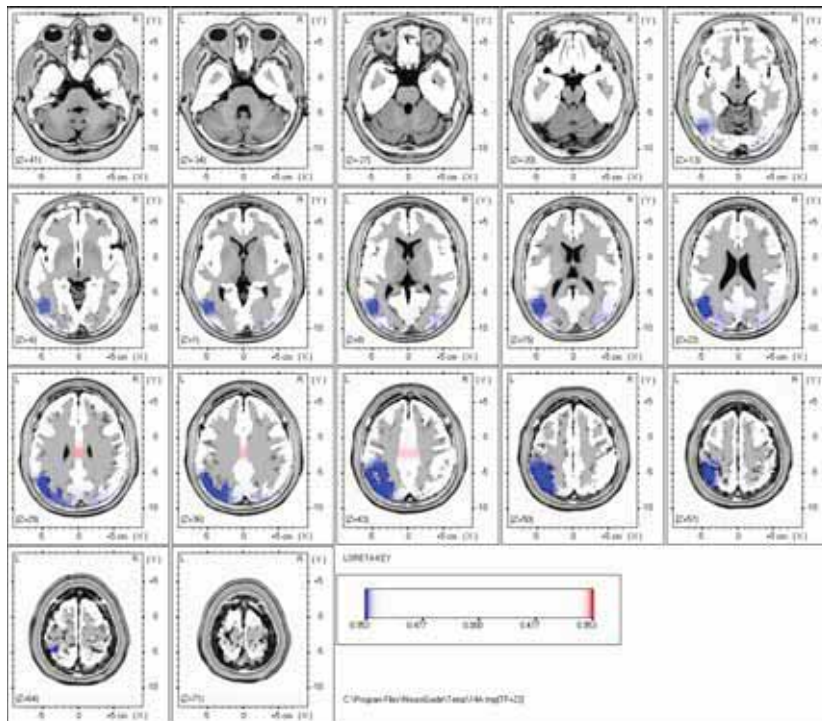


Figure 85. Paired *t*-test for 23 Hz LORETA: Significant differences after 20 minutes of 0.5 Hz CES.

Summary of 24 Hz Changes in Current Density

Decreased Parietal Lobe Activation

- Left Precentral Gyrus (Brodmann Area 40)
- Left Superior Parietal Lobule (Brodmann Area 7)
- Left Inferior Parietal Lobule (Brodmann Area 39)
- Left Precuneus (Brodmann Area 19)

Decreased Temporal Lobe Activation

- Left Superior Temporal Gyrus (Brodmann Area 39)
- Left Middle Temporal Gyrus (Brodmann Area 39)

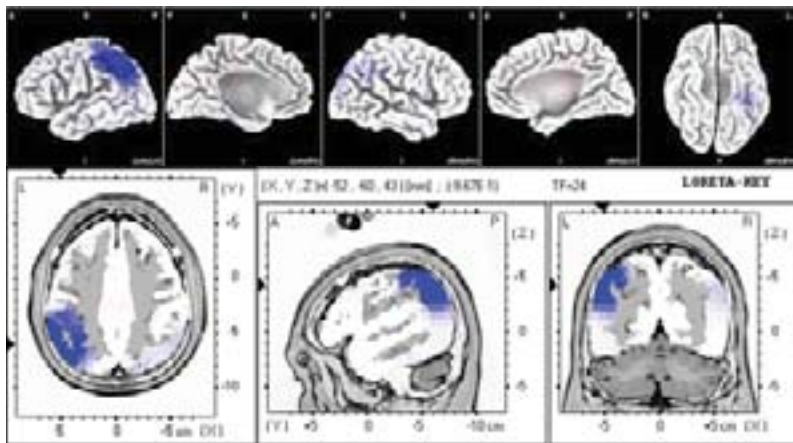


Figure 86. Paired t -test for 24 Hz LORETA: Significant differences after 20 minutes of 0.5 Hz CES.

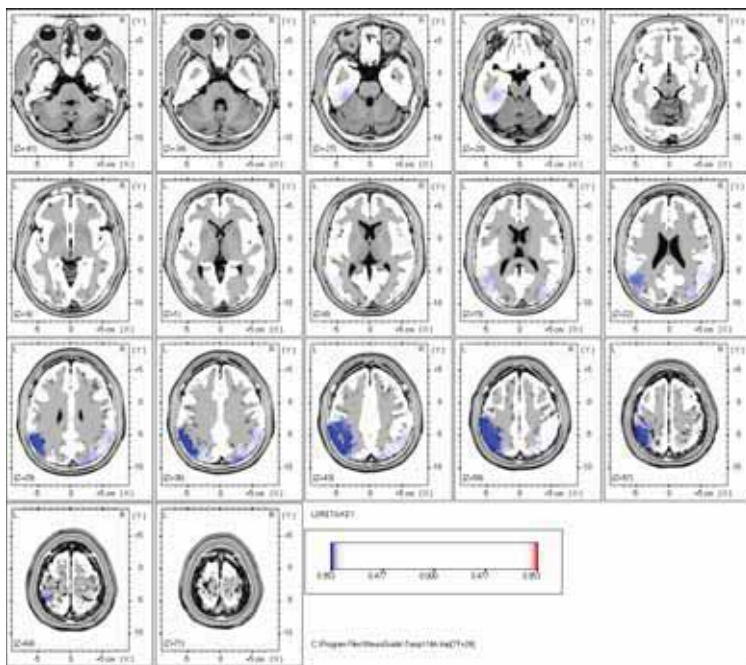


Figure 87. Paired t -test for 24 Hz LORETA: Significant differences after 20 minutes of 0.5 Hz CES.

Summary of 25 Hz Changes in Current Density

Decreased Frontal Lobe Activation

- Left Superior Frontal Gyrus (Brodmann Area 9)
- Left Middle Frontal Gyrus (Brodmann Area 9)
- Left Inferior Frontal Gyrus (Brodmann Area 9)
- Left Precentral Gyrus (Brodmann Area 4)

Decreased Temporal Lobe Activation

- Left Superior Temporal Gyrus (Brodmann Area 39)
- Left Inferior Temporal Gyrus (Brodmann Area 20)
- Left Fusiform Gyrus (Brodmann Area 20)

Decreased Limbic Lobe Activation

- Left Parahippocampal Gyrus (Brodmann Area 34)
- Left Uncus (Brodmann Area 28)

Decreased Parietal Lobe Activation

- Left Precentral Gyrus (Brodmann Area 40)
- Left Inferior Parietal Lobule (Brodmann Area 39)
- Left Precuneus (Brodmann Area 19)

Decreased Occipital Lobe

- Right and Left Cuneus (Brodmann Area 19)

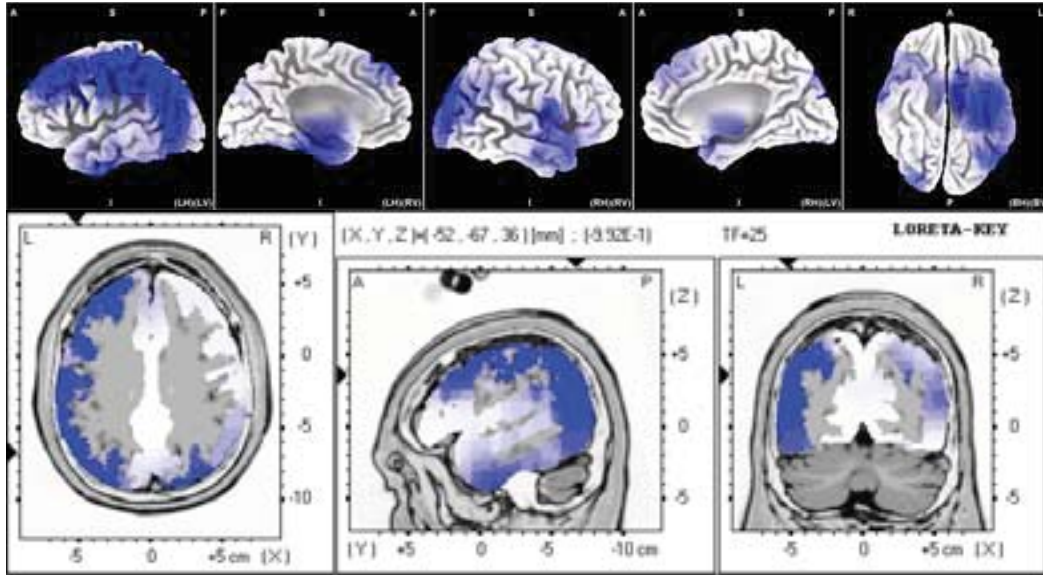


Figure 88. Paired t -test for 25 Hz LORETA: Significant differences after 20 minutes of 0.5 Hz CES.

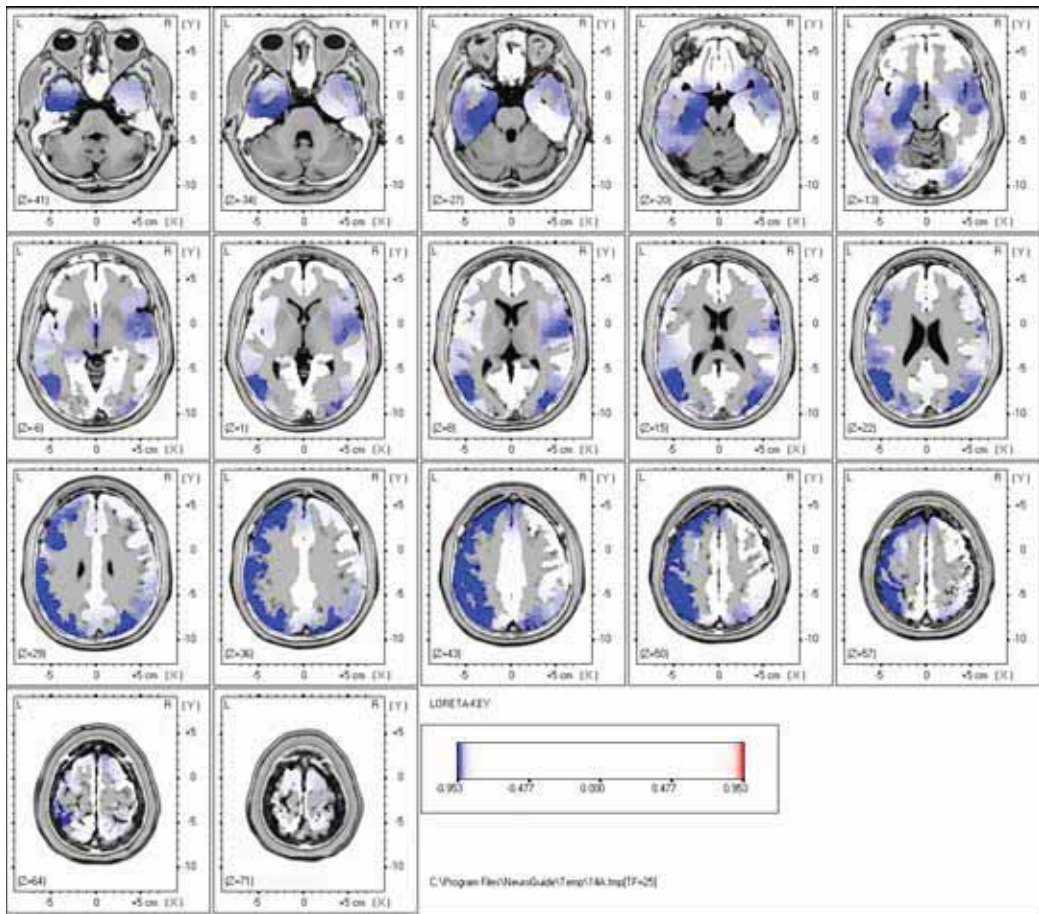


Figure 89. Paired t -test for 25 Hz LORETA: Significant differences after 20 minutes of 0.5 Hz CES.

Summary of 26 Hz Changes in Current Density

Decreased Frontal Lobe Activation

- Left Superior Frontal Gyrus (Brodmann Area 9)
- Left Middle Frontal Gyrus (Brodmann Area 9)
- Left Inferior Frontal Gyrus (Brodmann Area 9)
- Left Precentral Gyrus (Brodmann Area 4)

Decreased Temporal Lobe Activation

- Left Superior Temporal Gyrus (Brodmann Area 39)
- Left Inferior Temporal Gyrus (Brodmann Area 20)
- Left Middle Temporal Gyrus (Brodmann Area 21)
- Left Fusiform Gyrus (Brodmann Area 20)

Decreased Limbic Lobe Activation

- Left Parahippocampal Gyrus (Brodmann Area 34)
- Left Uncus (Brodmann Area 28)

Decreased Parietal Lobe Activation

- Left Precentral Gyrus (Brodmann Area 40)
- Left Supramarginal Gyrus (Brodmann Area 40)
- Left Inferior Parietal Lobule (Brodmann Area 39)
- Left Angular Gyrus (Brodmann Area 39)

Decreased Occipital Lobe

- Left Cuneus (Brodmann Area 19)

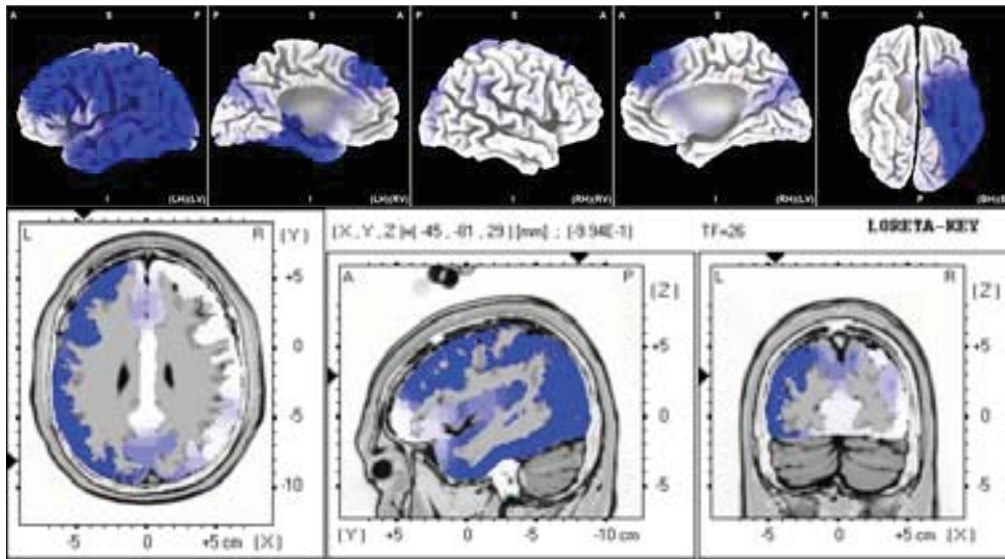


Figure 90. Paired t -test for 26 Hz LORETA: Significant differences after 20 minutes of 0.5 Hz CES.

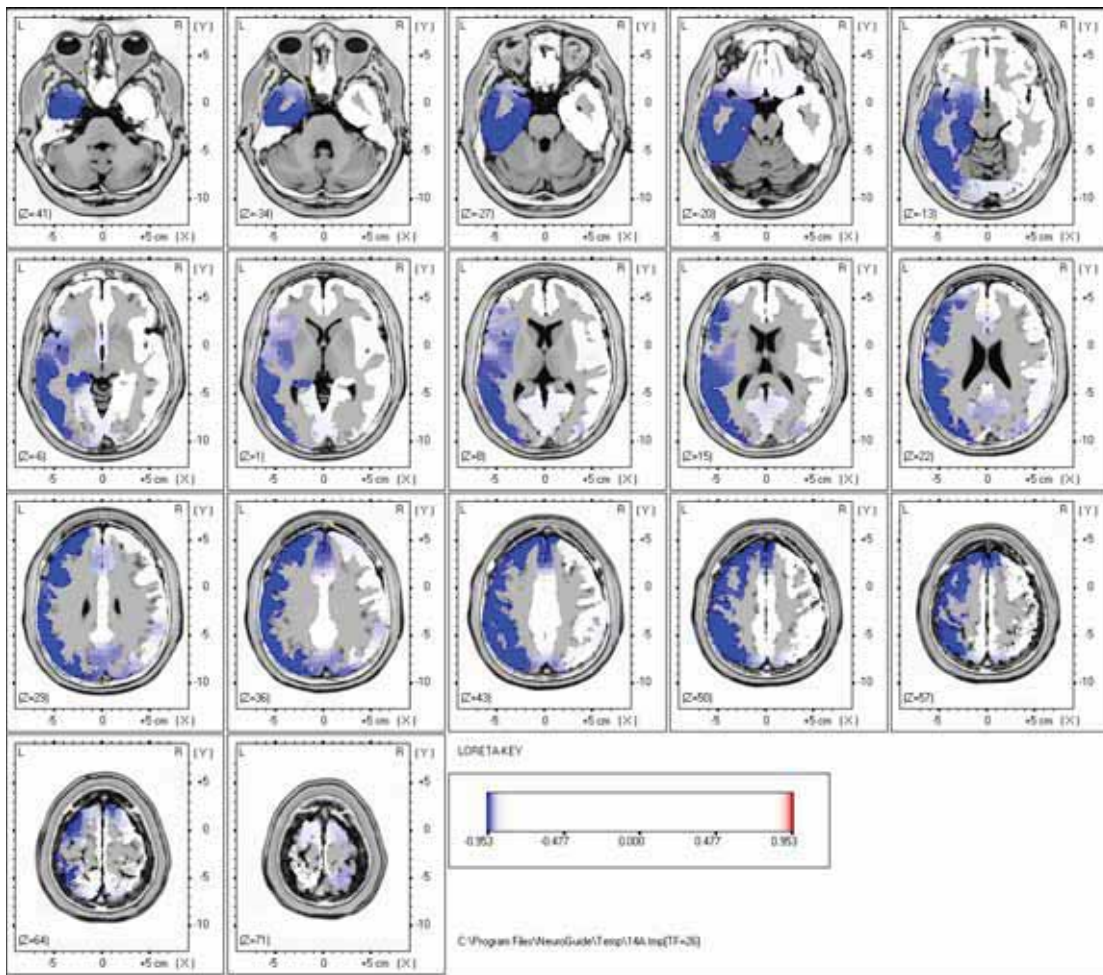


Figure 91. Paired t -test for 26 Hz LORETA: Significant Differences After 20 Minutes of 0.5 Hz CES.

Summary of 27 Hz Changes in Current Density

Decreased Frontal Lobe Activation

- Left Superior Frontal Gyrus (Brodmann Area 9)
- Left Middle Frontal Gyrus (Brodmann Area 9)
- Left Inferior Frontal Gyrus (Brodmann Area 9)

Decreased Temporal Lobe Activation

- Left Superior Temporal Gyrus (Brodmann Area 39)
- Left Inferior Temporal Gyrus (Brodmann Area 20)
- Left Middle Temporal Gyrus (Brodmann Area 21)
- Left Angular Gyrus (Brodmann Area 39)
- Left Fusiform Gyrus (Brodmann Area 20)

Decreased Limbic Lobe Activation

- Left Parahippocampal Gyrus (Brodmann Area 34)
- Left Uncus (Brodmann Area 28)

Decreased Parietal Lobe Activation

- Left Precentral Gyrus (Brodmann Area 40)
- Left Supramarginal Gyrus (Brodmann Area 40)
- Left Superior Parietal Lobule (Brodmann Area 7)
- Left Inferior Parietal Lobule (Brodmann Area 40)
- Left Precuneus (Brodmann Area 19)

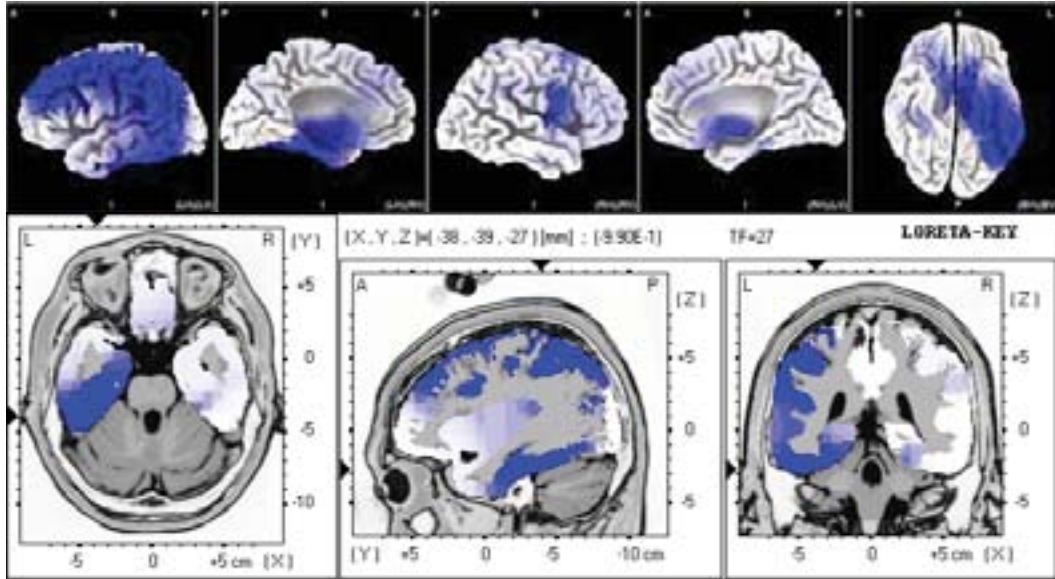


Figure 92. Paired t -test for 27 Hz LORETA: Significant differences after 20 minutes of 0.5 Hz CES.

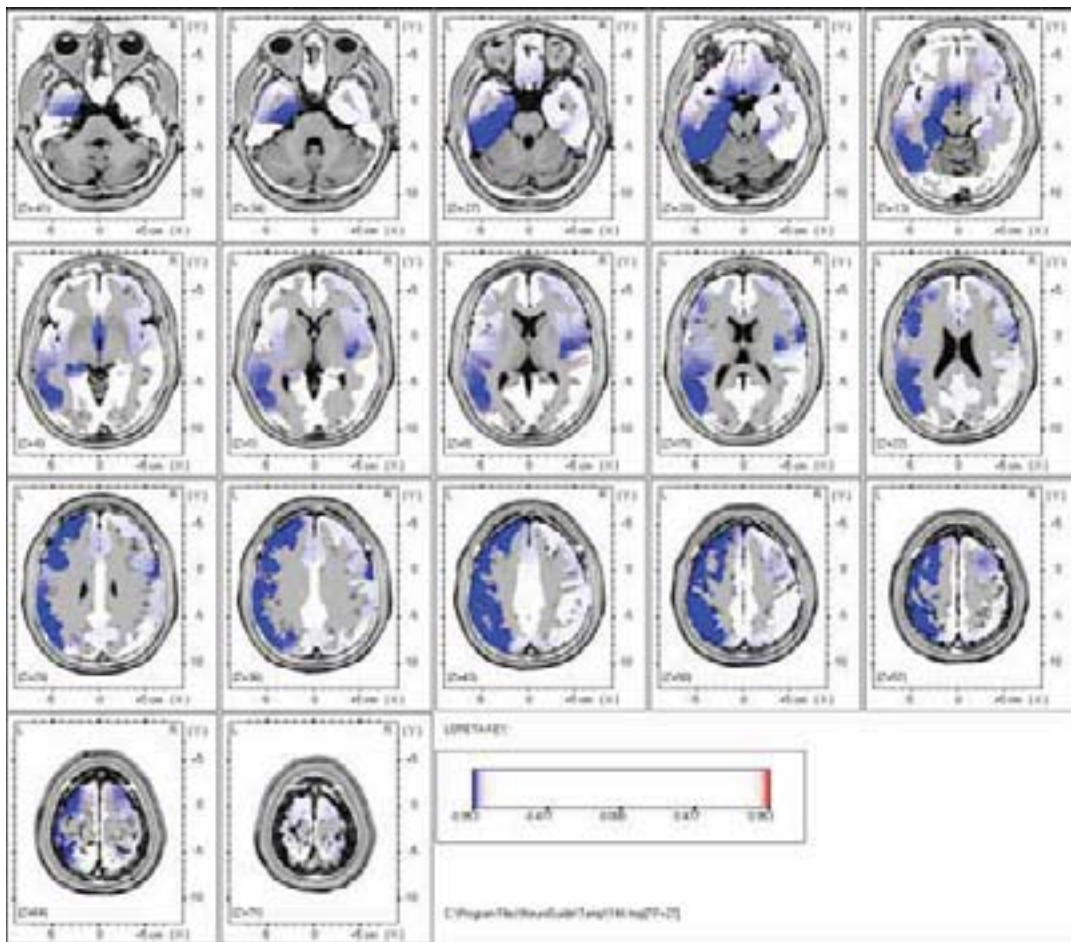


Figure 93. Paired t -test for 27 Hz LORETA: Significant differences after 20 minutes of 0.5 Hz CES.

Summary of 28 Hz Changes in Current Density

Decreased Frontal Lobe Activation

- Left and Right Superior Frontal Gyrus (Brodmann Area 10)
- Left and Right Middle Frontal Gyrus (Brodmann Area 9)
- Left Precentral Gyrus (Brodmann Area 6)
- Left Inferior Frontal Gyrus (Brodmann Area 9)
- Left Rectal Gyrus (Brodmann Area 4)

Decreased Temporal Lobe Activation

- Left Superior Temporal Gyrus (Brodmann Area 39)
- Left Inferior Temporal Gyrus (Brodmann Area 20)
- Left Middle Temporal Gyrus (Brodmann Area 21)
- Left Angular Gyrus (Brodmann Area 39)
- Left Fusiform Gyrus (Brodmann Area 20)

Decreased Limbic Lobe Activation

- Left Parahippocampal Gyrus (Brodmann Area 34)
- Left Hippocampus (Sub-Gyral)
- Left Uncus (Brodmann Area 28)
- Left and Right Anterior Cingulate (Brodmann Area 32)
- Left and Right Cingulate Gyrus (Brodmann Area 24)

Decreased Parietal Lobe Activation

- Right Postcentral Gyrus (Brodmann Area 2)
- Left Inferior Parietal Lobule (Brodmann Area 40)
- Right Superior Parietal Lobule
- Left Supramarginal Gyrus (Brodmann Area 40)

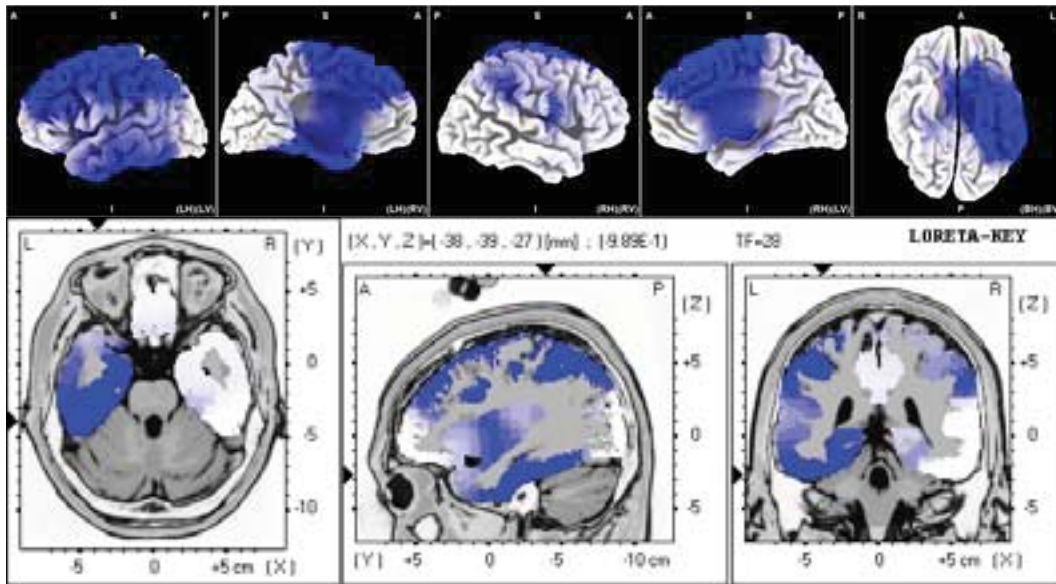


Figure 94. Paired t -test for 28 Hz LORETA: Significant differences after 20 minutes of 0.5 Hz CES.

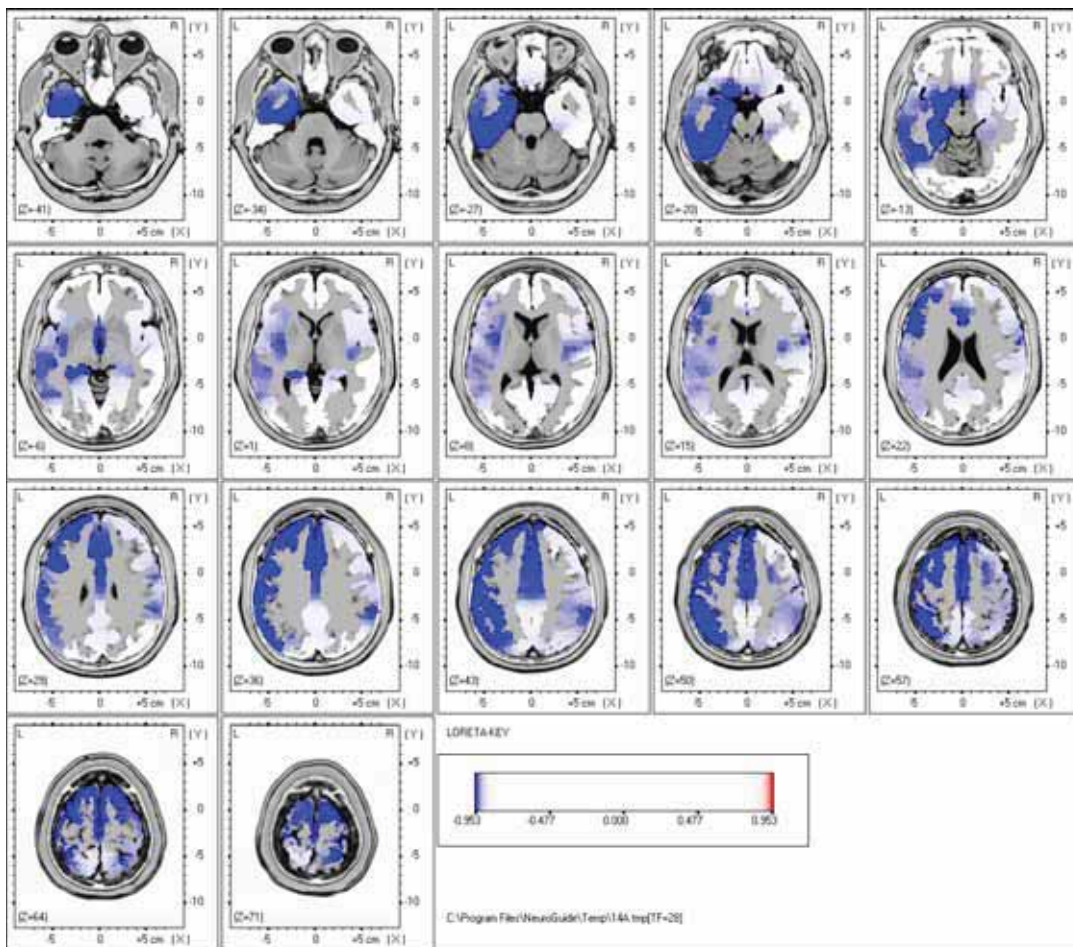


Figure 95. Paired t -test for 28 Hz LORETA: Significant Differences After 20 Minutes of 0.5 Hz CES.

Summary of 29 Hz Changes in Current Density

Decreased Frontal Lobe Activation

- Left and Right Superior Frontal Gyrus (Brodmann Area 10)
- Left Middle Frontal Gyrus (Brodmann Area 9)
- Left and Right Medial Frontal Gyrus (Brodmann Area 8)
- Left Precentral Gyrus (Brodmann Area 6)
- Left Inferior Frontal Gyrus (Brodmann Area 9)
- Left Subcallosal Gyrus (Brodmann Area 34)

Decreased Temporal Lobe Activation

- Left Fusiform Gyrus (Brodmann Area 20)

Decreased Limbic Lobe Activation

- Left Parahippocampal Gyrus (Brodmann Area 34)
- Left and Right Anterior Cingulate (Brodmann Area 25)

Decreased Parietal Lobe Activation

- Left Postcentral Gyrus (Brodmann Area 2)
- Left Inferior Parietal Lobule (Brodmann Area 40)
- Left Superior Parietal Lobule (Brodmann Area 7)
- Left Precuneus (Brodmann Area 7)

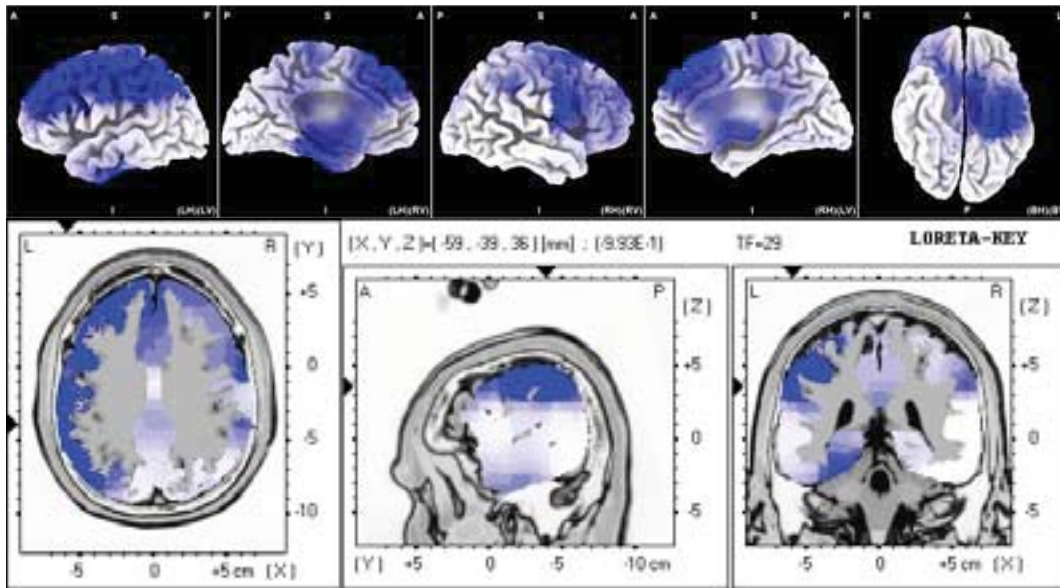


Figure 96. Paired t -test for 29 Hz LORETA: Significant Differences After 20 Minutes of 0.5 Hz CES.

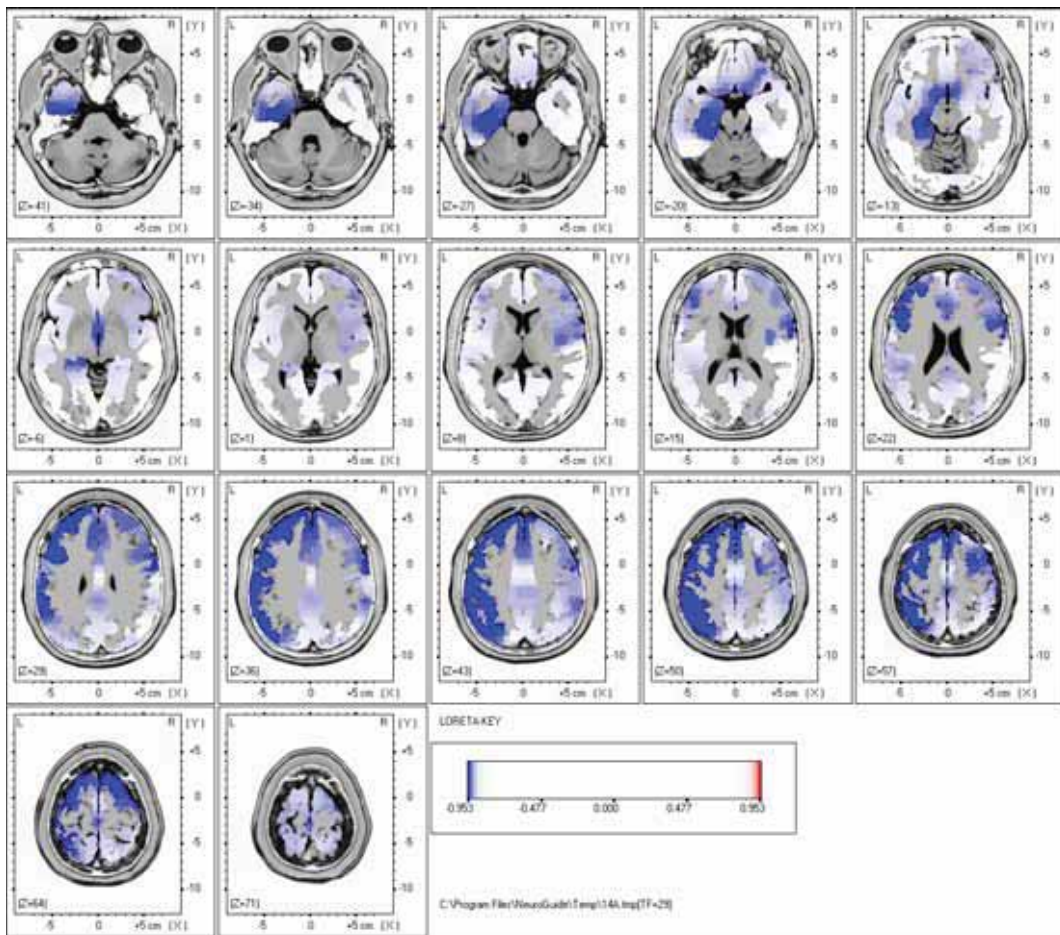


Figure 97. Paired t -test for 29 Hz LORETA: Significant Differences After 20 Minutes of 0.5 Hz CES.

Summary of 30 Hz Changes in Current Density

Decreased Frontal Lobe Activation

- Left and Right Superior Frontal Gyrus (Brodmann Area 10)
- Left and Right Middle Frontal Gyrus (Brodmann Area 9)
- Left and Right Medial Frontal Gyrus (Brodmann Area 8)
- Left Precentral Gyrus (Brodmann Area 6)
- Left Inferior Frontal Gyrus (Brodmann Area 9)
- Left Subcallosal Gyrus (Brodmann Area 34)

Decreased Temporal Lobe Activation

- Left and Right Hippocampus (Sub-Gyral)
- Left Fusiform Gyrus (Brodmann Area 36)

Decreased Limbic Lobe Activation

- Left and Right Parahippocampal Gyrus (Brodmann Area 27)
- Left and Right Anterior Cingulate (Brodmann Area 25)
- Left and Right Cingulate Gyrus (Brodmann Area 24)

Decreased Parietal Lobe Activation

- Left Postcentral Gyrus (Brodmann Area 2)
- Left Inferior Parietal Lobule (Brodmann Area 40)
- Left Superior Parietal Lobule (Brodmann Area 7)

Decreased Occipital Lobe Activation

- Lingual Gyrus (Brodmann Area 19)

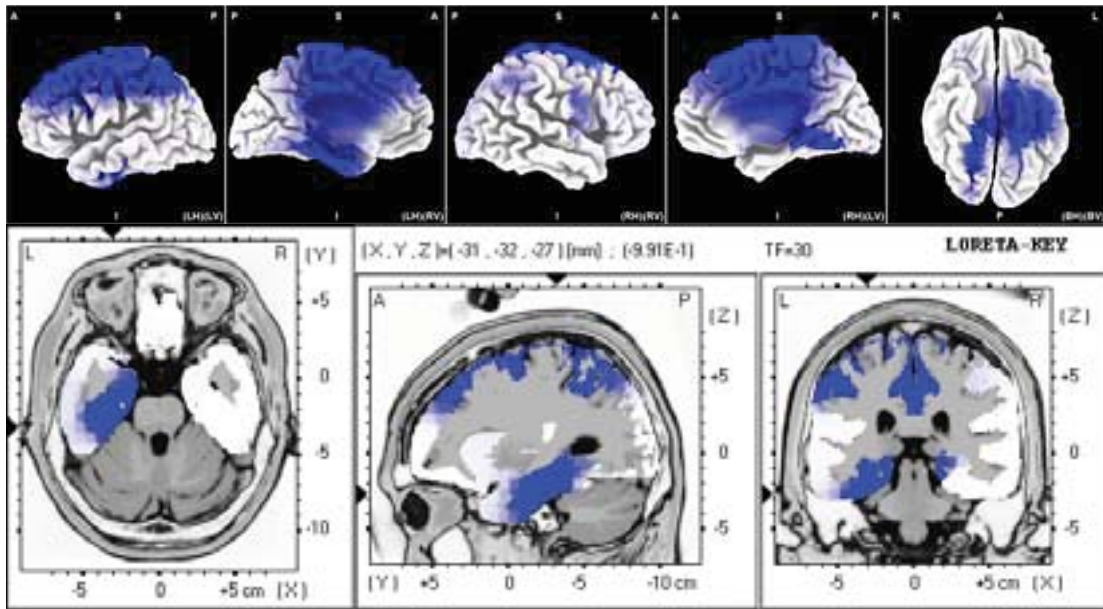


Figure 98. Paired t -test for 30 Hz LORETA: Significant differences after 20 minutes of 0.5 Hz CES.

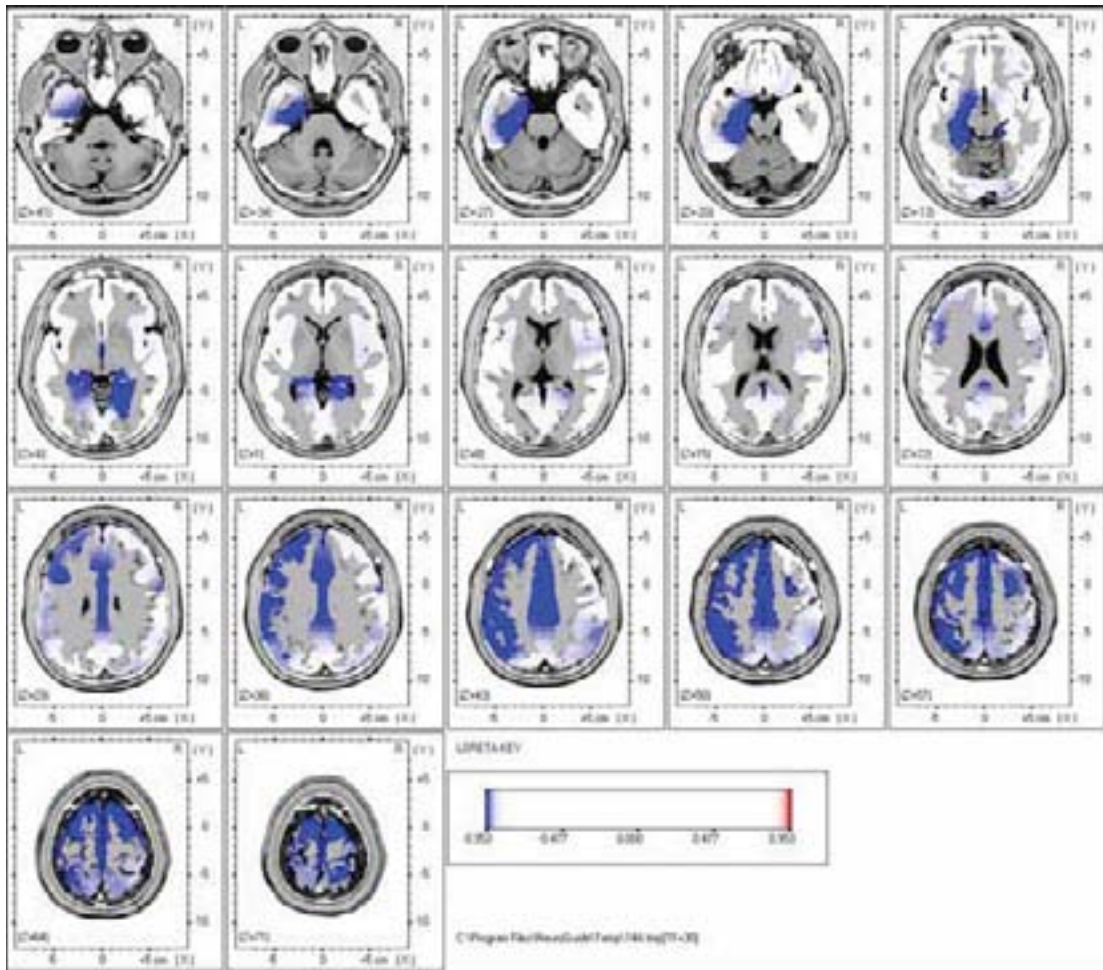


Figure 99. Paired t -test for 30 Hz LORETA: Significant differences after 20 minutes of 0.5 Hz CES.

Summary of 31 Hz Changes in Current Density

Decreased Frontal Lobe Activation

- Left and Right Superior Frontal Gyrus (Brodmann Area 10)
- Left Middle Frontal Gyrus (Brodmann Area 9)
- Left and Right Medial Frontal Gyrus (Brodmann Area 8)
- Left Precentral Gyrus (Brodmann Area 6)

Decreased Temporal Lobe Activation

- Left Fusiform Gyrus (Brodmann Area 20)
- Left Inferior Temporal Gyrus (Brodmann Area 20)

Decreased Limbic Lobe Activation

- Left Parahippocampal Gyrus (Brodmann Area 34)
- Left Hippocampus (Sub-Gyral)
- Left and Right Anterior Cingulate (Brodmann Area 25)
- Left Uncus (Brodmann Area 28)

Decreased Parietal Lobe Activation

- Left Postcentral Gyrus (Brodmann Area 2)
- Left Inferior Parietal Lobule (Brodmann Area 40)
- Left Superior Parietal Lobule (Brodmann Area 7)
- Left Precuneus (Brodmann Area 7)

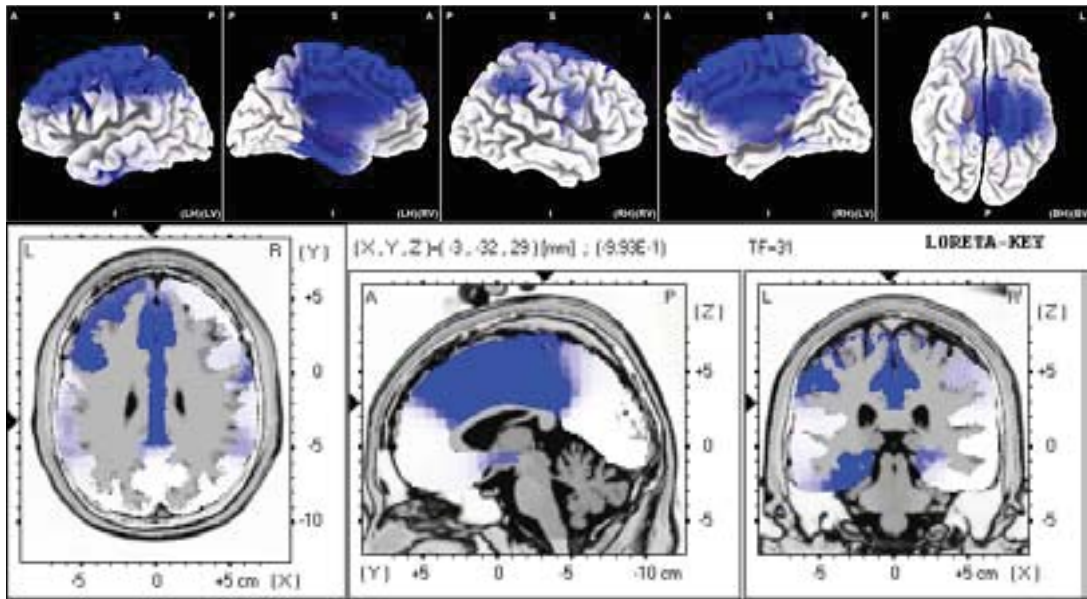


Figure 100. Paired t -test for 31 Hz LORETA: Significant differences after 20 minutes of 0.5 Hz CES.

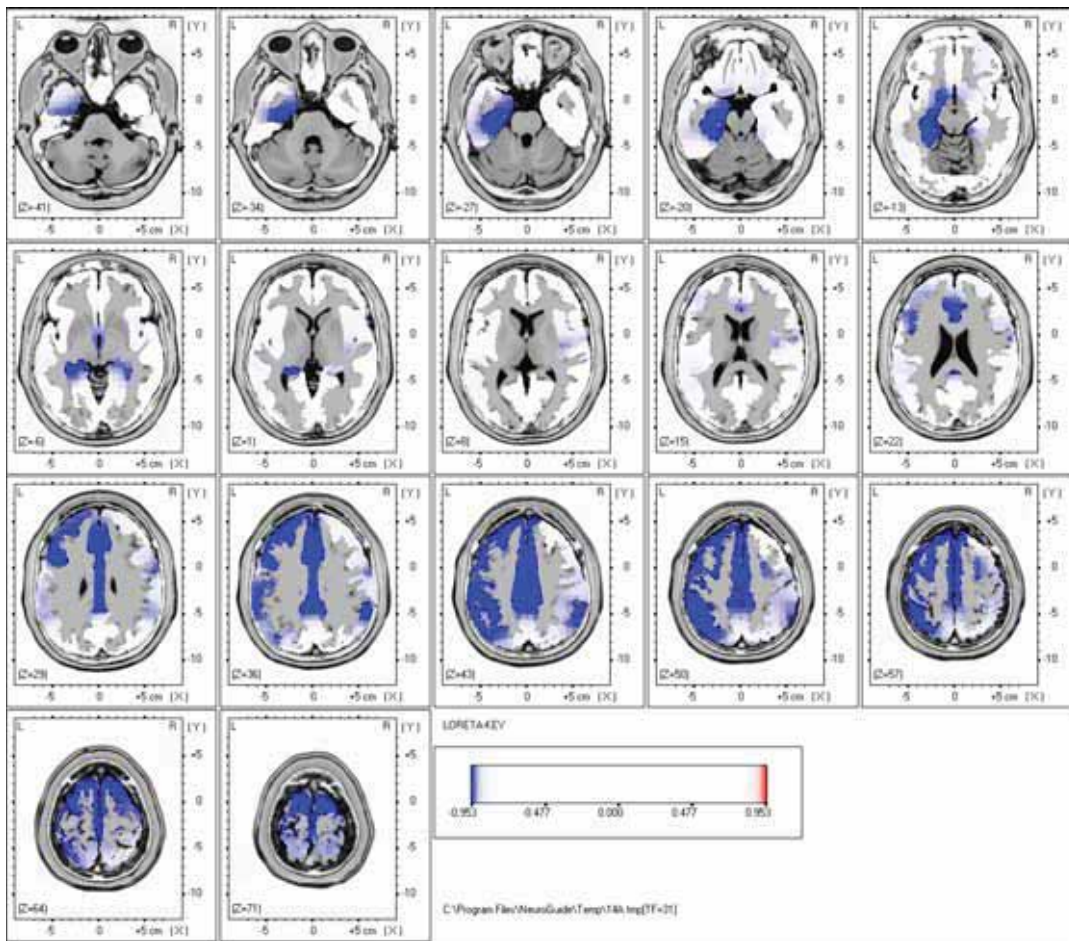


Figure 101. Paired t -test for 31 Hz LORETA: Significant differences after 20 minutes of 0.5 Hz CES.

Summary of 32 Hz Changes in Current Density

Decreased Frontal Lobe Activation

- Left Superior Frontal Gyrus (Brodmann Area 10)

Decreased Temporal Lobe Activation

- Left Hippocampus (Sub-Gyral)

Decreased Limbic Lobe Activation

- Left and Right Cingulate (Brodmann Area 24)
- Left Parahippocampal Gyrus (Brodmann Area 36)

Decreased Parietal Lobe Activation

- Left Postcentral Gyrus (Brodmann Area 2)
- Left Inferior Parietal Lobule (Brodmann Area 40)
- Left Superior Parietal Lobule (Brodmann Area 7)

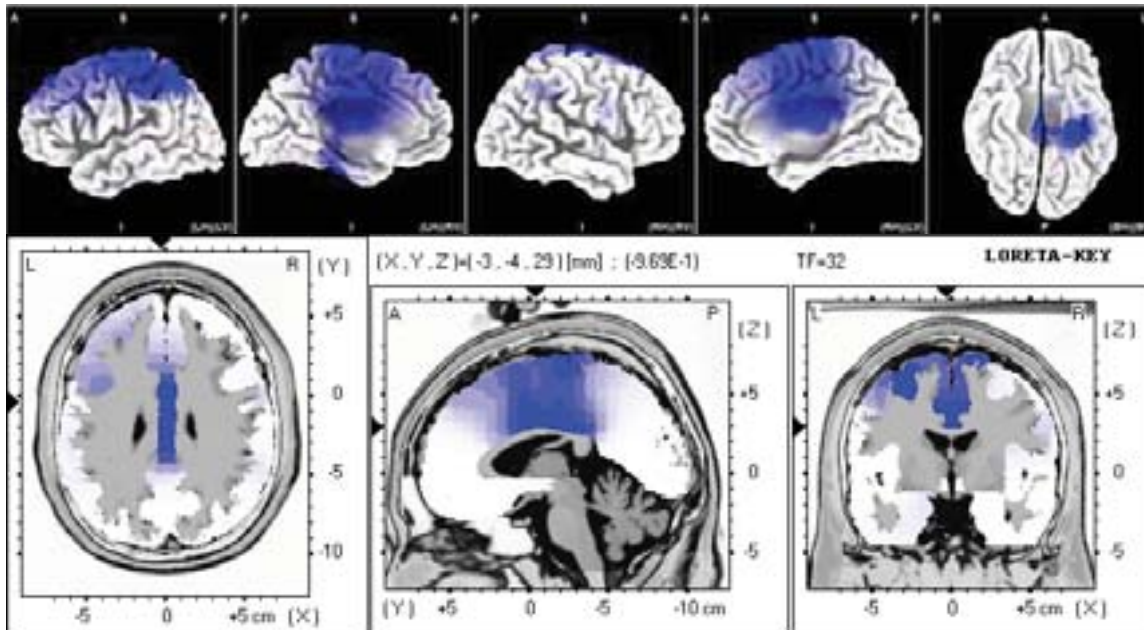


Figure 102. Paired *t*-test for 32 Hz LORETA: Significant differences after 20 minutes of 0.5 Hz CES.

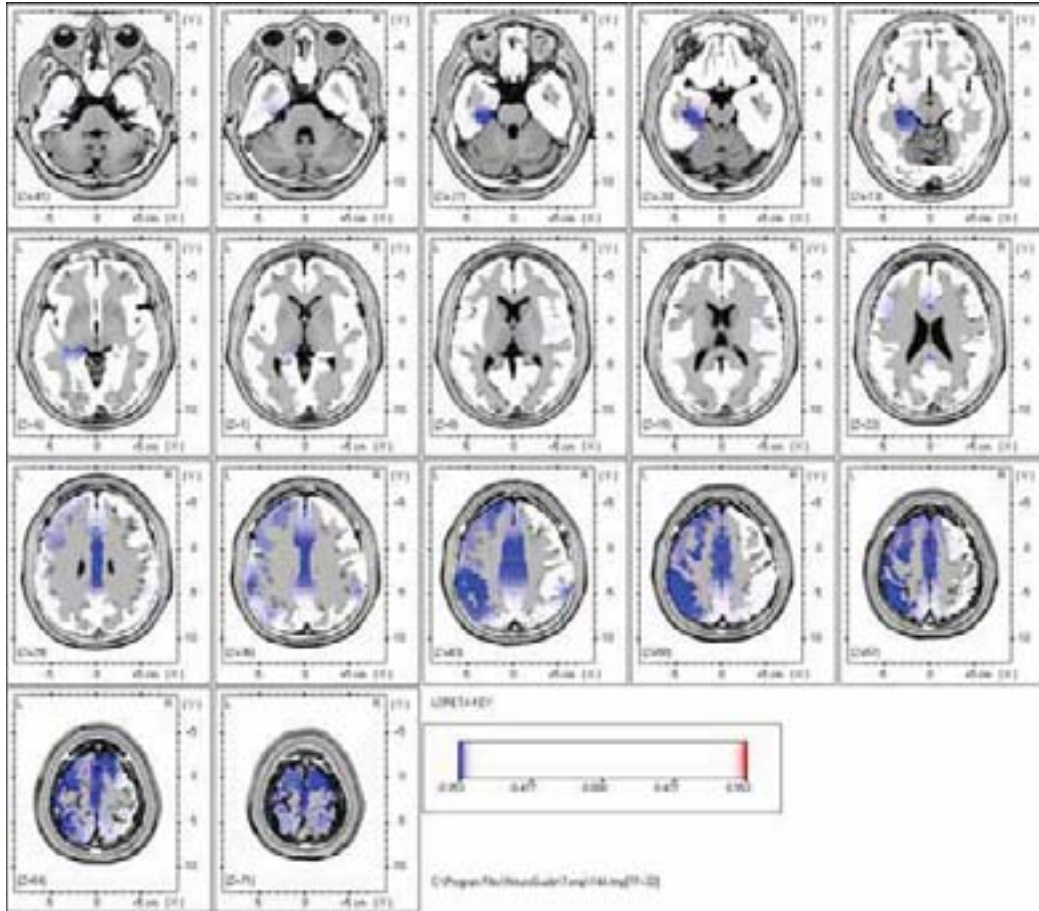


Figure 103. Paired t -test for 32 Hz LORETA: Significant differences after 20 minutes of 0.5 Hz CES.

Summary of 33 Hz Changes in Current Density

Decreased Frontal Lobe Activation

- Left Superior Frontal Gyrus (Brodmann Area 10)

Decreased Temporal Lobe Activation

- Left Fusiform Gyrus (Brodmann Area 20)
- Left Inferior Temporal Gyrus (Brodmann Area 20)

Decreased Parietal Lobe Activation

- Left Postcentral Gyrus (Brodmann Area 2)
- Left Inferior Parietal Lobule (Brodmann Area 40)
- Left Superior Parietal Lobule (Brodmann Area 7)

- Left Precuneus (Brodmann Area 7)

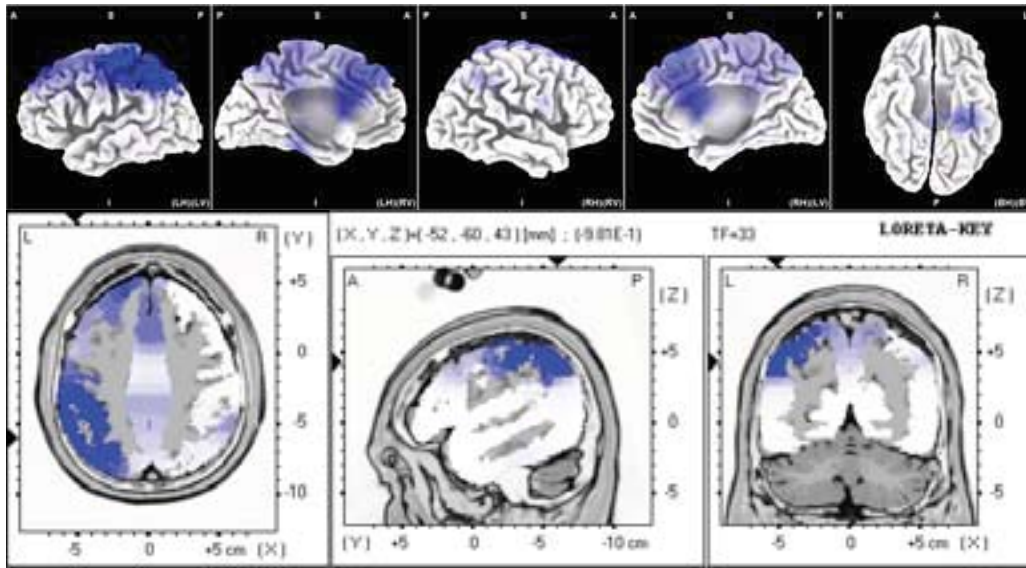


Figure 104. Paired t -test for 33 Hz LORETA: Significant differences after 20 minutes of 0.5 Hz CES.

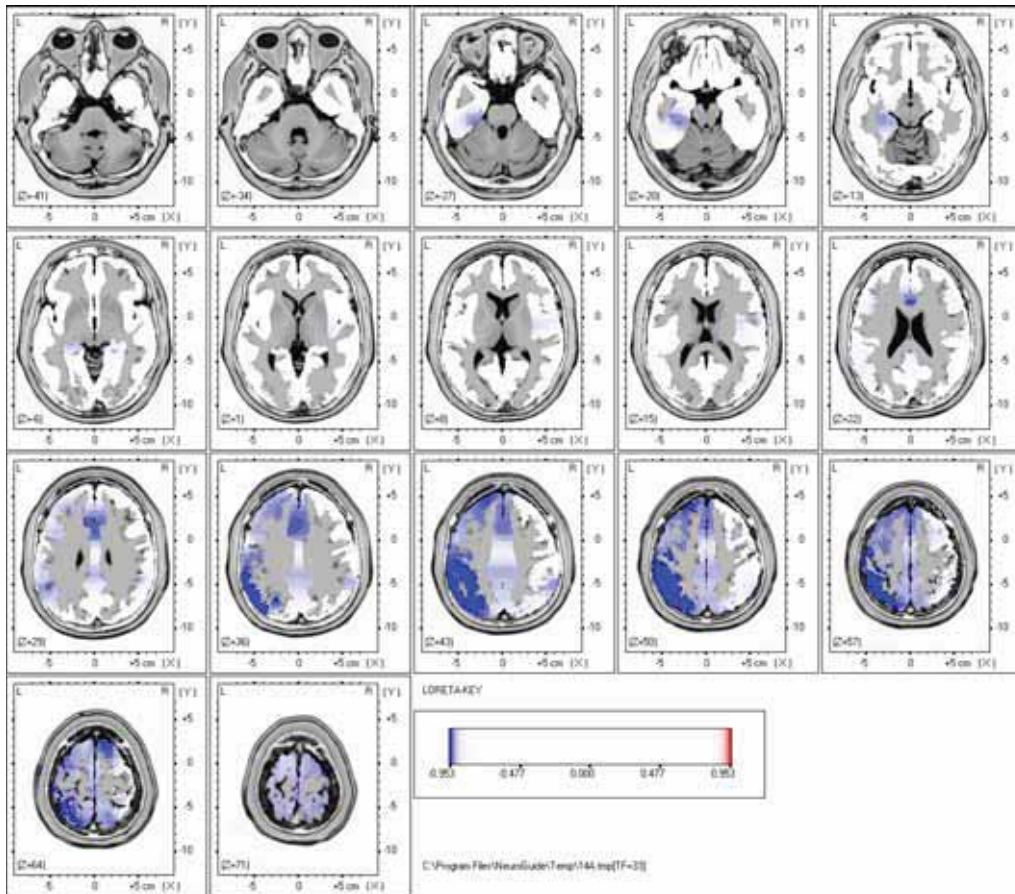


Figure 105. Paired t -test for 33 Hz LORETA: Significant differences after 20 minutes of 0.5 Hz CES.

Summary of 34 Hz Changes in Current Density

Decreased Frontal Lobe Activation

- Left and Right Superior Frontal Gyrus (Brodmann Area 10)
- Left Middle Frontal Gyrus (Brodmann Area 9)
- Left Precentral Gyrus (Brodmann Area 4)

Decreased Temporal Lobe Activation

- Left Fusiform Gyrus (Brodmann Area 20)
- Left Inferior Temporal Gyrus (Brodmann Area 37)
- Left Hippocampus Sub-Gyral)

Decreased Limbic Lobe Activation

- Left and Right Anterior Cingulate (Brodmann Area 24)
- Left and Right Cingulate Gyrus (Brodmann Area 23)
- Left Parahippocampal Gyrus (Brodmann Area 36)

Decreased Parietal Lobe Activation

- Left Postcentral Gyrus (Brodmann Area 2)
- Left Inferior Parietal Lobule (Brodmann Area 40)
- Left Superior Parietal Lobule (Brodmann Area 7)
- Left Precuneus (Brodmann Area 7)

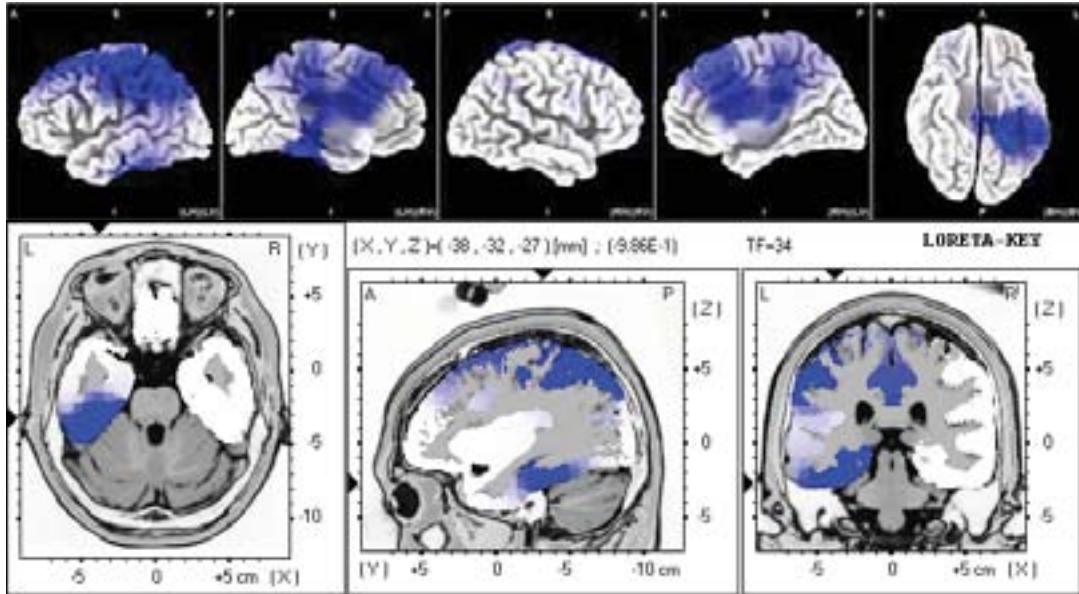


Figure 106. Paired t -test for 34 Hz LORETA: Significant differences after 20 minutes of 0.5 Hz CES.

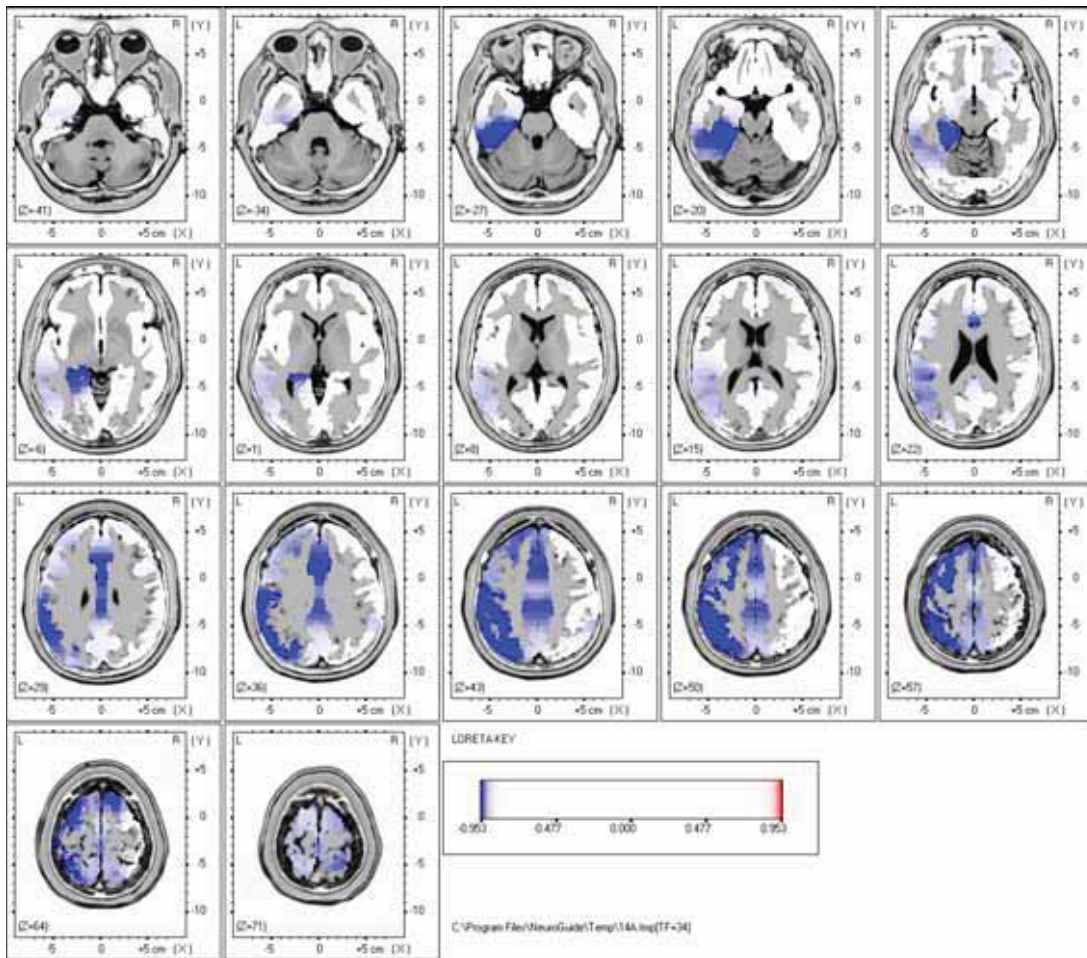


Figure 107. Paired t -test for 34 Hz LORETA: Significant differences after 20 minutes of 0.5 Hz CES.

Summary of 35 Hz Changes in Current Density

Decreased Frontal Lobe Activation

- Left Middle Frontal Gyrus (Brodmann Area 9)
- Left Precentral Gyrus (Brodmann Area 6)

Decreased Temporal Lobe Activation

- Left Fusiform Gyrus (Brodmann Area 20)
- Left Hippocampus (Sub-Gyral)

Decreased Limbic Lobe Activation

- Left and Right Parahippocampal Gyrus (Brodmann Area 34)
- Left and Right Hippocampus (Sub-Gyral)
- Left and Right Anterior Cingulate (Brodmann Area 25)
- Left Uncus (Brodmann Area 28)

Decreased Parietal Lobe Activation

- Left Postcentral Gyrus (Brodmann Area 2)
- Left Inferior Parietal Lobule (Brodmann Area 40)
- Left Superior Parietal Lobule (Brodmann Area 7)
- Left Precuneus (Brodmann Area 7)

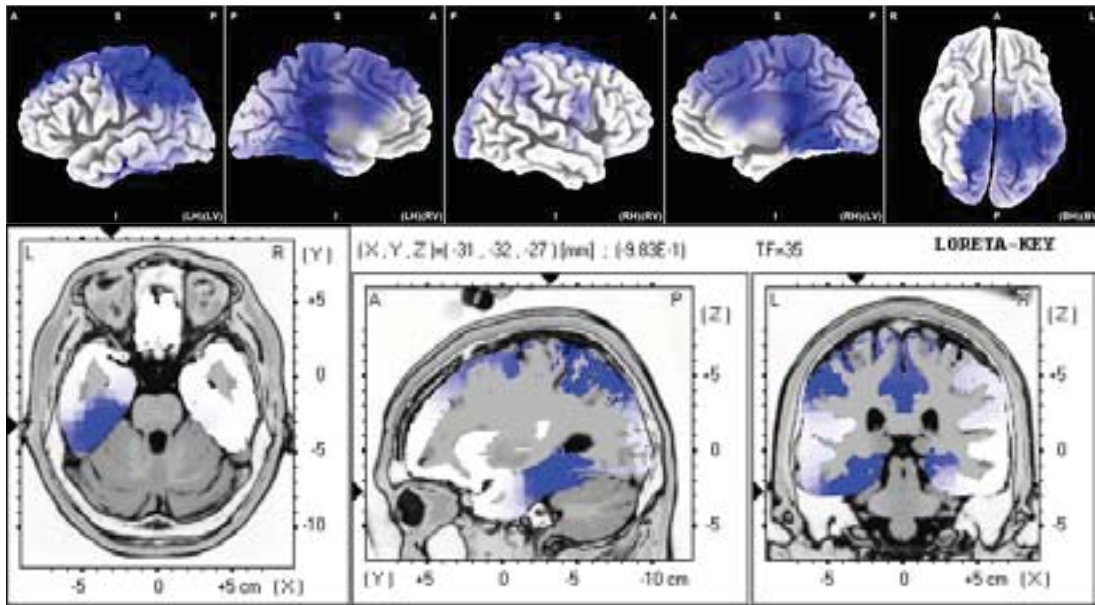


Figure 108. Paired t -test for 35 Hz LORETA: Significant differences after 20 minutes of 0.5 Hz CES.

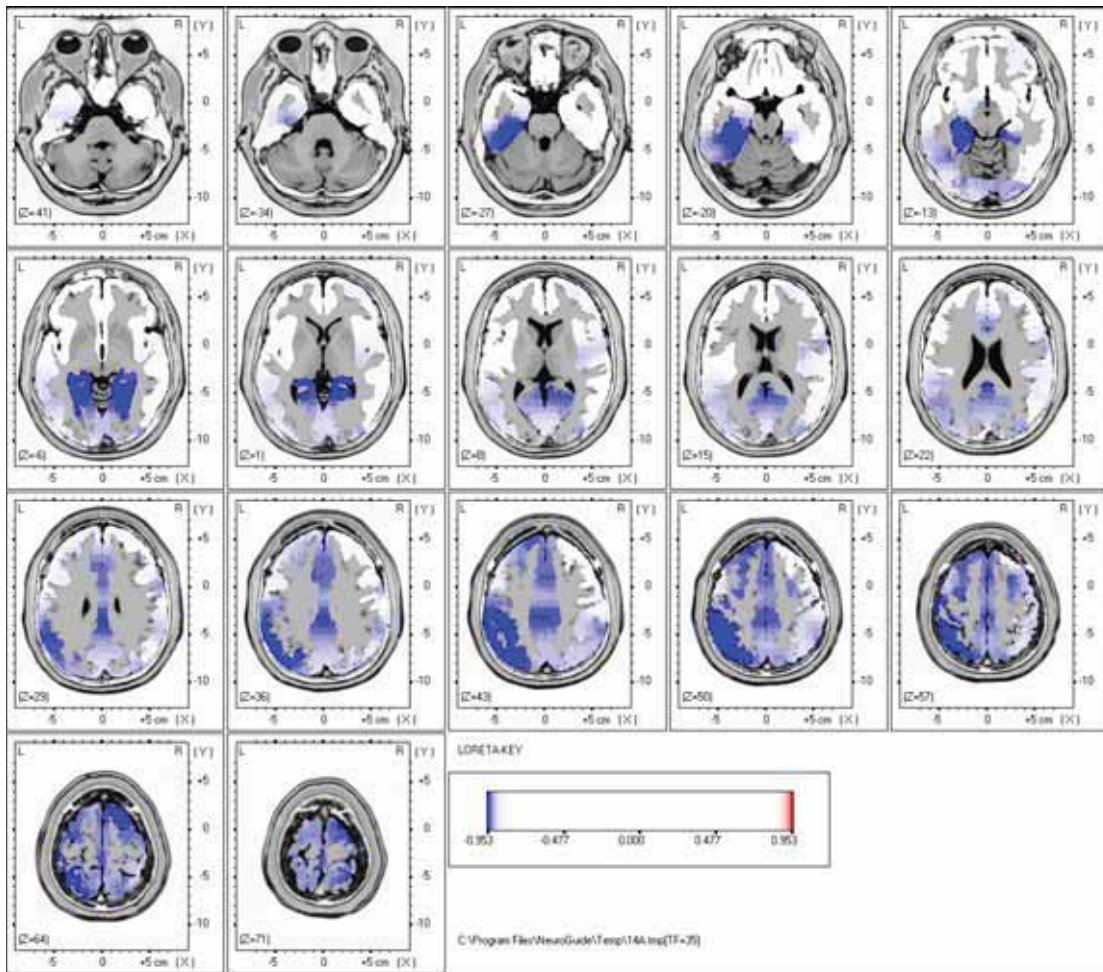


Figure 109. Paired t -test for 35 Hz LORETA: Significant differences after 20 minutes of 0.5 Hz CES.

Summary of 36 Hz Changes in Current Density

Decreased Frontal Lobe Activation

- Left Superior Frontal Gyrus (Brodmann Area 8)
- Left Middle Frontal Gyrus (Brodmann Area 8)

Decreased Temporal Lobe Activation

- Left Fusiform Gyrus (Brodmann Area 20)
- Left Hippocampus (Sub-Gyral)

Decreased Limbic Lobe Activation

- Left Parahippocampal Gyrus (Brodmann Area 34)

Decreased Parietal Lobe Activation

- Left Postcentral Gyrus (Brodmann Area 2)
- Left Inferior Parietal Lobule (Brodmann Area 40)
- Left Superior Parietal Lobule (Brodmann Area 7)
- Left Precuneus (Brodmann Area 7)

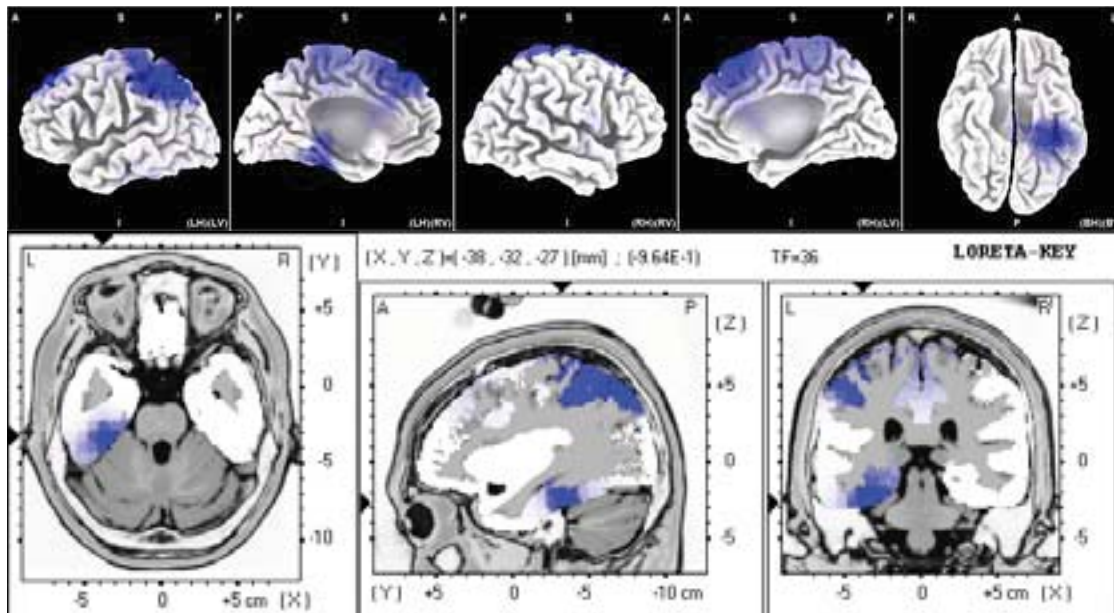


Figure 110. Paired *t*-test for 36 Hz LORETA: Significant differences after 20 minutes of 0.5 Hz CES.

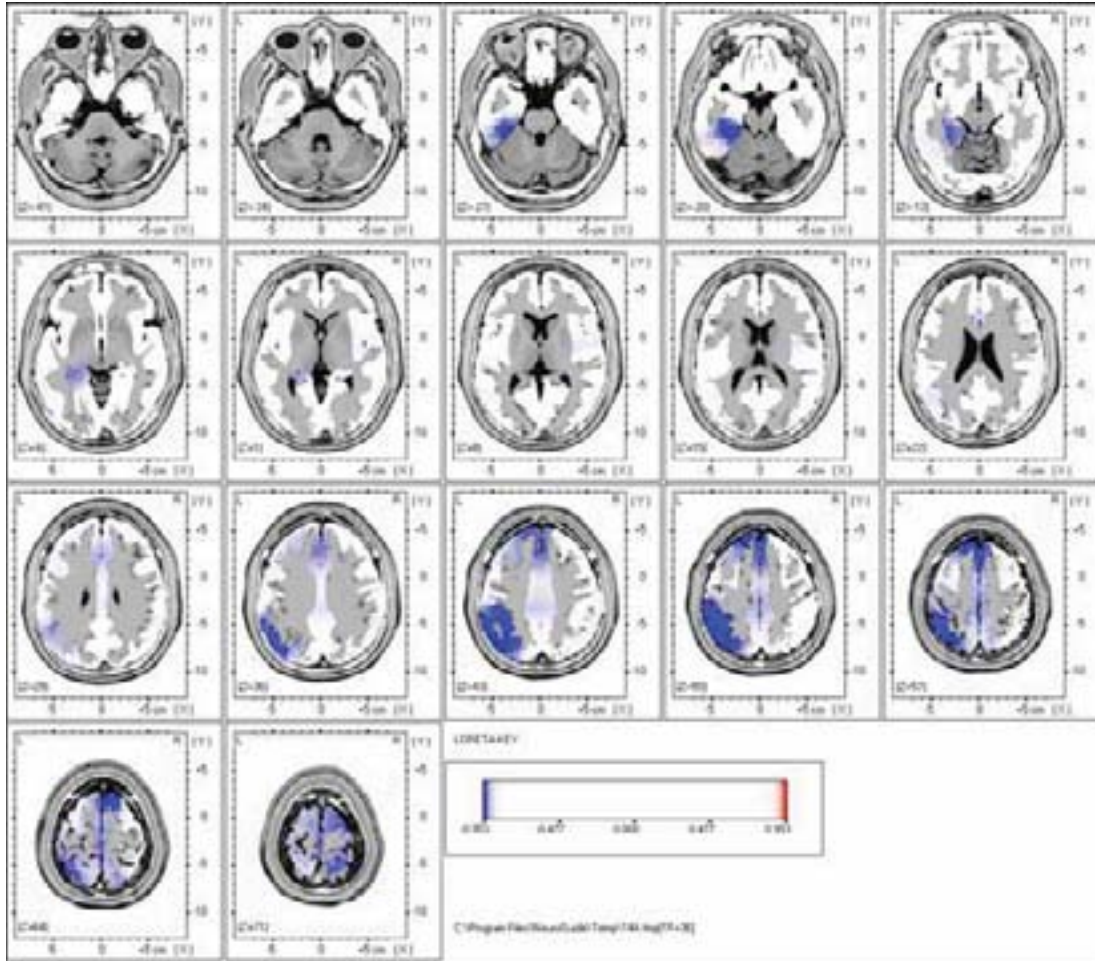


Figure 111. Paired t -test for 36 Hz LORETA: Significant differences after 20 minutes of 0.5 Hz CES.

Summary of 37 Hz Changes in Current Density

Decreased Frontal Lobe Activation

- Left and Right Superior Frontal Gyrus (Brodmann Area 8)

Decreased Temporal Lobe Activation

- Left Fusiform Gyrus (Brodmann Area 20)

Decreased Limbic Lobe Activation

- Left Parahippocampal Gyrus (Brodmann Area 34)

Decreased Parietal Lobe Activation

- Left Postcentral Gyrus (Brodmann Area 2)
- Left Inferior Parietal Lobule (Brodmann Area 40)

- Left Superior Parietal Lobule (Brodmann Area 7)
- Left Precuneus (Brodmann Area 7)

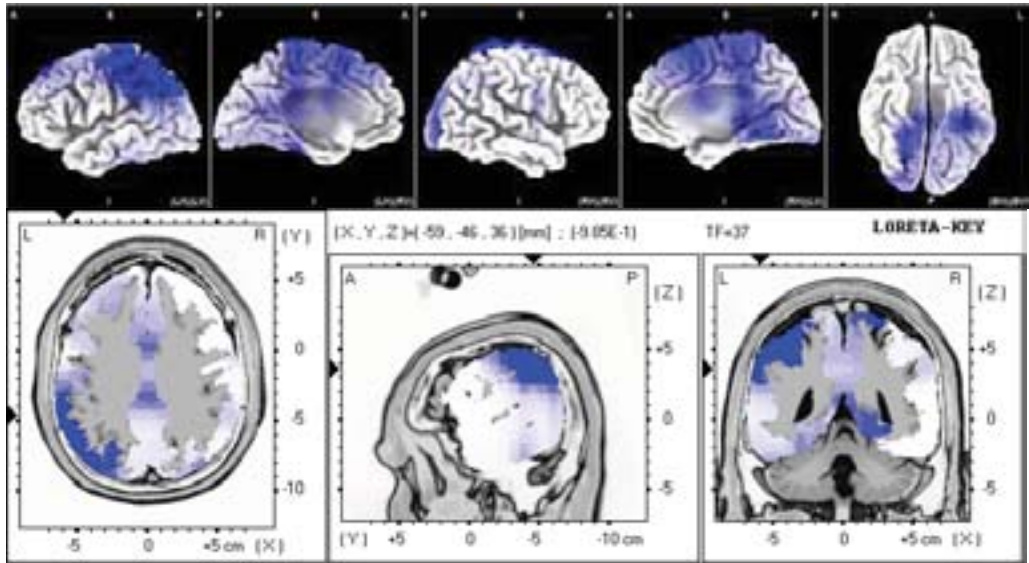


Figure 112. Paired t -test for 37 Hz LORETA: Significant differences after 20 minutes of 0.5 Hz CES.

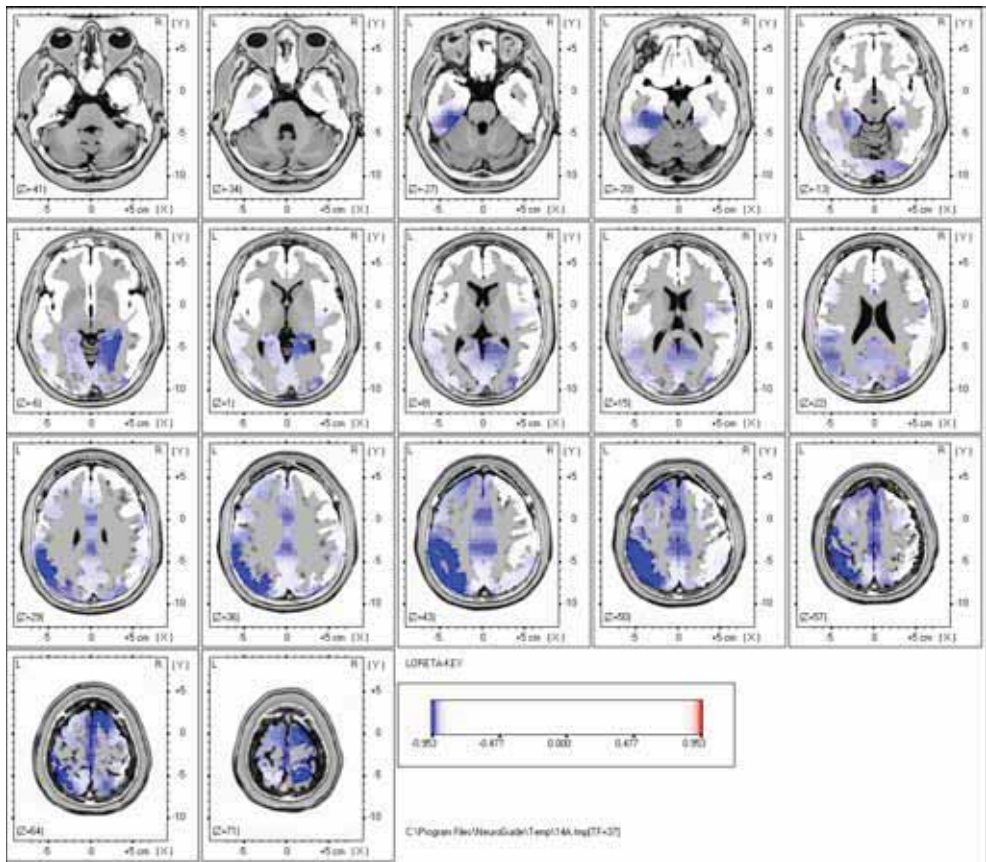


Figure 113. Paired t -test for 37 Hz LORETA: Significant differences after 20 minutes of 0.5 Hz CES.

Summary of 38 Hz Changes in Current Density

Decreased Frontal Lobe Activation

- Left Superior Frontal Gyrus (Brodmann Area 8)
- Left Middle Frontal Gyrus (Brodmann Area 9)
- Left and Right Medial Frontal Gyrus (Brodmann Area 8)
- Left Precentral Gyrus (Brodmann Area 4)

Decreased Temporal Lobe Activation

- Left Fusiform Gyrus (Brodmann Area 20)

Decreased Limbic Lobe Activation

- Left and Right Cingulate Gyrus (Brodmann Area 32)
- Left Parahippocampal Gyrus (Brodmann Area 34)
- Left Hippocampus (Sub-Gyral)

Decreased Parietal Lobe Activation

- Left and Right Postcentral Gyrus (Brodmann Area 2)
- Left Inferior Parietal Lobule (Brodmann Area 40)
- Left Superior Parietal Lobule (Brodmann Area 7)
- Left Precuneus (Brodmann Area 7)

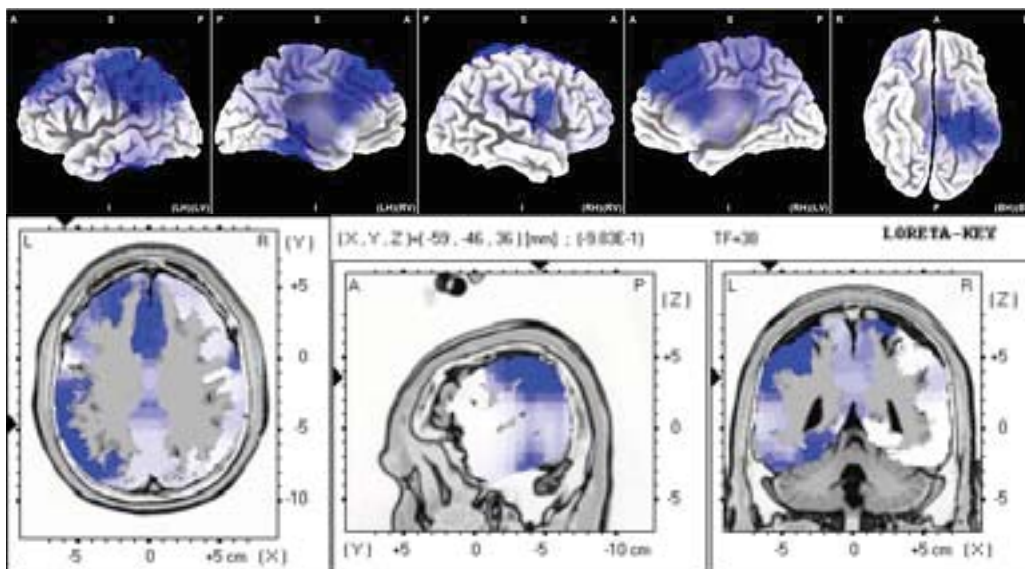


Figure 114. Paired *t*-test for 38 Hz LORETA: Significant differences after 20 minutes of 0.5 Hz CES.

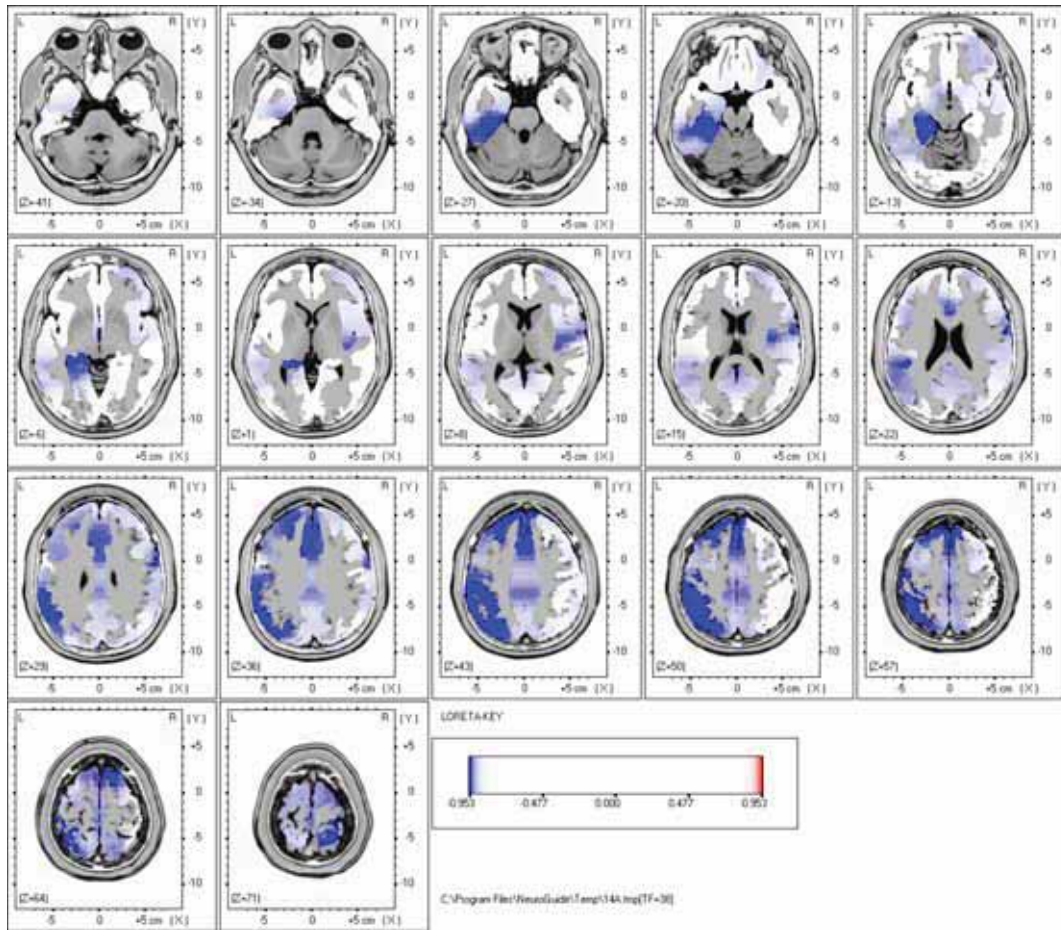


Figure 115. Paired t -test for 38 Hz LORETA: Significant differences after 20 minutes of 0.5 Hz CES.

Summary of 39 Hz Changes in Current Density

Decreased Frontal Lobe Activation

- Left Superior Frontal Gyrus (Brodmann Area 8)
- Left Middle Frontal Gyrus (Brodmann Area 9)
- Left and Right Medial Frontal Gyrus (Brodmann Area 8)
- Left Precentral Gyrus (Brodmann Area 4)

Decreased Temporal Lobe Activation

- Left Fusiform Gyrus (Brodmann Area 20)

Decreased Limbic Lobe Activation

- Left Parahippocampal Gyrus (Brodmann Area 34)

Decreased Parietal Lobe Activation

- Left Postcentral Gyrus (Brodmann Area 2)
- Left Inferior Parietal Lobule (Brodmann Area 40)
- Left Superior Parietal Lobule (Brodmann Area 7)
- Left Precuneus (Brodmann Area 7)

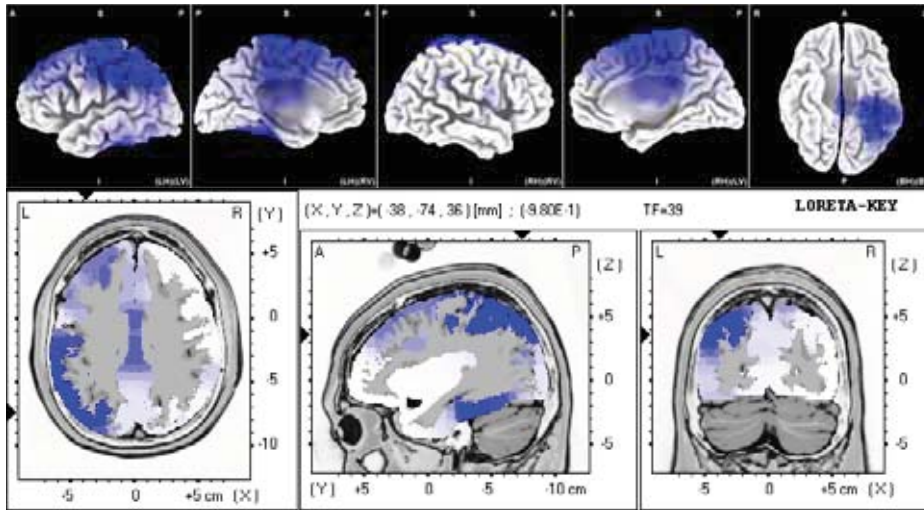


Figure 116. Paired *t*-test for 39 Hz LORETA: Significant differences after 20 minutes of 0.5 Hz CES.

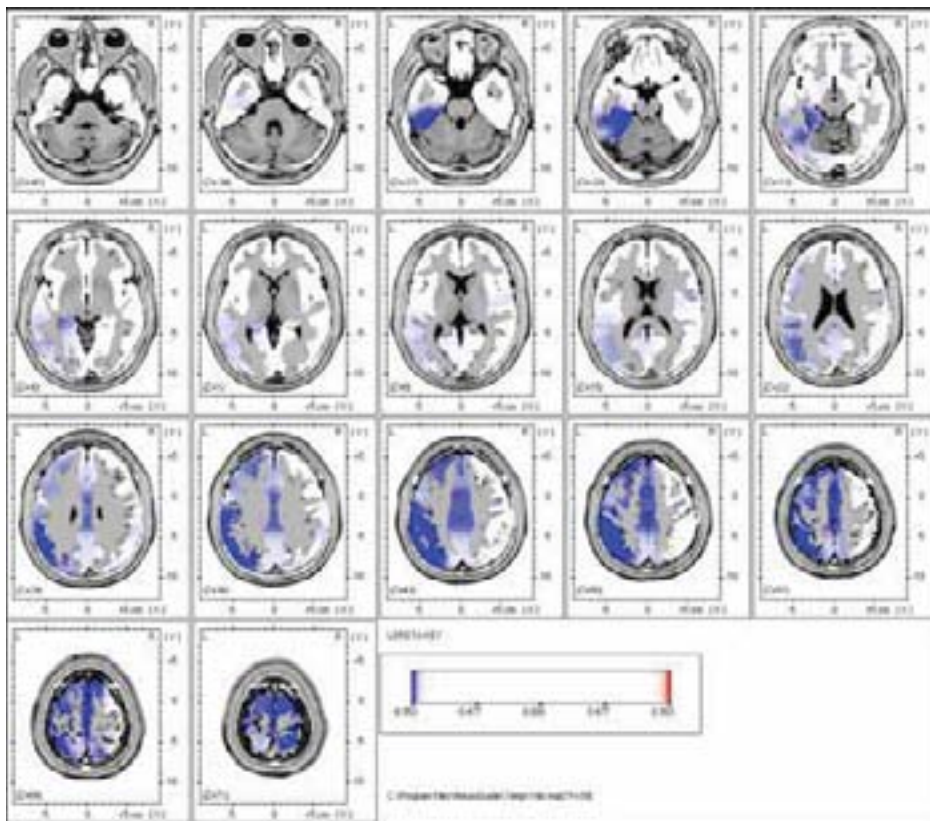


Figure 117. Paired *t*-test for 39 Hz LORETA: Significant differences after 20 minutes of 0.5 Hz CES.

Summary of 40 Hz Changes in Current Density

Decreased Temporal Lobe Activation

- Left Fusiform Gyrus (Brodmann Area 20)

Decreased Limbic Lobe Activation

- Left Parahippocampal Gyrus (Brodmann Area 34)

Decreased Parietal Lobe Activation

- Left Postcentral Gyrus (Brodmann Area 2)
- Left Inferior Parietal Lobule (Brodmann Area 40)
- Left Superior Parietal Lobule (Brodmann Area 7)
- Left Precuneus (Brodmann Area 19)

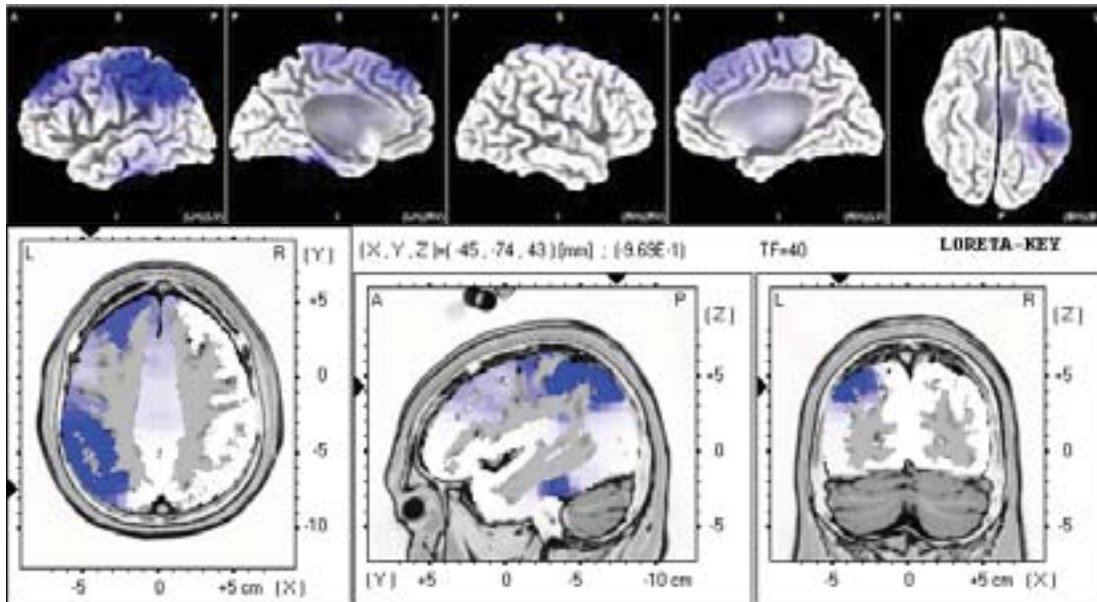


Figure 118. Paired *t*-test for 40 Hz LORETA: Significant differences after 20 minutes of 0.5 Hz CES.

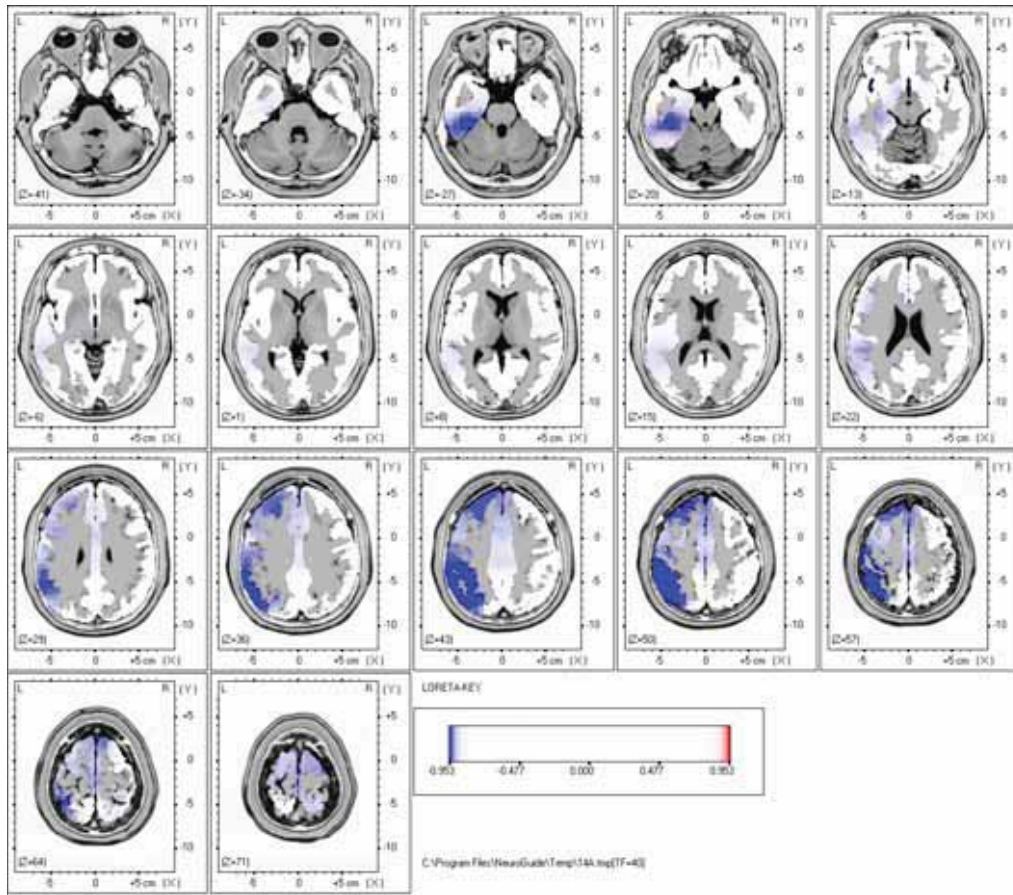


Figure 119. Paired t -test for 40 Hz LORETA: Significant differences after 20 minutes of 0.5 Hz CES.

LORETA Paired t -Test Results for 100 Hz CES in 1 Hz Increments

The following figures present the results of the LORETA paired t -test for the 100 Hz CES group. These images represent statistically significant changes at the .05 level after 20 minutes of 0.5 Hz CES. Red indicates a statistically significant increase in activity after CES while blue indicates a statistically significant decrease in activity after CES.

Summary of 1 Hz Changes in Current Density

Decreased Frontal Lobe Activation

- Left Superior Frontal Gyrus (Brodmann Area 8)
- Left Middle Frontal Gyrus (Brodmann Area 8)

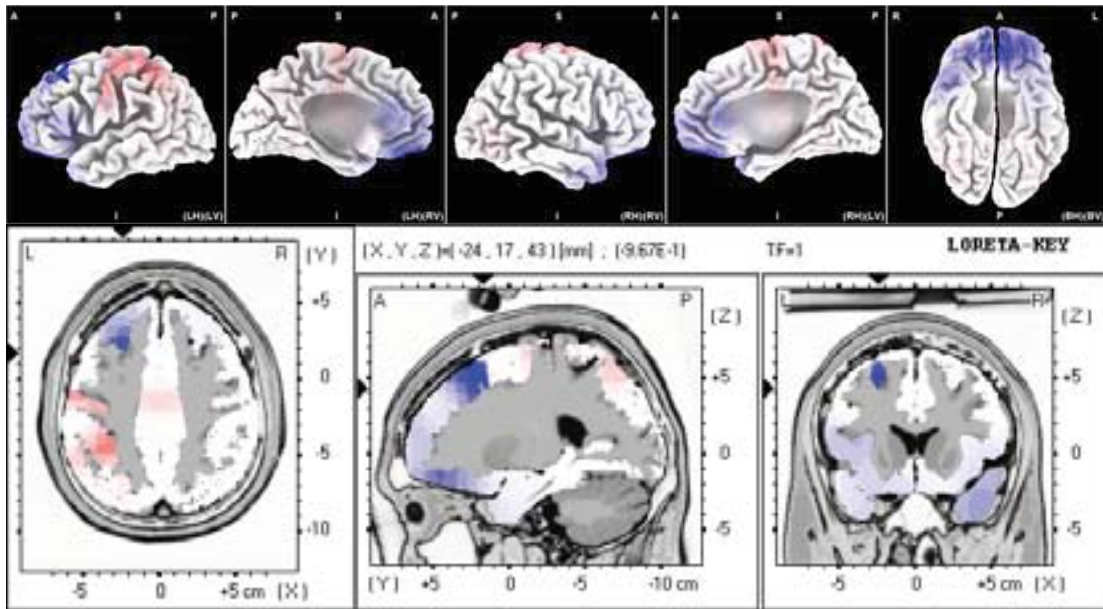


Figure 120. Paired t -test for 1 Hz LORETA: Significant differences after 20 minutes of 100 Hz CES.

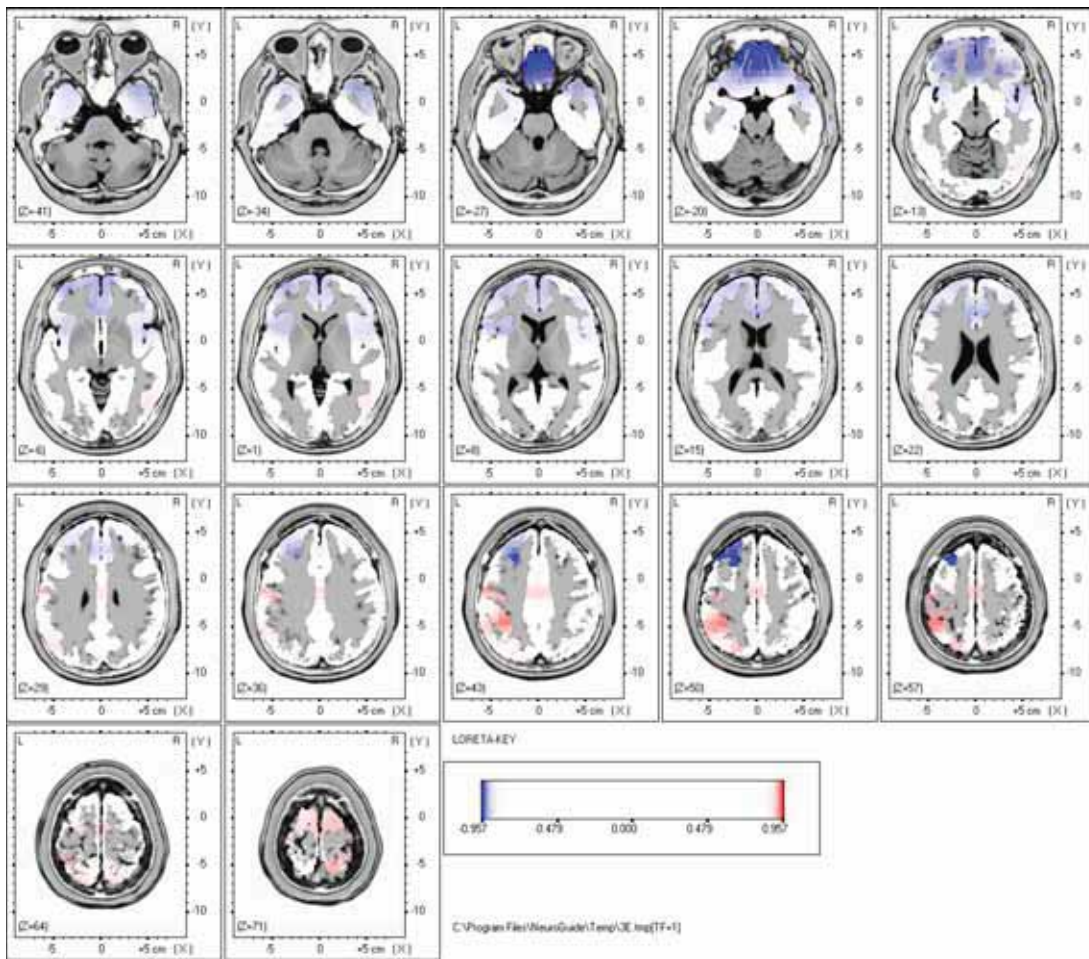


Figure 121. Paired t -test for 1 Hz LORETA: Significant differences after 20 minutes of 100 Hz CES.

Summary of 2 Hz Changes in Current Density

Decreased Frontal Lobe Activation

- Right and Left Superior Frontal Gyrus (Brodmann Area 10)
- Right Middle Frontal Gyrus (Brodmann Area 8)
- Right and Left Medial Frontal Gyrus (Brodmann Area 8)
- Right and Left Orbital Gyrus (Brodmann Area 11)
- Right and Left Rectal Gyrus (Brodmann Area 11)
- Right Inferior Frontal Gyrus (Brodmann Area 47)

Decreased Limbic Lobe Activation

- Left and Right Anterior Cingulate (Brodmann Area 32)

Increased Frontal Lobe Activation

- Left Precentral Gyrus (Brodmann Area 6)
- Left Middle Frontal Gyrus (Brodmann Area 6)

Increased Parietal Lobe Activation

- Left Postcentral Gyrus (Brodmann Area 2)
- Left Inferior Parietal Lobule (Brodmann Area 40)
- Left Superior Parietal Lobule (Brodmann Area 7)
- Left Precuneus (Brodmann Area 7)

Increased Limbic Lobe Activation

- Right and Left Cingulate Gyrus (Brodmann Area 24)

Increased Temporal Lobe Activation

- Left Transverse Temporal Gyrus

Increased Sub-Lobar Activation

- Left Insula

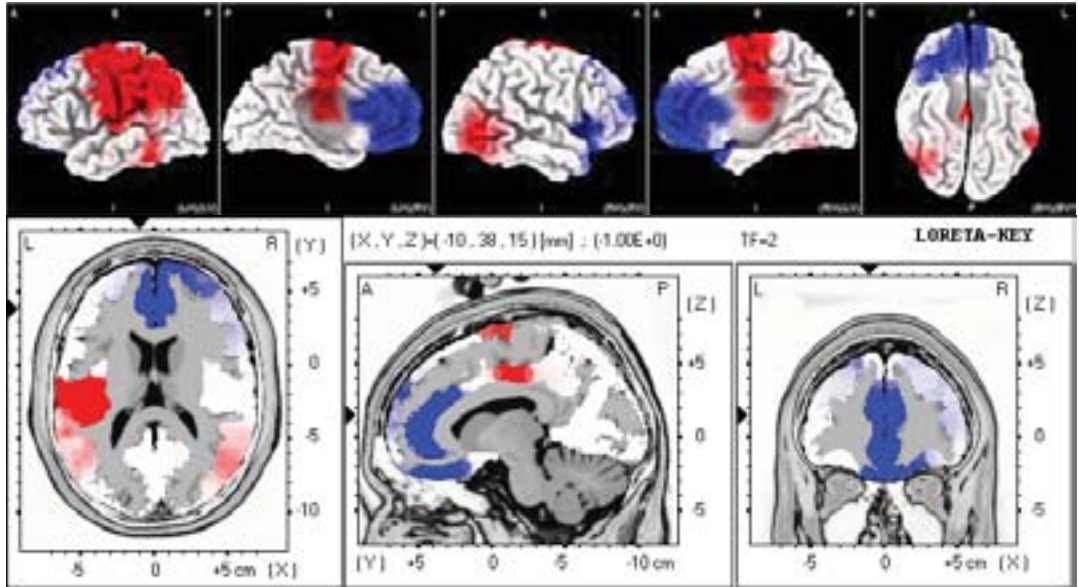


Figure 122. Paired t -test for 2 Hz LORETA: Significant differences after 20 minutes of 100 Hz CES.

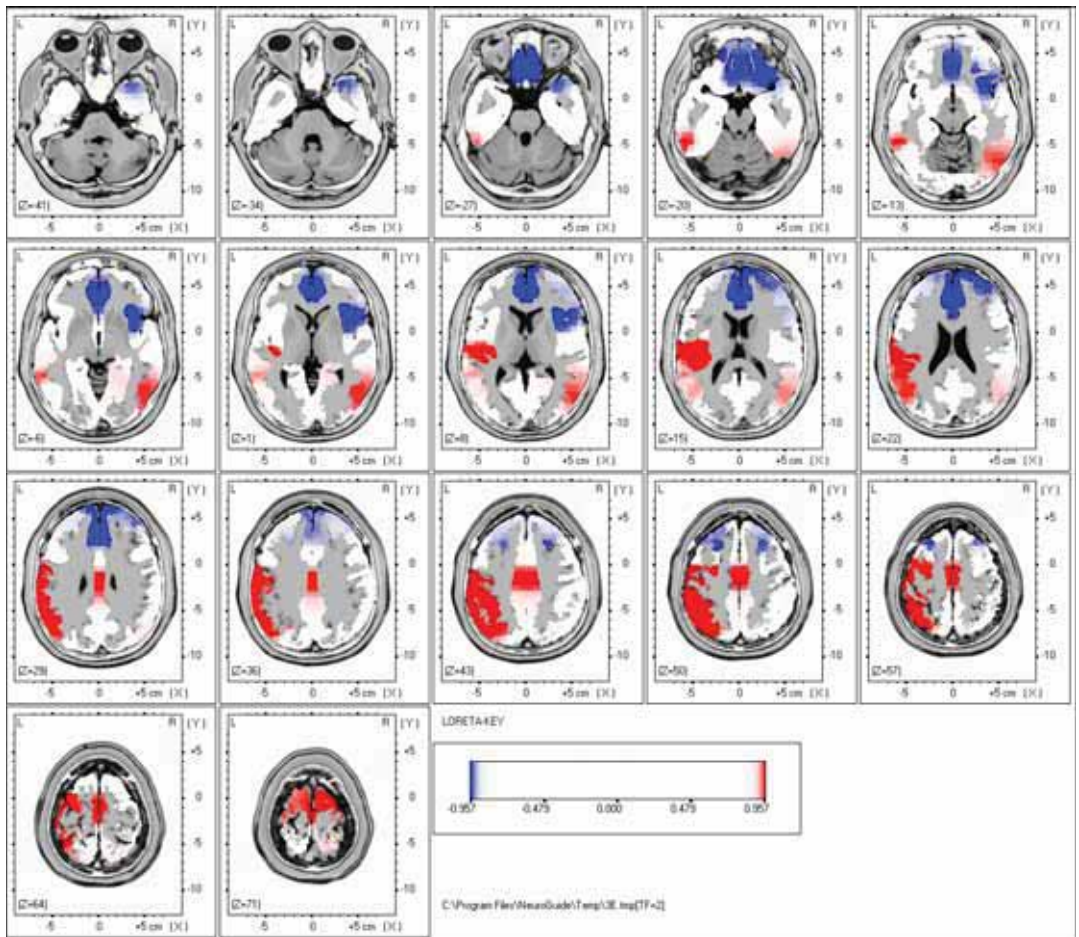


Figure 123. Paired t -test for 2 Hz LORETA: Significant differences after 20 minutes of 100 Hz CES.

Summary of 3 Hz Changes in Current Density

Decreased Frontal Lobe Activation

- Left Superior Frontal Gyrus (Brodmann Area 10)
- Right and Left Medial Frontal Gyrus (Brodmann Area 8)

Increased Frontal Lobe Activation

- Left Precentral Gyrus (Brodmann Area 4)

Increased Parietal Lobe Activation

- Left Postcentral Gyrus (Brodmann Area 2)
- Left Inferior Parietal Lobule (Brodmann Area 40)

Increased Temporal Lobe Activation

- Left Transverse Temporal Gyrus (Brodmann Area 41)
- Left Superior Temporal Gyrus (Brodmann Area 29)
- Right Hippocampus (Sub-Gyral)

Increased Sub-Lobar Activation

- Left Insula (Brodmann Area 13)

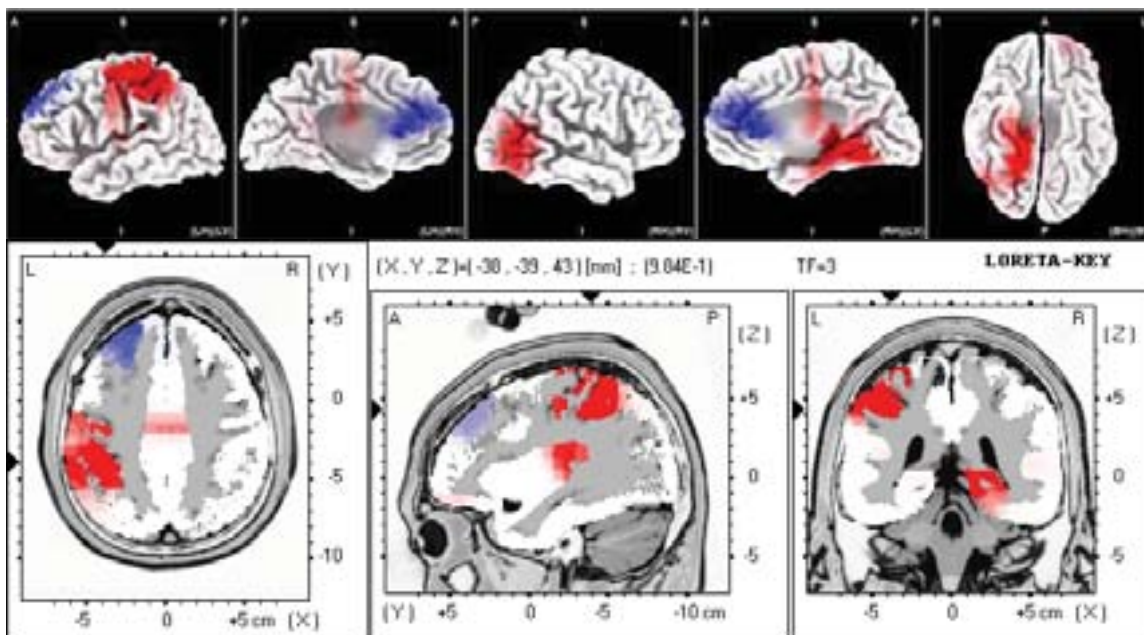


Figure 124. Paired *t*-test for 3 Hz LORETA: Significant differences after 20 minutes of 100 Hz CES.

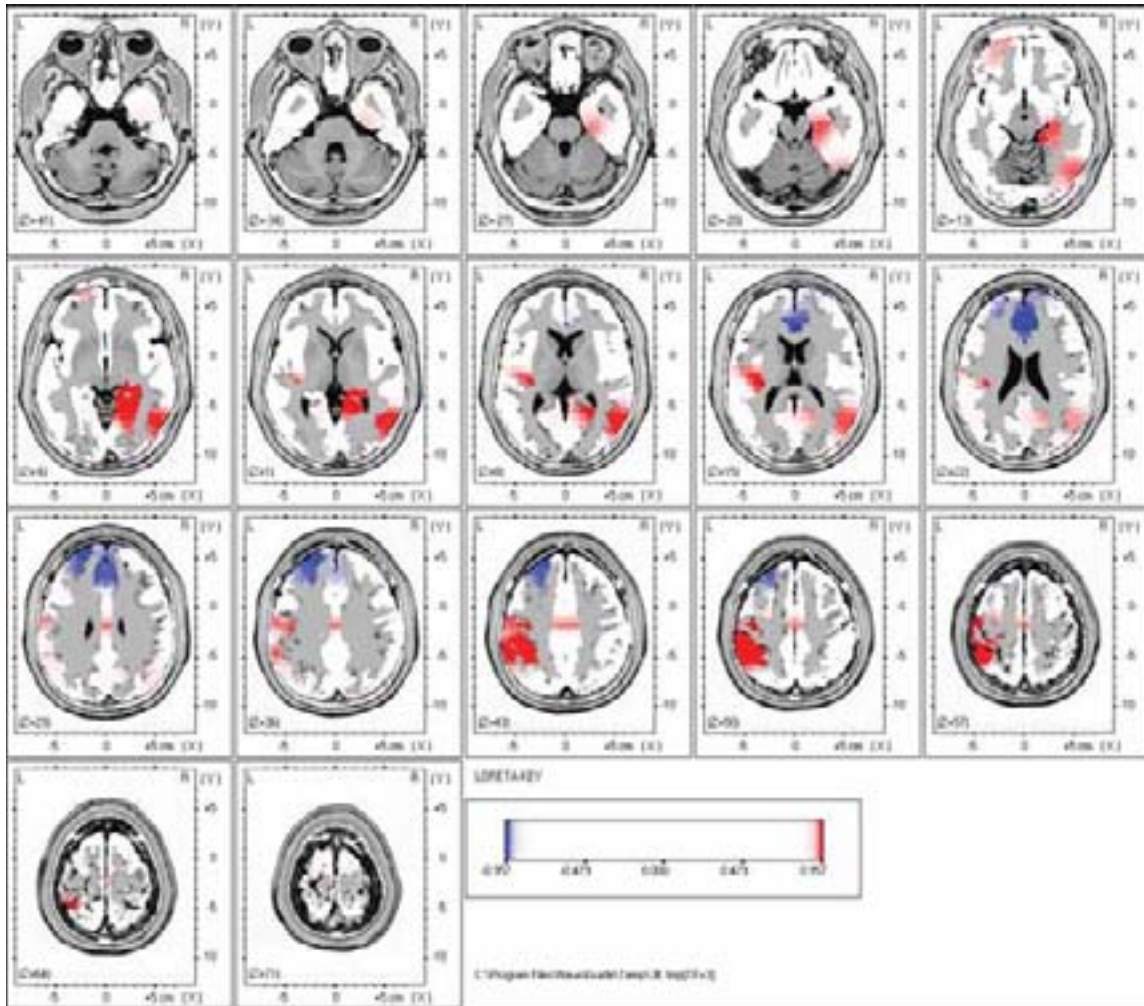


Figure 125. Paired *t*-test for 3 Hz LORETA: Significant differences after 20 minutes of 100 Hz CES.

Summary of 4 Hz Changes in Current Density

Increased Parietal Lobe Activation

- Left Inferior Parietal Lobule (Brodmann Area 40)
- Left Supramarginal Gyrus (Brodmann Area 40)
- Left Angular Gyrus (Brodmann Area 39)

Increased Temporal Lobe Activation

- Right and Left Superior Temporal Gyrus (Brodmann Area 29)
- Right Middle Temporal Gyrus (Brodmann Area 39)
- Right Hippocampus (Sub-Gyral)

Increased Limbic Lobe Activation

- Right Parahippocampal Gyrus (Brodmann Area 19)
- Right Posterior Cingulate (Brodmann Area 30)

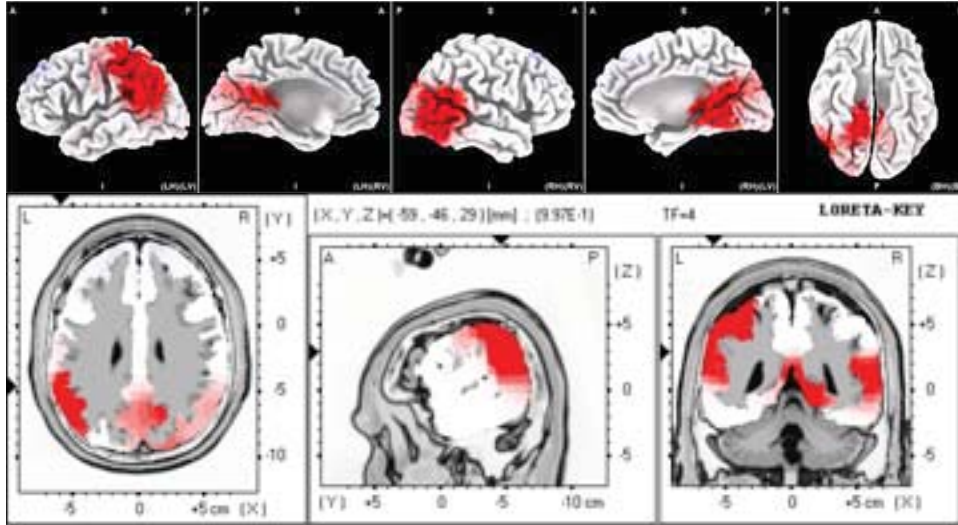


Figure 126. Paired *t*-test for 4 Hz LORETA: Significant differences after 20 minutes of 100 Hz CES.

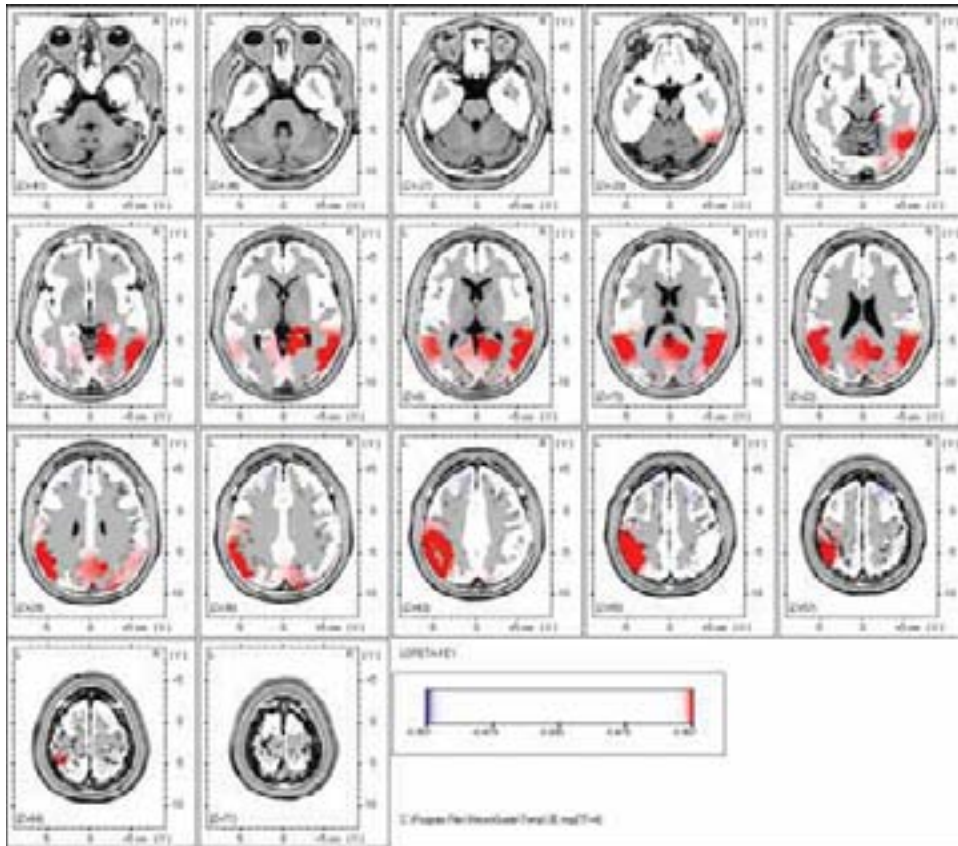


Figure 127. Paired *t*-test for 4 Hz LORETA: Significant differences after 20 minutes of 100 Hz CES.

Summary of 5 Hz Changes in Current Density

Decreased Frontal Lobe Activation

- Right Superior Frontal Gyrus (Brodmann Area 10)
- Right and Left Medial Frontal Gyrus (Brodmann Area 9)

Increased Frontal Lobe Activation

- Left Precentral Gyrus (Brodmann Area 6)

Increased Parietal Lobe Activation

- Left Postcentral Gyrus (Brodmann Area 2)
- Left and Right Inferior Parietal Lobule (Brodmann Area 40)
- Left and Right Supramarginal Gyrus (Brodmann Area 40)
- Left and Right Angular Gyrus (Brodmann Area 39)
- Left and Right Precuneus (Brodmann Area 19)

Increased Temporal Lobe Activation

- Right and Left Superior Temporal Gyrus (Brodmann Area 29)
- Right Middle Temporal Gyrus (Brodmann Area 39)
- Right Hippocampus (Sub-Gyral)

Increased Limbic Lobe Activation

- Right and Left Parahippocampal Gyrus (Brodmann Area 19)
- Right and Left Posterior Cingulate (Brodmann Area 30)
- Right and Left Hippocampus (Sub-Gyral)

Increased Occipital Lobe Activation

- Right and Left Lingual Gyrus (Brodmann Area 18)
- Right Inferior Occipital Gyrus (Brodmann Area 18)

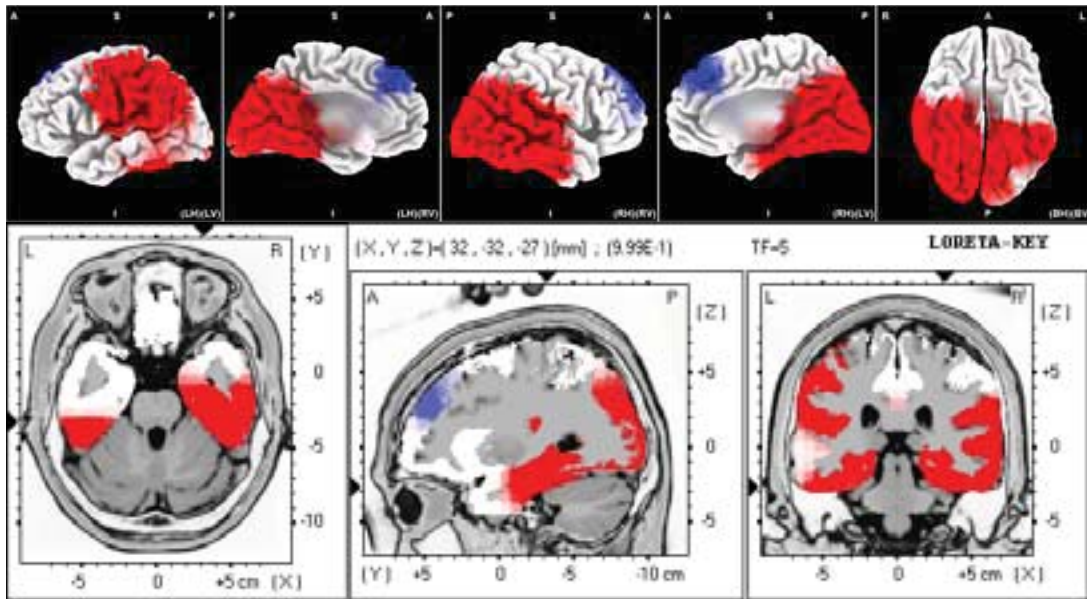


Figure 128. Paired t -test for 5 Hz LORETA: Significant differences after 20 minutes of 100 Hz CES.

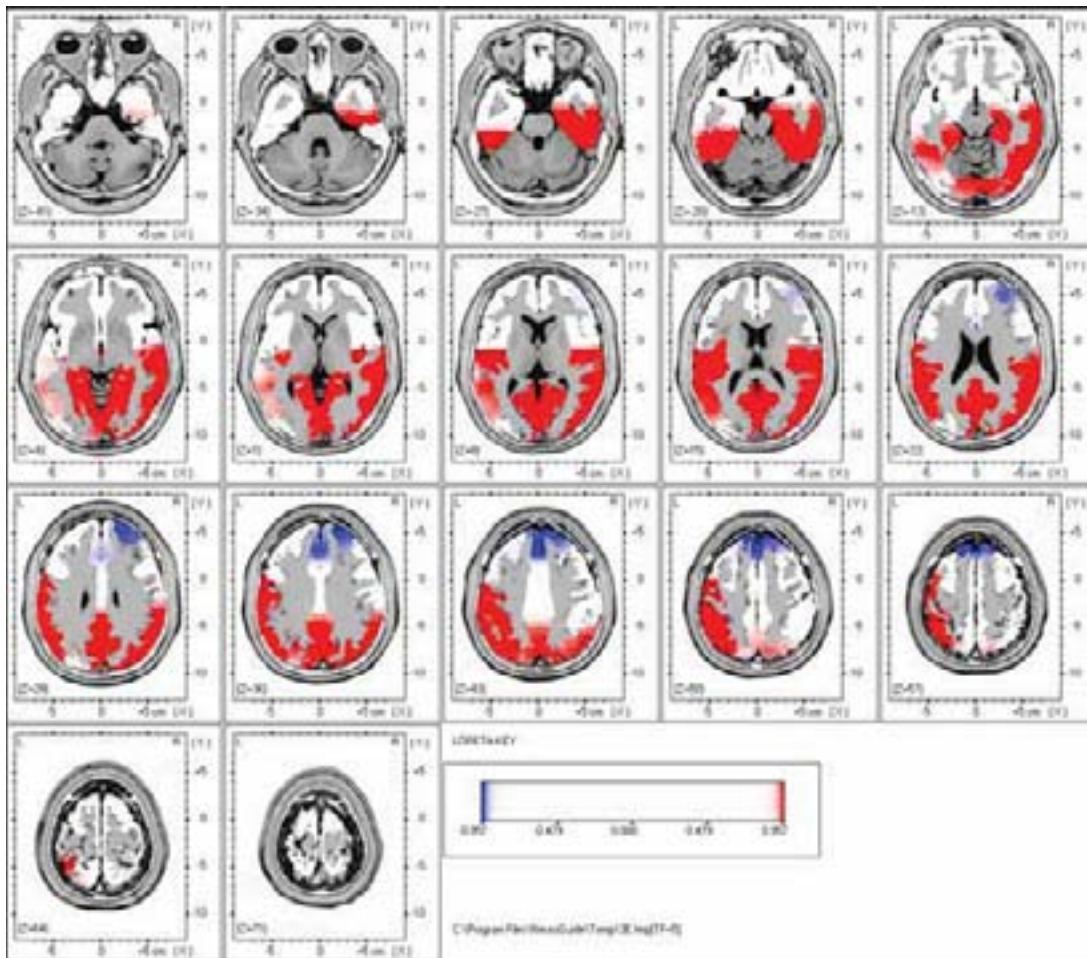


Figure 129. Paired t -test for 5 Hz LORETA: Significant differences after 20 minutes of 100 Hz CES.

Summary of 6 Hz Changes in Current Density

Increased Frontal Lobe Activation

- Right and Left Superior Frontal Gyrus (Brodmann Area 10)
- Right and Left Inferior Frontal Gyrus (Brodmann Area 47)
- Right and Left Medial Frontal Gyrus (Brodmann Area 10)
- Right and Left Orbital Gyrus (Brodmann Area 11)
- Right and Left Rectal Gyrus (Brodmann Area 11)
- Left Precentral Gyrus (Brodmann Area 4)
- Right and Left Subcallosal Gyrus (Brodmann Area 34)

Increased Parietal Lobe Activation

- Right and Left Postcentral Gyrus (Brodmann Area 40)
- Left and Right Inferior Parietal Lobule (Brodmann Area 40)
- Left and Right Supramarginal Gyrus (Brodmann Area 40)

Increased Temporal Lobe Activation

- Right and Left Superior Temporal Gyrus (Brodmann Area 29)
- Right and Left Transverse Temporal Gyrus (Brodmann Area 41)
- Left and Right Middle Temporal Gyrus (Brodmann Area 39)
- Right Inferior Temporal Gyrus (Brodmann Area 20)
- Right and Left Fusiform Gyrus (Brodmann Area 37)

Increased Limbic Lobe Activation

- Right Hippocampus (Brodmann Area 27)
- Right and Left Parahippocampal Gyrus (Brodmann Area 19)
- Right and Left Anterior Cingulate (Brodmann Area 25)
- Right and Left Cingulate Gyrus (Brodmann Area 24)
- Right and Left Posterior Cingulate (Brodmann Area 30)
- Right Uncus (Brodmann Area 28)

Increased Sub-lobar

- Right and Left Insula (Brodmann Area 13)

Increased Occipital Lobe Activation

- Right Superior Occipital Gyrus (Brodmann Area 19)
- Right Lingual Gyrus (Brodmann Area 18)

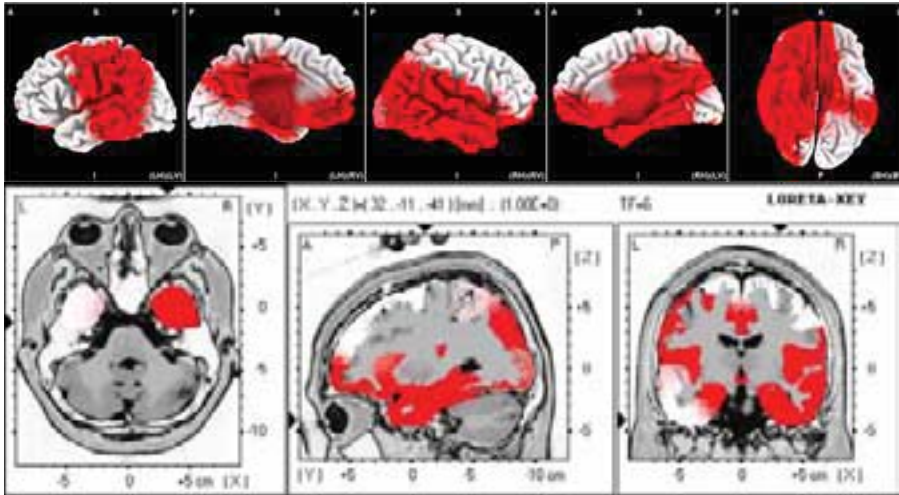


Figure 130. Paired t -test for 6 Hz LORETA: Significant differences after 20 minutes of 100 Hz CES.

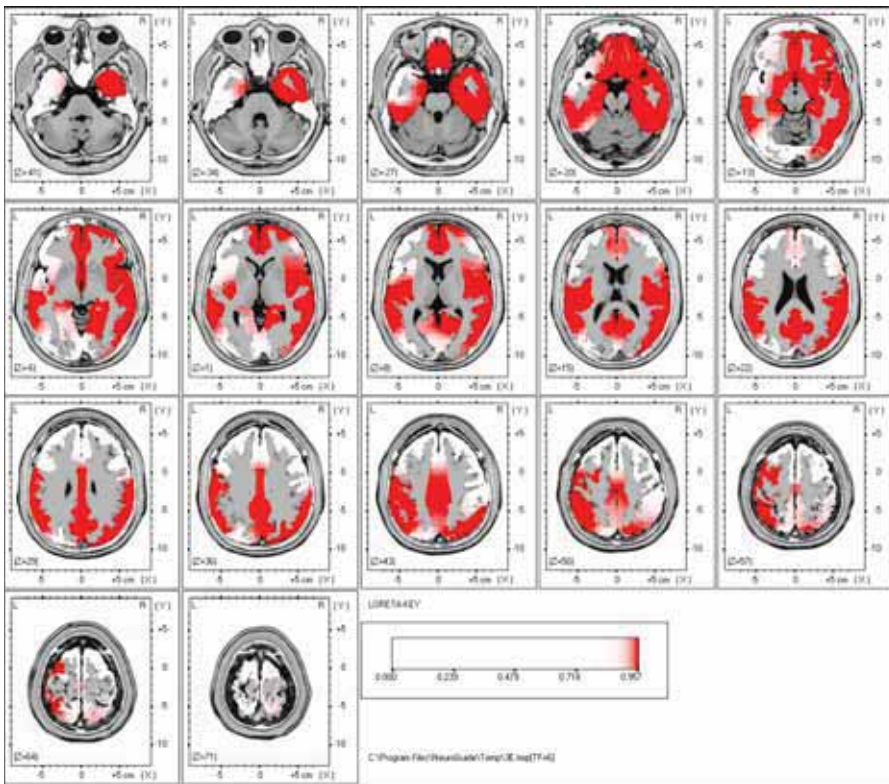


Figure 131. Paired t -test for 6 Hz LORETA: Significant differences after 20 minutes of 100 Hz CES.

Summary of 7 Hz Changes in Current Density

Increased Frontal Lobe Activation

- Right and Left Superior Frontal Gyrus (Brodmann Area 10)
- Right and Left Inferior Frontal Gyrus (Brodmann Area 47)
- Right and Left Medial Frontal Gyrus (Brodmann Area 10)
- Right and Left Orbital Gyrus (Brodmann Area 11)
- Right and Left Rectal Gyrus (Brodmann Area 11)
- Left Precentral Gyrus (Brodmann Area 4)
- Right and Left Subcallosal Gyrus (Brodmann Area 34)

Increased Parietal Lobe Activation

- Right and Left Postcentral Gyrus (Brodmann Area 40)
- Left and Right Inferior Parietal Lobule (Brodmann Area 40)
- Right and Left Superior Parietal Lobule (Brodmann Area 7)
- Right and Left Precuneus (Brodmann Area 7)

Increased Temporal Lobe Activation

- Right and Left Superior Temporal Gyrus (Brodmann Area 29)
- Right and Left Transverse Temporal Gyrus (Brodmann Area 41)
- Right and Left Middle Temporal Gyrus (Brodmann Area 39)
- Right and Left Inferior Temporal Gyrus (Brodmann Area 20)
- Right and Left Fusiform Gyrus (Brodmann Area 37)

Increased Limbic Lobe Activation

- Right and Left Hippocampus (Brodmann Area 27)
- Right and Left Parahippocampal Gyrus (Brodmann Area 19)

- Right and Left Cingulate Gyrus (Brodmann Area 24)
- Right and Left Posterior Cingulate (Brodmann Area 30)
- Right and Left Uncus (Brodmann Area 28)

Increased Sub-lobar

- Right and Left Insula (Brodmann Area 13)

Increased Occipital Lobe Activation

- Right Superior Occipital Gyrus (Brodmann Area 19)
- Right Inferior Occipital Gyrus (Brodmann Area 18)
- Right Middle Occipital Gyrus (Brodmann Area 18)
- Right and Left Lingual Gyrus (Brodmann Area 18)

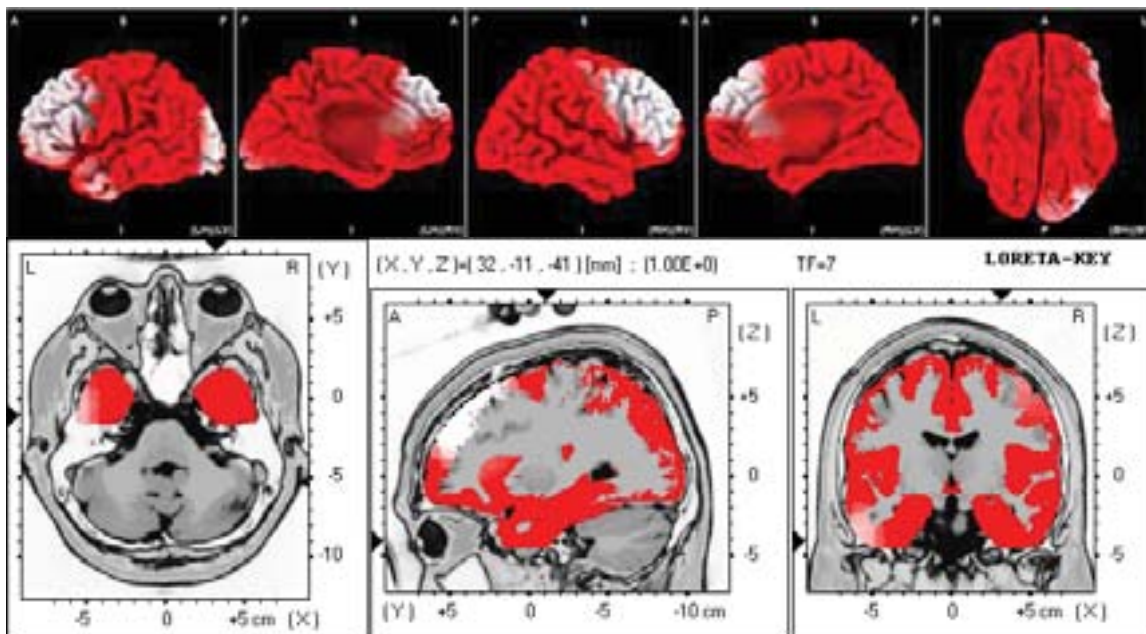


Figure 132. Paired *t*-test for 7 Hz LORETA: Significant differences after 20 minutes of 100 Hz CES.

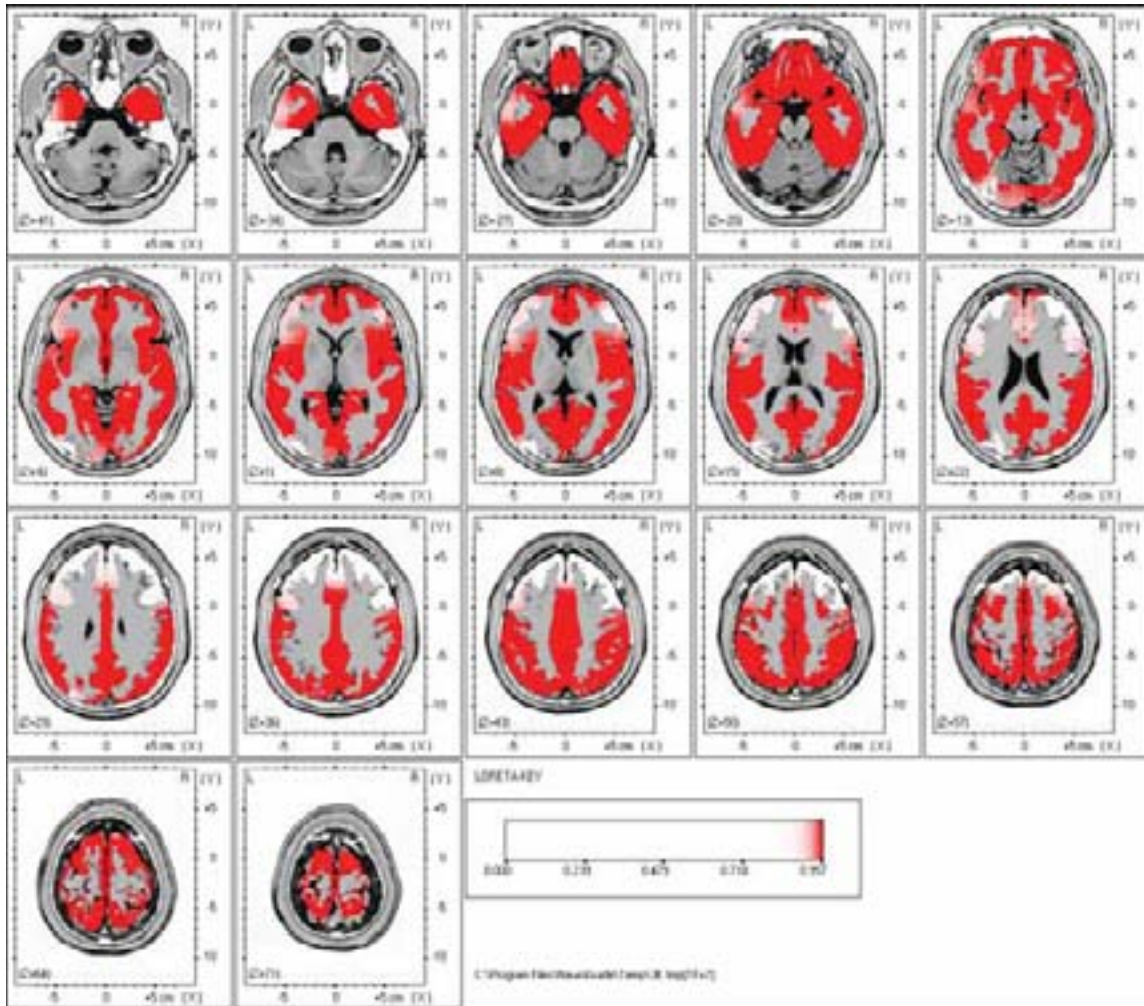


Figure 133. Paired t -test for 7 Hz LORETA: Significant differences after 20 minutes of 100 Hz CES.

Summary of 8 Hz Changes in Current Density

Increased Frontal Lobe Activation

- Right Superior Frontal Gyrus (Brodmann Area 10)
- Right Inferior Frontal Gyrus (Brodmann Area 47)
- Right Middle Frontal Gyrus (Brodmann Area 10)
- Right and Left Medial Frontal Gyrus (Brodmann Area 10)
- Right and Left Orbital Gyrus (Brodmann Area 11)
- Right and Left Rectal Gyrus (Brodmann Area 11)
- Right and Left Subcallosal Gyrus (Brodmann Area 34)

Increased Parietal Lobe Activation

- Right and Left Postcentral Gyrus (Brodmann Area 40)
- Right and Left Inferior Parietal Lobule (Brodmann Area 40)
- Right and Left Supramarginal Gyrus (Brodmann Area 40)
- Right and Left Angular Gyrus (Brodmann Area 39)
- Right and Left Superior Parietal Lobule (Brodmann Area 7)
- Right and Left Precuneus (Brodmann Area 7)

Increased Temporal Lobe Activation

- Right Superior Temporal Gyrus (Brodmann Area 29)
- Right and Left Transverse Temporal Gyrus (Brodmann Area 41)
- Right Middle Temporal Gyrus (Brodmann Area 39)
- Right Inferior Temporal Gyrus (Brodmann Area 20)
- Right and Left Fusiform Gyrus (Brodmann Area 37)

Increased Limbic Lobe Activation

- Right and Left Hippocampus (Brodmann Area 27)
- Right and Left Parahippocampal Gyrus (Brodmann Area 19)
- Right and Left Anterior Cingulate (Brodmann Area 32)
- Right and Left Cingulate Gyrus (Brodmann Area 24)
- Right and Left Posterior Cingulate (Brodmann Area 30)
- Right and Left Uncus (Brodmann Area 28)

Increased Sub-lobar

- Right and Left Insula (Brodmann Area 13)

Increased Occipital Lobe Activation

- Right and Left Superior Occipital Gyrus (Brodmann Area 19)
- Right Inferior Occipital Gyrus (Brodmann Area 18)
- Right and Left Middle Occipital Gyrus (Brodmann Area 18)

- Right and Left Lingual Gyrus (Brodmann Area 18)
- Right and Left Cuneus (Brodmann Area 18)

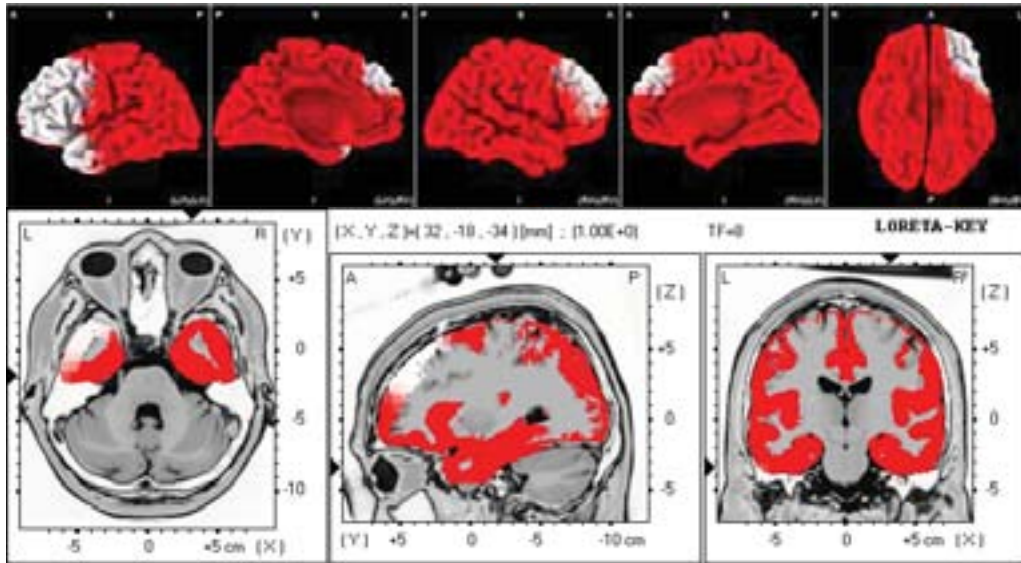


Figure 134. Paired t -test for 8 Hz LORETA: Significant differences after 20 minutes of 100 Hz CES.

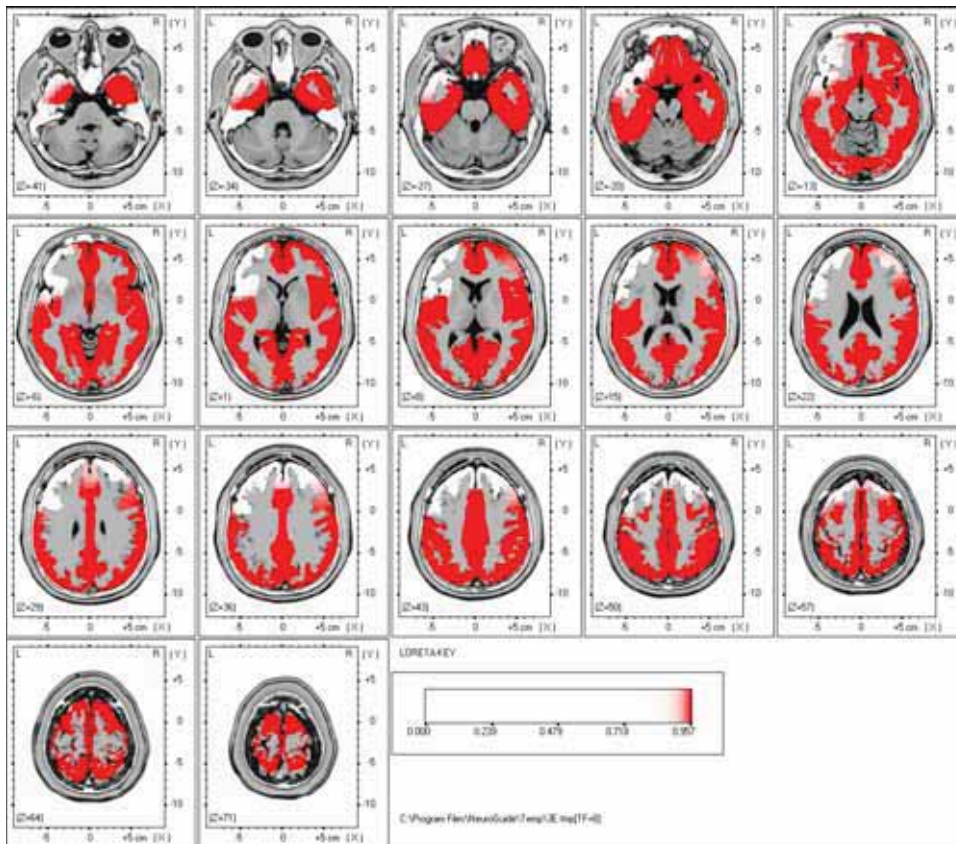


Figure 135. Paired t -test for 8 Hz LORETA: Significant differences after 20 minutes of 100 Hz CES.

Summary of 9 Hz Changes in Current Density

Increased Frontal Lobe Activation

- Right Superior Frontal Gyrus (Brodmann Area 10)
- Right Inferior Frontal Gyrus (Brodmann Area 47)
- Right Middle Frontal Gyrus (Brodmann Area 10)
- Right and Left Medial Frontal Gyrus (Brodmann Area 10)
- Right and Left Orbital Gyrus (Brodmann Area 11)
- Right and Left Rectal Gyrus (Brodmann Area 11)
- Right and Left Subcallosal Gyrus (Brodmann Area 34)

Increased Parietal Lobe Activation

- Right and Left Postcentral Gyrus (Brodmann Area 40)
- Right and Left Inferior Parietal Lobule (Brodmann Area 40)
- Right and Left Supramarginal Gyrus (Brodmann Area 40)
- Right and Left Angular Gyrus (Brodmann Area 39)
- Right and Left Superior Parietal Lobule (Brodmann Area 7)
- Right and Left Precuneus (Brodmann Area 7)

Increased Temporal Lobe Activation

- Right and Left Superior Temporal Gyrus (Brodmann Area 29)
- Right and Left Transverse Temporal Gyrus (Brodmann Area 41)
- Right and Left Middle Temporal Gyrus (Brodmann Area 39)
- Right and Left Inferior Temporal Gyrus (Brodmann Area 20)
- Right and Left Fusiform Gyrus (Brodmann Area 37)

Increased Limbic Lobe Activation

- Right and Left Hippocampus (Brodmann Area 27)
- Right and Left Parahippocampal Gyrus (Brodmann Area 19)
- Right and Left Anterior Cingulate (Brodmann Area 32)
- Right and Left Cingulate Gyrus (Brodmann Area 24)
- Right and Left Posterior Cingulate (Brodmann Area 30)
- Right and Left Uncus (Brodmann Area 28)

Increased Sub-lobar

- Right and Left Insula (Brodmann Area 13)

Increased Occipital Lobe Activation

- Right and Left Superior Occipital Gyrus (Brodmann Area 19)
- Right and Left Inferior Occipital Gyrus (Brodmann Area 18)
- Right and Left Middle Occipital Gyrus (Brodmann Area 18)
- Right and Left Lingual Gyrus (Brodmann Area 18)
- Right and Left Cuneus (Brodmann Area 18)

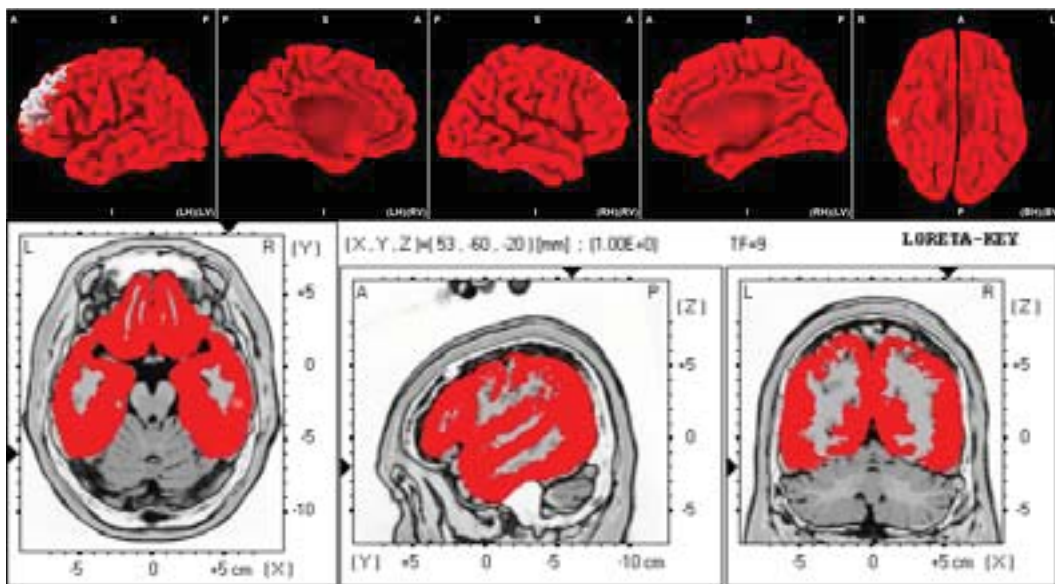


Figure 136. Paired *t*-test for 9 Hz LORETA: Significant differences after 20 minutes of 100 Hz CES.

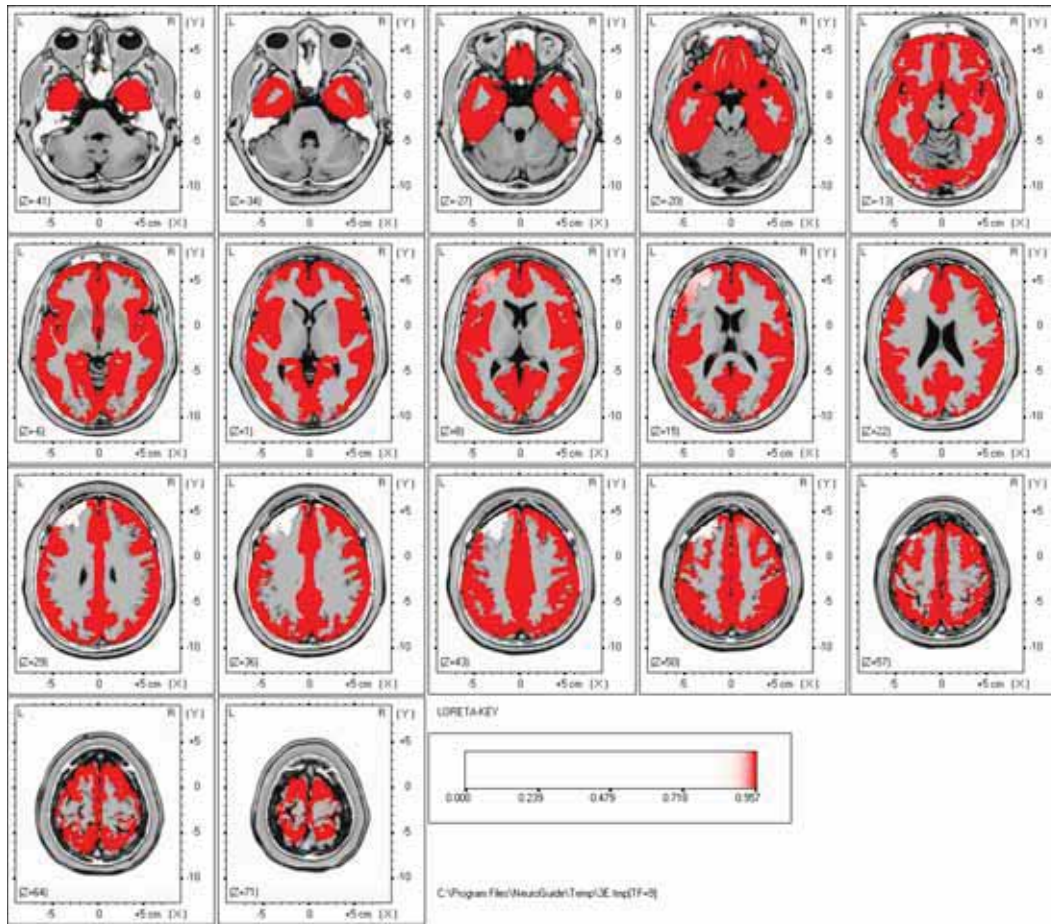


Figure 137. Paired t -test for 9 Hz LORETA: Significant differences after 20 minutes of 100 Hz CES.

Summary of 10 Hz Changes in Current Density

Increased Frontal Lobe Activation

- Right Inferior Frontal Gyrus (Brodmann Area 47)
- Right and Left Medial Frontal Gyrus (Brodmann Area 10)
- Right and Left Orbital Gyrus (Brodmann Area 11)
- Right and Left Rectal Gyrus (Brodmann Area 11)
- Right and Left Subcallosal Gyrus (Brodmann Area 34)

Increased Parietal Lobe Activation

- Right and Left Postcentral Gyrus (Brodmann Area 40)
- Right and Left Inferior Parietal Lobule (Brodmann Area 40)
- Right and Left Supramarginal Gyrus (Brodmann Area 40)

- Right and Left Angular Gyrus (Brodmann Area 39)
- Right and Left Superior Parietal Lobule (Brodmann Area 7)
- Right and Left Precuneus (Brodmann Area 7)

Increased Temporal Lobe Activation

- Right Superior Temporal Gyrus (Brodmann Area 29)
- Right and Left Transverse Temporal Gyrus (Brodmann Area 41)
- Right and Left Middle Temporal Gyrus (Brodmann Area 39)
- Right and Left Inferior Temporal Gyrus (Brodmann Area 20)
- Right and Left Fusiform Gyrus (Brodmann Area 37)

Increased Limbic Lobe Activation

- Right and Left Hippocampus (Brodmann Area 27)
- Right and Left Parahippocampal Gyrus (Brodmann Area 19)
- Right and Left Anterior Cingulate (Brodmann Area 32)
- Right and Left Cingulate Gyrus (Brodmann Area 24)
- Right and Left Posterior Cingulate (Brodmann Area 30)
- Right and Left Uncus (Brodmann Area 28)

Increased Sub-lobar

- Right and Left Insula (Brodmann Area 13)

Increased Occipital Lobe Activation

- Right and Left Superior Occipital Gyrus (Brodmann Area 19)
- Right and Left Inferior Occipital Gyrus (Brodmann Area 18)
- Right and Left Middle Occipital Gyrus (Brodmann Area 18)
- Right and Left Lingual Gyrus (Brodmann Area 18)
- Right and Left Cuneus (Brodmann Area 18)

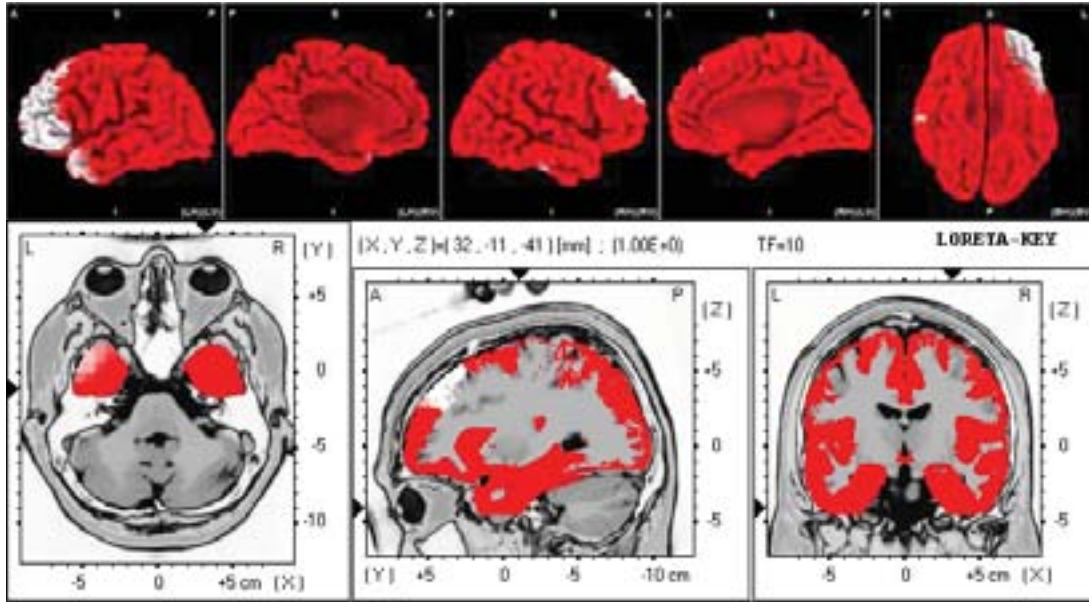


Figure 138. Paired t -test for 10 Hz LORETA: Significant differences after 20 minutes of 100 Hz CES.

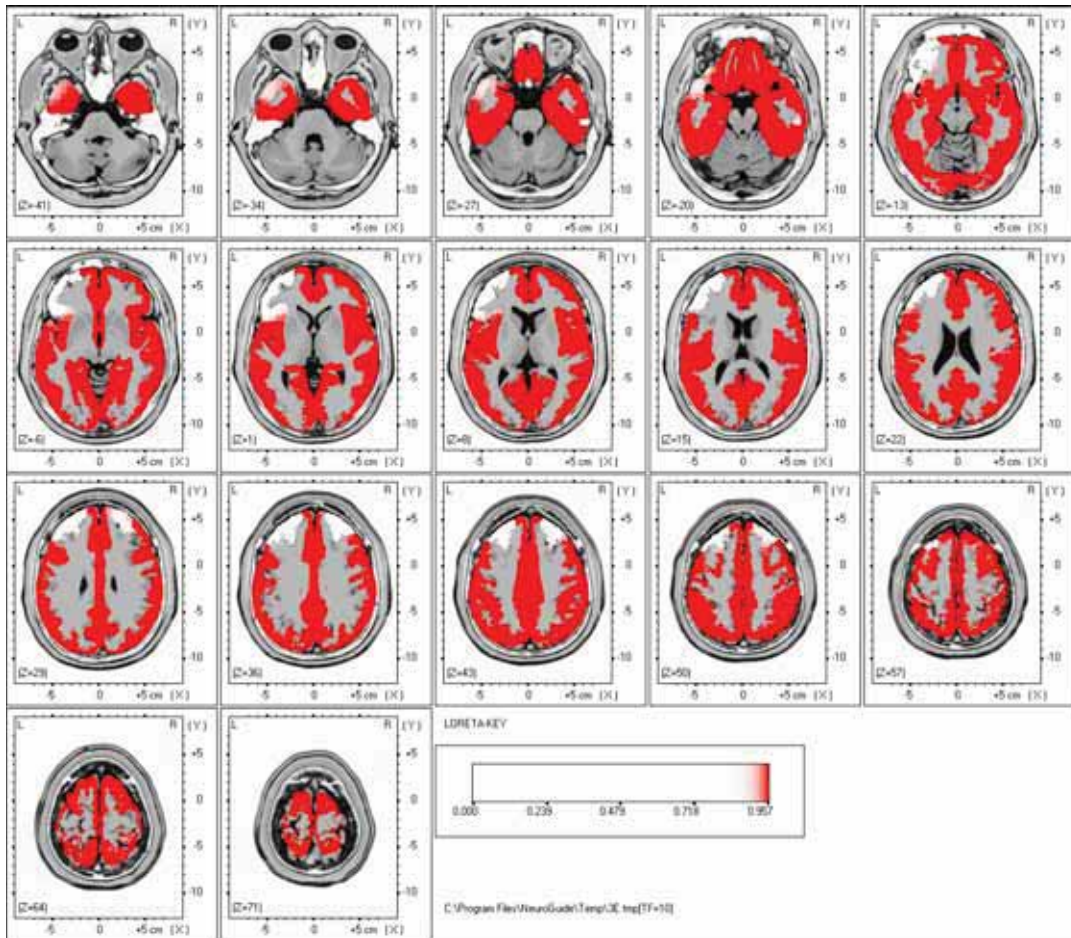


Figure 139. Paired t -test for 10 Hz LORETA: Significant differences after 20 minutes of 100 Hz CES.

Summary of 11 Hz Changes in Current Density

Increased Frontal Lobe Activation

- Right and Left Superior Frontal Gyrus (Brodmann Area 11)
- Right and Left Inferior Frontal Gyrus (Brodmann Area 44)
- Right and Left Medial Frontal Gyrus (Brodmann Area 25)
- Right and Left Rectal Gyrus (Brodmann Area 11)
- Right and Left Subcallosal Gyrus (Brodmann Area 34)
- Left Precentral Gyrus (Brodmann Area 44)
- Left Middle Frontal Gyrus (Brodmann Area 9)
- Right and Left Rectal Gyrus (Brodmann Area 11)

Increased Parietal Lobe Activation

- Left Postcentral Gyrus (Brodmann Area 40)
- Left Inferior Parietal Lobule (Brodmann Area 40)
- Right and Left Supramarginal Gyrus (Brodmann Area 40)
- Right and Left Angular Gyrus (Brodmann Area 39)
- Right and Left Superior Parietal Lobule (Brodmann Area 7)
- Right and Left Precuneus (Brodmann Area 7)

Increased Temporal Lobe Activation

- Left Superior Temporal Gyrus (Brodmann Area 29)
- Left Transverse Temporal Gyrus (Brodmann Area 41)
- Right and Left Middle Temporal Gyrus (Brodmann Area 39)
- Right Inferior Temporal Gyrus (Brodmann Area 20)

Increased Limbic Lobe Activation

- Right and Left Hippocampus (Brodmann Area 27)
- Right and Left Parahippocampal Gyrus (Brodmann Area 19)
- Right and Left Cingulate Gyrus (Brodmann Area 24)

- Right and Left Posterior Cingulate (Brodmann Area 30)
- Right and Left Uncus (Brodmann Area 28)

Increased Sub-lobar

- Left Insula (Brodmann Area 13)

Increased Occipital Lobe Activation

- Right and Left Superior Occipital Gyrus (Brodmann Area 19)
- Right Inferior Occipital Gyrus (Brodmann Area 18)
- Right and Left Middle Occipital Gyrus (Brodmann Area 18)
- Right and Left Lingual Gyrus (Brodmann Area 18)
- Right and Left Cuneus (Brodmann Area 18)

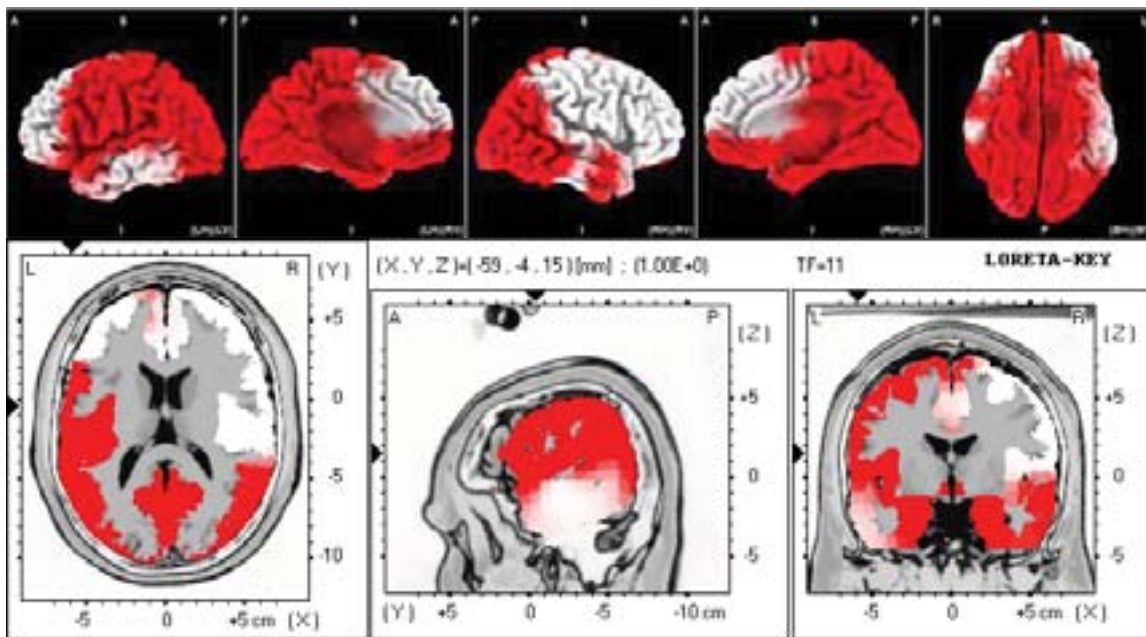


Figure 140. Paired *t*-test for 11 Hz LORETA: Significant differences after 20 minutes of 100 Hz CES.

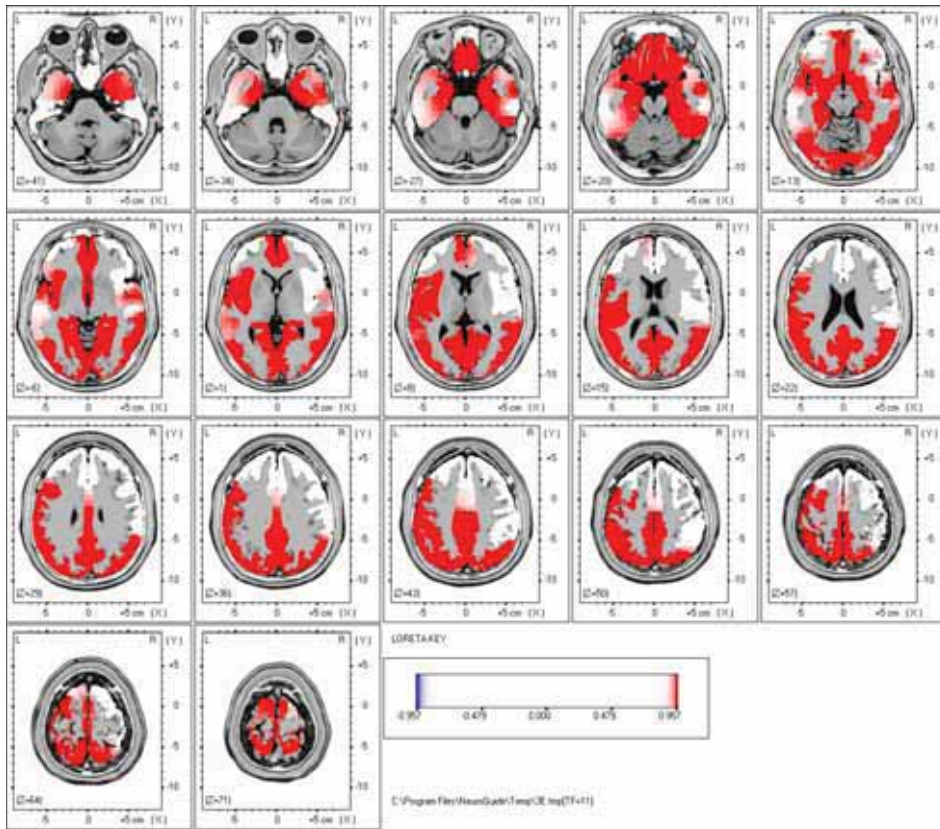


Figure 141. Paired t -test for 11 Hz LORETA: Significant differences after 20 minutes of 100 Hz CES.

Summary of 12 Hz Changes in Current Density

Increased Parietal Lobe Activation

- Left Inferior Parietal Lobule (Brodmann Area 40)

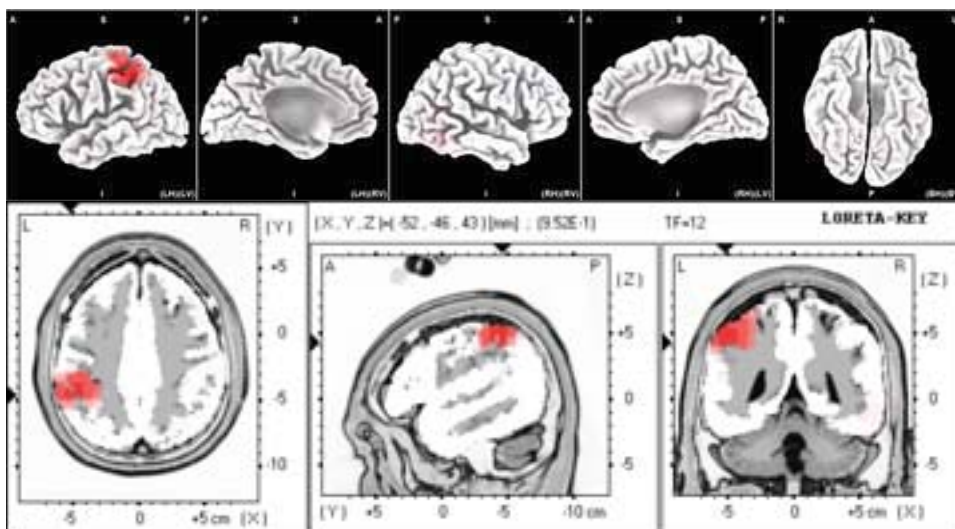


Figure 142. Paired t -test for 12 Hz LORETA: Significant differences after 20 minutes of 100 Hz CES.

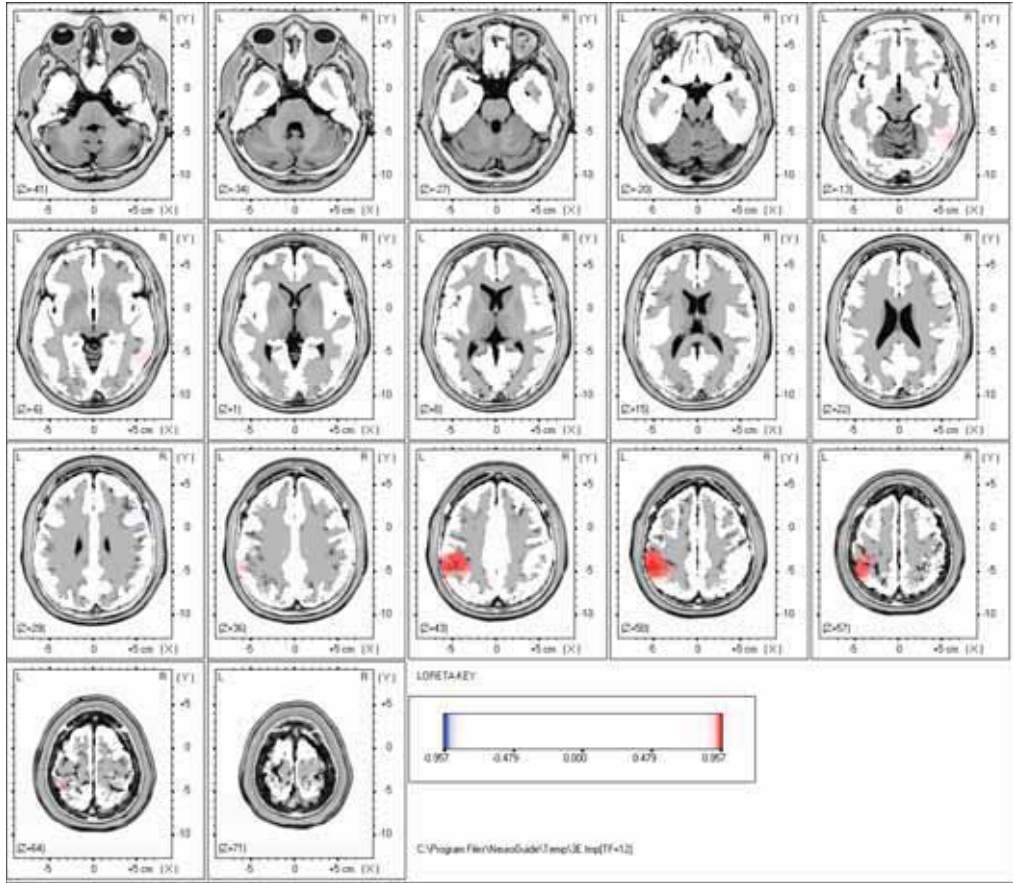


Figure 143. Paired t -test for 12 Hz LORETA: Significant differences after 20 minutes of 100 Hz CES.

Summary of 13 Hz Changes in Current Density

There were no statistically significant changes in 13 Hz current density from baseline.

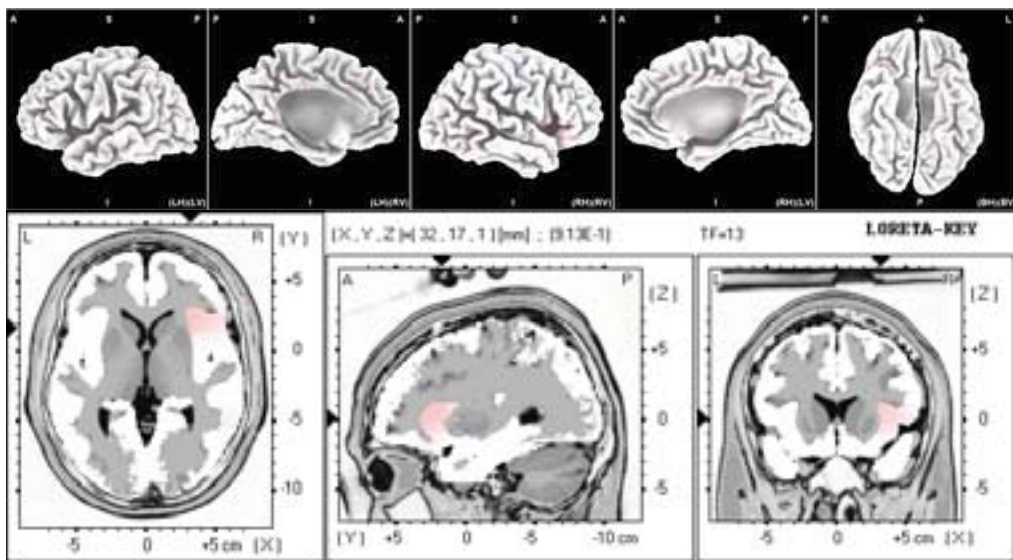


Figure 144. Paired t -test for 13 Hz LORETA: Significant differences after 20 minutes of 100 Hz CES.

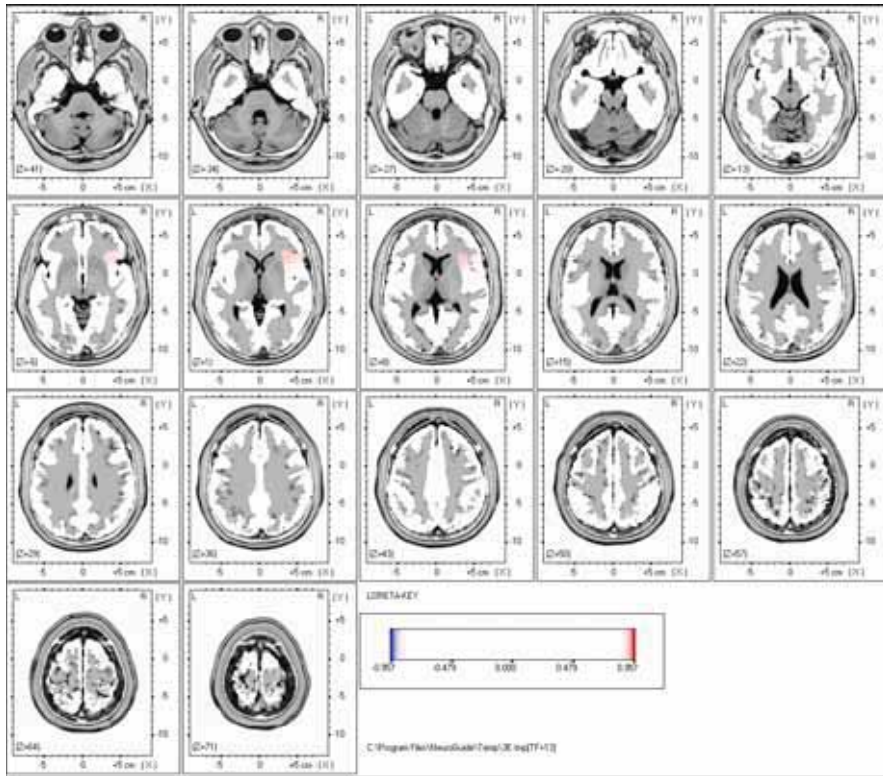


Figure 145. Paired t -test for 13 Hz LORETA: Significant differences after 20 minutes of 100 Hz CES.

Summary of 14 Hz Changes in Current Density

Increased Frontal Lobe Activation

- Right Middle Frontal Gyrus (Brodmann Area 9)

Increased Temporal Lobe Activation

- Right Middle Temporal Gyrus (Brodmann Area 39)

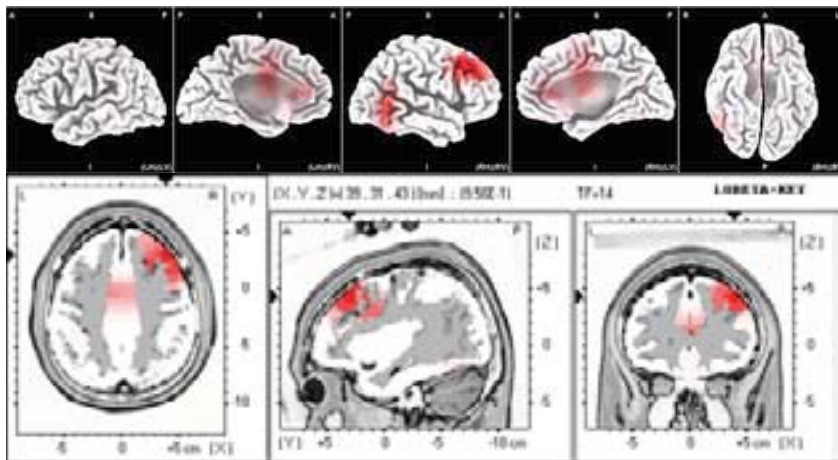


Figure 146. Paired t -test for 14 Hz LORETA: Significant differences after 20 minutes of 100 Hz CES.

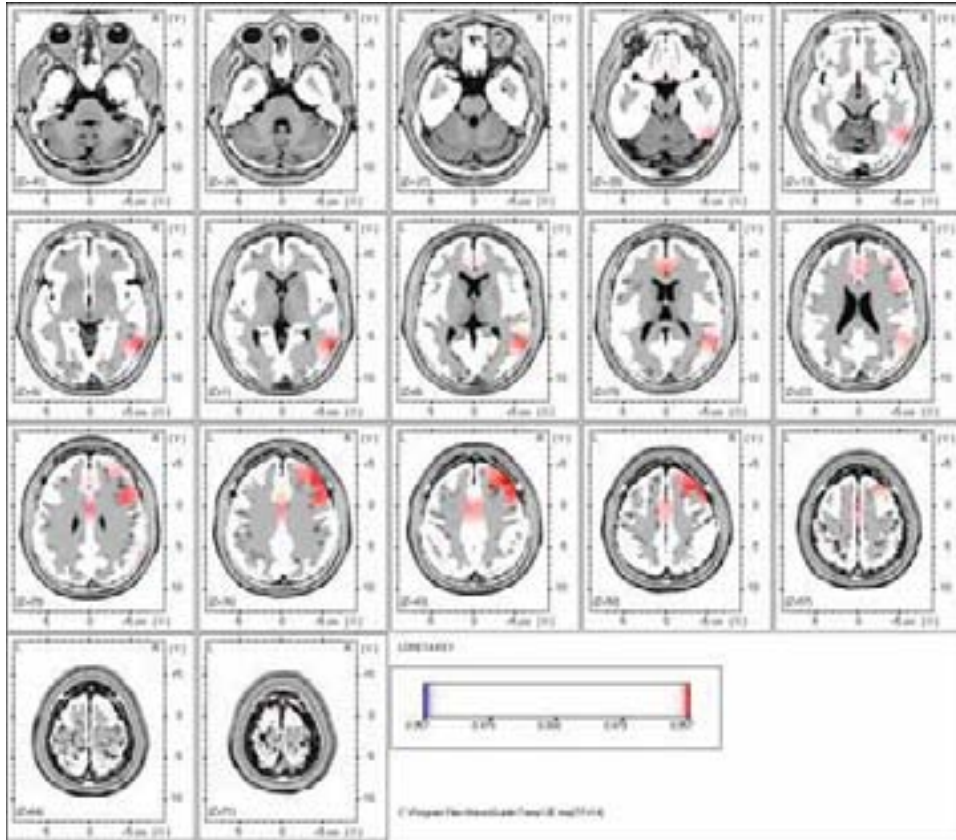


Figure 147. Paired t -test for 14 Hz LORETA: Significant differences after 20 minutes of 100 Hz CES.

Summary of 15 Hz Changes in Current Density

Increased Frontal Lobe Activation

- Right Superior Frontal Gyrus (Brodmann Area 11)
- Right Inferior Frontal Gyrus (Brodmann Area 44)
- Right Precentral Gyrus (Brodmann Area 44)
- Right Middle Frontal Gyrus (Brodmann Area 9)

Increased Parietal Lobe Activation

- Right Postcentral Gyrus (Brodmann Area 40)
- Right and Left Inferior Parietal Lobule (Brodmann Area 40)
- Right Superior Parietal Lobule (Brodmann Area 7)
- Right Angular Gyrus (Brodmann Area 39)
- Right Precuneus (Brodmann Area 19)

Increased Temporal Lobe Activation

- Right Superior Temporal Gyrus (Brodmann Area 38)
- Right Inferior Temporal Gyrus (Brodmann Area 47)
- Right Fusiform Gyrus (Brodmann Area 20)
- Right Middle Temporal Gyrus (Brodmann Area 39)

Increased Limbic Lobe Activation

- Right Hippocampus (Brodmann Area 27)
- Right and Left Parahippocampal Gyrus (Brodmann Area 19)
- Right and Left Cingulate Gyrus (Brodmann Area 24)
- Right and Left Posterior Cingulate (Brodmann Area 30)
- Right Uncus (Brodmann Area 28)

Increased Sub-lobar

- Right Insula (Brodmann Area 13)

Increased Occipital Lobe Activation

- Right Superior Occipital Gyrus (Brodmann Area 19)
- Right Inferior Occipital Gyrus (Brodmann Area 18)
- Right Middle Occipital Gyrus (Brodmann Area 18)

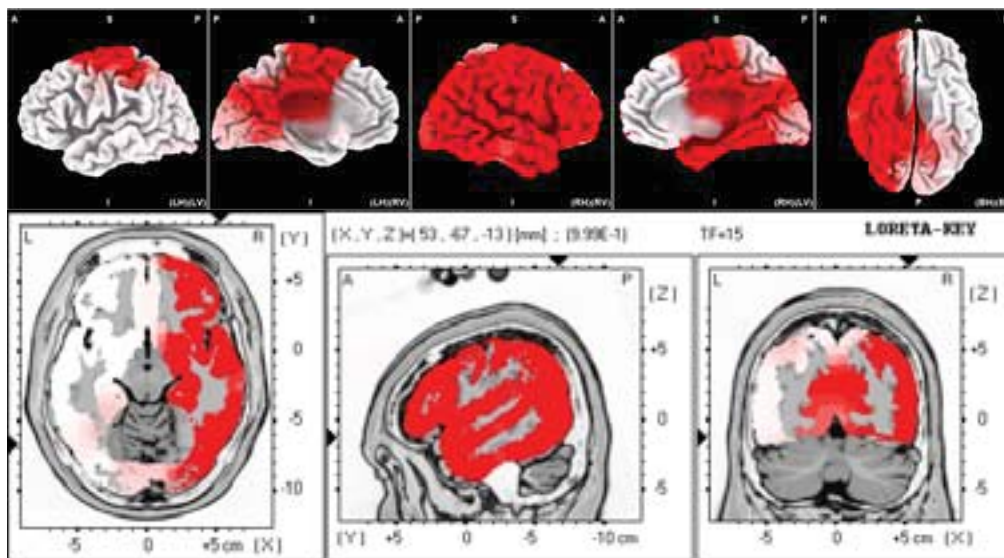


Figure 148. Paired *t*-test for 15 Hz LORETA: Significant differences after 20 minutes of 100 Hz CES.

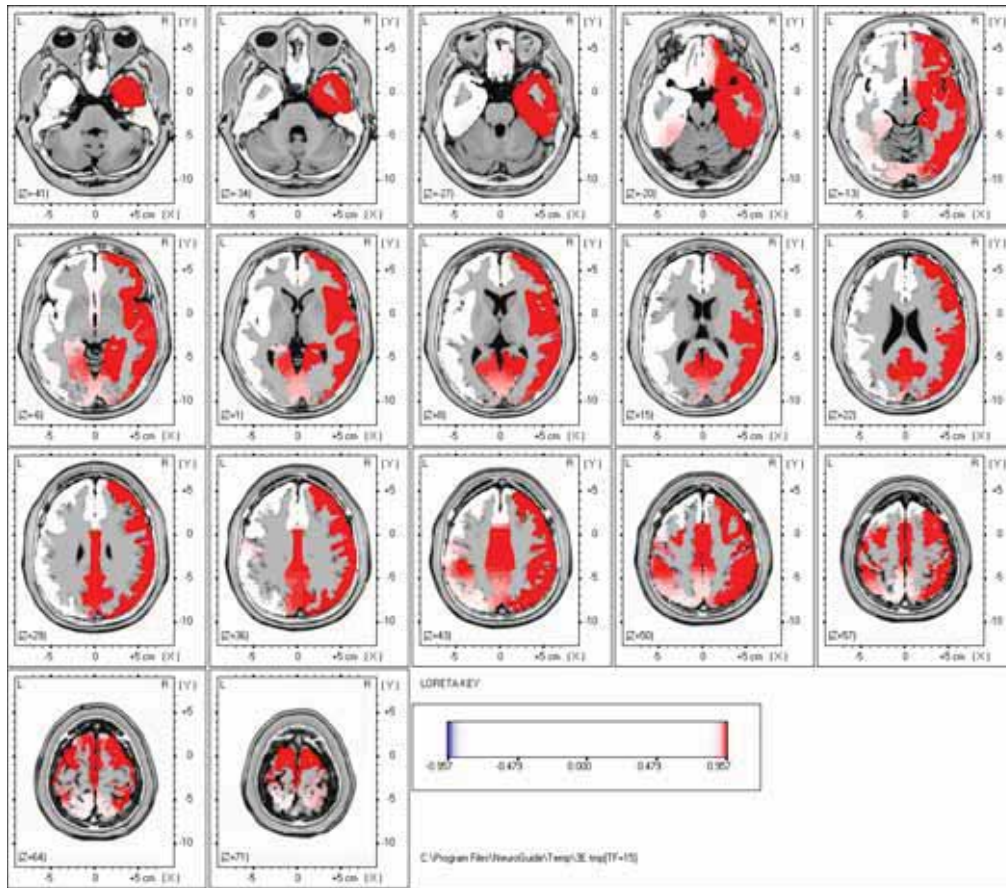


Figure 149. Paired t -test for 15 Hz LORETA: significant differences after 20 minutes of 100 Hz CES.

Summary of 16 Hz Changes in Current Density

Increased Frontal Lobe Activation

- Right Superior Frontal Gyrus (Brodmann Area 11)
- Right Inferior Frontal Gyrus (Brodmann Area 47)
- Right Medial Frontal Gyrus (Brodmann Area 10)

Increased Parietal Lobe Activation

- Right and Left Postcentral Gyrus (Brodmann Area 40)
- Right and Left Superior Parietal Lobule (Brodmann Area 7)
- Right and Left Inferior Parietal Lobule (Brodmann Area 40)
- Right and Left Precuneus (Brodmann Area 7)

Increased Temporal Lobe Activation

- Right Superior Temporal Gyrus (Brodmann Area 29)
- Right Middle Temporal Gyrus (Brodmann Area 39)
- Right Inferior Temporal Gyrus (Brodmann Area 20)
- Right Fusiform Gyrus (Brodmann Area 37)

Increased Limbic Lobe Activation

- Right and Left Hippocampus (Brodmann Area 27)
- Right and Left Parahippocampal Gyrus (Brodmann Area 19)
- Right and Left Cingulate Gyrus (Brodmann Area 24)
- Right and Left Posterior Cingulate (Brodmann Area 30)
- Right Uncus (Brodmann Area 28)

Increased Sub-lobar

- Right and Left Insula (Brodmann Area 13)

Increased Occipital Lobe Activation

- Right and Left Superior Occipital Gyrus (Brodmann Area 19)
- Right and Left Inferior Occipital Gyrus (Brodmann Area 18)
- Right and Left Middle Occipital Gyrus (Brodmann Area 18)
- Right and Left Lingual Gyrus (Brodmann Area 18)
- Right and Left Cuneus (Brodmann Area 18)

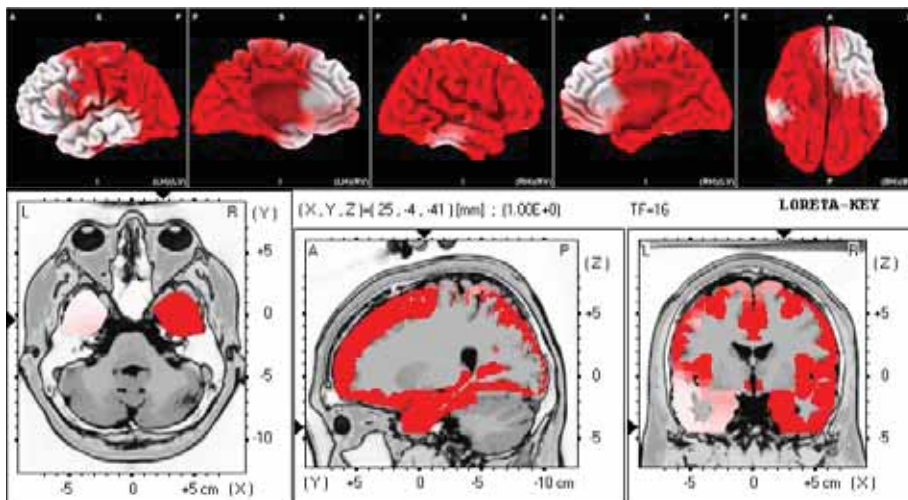


Figure 150. Paired *t*-test for 16 Hz LORETA: significant differences after 20 minutes of 100 Hz CES.

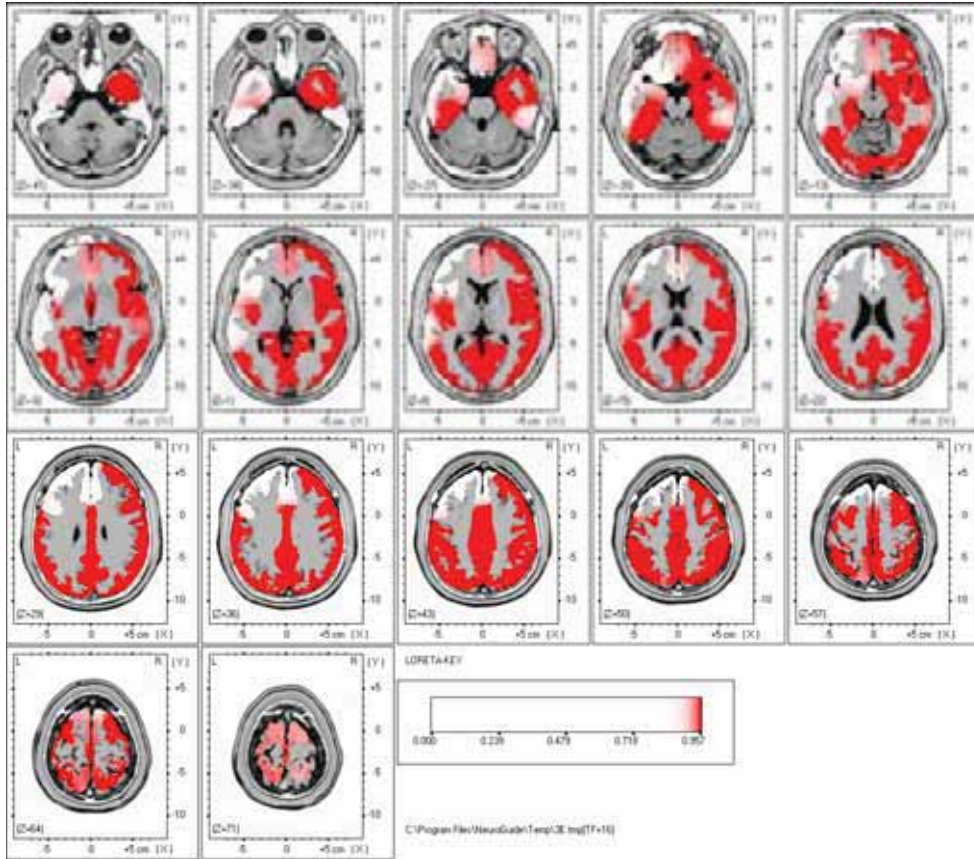


Figure 151. Paired t -test for 16 Hz LORETA: significant differences after 20 minutes of 100 Hz CES.

Summary of 17 Hz Changes in Current Density

Increased Frontal Lobe Activation

- Right Superior Frontal Gyrus (Brodmann Area 11)
- Right Inferior Frontal Gyrus (Brodmann Area 47)
- Right and Left Medial Frontal Gyrus (Brodmann Area 25)
- Right and Left Orbital Gyrus (Brodmann Area 11)
- Right and Left Rectal Gyrus (Brodmann Area 11)

Increased Parietal Lobe Activation

- Right and Left Postcentral Gyrus (Brodmann Area 40)
- Right and Left Superior Parietal Lobule (Brodmann Area 7)

- Right and Left Inferior Parietal Lobule (Brodmann Area 40)
- Right and Left Precuneus (Brodmann Area 7)

Increased Temporal Lobe Activation

- Right Superior Temporal Gyrus (Brodmann Area 29)
- Right Middle Temporal Gyrus (Brodmann Area 39)
- Right Inferior Temporal Gyrus (Brodmann Area 20)
- Right Transverse Temporal Gyrus (Brodmann Area 42)
- Right and Left Fusiform Gyrus (Brodmann Area 37)

Increased Limbic Lobe Activation

- Right Hippocampus (Brodmann Area 27)
- Right and Left Parahippocampal Gyrus (Brodmann Area 19)
- Right and Left Cingulate Gyrus (Brodmann Area 24)
- Right and Left Posterior Cingulate (Brodmann Area 30)
- Right Uncus (Brodmann Area 28)

Increased Sub-lobar

- Right and Left Insula (Brodmann Area 13)

Increased Occipital Lobe Activation

- Right and Left Superior Occipital Gyrus (Brodmann Area 19)
- Right and Left Inferior Occipital Gyrus (Brodmann Area 18)
- Right and Left Middle Occipital Gyrus (Brodmann Area 18)
- Right and Left Lingual Gyrus (Brodmann Area 18)
- Right and Left Cuneus (Brodmann Area 18)

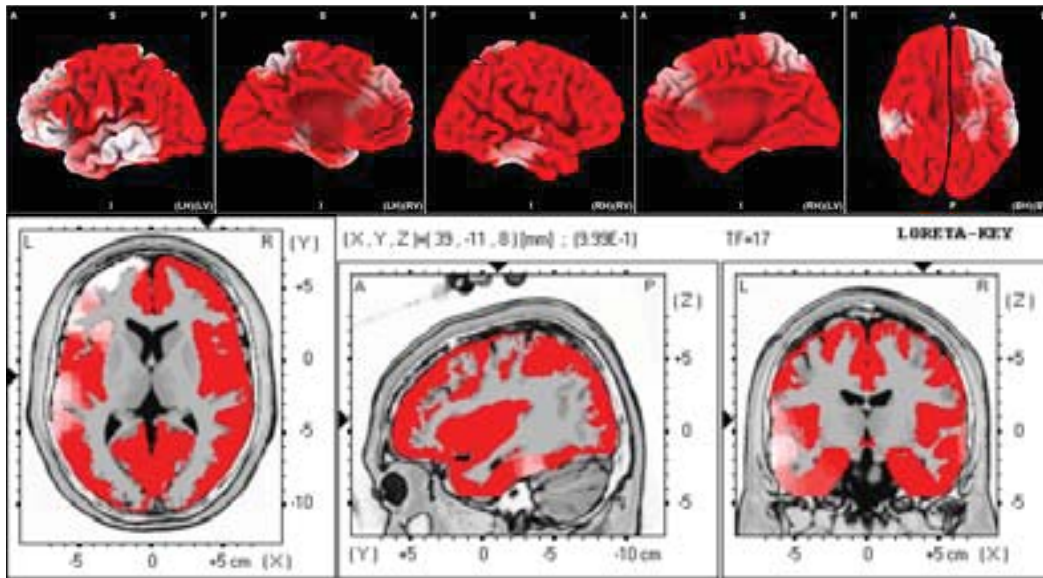


Figure 152. Paired t -test for 17 Hz LORETA: significant differences after 20 minutes of 100 Hz CES.

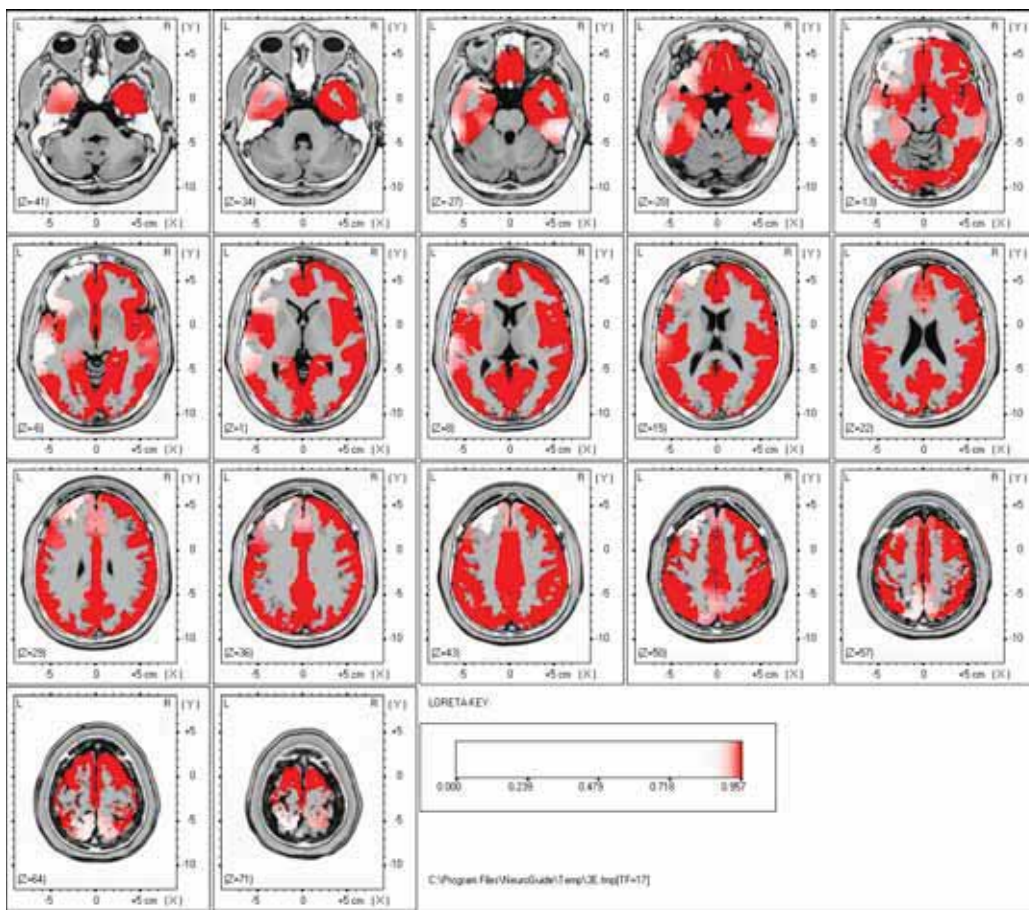


Figure 153. Paired t -test for 17 Hz LORETA: significant differences after 20 minutes of 100 Hz CES.

Summary of 18 Hz Changes in Current Density

Increased Frontal Lobe Activation

- Right Superior Frontal Gyrus (Brodmann Area 11)
- Right Middle Frontal Gyrus (Brodmann Area 46)
- Right Inferior Frontal Gyrus (Brodmann Area 45)
- Right Medial Frontal Gyrus (Brodmann Area 25)
- Right Precentral Gyrus (Brodmann Area 4)

Increased Parietal Lobe Activation

- Right and Left Postcentral Gyrus (Brodmann Area 40)
- Right and Left Superior Parietal Lobule (Brodmann Area 7)
- Right and Left Inferior Parietal Lobule (Brodmann Area 40)
- Right and Left Precuneus (Brodmann Area 7)

Increased Temporal Lobe Activation

- Right Superior Temporal Gyrus (Brodmann Area 29)
- Right Middle Temporal Gyrus (Brodmann Area 39)

Increased Limbic Lobe Activation

- Right Hippocampus (Brodmann Area 27)
- Right Parahippocampal Gyrus (Brodmann Area 19)
- Right and Left Cingulate Gyrus (Brodmann Area 24)
- Right and Left Posterior Cingulate (Brodmann Area 30)
- Right Uncus (Brodmann Area 28)

Increased Sub-lobar

- Right and Left Insula (Brodmann Area 13)

Increased Occipital Lobe Activation

- Right Superior Occipital Gyrus (Brodmann Area 19)
- Right Inferior Occipital Gyrus (Brodmann Area 18)

- Right Middle Occipital Gyrus (Brodmann Area 18)
- Right Lingual Gyrus (Brodmann Area 18)
- Right Cuneus (Brodmann Area 18)

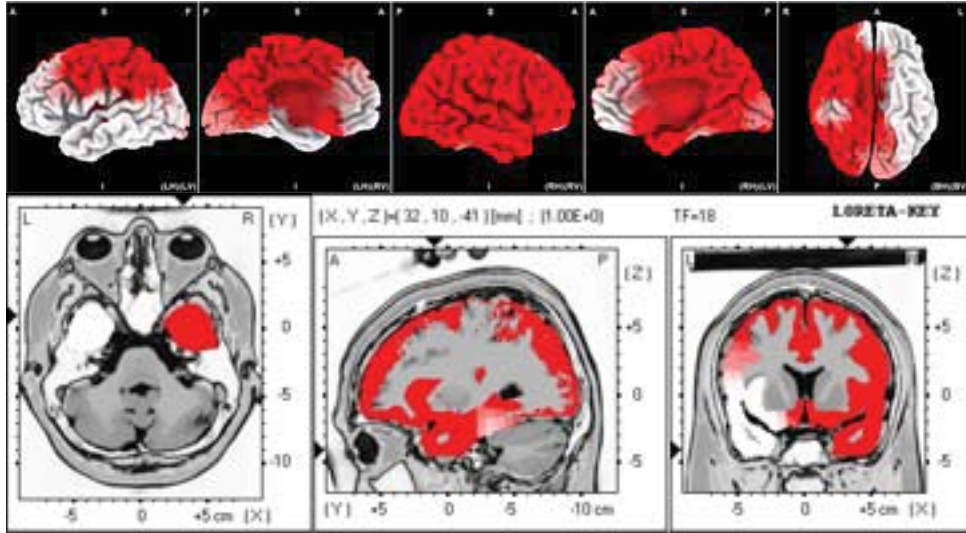


Figure 154. Paired t -test for 18 Hz LORETA: Significant differences after 20 minutes of 100 Hz CES.

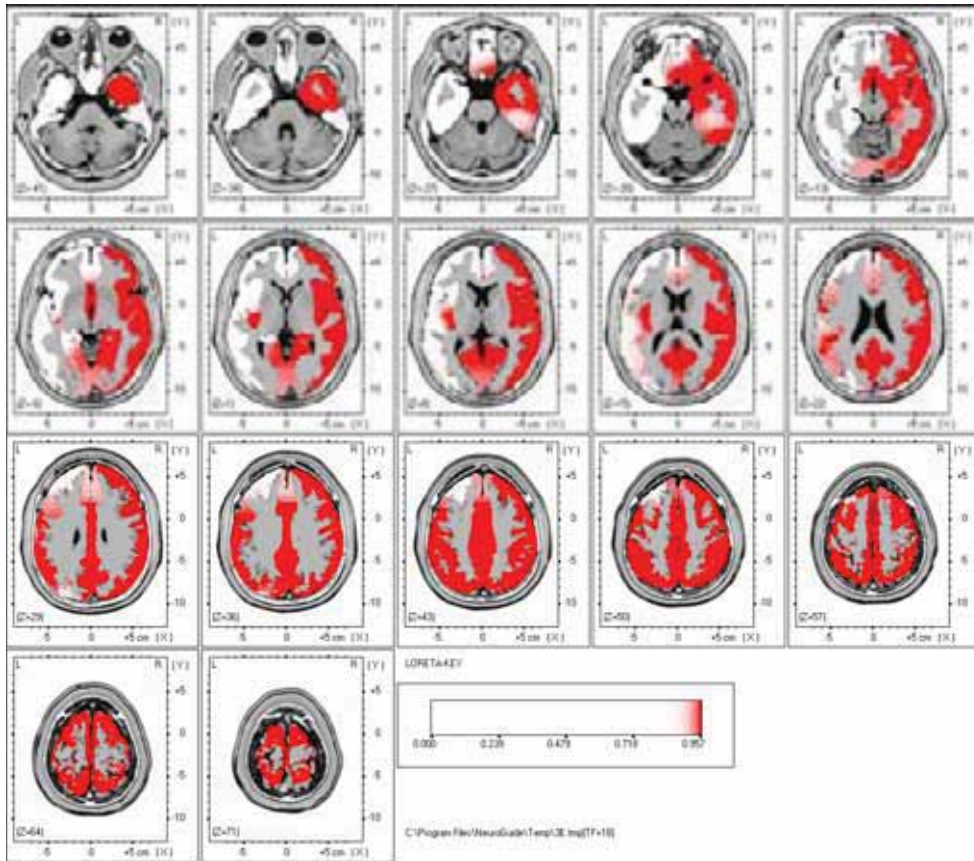


Figure 155. Paired t -test for 18 Hz LORETA: Significant differences after 20 minutes of 100 Hz CES.

Summary of 19 Hz Changes in Current Density

Increased Frontal Lobe Activation

- Right Middle Frontal Gyrus (Brodmann Area 46)
- Right Inferior Frontal Gyrus (Brodmann Area 45)
- Right and Left Subcallosal Gyrus (Brodmann Area 34)
- Right and Left Precentral Gyrus (Brodmann Area 6)

Increased Parietal Lobe Activation

- Right and Left Postcentral Gyrus (Brodmann Area 40)
- Right and Left Superior Parietal Lobule (Brodmann Area 7)
- Right and Left Inferior Parietal Lobule (Brodmann Area 40)
- Right and Left Precuneus (Brodmann Area 7)

Increased Temporal Lobe Activation

- Right Superior Temporal Gyrus (Brodmann Area 42)
- Right Supramarginal Gyrus (Brodmann Area 40)

Increased Limbic Lobe Activation

- Right and Left Anterior Cingulate (Brodmann Area 33)
- Right and Left Cingulate Gyrus (Brodmann Area 24)
- Right and Left Posterior Cingulate (Brodmann Area 30)

Increased Sub-lobar

- Right Insula (Brodmann Area 13)

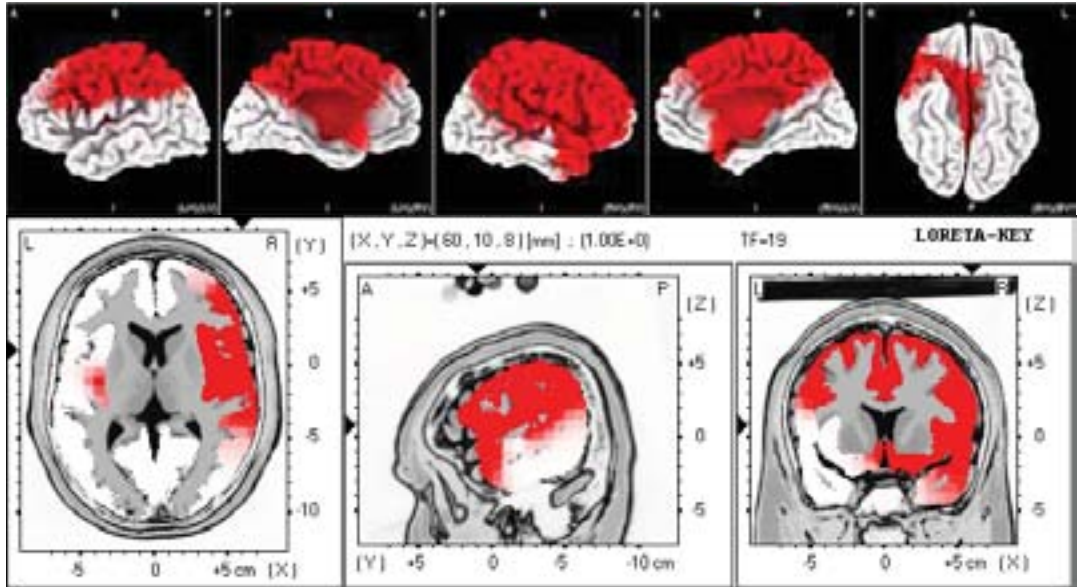


Figure 156. Paired t -test for 19 Hz LORETA: significant differences after 20 minutes of 100 Hz CES.

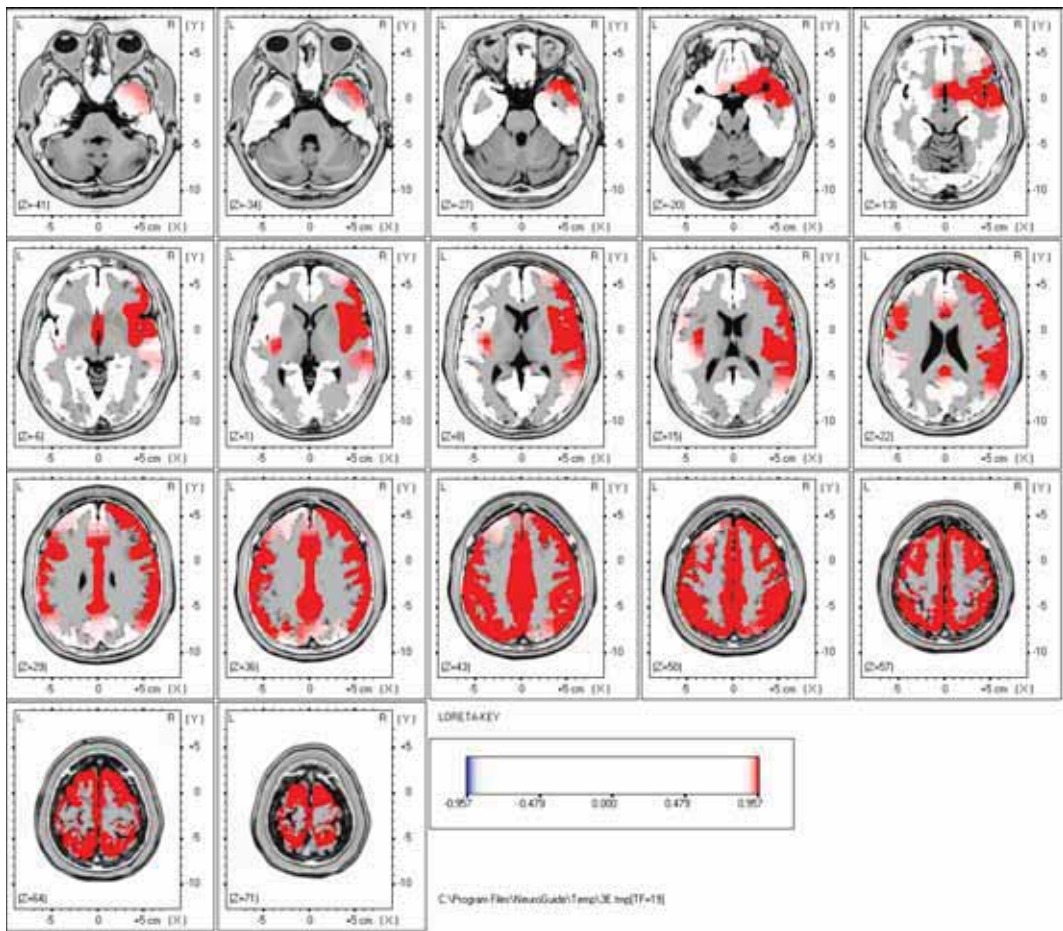


Figure 157. Paired t -test for 19 Hz LORETA: significant differences after 20 minutes of 100 Hz CES.

Summary of 20 Hz Changes in Current Density

Increased Frontal Lobe Activation

- Right Superior Frontal Gyrus (Brodmann Area 10)
- Right Middle Frontal Gyrus (Brodmann Area 46)
- Right Inferior Frontal Gyrus (Brodmann Area 45)
- Right Subcallosal Gyrus (Brodmann Area 34)
- Right Precentral Gyrus (Brodmann Area 6)

Increased Parietal Lobe Activation

- Right and Left Postcentral Gyrus (Brodmann Area 40)
- Right and Left Superior Parietal Lobule (Brodmann Area 7)
- Right and Left Inferior Parietal Lobule (Brodmann Area 40)

Increased Temporal Lobe Activation

- Right Superior Temporal Gyrus (Brodmann Area 42)
- Right Middle Temporal Gyrus (Brodmann Area 21)
- Right Inferior Temporal Gyrus (Brodmann Area 20)

Increased Limbic Lobe Activation

- Right Uncus (Brodmann Area 34)
- Right Parahippocampal Gyrus (Brodmann Area 35)
- Right and Left Anterior Cingulate (Brodmann Area 33)
- Right and Left Cingulate Gyrus (Brodmann Area 24)

Increased Sub-lobar

- Right Insula (Brodmann Area 13)

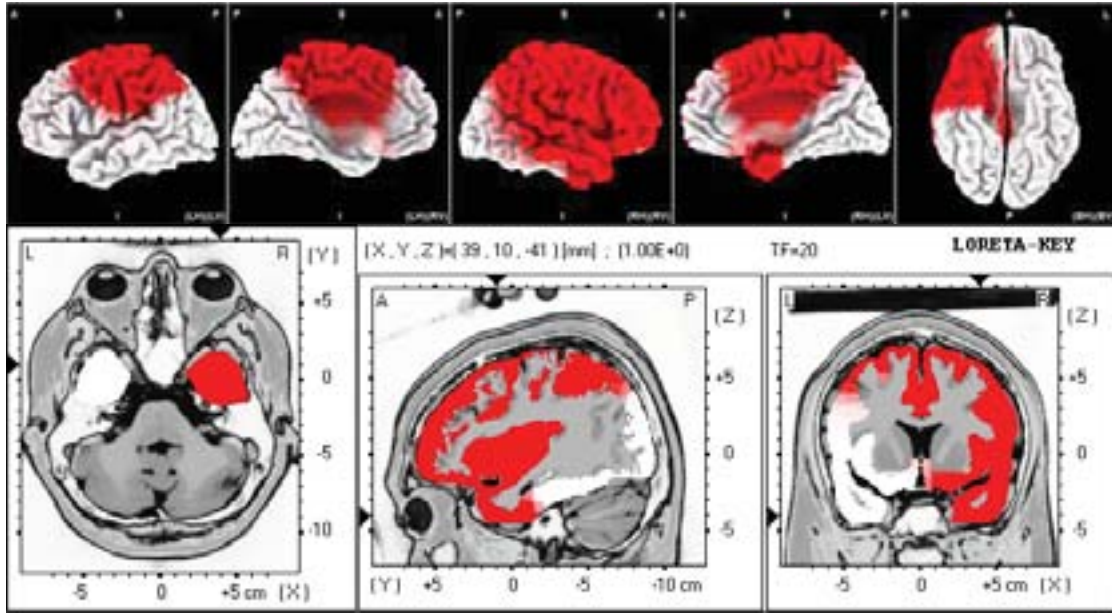


Figure 158. Paired t -test for 20 Hz LORETA: Significant differences after 20 minutes of 100 Hz CES.

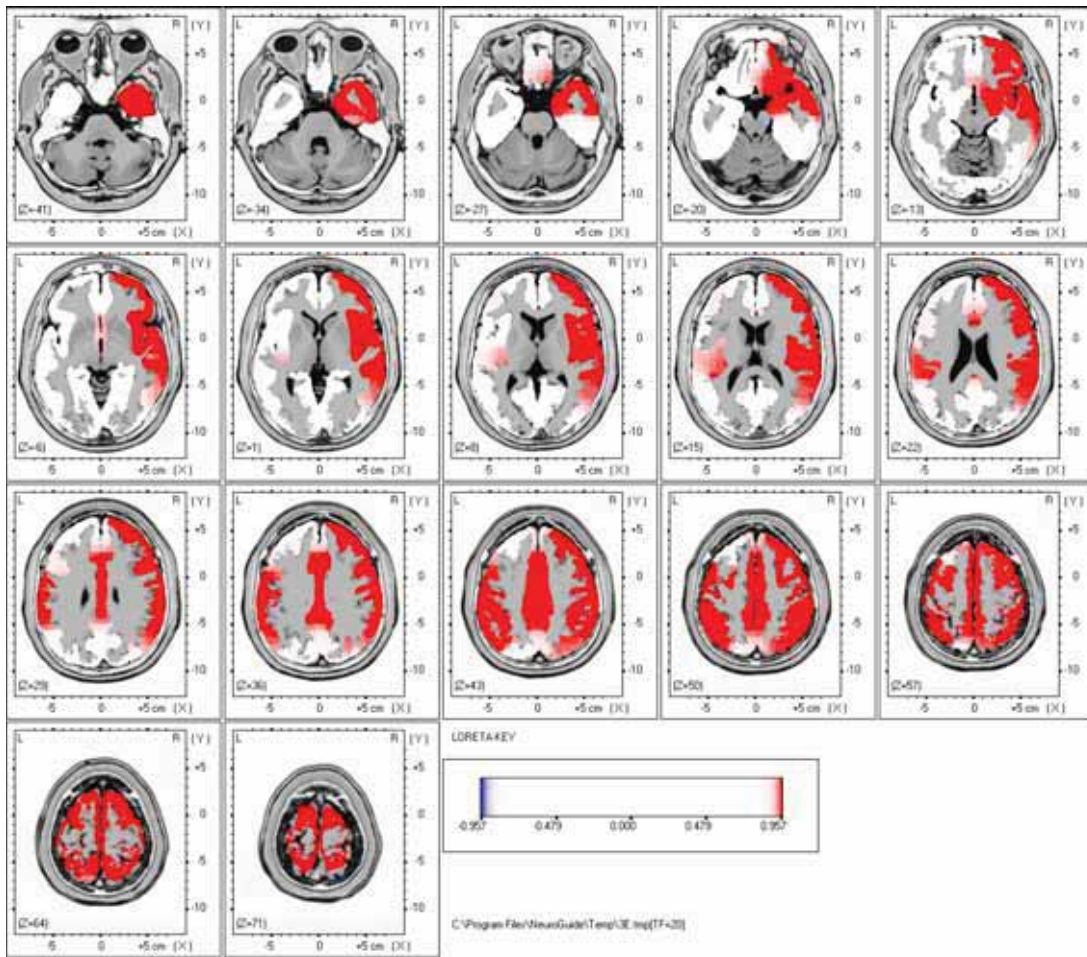


Figure 159. Paired t -test for 20 Hz LORETA: Significant differences after 20 minutes of 100 Hz CES.

Summary of 21 Hz Changes in Current Density

Increased Frontal Lobe Activation

- Right Superior Frontal Gyrus (Brodmann Area 11)
- Right Middle Frontal Gyrus (Brodmann Area 46)
- Right Inferior Frontal Gyrus (Brodmann Area 45)
- Right Subcallosal Gyrus (Brodmann Area 34)
- Right Precentral Gyrus (Brodmann Area 6)
- Right and Left Rectal Gyrus (Brodmann Area 11)

Increased Parietal Lobe Activation

- Right and Left Postcentral Gyrus (Brodmann Area 40)
- Right and Left Inferior Parietal Lobule (Brodmann Area 40)
- Right Supramarginal Gyrus (Brodmann Area 40)

Increased Temporal Lobe Activation

- Right Superior Temporal Gyrus (Brodmann Area 38)
- Right Middle Temporal Gyrus (Brodmann Area 21)
- Right Inferior Temporal Gyrus (Brodmann Area 20)
- Right Transverse Temporal Gyrus (Brodmann Area 42)

Increased Limbic Lobe Activation

- Right and Left Anterior Cingulate (Brodmann Area 32)
- Right and Left Cingulate Gyrus (Brodmann Area 24)

Increased Sub-lobar

- Right Insula (Brodmann Area 13)

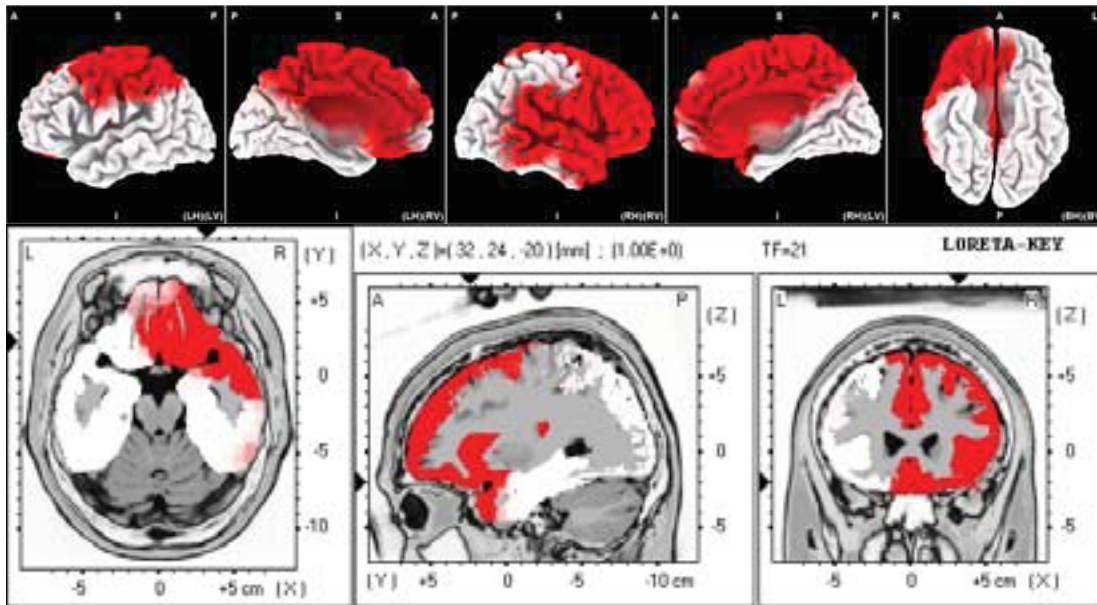


Figure 160. Paired t -test for 21 Hz LORETA: Significant differences after 20 minutes of 100 Hz CES.

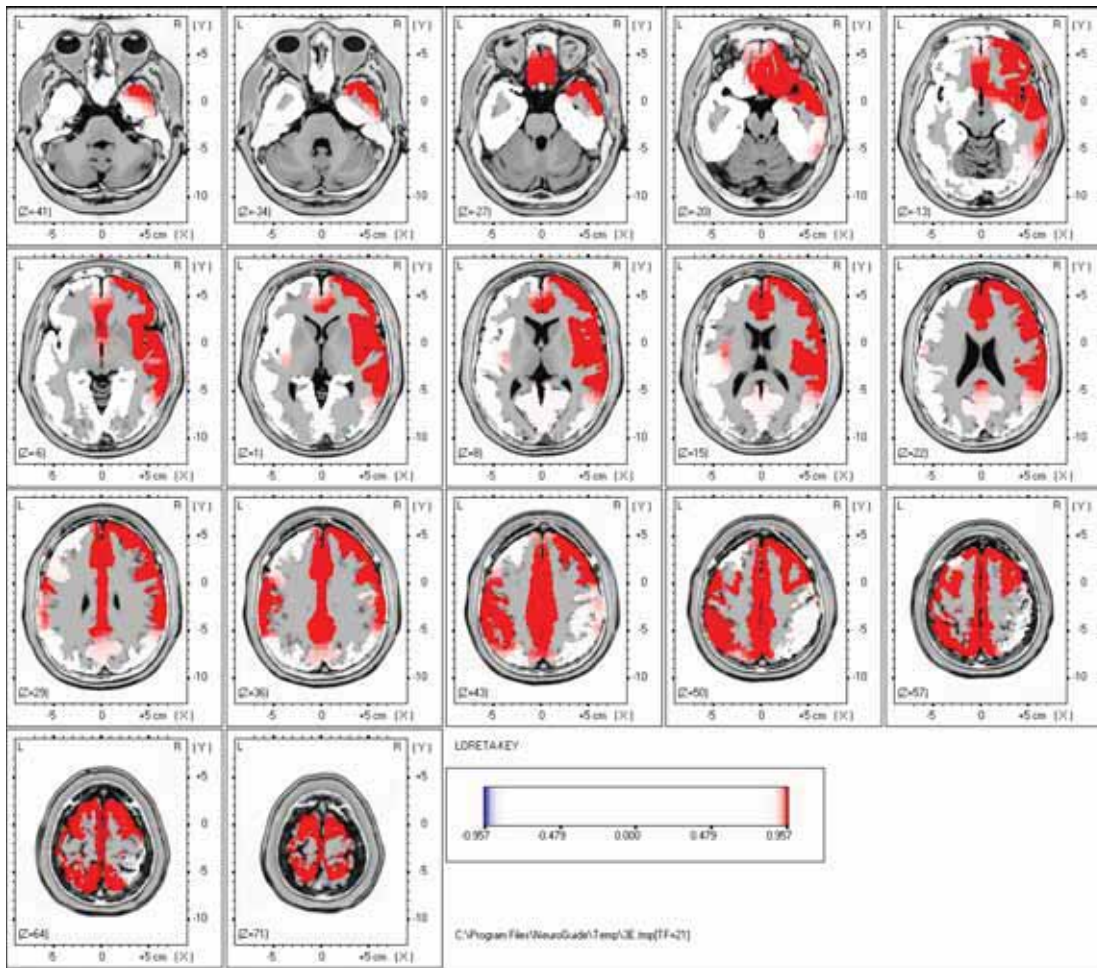


Figure 161. Paired t -test for 21 Hz LORETA: Significant differences after 20 minutes of 100 Hz CES.

Summary of 22 Hz Changes in Current Density

Increased Frontal Lobe Activation

- Right Superior Frontal Gyrus (Brodmann Area 11)
- Right Middle Frontal Gyrus (Brodmann Area 46)
- Right Inferior Frontal Gyrus (Brodmann Area 45)
- Right Subcallosal Gyrus (Brodmann Area 34)

Increased Parietal Lobe Activation

- Left Postcentral Gyrus (Brodmann Area 2)
- Left Inferior Parietal Lobule (Brodmann Area 40)
- Left Superior Parietal Lobule (Brodmann Area 7)
- Left Precuneus (Brodmann Area 7)

Increased Temporal Lobe Activation

- Right Superior Temporal Gyrus (Brodmann Area 38)
- Right Middle Temporal Gyrus (Brodmann Area 21)
- Right Inferior Temporal Gyrus (Brodmann Area 20)

Increased Limbic Lobe Activation

- Right and Left Anterior Cingulate (Brodmann Area 32)
- Right and Left Cingulate Gyrus (Brodmann Area 24)
- Right Uncus (Brodmann Area 38)

Increased Sub-lobar

- Right Insula (Brodmann Area 13)

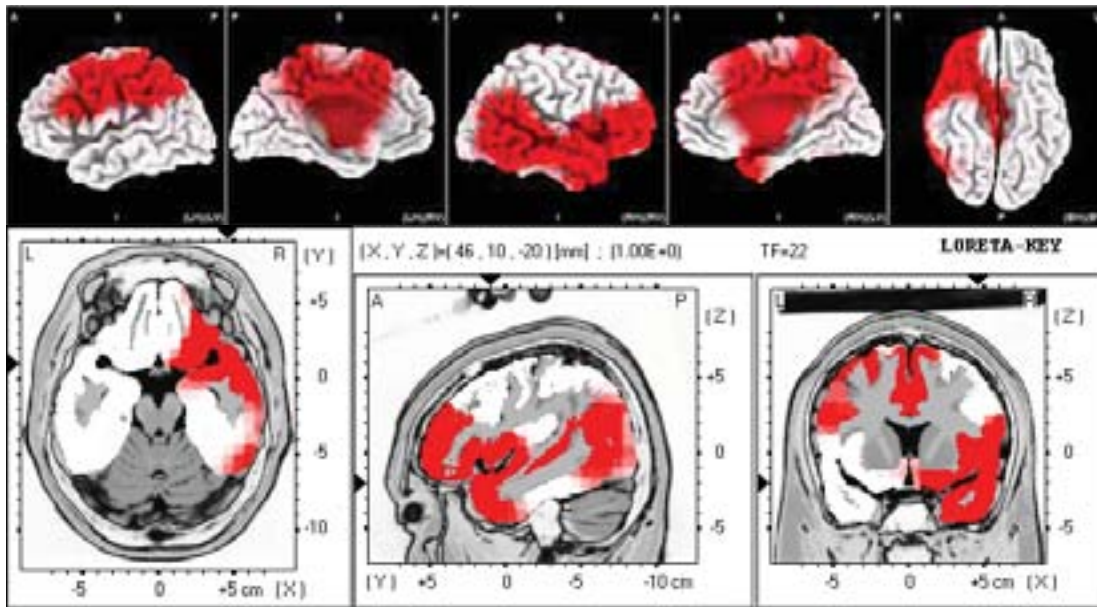


Figure 162. Paired t -test for 22 Hz LORETA: Significant differences after 20 minutes of 100 Hz CES.

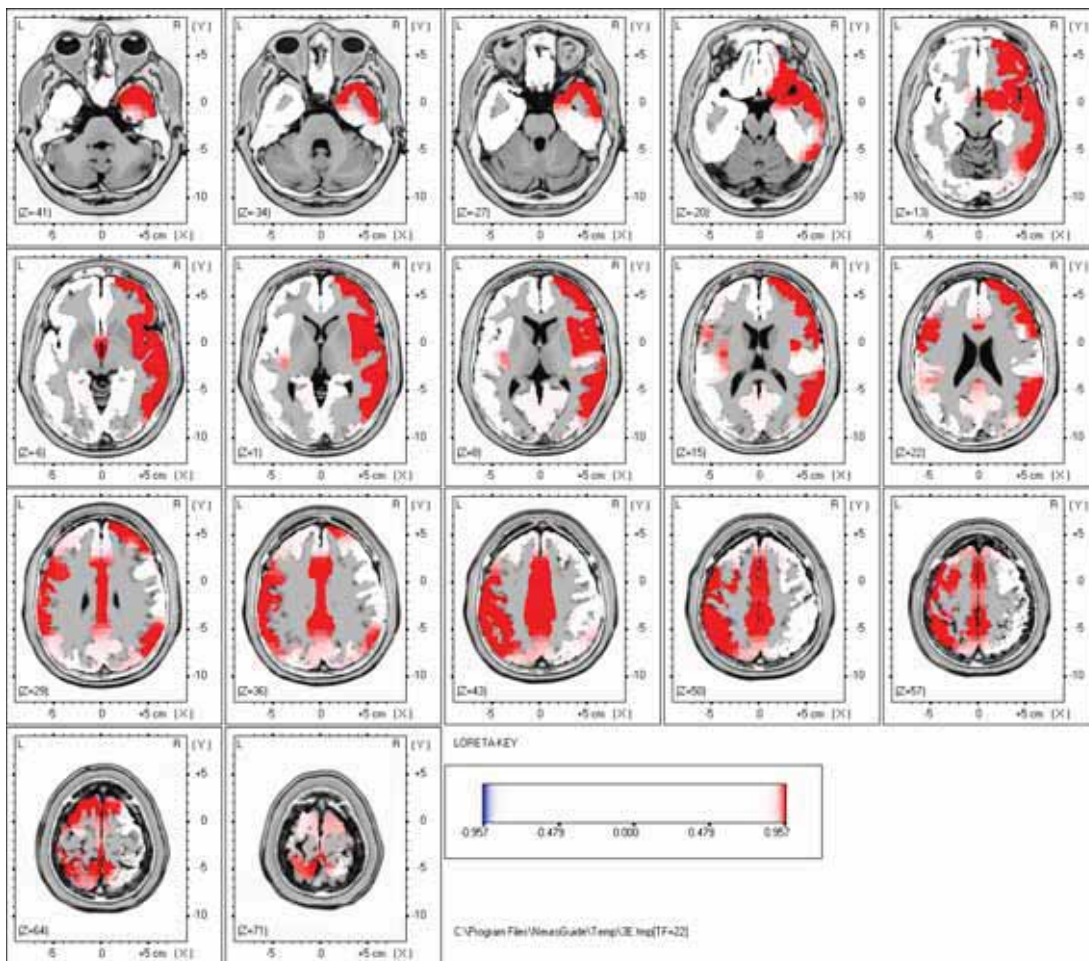


Figure 163. Paired t -test for 22 Hz LORETA: Significant differences after 20 minutes of 100 Hz CES.

Summary of 23 Hz Changes in Current Density

Increased Frontal Lobe Activation

- Right Superior Frontal Gyrus (Brodmann Area 8)
- Right Middle Frontal Gyrus (Brodmann Area 46)
- Right Inferior Frontal Gyrus (Brodmann Area 47)
- Right and Left Medial Frontal Gyrus
- Left Precentral Gyrus (Brodmann Area 4)

Increased Limbic Lobe Activation

- Right and Left Anterior Cingulate (Brodmann Area 32)
- Right and Left Cingulate Gyrus (Brodmann Area 24)
- Right and Left Posterior Cingulate (Brodmann Area 29)
- Right Uncus (Brodmann Area 38)

Increased Sub-lobar

- Left Insula (Brodmann Area 13)

Increased Parietal Lobe Activation

- Right and Left Postcentral Gyrus (Brodmann Area 7)
- Left Superior Parietal Lobule (Brodmann Area 7)
- Right and Left Precuneus (Brodmann Area 7)

Increased Temporal Lobe Activation

- Right Middle Temporal Gyrus (Brodmann Area 21)

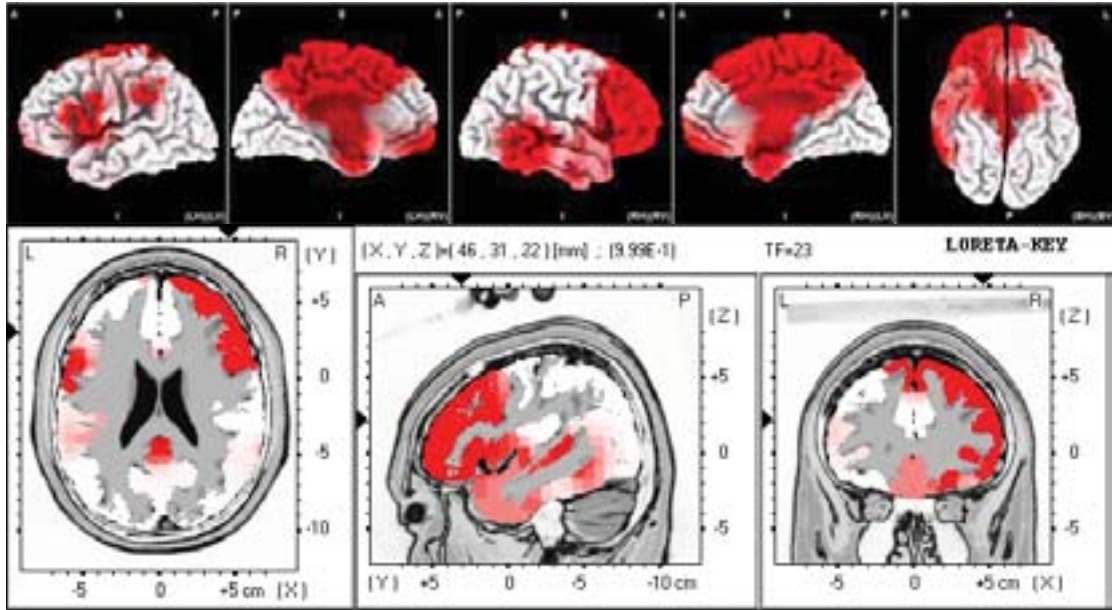


Figure 164. Paired t -test for 23 Hz LORETA: Significant differences after 20 minutes of 100 Hz CES.

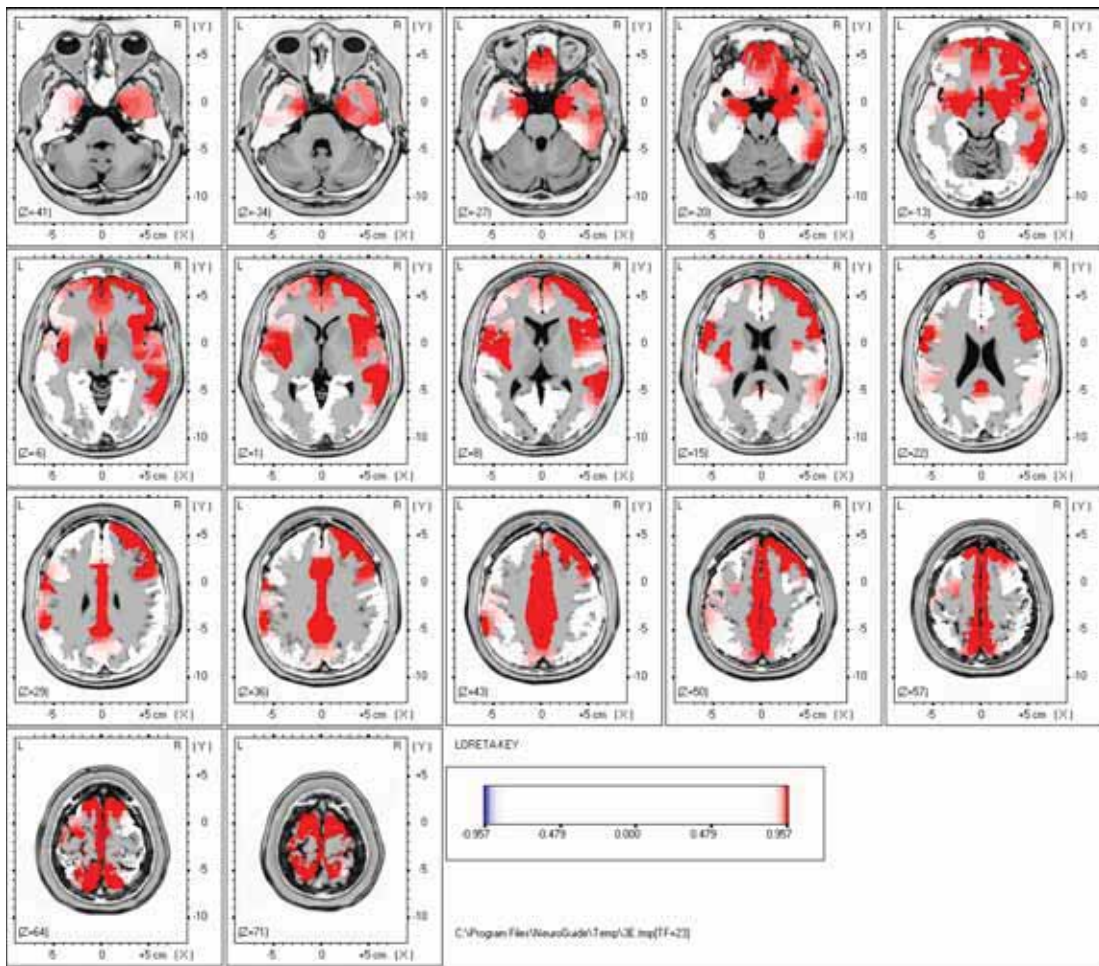


Figure 165. Paired t -test for 23 Hz LORETA: Significant differences after 20 minutes of 100 Hz CES.

Summary of 24 Hz Changes in Current Density

Increased Frontal Lobe Activation

- Right Superior Frontal Gyrus (Brodmann Area 10)
- Right Middle Frontal Gyrus (Brodmann Area 10)
- Right Inferior Frontal Gyrus (Brodmann Area 9)
- Right and Left Paracentral Lobule (Brodmann Area 6)
- Right and Left Medial Frontal Gyrus (Brodmann Area 6)

Increased Limbic Lobe Activation

- Right and Left Anterior Cingulate (Brodmann Area 32)
- Right and Left Cingulate Gyrus (Brodmann Area 24)
- Right and Left Posterior Cingulate (Brodmann Area 29)

Increased Sub-lobar

- Left Insula (Brodmann Area 13)

Increased Parietal Lobe Activation

- Right and Left Superior Paracentral Lobule (Brodmann Area 4)
- Right and Left Precuneus (Brodmann Area 7)

Increased Temporal Lobe Activation

- Right Middle Temporal Gyrus (Brodmann Area 21)

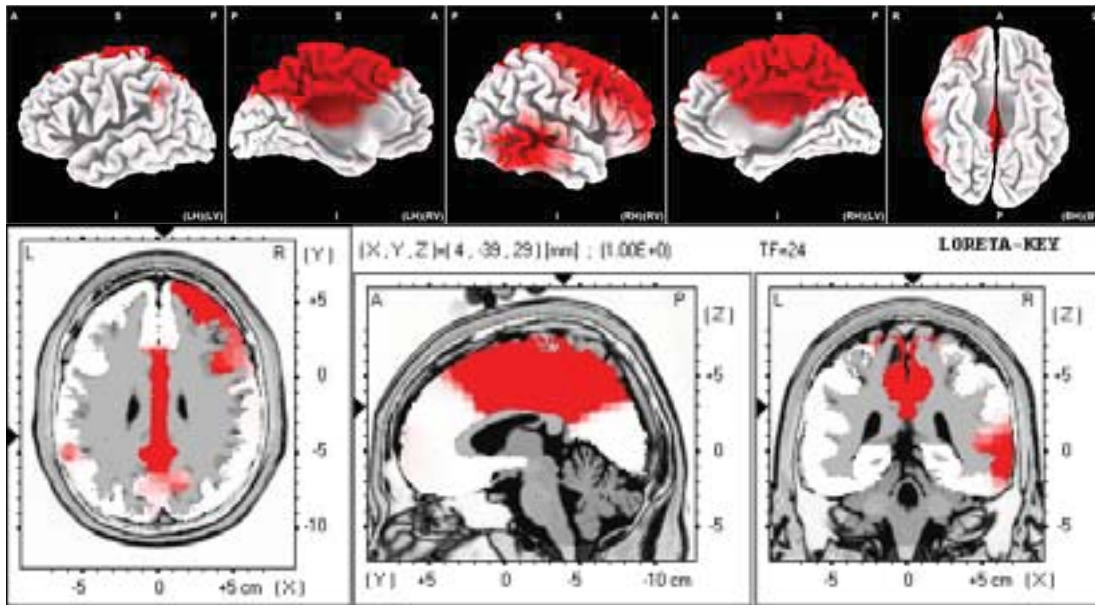


Figure 166. Paired t -test for 24 Hz LORETA: Significant differences after 20 minutes of 100 Hz CES.

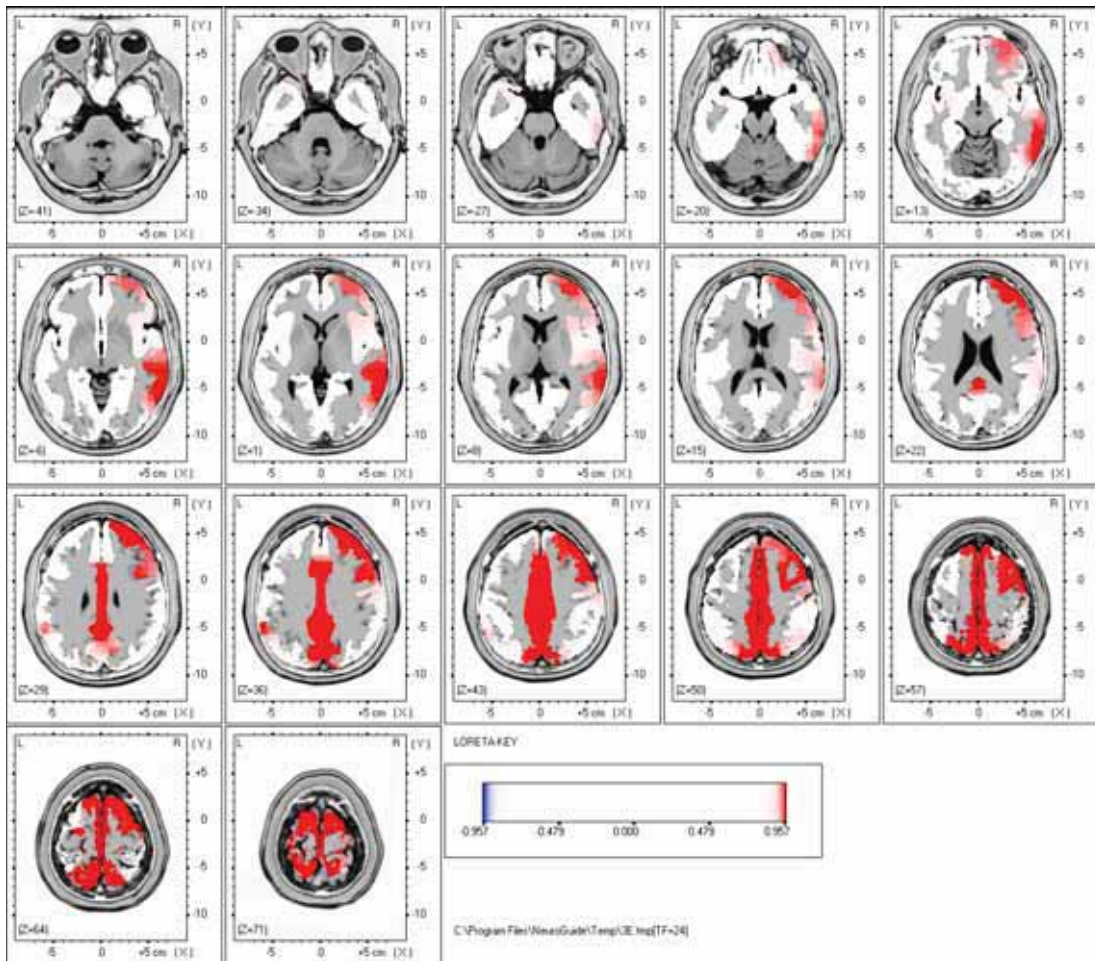


Figure 167. Paired t -test for 24 Hz LORETA: Significant differences after 20 minutes of 100 Hz CES.

Summary of 25 Hz Changes in Current Density

Increased Frontal Lobe Activation

- Right Superior Frontal Gyrus (Brodmann Area 8)
- Right and Left Medial Frontal Gyrus (Brodmann Area 6)
- Right and Left Paracentral Lobule (Brodmann Area 6)

Increased Limbic Lobe Activation

- Right and Left Anterior Cingulate Gyrus (Brodmann Area 33)
- Right and Left Cingulate Gyrus (Brodmann Area 24)

Increased Parietal Lobe Activation

- Right and Left Superior Paracentral Lobule (Brodmann Area 4)
- Right and Left Precuneus (Brodmann Area 7)

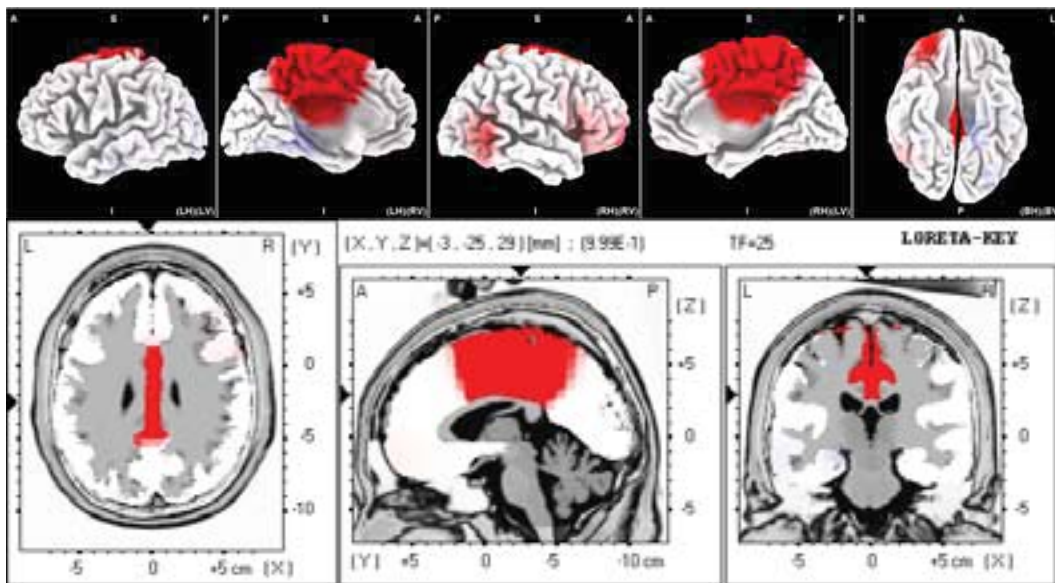


Figure 168. Paired *t*-test for 25 Hz LORETA: Significant differences after 20 minutes of 100 Hz CES.

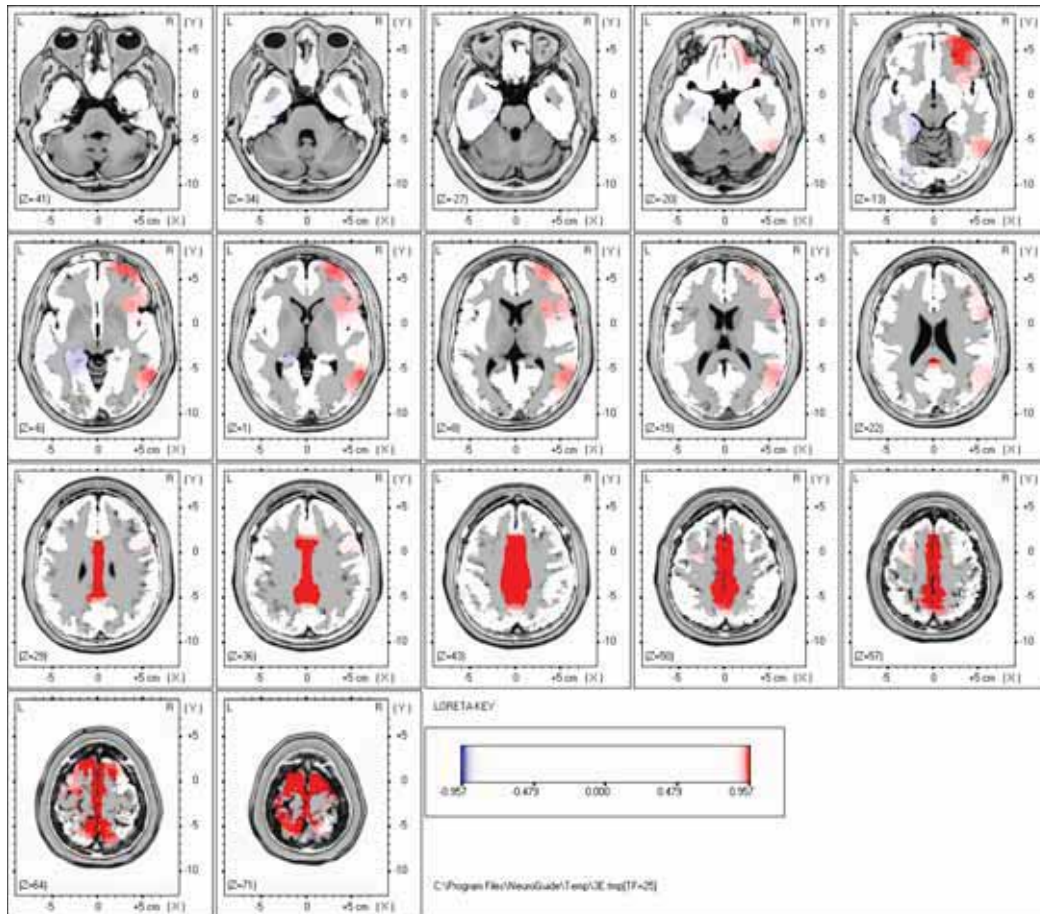


Figure 169. Paired t -test for 25 Hz LORETA: Significant differences after 20 minutes of 100 Hz CES.

Summary of 26 Hz Changes in Current Density

Increased Frontal Lobe Activation

- Right and Left Superior Frontal Gyrus (Brodmann Area 6)
- Left Middle Frontal Gyrus (Brodmann Area 6)
- Right and Left Medial Frontal Gyrus (Brodmann Area 6)

Increased Limbic Lobe Activation

- Right and Left Anterior Cingulate (Brodmann Area 32)
- Right and Left Cingulate Gyrus (Brodmann Area 24)
- Right and Left Posterior Cingulate (Brodmann Area 29)

Increased Parietal Lobe Activation

- Left Postcentral Gyrus (Brodmann Area 40)

- Left Inferior Parietal Lobule (Brodmann Area 40)

Decreased Occipital Lobe Activation

- Left Inferior Occipital Gyrus (Brodmann Area 18)
- Left Middle Occipital Gyrus (Brodmann Area 18)
- Left Cuneus (Brodmann Area 18)
- Right and Left Lingual Gyrus (Brodmann Area 18)
- Left Precuneus (Brodmann Area 19)

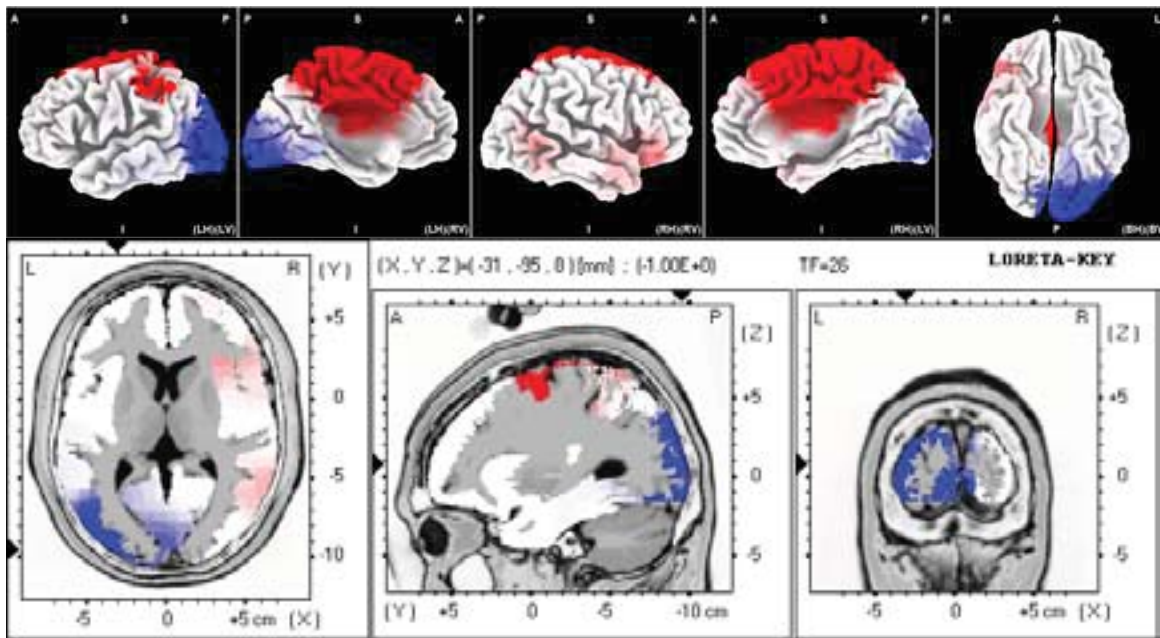


Figure 170. Paired t -test for 26 Hz LORETA: Significant differences after 20 minutes of 100 Hz CES.

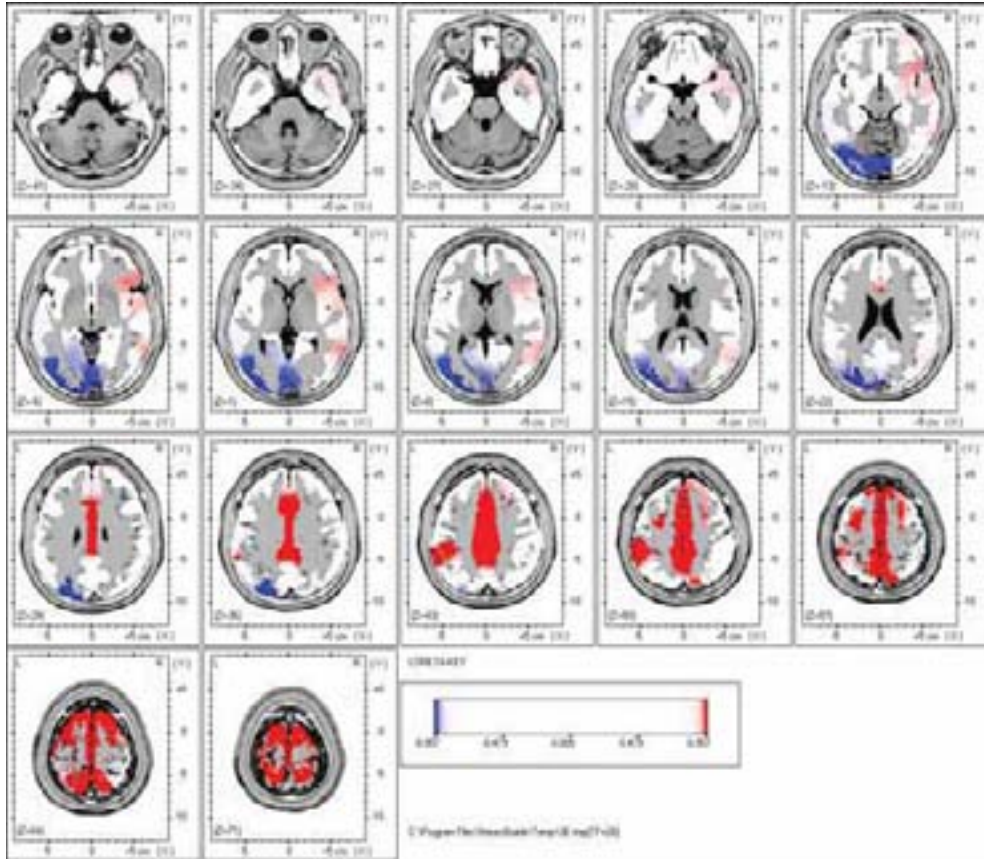


Figure 171. Paired t -test for 26 Hz LORETA: Significant differences after 20 minutes of 100 Hz CES.

Summary of 27 Hz Changes in Current Density

Increased Frontal Lobe Activation

- Right and Left Superior Frontal Gyrus (Brodmann Area 10)
- Right and Left Middle Frontal Gyrus (Brodmann Area 6)
- Right Inferior Frontal Gyrus (Brodmann Area 9)
- Right and Left Paracentral Lobule (Brodmann Area 6)
- Right and Left Medial Frontal Gyrus (Brodmann Area 8)

Increased Limbic Lobe Activation

- Right and Left Anterior Cingulate (Brodmann Area 32)
- Right and Left Cingulate Gyrus (Brodmann Area 24)

Increased Parietal Lobe Activation

- Right Postcentral Gyrus (Brodmann Area 2)
- Right and Left Inferior Parietal Lobule (Brodmann Area 40)
- Right and Left Superior Parietal Lobule (Brodmann Area 7)
- Right and Left Precuneus (Brodmann Area 7)
- Right and Left Superior Paracentral Lobule (Brodmann Area 4)
- Right and Left Precuneus (Brodmann Area 7)

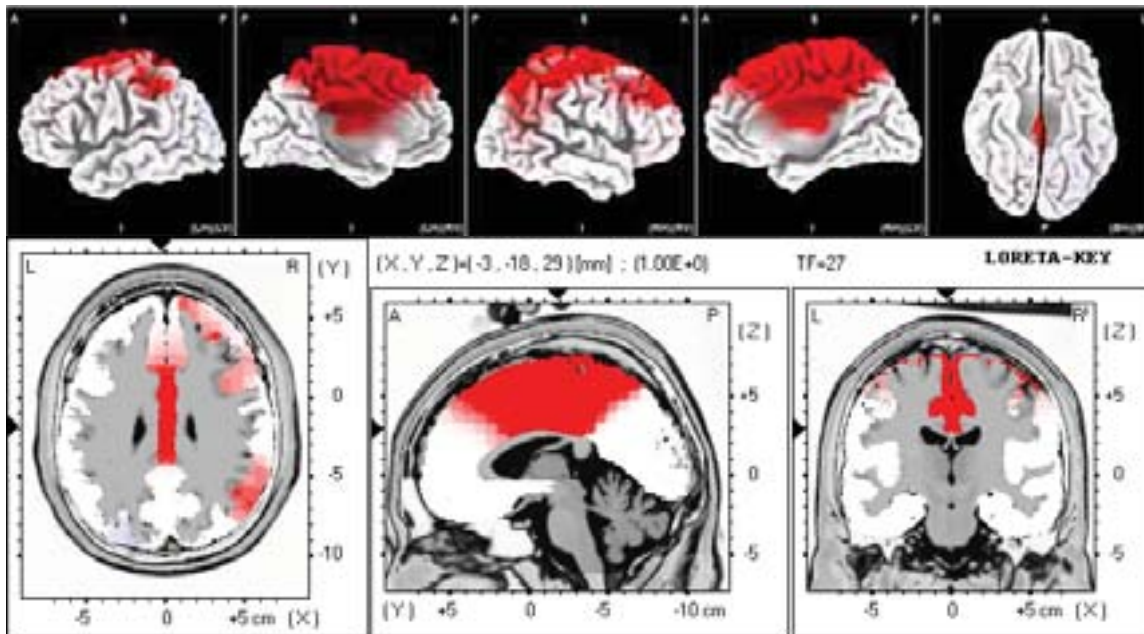


Figure 172. Paired t -test for 27 Hz LORETA: Significant differences after 20 minutes of 100 Hz CES.

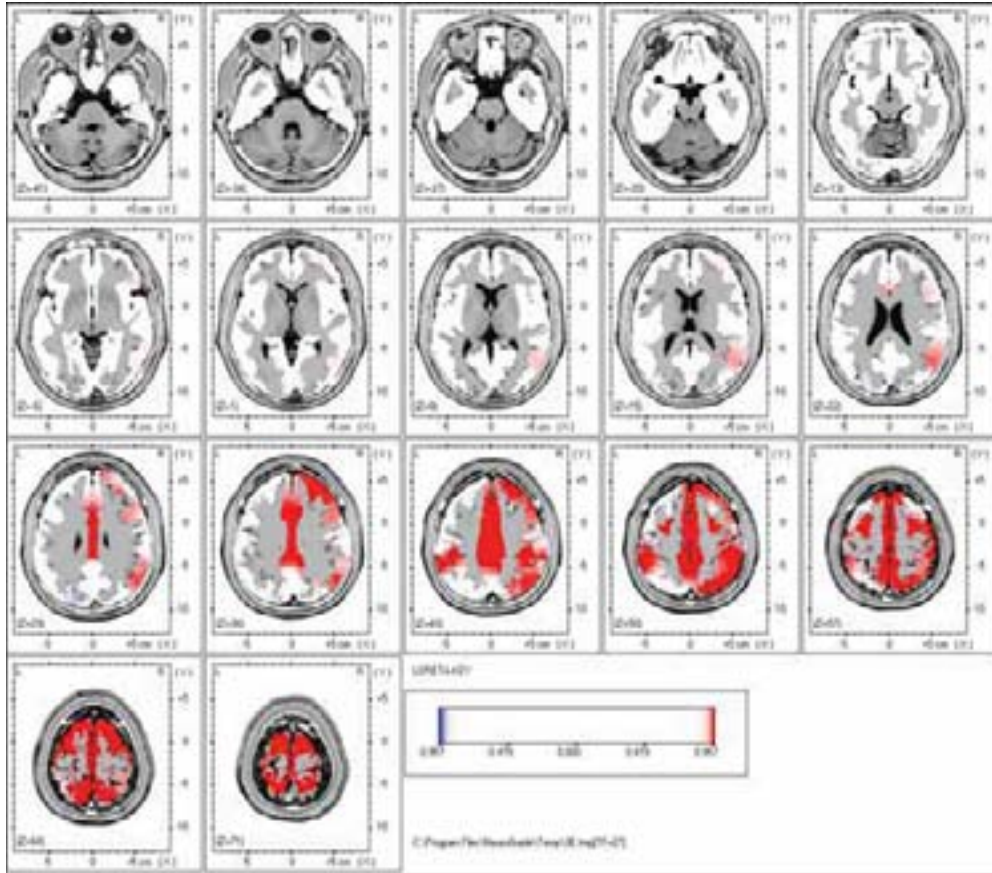


Figure 173. Paired t -test for 27 Hz LORETA: Significant differences after 20 minutes of 100 Hz CES.

Summary of 28 Hz Changes in Current Density

Increased Frontal Lobe Activation

- Right and Left Superior Frontal Gyrus (Brodmann Area 10)
- Left Middle Frontal Gyrus (Brodmann Area 6)
- Right and Left Paracentral Lobule (Brodmann Area 5)

Increased Limbic Lobe Activation

- Right and Left Cingulate Gyrus (Brodmann Area 31)

Increased Parietal Lobe Activation

- Right and Left Postcentral Gyrus (Brodmann Area 7)
- Right and Left Precuneus (Brodmann Area 7)
- Right Superior Parietal Lobule (Brodmann Area 7)

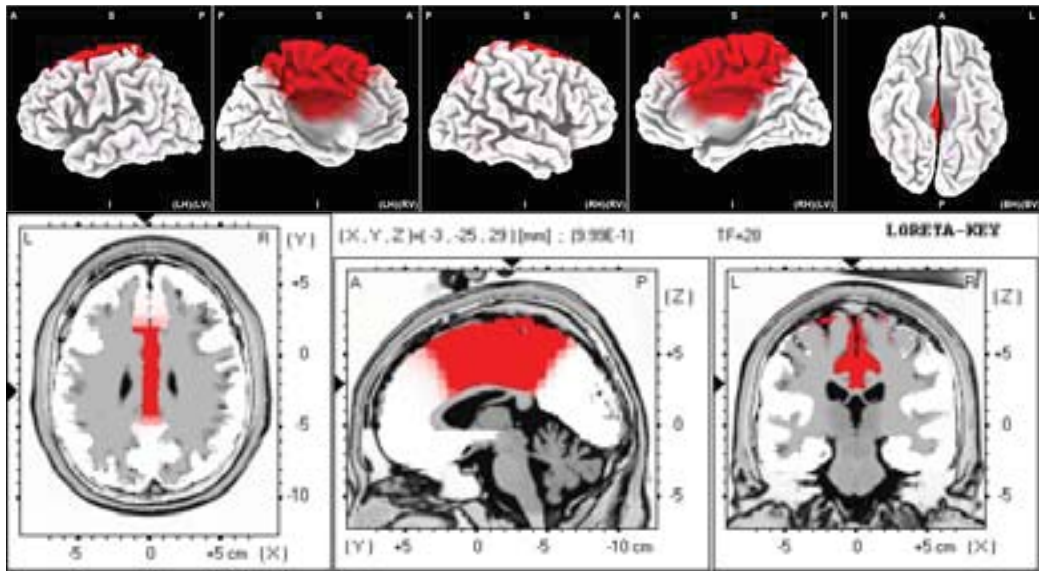


Figure 174. Paired t -test for 28 Hz LORETA: Significant differences after 20 minutes of 100 Hz CES.

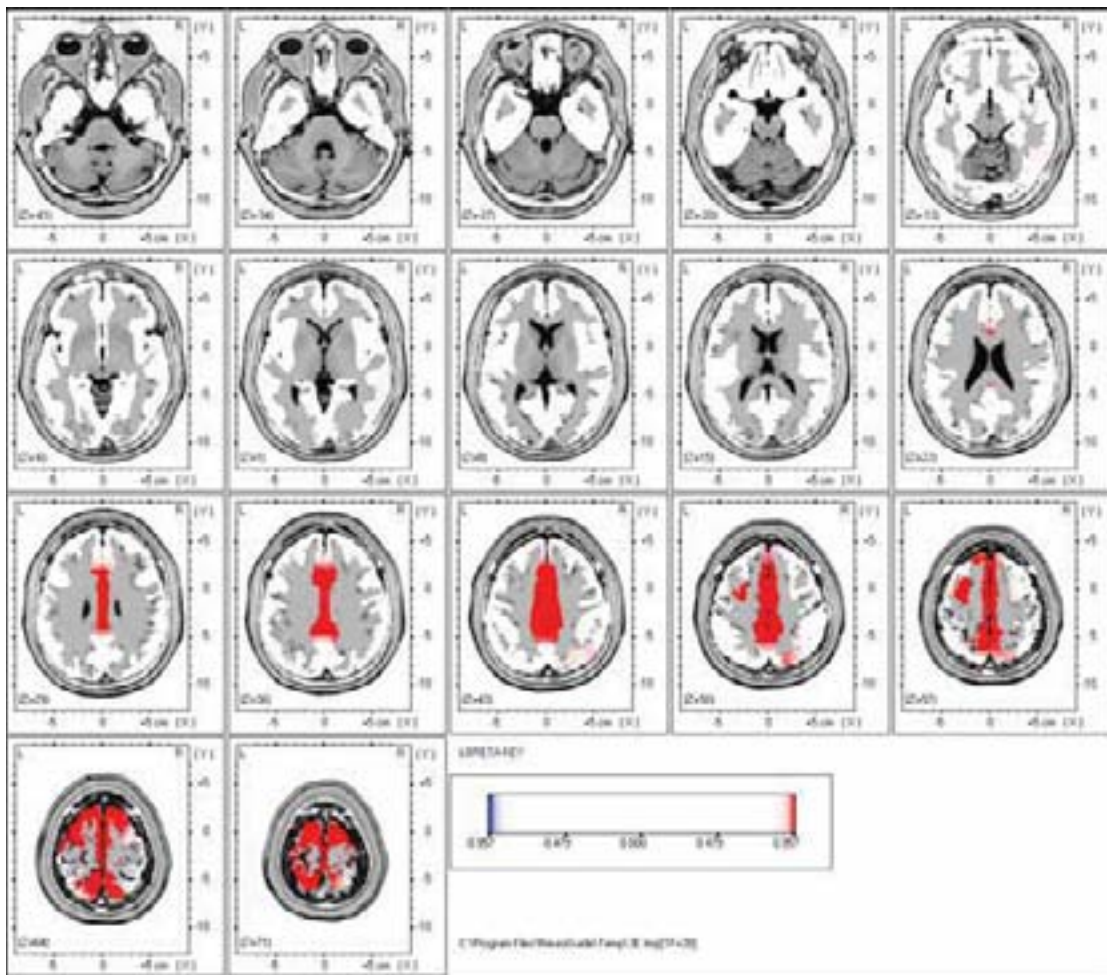


Figure 175. Paired t -test for 28 Hz LORETA: Significant differences after 20 minutes of 100 Hz CES.

Summary of 29 Hz Changes in Current Density

Decreased Frontal Lobe Activation

- Right and Left Rectal Gyrus (Brodmann Area 11)
- Right and Left Medial Frontal Gyrus (Brodmann Area 11)
- Right and Left Subcallosal Gyrus (Brodmann Area 25)

Decreased Limbic Lobe Activation

- Right and Left Anterior Cingulate (Brodmann Area 24)

Decreased Occipital Lobe Activation

- Left Cuneus (Brodmann Area 19)
- Left Superior Occipital Gyrus (Brodmann Area 19)

Decreased Parietal Lobe Activation

- Left Precuneus (Brodmann Area 19)

Increased Frontal Lobe Activation

- Right Superior Frontal Gyrus (Brodmann Area 6)
- Right and Left Medial Frontal Gyrus (Brodmann Area 6)
- Right Middle Frontal Gyrus (Brodmann Area 6)
- Right Precentral Gyrus (Brodmann Area 4)

Increased Limbic Lobe Activation

- Right and Left Cingulate Gyrus (Brodmann Area 31)

Increased Parietal Lobe Activation

- Right Postcentral Gyrus (Brodmann Area 2)
- Right Inferior Parietal Lobule (Brodmann Area 40)

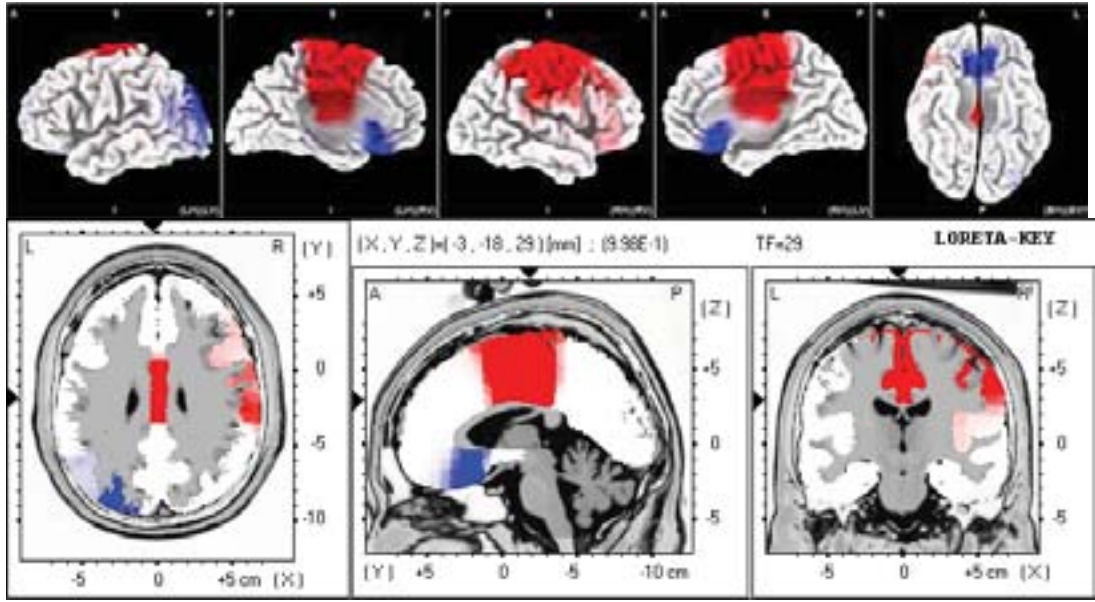


Figure 176. Paired t -test for 29 Hz LORETA: Significant differences after 20 minutes of 100 Hz CES.

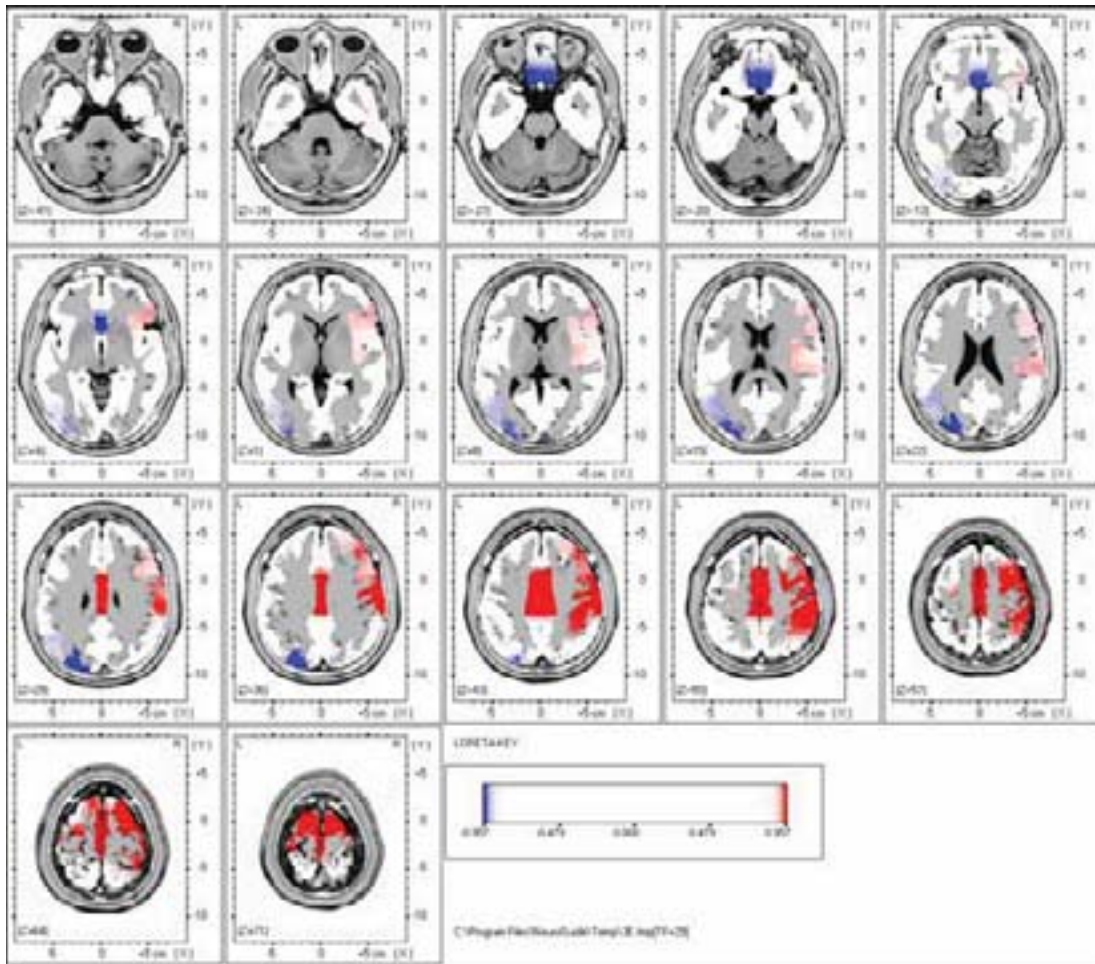


Figure 177. Paired t -test for 29 Hz LORETA: Significant differences after 20 minutes of 100 Hz CES.

Summary of 30 Hz Changes in Current Density

Decreased Frontal Lobe Activation

- Right and Left Medial Frontal Gyrus (Brodmann Area 11)

Decreased Temporal Lobe Activation

- Left Superior Temporal Gyrus (Brodmann Area 22)

Decreased Occipital Lobe Activation

- Left Superior Occipital Gyrus (Brodmann Area 19)

Decreased Parietal Lobe Activation

- Left Precuneus (Brodmann Area 19)

Increased Frontal Lobe Activation

- Right Superior Frontal Gyrus (Brodmann Area 6)
- Right and Left Medial Frontal Gyrus (Brodmann Area 6)
- Right and Left Middle Frontal Gyrus (Brodmann Area 6)
- Right Precentral Gyrus (Brodmann Area 4)
- Right and Left Paracentral Lobule (Brodmann Area 5)

Increased Limbic Lobe Activation

- Right and Left Cingulate Gyrus (Brodmann Area 23)

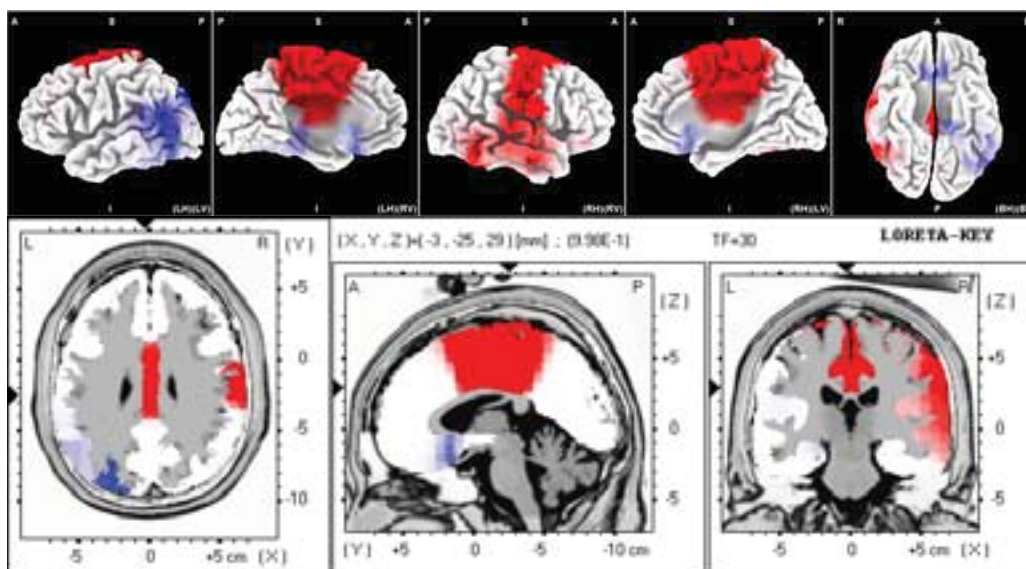


Figure 178. Paired t -test for 30 Hz LORETA: Significant differences after 20 minutes of 100 Hz CES.

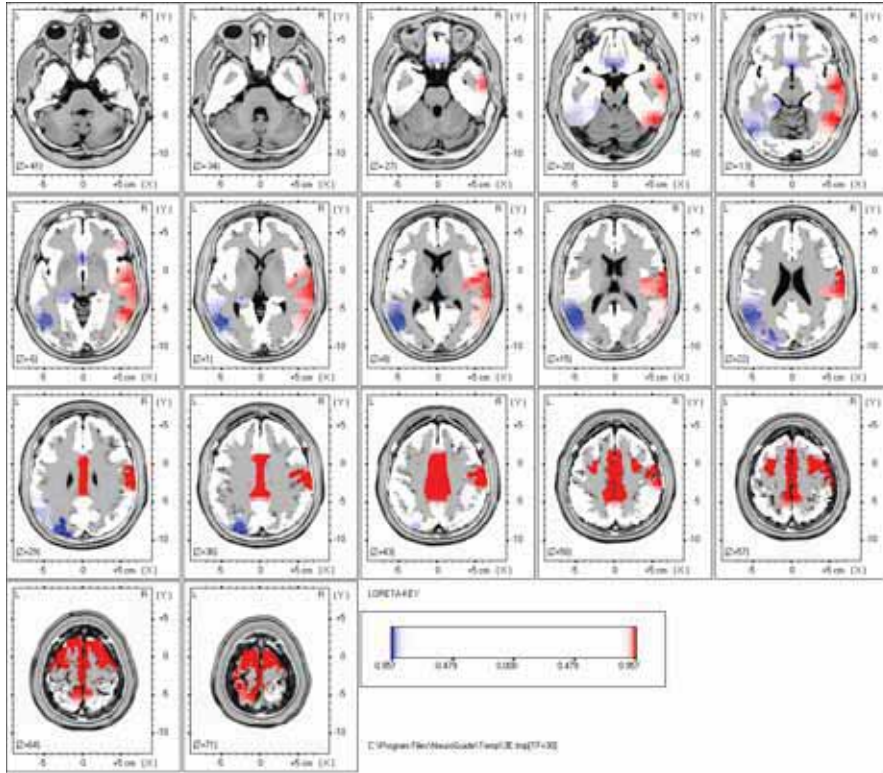


Figure 179. Paired t -test for 30 Hz LORETA: Significant differences after 20 minutes of 100 Hz CES.

Summary of 31 Hz Changes in Current Density

Increased Frontal Lobe Activation

- Right Superior Frontal Gyrus (Brodmann Area 6)
- Right and Left Medial Frontal Gyrus (Brodmann Area 6)
- Right Middle Frontal Gyrus (Brodmann Area 6)
- Right Precentral Gyrus (Brodmann Area 4)
- Right and Left Paracentral Lobule (Brodmann Area 5)

Increased Temporal Lobe Activation

- Right Inferior Temporal Gyrus (Brodmann Area 20)
- Right Fusiform Gyrus (Brodmann Area 20)
- Right Temporal Gyrus (Brodmann Area 21)
- Right Superior Temporal Gyrus (Brodmann Area 22)

Increased Sub-lobar

- Right Insula (Brodmann Area 13)

Increased Parietal Lobe Activation

- Right Postcentral Gyrus (Brodmann Area 23)
- Right Inferior Parietal Lobule (Brodmann Area 40)
- Right and Left Superior Parietal Lobule (Brodmann Area 7)
- Right and Left Precuneus (Brodmann Area 7)

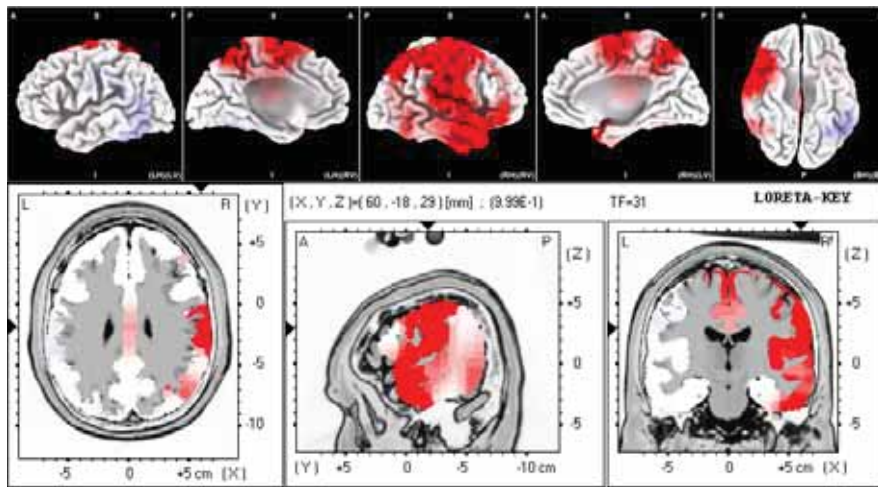


Figure 180. Paired t -test for 31 Hz LORETA: Significant differences after 20 minutes of 100 Hz CES.

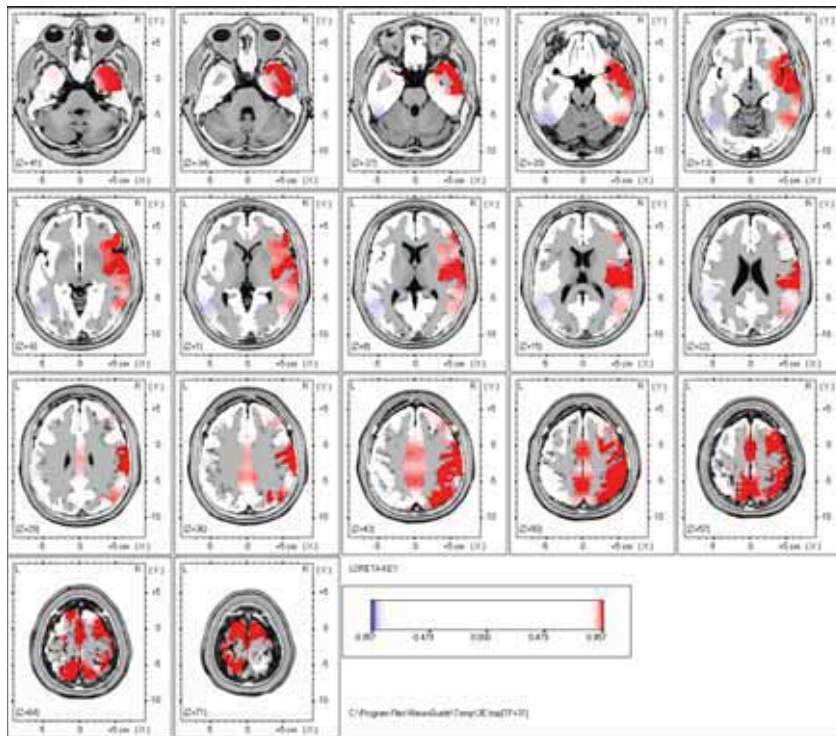


Figure 181. Paired t -test for 31 Hz LORETA: Significant differences after 20 minutes of 100 Hz CES.

Summary of 32 Hz Changes in Current Density

Increased Frontal Lobe Activation

- Right and Left Superior Frontal Gyrus (Brodmann Area 6)
- Right and Left Medial Frontal Gyrus (Brodmann Area 6)
- Right Middle Frontal Gyrus (Brodmann Area 6)
- Right and Left Medial Frontal Gyrus (Brodmann Area 6)
- Right Inferior Frontal Gyrus (Brodmann Area 47)
- Right and Left Paracentral Lobule (Brodmann Area 6)

Increased Limbic Lobe Activation

- Right and Left Cingulate Gyrus (Brodmann Area 32)

Increased Parietal Lobe Activation

- Inferior Parietal Lobule (Brodmann Area 40)

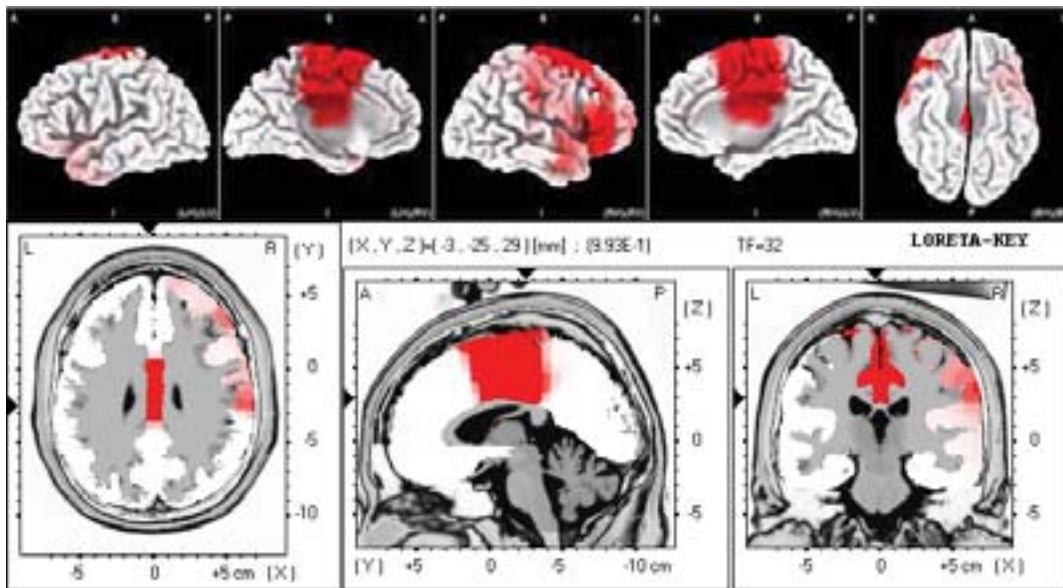


Figure 182. Paired *t*-test for 32 Hz LORETA: Significant differences after 20 minutes of 100 Hz CES.

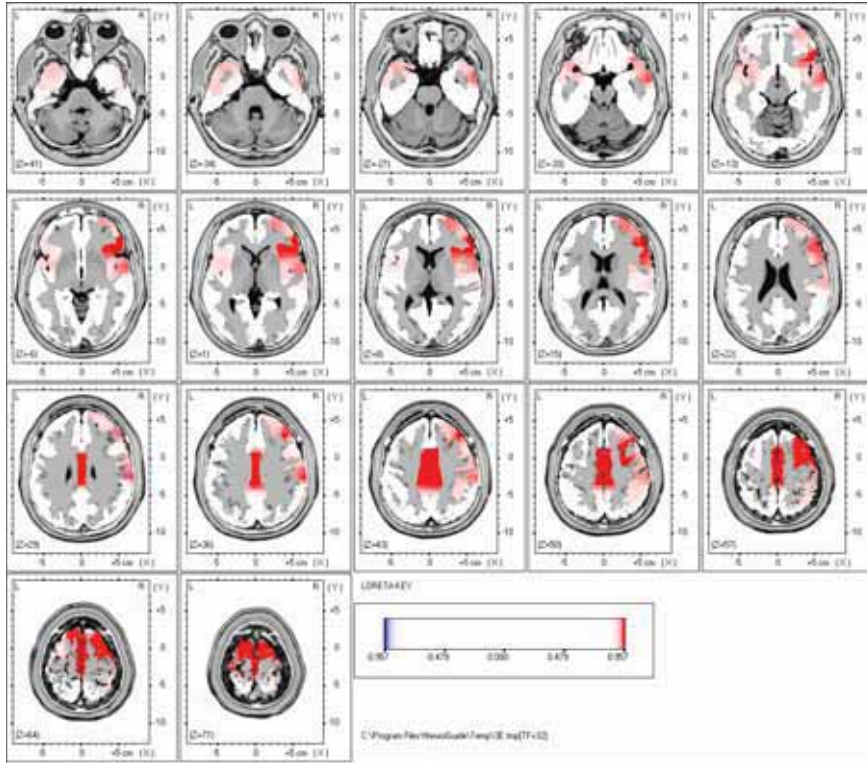


Figure 183. Paired t -test for 32 Hz LORETA: Significant differences after 20 minutes of 100 Hz CES.

Summary of 33 Hz Changes in Current Density

Increased Frontal Lobe Activation

- Right and Left Superior Frontal Gyrus (Brodmann Area 6)

Increased Limbic Lobe Activation

- Right and Left Cingulate Gyrus (Brodmann Area 24)

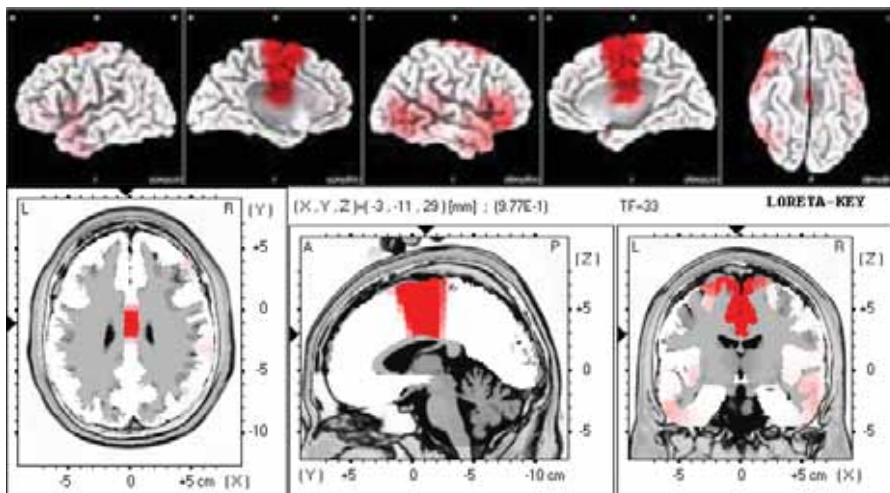


Figure 184. Paired t -test for 33 Hz LORETA: Significant differences after 20 minutes of 100 Hz CES.

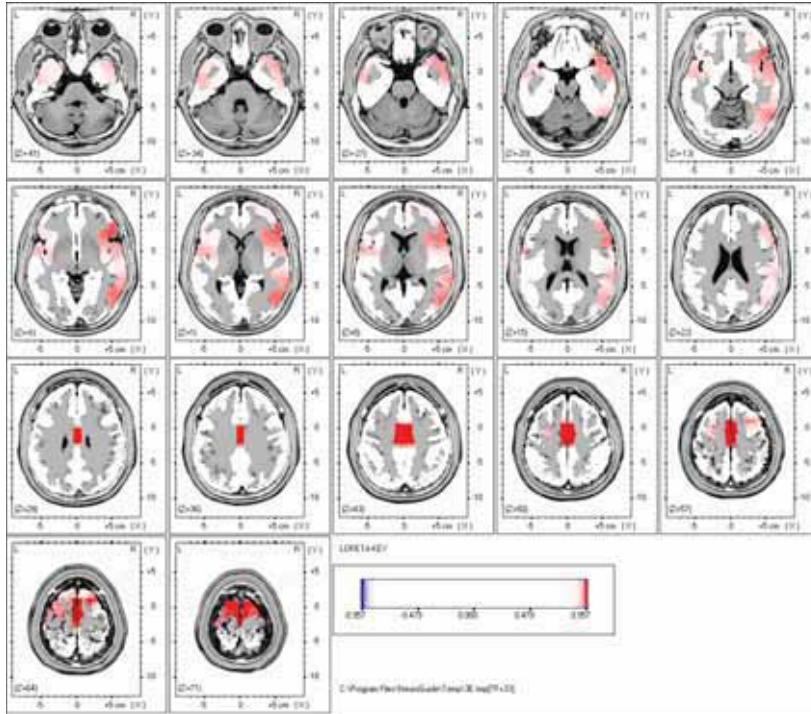


Figure 185. Paired t -test for 33 Hz LORETA: Significant differences after 20 minutes of 100 Hz CES.

Summary of 34 Hz Changes in Current Density

Decreased Limbic Lobe Activation

- Right and Left Anterior Cingulate (Brodmann Area 25)

Increased Frontal Lobe Activation

- Right and Left Superior Frontal Gyrus (Brodmann Area 6)
- Right and Left Medial Frontal Gyrus (Brodmann Area 6)
- Left Middle Frontal Gyrus (Brodmann Area 6)

Increased Limbic Lobe Activation

- Right and Left Cingulate Gyrus (Brodmann Area 24)
- Right Uncus (Brodmann Area 20)

Increased Temporal Lobe Activation

- Right Inferior Temporal Gyrus (Brodmann Area 20)
- Right Fusiform Gyrus (Brodmann Area 20)
- Right Middle Temporal Gyrus (Brodmann Area 21)

Increased Sub-lobar

- Right Insula (Brodmann Area 13)

Increased Parietal Lobe Activation

- Right Inferior Parietal Lobule (Brodmann Area 40)

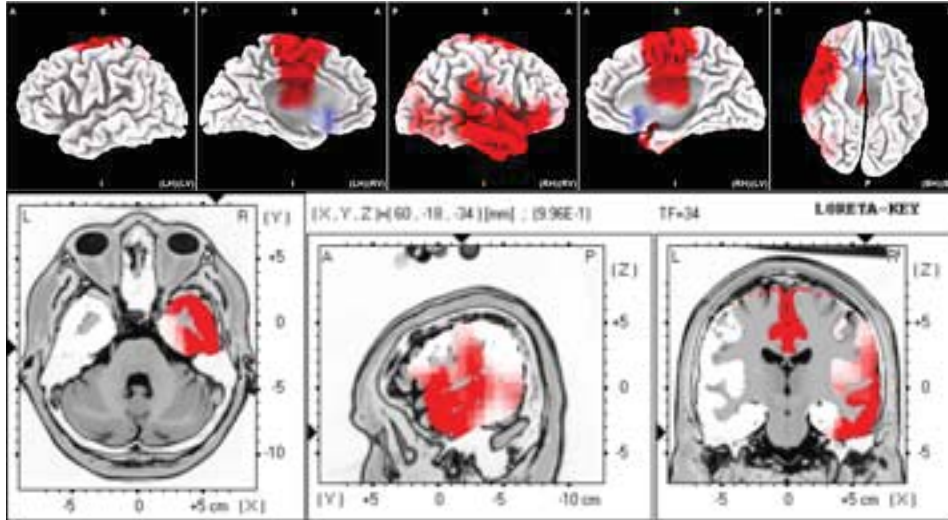


Figure 186. Paired t -test for 34 Hz LORETA: Significant differences after 20 minutes of 100 Hz CES.

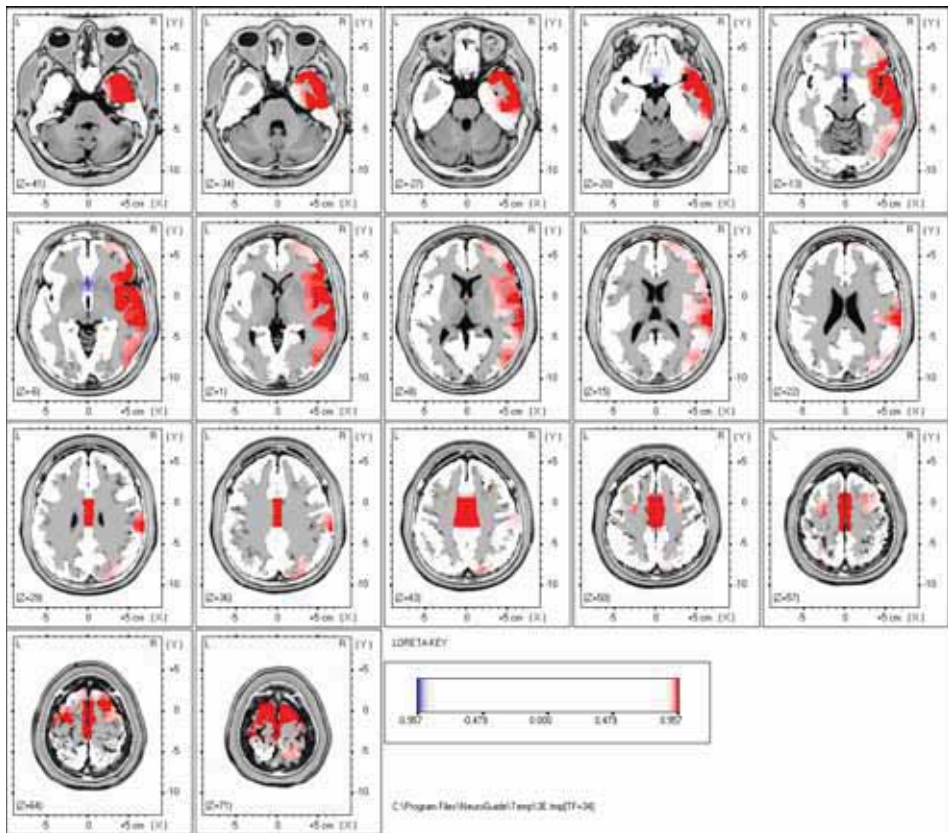


Figure 187. Paired t -test for 34 Hz LORETA: Significant differences after 20 minutes of 100 Hz CES.

Summary of 35 Hz Changes in Current Density

Increased Frontal Lobe Activation

- Right and Left Superior Frontal Gyrus (Brodmann Area 6)
- Right and Left Medial Frontal Gyrus (Brodmann Area 6)
- Left Middle Frontal Gyrus (Brodmann Area 6)
- Right Precentral Gyrus (Brodmann Area 6)

Increased Limbic Lobe Activation

- Right and Left Cingulate Gyrus (Brodmann Area 24)

Increased Temporal Lobe Activation

- Right Inferior Temporal Gyrus (Brodmann Area 20)
- Right Fusiform Gyrus (Brodmann Area 20)
- Right Middle Temporal Gyrus (Brodmann Area 21)
- Right Superior Temporal Gyrus (Brodmann Area 22)

Increased Parietal Lobe Activation

- Postcentral Gyrus (Brodmann Area 2)

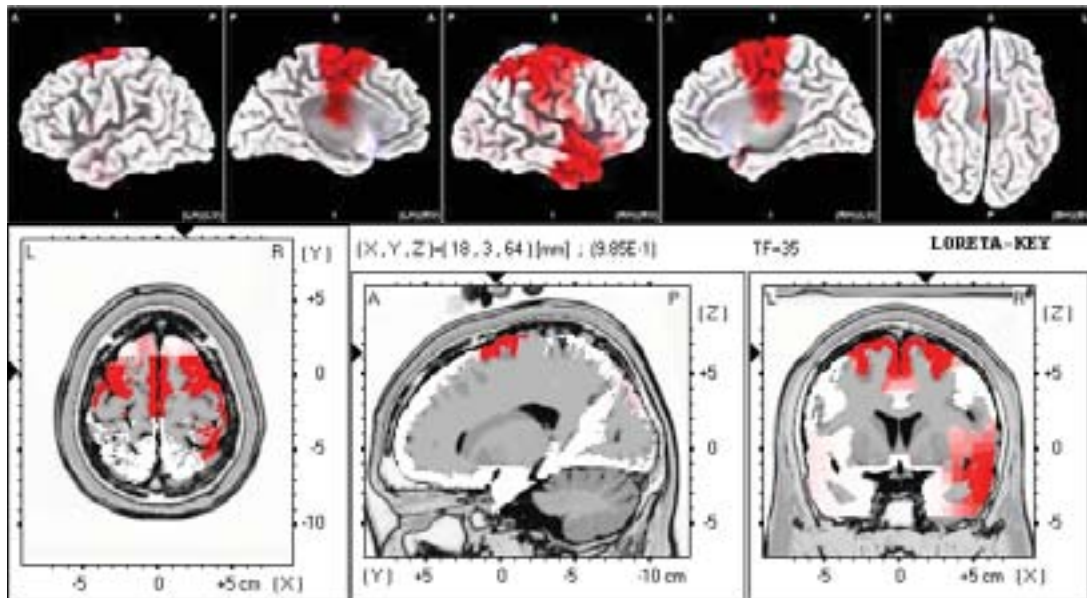


Figure 188. Paired *t*-test for 35 Hz LORETA: Significant differences after 20 minutes of 100 Hz CES.

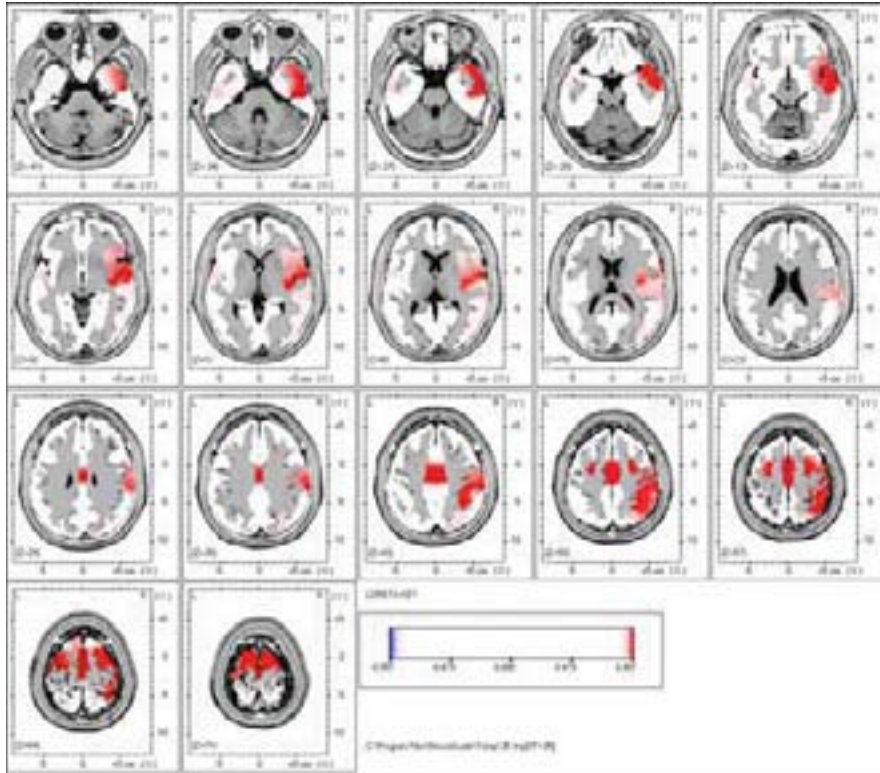


Figure 189. Paired t -test for 35 Hz LORETA: Significant differences after 20 minutes of 100 Hz CES.

Summary of 36 Hz Changes in Current Density

Increased Parietal Lobe Activation

- Right Inferior Parietal Lobule (Brodmann Area 40)
- Right Superior Parietal Lobule (Brodmann Area 7)

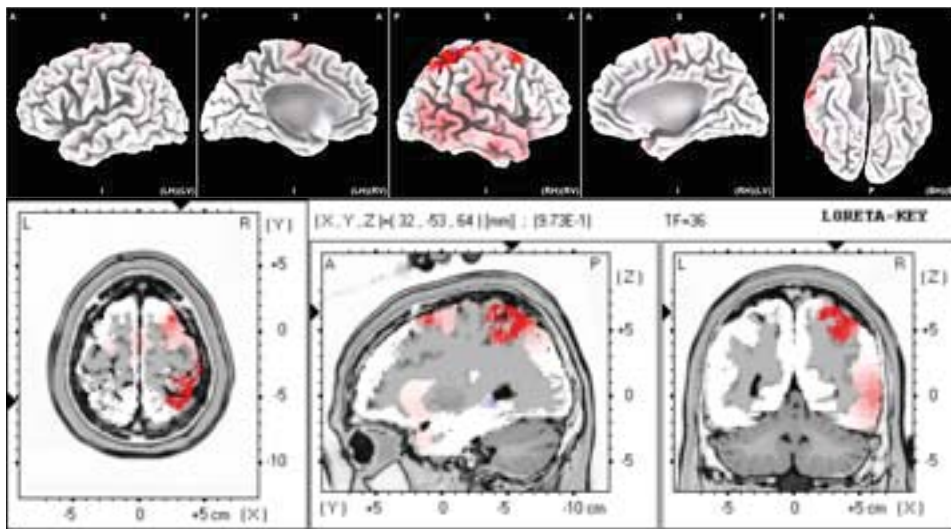


Figure 190. Paired t -test for 36 Hz LORETA: Significant differences after 20 minutes of 100 Hz CES.

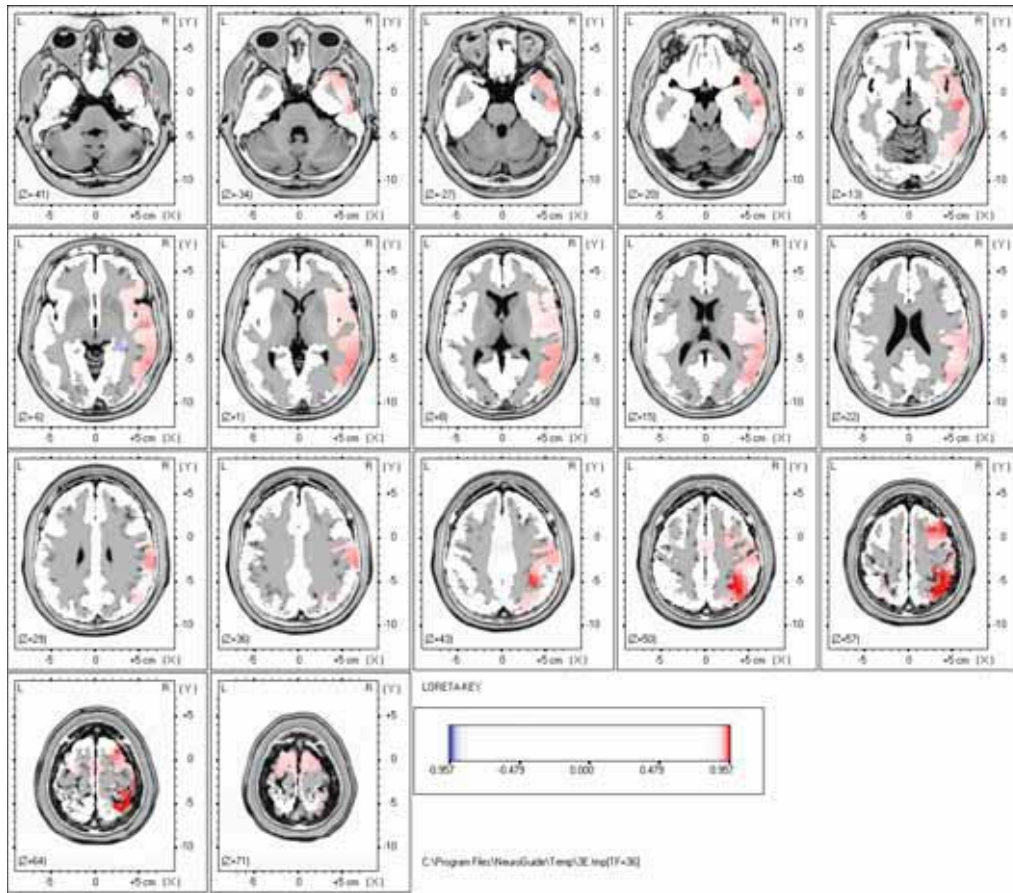


Figure 191. Paired t -test for 36 Hz LORETA: Significant differences after 20 minutes of 100 Hz CES.

Summary of 37 Hz Changes in Current Density

Decreased Limbic Lobe Activation

- Right Parahippocampal Gyrus (Brodmann Area 35)

Increased Frontal Lobe Activation

- Right and Left Medial Frontal Gyrus

Increased Limbic Lobe Activation

- Right and Left Cingulate Gyrus (Brodmann Area 24)

Increased Temporal Lobe Activation

- Right Inferior Temporal Gyrus (Brodmann Area 20)
- Right Fusiform Gyrus (Brodmann Area 20)
- Right Middle Temporal Gyrus (Brodmann Area 21)

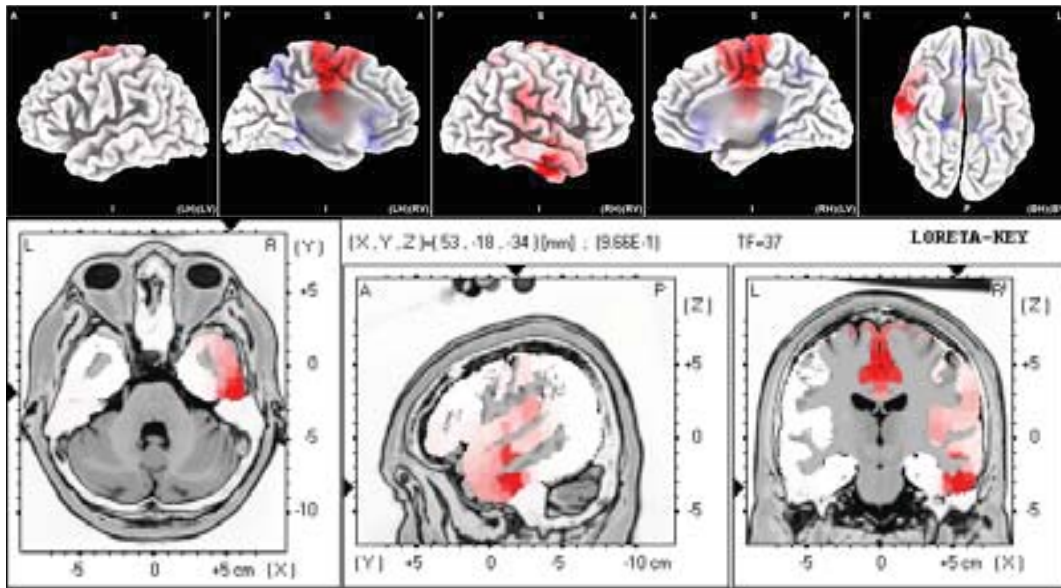


Figure 192. Paired t -test for 37 Hz LORETA: Significant differences after 20 minutes of 100 Hz CES.

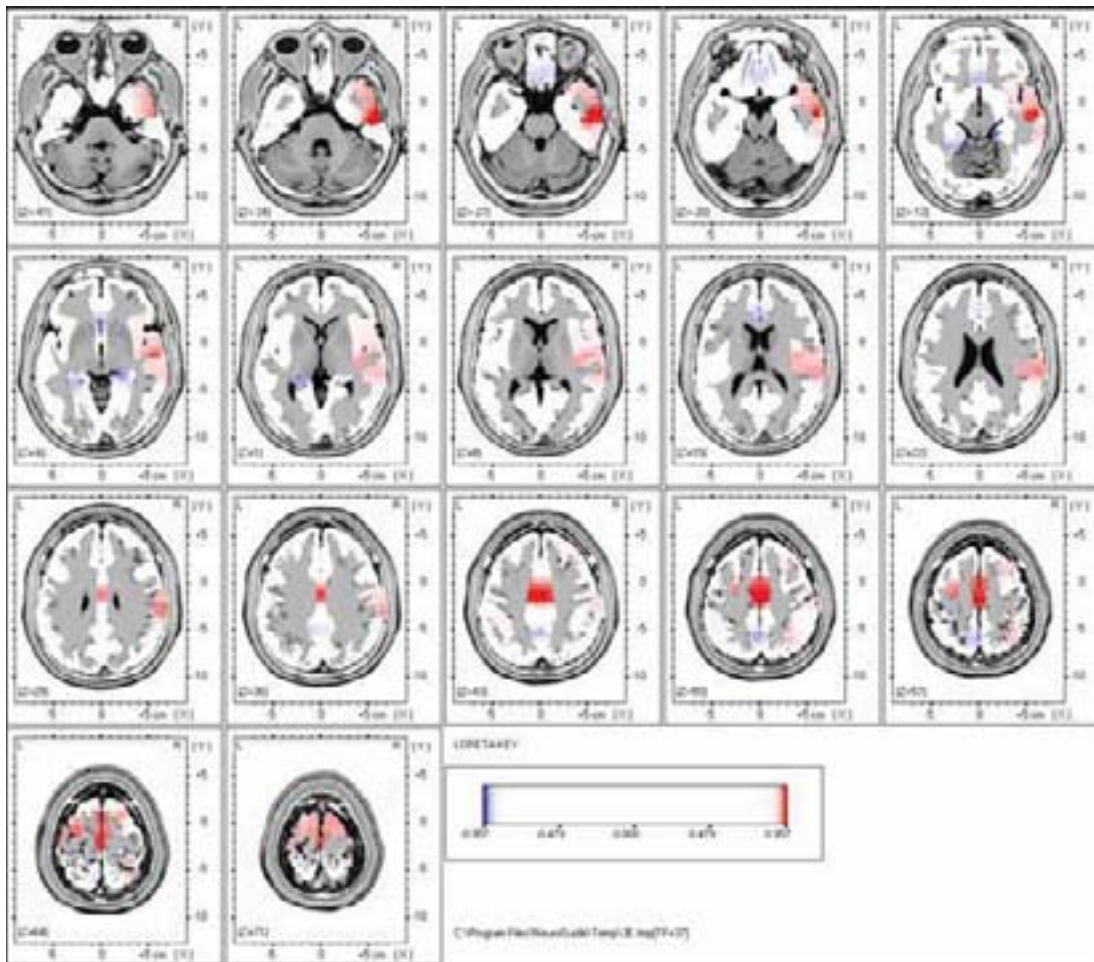


Figure 193. Paired t -test for 37 Hz LORETA: Significant differences after 20 minutes of 100 Hz CES.

Summary of 38 Hz Changes in Current Density

Increased Frontal Lobe Activation

- Right Middle Frontal Gyrus (Brodmann Area 8)
- Right Precentral Gyrus (Brodmann Area 9)

Increased Temporal Lobe Activation

- Right Inferior Temporal Gyrus (Brodmann Area 20)
- Right Fusiform Gyrus (Brodmann Area 20)

Increased Parietal Lobe Activation

- Postcentral Gyrus (Brodmann Area 3)

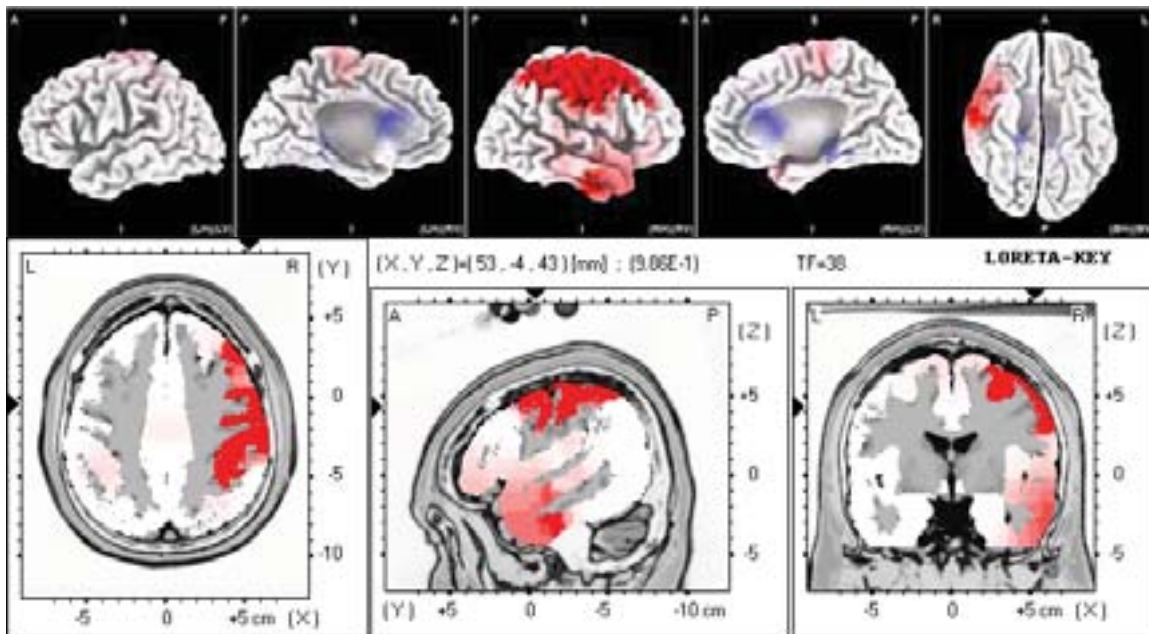


Figure 194. Paired *t*-test for 38 Hz LORETA: Significant differences after 20 minutes of 100 Hz CES.

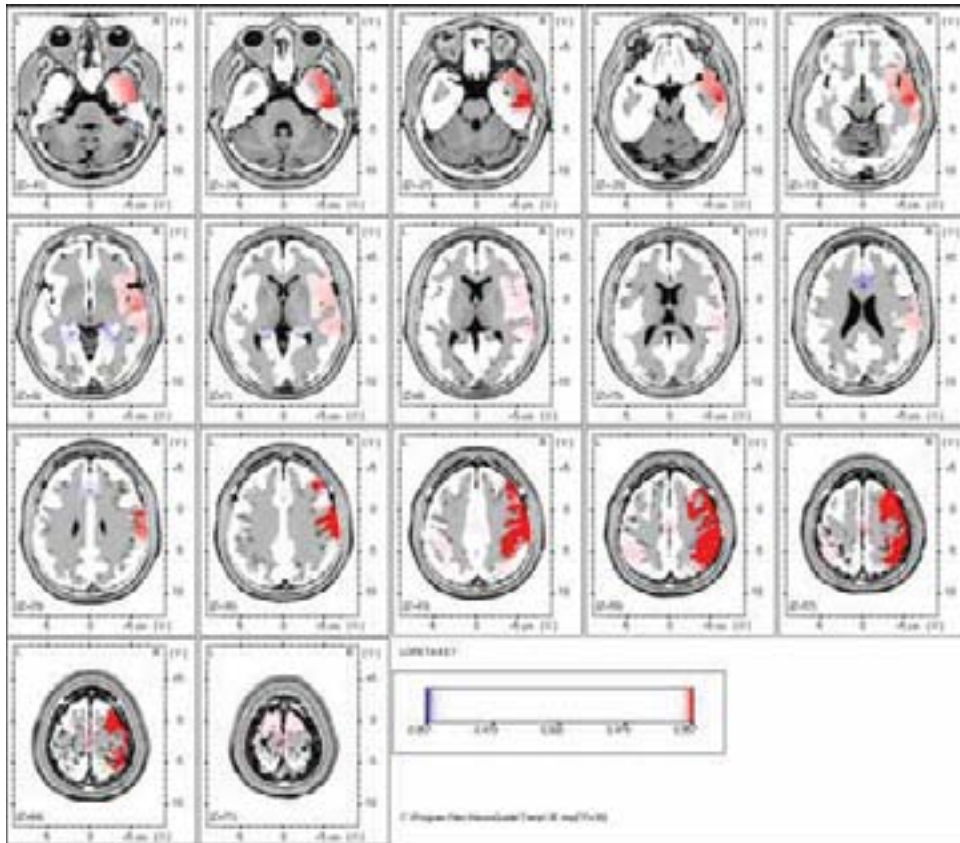


Figure 195. Paired t -test for 38 Hz LORETA: Significant differences after 20 minutes of 100 Hz CES.

Summary of 39 Hz Changes in Current Density

Decreased Frontal Lobe Activation

- Right and Left Subcallosal Gyrus (Brodmann Area 25)

Decreased Limbic Lobe Activation

- Right and Left Anterior Cingulate (Brodmann Area 32)
- Right and Left Posterior Cingulate (Brodmann Area 30)
- Right and Left Hippocampus (Sub-Gyral)
- Right and Left Parahippocampal Gyrus (Brodmann Area 37)

Increased Frontal Lobe Activation

- Right and Left Medial Frontal Gyrus (Brodmann Area 6)

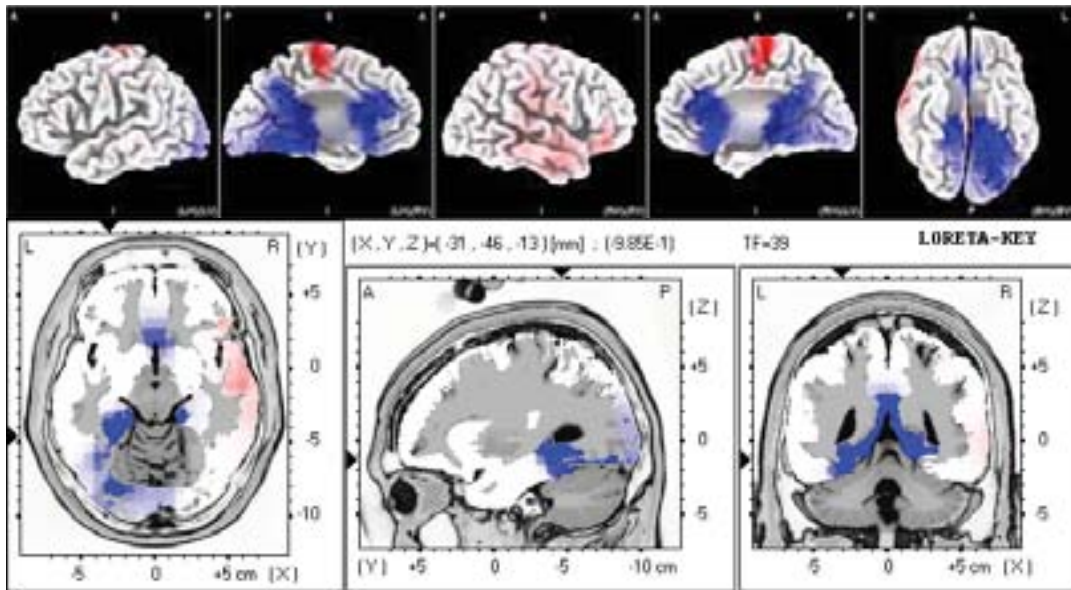


Figure 196. Paired t -test for 39 Hz LORETA: Significant differences after 20 minutes of 100 Hz CES.

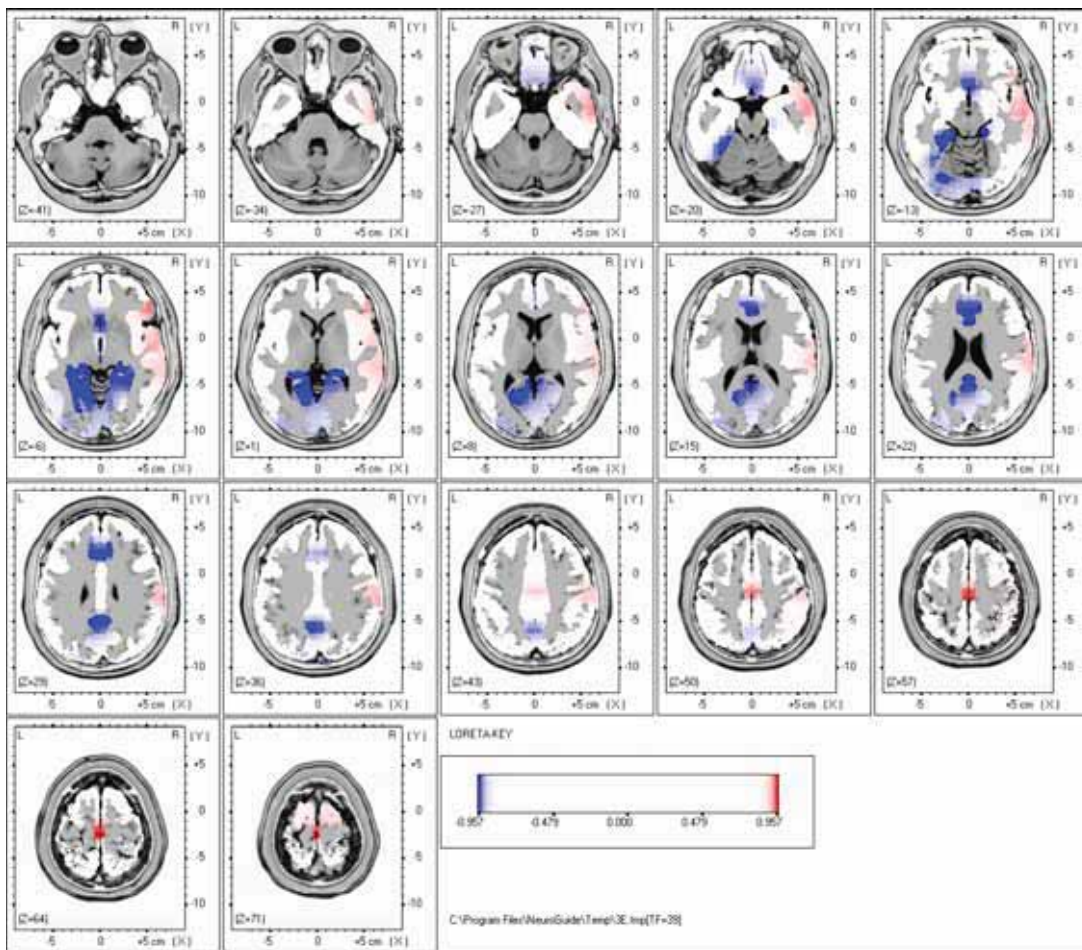


Figure 197. Paired t -test for 39 Hz LORETA: Significant differences after 20 minutes of 100 Hz CES.

Summary of 40 Hz Changes in Current Density

Decreased Frontal Lobe Activation

- Right and Left Medial Frontal Gyrus (Brodmann Area 9)
- Right and Left Rectal Gyrus (Brodmann Area 11)
- Right and Left Subcallosal Gyrus (Brodmann Area 25)
- Left Superior Frontal Gyrus (Brodmann Area 11)

Decreased Temporal Lobe Activation

- Left Fusiform Gyrus (Brodmann Area 37)

Decreased Limbic Lobe Activation

- Right and Left Anterior Cingulate (Brodmann Area 24)
- Right and Left Posterior Cingulate (Brodmann Area 30)
- Right and Left Hippocampus (Sub-Gyral)
- Right and Left Parahippocampal Gyrus (Brodmann Area 30)

Decreased Occipital Lobe Activation

- Left Cuneus (Brodmann Area 19)
- Left Superior Occipital Gyrus (Brodmann Area 19)
- Left Middle Occipital Gyrus (Brodmann Area 18)
- Left Inferior Occipital Gyrus (Brodmann Area 18)
- Right and Left Lingual Gyrus (Brodmann Area 18)

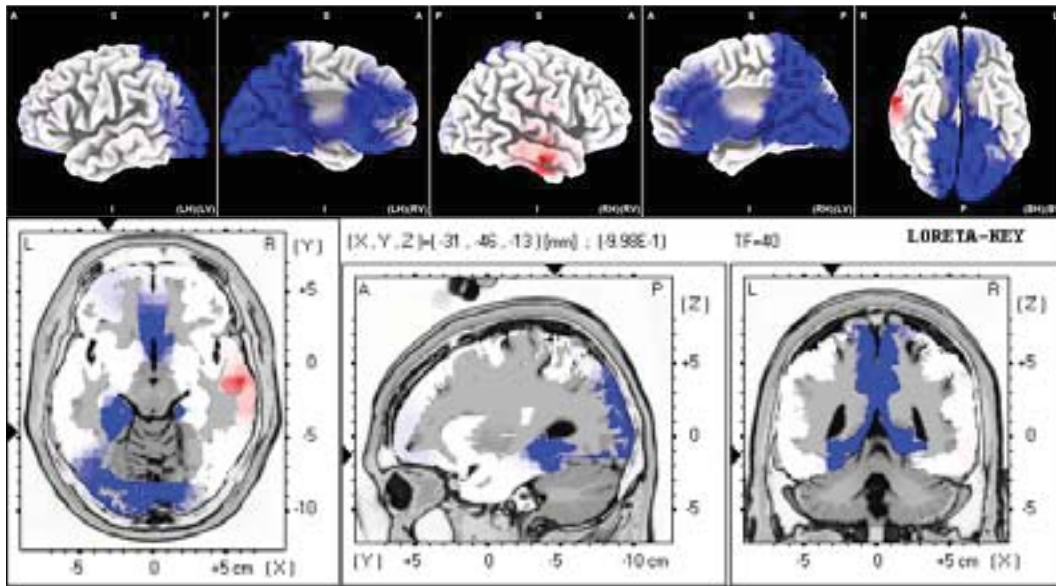


Figure 198. Paired t -test for 40 Hz LORETA: Significant differences after 20 minutes of 100 Hz CES.

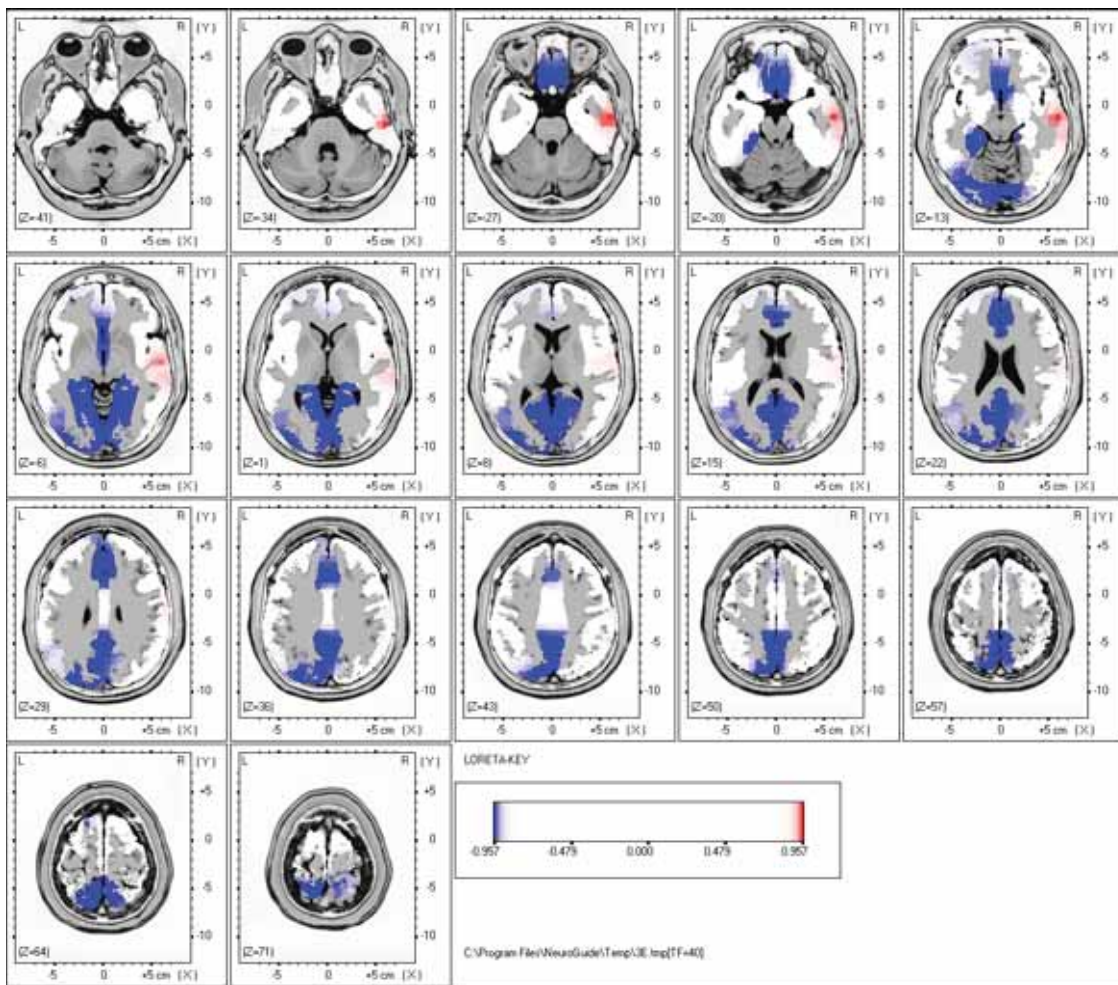


Figure 199. Paired t -test for 40 Hz LORETA: Significant differences after 20 minutes of 100 Hz CES.

Common Changes in qEEG Relative Power and LORETA

The paired *t*-tests revealed that in both relative power and in LORETA there were statistically significant changes after CES. Both found an increase in alpha activity with a decrease in beta activity. The LORETA found an increase in theta current density activity that was not found in either group of CES on the relative power results. Likewise relative power analysis found a decrease in delta activity that was not found in both groups on the LORETA, but was found in the 0.5 Hz CES LORETA results. A summary of the changes common to both groups in relative power and in LORETA is presented in table 11.

Table 11

Summary of Changes in Relative Power and LORETA Current Density (CD) for Both Groups after 20 Minutes of CES

Location	Increased Power	Decreased Power	Increased CD	Decreased CD	Common Changes
Frontal Lobe	<i>Alpha</i>	Delta, Gamma	<i>Theta, Alpha</i>	Gamma	<i>Alpha, Gamma</i>
Temporal Lobe	<i>Alpha</i>	Delta, Beta 3, Gamma	<i>Theta, Alpha</i>	Gamma	<i>Alpha, Gamma</i>
Limbic Lobe	NA	NA	<i>Theta, Alpha</i>	Gamma	
Parietal Lobe	<i>Alpha</i>	Delta, Theta, Beta 2, Beta 3, Gamma	<i>Theta, Alpha</i>	Gamma	<i>Alpha, Gamma</i>
Occipital Lobe	<i>Alpha (100 Hz only)</i>	Delta, Beta 1, Beta 3, Gamma	<i>Theta, Alpha</i>	Gamma	Gamma
Sub-Lobar	NA	NA	<i>Theta, Alpha</i>		
Summary for All Locations	<i>Alpha</i>	Delta, Theta, Beta	<i>Theta, Alpha</i>	Gamma (Beta)	<i>Alpha, Beta</i>

Findings for Hypothesis 17:

Given the discovery of a significant difference in the mean current density of voxels in the alpha band for 0.5 Hz CES between the baseline and treatment groups, the null hypothesis 17

was rejected ($H17_0: \mu_{.5\alpha CDB} = \mu_{.5\alpha CDE}$) in favor of the alternate hypothesis 17 ($H17_A: \mu_{.5\alpha CDB} \neq \mu_{.5\alpha CDE}$). It was found that immediately after a single 20-minute session of 0.5 Hz CES, there was a statistically significant change in the mean current density of voxels in the alpha band at one or more electrode sites.

Findings for Hypothesis 18:

Given the discovery of a significant difference in the mean current density of voxels in the alpha band for 100 Hz CES between the baseline and treatment groups, the null hypothesis 18 was rejected ($H18_0: \mu_{100\alpha CDB} = \mu_{100\alpha CDE}$) in favor of the alternate hypothesis 18 ($H18_A: \mu_{100\alpha CDB} \neq \mu_{100\alpha CDE}$). It was found that immediately after a single 20-minute session of 100 Hz CES, there was a statistically significant change in the mean current density of voxels in the alpha band at one or more electrode sites.

Findings for Hypothesis 19:

Given the discovery of a significant difference in the mean current density of voxels in the delta band for 0.5 Hz CES between the baseline and treatment groups, the null hypothesis 19 was rejected ($H19_0: \mu_{.5\Delta CDB} = \mu_{.5\Delta CDE}$) in favor of the alternate hypothesis 19 ($H19_A: \mu_{.5\Delta CDB} \neq \mu_{.5\Delta CDE}$). It was found that immediately after a single 20-minute session of 0.5 Hz CES, there was a statistically significant change in the mean current density of voxels in the delta band at one or more electrode sites.

Findings for Hypothesis 20:

Given the discovery of a significant difference in the mean current density of voxels in

the delta band for 100 Hz CES between the baseline and treatment groups, the null hypothesis 20 was rejected ($H20_0: \mu_{100\Delta CDB} = \mu_{100\Delta CDE}$) in favor of the alternate hypothesis 20 ($H20_A: \mu_{100\Delta CDB} \neq \mu_{100\Delta CDE}$). It was found that immediately after a single 20-minute session of 100 Hz CES, there was a statistically significant change in the mean current density of voxels in the delta band at one or more electrode sites.

Findings for Hypothesis 21:

Given the discovery of a significant difference in the mean current density of voxels in the theta band for 0.5 Hz CES between the baseline and treatment groups, the null hypothesis 21 was rejected ($H21_0: \mu_{.5\Theta CDB} = \mu_{.5\Theta CDE}$) in favor of the alternate hypothesis 21 ($H21_A: \mu_{.5\Theta CDB} \neq \mu_{.5\Theta CDE}$). It was found that immediately after a single 20-minute session of 0.5 Hz CES, there was a statistically significant change in the mean current density of voxels in the theta band at one or more electrode sites.

Findings for Hypothesis 22:

Given the discovery of a significant difference in the mean current density of voxels in the theta band for 100 Hz CES between the baseline and treatment groups, the null hypothesis 22 was rejected ($H22_0: \mu_{100\Theta CDB} = \mu_{100\Theta CDE}$) in favor of the alternate hypothesis 22 ($H22_A: \mu_{100\Theta CDB} \neq \mu_{100\Theta CDE}$). It was found that immediately after a single 20-minute session of 100 Hz CES, there was a statistically significant change in the mean current density of voxels in the theta band at one or more electrode sites.

Findings for Hypothesis 23:

Given the discovery of a significant difference in the mean current density of voxels in the beta band for 0.5 Hz CES between the baseline and treatment groups, the null hypothesis 23 was rejected ($H_{23_0}: \mu_{.5\beta CDB} = \mu_{.5\beta CDE}$) in favor of the alternate hypothesis 23 ($H_{23_A}: \mu_{.5\beta CDB} \neq \mu_{.5\beta CDE}$). It was found that immediately after a single 20-minute session of 0.5 Hz CES, there was a statistically significant change in the mean current density of voxels in the beta band at one or more electrode sites.

Findings for Hypothesis 24:

Given the discovery of a significant difference in the mean current density of voxels in the beta band for 100 Hz CES between the baseline and treatment groups, the null hypothesis 23 was rejected ($H_{24_0}: \mu_{100\beta CDB} = \mu_{100\beta CDE}$) in favor of the alternate hypothesis 23 ($H_{24_A}: \mu_{100\beta CDB} \neq \mu_{100\beta CDE}$). It was found that immediately after a single 20-minute session of 100 Hz CES, there was a statistically significant change in the mean current density of voxels in the beta band at one or more electrode sites.

CHAPTER 4

DISCUSSION

Introduction

The data from this study demonstrated that cranial electrotherapy stimulation (CES) does have a significant effect on cortical and subcortical activity as measured by qEEG and LORETA. On qEEG, the response to both frequencies of CES was substantially similar involving a decrease in delta and beta relative power activity with an increase in alpha relative power activity. The response to the 0.5 Hz CES as measured by LORETA was reasonably consistent with the qEEG relative power findings and the qEEG current density measure (Laplacian montage). However, the LORETA results of the 100 Hz CES included substantially more activity than that found in the 0.5 Hz LORETA and 0.5 Hz and 100 Hz qEEG relative power. Because the LORETA results for the 100 Hz CES include substantial additional activity that is not seen on any of the other imaging, interpretation of this activity must be done cautiously.

Summary of the Relative Power Findings

Statistically significant changes in EEG were found in the relative power alpha, delta and beta bands for both CES frequencies. There was an increase in alpha power with a concomitant decrease in delta and beta power. The pattern of statistically significant changes observed in relative power was consistent with the affective changes described in the literature on CES. The null hypothesis was supported for the theta band activity, where there was no statistically significant change in cortical activity on the qEEG. The changes that were statistically significant passed three levels of control for type I error, in that they occurred as part of a pattern, they were found in both CES groups, and they were found in an alternate referential montage (average

reference). Despite the similarity of response to both frequencies of CES, the relative power results were not identical. The 100 Hz CES suppressed a wider range of beta frequency activity than the 0.5 Hz CES. Conversely it was found that the 0.5 Hz CES suppressed more of the delta frequency activity than the 100 Hz CES.

Summary of Coherence Findings

A common increase in EEG coherence was found for theta and beta frequencies in both conditions of CES. The 0.5 Hz CES decreased delta coherence in linked ears and average reference montages, but the decrease in delta coherence did not occur with the 100 Hz CES. The EEG is unable to detect activity in the white matter tracks connecting the various regions of the brain; however, coherence allows for the use of EEG data to infer the activity in these subcortical tracks. The observed changes in coherence from CES were primarily increased coherence in alpha with some additional increase in theta. The increase in alpha coherence is not surprising given the extent of increased production of alpha in relative power. While coherence is independent of amplitude, the increase in production of alpha suggests that the thalamus, the primary generator of alpha, has become more active. An increase in alpha frequency input to different cortical regions from a common subcortical generator would increase alpha coherence. Given that the thalamus is the primary generator of alpha, although not the only generator, it is likely that the thalamus is the source of the increased production of alpha. Unfortunately the LORETA was not able to confirm this supposition, since the increased alpha activity registered by LORETA occupied all cortical and subcortical grey matter voxels represented by LORETA. Coherence may also reflect changes in the amount of some presynaptic neurotransmitters as well as some postsynaptic responses to neurotransmitters (Purves, 1988), in which case the changes

in coherence may reflect the increase of neurotransmitters associated with alpha and theta frequencies. If this is the case, then the findings in the LORETA may reflect both an increase in alpha generation by the thalamus and changes in the level/and or response to neurotransmitters in the synaptic cleft. Regardless of the source of the increase in coherence, the association of the theta coherence with the alpha in terms of frequency and location suggests that it is part of the same pattern of activation as the alpha coherence, and may be a continuation of the same activity in alpha into lower frequencies.

Summary of Amplitude Asymmetry Findings

There were changes in amplitude asymmetry noted in both CES groups, however the patterns of changes were not the same. In the 0.5 Hz CES group, an increase in alpha amplitude asymmetry was noted in both a linked ears and common reference montage. These changes in alpha asymmetry were not seen in either montage of the 100 Hz group and appear to be specific to the 0.5 Hz CES. There were no other validated changes in asymmetry with the 0.5 Hz group. The 100 Hz CES produced both decreased and increased asymmetry in delta as well as a decrease in theta asymmetry in both montages.

Summary of Phase Lag Findings

There was an increase in alpha frequency phase lag in both CES groups, however none of the changes involved the same electrode pairs. A comparison of the linked ears montage and the average reference montage found only two electrode pairs in the 100 Hz CES group and one electrode pair in the 0.5 Hz CES group with common changes in phase lag. Therefore, while the

null hypothesis was rejected for phase lag the changes were minimal. In short CES does not appear to have a strong effect on phase lag.

Summary of Power Ratio Findings

Power ratios are an index of EEG power reflecting changes in the balance of EEG power by frequency band. The effect of CES on the power ratios was essentially identical in both 0.5 Hz and 100 Hz CES. There were significant ratio decreases found in delta/theta, delta/alpha and theta/alpha, with significant ratio increases in theta/gamma, alpha/beta, alpha/gamma and beta/gamma. The changes in power ratios in response to CES are congruent with the changes found in relative power.

Summary of LORETA Findings

The results of the LORETA analysis revealed changes in current density common to both the 0.5 Hz CES group and the 100 Hz CES group. There was agreement in LORETA between the two CES groups for statistically significant increases in theta and alpha frequency current density, with a significant decrease in beta frequencies. Since these changes were observed with both frequencies of CES, they can reasonably be assumed to represent real changes in activity and do not represent type I error. In terms of location, the increased current density was found in all lobes, subcortical regions of interest and across most of the cortex. All gray matter voxels represented by LORETA showed response to CES. The increase or decrease in current density varied by frequency and location within the brain. In any frequency in which CES increased current density, there was an increase in limbic activity. This data suggests that the limbic system responds in more frequencies of current density than the rest of the brain.

The LORETA results suggest that the entire brain is responding to CES. In some frequencies there was a current density increase in every lobe and every region of interest within the brain, while in other frequencies the current density decreased within every lobe and every region of interest. For both the qEEG and LORETA there are frequency specific responses that occurred as a result of CES, but it is clear from the LORETA that in some frequencies these responses were global.

The LORETA finding that CES increases alpha frequency activity in both 0.5 Hz and 100 Hz CES is not surprising given that a pattern of increased alpha was seen in relative power qEEG. The alpha frequency response of current density was extensive and involved all subcortical regions of interest estimated by LORETA. It is largely from the alpha response to CES on LORETA that it can be inferred that CES evokes changes in most of the brain. This data suggests that, as predicted by the proposed theory of CES, the vesicles of most, or all, neurons are being stimulated by CES.

It is surprising to see increases in theta current density for both groups of CES in the LORETA analysis, when the relative power qEEG did not find any increase in theta. However, an increase in theta was found in the coherence measure of the qEEG, suggesting the theta is a consequence of volume conduction from a subcortical generator, or the result of changes in neurotransmitter levels. It may be that the activation of limbic structures by CES is extending the response seen with increased alpha into theta current densities. More study will be required of this aspect of the response to CES to determine what is the source and implication of the increase in theta activity seen on the LORETA and qEEG coherence.

The LORETA of the 0.5 Hz CES group was found to have a decrease in beta activity. The LORETA results for beta activity in the 0.5 Hz CES group is generally consistent with the

findings in the relative power qEEG. The LORETA of 100 Hz CES indicated widespread increases in activity in delta and beta frequencies not seen in the LORETA of the 0.5 Hz group. This activity did not pass methodological controls for type I error and likely represents false positive results. The only widespread decrease in 100 Hz LORETA beta activity occurred in the last two frequencies of the data (39 & 40 Hz). The pattern of decrease in beta activity seen with 0.5 Hz LORETA was primarily in the left hemisphere, while the pattern of increased beta activity seen with 100 Hz LORETA was primarily in the right hemisphere. Because of the likelihood that it represents artifact, the increase in delta and beta activity seen with the 100 Hz CES should be considered with caution.

LORETA Artifact in the 100 Hz CES Group

The lack of agreement between some of the LORETA results for the 100 Hz CES group and the 0.5 Hz CES LORETA is a concern requiring careful consideration. The increase in delta and beta activity in 100 Hz CES LORETA is widespread and varies considerably from the findings in the 0.5 Hz CES and the qEEG for both 0.5 Hz and 100 Hz CES groups. It is difficult to understand how the effect of 100 Hz CES, as measured by LORETA, could actually vary so substantially from the effect of 0.5 Hz CES and not be reflected in the qEEG. The question is whether or not this discrepant activity is real or artifact. Due to the extraordinarily large number of paired *t*-tests conducted in the LORETA analysis (193, 914) for each CES group, any findings that do not occur in both groups should be considered artifact. It is also a remote possibility that there are unique responses to 100 Hz CES that do not appear on the 0.5 Hz LORETA, or the 100 Hz CES qEEG. Since the LORETA estimates current density, it may be that the activity seen in the 100 Hz LORETA analyses is not visible on EEG. It is possible for substantial cortical

activity to be present and not register on an EEG. Even though the LORETA method uses EEG to estimate current density, actual current density is not visible on the EEG. The EEG measures are unable to detect about 2/3rds of the electrical activity at the cortex (Thompson & Thompson, 2003). These measures are based on extracellular potentials and not lateral current flow. Direct measures of current flow are possible with MEG, but that data does not register any EEG activity. If this is the case, then the discrepant activity should be visible on the other method of estimating current density used in the study, the Laplacian montage.

In the qEEG a cluster of activity spanning several frequencies would pass the test for type I error since random activity by definition does not occur in organized groups. However, it is known that in the case of point source activity, the LORETA can produce phantom clusters of activity that appear to be a real, but in fact are an artifact. Therefore, it is not sufficient just to identify a cluster of activity in LORETA to control for type I error, the activity has to be found in another (independent) group or montage to control for false positive results. While the assumptions and calculations in the Laplacian montage are different from those in the LORETA, both are estimates of current density and therefore should to some degree represent the same activity on the cortex. A paired *t*-test of the 100 Hz CES data was conducted with a Laplacian montage to compare with the cortical aspects of the LORETA analysis.

The 100 Hz CES Laplacian montage showed a decrease in delta and beta activation, and an increase in alpha. The results of the 100 Hz CES Laplacian montage were consistent with the 0.5 Hz LORETA and the 100 Hz CES qEEG (amplitude based relative power), but not with the 100 Hz CES LORETA. However, the Laplacian montage did yield a significant finding which probably reveals the source of the discrepant activity in 100 Hz LORETA analyses. The Laplacian found a focal increase in current density for the 100 Hz group frontally at two sites (F4

and T4). This activity is highly localized, but is present in multiple frequencies. The focal activity found in the 100 Hz CES Laplacian montage is present in the delta and beta frequencies; the same frequencies the 100 Hz LORETA analysis found activity not seen in the 0.5 Hz LORETA or 100 Hz qEEG. The discovery of this focal activity on the Laplacian montage suggests that the discrepant activity seen in the 100 Hz LORETA in delta and beta is an artifact; it is phantom activity of the type produced by LORETA when it encounters focal activity. Therefore, the Laplacian montage did not validate the extensive pattern of increased beta frequency current density found with the LORETA analysis of the 100 Hz group, but it did find focal activity of the type known to create phantom activity on the LORETA. Further research will be needed to confirm that the discrepant LORETA activity in 100 Hz CES is artifact and not actual activity. Until the follow-up research is done, the findings of LORETA involving an increase in delta activity and beta with 100 Hz CES should be considered with caution.

Activation/Adaptation Model of CES

Previous research has found that the electrical currents from CES are uniformly distributed through the entire volume of the brain, and that these currents induce activation of the vesicles to release neurotransmitters. The activation/adaptation model of CES proposed in this paper proposes that the activation of vesicles by CES and the subsequent increase in neurotransmitters is responsible for the neurochemical, electrical (EEG and current density) and therapeutic changes seen with CES. The theory further predicts that the activation of vesicles is not restricted to selected subcortical structures such as the thalamus or pituitary gland, but occurs throughout the brain. A consequence is that in response to CES, the activity of neurons and thus the electrical activity of the brain should change throughout the entire brain. The LORETA

results do indeed show changes in some frequencies that do occur in every voxel of grey matter. This finding provides some support for a prediction made by the proposed theory that all of the brain is responding to CES. It is support for the idea that the consequence of the CES current reaching all the areas of the brain equally is that the response of the neurons is not limited to known subcortical generators of EEG, or neurotransmitters, but extends throughout the brain.

Further Implications of the Findings

The effects of CES on relative power qEEG are consistent with the previously published research on the effects of CES on human EEG. The changes in relative power suggest that the primary effect of CES is to increase alpha activity, and thus relaxation, with secondary effects to decrease delta (inattention) and beta (anxiety).

Given the effect of CES to increase alpha and decrease beta, it would appear that CES may be useful in any situation where a person may wish to increase relaxation and reduce stress. The results of the study and the existing literature suggest that anyone experiencing stress may benefit from occasion or routine use of CES to relieve the symptoms of that stress. In this application CES would be a supportive therapy; not be a treatment for stress, but a temporary relief from the symptoms of stress. CES could provide quick support in times of routine, but temporary stress such as life transitions, or exams, or public speaking. For more serious or persistent sources of stress, CES could facilitate change when prescribed by a therapist. In this application the CES would be used to provide sufficient temporary relief from the stress that an individual can work with the therapist and initiate the appropriate changes to their lives.

The observed reduction of beta activity with the increase in alpha is a pattern that would be expected to degrade complex attention; therefore CES should probably not be used during

driving or any important task requiring attention to detail.

It was also found that the 100 Hz CES suppressed a much wider range of beta frequency activity than the 0.5 Hz CES; this difference could not be verified by the current study so any interpretation of it should be done cautiously. Should future studies confirm the finding of a difference due to the frequency of stimulation, the difference may have implications for treatment. Excessive beta frequency activity is associated with anxiety; therefore, the wider range of beta activity that is suppressed by 100 Hz CES suggest that it may be a more effective frequency for the treatment of anxiety than 0.5 Hz. It may be that 100 Hz CES is also a better frequency of CES for any complaints involving excessive beta activity, such as a disturbance in sleep onset due to rumination, irritability, and some forms of alcoholism.

In general both frequencies of CES should be beneficial for alcoholics who have a deficit in their production of alpha, since CES can provide an alternative to alcohol for increasing alpha production. Some alcoholics also have an excess of beta activity, which produces anxiety and irritability. It is in this group that the 100 Hz frequency CES may be a more effective treatment, since it would both increase alpha and decrease a broader range of beta activity. Further research will be required to clarify to what extent CES is beneficial in the treatment of alcoholism; however the existing literature and the relative power results suggest that CES can be a highly effective adjunct to traditional psychosocial treatment because it probably treats some of the physiological aspects of alcoholism. Additionally, it should also be noted that many non-alcoholics periodically abuse alcohol as a method of coping with stress, and that for these alcoholics CES can provides a safe, non-addictive method of quickly reducing feelings of stress.

One of the three FDA indications for CES is for the treatment of depression. Because depression involves an affective state spanning several months to several years, the success of

CES in treating depression suggests a persistent effect from regular CES on brain activity. In terms of EEG, this suggests that a course of treatment with CES may produce lasting changes in EEG associated with recovery from depression. Depression is associated in many individuals with a frontal alpha EEG asymmetry. The alpha power asymmetry associated with depression can be found in resting EEG and is stable over time (Allen, Urry, Hitt & Coan, 2004; Henriques, & Davidson, 1990; Henriques & Davidson 1991). Over 40 studies have found the association between depression and alpha asymmetry (Coan & Allen, 2003) although a more recent study failed to find any association between alpha asymmetry and depression (Vuga et al., 2005). It was not expected that a single exposure to CES in an experimental group would reveal changes in EEG associated with the treatment of depression, however a suggestion of this sort change was found in the 0.5 Hz CES group. For the 0.5 Hz CES group changes were seen in frontal alpha asymmetry involving an increase in left alpha asymmetry in both the linked ears and average reference montages. The same changes were not seen with the 100 Hz CES group. Both frequencies of CES should effectively treat depression, however the observed changes in alpha asymmetry suggest that the 0.5 Hz CES may be more effective in the treatment of depression than the 100 Hz CES. A treatment study comparing 0.5 Hz and 100 Hz CES for the treatment of depression would clarify if 0.5 Hz CES actually is a more effective frequency for treating depression.

The changes observed in relative power with both groups of CES suggest that some forms of attention deficit or oppositional defiant disorders may benefit from the use of CES. The presence of slow wave activity has been associated with attentional problems (Laibow, 1999). The ability of CES to decrease delta relative power activity may benefit attention (and perhaps

motor hyperactivity) while the increase of alpha relative power and decrease of beta relative power may decrease irritability.

Limitations of the Study

One of the primary limitations of the current study is that it did not directly measure changes in subcortical activity. The current study utilized data gathered from scalp EEG to infer subcortical current densities through the LORETA method. The LORETA method estimates subcortical current density from scalp EEG data, even though the EEG data is blind to current density activity. Therefore, estimations of changes were generated, but there was no direct measurement of the changes in subcortical current density from CES. Thus, any conclusions about the changes in subcortical activity found in this study should be considered preliminary until direct measurements have been made using a functional neuroimaging technology such as fMRI or PET.

Another limitation of the study was the lack of information about the effects of CES beyond a single exposure. All conclusions from the current study are limited to the immediate effects of a single session of CES and do not provide any information about the EEG and therapeutic changes that occur over time with a full course of treatment.

A third limitation of the study was the lack of a double blind design. The study was initially designed with a double blind protocol involving the use of a sham CES device. Other studies have used double blind methodologies with CES and demonstrated robust effects, however those studies did not involve the recording of EEG. Due to the noticeable effect of CES on EEG it proved impossible to both blind the researcher and obtain useful (artifact free) EEG data.

Given these limitations, further research is needed which can directly measure both EEG and subcortical activity in a double blind manner, as well as the concomitant changes in therapeutic measures that occur over a course of treatment with CES.

Conclusions

A review of the literature on CES found that the application of a low level current to the head can have profound cognitive, affective and motor effects that are beneficial in the treatment of pain, anxiety, depression, sleep disorders, stress, aggression, substance abuse treatment and movement disorders. Given that CES is the application of a low level current, its effect on the electrical activity of the brain is of particular interest. The current study investigated the effects of CES on the electrical activity of the brain through qEEG and LORETA. Original data has been presented which objectively evaluated the cortical and subcortical effects of CES through EEG. A single session of CES was found to have a significant impact on cortical and subcortical brain activity as measured by the qEEG and LORETA techniques. When used clinically, a single session of CES can be expected to provide increased alpha relative power with concomitant decreased delta and beta relative power. This impact on brain activity from CES is congruent with the cognitive and affective changes reported in the literature. The estimation of subcortical current densities support the supposition that CES has an effect on more than just select subcortical structures projecting to the cortex, but appears to have effects on all the gray matter of the brain. The current density data provides support to the idea that to some degree vesicles are activated throughout the brain and that the increase of neurotransmitters associated with CES may not be a localized phenomena. Both 0.5 Hz CES and 100 Hz CES were found to be substantially similar in their effects on the EEG; although there were differences suggesting

some frequencies of CES may be more effective for some applications. Further research is still needed to identify the central effects of CES on clinical populations when CES is used across a course of treatment.

It is important to understand the changes CES induces within the brain and where those changes occur with the application of CES. A better understanding of these biological effects can contribute to improving our understanding of the clinical effects of CES and the appropriate clinical use of CES. The current study was not designed to evaluate the effectiveness of CES for clinical use, but the literature on CES shows that it holds great promise as a therapy. It is hoped that the findings of this study will be useful in furthering an understanding CES, and that it will also help guide future clinical research regarding who may benefit from CES treatment.

APPENDIX A

SUPPLEMENTARY INFORMATION FOR THE .5 HZ CES LINKED EARS MONTAGE

Table A 1

0.5 Hz Linked Ears FFT Relative Power Group Paired t-Test (p-Value)

	Delta	Theta	Alpha	Beta	High Beta	Beta 1	Beta 2	Beta 3
	1.0 - 3.5 Hz	4.0 - 7.5 Hz	8.0 - 12.0 Hz	12.5 - 25.0 Hz	25.5 - 30.0 Hz	12.0 - 15.0 Hz	15.0 - 17.5 Hz	18.0 - 25.0 Hz
FP1	0.001	0.692	0.003	0.324	0.026	0.839	0.781	0.14
FP2	0	0.95	0.002	0.339	0.142	0.929	0.716	0.137
F3	0	0.898	0.002	0.206	0.003	0.524	0.543	0.082
F4	0	0.99	0.003	0.15	0.025	0.373	0.404	0.049
C3	0	0.854	0.011	0.172	0.009	0.672	0.269	0.06
C4	0	0.704	0.016	0.087	0.037	0.207	0.168	0.039
P3	0.001	0.977	0.043	0.042	0.004	0.086	0.219	0.012
P4	0.004	0.797	0.057	0.031	0.016	0.035	0.209	0.023
O1	0.045	0.563	0.222	0.008	0	0.008	0.351	0.001
O2	0.036	0.95	0.223	0.012	0.003	0.028	0.223	0.009
F7	0	0.464	0.001	0.231	0.026	0.37	0.632	0.18
F8	0.001	0.984	0.002	0.28	0.046	0.878	0.421	0.102
T3	0.004	0.427	0	0.216	0.028	0.813	0.232	0.216
T4	0.033	0.12	0.016	0.106	0.234	0.56	0.104	0.103
T5	0.015	0.561	0.118	0.037	0.002	0.055	0.329	0.008
T6	0.073	0.335	0.192	0.053	0.033	0.237	0.076	0.033
Fz	0	0.697	0.004	0.226	0.007	0.555	0.667	0.051
Cz	0	0.958	0.029	0.148	0.012	0.21	0.269	0.068
Pz	0.001	0.959	0.026	0.031	0.003	0.038	0.252	0.009
AUX1	0.662	0.942	0.307	0.31	0.356	0.398	0.387	0.268
AUX2	0.797	0.238	0.312	0.708	0.363	0.473	0.792	0.539
AUX3	0.777	0.315	0.395	0.559	0.89	0.524	0.312	0.624
AUX4	0.435	0.683	0.986	0.82	0.192	0.657	0.845	0.133

Table A 2

0.5 Hz CES Single Hz FFT Relative Power Group Paired t-Test (p-Value)

	1 Hz	2 Hz	3 Hz	4 Hz	5 Hz
FP1	0	0.005	0.073	0.071	0.49
FP2	0	0.005	0.017	0.022	0.323
F3	0	0.001	0.015	0.007	0.586
F4	0	0.001	0.044	0.004	0.512
C3	0.003	0.001	0.004	0.006	0.996
C4	0.001	0.001	0.014	0.001	0.38
P3	0.004	0.007	0.02	0.038	0.579
P4	0.006	0.015	0.121	0.019	0.707
O1	0.006	0.124	0.429	0.589	0.921
O2	0.01	0.095	0.186	0.288	0.984
F7	0	0.002	0.1	0.107	0.859
F8	0.001	0.047	0.014	0.026	0.339
T3	0.005	0.008	0.133	0.272	0.46
T4	0.069	0.074	0.211	0.489	0.518
T5	0.008	0.043	0.239	0.137	0.675
T6	0.052	0.106	0.247	0.111	0.51
Fz	0	0.001	0.018	0.002	0.4
Cz	0.002	0	0.008	0.004	0.691
Pz	0.002	0.004	0.028	0.018	0.525
AUX1	0.764	0.534	0.85	0.006	0.888
AUX2	0.833	0.926	0.529	0.47	0.5
AUX3	0.439	0.901	0.72	0.355	0.321
AUX4	0.364	0.449	0.491	0.212	0.723

Table A 3

0.5 Hz CES Single Hz FFT Relative Power Group Paired t-Test (p-Value)

	6 Hz	7 Hz	8 Hz	9 Hz	10 Hz
FP1	0.515	0.072	0.002	0.012	0.242
FP2	0.663	0.12	0.001	0.021	0.18
F3	0.997	0.123	0.002	0.006	0.391
F4	0.732	0.131	0.002	0.018	0.276
C3	0.687	0.139	0.007	0.011	0.805
C4	0.923	0.269	0.004	0.011	0.517
P3	0.676	0.264	0.031	0.04	0.243
P4	0.452	0.237	0.009	0.03	0.303
O1	0.494	0.265	0.173	0.178	0.475
O2	0.826	0.584	0.092	0.193	0.591
F7	0.443	0.082	0.003	0.008	0.093
F8	0.634	0.155	0.005	0.035	0.084
T3	0.23	0.039	0.003	0.005	0.299
T4	0.11	0.084	0.004	0.136	0.179
T5	0.494	0.082	0.022	0.11	0.722
T6	0.243	0.11	0.023	0.214	0.377
Fz	0.87	0.176	0.003	0.01	0.492
Cz	0.724	0.184	0.008	0.012	0.668
Pz	0.614	0.248	0.015	0.015	0.224
AUX1	0.487	0.481	0.177	0.325	0.476
AUX2	0.266	0.097	0.448	0.173	0.203
AUX3	0.366	0.367	0.923	0.523	0.173
AUX4	0.795	0.574	0.708	0.818	0.446

Table A 4

0.5 Hz CES Single Hz FFT Relative Power Group Paired t-Test (p-Value)

	11 Hz	12 Hz	13 Hz	14 Hz	15 Hz
FP1	0.769	0.471	0.804	0.931	0.867
FP2	0.789	0.827	0.768	0.92	0.951
F3	0.401	0.471	0.737	0.518	0.53
F4	0.315	0.337	0.47	0.347	0.426
C3	0.183	0.837	0.969	0.562	0.323
C4	0.354	0.493	0.518	0.193	0.149
P3	0.116	0.234	0.202	0.358	0.36
P4	0.4	0.059	0.185	0.138	0.568
O1	0.218	0.017	0.005	0.31	0.506
O2	0.508	0.054	0.044	0.054	0.206
F7	0.878	0.438	0.306	0.492	0.822
F8	0.966	0.968	0.644	0.954	0.56
T3	0.907	0.294	0.636	0.163	0.392
T4	0.734	0.894	0.997	0.292	0.122
T5	0.058	0.257	0.056	0.151	0.243
T6	0.769	0.306	0.576	0.109	0.171
Fz	0.243	0.312	0.92	0.601	0.55
Cz	0.157	0.191	0.352	0.585	0.308
Pz	0.224	0.071	0.093	0.427	0.466
AUX1	0.548	0.44	0.4	0.397	0.327
AUX2	0.662	0.924	0.675	0.299	0.656
AUX3	0.068	0.342	0.733	0.763	0.455
AUX4	0.315	0.787	0.575	0.589	0.72

Table A 5

0.5 Hz CES Single Hz FFT Relative Power Group Paired t-Test (p-Value)

	16 Hz	17 Hz	18 Hz	19 Hz	20 Hz
FP1	0.619	0.626	0.367	0.07	0.098
FP2	0.556	0.741	0.337	0.139	0.039
F3	0.825	0.406	0.188	0.116	0.053
F4	0.348	0.486	0.115	0.113	0.027
C3	0.861	0.053	0.096	0.02	0.034
C4	0.291	0.183	0.016	0.03	0.039
P3	0.703	0.036	0.122	0.018	0.01
P4	0.336	0.075	0.2	0.082	0.029
O1	0.692	0.078	0.149	0.039	0.006
O2	0.424	0.105	0.469	0.177	0.005
F7	0.707	0.419	0.529	0.062	0.12
F8	0.31	0.468	0.257	0.445	0.227
T3	0.555	0.09	0.439	0.194	0.148
T4	0.112	0.177	0.055	0.224	0.22
T5	0.777	0.194	0.238	0.021	0.008
T6	0.131	0.02	0.302	0.196	0.013
Fz	0.866	0.708	0.162	0.112	0.026
Cz	0.479	0.17	0.053	0.091	0.045
Pz	0.736	0.046	0.076	0.02	0.016
AUX1	0.345	0.568	0.369	0.229	0.33
AUX2	0.451	0.474	0.881	0.608	0.358
AUX3	0.885	0.114	0.458	0.437	0.242
AUX4	0.931	0.869	0.076	0.751	0.372

Table A 6

0.5 Hz CES Single Hz FFT Relative Power Group Paired t-Test (p-Value)

	21 Hz	22 Hz	23 Hz	24 Hz	25 Hz
FP1	0.238	0.185	0.176	0.11	0.052
FP2	0.183	0.189	0.168	0.077	0.166
F3	0.224	0.118	0.146	0.035	0.008
F4	0.139	0.057	0.033	0.086	0.058
C3	0.358	0.098	0.255	0.061	0.052
C4	0.121	0.074	0.133	0.073	0.222
P3	0.03	0.004	0.094	0.051	0.02
P4	0.018	0.025	0.059	0.024	0.087
O1	0.017	0	0.003	0.001	0.001
O2	0.012	0.015	0.01	0.026	0.018
F7	0.519	0.457	0.179	0.026	0.073
F8	0.065	0.07	0.048	0.023	0.048
T3	0.357	0.255	0.36	0.127	0.151
T4	0.198	0.1	0.04	0.082	0.373
T5	0.02	0.002	0.004	0.011	0.008
T6	0.023	0.157	0.017	0.031	0.123
Fz	0.145	0.063	0.071	0.05	0.041
Cz	0.216	0.105	0.168	0.078	0.037
Pz	0.013	0.002	0.051	0.02	0.013
AUX1	0.385	0.212	0.453	0.327	0.559
AUX2	0.323	0.215	0.047	0.006	0.609
AUX3	0.884	0.83	0.408	0.972	0.465
AUX4	0.098	0.149	0.201	0.122	0.849

Table A 7

0.5 Hz CES Single Hz FFT Relative Power Group Paired t-Test (p-Value)

	26 Hz	27 Hz	28 Hz	29 Hz	30 Hz
FP1	0.118	0.021	0.01	0.023	0.088
FP2	0.184	0.182	0.166	0.13	0.118
F3	0.005	0.002	0.001	0.025	0.017
F4	0.045	0.013	0.008	0.082	0.032
C3	0.018	0.004	0.006	0.038	0.037
C4	0.146	0.011	0.008	0.104	0.064
P3	0.005	0.003	0.007	0.018	0.026
P4	0.074	0.011	0.008	0.042	0.015
O1	0	0.002	0.001	0.001	0.002
O2	0.049	0.002	0	0.011	0.002
F7	0.14	0.062	0.007	0.02	0.014
F8	0.071	0.058	0.035	0.059	0.054
T3	0.062	0.011	0.021	0.046	0.051
T4	0.156	0.167	0.229	0.366	0.348
T5	0.002	0.001	0.003	0.011	0.009
T6	0.178	0.017	0.011	0.053	0.039
Fz	0.011	0.003	0.002	0.066	0.04
Cz	0.036	0.012	0.002	0.064	0.027
Pz	0.007	0.002	0.005	0.024	0.013
AUX1	0.528	0.344	0.394	0.266	0.548
AUX2	0.778	0.318	0.624	0.448	0.572
AUX3	0.425	0.692	0.926	0.592	0.85
AUX4	0.149	0.335	0.222	0.206	0.694

Table A 8

0.5 Hz CES Single Hz FFT Relative Power Group Paired t-Test (p-Value)

	31 Hz	32 Hz	33 Hz	34 Hz	35 Hz
FP1	0.038	0.156	0.346	0.356	0.433
FP2	0.016	0.026	0.041	0.028	0.026
F3	0.005	0.019	0.039	0.02	0.024
F4	0.034	0.117	0.143	0.099	0.118
C3	0.02	0.137	0.077	0.019	0.045
C4	0.043	0.227	0.132	0.123	0.151
P3	0.061	0.048	0.034	0.018	0.028
P4	0.027	0.077	0.03	0.074	0.103
O1	0.013	0.003	0.001	0.002	0.001
O2	0.013	0.01	0.004	0.016	0.004
F7	0.006	0.018	0.08	0.025	0.026
F8	0.056	0.077	0.076	0.033	0.085
T3	0.056	0.086	0.065	0.025	0.018
T4	0.313	0.4	0.187	0.199	0.12
T5	0.069	0.104	0.052	0.024	0.021
T6	0.102	0.184	0.077	0.115	0.104
Fz	0.005	0.051	0.175	0.032	0.097
Cz	0.002	0.049	0.052	0.009	0.097
Pz	0.015	0.029	0.018	0.012	0.018
AUX1	0.75	0.649	0.959	0.855	0.36
AUX2	0.323	0.438	0.264	0.215	0.026
AUX3	0.405	0.671	0.749	0.627	0.354
AUX4	0.062	0.431	0.378	0.082	0.337

Table A 9

0.5 Hz CES Single Hz FFT Relative Power Group Paired t-Test (p-Value)

	36 Hz	37 Hz	38 Hz	39 Hz	40 Hz
FP1	0.292	0.245	0.313	0.206	0.148
FP2	0.018	0.03	0.081	0.061	0.075
F3	0.046	0.028	0.081	0.032	0.047
F4	0.147	0.17	0.256	0.311	0.234
C3	0.14	0.08	0.059	0.092	0.128
C4	0.195	0.266	0.181	0.347	0.34
P3	0.082	0.084	0.058	0.086	0.113
P4	0.071	0.19	0.106	0.207	0.205
O1	0.001	0.013	0.003	0.014	0.013
O2	0.008	0.013	0.013	0.045	0.018
F7	0.052	0.024	0.042	0.05	0.045
F8	0.114	0.078	0.14	0.219	0.12
T3	0.281	0.089	0.149	0.05	0.148
T4	0.193	0.204	0.159	0.341	0.312
T5	0.033	0.044	0.022	0.037	0.019
T6	0.139	0.084	0.153	0.232	0.163
Fz	0.032	0.101	0.24	0.108	0.124
Cz	0.068	0.077	0.041	0.057	0.146
Pz	0.026	0.059	0.046	0.105	0.14
AUX1	0.38	0.526	0.331	0.913	0.933
AUX2	0.6	0.492	0.642	0.859	0.718
AUX3	0.304	0.353	0.206	0.662	0.476
AUX4	0.158	0.405	0.395	0.413	0.376

Table A 10

0.5 Hz CES Baseline FFT Relative Power Group Means (%)

	Delta	Theta	Alpha	Beta	High Beta	Beta 1	Beta 2	Beta 3
	1.0 - 3.5 Hz	4.0 - 7.5 Hz	8.0 - 12.0 Hz	12.5 - 25.0 Hz	25.5 - 30.0 Hz	12.0 - 15.0 Hz	15.0 - 17.5 Hz	18.0 - 25.0 Hz
FP1	21.084	21.457	35.45	16.032	3.421	6.035	4.163	7.758
FP2	21.64	21.572	35.112	16.228	3.056	6.02	4.163	7.947
F3	20.034	23.969	36.652	15.405	2.355	5.993	4.158	7.205
F4	19.841	23.736	36.207	15.953	2.506	6.169	4.27	7.492
C3	18.914	21.189	41.199	15.28	2.092	6.302	4.153	6.976
C4	19.003	21.275	40.479	15.72	2.114	6.649	4.259	7.115
P3	15.43	16.387	51.442	14.067	1.624	6.412	3.753	6.282
P4	15.153	16.145	51.979	14.244	1.482	6.775	3.797	6.188
O1	12.035	12.258	58.91	13.54	1.837	6.658	3.174	6.197
O2	12.023	12.367	58.827	13.843	1.689	6.836	3.315	6.285
F7	21.218	21.466	34.156	16.985	3.343	6.387	4.453	8.175
F8	21.436	20.896	33.58	17.694	3.466	6.477	4.584	8.661
T3	19.785	19.479	34.524	19.373	3.616	7.649	5.264	8.897
T4	17.922	17.933	34.32	21.337	4.002	7.865	5.885	10.063
T5	15.415	15.651	48.559	16.268	2.322	7.297	4.27	7.256
T6	15.571	15.36	49.471	15.803	2.101	7.323	4.227	6.826
Fz	20.107	25.043	37.202	14.416	1.973	5.784	3.904	6.623
Cz	19.552	21.936	40.889	14.458	2.006	5.91	3.872	6.692
Pz	15.477	16.455	52.731	12.973	1.44	6.212	3.429	5.672
AUX1	13.814	14.813	22.599	27.502	12.477	8.021	6.412	15.538
AUX2	9.571	13.978	21.411	32.049	11.084	9.036	7.415	18.274
AUX3	9.702	13.162	25.618	31.016	10.571	8.894	7.342	17.469
AUX4	10.107	13.526	26.888	29.052	10.32	8.468	6.683	16.56

Table A 11

0.5 Hz CES Baseline FFT Relative Power Group Standard Deviation (%)

	Delta	Theta	Alpha	Beta	High Beta	Beta 1	Beta 2	Beta 3
	1.0 - 3.5 Hz	4.0 - 7.5 Hz	8.0 - 12.0 Hz	12.5 - 25.0 Hz	25.5 - 30.0 Hz	12.0 - 15.0 Hz	15.0 - 17.5 Hz	18.0 - 25.0 Hz
FP1	7.235	8.295	12.516	6.337	2.085	1.916	2.069	3.839
FP2	7.428	8.036	12.036	6.544	1.816	1.913	1.969	4.17
F3	7.659	8.726	12.327	6.585	1.56	2.167	2.142	3.959
F4	7.97	8.494	11.696	6.784	1.791	2.125	2.139	4.185
C3	7.964	8.358	12.916	6.604	1.622	2.223	2.208	3.706
C4	8.213	8.299	12.373	6.321	1.532	2.349	2.173	3.526
P3	9.236	8.812	17.503	7.162	1.62	2.825	2.171	3.912
P4	9.079	8.781	17.054	7.082	1.231	2.969	2.385	3.604
O1	10.054	8.375	21.106	7.96	2.665	3.185	1.995	4.63
O2	9.125	8.022	19.636	7.643	2.074	3.158	2.145	4.319
F7	7.388	8.827	12.434	6.621	2.04	2.116	2.168	3.851
F8	8.835	7.631	11.81	6.503	2.181	2.219	2.038	3.736
T3	7.44	8.698	10.796	7.995	2.523	2.699	2.505	4.658
T4	7.568	8.879	12.481	10.224	3.631	2.818	3.213	6.809
T5	8.618	8.715	17.236	8.495	2.654	3.21	2.448	4.62
T6	10.913	9.231	18.336	8.538	2.065	3.385	2.765	4.388
Fz	7.968	9.031	12.358	6.526	1.376	2.007	2.113	3.896
Cz	8.217	8.115	13.148	6.209	1.457	2.17	2.036	3.56
Pz	9.417	8.906	17.761	6.246	1.321	2.852	1.954	3.266
AUX1	10.742	4.111	9.545	8.967	15.084	2.497	2.216	5.274
AUX2	2.749	6.542	16.287	8.842	3.558	2.07	2.039	5.497
AUX3	3.727	3.453	16.331	7.901	3.293	2.046	2.001	4.555
AUX4	5.516	4.195	17.547	9.137	4.224	2.389	2.324	5.396

Table A 12

0.5 Hz CES FFT Relative Power Post CES Group Mean (%)

	Delta	Theta	Alpha	Beta	High Beta	Beta 1	Beta 2	Beta 3
	1.0 - 3.5 Hz	4.0 - 7.5 Hz	8.0 - 12.0 Hz	12.5 - 25.0 Hz	25.5 - 30.0 Hz	12.0 - 15.0 Hz	15.0 - 17.5 Hz	18.0 - 25.0 Hz
FP1	17.228	22.255	40.258	15.345	2.667	6.039	4.119	7.092
FP2	17.101	22.363	40.101	15.583	2.844	6.073	4.093	7.305
F3	16.391	24.632	41.082	14.619	1.958	5.855	4.005	6.643
F4	16.22	24.535	40.881	14.859	2.087	5.939	4.013	6.783
C3	15.894	22.042	44.482	14.607	1.824	6.269	3.949	6.483
C4	15.969	21.926	44.205	14.795	1.884	6.401	3.943	6.617
P3	13.263	16.925	54.287	13.187	1.417	6.111	3.565	5.704
P4	13.21	16.802	54.698	13.117	1.313	6.273	3.518	5.595
O1	10.457	13.033	61.302	12.524	1.53	6.13	3.072	5.602
O2	10.469	12.858	61.672	12.589	1.388	6.298	3.104	5.579
F7	17.942	22.163	38.658	16.041	2.863	6.184	4.301	7.577
F8	18.248	21.33	38.396	16.689	2.941	6.463	4.298	7.893
T3	17.146	20.257	38.652	18.246	3.003	7.672	4.847	8.241
T4	16.182	18.995	37.601	19.506	3.698	7.524	5.054	9.252
T5	13.614	16.364	51.303	15.29	1.914	6.995	4.05	6.672
T6	13.432	16.299	52.313	14.664	1.864	6.891	3.839	6.343
Fz	16.323	25.664	41.358	13.786	1.743	5.688	3.804	6.109
Cz	16.325	22.845	44.336	13.702	1.777	5.661	3.645	6.266
Pz	13.149	16.968	55.879	11.986	1.238	5.765	3.231	5.086
AUX1	13.642	15.195	24.168	28.464	9.666	8.165	6.588	16.251
AUX2	9.956	12.507	20.917	32.532	11.7	9.574	7.618	18.104
AUX3	9.941	13.027	24.861	31.029	10.762	8.823	7.248	17.596
AUX4	9.735	13.925	27.285	29.924	9.814	9.236	7.097	16.401

Table A 13

0.5 Hz CES FFT Relative Power Post CES Group Standard Deviation (%)

	Delta	Theta	Alpha	Beta	High Beta	Beta 1	Beta 2	Beta 3
	1.0 - 3.5 Hz	4.0 - 7.5 Hz	8.0 - 12.0 Hz	12.5 - 25.0 Hz	25.5 - 30.0 Hz	12.0 - 15.0 Hz	15.0 - 17.5 Hz	18.0 - 25.0 Hz
FP1	6.352	10.487	12.923	6.817	1.599	2.187	2.064	3.767
FP2	5.767	10.878	12.564	7.078	2.126	2.122	1.972	4.277
F3	5.272	11.515	12.672	6.749	1.336	2.216	2.026	3.734
F4	5.39	11.483	12.374	6.685	1.388	2.162	1.949	3.838
C3	5.921	10.602	13.401	6.614	1.383	2.384	2.038	3.51
C4	6.038	11.437	12.757	6.191	1.341	2.359	1.903	3.433
P3	7.487	10.019	17.389	6.982	1.473	2.66	2.093	3.732
P4	7.2	9.976	16.104	6.426	1.102	2.732	2.055	3.216
O1	7.961	9.877	20.538	7.917	2.253	2.943	2.189	4.54
O2	7.821	9.403	19.343	7.353	1.758	3.091	2.169	4.022
F7	6.239	9.994	12.611	6.594	1.74	2.159	1.949	3.855
F8	7.697	9.262	12.295	6.162	1.928	2.155	1.669	3.698
T3	6.152	9.55	11.293	7.3	2.067	2.663	2.009	4.498
T4	6.231	9.773	12.519	9.09	3.195	2.493	2.177	6.613
T5	7.209	9.866	17.61	8.528	2.303	3.268	2.312	4.824
T6	7.551	10.492	17.632	7.962	1.881	3.142	2.504	4.237
Fz	5.41	12.267	12.842	6.535	1.233	2.165	1.984	3.554
Cz	5.964	11.343	13.386	6.018	1.253	2.113	1.844	3.398
Pz	7.473	10.093	16.715	5.746	1.164	2.458	1.756	2.995
AUX1	10.046	5.17	9.076	7.747	3.617	2.01	1.926	5.016
AUX2	5.72	3.731	16.941	8.149	3.339	2.979	2.13	5.248
AUX3	5.795	4.341	16.9	7.911	3.315	2.021	2.003	4.783
AUX4	6.202	6.31	18.273	10.853	4.103	5.436	3.509	5.854

APPENDIX B

SUPPLEMENTARY INFORMATION FOR THE 100 HZ CES LINKED EARS MONTAGE

Table B 1

100 Hz CES FFT Relative Power Group Paired t-Test (p-Value)

	Delta	Theta	Alpha	Beta	High Beta	Beta 1	Beta 2	Beta 3
	1.0 - 3.5 Hz	4.0 - 7.5 Hz	8.0 - 12.0 Hz	12.5 - 25.0 Hz	25.5 - 30.0 Hz	12.0 - 15.0 Hz	15.0 - 17.5 Hz	18.0 - 25.0 Hz
FP1	0.001	0.771	0	0.121	0.004	0.03	0.999	0.167
FP2	0.001	0.968	0.001	0.228	0.005	0.092	0.753	0.221
F3	0.001	0.399	0.006	0.433	0.094	0.085	0.85	0.801
F4	0.002	0.469	0.019	0.63	0.022	0.192	0.518	0.813
C3	0.026	0.703	0.007	0.262	0.046	0.003	0.802	0.726
C4	0.056	0.776	0.007	0.215	0.004	0.008	0.317	0.319
P3	0.029	0.361	0.004	0	0	0	0.219	0.015
P4	0.006	0.56	0	0	0	0	0.199	0.013
O1	0.024	0.121	0.002	0	0	0.001	0.034	0.009
O2	0.043	0.231	0.001	0	0	0	0.108	0.002
F7	0.011	0.762	0.002	0.163	0.015	0.014	0.668	0.266
F8	0.008	0.541	0.016	0.34	0.016	0.321	0.574	0.111
T3	0.053	0.491	0.001	0.011	0.029	0.001	0.587	0.095
T4	0.194	0.231	0.002	0.135	0.076	0.008	0.866	0.211
T5	0.01	0.388	0.001	0.002	0	0	0.345	0.037
T6	0.061	0.738	0.003	0.001	0.001	0	0.432	0.01
Fz	0.001	0.45	0.008	0.579	0.039	0.136	0.872	0.968
Cz	0.07	0.664	0.01	0.262	0.096	0.014	0.962	0.667
Pz	0.012	0.307	0.001	0.001	0.001	0	0.146	0.011
AUX1	0.008	0.844	0.001	0.825	0.03	0.176	0.381	0.328
AUX2	0.144	0.207	0.77	0.263	0.337	0.045	0.08	0.422
AUX3	0.184	0.16	0.894	0.423	0.208	0.121	0.192	0.457
AUX4	0.228	0.157	0.826	0.4	0.231	0.163	0.151	0.45

Table B 2

100 Hz CES FFT Relative Power Group Paired t-Test (p-Value)

	1 Hz	2 Hz	3 Hz	4 Hz	5 Hz
FP1	0.066	0.001	0.003	0.152	0.323
FP2	0.069	0.001	0.004	0.173	0.374
F3	0.204	0.004	0.002	0.115	0.163
F4	0.223	0.001	0.011	0.08	0.187
C3	0.452	0.027	0.023	0.194	0.1
C4	0.385	0.019	0.19	0.258	0.35
P3	0.131	0.022	0.067	0.085	0.11
P4	0.149	0.002	0.065	0.108	0.049
O1	0.042	0.025	0.059	0.086	0.092
O2	0.09	0.035	0.163	0.116	0.136
F7	0.141	0.057	0.005	0.254	0.351
F8	0.072	0.006	0.041	0.664	0.586
T3	0.545	0.166	0.038	0.688	0.66
T4	0.417	0.07	0.421	0.91	0.929
T5	0.056	0.018	0.023	0.063	0.117
T6	0.211	0.023	0.152	0.173	0.572
Fz	0.188	0.001	0.003	0.065	0.088
Cz	0.601	0.04	0.037	0.103	0.079
Pz	0.127	0.01	0.031	0.039	0.023
AUX1	0.018	0.023	0.158	0.412	0.199
AUX2	0.176	0.128	0.127	0.231	0.32
AUX3	0.238	0.167	0.147	0.225	0.154
AUX4	0.233	0.207	0.238	0.253	0.195

Table B 3

100 Hz CES FFT Relative Power Group Paired t-Test (p-Value)

	6 Hz	7 Hz	8 Hz	9 Hz	10 Hz
FP1	0.28	0.888	0.004	0.013	0.252
FP2	0.156	0.824	0.006	0.02	0.283
F3	0.565	0.659	0.042	0.03	0.438
F4	0.346	0.707	0.066	0.039	0.643
C3	0.5	0.401	0.027	0.019	0.416
C4	0.181	0.285	0.017	0.012	0.192
P3	0.407	0.312	0.042	0.01	0.462
P4	0.632	0.267	0.121	0.025	0.114
O1	0.106	0.932	0.213	0.059	0.128
O2	0.176	0.979	0.899	0.351	0.01
F7	0.491	0.685	0.003	0.019	0.315
F8	0.216	0.143	0.003	0.03	0.41
T3	0.251	0.174	0.003	0.003	0.275
T4	0.405	0.013	0.001	0.002	0.281
T5	0.434	0.431	0.078	0.067	0.11
T6	0.77	0.034	0.152	0.205	0.256
Fz	0.265	0.724	0.05	0.02	0.629
Cz	0.353	0.367	0.017	0.017	0.374
Pz	0.366	0.356	0.038	0.006	0.146
AUX1	0.54	0.143	0.019	0.01	0.179
AUX2	0.253	0.181	0.582	0.891	0.704
AUX3	0.234	0.189	0.311	0.573	0.957
AUX4	0.246	0.084	0.232	0.485	0.957

Table B 4

100 Hz CES FFT Relative Power Group Paired t-Test (p-Value)

	11 Hz	12 Hz	13 Hz	14 Hz	15 Hz
FP1	0.704	0.016	0.006	0.983	0.788
FP2	0.613	0.008	0.025	0.877	0.743
F3	0.783	0.014	0.073	0.942	0.306
F4	0.894	0.008	0.124	0.617	0.77
C3	0.709	0.006	0.015	0.122	0.532
C4	0.136	0.003	0.019	0.559	0.621
P3	0.994	0.012	0	0.001	0.038
P4	0.461	0.007	0	0.001	0.082
O1	0.854	0.005	0.002	0.003	0.01
O2	0.697	0.009	0	0.004	0.053
F7	0.852	0.004	0.013	0.61	0.372
F8	0.724	0.028	0.07	0.741	0.204
T3	0.877	0.001	0.038	0.022	0.066
T4	0.249	0.005	0.012	0.155	0.788
T5	0.582	0.002	0	0.001	0.05
T6	0.706	0.001	0	0.001	0.5
Fz	0.889	0.013	0.098	0.589	0.558
Cz	0.165	0.002	0.025	0.558	0.648
Pz	0.587	0.015	0	0.001	0.077
AUX1	0.503	0.08	0.242	0.83	0.85
AUX2	0.418	0.213	0.038	0.081	0.076
AUX3	0.222	0.152	0.176	0.114	0.155
AUX4	0.259	0.184	0.132	0.269	0.147

Table B 5

100 Hz CES FFT Relative Power Group Paired t-Test (p-Value)

	16 Hz	17 Hz	18 Hz	19 Hz	20 Hz
FP1	0.906	0.929	0.113	0.617	0.225
FP2	0.569	0.866	0.103	0.327	0.394
F3	0.925	0.584	0.078	0.857	0.497
F4	0.555	0.514	0.045	0.937	0.555
C3	0.639	0.288	0.161	0.265	0.485
C4	0.629	0.147	0.41	0.895	0.965
P3	0.606	0.665	0.295	0.266	0.121
P4	0.497	0.564	0.061	0.168	0.385
O1	0.247	0.095	0.027	0.008	0.038
O2	0.599	0.069	0.004	0.003	0.046
F7	0.558	0.622	0.349	0.667	0.279
F8	0.563	0.577	0.277	0.092	0.102
T3	0.79	0.577	0.86	0.434	0.142
T4	0.648	0.901	0.715	0.077	0.695
T5	0.97	0.642	0.714	0.077	0.208
T6	0.723	0.259	0.028	0.052	0.192
Fz	0.671	0.594	0.025	0.694	0.614
Cz	0.956	0.521	0.136	0.555	0.392
Pz	0.36	0.417	0.137	0.2	0.129
AUX1	0.174	0.319	0.127	0.371	0.073
AUX2	0.084	0.098	0.164	0.291	0.389
AUX3	0.227	0.208	0.283	0.215	0.548
AUX4	0.19	0.134	0.209	0.235	0.486

Table B 6

100 Hz CES FFT Relative Power Group Paired t-Test (p-Value)

	21 Hz	22 Hz	23 Hz	24 Hz	25 Hz
FP1	0.041	0.001	0.276	0.158	0.084
FP2	0.064	0.022	0.357	0.097	0.17
F3	0.62	0.054	0.173	0.085	0.525
F4	0.125	0.179	0.621	0.288	0.355
C3	0.501	0.224	0.02	0.024	0.118
C4	0.122	0.057	0.02	0.043	0
P3	0.025	0.171	0.003	0	0.002
P4	0.046	0.03	0.003	0.001	0
O1	0.041	0.176	0.094	0	0
O2	0.043	0.086	0.01	0	0
F7	0.307	0.003	0.073	0.022	0.196
F8	0.025	0.059	0.12	0.223	0.157
T3	0.279	0.005	0.013	0.046	0.136
T4	0.448	0.135	0.563	0.506	0.089
T5	0.052	0.065	0.01	0	0
T6	0.066	0.035	0.008	0.002	0.002
Fz	0.309	0.177	0.56	0.153	0.455
Cz	0.078	0.282	0.293	0.462	0.177
Pz	0.012	0.086	0.025	0.001	0
AUX1	0.124	0.43	0.894	0.573	0.898
AUX2	0.742	0.471	0.219	0.2	0.364
AUX3	0.721	0.485	0.231	0.294	0.214
AUX4	0.707	0.476	0.353	0.234	0.216

Table B 7

100 Hz CES FFT Relative Power Group Paired t-Test (p-Value)

	26 Hz	27 Hz	28 Hz	29 Hz	30 Hz
FP1	0.042	0.015	0.018	0.007	0
FP2	0.042	0.005	0.025	0.003	0.007
F3	0.357	0.14	0.155	0.121	0.009
F4	0.137	0.058	0.054	0.013	0.009
C3	0.106	0.071	0.2	0.043	0.012
C4	0.023	0.047	0.027	0.009	0.008
P3	0.003	0	0.004	0.001	0
P4	0.001	0.009	0.002	0	0.001
O1	0	0	0	0	0
O2	0	0	0	0	0.002
F7	0.039	0.062	0.029	0.012	0.001
F8	0.023	0.031	0.044	0.006	0.024
T3	0.033	0.02	0.1	0.033	0.019
T4	0.087	0.306	0.117	0.071	0.061
T5	0	0	0	0	0
T6	0.001	0.037	0.017	0	0.001
Fz	0.311	0.092	0.149	0.019	0.009
Cz	0.694	0.356	0.175	0.038	0.015
Pz	0.005	0.005	0.004	0	0
AUX1	0.02	0.024	0.338	0.019	0.033
AUX2	0.382	0.348	0.298	0.292	0.24
AUX3	0.249	0.214	0.146	0.175	0.266
AUX4	0.228	0.283	0.212	0.184	0.275

Table B 8

100 Hz CES FFT Relative Power Group Paired t-Test (p-Value)

	31 Hz	32 Hz	33 Hz	34 Hz	35 Hz
FP1	0.008	0.001	0	0.001	0
FP2	0.003	0.001	0.002	0.002	0
F3	0.007	0.02	0.024	0.033	0.014
F4	0.002	0.012	0.009	0.002	0.001
C3	0.01	0	0.017	0.008	0.002
C4	0.001	0.008	0.005	0.001	0.005
P3	0	0	0.006	0	0.002
P4	0	0	0	0	0.001
O1	0	0	0.001	0	0
O2	0	0	0	0	0
F7	0.068	0.048	0.127	0.274	0.188
F8	0.006	0.014	0.011	0.038	0.004
T3	0.002	0.019	0.147	0.086	0.147
T4	0.029	0.065	0.09	0.062	0.262
T5	0	0.001	0.008	0.002	0.001
T6	0	0	0.001	0	0.001
Fz	0.004	0.014	0.015	0.006	0.002
Cz	0.005	0.008	0.011	0.004	0.005
Pz	0	0	0	0	0
AUX1	0.003	0.043	0.017	0.115	0.064
AUX2	0.19	0.234	0.24	0.247	0.221
AUX3	0.206	0.21	0.241	0.251	0.192
AUX4	0.21	0.167	0.191	0.157	0.183

Table B 9

100 Hz CES FFT Relative Power Group Paired t-Test (p-Value)

	36 Hz	37 Hz	38 Hz	39 Hz	40 Hz
FP1	0	0	0	0	0
FP2	0.01	0.001	0.001	0	0
F3	0.025	0.022	0.003	0.003	0
F4	0.006	0.005	0	0	0
C3	0.021	0.03	0	0.003	0
C4	0.001	0.003	0	0.002	0
P3	0.002	0.001	0	0.003	0
P4	0	0	0.001	0.001	0
O1	0	0	0	0	0
O2	0	0	0	0	0
F7	0.206	0.09	0.046	0.015	0.021
F8	0.006	0.006	0.01	0	0.002
T3	0.222	0.176	0.095	0.164	0.047
T4	0.124	0.126	0.189	0.113	0.046
T5	0.003	0	0.002	0.004	0
T6	0	0	0.002	0.004	0.001
Fz	0.005	0.01	0.001	0	0
Cz	0.002	0.001	0	0	0
Pz	0	0	0	0	0
AUX1	0.048	0.016	0.006	0.002	0.006
AUX2	0.195	0.095	0.119	0.152	0.122
AUX3	0.233	0.256	0.244	0.302	0.148
AUX4	0.303	0.216	0.161	0.126	0.15

Table B 10

100 Hz CES Baseline Means FFT Relative Power (%)

	Delta	Theta	Alpha	Beta	High Beta	Beta 1	Beta 2	Beta 3
	1.0 - 3.5 Hz	4.0 - 7.5 Hz	8.0 - 12.0 Hz	12.5 - 25.0 Hz	25.5 - 30.0 Hz	12.0 - 15.0 Hz	15.0 - 17.5 Hz	18.0 - 25.0 Hz
FP1	17.716	17.032	38.819	19.997	3.359	9.445	5.257	8.559
FP2	18.369	17.131	38.622	19.816	3.22	9.543	5.214	8.326
F3	17.387	19.033	39.17	19.952	2.484	9.251	5.543	8.402
F4	17.452	18.855	38.962	20.186	2.583	9.481	5.583	8.385
C3	17.481	17.408	40.177	20.567	2.493	9.305	5.603	8.928
C4	17.095	16.769	40.465	21.222	2.616	9.911	5.734	8.894
P3	14.333	13.743	47.194	21.657	1.83	11.609	5.367	8.82
P4	13.846	13.291	48.673	21.117	1.846	11.567	5.316	8.378
O1	10.986	10.466	56.034	20.328	1.305	13.228	4.323	7.713
O2	10.191	10.255	57.759	19.606	1.306	12.762	4.231	7.508
F7	17.707	17.307	37.695	20.83	3.408	9.17	5.548	9.246
F8	18.682	16.644	36.575	21.563	3.444	9.629	5.732	9.361
T3	17.632	16.142	34.384	24.711	3.598	10.942	6.46	10.812
T4	16.798	15.356	35.39	24.465	4.183	10.505	6.57	10.622
T5	13.857	12.401	47.517	23.01	1.832	12.564	5.556	9.357
T6	13.211	12.459	49.877	21.369	1.808	12.095	5.339	8.297
Fz	17.464	19.834	39.431	19.333	2.245	9.373	5.391	7.848
Cz	17.952	18.084	40.403	19.458	2.488	9.123	5.249	8.252
Pz	15.004	14.258	47.337	20.292	1.863	10.48	5.406	8.177
AUX1	24.833	18.503	28.897	18.838	4.599	8.618	4.668	8.376
AUX2	6.916	12.178	27.768	30.79	10.627	8.133	7.956	17.085
AUX3	6.499	12.617	28.655	29.957	11.016	8.253	7.095	16.979
AUX4	6.333	12.408	29.387	29.823	10.709	8.098	7.179	16.937

Table B 11

100 Hz CES Baseline Standard Deviations FFT Relative Power (%)

	Delta	Theta	Alpha	Beta	High Beta	Beta 1	Beta 2	Beta 3
	1.0 - 3.5 Hz	4.0 - 7.5 Hz	8.0 - 12.0 Hz	12.5 - 25.0 Hz	25.5 - 30.0 Hz	12.0 - 15.0 Hz	15.0 - 17.5 Hz	18.0 - 25.0 Hz
FP1	5.731	5.852	13.891	8.015	2.779	6.328	2.397	3.844
FP2	5.942	5.821	12.994	7.928	2.499	6.412	2.35	3.441
F3	5.443	5.558	13.374	7.399	1.973	5.859	2.382	3.379
F4	5.22	5.847	13.24	8.206	2.017	6.221	2.798	3.482
C3	5.34	4.713	13.688	7.469	2.072	5.044	2.768	3.809
C4	5.61	5.275	14.637	9.35	2.025	5.9	3.827	4.018
P3	5.085	4.433	13.955	10.544	1.204	10.349	3.465	4.892
P4	5.217	4.985	15.055	10.989	1.268	9.814	4.43	4.862
O1	5.218	4.363	14.687	12.641	0.762	14.864	2.933	5.446
O2	4.961	4.897	15.677	12.195	0.81	13.823	3.248	5.453
F7	5.333	5.6	13.348	7.16	2.652	5.051	1.955	3.457
F8	5.859	5.617	13.112	8.123	2.836	5.614	2.409	3.712
T3	4.492	5.077	12.554	7.921	2.777	4.015	2.333	6.206
T4	5.578	5.958	14.298	10.088	4.177	4.949	3.183	5.321
T5	5.255	3.96	13.188	11.735	0.985	11.461	3.443	5.979
T6	4.73	4.943	13.424	10.932	1.119	9.933	4.062	4.944
Fz	5.428	6.28	13.392	7.885	1.817	6.259	2.553	3.456
Cz	5.813	5.206	13.827	7.743	1.948	5.903	2.738	3.752
Pz	5.585	4.555	14.773	9.921	1.361	8.233	3.89	4.691
AUX1	7.086	4.114	9.613	5.062	2.814	4.38	1.451	2.702
AUX2	3.934	2.272	30.3	16.264	5.671	4.12	5.84	8.909
AUX3	3.297	2.098	30.139	15.508	5.804	4.209	3.717	8.865
AUX4	3.31	2.433	29.943	15.529	5.848	4.103	3.774	9.027

Table B 12

100 Hz Post CES Group Means FFT Relative Power (%)

	Delta	Theta	Alpha	Beta	High Beta	Beta 1	Beta 2	Beta 3
	1.0 - 3.5 Hz	4.0 - 7.5 Hz	8.0 - 12.0 Hz	12.5 - 25.0 Hz	25.5 - 30.0 Hz	12.0 - 15.0 Hz	15.0 - 17.5 Hz	18.0 - 25.0 Hz
FP1	15.643	16.913	43.47	19.089	2.717	8.594	5.292	8.226
FP2	15.905	17.264	43.245	19.135	2.495	8.851	5.36	8.035
F3	15.472	18.643	42.841	19.676	2.04	8.502	5.662	8.401
F4	15.523	18.611	42.341	20.124	2.07	8.879	5.849	8.431
C3	16.295	17.266	43.019	20.157	2.015	8.263	5.706	9.009
C4	15.744	16.916	43.558	20.53	2.041	8.832	5.889	8.782
P3	13.214	13.644	51.871	19.081	1.378	9.85	4.981	8.12
P4	12.676	13.231	53.171	18.692	1.428	9.776	4.952	7.768
O1	9.696	9.875	61.968	16.839	0.994	10.536	3.902	6.833
O2	9.184	9.887	63.064	16.292	0.979	10.301	3.964	6.426
F7	16.205	17.042	41.845	19.984	2.725	8.363	5.545	8.936
F8	16.339	17.018	40.899	20.872	2.733	9.251	6.007	8.806
T3	16.863	16.56	38.067	22.77	3.052	9.58	6.249	9.901
T4	15.634	15.907	39.186	23.091	3.335	9.512	6.438	10.133
T5	12.238	12.243	52.883	20.189	1.385	10.198	5.26	8.731
T6	11.898	13.071	53.884	18.823	1.437	9.816	5.139	7.622
Fz	15.272	19.586	42.989	19.187	1.819	8.72	5.541	7.907
Cz	16.789	17.984	43.292	18.731	2.109	8.004	5.236	8.207
Pz	13.544	14.073	52.218	17.987	1.401	9.145	4.957	7.467
AUX1	21.869	18.755	32.627	19.09	4.052	8.112	4.867	8.738
AUX2	5.957	11.3	31.855	29.433	10.936	6.973	6.046	18.506
AUX3	5.824	11.573	32.015	30.403	9.888	7.457	6.431	18.681
AUX4	5.917	11.447	32.498	30.1	9.884	7.509	6.282	18.505

Table B 13

100 Hz Post CES Standard Deviations FFT Relative Power (%)

	Delta	Theta	Alpha	Beta	High Beta	Beta 1	Beta 2	Beta 3
	1.0 - 3.5 Hz	4.0 - 7.5 Hz	8.0 - 12.0 Hz	12.5 - 25.0 Hz	25.5 - 30.0 Hz	12.0 - 15.0 Hz	15.0 - 17.5 Hz	18.0 - 25.0 Hz
FP1	5.758	6.254	14.316	7.54	2.04	5.303	2.41	3.79
FP2	5.37	6.59	13.867	7.559	1.509	5.493	2.451	3.53
F3	5.267	6.463	14.072	7.886	1.233	4.782	2.753	3.634
F4	4.807	6.843	13.93	8.49	1.242	5.109	3.028	3.756
C3	5.856	5.382	13.45	8.11	1.202	4.056	2.644	4.376
C4	5.045	5.576	14.047	8.971	1.188	4.777	3.169	4.283
P3	6.285	5.787	14.211	8.586	0.767	8.615	2.849	4.79
P4	5.668	5.959	14.962	9.387	0.877	8.079	3.506	4.891
O1	5.601	4.702	13.957	9.31	0.633	11.358	2.437	5.029
O2	5.019	5.194	13.886	9.066	0.552	10.184	2.717	4.451
F7	5.187	5.555	13.183	7.339	1.72	4.267	2.243	3.832
F8	5.149	6.09	13.059	7.736	1.643	4.998	2.816	3.497
T3	4.912	5.596	11.689	7.819	2.379	3.795	2.103	5.066
T4	4.482	5.733	13.171	8.83	2.689	4.189	2.726	5.066
T5	5.146	4.978	13.413	10.065	0.691	9.02	2.908	6.235
T6	4.363	6.195	14.032	9.973	0.834	7.371	3.605	5.115
Fz	5.155	7.503	14.194	8.094	1.099	5.154	2.784	3.58
Cz	6.206	6.076	14.126	7.325	1.391	4.494	2.278	3.75
Pz	6.265	6.149	14.688	8.217	0.877	7.295	2.923	4.408
AUX1	6.495	4.808	11.271	5.343	2.427	3.716	1.541	3.12
AUX2	3.594	3.595	33.993	19.978	7.357	4.219	3.852	16.819
AUX3	3.439	3.623	34.167	20.319	6.284	4.495	4.016	16.825
AUX4	3.582	3.881	33.963	20.28	6.46	4.543	3.927	16.85

APPENDIX C
COMMON AVERAGE REFERENCE MONTAGE

FFT Relative Power Group Paired t-Test (P-Value)

Intrahemispheric: LEFT

	DELTA	THETA	ALPHA	BETA	HIGH BETA	BETA 1	BETA 2	BETA 3
FP1 - AVE	0.025	0.828	0.050	0.462	0.045	0.298	0.695	0.365
F3 - AVE	0.012	0.481	0.006	0.048	0.001	0.109	0.184	0.044
C3 - AVE	0.009	0.631	0.084	0.345	0.047	0.335	0.338	0.181
P3 - AVE	0.012	0.940	0.144	0.050	0.007	0.097	0.373	0.013
O1 - AVE	0.096	0.658	0.543	0.015	0.003	0.005	0.457	0.001
F7 - AVE	0.031	0.944	0.012	0.119	0.016	0.038	0.457	0.143
T3 - AVE	0.013	0.177	0.013	0.273	0.027	0.915	0.605	0.121
T5 - AVE	0.026	0.216	0.172	0.039	0.002	0.044	0.396	0.004

Intrahemispheric: RIGHT

	DELTA	THETA	ALPHA	BETA	HIGH BETA	BETA 1	BETA 2	BETA 3
FP2 - AVE	0.003	0.616	0.036	0.257	0.099	0.438	0.620	0.185
F4 - AVE	0.009	0.674	0.008	0.082	0.018	0.065	0.343	0.055
C4 - AVE	0.006	0.574	0.037	0.062	0.047	0.100	0.104	0.062
P4 - AVE	0.230	0.949	0.204	0.046	0.023	0.025	0.357	0.077
O2 - AVE	0.053	0.763	0.368	0.038	0.002	0.040	0.496	0.017
F8 - AVE	0.014	0.663	0.060	0.304	0.051	0.490	0.639	0.166
T4 - AVE	0.008	0.247	0.016	0.230	0.345	0.527	0.246	0.278
T6 - AVE	0.227	0.370	0.261	0.049	0.010	0.324	0.084	0.013

Intrahemispheric: CENTER

	DELTA	THETA	ALPHA	BETA	HIGH BETA	BETA 1	BETA 2	BETA 3
Fz - AVE	0.004	0.259	0.017	0.069	0.001	0.081	0.527	0.039
Cz - AVE	0.002	0.718	0.137	0.151	0.013	0.062	0.157	0.151
Pz - AVE	0.004	0.318	0.034	0.028	0.021	0.012	0.300	0.018

Figure C 1. Relative power paired *t*-test table for the 0.5 Hz average reference montage. Statistically significant (.05 or better) decreases in activation after 0.5 Hz CES are indicated in blue. Statistically significant increases in activation are indicated in red.

Table C 1

0.5 Hz CES Av. Ref. FFT Relative Power Group Paired t-Test (p-Value)

	Delta	Theta	Alpha	Beta	High Beta	Beta 1	Beta 2	Beta 3
	1.0 - 3.5 Hz	4.0 - 7.5 Hz	8.0 - 12.0 Hz	12.5 - 25.0 Hz	25.5 - 30.0 Hz	12.0 - 15.0 Hz	15.0 - 17.5 Hz	18.0 - 25.0 Hz
FP1	0.025	0.828	0.05	0.462	0.045	0.298	0.695	0.365
FP2	0.003	0.616	0.036	0.257	0.099	0.438	0.62	0.185
F3	0.012	0.481	0.006	0.048	0.001	0.109	0.184	0.044
F4	0.009	0.674	0.008	0.082	0.018	0.065	0.343	0.055
C3	0.009	0.631	0.084	0.345	0.047	0.335	0.338	0.181
C4	0.006	0.574	0.037	0.062	0.047	0.1	0.104	0.062
P3	0.012	0.94	0.144	0.05	0.007	0.097	0.373	0.013
P4	0.23	0.949	0.204	0.046	0.023	0.025	0.357	0.077
O1	0.096	0.658	0.543	0.015	0.003	0.005	0.457	0.001
O2	0.053	0.763	0.368	0.038	0.002	0.04	0.496	0.017
F7	0.031	0.944	0.012	0.119	0.016	0.038	0.457	0.143
F8	0.014	0.663	0.06	0.304	0.051	0.49	0.639	0.166
T3	0.013	0.177	0.013	0.273	0.027	0.915	0.605	0.121
T4	0.008	0.247	0.016	0.23	0.345	0.527	0.246	0.278
T5	0.026	0.216	0.172	0.039	0.002	0.044	0.396	0.004
T6	0.227	0.37	0.261	0.049	0.01	0.324	0.084	0.013
Fz	0.004	0.259	0.017	0.069	0.001	0.081	0.527	0.039
Cz	0.002	0.718	0.137	0.151	0.013	0.062	0.157	0.151
Pz	0.004	0.318	0.034	0.028	0.021	0.012	0.3	0.018

Table C 2

0.5 Hz CES Av. Ref. FFT Relative Power Group Paired t-Test (p-Value)

	1 Hz	2 Hz	3 Hz	4 Hz	5 Hz
FP1	0.013	0.072	0.259	0.022	0.532
FP2	0.002	0.032	0.051	0.003	0.506
F3	0.012	0.042	0.088	0.017	0.35
F4	0.002	0.058	0.066	0.015	0.431
C3	0.093	0.04	0.002	0.196	0.918
C4	0.031	0.028	0.007	0.002	0.341
P3	0.007	0.063	0.046	0.218	0.479
P4	0.057	0.608	0.432	0.165	0.472
O1	0.005	0.186	0.597	0.337	0.957
O2	0.007	0.119	0.187	0.28	0.7
F7	0.028	0.148	0.128	0.238	0.969
F8	0.018	0.142	0.016	0.075	0.269
T3	0.029	0.031	0.081	0.351	0.635
T4	0.023	0.036	0.027	0.626	0.679
T5	0.013	0.06	0.182	0.073	0.813
T6	0.14	0.372	0.21	0.282	0.929
Fz	0.002	0.024	0.047	0.004	0.304
Cz	0.037	0.004	0.004	0.006	0.626
Pz	0.003	0.03	0.053	0.07	0.167

Table C 3

0.5 Hz CES Av. Ref. FFT Relative Power Group Paired t-Test (p-Value)

	6 Hz	7 Hz	8 Hz	9 Hz	10 Hz
FP1	0.922	0.244	0.021	0.052	0.199
FP2	0.581	0.252	0.026	0.085	0.171
F3	0.218	0.139	0.017	0.022	0.219
F4	0.644	0.203	0.056	0.083	0.096
C3	0.85	0.144	0.15	0.091	0.79
C4	0.563	0.446	0.013	0.045	0.645
P3	0.871	0.289	0.166	0.133	0.411
P4	0.925	0.511	0.216	0.076	0.418
O1	0.805	0.235	0.197	0.277	0.788
O2	0.424	0.707	0.211	0.204	0.812
F7	0.874	0.492	0.008	0.06	0.109
F8	0.488	0.584	0.102	0.075	0.188
T3	0.08	0.024	0.001	0.026	0.299
T4	0.216	0.118	0.005	0.019	0.312
T5	0.341	0.016	0.007	0.111	0.367
T6	0.407	0.051	0.042	0.133	0.965
Fz	0.157	0.404	0.062	0.046	0.499
Cz	0.903	0.315	0.042	0.085	0.707
Pz	0.296	0.806	0.169	0.034	0.116

Table C 4

0.5 Hz CES Av. Ref. FFT Relative Power Group Paired t-Test (p-Value)

	11 Hz	12 Hz	13 Hz	14 Hz	15 Hz
FP1	0.674	0.133	0.294	0.834	0.934
FP2	0.609	0.349	0.963	0.364	0.763
F3	0.767	0.115	0.117	0.248	0.351
F4	0.381	0.048	0.127	0.054	0.225
C3	0.867	0.123	0.741	0.99	0.618
C4	0.868	0.624	0.243	0.015	0.025
P3	0.158	0.134	0.144	0.454	0.627
P4	0.712	0.049	0.045	0.09	0.813
O1	0.126	0.002	0.006	0.394	0.514
O2	0.472	0.063	0.023	0.323	0.275
F7	0.983	0.185	0.003	0.328	0.497
F8	0.577	0.655	0.575	0.241	0.781
T3	0.812	0.979	0.826	0.814	0.952
T4	0.934	0.817	0.334	0.636	0.224
T5	0.028	0.007	0.086	0.332	0.36
T6	0.41	0.627	0.269	0.243	0.24
Fz	0.346	0.035	0.173	0.269	0.449
Cz	0.22	0.195	0.017	0.654	0.198
Pz	0.439	0.014	0.008	0.554	0.867

Table C 5

0.5 Hz CES Av. Ref. FFT Relative Power Group Paired t-Test (p-Value)

	16 Hz	17 Hz	18 Hz	19 Hz	20 Hz
FP1	0.69	0.424	0.739	0.236	0.327
FP2	0.497	0.625	0.746	0.234	0.065
F3	0.242	0.11	0.21	0.087	0.13
F4	0.281	0.657	0.192	0.103	0.032
C3	0.664	0.116	0.303	0.035	0.211
C4	0.37	0.161	0.016	0.001	0.126
P3	0.588	0.172	0.059	0.006	0.009
P4	0.541	0.072	0.41	0.186	0.057
O1	0.677	0.264	0.136	0.018	0.003
O2	0.704	0.457	0.572	0.375	0.02
F7	0.533	0.39	0.886	0.132	0.319
F8	0.755	0.404	0.579	0.665	0.151
T3	0.867	0.309	0.304	0.197	0.139
T4	0.469	0.114	0.341	0.337	0.183
T5	0.611	0.385	0.137	0.005	0.005
T6	0.12	0.023	0.081	0.073	0.025
Fz	0.519	0.82	0.344	0.111	0.042
Cz	0.336	0.1	0.134	0.119	0.073
Pz	0.705	0.033	0.107	0.03	0.028

Table C 6

0.5 Hz CES Av. Ref. FFT Relative Power Group Paired t-Test (p-Value)

	21 Hz	22 Hz	23 Hz	24 Hz	25 Hz
FP1	0.275	0.442	0.539	0.509	0.085
FP2	0.094	0.197	0.466	0.169	0.095
F3	0.028	0.093	0.079	0.018	0.002
F4	0.043	0.054	0.086	0.073	0.021
C3	0.609	0.606	0.602	0.133	0.04
C4	0.324	0.196	0.278	0.075	0.397
P3	0.061	0.049	0.411	0.132	0.024
P4	0.073	0.161	0.122	0.017	0.152
O1	0.001	0.001	0.001	0.034	0.021
O2	0	0.011	0.012	0.046	0.02
F7	0.124	0.245	0.235	0.039	0.02
F8	0.094	0.061	0.256	0.061	0.024
T3	0.128	0.098	0.199	0.123	0.103
T4	0.573	0.395	0.352	0.311	0.169
T5	0.005	0.004	0.004	0.015	0.012
T6	0.012	0.115	0.006	0.029	0.056
Fz	0.016	0.031	0.149	0.057	0.015
Cz	0.216	0.378	0.541	0.274	0.045
Pz	0.073	0.005	0.057	0.011	0.025

Table C 7

0.5 Hz CES Av. Ref. FFT Relative Power Group Paired t-Test (p-Value)

	26 Hz	27 Hz	28 Hz	29 Hz	30 Hz
FP1	0.141	0.037	0.028	0.025	0.138
FP2	0.138	0.171	0.156	0.055	0.084
F3	0.001	0.001	0.001	0.002	0.004
F4	0.02	0.026	0.012	0.02	0.028
C3	0.095	0.014	0.016	0.134	0.039
C4	0.133	0.038	0.005	0.07	0.048
P3	0.008	0.026	0.009	0.033	0.028
P4	0.092	0.073	0.014	0.01	0.004
O1	0.002	0.012	0.003	0.002	0.012
O2	0.015	0.009	0.001	0.002	0.001
F7	0.047	0.045	0.002	0.038	0.011
F8	0.099	0.057	0.045	0.071	0.061
T3	0.052	0.014	0.007	0.127	0.039
T4	0.264	0.223	0.444	0.481	0.496
T5	0	0.001	0.002	0.012	0.008
T6	0.053	0.008	0.008	0.013	0.01
Fz	0	0.003	0.001	0.004	0.003
Cz	0.06	0.034	0.001	0.02	0.004
Pz	0.021	0.076	0.015	0.024	0.007

Table C 8

0.5 Hz CES Av. Ref. FFT Relative Power Group Paired t-Test (p-Value)

	31 Hz	32 Hz	33 Hz	34 Hz	35 Hz
FP1	0.056	0.15	0.301	0.247	0.291
FP2	0.015	0.019	0.017	0.008	0.016
F3	0.001	0.003	0.005	0.001	0.001
F4	0.028	0.022	0.031	0.026	0.065
C3	0.015	0.116	0.09	0.033	0.062
C4	0.012	0.064	0.063	0.06	0.075
P3	0.016	0.005	0.031	0.017	0.028
P4	0.008	0.012	0.015	0.073	0.041
O1	0.002	0.002	0.017	0.001	0
O2	0.002	0.004	0.015	0.005	0.003
F7	0.003	0.013	0.04	0.031	0.013
F8	0.042	0.099	0.103	0.062	0.156
T3	0.017	0.052	0.031	0.032	0.03
T4	0.266	0.417	0.328	0.497	0.251
T5	0.008	0.026	0.016	0.004	0.011
T6	0.006	0.042	0.039	0.046	0.02
Fz	0	0.001	0.011	0.001	0.006
Cz	0	0	0.003	0	0.018
Pz	0.007	0.002	0.01	0.008	0.008

Table C 9

0.5 Hz CES Av. Ref. FFT Relative Power Group Paired t-Test (p-Value)

	36 Hz	37 Hz	38 Hz	39 Hz	40 Hz
FP1	0.308	0.308	0.169	0.196	0.135
FP2	0.006	0.016	0.022	0.047	0.027
F3	0.003	0.001	0.002	0.003	0.002
F4	0.034	0.08	0.079	0.201	0.103
C3	0.206	0.094	0.114	0.128	0.111
C4	0.231	0.129	0.061	0.26	0.332
P3	0.072	0.033	0.034	0.046	0.023
P4	0.106	0.035	0.06	0.112	0.112
O1	0.002	0.003	0.002	0.01	0.02
O2	0.006	0.001	0.01	0.008	0.017
F7	0.03	0.027	0.005	0.06	0.038
F8	0.114	0.149	0.171	0.335	0.138
T3	0.224	0.114	0.065	0.09	0.069
T4	0.373	0.222	0.285	0.427	0.621
T5	0.011	0.011	0.006	0.028	0.005
T6	0.047	0.003	0.048	0.032	0.055
Fz	0	0.002	0.005	0.005	0.005
Cz	0.002	0.004	0.004	0.006	0.038
Pz	0.011	0.016	0.021	0.037	0.038

FFT Relative Power Group Paired *t*-Test (P-Value)

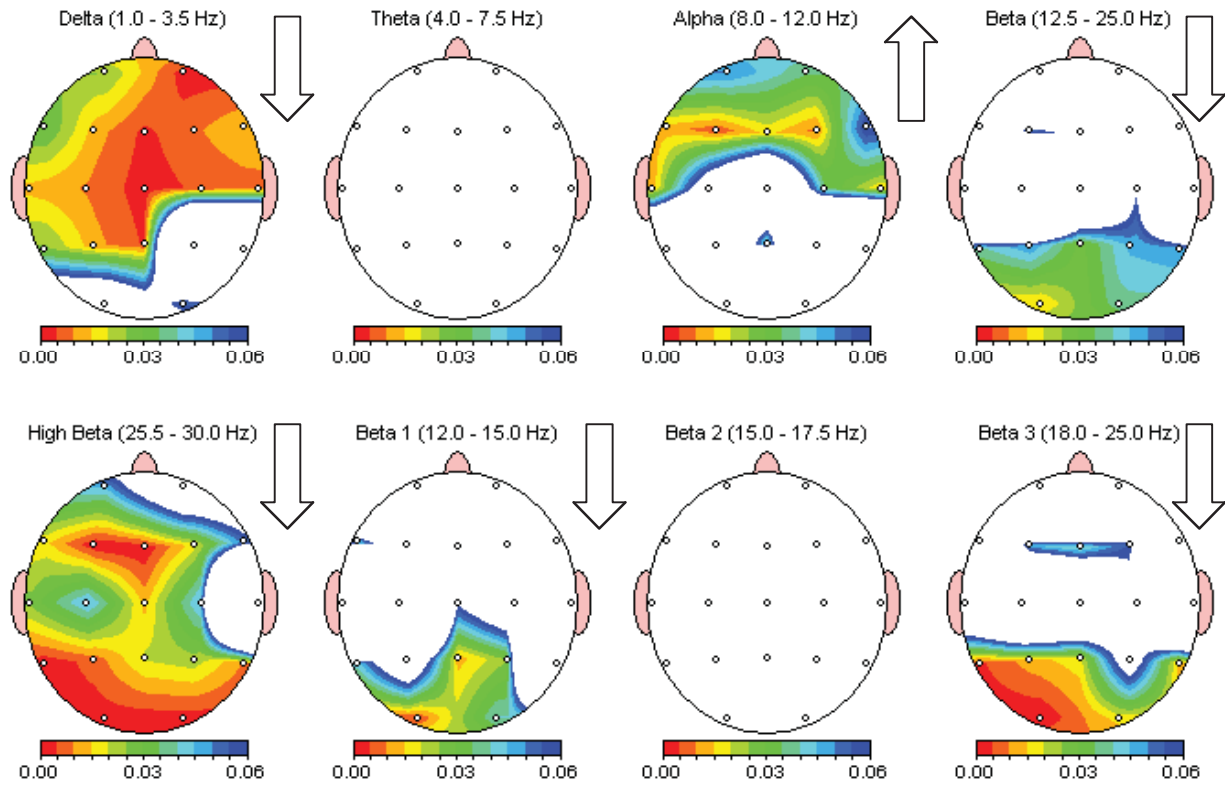


Figure C 2. Relative power paired *t*-test topographical map for the 0.5 Hz average reference montage.

FFT Relative Power Group Paired t-Test (P-Value)

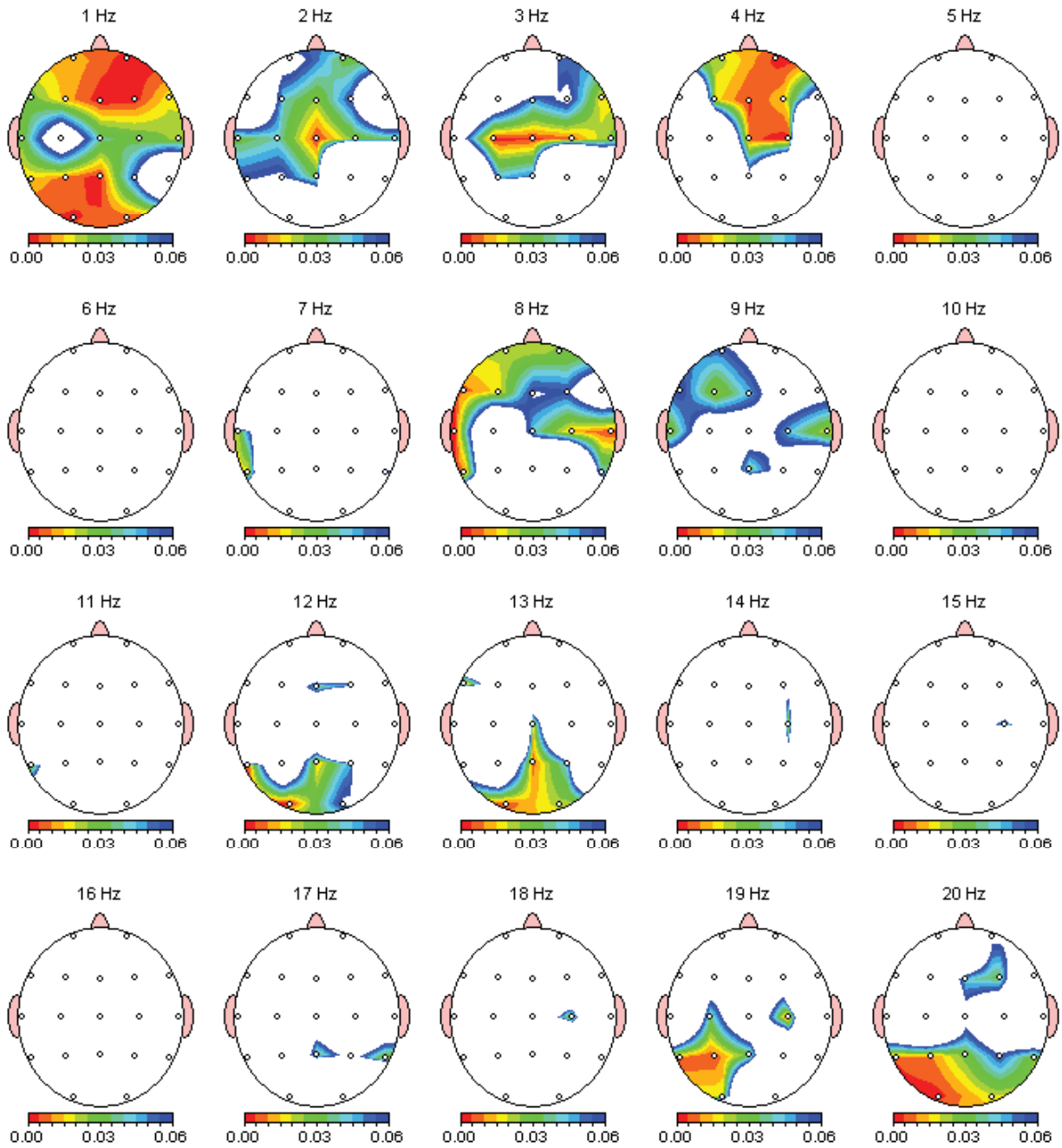


Figure C 3. Relative power paired *t*-test topographical map for the 0.5 Hz average reference montage.

FFT Relative Power Group Paired t-Test (P-Value)

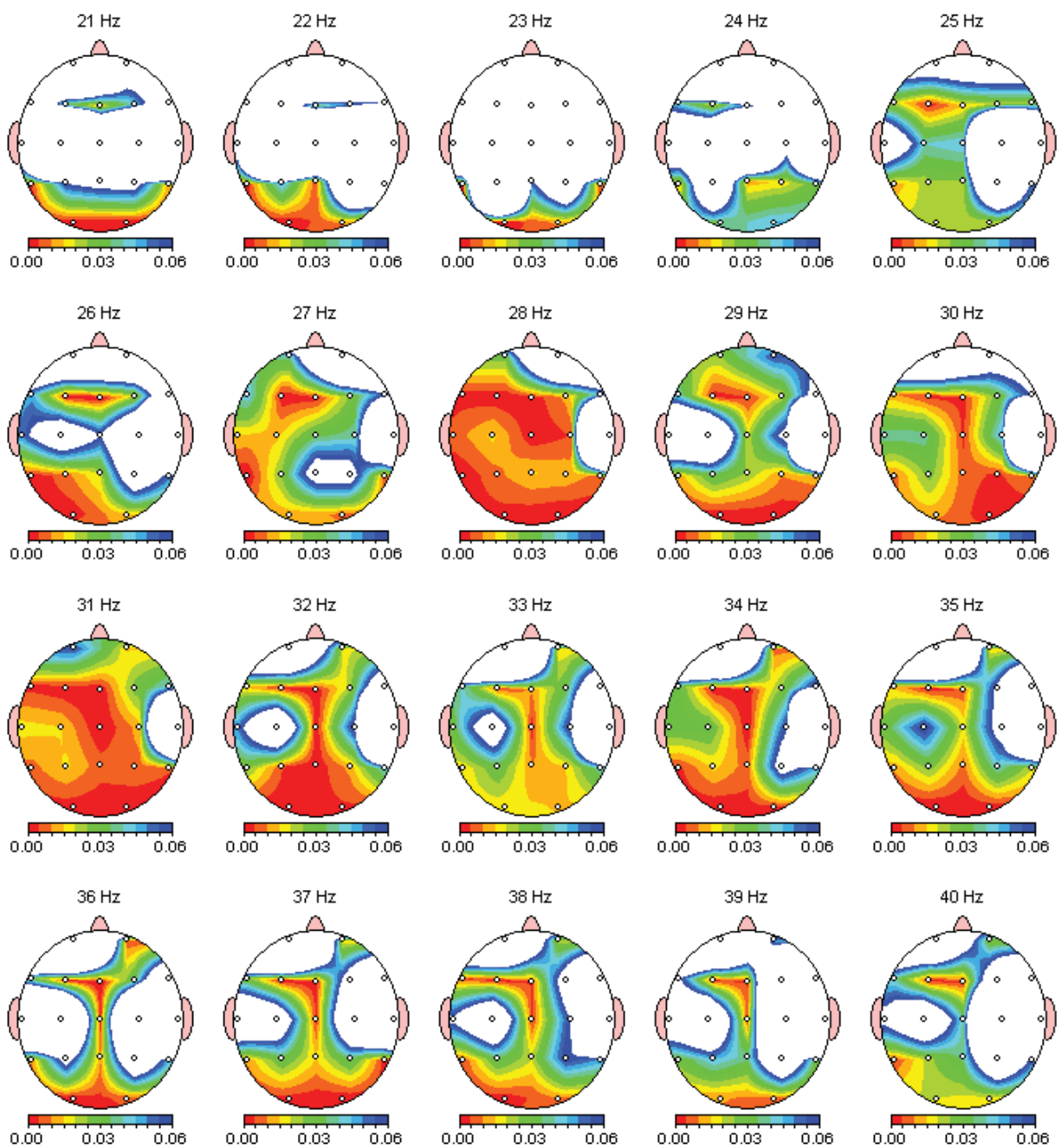


Figure C 4. Relative power paired *t*-test topographical map for the 0.5 Hz average reference montage.

FFT Coherence Group Paired t-Test (P-Value)

Intrahemispheric: LEFT

	DELTA	THETA	ALPHA	BETA
FP1 F3	0.034	0.311	0.475	0.278
FP1 C3	0.028	0.834	0.159	0.727
FP1 P3	0.329	0.208	0.062	0.080
FP1 O1	0.988	0.084	0.240	0.324
FP1 F7	0.057	0.390	0.630	0.897
FP1 T3	0.263	0.404	0.607	0.522
FP1 T5	0.908	0.031	0.071	0.064
F3 C3	0.186	0.204	0.333	0.636
F3 P3	0.031	0.140	0.007	0.014
F3 O1	0.202	0.035	0.019	0.021
F3 F7	0.026	0.786	0.259	0.276
F3 T3	0.271	0.218	0.781	0.349
F3 T5	0.176	0.002	0.000	0.003
C3 P3	0.007	0.066	0.392	0.363
C3 O1	0.493	0.531	0.158	0.660
C3 F7	0.853	0.045	0.212	0.990
C3 T3	0.363	0.495	0.891	0.362
C3 T5	0.090	0.760	0.435	0.665
P3 O1	0.579	0.158	0.197	0.545
P3 F7	0.247	0.325	0.020	0.181
P3 T3	0.308	0.225	0.434	0.570
P3 T5	0.377	0.436	0.895	0.114
O1 F7	0.146	0.276	0.177	0.474
O1 T3	0.339	0.051	0.457	0.983
O1 T5	0.916	0.043	0.074	0.058
F7 T3	0.897	0.935	0.982	0.497
F7 T5	0.266	0.128	0.073	0.879
T3 T5	0.966	0.721	0.793	0.933

Intrahemispheric: RIGHT

	DELTA	THETA	ALPHA	BETA
FP2 F4	0.883	0.564	0.802	0.113
FP2 C4	0.740	0.294	0.109	0.539
FP2 P4	0.980	0.947	0.198	0.332
FP2 O2	0.295	0.304	0.333	0.320
FP2 F8	0.306	0.118	0.254	0.151
FP2 T4	0.345	0.179	0.742	0.477
FP2 T6	0.304	0.595	0.182	0.210
F4 C4	0.696	0.029	0.444	0.777
F4 P4	0.794	0.981	0.181	0.113
F4 O2	0.574	0.134	0.012	0.116
F4 F8	0.616	0.679	0.750	0.540
F4 T4	0.689	0.193	0.826	0.943
F4 T6	0.181	0.029	0.004	0.004
C4 P4	0.962	0.361	0.947	0.614
C4 O2	0.905	0.097	0.109	0.253
C4 F8	0.596	0.693	0.922	0.620
C4 T4	0.816	0.682	0.210	0.318
C4 T6	0.600	0.586	0.139	0.575
P4 O2	0.317	0.792	0.644	0.953
P4 F8	0.371	0.233	0.022	0.056
P4 T4	0.348	0.722	0.091	0.388
P4 T6	0.925	0.493	0.278	0.663
O2 F8	0.260	0.387	0.169	0.219
O2 T4	0.507	0.898	0.017	0.749
O2 T6	0.189	0.284	0.336	0.002
F8 T4	0.990	0.328	0.585	0.396
F8 T6	0.176	0.205	0.362	0.595
T4 T6	0.599	0.933	0.805	0.932

Interhemispheric: HOMOLOGOUS PAIRS

	DELTA	THETA	ALPHA	BETA
FP1 FP2	0.304	0.034	0.206	0.782
C3 C4	0.959	0.113	0.041	0.759
O1 O2	0.910	0.291	0.000	0.203
T3 T4	0.291	0.738	0.697	0.154

	DELTA	THETA	ALPHA	BETA
F3 F4	0.119	0.017	0.013	0.041
P3 P4	0.678	0.789	0.001	0.204
F7 F8	0.136	0.311	0.212	0.297
T5 T6	0.672	0.008	0.001	0.457

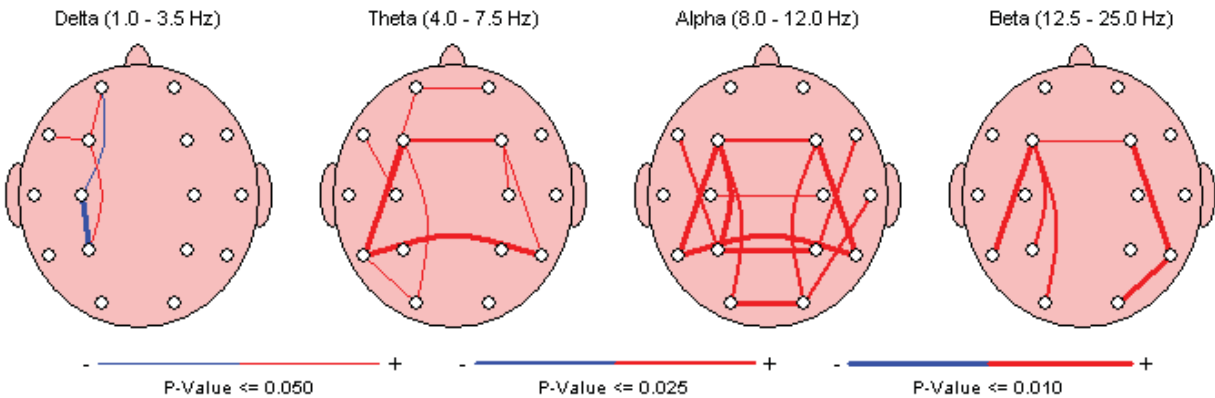


Figure C 5. Coherence for the 0.5 Hz CES average reference montage.

FFT Amplitude Asymmetry Group Paired t-Test (P-Value)

Intrahemispheric: LEFT

	DELTA	THETA	ALPHA	BETA
FP1 F3	0.602	0.669	0.259	0.503
FP1 C3	0.961	0.538	0.564	0.974
FP1 P3	0.953	0.124	0.613	0.829
FP1 O1	0.314	0.028	0.797	0.958
FP1 F7	0.737	0.800	0.159	0.587
FP1 T3	0.612	0.847	0.042	0.589
FP1 T5	0.247	0.014	0.833	0.878
F3 C3	0.314	0.872	0.191	0.393
F3 P3	0.399	0.439	0.222	0.306
F3 O1	0.673	0.069	0.513	0.716
F3 F7	0.853	0.595	0.022	0.902
F3 T3	0.291	0.926	0.002	0.668
F3 T5	0.466	0.039	0.665	0.492
C3 P3	0.901	0.510	0.675	0.768
C3 O1	0.270	0.110	0.903	0.765
C3 F7	0.891	0.469	0.832	0.438
C3 T3	0.500	0.903	0.685	0.327
C3 T5	0.117	0.039	0.504	0.926
P3 O1	0.242	0.144	0.934	0.605
P3 F7	0.806	0.143	0.883	0.233
P3 T3	0.543	0.544	0.380	0.317
P3 T5	0.090	0.038	0.580	0.850
O1 F7	0.518	0.015	0.929	0.605
O1 T3	0.076	0.065	0.779	0.419
O1 T5	0.868	0.578	0.758	0.791
F7 T3	0.302	0.688	0.053	0.763
F7 T5	0.366	0.009	0.475	0.417
T3 T5	0.065	0.063	0.158	0.310

Intrahemispheric: RIGHT

	DELTA	THETA	ALPHA	BETA
FP2 F4	0.121	0.097	0.143	0.992
FP2 C4	0.267	0.498	0.504	0.970
FP2 P4	0.008	0.576	0.076	0.816
FP2 O2	0.221	0.070	0.784	0.414
FP2 F8	0.518	0.591	0.146	0.797
FP2 T4	0.769	0.663	0.174	0.691
FP2 T6	0.216	0.029	0.944	0.729
F4 C4	0.983	0.541	0.562	0.922
F4 P4	0.202	0.271	0.015	0.919
F4 O2	0.847	0.397	0.833	0.419
F4 F8	0.606	0.100	0.051	0.889
F4 T4	0.252	0.382	0.031	0.396
F4 T6	0.332	0.161	0.432	0.751
C4 P4	0.148	0.705	0.196	0.638
C4 O2	0.867	0.495	0.822	0.612
C4 F8	0.446	0.473	0.215	0.762
C4 T4	0.167	0.842	0.103	0.590
C4 T6	0.356	0.282	0.921	0.959
P4 O2	0.174	0.184	0.444	0.224
P4 F8	0.078	0.541	0.494	0.973
P4 T4	0.012	0.949	0.951	0.791
P4 T6	0.776	0.085	0.208	0.312
O2 F8	0.552	0.092	0.502	0.399
O2 T4	0.097	0.232	0.581	0.236
O2 T6	0.481	0.644	0.823	0.374
F8 T4	0.436	0.295	0.524	0.764
F8 T6	0.329	0.045	0.500	0.579
T4 T6	0.083	0.110	0.419	0.321

Interhemispheric: HOMOLOGOUS PAIRS

	DELTA	THETA	ALPHA	BETA
FP1 FP2	0.210	0.650	0.861	0.863
C3 C4	0.595	0.924	0.151	0.979
O1 O2	0.529	0.499	0.683	0.326
T3 T4	0.880	0.983	0.551	0.812

	DELTA	THETA	ALPHA	BETA
F3 F4	0.791	0.230	0.731	0.666
P3 P4	0.040	0.399	0.419	0.152
F7 F8	0.472	0.704	0.821	0.681
T5 T6	0.555	0.597	0.944	0.894

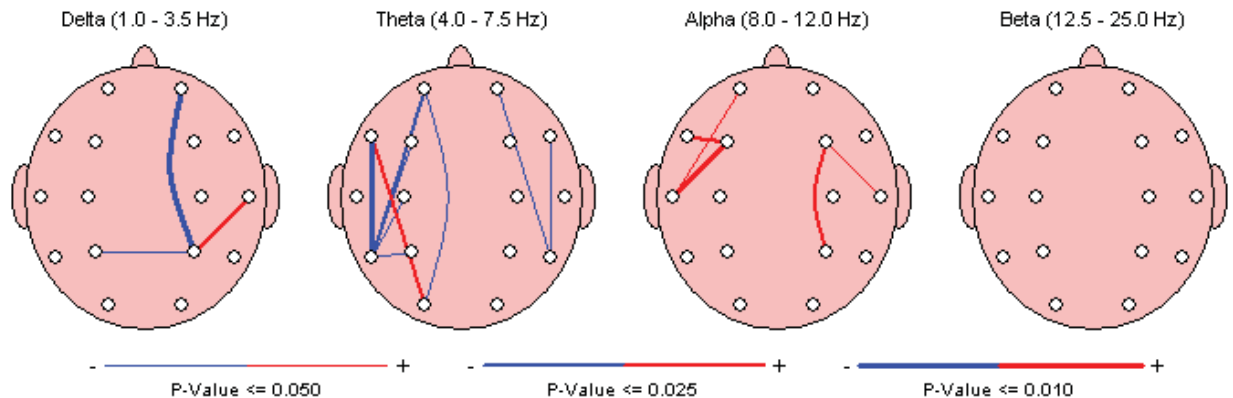


Figure C 6. Amplitude asymmetry for 0.5 Hz CES average reference montage.

FFT Phase Lag Group Paired t-Test (P-Value)

Intrahemispheric: LEFT

	DELTA	THETA	ALPHA	BETA
FP1 F3	0.424	0.247	0.609	0.398
FP1 C3	0.340	0.789	0.490	0.071
FP1 P3	0.350	0.627	0.006	0.372
FP1 O1	0.866	0.903	0.291	0.167
FP1 F7	0.198	0.270	0.532	0.603
FP1 T3	0.131	0.985	0.341	0.399
FP1 T5	0.091	0.839	0.058	0.543
F3 C3	0.896	0.171	0.769	0.658
F3 P3	0.154	0.163	0.516	0.290
F3 O1	0.835	0.002	0.054	0.126
F3 F7	0.113	0.977	0.723	0.368
F3 T3	0.510	0.646	0.230	0.850
F3 T5	0.114	0.174	0.107	0.469
C3 P3	0.476	0.728	0.047	0.754
C3 O1	0.919	0.176	0.487	0.470
C3 F7	0.997	0.684	0.233	0.649
C3 T3	0.179	0.653	0.434	0.572
C3 T5	0.047	0.848	0.081	0.364
P3 O1	0.114	0.995	0.689	0.791
P3 F7	0.150	0.317	0.194	0.810
P3 T3	0.655	0.977	0.387	0.408
P3 T5	0.605	0.823	0.197	0.661
O1 F7	0.359	0.127	0.040	0.425
O1 T3	0.306	0.238	0.513	0.780
O1 T5	0.761	0.228	0.094	0.405
F7 T3	0.659	0.467	0.269	0.641
F7 T5	0.447	0.250	0.036	0.082
T3 T5	0.585	0.172	0.549	0.602

Intrahemispheric: RIGHT

	DELTA	THETA	ALPHA	BETA
FP2 F4	0.080	0.905	0.978	0.354
FP2 C4	0.169	0.834	0.164	0.060
FP2 P4	0.274	0.132	0.024	0.129
FP2 O2	0.900	0.721	0.107	0.882
FP2 F8	0.516	0.934	0.169	0.089
FP2 T4	0.142	0.236	0.329	0.365
FP2 T6	0.325	0.410	0.217	0.257
F4 C4	0.025	0.876	0.704	0.078
F4 P4	0.139	0.151	0.059	0.116
F4 O2	0.128	0.555	0.026	0.986
F4 F8	0.500	0.913	0.938	0.809
F4 T4	0.323	0.118	0.849	0.764
F4 T6	0.433	0.400	0.262	0.444
C4 P4	0.980	0.678	0.445	0.321
C4 O2	0.270	0.804	0.336	0.128
C4 F8	0.592	0.553	0.394	0.410
C4 T4	0.279	0.438	0.487	0.966
C4 T6	0.438	0.267	0.143	0.556
P4 O2	0.975	0.109	0.887	0.143
P4 F8	0.364	0.150	0.031	0.072
P4 T4	0.958	0.667	0.579	0.209
P4 T6	0.652	0.944	0.768	0.687
O2 F8	0.594	0.764	0.231	0.411
O2 T4	0.994	0.423	0.727	0.392
O2 T6	0.421	0.331	0.986	0.190
F8 T4	0.795	0.337	0.505	0.557
F8 T6	0.623	0.118	0.304	0.308
T4 T6	0.306	0.861	0.900	0.471

Interhemispheric: HOMOLOGOUS PAIRS

	DELTA	THETA	ALPHA	BETA
FP1 FP2	0.857	0.541	0.066	0.422
C3 C4	0.600	0.826	0.384	0.226
O1 O2	0.998	0.399	0.009	0.023
T3 T4	0.832	0.896	0.444	0.170

	DELTA	THETA	ALPHA	BETA
F3 F4	0.113	0.112	0.144	0.992
P3 P4	0.141	0.421	0.059	0.605
F7 F8	0.806	0.033	0.324	0.040
T5 T6	0.122	0.412	0.036	0.772

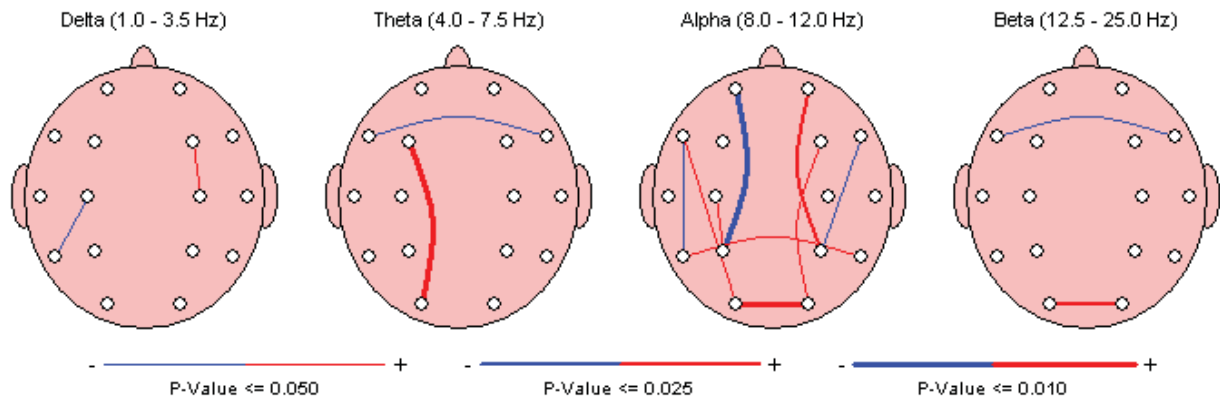


Figure C 7. Phase lag for the 0.5 Hz CES average reference montage.

FFT Power Ratio Group Paired t-Test (P-Value)

Intrahemispheric: LEFT

	D/T	D/A	D/B	D/G	T/A	T/B	T/G	A/B	A/G	B/G
FP1 - AVE	0.060	0.021	0.398	0.543	0.053	0.590	0.068	0.054	0.009	0.007
F3 - AVE	0.036	0.004	0.673	0.205	0.029	0.240	0.006	0.001	0.000	0.000
C3 - AVE	0.001	0.015	0.191	1.000	0.419	0.340	0.057	0.055	0.008	0.031
P3 - AVE	0.004	0.027	0.135	0.700	0.377	0.104	0.016	0.031	0.002	0.016
O1 - AVE	0.002	0.204	0.653	0.747	0.914	0.036	0.008	0.125	0.043	0.069
F7 - AVE	0.043	0.012	0.527	0.491	0.069	0.233	0.040	0.003	0.001	0.014
T3 - AVE	0.000	0.007	0.278	0.532	0.600	0.144	0.024	0.018	0.004	0.012
T5 - AVE	0.001	0.055	0.460	0.247	0.819	0.017	0.002	0.062	0.006	0.001

Intrahemispheric: RIGHT

	D/T	D/A	D/B	D/G	T/A	T/B	T/G	A/B	A/G	B/G
FP2 - AVE	0.018	0.005	0.168	0.836	0.025	0.493	0.187	0.027	0.019	0.150
F4 - AVE	0.023	0.004	0.538	0.596	0.030	0.216	0.044	0.010	0.004	0.011
C4 - AVE	0.020	0.007	0.326	0.941	0.085	0.331	0.137	0.007	0.009	0.104
P4 - AVE	0.207	0.196	0.967	0.386	0.475	0.123	0.036	0.035	0.009	0.123
O2 - AVE	0.009	0.107	0.253	0.873	0.530	0.271	0.003	0.112	0.019	0.016
F8 - AVE	0.040	0.019	0.280	0.617	0.073	0.565	0.106	0.047	0.011	0.021
T4 - AVE	0.000	0.001	0.267	0.624	0.251	0.163	0.246	0.023	0.084	0.576
T6 - AVE	0.053	0.233	0.828	0.674	0.682	0.060	0.011	0.029	0.012	0.076

Intrahemispheric: CENTER

	D/T	D/A	D/B	D/G	T/A	T/B	T/G	A/B	A/G	B/G
Fz - AVE	0.045	0.003	0.232	0.844	0.044	0.390	0.003	0.004	0.000	0.000
Cz - AVE	0.009	0.011	0.156	0.851	0.314	0.347	0.046	0.070	0.010	0.025
Pz - AVE	0.018	0.007	0.239	0.975	0.076	0.258	0.067	0.006	0.003	0.122

Figure C 8. Power ratios for the 0.5 Hz CES average reference montage.

FFT Power Ratio Group Paired t-Test (P-Value)

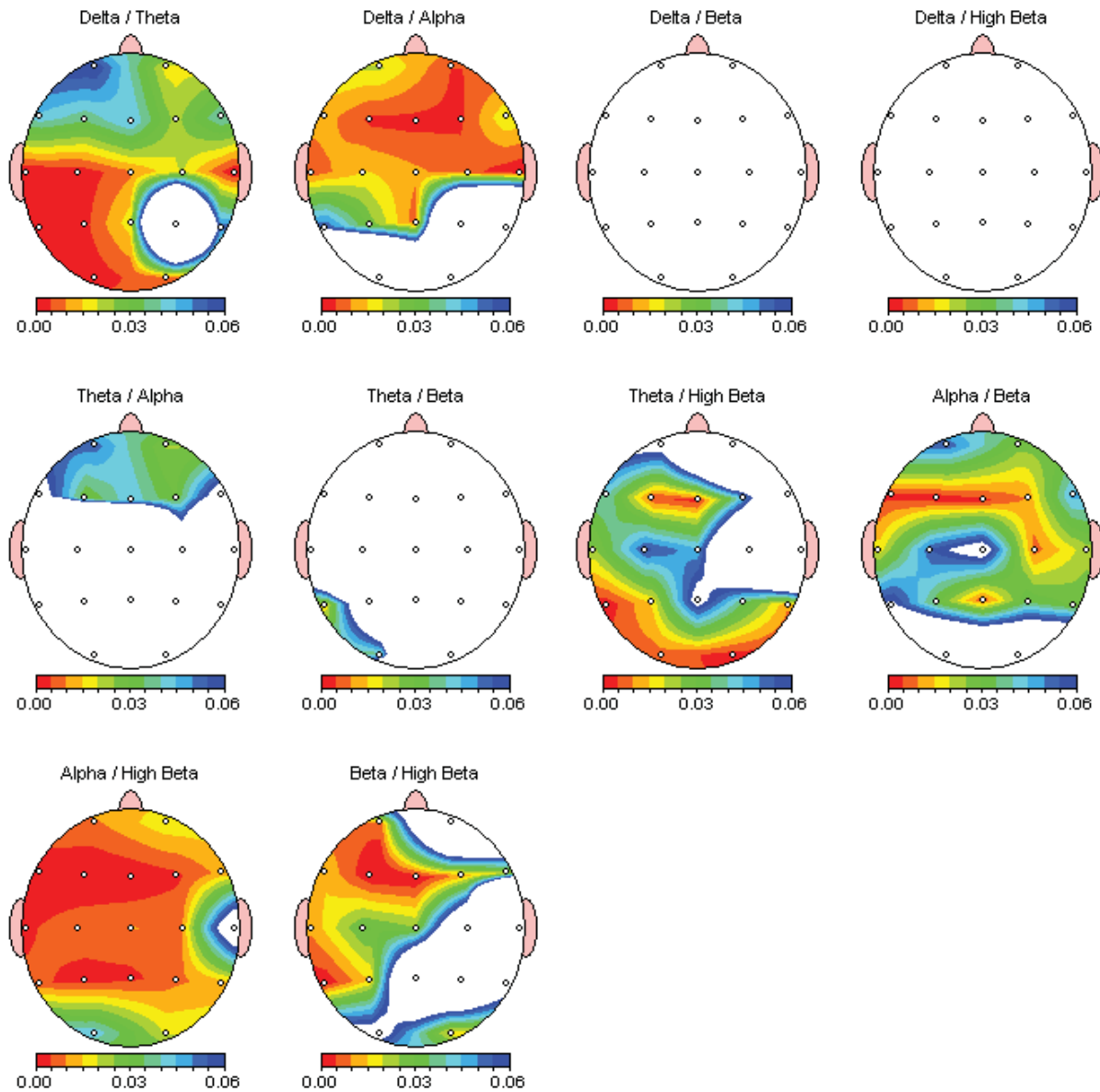


Figure C 9. Power ratios for the 0.5 Hz CES average reference montage. Color indicates a significant p -value between .00 and .05. White indicates no statistically significant result.

Table C 10

0.5 Hz Av. Ref. FFT Relative Power Baseline Group Mean (%)

	Delta	Theta	Alpha	Beta	High Beta	Beta 1	Beta 2	Beta 3
	1.0 - 3.5 Hz	4.0 - 7.5 Hz	8.0 - 12.0 Hz	12.5 - 25.0 Hz	25.5 - 30.0 Hz	12.0 - 15.0 Hz	15.0 - 17.5 Hz	18.0 - 25.0 Hz
FP1	20.144	16.647	42.708	14.66	3.394	5.877	3.527	7.355
FP2	21.032	16.7	42.172	14.903	2.956	5.826	3.54	7.614
F3	13.921	18.402	45.868	17.064	2.873	6.596	4.214	8.587
F4	14.449	18.016	45.162	17.408	3.005	6.717	4.262	8.749
C3	14.655	18.452	41.958	20.056	3.067	7.623	5.201	9.841
C4	14.548	18.466	40.081	21.29	3.354	8.438	5.582	10.256
P3	12.619	14.296	52.755	17.189	2.005	7.214	4.535	8.148
P4	11.241	14.17	54.483	17.356	1.716	7.999	4.59	7.792
O1	9.075	11.352	61.704	14.515	1.927	6.934	3.433	6.722
O2	9.474	11.447	61.861	14.537	1.595	7.011	3.565	6.635
F7	21.008	18.157	40.704	15.042	2.841	6.176	3.665	7.343
F8	22.244	17.612	39.648	15.427	2.832	6.163	3.795	7.604
T3	16.533	18.366	38.448	19.921	3.594	8.292	5.026	9.323
T4	15.665	17.557	37.294	21.329	3.911	8.358	5.884	9.788
T5	11.282	15.452	50.011	18.923	2.533	8.168	5.054	8.48
T6	11.2	15.252	51.91	17.915	2.126	8.118	4.993	7.599
Fz	13.925	20.585	47.244	14.923	2.106	6.074	3.718	7.293
Cz	17.229	20.695	41.388	16.486	2.829	5.999	4.2	8.344
Pz	13.59	14.622	54.939	14.135	1.684	6.587	3.705	6.4

Table C 11

0.5 Hz Av. Ref. FFT Relative Power Group Baseline Standard Deviation (%)

	Delta	Theta	Alpha	Beta	High Beta	Beta 1	Beta 2	Beta 3
	1.0 - 3.5 Hz	4.0 - 7.5 Hz	8.0 - 12.0 Hz	12.5 - 25.0 Hz	25.5 - 30.0 Hz	12.0 - 15.0 Hz	15.0 - 17.5 Hz	18.0 - 25.0 Hz
FP1	9.171	8.693	18.467	6.332	2.534	2.31	1.761	3.937
FP2	8.758	8.211	18.027	6.946	2.109	2.254	1.7	4.678
F3	6.373	9.672	18.074	8.413	2.239	2.476	2.395	5.292
F4	7.301	8.888	16.791	8.39	2.144	2.32	2.225	5.526
C3	5.609	8.086	13.56	8.32	2.178	2.551	2.702	5.172
C4	6.35	8.055	11.722	8.172	2.307	2.858	2.725	4.948
P3	7.969	8.995	18.696	9.74	1.788	3.143	2.892	5.795
P4	6.917	9.017	18.114	9.83	1.183	3.464	3.439	5.185
O1	7.629	8.17	20.449	8.942	2.902	3.354	2.422	5.224
O2	7.735	7.728	18.579	8.583	1.768	3.295	2.75	4.83
F7	9.185	8.966	17.029	6.377	1.918	2.361	1.72	3.654
F8	9.537	7.699	15.791	5.81	1.519	2.328	1.572	3.225
T3	6.853	8.75	13.306	8.567	2.379	3.312	2.236	5.601
T4	6.552	9.232	12.685	9.858	3.539	2.664	3.08	6.36
T5	5.948	8.834	15.681	9.506	2.472	3.644	2.931	5.267
T6	9.86	9.775	17.503	9.497	1.887	3.72	3.231	4.977
Fz	6.847	10.57	17.648	8.312	1.656	2.197	2.438	5.174
Cz	6.728	7.852	13.739	7.593	2.108	1.937	2.431	4.811
Pz	9.075	9.042	19.828	7.734	1.553	3.243	2.47	4.267

Table C 12

0.5 Hz CES Av. Ref FFT Relative Power Post CES Group Mean (%)

	Delta	Theta	Alpha	Beta	High Beta	Beta 1	Beta 2	Beta 3
	1.0 - 3.5 Hz	4.0 - 7.5 Hz	8.0 - 12.0 Hz	12.5 - 25.0 Hz	25.5 - 30.0 Hz	12.0 - 15.0 Hz	15.0 - 17.5 Hz	18.0 - 25.0 Hz
FP1	18.284	16.733	46.266	14.019	2.617	5.648	3.465	6.906
FP2	18.452	16.912	45.759	14.318	2.726	5.705	3.518	7.104
F3	12.384	18.339	50.233	15.533	2.194	6.173	3.933	7.63
F4	12.541	18.052	49.633	15.892	2.395	6.269	3.988	7.84
C3	13.273	18.997	44.204	19.351	2.69	7.922	4.924	9.254
C4	13.031	18.812	43.676	19.936	2.845	8.116	5.118	9.578
P3	11.231	14.621	55.307	16.082	1.791	6.903	4.305	7.41
P4	10.825	14.389	56.442	15.938	1.52	7.371	4.338	6.981
O1	8.26	12.039	64.044	13.062	1.509	6.277	3.244	5.871
O2	8.054	11.655	64.968	13.207	1.272	6.573	3.383	5.768
F7	19.479	18.219	43.893	14.123	2.442	5.777	3.517	6.856
F8	20.261	17.604	42.972	14.825	2.456	6.034	3.679	7.207
T3	14.735	19.678	41.184	18.785	3.012	8.162	4.76	8.505
T4	13.543	18.413	40.529	20.033	3.598	8.071	5.267	9.287
T5	9.981	16.409	52.995	17.191	1.951	7.714	4.696	7.348
T6	9.612	16.286	54.717	16.291	1.827	7.644	4.508	6.804
Fz	11.932	20.376	51.017	13.931	1.774	5.787	3.592	6.61
Cz	15.126	21.265	44.404	15.63	2.441	5.731	3.844	7.983
Pz	12.094	14.476	58.496	12.798	1.385	5.965	3.446	5.645

Table C 13

0.5 Hz CES Av. Ref. FFT Relative Power Group Post CES Standard Deviation (%)

	Delta	Theta	Alpha	Beta	High Beta	Beta 1	Beta 2	Beta 3
	1.0 - 3.5 Hz	4.0 - 7.5 Hz	8.0 - 12.0 Hz	12.5 - 25.0 Hz	25.5 - 30.0 Hz	12.0 - 15.0 Hz	15.0 - 17.5 Hz	18.0 - 25.0 Hz
FP1	9.171	8.693	18.467	6.332	2.534	2.31	1.761	3.937
FP2	8.758	8.211	18.027	6.946	2.109	2.254	1.7	4.678
F3	6.373	9.672	18.074	8.413	2.239	2.476	2.395	5.292
F4	7.301	8.888	16.791	8.39	2.144	2.32	2.225	5.526
C3	5.609	8.086	13.56	8.32	2.178	2.551	2.702	5.172
C4	6.35	8.055	11.722	8.172	2.307	2.858	2.725	4.948
P3	7.969	8.995	18.696	9.74	1.788	3.143	2.892	5.795
P4	6.917	9.017	18.114	9.83	1.183	3.464	3.439	5.185
O1	7.629	8.17	20.449	8.942	2.902	3.354	2.422	5.224
O2	7.735	7.728	18.579	8.583	1.768	3.295	2.75	4.83
F7	9.185	8.966	17.029	6.377	1.918	2.361	1.72	3.654
F8	9.537	7.699	15.791	5.81	1.519	2.328	1.572	3.225
T3	6.853	8.75	13.306	8.567	2.379	3.312	2.236	5.601
T4	6.552	9.232	12.685	9.858	3.539	2.664	3.08	6.36
T5	5.948	8.834	15.681	9.506	2.472	3.644	2.931	5.267
T6	9.86	9.775	17.503	9.497	1.887	3.72	3.231	4.977
Fz	6.847	10.57	17.648	8.312	1.656	2.197	2.438	5.174
Cz	6.728	7.852	13.739	7.593	2.108	1.937	2.431	4.811
Pz	9.075	9.042	19.828	7.734	1.553	3.243	2.47	4.267

Montage: AveRef

FFT Relative Power Group Paired t-Test (P-Value)

Intrahemispheric: LEFT

	DELTA	THETA	ALPHA	BETA	HIGH BETA	BETA 1	BETA 2	BETA 3
FP1 - AVE	0.001	0.226	0.000	0.001	0.003	0.000	0.053	0.012
F3 - AVE	0.000	0.063	0.000	0.034	0.118	0.003	0.145	0.238
C3 - AVE	0.069	0.242	0.004	0.036	0.023	0.000	0.910	0.302
P3 - AVE	0.046	0.244	0.002	0.001	0.001	0.000	0.078	0.017
O1 - AVE	0.029	0.136	0.003	0.001	0.000	0.002	0.027	0.012
F7 - AVE	0.001	0.229	0.000	0.012	0.003	0.002	0.284	0.036
T3 - AVE	0.048	0.827	0.002	0.015	0.020	0.044	0.550	0.049
T5 - AVE	0.076	0.619	0.007	0.018	0.000	0.002	0.531	0.047

Intrahemispheric: RIGHT

	DELTA	THETA	ALPHA	BETA	HIGH BETA	BETA 1	BETA 2	BETA 3
FP2 - AVE	0.002	0.199	0.000	0.005	0.006	0.001	0.159	0.028
F4 - AVE	0.000	0.022	0.000	0.013	0.004	0.001	0.187	0.209
C4 - AVE	0.060	0.557	0.005	0.033	0.019	0.000	0.841	0.215
P4 - AVE	0.023	0.349	0.000	0.000	0.000	0.000	0.118	0.011
O2 - AVE	0.080	0.255	0.001	0.000	0.000	0.001	0.275	0.006
F8 - AVE	0.002	0.237	0.003	0.014	0.009	0.000	0.638	0.055
T4 - AVE	0.054	0.436	0.004	0.035	0.028	0.002	0.535	0.602
T6 - AVE	0.392	0.615	0.090	0.014	0.015	0.001	0.553	0.092

Intrahemispheric: CENTER

	DELTA	THETA	ALPHA	BETA	HIGH BETA	BETA 1	BETA 2	BETA 3
Fz - AVE	0.000	0.055	0.000	0.016	0.003	0.001	0.074	0.327
Cz - AVE	0.165	0.096	0.010	0.095	0.533	0.002	0.445	0.873
Pz - AVE	0.004	0.060	0.000	0.001	0.001	0.000	0.015	0.013

Figure C 10. Relative power *p*-value tables for the 100 Hz CES average reference montage.

Table C 14

100 Hz CES Av. Ref FFT Relative Power Group Paired t-Test (p-Value)

	Delta	Theta	Alpha	Beta	High Beta	Beta 1	Beta 2	Beta 3
	1.0 - 3.5 Hz	4.0 - 7.5 Hz	8.0 - 12.0 Hz	12.5 - 25.0 Hz	25.5 - 30.0 Hz	12.0 - 15.0 Hz	15.0 - 17.5 Hz	18.0 - 25.0 Hz
FP1	0.001	0.226	0	0.001	0.003	0	0.053	0.012
FP2	0.002	0.199	0	0.005	0.006	0.001	0.159	0.028
F3	0	0.063	0	0.034	0.118	0.003	0.145	0.238
F4	0	0.022	0	0.013	0.004	0.001	0.187	0.209
C3	0.069	0.242	0.004	0.036	0.023	0	0.91	0.302
C4	0.06	0.557	0.005	0.033	0.019	0	0.841	0.215
P3	0.046	0.244	0.002	0.001	0.001	0	0.078	0.017
P4	0.023	0.349	0	0	0	0	0.118	0.011
O1	0.029	0.136	0.003	0.001	0	0.002	0.027	0.012
O2	0.08	0.255	0.001	0	0	0.001	0.275	0.006
F7	0.001	0.229	0	0.012	0.003	0.002	0.284	0.036
F8	0.002	0.237	0.003	0.014	0.009	0	0.638	0.055
T3	0.048	0.827	0.002	0.015	0.02	0.044	0.55	0.049
T4	0.054	0.436	0.004	0.035	0.028	0.002	0.535	0.602
T5	0.076	0.619	0.007	0.018	0	0.002	0.531	0.047
T6	0.392	0.615	0.09	0.014	0.015	0.001	0.553	0.092
Fz	0	0.055	0	0.016	0.003	0.001	0.074	0.327
Cz	0.165	0.096	0.01	0.095	0.533	0.002	0.445	0.873
Pz	0.004	0.06	0	0.001	0.001	0	0.015	0.013

Table C 15

100 Hz CES Av. Ref FFT Relative Power Group Paired t-Test (p-Value)

	1 Hz	2 Hz	3 Hz	4 Hz	5 Hz
FP1	0.023	0	0.024	0.047	0.043
FP2	0.032	0.001	0.005	0.016	0.006
F3	0.003	0	0	0.004	0.039
F4	0.029	0	0	0.004	0.005
C3	0.445	0.114	0.013	0.031	0.014
C4	0.176	0.028	0.165	0.07	0.207
P3	0.083	0.054	0.073	0.059	0.038
P4	0.231	0.01	0.035	0.013	0.042
O1	0.046	0.031	0.029	0.063	0.12
O2	0.141	0.059	0.121	0.033	0.314
F7	0.021	0.001	0.078	0.032	0.046
F8	0.027	0.002	0.014	0.035	0.004
T3	0.197	0.151	0.074	0.269	0.039
T4	0.178	0.058	0.046	0.174	0.112
T5	0.155	0.26	0.011	0.149	0.086
T6	0.529	0.35	0.233	0.157	0.697
Fz	0.006	0	0	0.003	0.011
Cz	0.776	0.123	0.017	0.001	0.06
Pz	0.018	0.006	0.026	0.001	0.004

Table C 16

100 Hz CES Av. Ref FFT Relative Power Group Paired t-Test (p-Value)

	6 Hz	7 Hz	8 Hz	9 Hz	10 Hz
FP1	0.214	0.126	0.04	0.01	0.004
FP2	0.856	0.201	0.123	0.037	0.003
F3	0.248	0.879	0.277	0.033	0.003
F4	0.224	0.239	0.691	0.217	0.003
C3	0.668	0.435	0.178	0.027	0.251
C4	0.903	0.75	0.045	0.053	0.033
P3	0.265	0.344	0.084	0.01	0.394
P4	0.264	0.263	0.279	0.017	0.004
O1	0.13	0.632	0.495	0.468	0.175
O2	0.364	0.774	0.88	0.65	0.02
F7	0.27	0.172	0.067	0.011	0.024
F8	0.495	0.171	0.191	0.135	0.029
T3	0.87	0.153	0.055	0.01	0.206
T4	0.615	0.02	0.003	0.003	0.376
T5	0.818	0.758	0.04	0.268	0.394
T6	0.734	0.08	0.088	0.655	0.699
Fz	0.567	0.316	0.368	0.051	0.004
Cz	0.352	0.631	0.041	0.083	0.251
Pz	0.058	0.301	0.023	0	0.047

Table C 17

100 Hz CES Av. Ref FFT Relative Power Group Paired t-Test (p-Value)

	11 Hz	12 Hz	13 Hz	14 Hz	15 Hz
FP1	0.959	0.01	0	0.002	0.083
FP2	0.86	0.008	0	0.002	0.086
F3	0.622	0.016	0	0.068	0.071
F4	0.405	0	0	0.043	0.112
C3	0.732	0	0.001	0.035	0.36
C4	0.385	0.001	0.003	0.029	0.79
P3	0.896	0.005	0	0.001	0.013
P4	0.392	0	0	0	0.01
O1	0.759	0.002	0.003	0.017	0.041
O2	0.635	0.003	0	0.016	0.105
F7	0.654	0.018	0	0.017	0.149
F8	0.685	0.003	0	0.002	0.317
T3	0.501	0.03	0.063	0.28	0.151
T4	0.874	0.005	0.007	0.006	0.152
T5	0.763	0.001	0.002	0.11	0.421
T6	0.567	0	0	0.008	0.462
Fz	0.515	0.003	0	0.153	0.035
Cz	0.605	0	0.004	0.208	0.423
Pz	0.654	0.006	0	0	0.012

Table C 18

100 Hz CES Av. Ref FFT Relative Power Group Paired t-Test (p-Value)

	16 Hz	17 Hz	18 Hz	19 Hz	20 Hz
FP1	0.226	0.028	0.44	0.137	0.214
FP2	0.97	0.039	0.717	0.043	0.511
F3	0.427	0.171	0.935	0.409	0.361
F4	0.905	0.132	0.354	0.276	0.565
C3	0.225	0.911	0.224	0.61	0.688
C4	0.828	0.392	0.436	0.468	0.752
P3	0.792	0.134	0.863	0.071	0.189
P4	0.803	0.206	0.273	0.113	0.47
O1	0.134	0.025	0.179	0.003	0.018
O2	0.966	0.181	0.384	0.008	0.029
F7	0.851	0.185	0.141	0.301	0.195
F8	0.457	0.315	0.764	0.113	0.66
T3	0.289	0.275	0.068	0.095	0.163
T4	0.646	0.561	0.351	0.266	0.504
T5	0.816	0.369	0.969	0.037	0.162
T6	0.848	0.242	0.463	0.21	0.164
Fz	0.515	0.079	0.473	0.398	0.493
Cz	0.323	0.813	0.195	0.737	0.167
Pz	0.187	0.012	0.064	0.102	0.148

Table C 19

100 Hz CES Av. Ref FFT Relative Power Group Paired t-Test (p-Value)

	21 Hz	22 Hz	23 Hz	24 Hz	25 Hz
FP1	0.029	0.004	0.027	0.003	0.013
FP2	0.068	0.006	0.136	0.006	0.02
F3	0.412	0.118	0.124	0.017	0.198
F4	0.076	0.086	0.176	0	0.015
C3	0.597	0.035	0.013	0.001	0.05
C4	0.296	0.061	0.026	0.009	0.001
P3	0.05	0.21	0.008	0	0.003
P4	0.044	0.003	0.003	0	0.001
O1	0.104	0.083	0.077	0.002	0.001
O2	0.036	0.007	0.007	0	0.001
F7	0.076	0.016	0.077	0.018	0.003
F8	0.054	0.192	0.076	0.002	0.006
T3	0.148	0.062	0.116	0.229	0.027
T4	0.821	0.313	0.716	0.141	0.061
T5	0.067	0.142	0.04	0.001	0.001
T6	0.196	0.027	0.072	0.021	0.1
Fz	0.32	0.066	0.343	0	0.053
Cz	0.453	0.408	0.484	0.967	0.487
Pz	0.025	0.042	0.169	0.006	0

Table C 20

100 Hz CES Av. Ref FFT Relative Power Group Paired t-Test (p-Value)

	26 Hz	27 Hz	28 Hz	29 Hz	30 Hz
FP1	0.018	0.013	0.065	0.001	0.005
FP2	0.009	0.003	0.048	0.003	0.01
F3	0.127	0.175	0.291	0.185	0.038
F4	0.044	0.003	0.024	0.002	0.004
C3	0.091	0.089	0.129	0.013	0.044
C4	0.033	0.04	0.029	0.096	0.026
P3	0.022	0.002	0.003	0.002	0
P4	0.002	0.012	0.001	0	0.001
O1	0.001	0	0.004	0.001	0.002
O2	0.004	0.001	0.002	0	0.031
F7	0.019	0.018	0.01	0.005	0.004
F8	0.027	0.013	0.028	0.004	0.011
T3	0.09	0.029	0.014	0.005	0.012
T4	0.064	0.021	0.099	0.034	0.009
T5	0	0	0.001	0	0
T6	0.016	0.031	0.115	0.007	0.005
Fz	0.041	0.024	0.063	0.003	0.002
Cz	0.543	0.928	0.615	0.1	0.13
Pz	0.01	0.012	0.003	0	0

Table C 21

100 Hz CES Av. Ref FFT Relative Power Group Paired t-Test (p-Value)

	31 Hz	32 Hz	33 Hz	34 Hz	35 Hz
FP1	0	0	0	0	0
FP2	0.001	0	0.001	0.001	0
F3	0.01	0.086	0.023	0.036	0.008
F4	0.007	0.001	0	0	0.001
C3	0.025	0	0.002	0.009	0.003
C4	0.034	0.023	0.012	0.002	0.024
P3	0.002	0.001	0.009	0.001	0.003
P4	0	0	0	0	0.001
O1	0.001	0	0	0	0
O2	0.001	0	0	0	0
F7	0.003	0.03	0.087	0.018	0.039
F8	0.012	0.003	0.001	0.006	0.003
T3	0.004	0.034	0.133	0.046	0.27
T4	0.131	0.077	0.072	0.12	0.429
T5	0.004	0.006	0.004	0.001	0.002
T6	0	0	0.001	0.002	0.002
Fz	0.023	0.01	0	0.001	0
Cz	0.063	0.139	0.067	0.045	0.007
Pz	0	0	0	0	0

Table C 22

100 Hz CES Av. Ref FFT Relative Power Group Paired t-Test (p-Value)

	36 Hz	37 Hz	38 Hz	39 Hz	40 Hz
FP1	0	0	0	0	0
FP2	0.004	0	0	0	0
F3	0.035	0.016	0.039	0.012	0.008
F4	0	0	0	0	0
C3	0.006	0.025	0	0.001	0
C4	0.011	0.012	0.006	0.01	0.002
P3	0.003	0	0.001	0.001	0
P4	0	0	0.001	0	0
O1	0.001	0	0	0	0
O2	0.001	0	0	0	0
F7	0.045	0.003	0.009	0.007	0.01
F8	0.004	0.003	0.018	0.004	0.002
T3	0.132	0.305	0.097	0.04	0.069
T4	0.182	0.247	0.144	0.152	0.088
T5	0.002	0	0.001	0	0
T6	0.001	0.001	0.003	0.002	0.006
Fz	0	0	0.001	0	0
Cz	0.001	0.001	0	0	0.001
Pz	0	0	0	0	0

Montage: AveRef

FFT Relative Power Group Paired t-Test (P-Value)

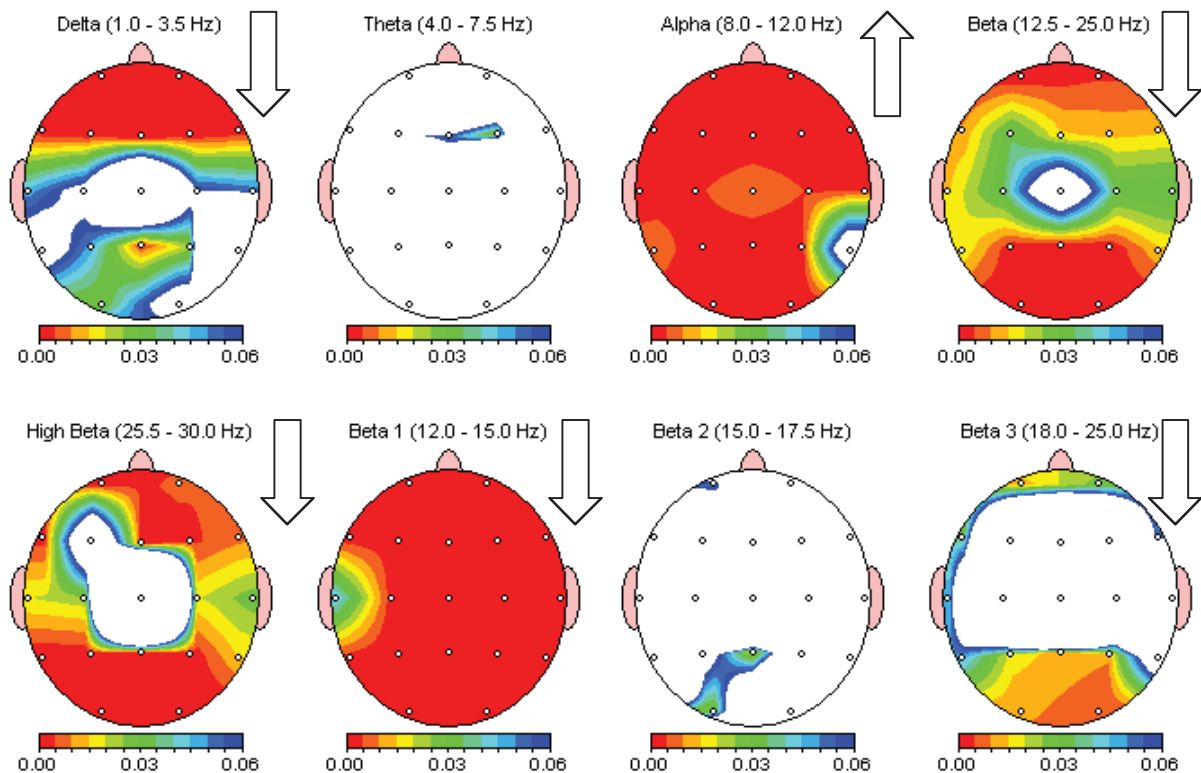


Figure C 11. Relative power p -value topographic map for the 100 Hz CES average reference montage. Color indicates statistically significant change. The arrows indicate the direction of change. White indicates no statistically significant change from baseline.

Montage: AveRef

FFT Coherence Group Paired t-Test (P-Value)

Intrahemispheric: LEFT

	DELTA	THETA	ALPHA	BETA
FP1 F3	0.697	0.191	0.005	0.638
FP1 C3	0.300	0.206	0.778	0.005
FP1 P3	0.028	0.480	0.079	0.375
FP1 O1	0.738	0.742	0.087	0.098
FP1 F7	0.193	0.388	0.414	0.845
FP1 T3	0.502	0.800	0.905	0.381
FP1 T5	0.001	0.532	0.553	0.857
F3 C3	0.146	0.172	0.462	0.954
F3 P3	0.039	0.960	0.042	0.499
F3 O1	0.581	0.571	0.065	0.484
F3 F7	0.186	0.184	0.022	0.968
F3 T3	0.031	0.232	0.636	0.496
F3 T5	0.111	0.799	0.333	0.591
C3 P3	0.177	0.098	0.546	0.083
C3 O1	0.284	0.441	0.698	0.029
C3 F7	0.392	0.349	0.086	0.197
C3 T3	0.224	0.054	0.001	0.212
C3 T5	0.204	0.581	0.429	0.538
P3 O1	0.923	0.237	0.025	0.066
P3 F7	0.168	0.287	0.217	0.913
P3 T3	0.989	0.352	0.001	0.106
P3 T5	0.007	0.829	0.223	0.975
O1 F7	0.553	0.679	0.252	0.852
O1 T3	0.444	0.576	0.182	0.502
O1 T5	0.672	0.071	0.805	0.841
F7 T3	0.718	0.387	0.762	0.957
F7 T5	0.119	0.652	0.677	0.406
T3 T5	0.236	0.312	0.759	0.012

Intrahemispheric: RIGHT

	DELTA	THETA	ALPHA	BETA
FP2 F4	0.000	0.000	0.000	0.631
FP2 C4	0.044	0.715	0.119	0.915
FP2 P4	0.032	0.681	0.712	0.235
FP2 O2	0.377	0.032	0.012	0.743
FP2 F8	0.001	0.049	0.025	0.460
FP2 T4	0.557	0.653	0.836	0.386
FP2 T6	0.230	0.046	0.126	0.131
F4 C4	0.267	0.188	0.495	0.785
F4 P4	0.491	0.463	0.271	0.509
F4 O2	0.591	0.524	0.015	0.602
F4 F8	0.042	0.003	0.004	0.301
F4 T4	0.992	0.097	0.153	0.079
F4 T6	0.049	0.322	0.324	0.294
C4 P4	0.455	0.532	0.319	0.994
C4 O2	0.689	0.452	0.107	0.977
C4 F8	0.622	0.626	0.071	0.812
C4 T4	0.978	0.330	0.026	0.296
C4 T6	0.934	0.458	0.247	0.607
P4 O2	0.972	0.757	0.676	0.542
P4 F8	0.546	0.982	0.618	0.693
P4 T4	0.505	0.160	0.723	0.539
P4 T6	0.508	0.394	0.909	0.680
O2 F8	0.322	0.298	0.009	0.825
O2 T4	0.419	0.115	0.012	0.084
O2 T6	0.391	0.191	0.461	0.232
F8 T4	0.682	0.548	0.422	0.977
F8 T6	0.603	0.418	0.011	0.218
T4 T6	0.326	0.056	0.960	0.941

Interhemispheric: HOMOLOGOUS PAIRS

	DELTA	THETA	ALPHA	BETA
FP1 FP2	0.166	0.041	0.002	0.372
C3 C4	0.169	0.081	0.005	0.317
O1 O2	0.741	0.915	0.051	0.706
T3 T4	0.265	0.012	0.088	0.728

	DELTA	THETA	ALPHA	BETA
F3 F4	0.850	0.160	0.003	0.545
P3 P4	0.000	0.065	0.669	0.122
F7 F8	0.243	0.184	0.049	0.607
T5 T6	0.000	0.847	0.345	0.107

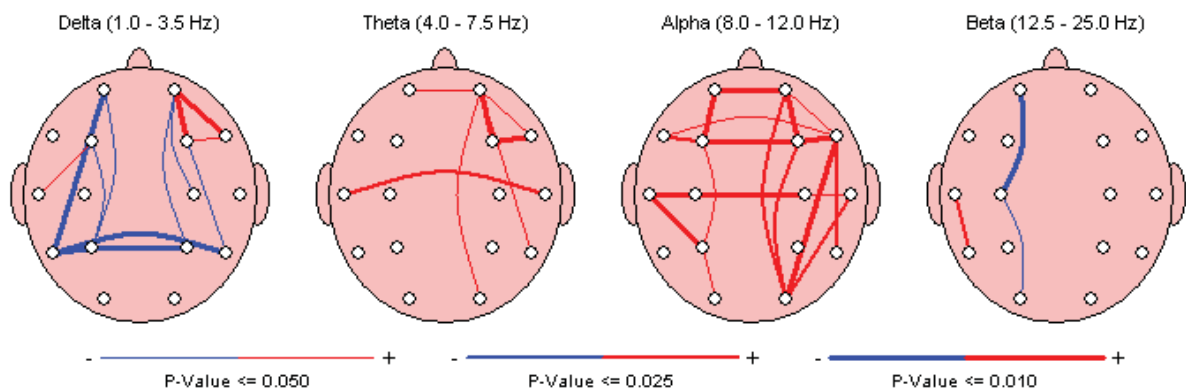


Figure C 12. Coherence tables and maps for the 100 Hz group average reference montage.

Montage: AveRef

FFT Amplitude Asymmetry Group Paired t-Test (P-Value)

Intrahemispheric: LEFT

	DELTA	THETA	ALPHA	BETA
FP1 F3	0.584	0.654	0.289	0.064
FP1 C3	0.001	0.240	0.391	0.048
FP1 P3	0.000	0.007	0.153	0.013
FP1 O1	0.870	0.920	0.945	0.765
FP1 F7	0.273	0.767	0.108	0.647
FP1 T3	0.115	0.908	0.184	0.965
FP1 T5	0.007	0.092	0.892	0.174
F3 C3	0.002	0.602	0.137	0.412
F3 P3	0.011	0.006	0.362	0.323
F3 O1	0.394	0.788	0.523	0.193
F3 F7	0.211	0.604	0.060	0.142
F3 T3	0.042	0.708	0.051	0.414
F3 T5	0.005	0.116	0.277	0.820
C3 P3	0.670	0.031	0.098	0.984
C3 O1	0.014	0.368	0.605	0.098
C3 F7	0.020	0.314	0.675	0.085
C3 T3	0.316	0.351	0.479	0.115
C3 T5	0.993	0.301	0.547	0.666
P3 O1	0.003	0.009	0.271	0.001
P3 F7	0.008	0.024	0.060	0.135
P3 T3	0.278	0.025	0.031	0.186
P3 T5	0.497	0.347	0.067	0.553
O1 F7	0.504	0.937	0.617	0.758
O1 T3	0.179	0.902	0.302	0.900
O1 T5	0.006	0.037	0.918	0.034
F7 T3	0.138	0.645	0.352	0.771
F7 T5	0.011	0.074	0.712	0.372
T3 T5	0.316	0.082	0.201	0.253

Intrahemispheric: RIGHT

	DELTA	THETA	ALPHA	BETA
FP2 F4	0.414	0.805	0.214	0.012
FP2 C4	0.243	0.577	0.738	0.409
FP2 P4	0.000	0.023	0.604	0.229
FP2 O2	0.043	0.489	0.922	0.906
FP2 F8	0.501	0.805	0.444	0.670
FP2 T4	0.229	0.206	0.536	0.315
FP2 T6	0.047	0.029	0.616	0.294
F4 C4	0.380	0.486	0.284	0.474
F4 P4	0.001	0.022	0.887	0.571
F4 O2	0.083	0.358	0.489	0.281
F4 F8	0.603	0.701	0.030	0.166
F4 T4	0.454	0.145	0.057	0.880
F4 T6	0.098	0.013	0.299	0.998
C4 P4	0.045	0.029	0.469	0.897
C4 O2	0.288	0.607	0.811	0.613
C4 F8	0.311	0.655	0.925	0.678
C4 T4	0.773	0.449	0.886	0.632
C4 T6	0.238	0.032	0.812	0.664
P4 O2	0.152	0.185	0.584	0.446
P4 F8	0.002	0.063	0.403	0.431
P4 T4	0.035	0.549	0.381	0.907
P4 T6	0.973	0.148	0.503	0.757
O2 F8	0.111	0.618	0.737	0.955
O2 T4	0.300	0.822	0.778	0.758
O2 T6	0.275	0.033	0.914	0.351
F8 T4	0.303	0.139	0.706	0.519
F8 T6	0.074	0.041	0.738	0.438
T4 T6	0.208	0.093	0.897	0.898

Interhemispheric: HOMOLOGOUS PAIRS

	DELTA	THETA	ALPHA	BETA
FP1 FP2	0.611	0.355	0.198	0.269
C3 C4	0.341	0.761	0.616	0.460
O1 O2	0.001	0.131	0.829	0.336
T3 T4	0.672	0.053	0.256	0.175

	DELTA	THETA	ALPHA	BETA
F3 F4	0.114	0.596	0.850	0.087
P3 P4	0.333	0.559	0.658	0.454
F7 F8	0.727	0.468	0.557	0.190
T5 T6	0.454	0.182	0.714	0.933

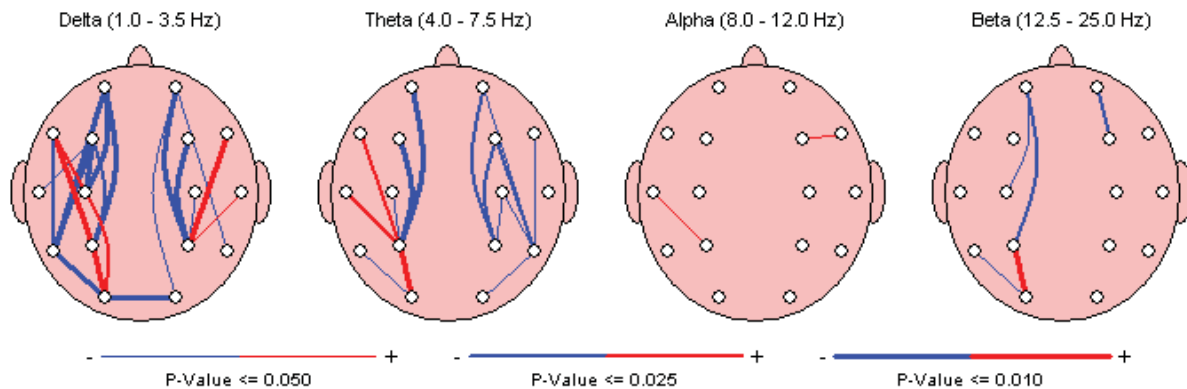


Figure C 13. Amplitude asymmetry for the 100 Hz group average reference montage.

Montage: AveRef

FFT Phase Lag Group Paired t-Test (P-Value)

Intrahemispheric: LEFT

	DELTA	THETA	ALPHA	BETA
FP1 F3	0.153	0.283	0.359	0.036
FP1 C3	0.170	0.302	0.070	0.983
FP1 P3	0.676	0.341	0.225	0.768
FP1 O1	0.355	0.950	0.156	0.036
FP1 F7	0.063	0.697	0.219	0.336
FP1 T3	0.030	0.125	0.711	0.569
FP1 T5	0.927	0.586	0.172	0.902
F3 C3	0.856	0.492	0.524	0.673
F3 P3	0.943	0.503	0.128	0.387
F3 O1	0.274	0.216	0.400	0.975
F3 F7	0.812	0.883	0.164	0.400
F3 T3	0.899	0.216	0.024	0.297
F3 T5	0.551	0.613	0.369	0.161
C3 P3	0.900	0.188	0.098	0.807
C3 O1	0.328	0.381	0.409	0.539
C3 F7	0.092	0.624	0.212	0.287
C3 T3	0.003	0.953	0.507	0.032
C3 T5	0.054	0.393	0.752	0.040
P3 O1	0.983	0.030	0.006	0.126
P3 F7	0.871	0.100	0.904	0.578
P3 T3	0.081	0.111	0.053	0.594
P3 T5	0.912	0.223	0.002	0.558
O1 F7	0.700	0.405	0.086	0.275
O1 T3	0.941	0.658	0.200	0.481
O1 T5	0.052	0.229	0.409	0.672
F7 T3	0.077	0.834	0.090	0.730
F7 T5	0.285	0.109	0.127	0.713
T3 T5	0.844	0.813	0.969	0.272

Intrahemispheric: RIGHT

	DELTA	THETA	ALPHA	BETA
FP2 F4	0.606	0.043	0.117	0.223
FP2 C4	0.622	0.076	0.400	0.306
FP2 P4	0.724	0.980	0.247	0.672
FP2 O2	0.578	0.650	0.212	0.055
FP2 F8	0.596	0.987	0.432	0.685
FP2 T4	0.367	0.379	0.436	0.048
FP2 T6	0.453	0.213	0.492	0.568
F4 C4	0.311	0.057	0.738	0.572
F4 P4	0.706	0.821	0.168	0.874
F4 O2	0.724	0.730	0.669	0.401
F4 F8	0.828	0.082	0.112	0.760
F4 T4	0.048	0.900	0.776	0.479
F4 T6	0.056	0.340	0.855	0.860
C4 P4	0.735	0.183	0.850	0.234
C4 O2	0.177	0.115	0.934	0.899
C4 F8	0.883	0.479	0.198	0.319
C4 T4	0.613	0.107	0.053	0.176
C4 T6	0.156	0.697	0.840	0.426
P4 O2	0.091	0.872	0.096	0.996
P4 F8	0.685	0.486	0.342	0.356
P4 T4	0.256	0.252	0.284	0.179
P4 T6	0.736	0.782	0.931	0.898
O2 F8	0.765	0.906	0.241	0.088
O2 T4	0.370	0.954	0.735	0.982
O2 T6	0.183	0.780	0.874	0.815
F8 T4	0.151	0.605	0.322	0.174
F8 T6	0.417	0.380	0.552	0.192
T4 T6	0.670	0.247	0.750	0.826

Interhemispheric: HOMOLOGOUS PAIRS

	DELTA	THETA	ALPHA	BETA
FP1 FP2	0.557	0.771	0.845	0.196
C3 C4	0.188	0.654	0.036	0.096
O1 O2	0.883	0.627	0.917	0.534
T3 T4	0.415	0.584	0.515	0.829

	DELTA	THETA	ALPHA	BETA
F3 F4	0.169	0.082	0.416	0.527
P3 P4	0.918	0.434	0.482	0.540
F7 F8	0.808	0.039	0.535	0.097
T5 T6	0.617	0.722	0.169	0.083

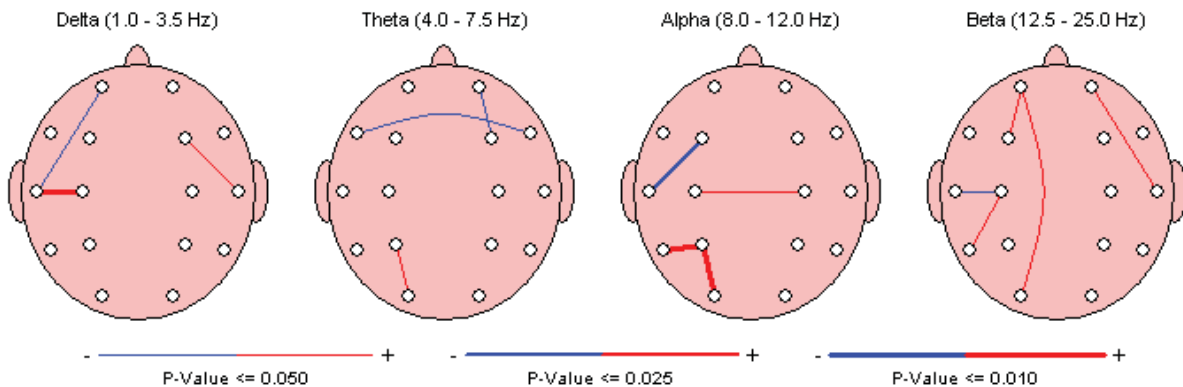


Figure C 14. Phase lag for the 100 Hz group average reference montage.

Montage: AveRef

FFT Power Ratio Group Paired t-Test (P-Value)

Intrahemispheric: LEFT

	D/T	D/A	D/B	D/G	T/A	T/B	T/G	A/B	A/G	B/G
FP1 - AVE	0.013	0.000	0.308	0.615	0.001	0.084	0.010	0.000	0.000	0.507
F3 - AVE	0.000	0.000	0.053	0.197	0.001	0.382	0.346	0.001	0.010	0.743
C3 - AVE	0.262	0.009	0.802	0.876	0.012	0.404	0.113	0.007	0.005	0.583
P3 - AVE	0.057	0.008	0.976	0.209	0.015	0.031	0.000	0.001	0.000	0.229
O1 - AVE	0.037	0.007	0.695	0.654	0.017	0.185	0.003	0.001	0.000	0.174
F7 - AVE	0.058	0.000	0.508	0.373	0.011	0.192	0.011	0.001	0.000	0.060
T3 - AVE	0.143	0.000	0.741	0.204	0.033	0.159	0.051	0.003	0.004	0.131
T5 - AVE	0.034	0.014	0.969	0.059	0.088	0.232	0.001	0.008	0.000	0.065

Intrahemispheric: RIGHT

	D/T	D/A	D/B	D/G	T/A	T/B	T/G	A/B	A/G	B/G
FP2 - AVE	0.014	0.000	0.294	0.938	0.002	0.136	0.024	0.000	0.000	0.276
F4 - AVE	0.022	0.000	0.097	0.201	0.001	0.860	0.216	0.000	0.000	0.316
C4 - AVE	0.046	0.016	0.661	0.315	0.080	0.333	0.022	0.004	0.007	0.164
P4 - AVE	0.292	0.000	0.195	0.061	0.008	0.067	0.001	0.000	0.000	0.374
O2 - AVE	0.111	0.010	0.744	0.348	0.022	0.227	0.027	0.000	0.000	0.484
F8 - AVE	0.023	0.001	0.232	0.987	0.015	0.159	0.045	0.003	0.002	0.162
T4 - AVE	0.045	0.002	0.466	0.803	0.062	0.114	0.063	0.004	0.005	0.185
T6 - AVE	0.187	0.209	0.555	0.160	0.755	0.049	0.002	0.023	0.016	0.305

Intrahemispheric: CENTER

	D/T	D/A	D/B	D/G	T/A	T/B	T/G	A/B	A/G	B/G
Fz - AVE	0.002	0.000	0.017	0.004	0.002	0.836	0.335	0.000	0.000	0.471
Cz - AVE	0.742	0.039	0.893	0.477	0.018	0.888	0.490	0.024	0.107	0.504
Pz - AVE	0.066	0.000	0.340	0.854	0.004	0.404	0.002	0.000	0.000	0.117

Figure C 15. Power ratios for the 100 Hz CES average reference montage.

Montage: AveRef

FFT Power Ratio Group Paired t-Test (P-Value)

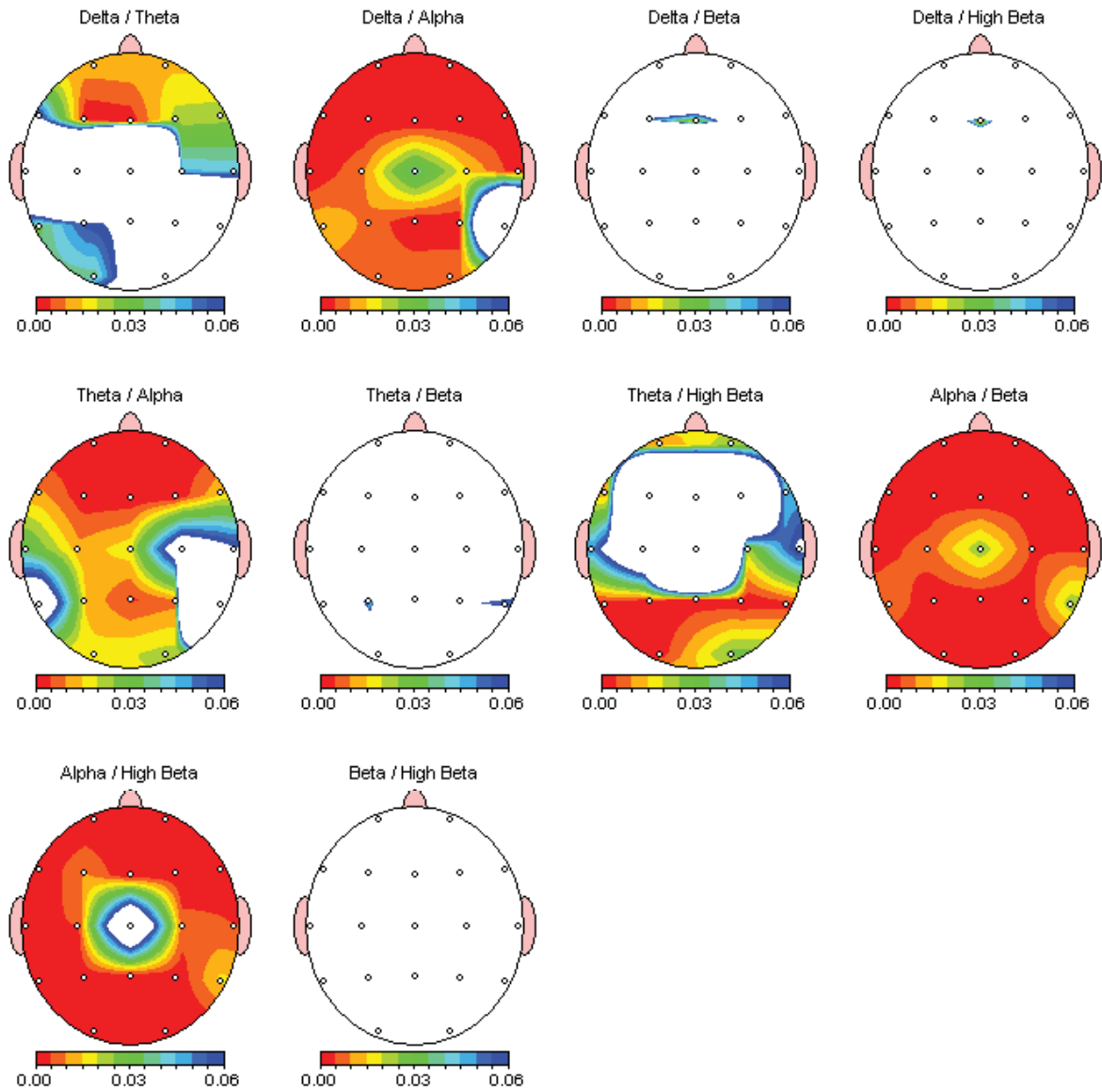


Figure C 16. Power ratios for the 100 Hz CES average reference montage. Color indicates a significant p -value between .00 and .05. White indicates no statistically significant result.

Table C 23

100 Hz CES Av. Ref FFT Relative Power Baseline Group Mean (%)

	Delta	Theta	Alpha	Beta	High Beta	Beta 1	Beta 2	Beta 3
	1.0 - 3.5 Hz	4.0 - 7.5 Hz	8.0 - 12.0 Hz	12.5 - 25.0 Hz	25.5 - 30.0 Hz	12.0 - 15.0 Hz	15.0 - 17.5 Hz	18.0 - 25.0 Hz
FP1	17.918	13.999	43.73	19.317	2.761	10.94	4.42	7.899
FP2	18.965	13.959	43.221	19.141	2.662	11.027	4.324	7.776
F3	13.241	14.329	47.287	21.43	2.284	11.783	5.06	8.99
F4	13.535	14.648	46.324	21.71	2.381	11.994	5.122	9.001
C3	13.085	14.784	43.269	24.308	2.915	11.655	5.656	11.186
C4	12.74	14.223	42.298	25.949	3.2	13.13	6.161	11.155
P3	11.69	11.737	48.106	25.292	2.075	13.389	5.787	10.877
P4	10.613	11.467	50.122	24.535	2.135	13.733	5.663	10.136
O1	8.478	9.199	59.511	20.844	1.241	13.685	4.357	7.941
O2	7.681	9.021	61.502	19.979	1.156	13.313	4.143	7.757
F7	18.697	16.066	41.53	19.538	2.445	10.749	4.532	7.993
F8	19.934	15.347	40.188	20.256	2.472	11.417	4.65	8.193
T3	14.532	15.849	37.513	25.898	3.326	12.365	6.63	10.734
T4	14.281	15.351	36.707	26.41	3.989	12.951	6.74	10.93
T5	9.974	11.356	49.9	25.684	1.88	13.352	6.512	10.526
T6	9.226	11.68	53.491	22.895	1.7	12.92	5.801	8.99
Fz	13.059	15.846	47.97	20.226	1.866	11.727	4.795	8.11
Cz	15.409	16.525	43.335	20.489	2.96	10.469	4.819	9.044
Pz	14.703	13.114	46.695	22.275	2.134	11.322	5.73	9.347

Table C 24

100 Hz CES Av. Ref. FFT Relative Power Baseline Group Standard Deviation (%)

	Delta	Theta	Alpha	Beta	High Beta	Beta 1	Beta 2	Beta 3
	1.0 - 3.5 Hz	4.0 - 7.5 Hz	8.0 - 12.0 Hz	12.5 - 25.0 Hz	25.5 - 30.0 Hz	12.0 - 15.0 Hz	15.0 - 17.5 Hz	18.0 - 25.0 Hz
FP1	6.857	4.052	13.965	9.578	2.368	11.712	3.019	3.897
FP2	7.077	4.051	13.278	9.134	2.074	11.626	2.739	3.489
F3	6.187	5.087	15.193	9.53	1.598	11.894	2.923	4.27
F4	5.285	4.705	14.185	9.952	1.751	12.169	2.913	4.241
C3	4.957	4.526	14.296	8.483	1.985	8.718	2.685	4.688
C4	5.744	5.084	14.871	11.522	1.871	10.654	3.935	4.873
P3	5.07	3.746	14.073	12.169	1.4	12.96	3.473	6.891
P4	4.798	4.733	15.799	12.594	1.587	11.981	4.708	6.414
O1	5.316	4.526	16.271	13.576	0.84	15.811	2.948	5.963
O2	4.746	4.77	16.552	13.245	0.817	15.077	3.288	6.099
F7	5.886	5.191	12.462	8.277	1.394	9.828	2.294	3.097
F8	6.417	4.686	11.57	7.831	1.417	10.64	1.974	2.713
T3	4.331	5.564	12.61	8.809	2.042	6.02	2.87	5.882
T4	5.438	5.683	13.479	9.729	3.956	7.932	2.313	5.605
T5	5.607	3.951	14.909	13.904	1.088	12.081	4.367	7.456
T6	4.179	4.732	13.963	12.11	1.195	10.595	3.986	6.16
Fz	6.06	5.96	15.593	10.507	1.499	12.491	3.109	4.512
Cz	6.461	5.151	15.274	9.513	2.943	10.531	2.632	5.272
Pz	6.381	3.989	14.837	10.802	1.625	9.319	4.047	5.974

Table C 25

100 Hz CES Av. Ref. FFT Relative Power Post CES Group Mean (%)

	Delta	Theta	Alpha	Beta	High Beta	Beta 1	Beta 2	Beta 3
	1.0 - 3.5 Hz	4.0 - 7.5 Hz	8.0 - 12.0 Hz	12.5 - 25.0 Hz	25.5 - 30.0 Hz	12.0 - 15.0 Hz	15.0 - 17.5 Hz	18.0 - 25.0 Hz
FP1	17.918	13.999	43.73	19.317	2.761	10.94	4.42	7.899
FP2	18.965	13.959	43.221	19.141	2.662	11.027	4.324	7.776
F3	13.241	14.329	47.287	21.43	2.284	11.783	5.06	8.99
F4	13.535	14.648	46.324	21.71	2.381	11.994	5.122	9.001
C3	13.085	14.784	43.269	24.308	2.915	11.655	5.656	11.186
C4	12.74	14.223	42.298	25.949	3.2	13.13	6.161	11.155
P3	11.69	11.737	48.106	25.292	2.075	13.389	5.787	10.877
P4	10.613	11.467	50.122	24.535	2.135	13.733	5.663	10.136
O1	8.478	9.199	59.511	20.844	1.241	13.685	4.357	7.941
O2	7.681	9.021	61.502	19.979	1.156	13.313	4.143	7.757
F7	18.697	16.066	41.53	19.538	2.445	10.749	4.532	7.993
F8	19.934	15.347	40.188	20.256	2.472	11.417	4.65	8.193
T3	14.532	15.849	37.513	25.898	3.326	12.365	6.63	10.734
T4	14.281	15.351	36.707	26.41	3.989	12.951	6.74	10.93
T5	9.974	11.356	49.9	25.684	1.88	13.352	6.512	10.526
T6	9.226	11.68	53.491	22.895	1.7	12.92	5.801	8.99
Fz	13.059	15.846	47.97	20.226	1.866	11.727	4.795	8.11
Cz	15.409	16.525	43.335	20.489	2.96	10.469	4.819	9.044
Pz	14.703	13.114	46.695	22.275	2.134	11.322	5.73	9.347

Table C 26

100 Hz CES Av. Ref. FFT Relative Power Post CES Group Standard Deviation (%)

	Delta	Theta	Alpha	Beta	High Beta	Beta 1	Beta 2	Beta 3
	1.0 - 3.5 Hz	4.0 - 7.5 Hz	8.0 - 12.0 Hz	12.5 - 25.0 Hz	25.5 - 30.0 Hz	12.0 - 15.0 Hz	15.0 - 17.5 Hz	18.0 - 25.0 Hz
FP1	6.857	4.052	13.965	9.578	2.368	11.712	3.019	3.897
FP2	7.077	4.051	13.278	9.134	2.074	11.626	2.739	3.489
F3	6.187	5.087	15.193	9.53	1.598	11.894	2.923	4.27
F4	5.285	4.705	14.185	9.952	1.751	12.169	2.913	4.241
C3	4.957	4.526	14.296	8.483	1.985	8.718	2.685	4.688
C4	5.744	5.084	14.871	11.522	1.871	10.654	3.935	4.873
P3	5.07	3.746	14.073	12.169	1.4	12.96	3.473	6.891
P4	4.798	4.733	15.799	12.594	1.587	11.981	4.708	6.414
O1	5.316	4.526	16.271	13.576	0.84	15.811	2.948	5.963
O2	4.746	4.77	16.552	13.245	0.817	15.077	3.288	6.099
F7	5.886	5.191	12.462	8.277	1.394	9.828	2.294	3.097
F8	6.417	4.686	11.57	7.831	1.417	10.64	1.974	2.713
T3	4.331	5.564	12.61	8.809	2.042	6.02	2.87	5.882
T4	5.438	5.683	13.479	9.729	3.956	7.932	2.313	5.605
T5	5.607	3.951	14.909	13.904	1.088	12.081	4.367	7.456
T6	4.179	4.732	13.963	12.11	1.195	10.595	3.986	6.16
Fz	6.06	5.96	15.593	10.507	1.499	12.491	3.109	4.512
Cz	6.461	5.151	15.274	9.513	2.943	10.531	2.632	5.272
Pz	6.381	3.989	14.837	10.802	1.625	9.319	4.047	5.974

APPENDIX D
LAPLACIAN MONTAGE

Montage: Laplacian

FFT Relative Power Group Paired t-Test (P-Value)

Intrahemispheric: LEFT

	DELTA	THETA	ALPHA	BETA	HIGH BETA	BETA 1	BETA 2	BETA 3
FP1 - CSD	0.391	0.720	0.022	0.795	0.205	0.360	0.653	0.913
F3 - CSD	0.561	0.068	0.000	0.511	0.026	0.258	0.691	0.567
C3 - CSD	0.699	0.462	0.276	0.841	0.154	0.182	0.669	0.878
P3 - CSD	0.022	0.823	0.022	0.004	0.005	0.252	0.105	0.000
O1 - CSD	0.967	0.271	0.769	0.076	0.048	0.231	0.662	0.003
F7 - CSD	0.445	0.259	0.000	0.767	0.141	0.595	0.758	0.769
T3 - CSD	0.423	0.205	0.032	0.366	0.041	0.715	0.946	0.116
T5 - CSD	0.545	0.095	0.569	0.379	0.054	0.703	0.990	0.058

Intrahemispheric: RIGHT

	DELTA	THETA	ALPHA	BETA	HIGH BETA	BETA 1	BETA 2	BETA 3
FP2 - CSD	0.641	0.267	0.004	0.750	0.282	0.727	0.647	0.654
F4 - CSD	0.585	0.273	0.020	0.604	0.153	0.399	0.937	0.557
C4 - CSD	0.426	0.991	0.002	0.195	0.026	0.134	0.040	0.573
P4 - CSD	0.254	0.649	0.046	0.005	0.005	0.046	0.048	0.001
O2 - CSD	0.435	0.808	0.353	0.527	0.068	0.732	0.856	0.307
F8 - CSD	0.504	0.649	0.009	0.412	0.065	0.526	0.758	0.346
T4 - CSD	0.247	0.269	0.031	0.720	0.520	0.710	0.578	0.627
T6 - CSD	0.595	0.086	0.138	0.161	0.410	0.287	0.247	0.152

Intrahemispheric: CENTER

	DELTA	THETA	ALPHA	BETA	HIGH BETA	BETA 1	BETA 2	BETA 3
Fz - CSD	0.530	0.643	0.008	0.499	0.066	0.094	0.253	0.848
Cz - CSD	0.215	0.864	0.019	0.133	0.002	0.023	0.014	0.389
Pz - CSD	0.116	0.941	0.097	0.020	0.018	0.022	0.043	0.037

Figure D 1. Relative power p -value tables for the 0.5 Hz CES Laplacian reference montage.

Table D 1

0.5 Hz CES Laplacian FFT Relative Power Group Paired t-Test (p-Value)

	Delta	Theta	Alpha	Beta	High Beta	Beta 1	Beta 2	Beta 3
	1.0 - 3.5 Hz	4.0 - 7.5 Hz	8.0 - 12.0 Hz	12.5 - 25.0 Hz	25.5 - 30.0 Hz	12.0 - 15.0 Hz	15.0 - 17.5 Hz	18.0 - 25.0 Hz
FP1	0.391	0.72	0.022	0.795	0.205	0.36	0.653	0.913
FP2	0.641	0.267	0.004	0.75	0.282	0.727	0.647	0.654
F3	0.561	0.068	0	0.511	0.026	0.258	0.691	0.567
F4	0.585	0.273	0.02	0.604	0.153	0.399	0.937	0.557
C3	0.699	0.452	0.276	0.841	0.154	0.182	0.669	0.878
C4	0.426	0.991	0.002	0.195	0.026	0.134	0.04	0.573
P3	0.022	0.823	0.022	0.004	0.005	0.252	0.105	0
P4	0.254	0.649	0.046	0.005	0.005	0.046	0.048	0.001
O1	0.967	0.271	0.769	0.076	0.048	0.231	0.662	0.003
O2	0.435	0.808	0.353	0.527	0.068	0.732	0.856	0.307
F7	0.445	0.259	0	0.767	0.141	0.595	0.758	0.769
F8	0.504	0.649	0.009	0.412	0.065	0.526	0.758	0.346
T3	0.423	0.205	0.032	0.366	0.041	0.715	0.946	0.116
T4	0.247	0.269	0.031	0.72	0.52	0.71	0.578	0.627
T5	0.545	0.095	0.569	0.379	0.054	0.703	0.99	0.058
T6	0.595	0.086	0.138	0.161	0.41	0.287	0.247	0.152
Fz	0.53	0.643	0.008	0.499	0.066	0.094	0.253	0.848
Cz	0.215	0.864	0.019	0.133	0.002	0.023	0.014	0.389
Pz	0.116	0.941	0.097	0.02	0.018	0.022	0.043	0.037

Table D 2

0.5 Hz CES Laplacian FFT Relative Power Group Paired t-Test (p-Value)

	1 Hz	2 Hz	3 Hz	4 Hz	5 Hz
FP1	0.355	0.333	0.913	0.855	0.863
FP2	0.351	0.989	0.776	0.879	0.231
F3	0.428	0.624	0.86	0.609	0.019
F4	0.49	0.344	0.839	0.962	0.287
C3	0.273	0.632	0.67	0.745	0.931
C4	0.428	0.322	0.288	0.102	0.222
P3	0.025	0.04	0.045	0.033	0.387
P4	0.169	0.3	0.733	0.273	0.582
O1	0.412	0.836	0.541	0.755	0.402
O2	0.232	0.575	0.487	0.882	0.913
F7	0.269	0.444	0.931	0.821	0.217
F8	0.303	0.876	0.519	0.894	0.985
T3	0.452	0.294	0.398	0.762	0.949
T4	0.119	0.455	0.408	0.593	0.956
T5	0.428	0.831	0.375	0.475	0.696
T6	0.528	0.644	0.549	0.69	0.863
Fz	0.254	0.908	0.453	0.916	0.403
Cz	0.472	0.173	0.068	0.13	0.868
Pz	0.082	0.199	0.32	0.093	0.913

Table D 3

0.5 Hz CES Laplacian FFT Relative Power Group Paired t-Test (p-Value)

	6 Hz	7 Hz	8 Hz	9 Hz	10 Hz
FP1	0.748	0.203	0.004	0.01	0.225
FP2	0.24	0.063	0.002	0.008	0.038
F3	0.167	0.038	0	0	0.009
F4	0.233	0.12	0.021	0.005	0.2
C3	0.529	0.044	0.054	0.287	0.981
C4	0.97	0.053	0.05	0.007	0.555
P3	0.954	0.059	0.062	0.008	0.128
P4	0.867	0.114	0.015	0.033	0.29
O1	0.154	0.271	0.814	0.709	0.837
O2	0.997	0.238	0.15	0.142	0.834
F7	0.45	0.077	0.002	0.021	0.011
F8	0.574	0.338	0.04	0.019	0.054
T3	0.077	0.003	0.009	0.018	0.229
T4	0.397	0.018	0.006	0.021	0.188
T5	0.278	0.016	0.011	0.462	0.067
T6	0.113	0.013	0.015	0.149	0.505
Fz	0.699	0.482	0.066	0.037	0.069
Cz	0.425	0.215	0.019	0.068	0.708
Pz	0.828	0.553	0.941	0.125	0.065

Table D 4

0.5 Hz CES Laplacian FFT Relative Power Group Paired t-Test (p-Value)

	11 Hz	12 Hz	13 Hz	14 Hz	15 Hz
FP1	0.413	0.413	0.584	0.263	0.664
FP2	0.545	0.907	0.944	0.376	0.233
F3	0.806	0.5	0.425	0.098	0.742
F4	0.415	0.662	0.194	0.597	0.713
C3	0.842	0.167	0.703	0.639	0.693
C4	0.119	0.681	0.067	0.008	0.011
P3	0.432	0.372	0.095	0.834	0.262
P4	0.523	0.082	0.006	0.209	0.4
O1	0.303	0.125	0.199	0.558	0.671
O2	0.939	0.712	0.488	0.736	0.759
F7	0.089	0.385	0.271	0.287	0.673
F8	0.107	0.4	0.432	0.274	0.604
T3	0.659	0.682	0.651	0.798	0.543
T4	0.282	0.801	0.781	0.842	0.472
T5	0.078	0.15	0.754	0.912	0.815
T6	0.787	0.408	0.264	0.23	0.399
Fz	0.496	0.793	0.087	0.064	0.059
Cz	0.849	0.976	0.006	0.014	0.012
Pz	0.716	0.087	0.003	0.176	0.134

Table D 5

0.5 Hz CES Laplacian FFT Relative Power Group Paired t-Test (p-Value)

	16 Hz	17 Hz	18 Hz	19 Hz	20 Hz
FP1	0.326	0.977	0.805	0.837	0.845
FP2	0.697	0.96	0.801	0.7	0.699
F3	0.856	0.502	0.836	0.689	0.755
F4	0.7	0.848	0.969	0.712	0.576
C3	0.844	0.606	0.665	0.592	0.783
C4	0.153	0.095	0.288	0.493	0.709
P3	0.186	0.058	0.056	0.008	0
P4	0.036	0.023	0.019	0	0.003
O1	0.664	0.228	0.154	0.067	0.007
O2	0.827	0.873	0.811	0.684	0.325
F7	0.749	0.861	0.934	0.478	0.879
F8	0.986	0.63	0.694	0.878	0.596
T3	0.886	0.712	0.509	0.27	0.084
T4	0.66	0.489	0.968	0.797	0.615
T5	0.851	0.649	0.695	0.153	0.023
T6	0.21	0.155	0.172	0.278	0.177
Fz	0.193	0.889	0.83	0.842	0.69
Cz	0.013	0.066	0.343	0.83	0.353
Pz	0.116	0.009	0.113	0.051	0.021

Table D 6

0.5 Hz CES Laplacian FFT Relative Power Group Paired t-Test (p-Value)

	21 Hz	22 Hz	23 Hz	24 Hz	25 Hz
FP1	0.766	0.965	0.871	0.968	0.442
FP2	0.478	0.421	0.412	0.743	0.479
F3	0.467	0.695	0.543	0.327	0.075
F4	0.577	0.327	0.525	0.413	0.164
C3	0.796	0.973	0.817	0.526	0.123
C4	0.626	0.562	0.796	0.32	0.124
P3	0	0.003	0.023	0.01	0.006
P4	0.005	0.001	0.008	0.011	0.009
O1	0.012	0.001	0.006	0.077	0.014
O2	0.146	0.282	0.034	0.311	0.037
F7	0.999	0.839	0.762	0.621	0.253
F8	0.112	0.279	0.224	0.117	0.055
T3	0.089	0.077	0.288	0.154	0.048
T4	0.401	0.528	0.431	0.419	0.239
T5	0.012	0.021	0.017	0.076	0.031
T6	0.05	0.319	0.082	0.207	0.261
Fz	0.899	0.886	0.949	0.186	0.332
Cz	0.444	0.533	0.625	0.161	0.047
Pz	0.045	0.092	0.028	0.032	0.093

Table D 7

0.5 Hz CES Laplacian FFT Relative Power Group Paired t-Test (p-Value)

	26 Hz	27 Hz	28 Hz	29 Hz	30 Hz
FP1	0.344	0.194	0.187	0.087	0.301
FP2	0.455	0.196	0.377	0.177	0.259
F3	0.028	0.018	0.023	0.044	0.088
F4	0.221	0.045	0.139	0.158	0.193
C3	0.172	0.17	0.205	0.114	0.145
C4	0.111	0.015	0.033	0.028	0.054
P3	0.006	0.008	0.007	0.013	0.027
P4	0.008	0.013	0.004	0.005	0.017
O1	0.004	0.158	0.124	0.08	0.206
O2	0.122	0.111	0.122	0.072	0.009
F7	0.155	0.274	0.081	0.148	0.165
F8	0.188	0.044	0.095	0.06	0.048
T3	0.021	0.028	0.02	0.091	0.147
T4	0.535	0.461	0.461	0.562	0.67
T5	0.02	0.024	0.038	0.137	0.179
T6	0.365	0.261	0.473	0.441	0.373
Fz	0.056	0.216	0.027	0.084	0.112
Cz	0.029	0.005	0.001	0.015	0.001
Pz	0.019	0.02	0.013	0.016	0.009

Table D 8

0.5 Hz CES Laplacian FFT Relative Power Group Paired t-Test (p-Value)

	31 Hz	32 Hz	33 Hz	34 Hz	35 Hz
FP1	0.151	0.285	0.412	0.312	0.323
FP2	0.183	0.208	0.191	0.14	0.216
F3	0.024	0.121	0.068	0.098	0.166
F4	0.232	0.398	0.293	0.272	0.455
C3	0.179	0.22	0.278	0.216	0.297
C4	0.037	0.136	0.204	0.266	0.073
P3	0.004	0.012	0.009	0.006	0.006
P4	0.006	0.004	0.016	0.016	0.026
O1	0.21	0.223	0.224	0.084	0.051
O2	0.112	0.199	0.232	0.188	0.073
F7	0.106	0.246	0.413	0.209	0.218
F8	0.089	0.178	0.124	0.124	0.096
T3	0.069	0.107	0.108	0.042	0.063
T4	0.508	0.797	0.604	0.663	0.546
T5	0.118	0.284	0.125	0.052	0.109
T6	0.44	0.566	0.408	0.444	0.491
Fz	0.061	0.176	0.107	0.101	0.093
Cz	0.001	0.003	0.014	0.024	0.021
Pz	0.011	0.008	0.007	0.014	0.02

Table D 9

0.5 Hz CES Laplacian FFT Relative Power Group Paired t-Test (p-Value)

	36 Hz	37 Hz	38 Hz	39 Hz	40 Hz
FP1	0.662	0.607	0.263	0.287	0.49
FP2	0.397	0.344	0.149	0.26	0.367
F3	0.161	0.184	0.097	0.151	0.076
F4	0.541	0.497	0.474	0.686	0.476
C3	0.632	0.354	0.35	0.21	0.366
C4	0.328	0.123	0.097	0.248	0.326
P3	0.022	0.021	0.013	0.045	0.033
P4	0.027	0.035	0.076	0.07	0.088
O1	0.112	0.1	0.135	0.095	0.289
O2	0.2	0.056	0.148	0.201	0.419
F7	0.358	0.287	0.187	0.264	0.351
F8	0.111	0.178	0.137	0.168	0.242
T3	0.221	0.12	0.075	0.075	0.075
T4	0.618	0.492	0.415	0.448	0.76
T5	0.154	0.134	0.109	0.186	0.092
T6	0.552	0.297	0.335	0.491	0.705
Fz	0.09	0.18	0.096	0.131	0.151
Cz	0.014	0.011	0.013	0.006	0.011
Pz	0.016	0.018	0.009	0.006	0.033

Montage: Laplacian

FFT Relative Power Group Paired t-Test (P-Value)

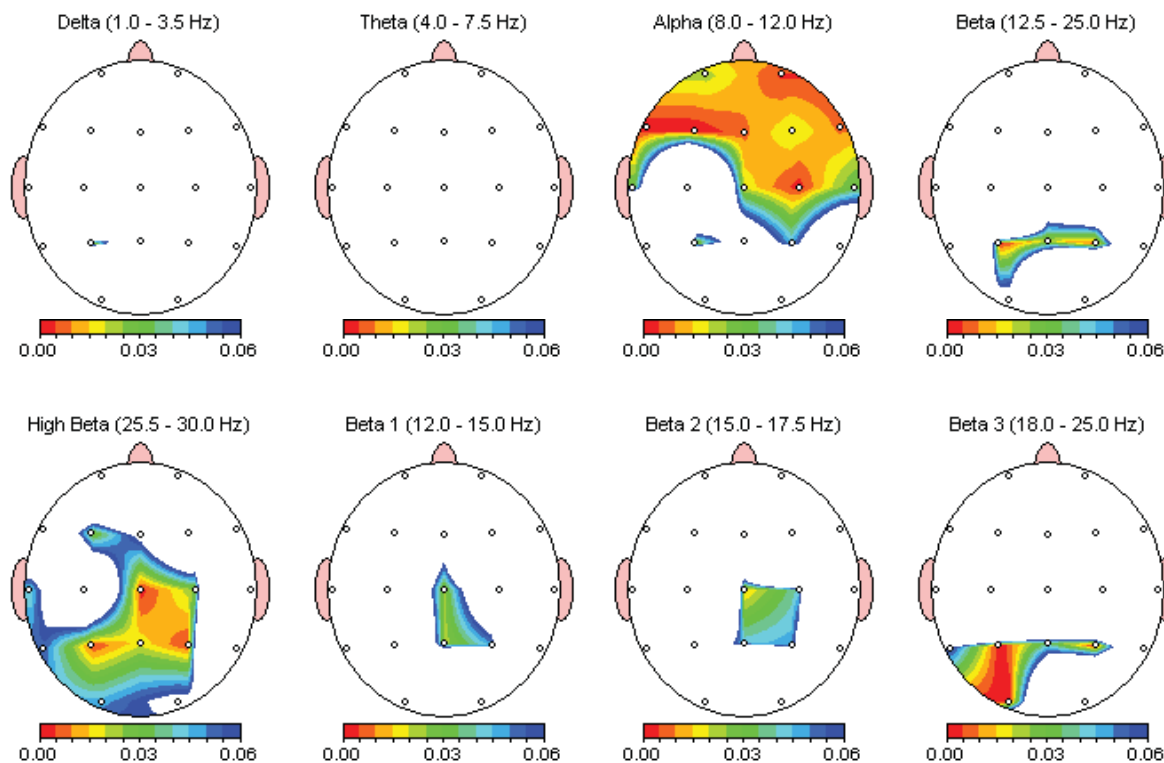


Figure D 2. Relative power p -value topographical map for the 0.5 Hz CES Laplacian reference montage.

Montage: Laplacian

FFT Relative Power Group Paired t-Test (P-Value)

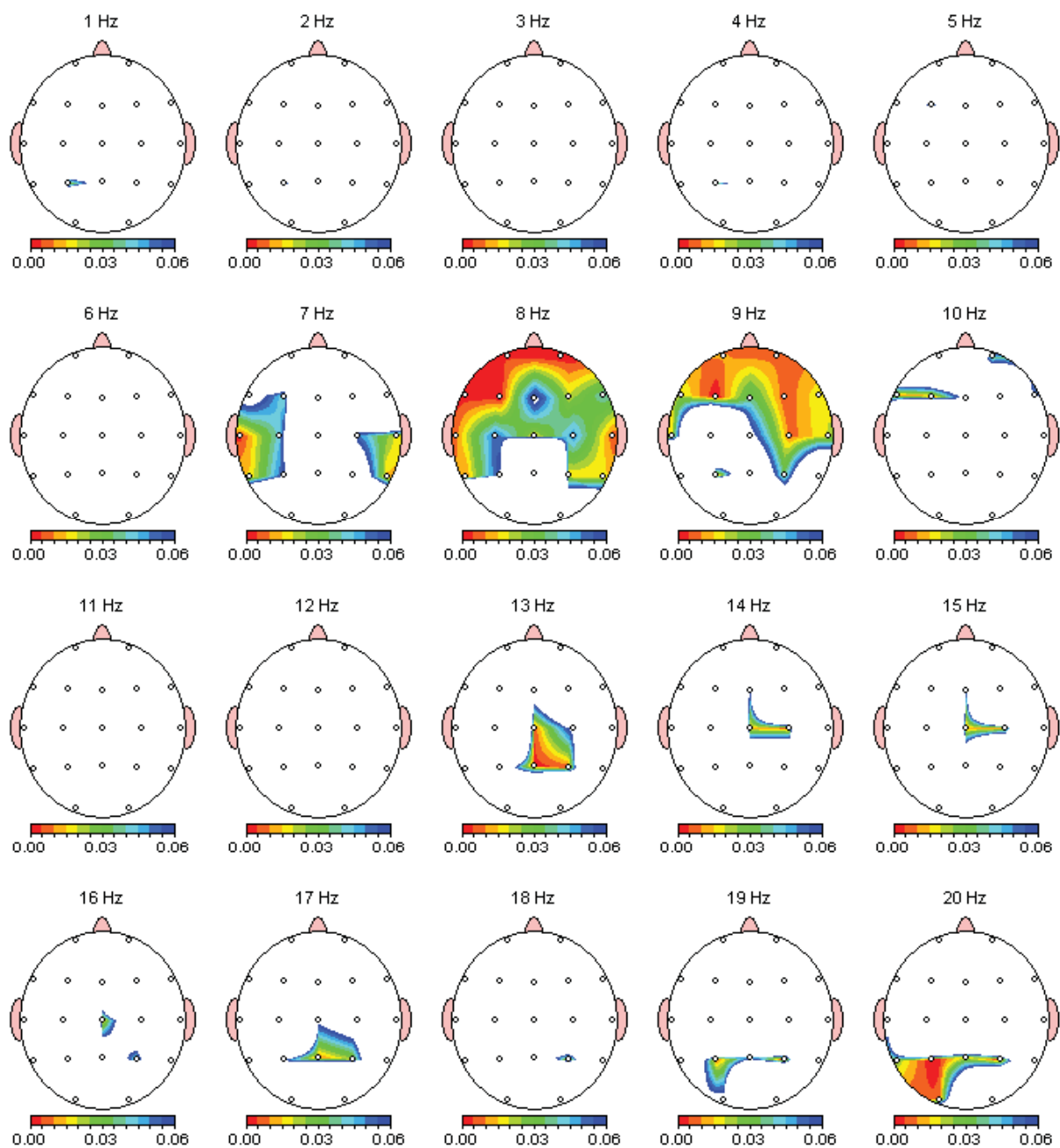


Figure D 3. Relative power p -value topographical map for the 0.5 Hz CES Laplacian reference montage.

Montage: Laplacian

FFT Relative Power Group Paired t-Test (P-Value)

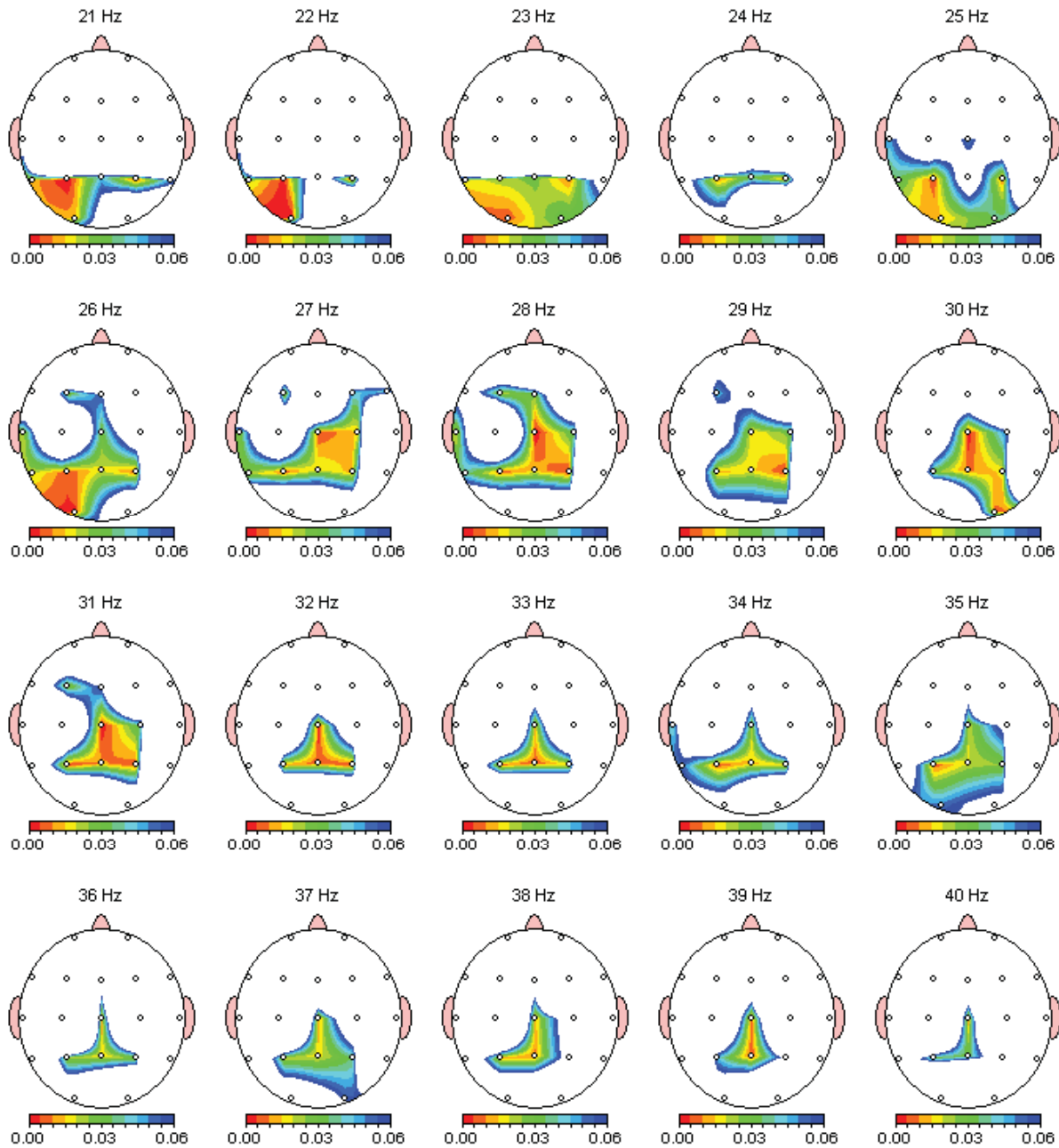


Figure D 4. Relative power p -value topographical map for the 0.5 Hz CES Laplacian reference montage.

Montage: Laplacian

FFT Coherence Group Paired t-Test (P-Value)

Intrahemispheric: LEFT

	DELTA	THETA	ALPHA	BETA
FP1 F3	0.526	0.476	0.002	0.307
FP1 C3	0.623	0.691	0.542	0.896
FP1 P3	0.675	0.016	0.136	0.877
FP1 O1	0.732	0.847	0.339	0.866
FP1 F7	0.935	0.528	0.010	0.944
FP1 T3	0.922	0.652	0.072	0.700
FP1 T5	0.999	0.034	0.246	0.883
F3 C3	0.365	0.139	0.865	0.030
F3 P3	0.818	0.286	0.012	0.595
F3 O1	0.722	0.466	0.030	0.021
F3 F7	0.220	0.706	0.147	0.435
F3 T3	0.350	0.536	0.384	0.581
F3 T5	0.141	0.175	0.048	0.024
C3 P3	0.566	0.202	0.475	0.759
C3 O1	0.427	0.721	0.898	0.850
C3 F7	0.390	0.637	0.990	0.230
C3 T3	0.342	0.261	0.424	0.447
C3 T5	0.820	0.681	0.488	0.851
P3 O1	0.376	0.088	0.116	0.910
P3 F7	0.779	0.032	0.166	0.199
P3 T3	0.333	0.415	0.149	0.360
P3 T5	0.688	0.040	0.645	0.541
O1 F7	0.598	0.680	0.076	0.879
O1 T3	0.562	0.377	0.029	0.382
O1 T5	0.534	0.994	0.508	0.226
F7 T3	0.807	0.427	0.005	0.266
F7 T5	0.168	0.361	0.679	0.904
T3 T5	0.965	0.504	0.576	0.796

Intrahemispheric: RIGHT

	DELTA	THETA	ALPHA	BETA
FP2 F4	0.053	0.106	0.001	0.595
FP2 C4	0.652	0.534	0.260	0.344
FP2 P4	0.260	0.027	0.057	0.411
FP2 O2	0.817	0.884	0.873	0.280
FP2 F8	0.369	0.956	0.056	0.017
FP2 T4	0.496	0.315	0.042	0.249
FP2 T6	0.695	0.012	0.001	0.486
F4 C4	0.994	0.453	0.825	0.767
F4 P4	0.947	0.035	0.013	0.776
F4 O2	0.067	0.479	0.063	0.572
F4 F8	0.449	0.717	0.175	0.667
F4 T4	0.928	0.794	0.236	0.740
F4 T6	0.095	0.939	0.014	0.253
C4 P4	0.887	0.728	0.629	0.614
C4 O2	0.822	0.274	0.543	0.217
C4 F8	0.566	0.170	0.201	0.417
C4 T4	0.274	0.200	0.700	0.383
C4 T6	0.502	0.392	0.132	0.667
P4 O2	0.381	0.597	0.068	0.272
P4 F8	0.373	0.232	0.030	0.626
P4 T4	0.997	0.750	0.055	0.410
P4 T6	0.817	0.678	0.060	0.332
O2 F8	0.538	0.769	0.492	0.350
O2 T4	0.517	0.796	0.774	0.715
O2 T6	0.353	0.174	0.238	0.045
F8 T4	0.439	0.715	0.016	0.300
F8 T6	0.692	0.179	0.067	0.324
T4 T6	0.504	0.557	0.661	0.912

Interhemispheric: HOMOLOGOUS PAIRS

	DELTA	THETA	ALPHA	BETA
FP1 FP2	0.541	0.828	0.010	0.909
C3 C4	0.815	0.168	0.820	0.081
O1 O2	0.799	0.220	0.173	0.634
T3 T4	0.941	0.953	0.050	0.654

	DELTA	THETA	ALPHA	BETA
F3 F4	0.222	0.010	0.003	0.469
P3 P4	0.408	0.130	0.004	0.145
F7 F8	0.980	0.880	0.000	0.084
T5 T6	0.154	0.796	0.075	0.127

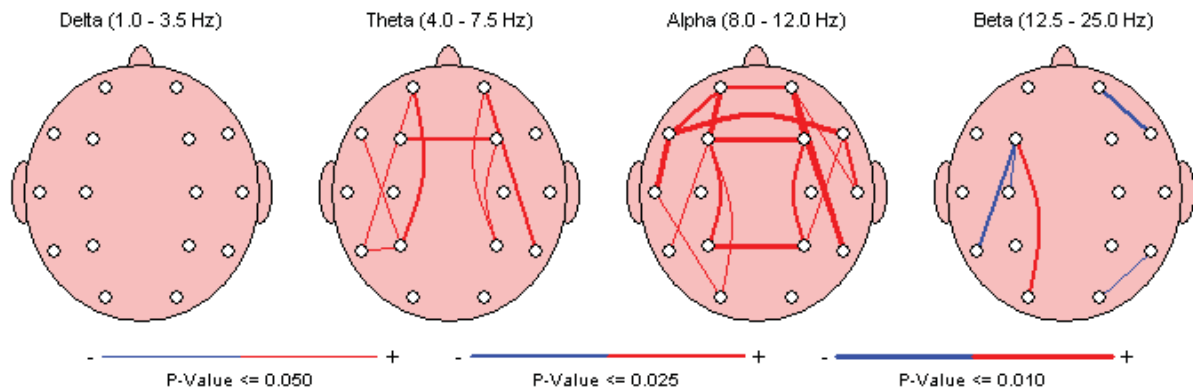


Figure D 5. Coherence tables and maps for the 0.5 Hz CES Laplacian reference montage.

Montage: Laplacian

FFT Amplitude Asymmetry Group Paired t-Test (P-Value)

Intrahemispheric: LEFT

	DELTA	THETA	ALPHA	BETA
FP1 F3	0.802	0.878	0.184	0.146
FP1 C3	0.882	0.456	0.191	0.693
FP1 P3	0.806	0.327	0.620	0.558
FP1 O1	0.249	0.255	0.438	0.499
FP1 F7	0.868	0.854	0.382	0.580
FP1 T3	0.995	0.747	0.082	0.526
FP1 T5	0.570	0.158	0.085	0.691
F3 C3	0.675	0.434	0.320	0.345
F3 P3	0.803	0.213	0.373	0.311
F3 O1	0.137	0.272	0.989	0.522
F3 F7	0.724	0.871	0.589	0.319
F3 T3	0.894	0.783	0.822	0.894
F3 T5	0.263	0.116	0.790	0.434
C3 P3	0.627	0.065	0.232	0.705
C3 O1	0.198	0.082	0.730	0.944
C3 F7	0.641	0.417	0.173	0.993
C3 T3	0.736	0.234	0.545	0.463
C3 T5	0.499	0.043	0.655	0.778
P3 O1	0.053	0.746	0.244	0.861
P3 F7	0.832	0.323	0.658	0.945
P3 T3	0.905	0.545	0.193	0.565
P3 T5	0.146	0.570	0.123	0.962
O1 F7	0.274	0.170	0.849	0.951
O1 T3	0.125	0.245	0.959	0.634
O1 T5	0.283	0.965	0.935	0.920
F7 T3	0.799	0.760	0.528	0.619
F7 T5	0.532	0.159	0.462	0.935
T3 T5	0.349	0.354	0.632	0.319

Intrahemispheric: RIGHT

	DELTA	THETA	ALPHA	BETA
FP2 F4	0.392	0.404	0.318	0.523
FP2 C4	0.875	0.704	0.728	0.765
FP2 P4	0.184	0.015	0.267	0.517
FP2 O2	0.654	0.786	0.336	0.935
FP2 F8	0.818	0.237	0.277	0.922
FP2 T4	0.866	0.647	0.873	0.722
FP2 T6	0.257	0.112	0.693	0.820
F4 C4	0.877	0.343	0.431	0.993
F4 P4	0.331	0.147	0.272	0.791
F4 O2	0.830	0.530	0.571	0.911
F4 F8	0.530	0.062	0.764	0.532
F4 T4	0.502	0.838	0.849	0.965
F4 T6	0.466	0.523	0.828	0.955
C4 P4	0.398	0.058	0.375	0.385
C4 O2	0.785	0.954	0.499	0.988
C4 F8	0.748	0.869	0.892	0.600
C4 T4	0.478	0.448	0.623	0.976
C4 T6	0.620	0.229	0.916	0.841
P4 O2	0.305	0.045	0.104	0.317
P4 F8	0.304	0.006	0.098	0.356
P4 T4	0.125	0.098	0.245	0.754
P4 T6	0.854	0.611	0.336	0.305
O2 F8	0.918	0.483	0.730	0.762
O2 T4	0.625	0.632	0.235	0.885
O2 T6	0.410	0.108	0.321	0.815
F8 T4	0.806	0.257	0.437	0.468
F8 T6	0.292	0.058	0.854	0.553
T4 T6	0.069	0.227	0.976	0.887

Interhemispheric: HOMOLOGOUS PAIRS

	DELTA	THETA	ALPHA	BETA
FP1 FP2	0.823	0.988	0.719	0.093
C3 C4	0.417	0.450	0.118	0.772
O1 O2	0.085	0.123	0.884	0.942
T3 T4	0.918	0.808	0.137	0.553

	DELTA	THETA	ALPHA	BETA
F3 F4	0.091	0.122	0.772	0.308
P3 P4	0.121	0.094	0.068	0.207
F7 F8	0.780	0.143	0.972	0.500
T5 T6	0.603	0.801	0.236	0.627

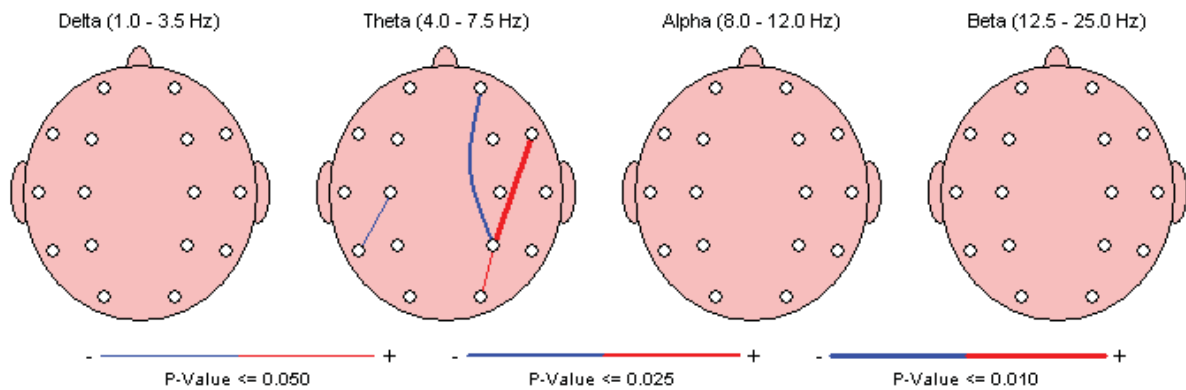


Figure D 6. Amplitude asymmetry for the 0.5 Hz CES Laplacian reference montage.

Montage: Laplacian

FFT Phase Lag Group Paired t-Test (P-Value)

Intrahemispheric: LEFT

	DELTA	THETA	ALPHA	BETA
FP1 F3	0.046	0.260	0.436	0.370
FP1 C3	0.302	0.779	0.669	0.171
FP1 P3	0.388	0.597	0.622	0.486
FP1 O1	0.891	0.330	0.198	0.582
FP1 F7	0.835	0.159	0.586	0.165
FP1 T3	0.316	0.313	0.678	0.439
FP1 T5	0.155	0.013	0.051	0.551
F3 C3	0.257	0.401	0.517	0.701
F3 P3	0.601	0.926	0.167	0.451
F3 O1	0.874	0.667	0.790	0.460
F3 F7	0.146	0.333	0.708	0.088
F3 T3	0.794	0.957	0.520	0.901
F3 T5	0.614	0.661	0.822	0.381
C3 P3	0.750	0.246	0.022	0.855
C3 O1	0.037	0.147	0.571	0.943
C3 F7	0.652	0.053	0.190	0.328
C3 T3	0.645	0.048	0.130	0.708
C3 T5	0.188	0.747	0.509	0.271
P3 O1	0.918	0.119	0.283	0.129
P3 F7	0.819	0.138	0.185	0.754
P3 T3	0.703	0.420	0.511	0.146
P3 T5	0.641	0.493	0.237	0.267
O1 F7	0.391	0.120	0.414	0.919
U1 I3	0.353	0.548	0.304	0.195
O1 T5	0.615	0.922	0.313	0.461
F7 T3	0.906	0.827	0.947	0.099
F7 T5	0.215	0.780	0.026	0.656
T3 T5	0.477	0.133	0.290	0.428

Intrahemispheric: RIGHT

	DELTA	THETA	ALPHA	BETA
FP2 F4	0.051	0.641	0.198	0.166
FP2 C4	0.680	0.638	0.675	0.410
FP2 P4	0.259	0.270	0.596	0.424
FP2 O2	0.050	0.462	0.738	0.332
FP2 F8	0.269	0.383	0.518	0.135
FP2 T4	0.097	0.803	0.539	0.071
FP2 T6	0.949	0.297	0.633	0.173
F4 C4	0.780	0.167	0.012	0.835
F4 P4	0.325	0.223	0.238	0.723
F4 O2	0.635	0.992	0.323	0.720
F4 F8	0.810	0.313	0.748	0.574
F4 T4	0.758	0.144	0.022	0.277
F4 T6	0.356	0.570	0.926	0.387
C4 P4	0.008	0.875	0.160	0.098
C4 O2	0.498	0.908	0.794	0.585
C4 F8	0.341	0.779	0.761	0.410
C4 T4	0.241	0.474	0.244	0.103
C4 T6	0.755	0.471	0.658	0.285
P4 O2	0.819	0.382	0.336	0.372
P4 F8	0.982	0.411	0.363	0.645
P4 T4	0.772	0.077	0.226	0.664
P4 T6	0.856	0.481	0.816	0.876
O2 F8	0.750	0.120	0.888	0.744
U2 I4	0.664	0.525	0.684	0.016
O2 T6	0.927	0.539	0.732	0.498
F8 T4	0.810	0.718	0.913	0.802
F8 T6	0.854	0.078	0.409	0.139
T4 T6	0.404	0.231	0.406	0.782

Interhemispheric: HOMOLOGOUS PAIRS

	DELTA	THETA	ALPHA	BETA
FP1 FP2	0.107	0.608	0.545	0.042
C3 C4	0.978	0.728	0.481	0.984
O1 O2	0.809	0.368	0.395	0.006
T3 T4	0.611	0.641	0.347	0.623

	DELTA	THETA	ALPHA	BETA
F3 F4	0.034	0.214	0.873	0.106
P3 P4	0.631	0.289	0.062	0.523
F7 F8	0.112	0.228	0.330	0.095
T5 T6	0.200	0.603	0.199	0.227

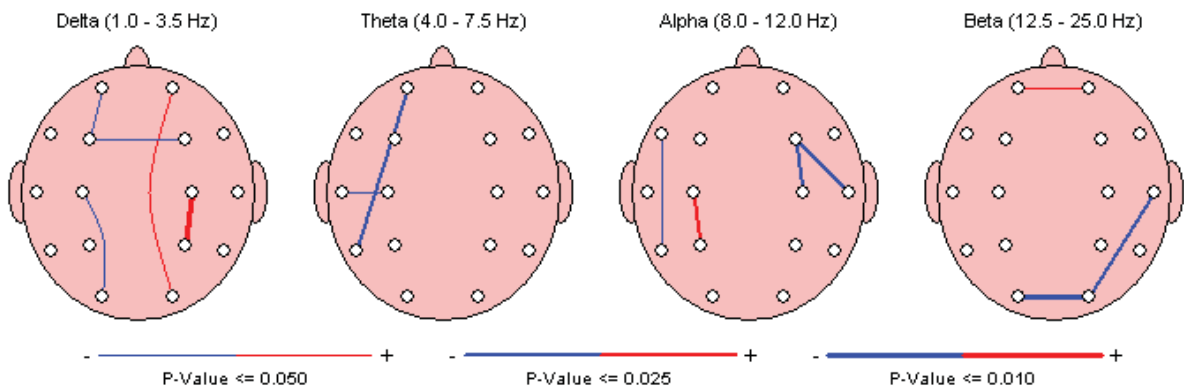


Figure D 7. Phase lag for the 0.5 Hz CES Laplacian reference montage.

Montage: Laplacian

FFT Power Ratio Group Paired t-Test (P-Value)

Intrahemispheric: LEFT

	D/T	D/A	D/B	D/G	T/A	T/B	T/G	A/B	A/G	B/G
FP1 - CSD	0.158	0.015	0.543	0.691	0.018	0.947	0.318	0.149	0.044	0.026
F3 - CSD	0.047	0.003	0.947	0.256	0.083	0.202	0.021	0.019	0.001	0.000
C3 - CSD	0.197	0.357	0.710	0.466	0.716	0.738	0.140	0.574	0.151	0.013
P3 - CSD	0.003	0.017	0.310	0.597	0.266	0.019	0.003	0.003	0.004	0.048
O1 - CSD	0.402	0.933	0.476	0.314	0.628	0.066	0.037	0.267	0.162	0.123
F7 - CSD	0.122	0.008	0.791	0.473	0.014	0.463	0.135	0.046	0.017	0.035
T3 - CSD	0.001	0.080	0.899	0.371	0.573	0.235	0.054	0.045	0.009	0.018
T5 - CSD	0.112	0.487	0.958	0.397	0.436	0.161	0.048	0.417	0.125	0.011

Intrahemispheric: RIGHT

	D/T	D/A	D/B	D/G	T/A	T/B	T/G	A/B	A/G	B/G
FP2 - CSD	0.068	0.004	0.904	0.657	0.003	0.402	0.216	0.036	0.032	0.187
F4 - CSD	0.036	0.030	0.925	0.547	0.383	0.348	0.140	0.122	0.054	0.045
C4 - CSD	0.297	0.018	0.989	0.373	0.014	0.418	0.080	0.006	0.003	0.045
P4 - CSD	0.145	0.128	0.869	0.313	0.283	0.014	0.004	0.005	0.004	0.052
O2 - CSD	0.170	0.371	0.632	0.872	0.694	0.528	0.094	0.252	0.065	0.039
F8 - CSD	0.228	0.010	0.972	0.348	0.006	0.487	0.147	0.031	0.014	0.019
T4 - CSD	0.011	0.030	0.519	0.906	0.169	0.419	0.381	0.072	0.137	0.503
T6 - CSD	0.088	0.275	0.797	0.869	0.680	0.077	0.183	0.011	0.071	0.861

Intrahemispheric: CENTER

	D/T	D/A	D/B	D/G	T/A	T/B	T/G	A/B	A/G	B/G
Fz - CSD	0.469	0.067	0.906	0.528	0.131	0.443	0.091	0.052	0.016	0.012
Cz - CSD	0.220	0.019	0.994	0.194	0.109	0.256	0.021	0.013	0.000	0.011
Pz - CSD	0.072	0.088	0.975	0.386	0.277	0.036	0.027	0.007	0.015	0.133

Figure D 8. Power ratios for the 0.5 Hz CES Laplacian reference montage.

Montage: Laplacian

FFT Power Ratio Group Paired t-Test (P-Value)

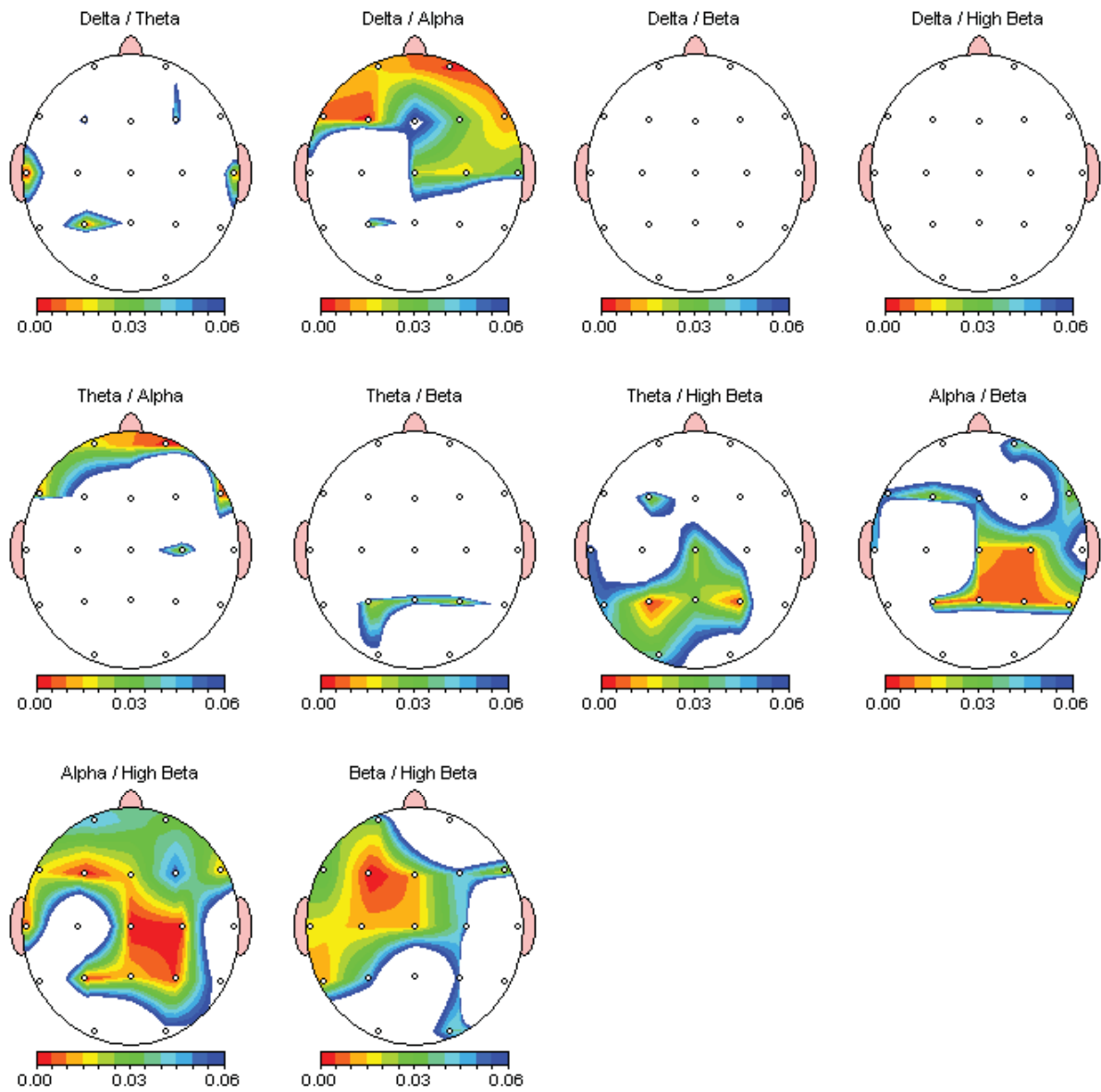


Figure D 9. Power ratios for the 0.5 Hz CES Laplacian reference montage.

Montage: Laplacian

FFT Relative Power Group Paired t-Test (P-Value)

Intrahemispheric: LEFT

	DELTA	THETA	ALPHA	BETA	HIGH BETA	BETA 1	BETA 2	BETA 3
FP1 - CSD	0.016	0.608	0.001	0.174	0.248	0.020	0.478	0.439
F3 - CSD	0.092	0.668	0.021	0.248	0.811	0.497	0.323	0.344
C3 - CSD	0.904	0.164	0.070	0.006	0.007	0.000	0.748	0.213
P3 - CSD	0.249	0.145	0.373	0.039	0.019	0.001	0.724	0.091
O1 - CSD	0.232	0.238	0.002	0.003	0.000	0.004	0.210	0.017
F7 - CSD	0.041	0.610	0.047	0.607	0.121	0.787	0.699	0.589
T3 - CSD	0.950	0.383	0.017	0.027	0.051	0.067	0.241	0.132
T5 - CSD	0.538	0.749	0.010	0.055	0.000	0.200	0.567	0.016

Intrahemispheric: RIGHT

	DELTA	THETA	ALPHA	BETA	HIGH BETA	BETA 1	BETA 2	BETA 3
FP2 - CSD	0.011	0.961	0.060	0.805	0.747	0.746	0.110	0.868
F4 - CSD	0.001	0.091	0.195	0.016	0.848	0.382	0.027	0.052
C4 - CSD	0.509	0.417	0.167	0.682	0.711	0.080	0.170	0.283
P4 - CSD	0.445	0.841	0.100	0.001	0.005	0.000	0.252	0.011
O2 - CSD	0.925	0.905	0.015	0.001	0.000	0.012	0.921	0.037
F8 - CSD	0.002	0.572	0.045	0.266	0.742	0.335	0.008	0.322
T4 - CSD	0.311	0.987	0.308	0.475	0.168	0.120	0.944	0.653
T6 - CSD	0.843	0.448	0.011	0.005	0.000	0.006	0.107	0.021

Intrahemispheric: CENTER

	DELTA	THETA	ALPHA	BETA	HIGH BETA	BETA 1	BETA 2	BETA 3
Fz - CSD	0.011	0.193	0.001	0.587	0.786	0.332	0.375	0.098
Cz - CSD	0.874	0.012	0.037	0.220	0.696	0.000	0.592	0.778
Pz - CSD	0.070	0.195	0.004	0.004	0.000	0.002	0.017	0.052

Figure D 10. Relative power table for the 100 Hz CES Laplacian reference montage.

Table D 10

100 Hz CES Laplacian FFT Relative Power Group Paired t-Test (p-Value)

	Delta	Theta	Alpha	Beta	High Beta	Beta 1	Beta 2	Beta 3
	1.0 - 3.5 Hz	4.0 - 7.5 Hz	8.0 - 12.0 Hz	12.5 - 25.0 Hz	25.5 - 30.0 Hz	12.0 - 15.0 Hz	15.0 - 17.5 Hz	18.0 - 25.0 Hz
FP1	0.016	0.608	0.001	0.174	0.248	0.02	0.478	0.439
FP2	0.011	0.961	0.06	0.805	0.747	0.745	0.11	0.868
F3	0.092	0.668	0.021	0.248	0.811	0.497	0.323	0.344
F4	0.001	0.091	0.195	0.016	0.848	0.382	0.027	0.052
C3	0.904	0.164	0.07	0.006	0.007	0	0.748	0.213
C4	0.509	0.417	0.167	0.682	0.711	0.08	0.17	0.283
P3	0.249	0.145	0.373	0.039	0.019	0.001	0.724	0.091
P4	0.445	0.841	0.1	0.001	0.005	0	0.252	0.011
O1	0.232	0.238	0.002	0.003	0	0.004	0.21	0.017
O2	0.925	0.905	0.015	0.001	0	0.012	0.921	0.037
F7	0.041	0.61	0.047	0.607	0.121	0.787	0.699	0.589
F8	0.002	0.572	0.045	0.266	0.742	0.335	0.008	0.322
T3	0.95	0.383	0.017	0.027	0.051	0.067	0.241	0.132
T4	0.311	0.987	0.308	0.475	0.168	0.12	0.944	0.653
T5	0.538	0.749	0.01	0.055	0	0.2	0.567	0.016
T6	0.843	0.448	0.011	0.005	0	0.006	0.107	0.021
Fz	0.011	0.193	0.001	0.587	0.786	0.332	0.375	0.098
Cz	0.874	0.012	0.037	0.22	0.696	0	0.592	0.778
Pz	0.07	0.195	0.004	0.004	0	0.002	0.017	0.052

Table D 11

100 Hz CES Laplacian FFT Relative Power Group Paired t-Test (p-Value)

	1 Hz	2 Hz	3 Hz	4 Hz	5 Hz
FP1	0.051	0.013	0.669	0.687	0.836
FP2	0.066	0.087	0.038	0.062	0.082
F3	0.167	0.072	0.275	0.204	0.975
F4	0.171	0	0.03	0.008	0.016
C3	0.75	0.443	0.097	0.098	0.081
C4	0.68	0.397	0.222	0.824	0.962
P3	0.397	0.137	0.732	0.632	0.406
P4	0.411	0.612	0.384	0.259	0.163
O1	0.289	0.203	0.249	0.372	0.163
O2	0.822	0.911	0.898	0.853	0.521
F7	0.081	0.087	0.683	0.137	0.315
F8	0.028	0.001	0.102	0.182	0.46
T3	0.877	0.581	0.609	0.521	0.859
T4	0.547	0.237	0.024	0.078	0.658
T5	0.621	0.654	0.265	0.522	0.754
T6	0.917	0.815	0.194	0.386	0.869
Fz	0.242	0.008	0.004	0.005	0.001
Cz	0.827	0.962	0.176	0.001	0.037
Pz	0.143	0.099	0.079	0.031	0.033

Table D 12

100 Hz CES Laplacian FFT Relative Power Group Paired t-Test (p-Value)

	6 Hz	7 Hz	8 Hz	9 Hz	10 Hz
FP1	0.591	0.02	0.022	0.039	0.108
FP2	0.27	0.014	0.007	0.194	0.345
F3	0.408	0.151	0.338	0.024	0.304
F4	0.79	0.621	0.768	0.31	0.521
C3	0.94	0.8	0.75	0.017	0.036
C4	0.283	0.11	0.022	0.002	0.055
P3	0.495	0.048	0.012	0.307	0.608
P4	0.753	0.121	0.004	0.37	0.421
O1	0.049	0.579	0.785	0.223	0.137
O2	0.341	0.997	0.639	0.873	0.093
F7	0.88	0.141	0.141	0.063	0.586
F8	0.458	0.044	0.651	0.756	0.021
T3	0.388	0.063	0.174	0.039	0.067
T4	0.566	0.182	0.035	0.198	0.363
T5	0.861	0.233	0.009	0.07	0.552
T6	0.816	0.201	0.206	0.683	0.194
Fz	0.385	0.125	0.017	0.003	0.247
Cz	0.048	0.446	0.011	0.022	0.037
Pz	0.302	0.506	0.008	0	0.012

Table D 13

100 Hz CES Laplacian FFT Relative Power Group Paired t-Test (p-Value)

	11 Hz	12 Hz	13 Hz	14 Hz	15 Hz
FP1	0.367	0.239	0.03	0.213	0.67
FP2	0.386	0.231	0.576	0.906	0.102
F3	0.088	0.646	0.563	0.332	0.906
F4	0.797	0.316	0.233	0.052	0.051
C3	0.693	0	0.001	0.001	0.073
C4	0.337	0.134	0.163	0.682	0.15
P3	0.254	0.003	0.004	0.118	0.487
P4	0.738	0	0	0.022	0.118
O1	0.465	0.005	0.012	0.008	0.1
O2	0.871	0.085	0.001	0.069	0.476
F7	0.401	0.571	0.343	0.905	0.8
F8	0.968	0.023	0.27	0.321	0.025
T3	0.893	0.028	0.153	0.268	0.046
T4	0.766	0.005	0.241	0.49	0.94
T5	0.485	0.186	0.093	0.536	0.424
T6	0.89	0.002	0.001	0.048	0.562
Fz	0.224	0.719	0.083	0.858	0.905
Cz	0.792	0	0.01	0.149	0.997
Pz	0.565	0.035	0.005	0.001	0.017

Table D 14

100 Hz CES Laplacian FFT Relative Power Group Paired t-Test (p-Value)

	16 Hz	17 Hz	18 Hz	19 Hz	20 Hz
FP1	0.999	0.193	0.509	0.238	0.6
FP2	0.118	0.414	0.84	0.059	0.961
F3	0.435	0.045	0.067	0.095	0.952
F4	0.079	0.013	0.047	0.027	0.266
C3	0.824	0.65	0.933	0.887	0.625
C4	0.31	0.091	0.077	0.205	0.009
P3	0.769	0.282	0.997	0.723	0.15
P4	0.178	0.953	0.66	0.086	0.067
O1	0.439	0.443	0.069	0.034	0.029
O2	0.579	0.807	0.614	0.048	0.095
F7	0.528	0.365	0.598	0.814	0.642
F8	0.002	0.103	0.074	0.382	0.079
T3	0.587	0.617	0.293	0.187	0.156
T4	0.685	0.897	0.411	0.161	0.391
T5	0.971	0.57	0.409	0.045	0.064
T6	0.295	0.012	0.004	0.019	0.083
Fz	0.49	0.157	0.24	0.133	0.102
Cz	0.076	0.924	0.411	0.767	0.835
Pz	0.028	0.05	0.073	0.295	0.325

Table D 15

100 Hz CES Laplacian FFT Relative Power Group Paired t-Test (p-Value)

	21 Hz	22 Hz	23 Hz	24 Hz	25 Hz
FP1	0.421	0.039	0.264	0.978	0.975
FP2	0.922	0.481	0.605	0.806	0.388
F3	0.389	0.495	0.888	0.508	0.79
F4	0.234	0.188	0.027	0.39	0.441
C3	0.497	0.596	0.128	0	0.014
C4	0.26	0.303	0.747	0.592	0.59
P3	0.05	0.489	0.002	0.045	0.047
P4	0.01	0.014	0	0.001	0.007
O1	0.113	0.258	0.045	0.001	0
O2	0.202	0.273	0.009	0	0.001
F7	0.597	0.55	0.969	0.501	0.087
F8	0.876	0.313	0.61	0.199	0.539
T3	0.189	0.335	0.652	0.218	0.057
T4	0.705	0.948	0.851	0.57	0.117
T5	0	0.029	0.057	0.007	0.002
T6	0.155	0.257	0.028	0.028	0.012
Fz	0.165	0.993	0.084	0.584	0.982
Cz	0.873	0.381	0.738	0.437	0.758
Pz	0.069	0.007	0.164	0.04	0.001

Table D 16

100 Hz CES Laplacian FFT Relative Power Group Paired t-Test (p-Value)

	26 Hz	27 Hz	28 Hz	29 Hz	30 Hz
FP1	0.625	0.423	0.362	0.07	0.067
FP2	0.992	0.744	0.723	0.408	0.943
F3	0.603	0.614	0.642	0.675	0.713
F4	0.4	0.665	0.876	0.945	0.282
C3	0.018	0.073	0.025	0.003	0.024
C4	0.196	0.65	0.712	0.23	0.856
P3	0.178	0.063	0.041	0.006	0.005
P4	0.007	0.074	0.048	0.003	0
O1	0	0	0.001	0	0
O2	0	0	0	0	0.01
F7	0.128	0.627	0.21	0.409	0.127
F8	0.954	0.659	0.702	0.955	0.79
T3	0.042	0.097	0.058	0.132	0.034
T4	0.29	0.205	0.366	0.171	0.333
T5	0	0.001	0.001	0.003	0
T6	0.005	0.002	0	0	0
Fz	0.561	0.198	0.653	0.793	0.552
Cz	0.181	0.269	0.942	0.644	0.554
Pz	0.004	0.006	0.002	0.001	0

Table D 17

100 Hz CES Laplacian FFT Relative Power Group Paired t-Test (p-Value)

	31 Hz	32 Hz	33 Hz	34 Hz	35 Hz
FP1	0.211	0.252	0.197	0.189	0.075
FP2	0.91	0.731	0.933	0.884	0.785
F3	0.612	0.487	0.732	0.502	0.643
F4	0.264	0.695	0.843	0.117	0.291
C3	0.001	0.003	0.007	0.028	0.068
C4	0.534	0.767	0.826	0.755	0.523
P3	0.012	0.078	0.109	0.012	0.066
P4	0.001	0.009	0	0.001	0.016
O1	0	0.009	0.023	0.012	0.007
O2	0.03	0.002	0.01	0	0.008
F7	0.972	0.56	0.439	0.72	0.654
F8	0.192	0.394	0.988	0.527	0.639
T3	0.041	0.222	0.639	0.377	0.657
T4	0.67	0.31	0.633	0.46	0.434
T5	0.002	0.005	0.013	0.031	0.035
T6	0.007	0	0.044	0.01	0.001
Fz	0.963	0.3	0.101	0.056	0.28
Cz	0.042	0.358	0.258	0.269	0.088
Pz	0.001	0	0	0	0

Table D 18

100 Hz CES Laplacian FFT Relative Power Group Paired t-Test (p-Value)

	36 Hz	37 Hz	38 Hz	39 Hz	40 Hz
FP1	0.137	0.095	0.093	0.02	0.004
FP2	0.748	0.181	0.444	0.371	0.2
F3	0.524	0.368	0.217	0.288	0.192
F4	0.547	0.952	0.251	0.009	0.06
C3	0.044	0.088	0.093	0.038	0.006
C4	0.616	0.819	0.245	0.747	0.994
P3	0.095	0.057	0	0.007	0.004
P4	0.009	0.03	0.003	0	0
O1	0.007	0	0.002	0	0
O2	0.001	0	0	0.001	0
F7	0.689	0.709	0.733	0.421	0.234
F8	0.847	0.571	0.528	0.859	0.956
T3	0.934	0.671	0.971	0.495	0.382
T4	0.615	0.64	0.657	0.735	0.57
T5	0.011	0.003	0.019	0.007	0.001
T6	0.024	0.004	0.02	0.054	0.009
Fz	0.005	0.174	0.015	0.002	0
Cz	0.044	0.019	0.004	0.01	0.002
Pz	0	0	0.001	0	0

Montage: Laplacian

FFT Relative Power Group Paired t-Test (P-Value)

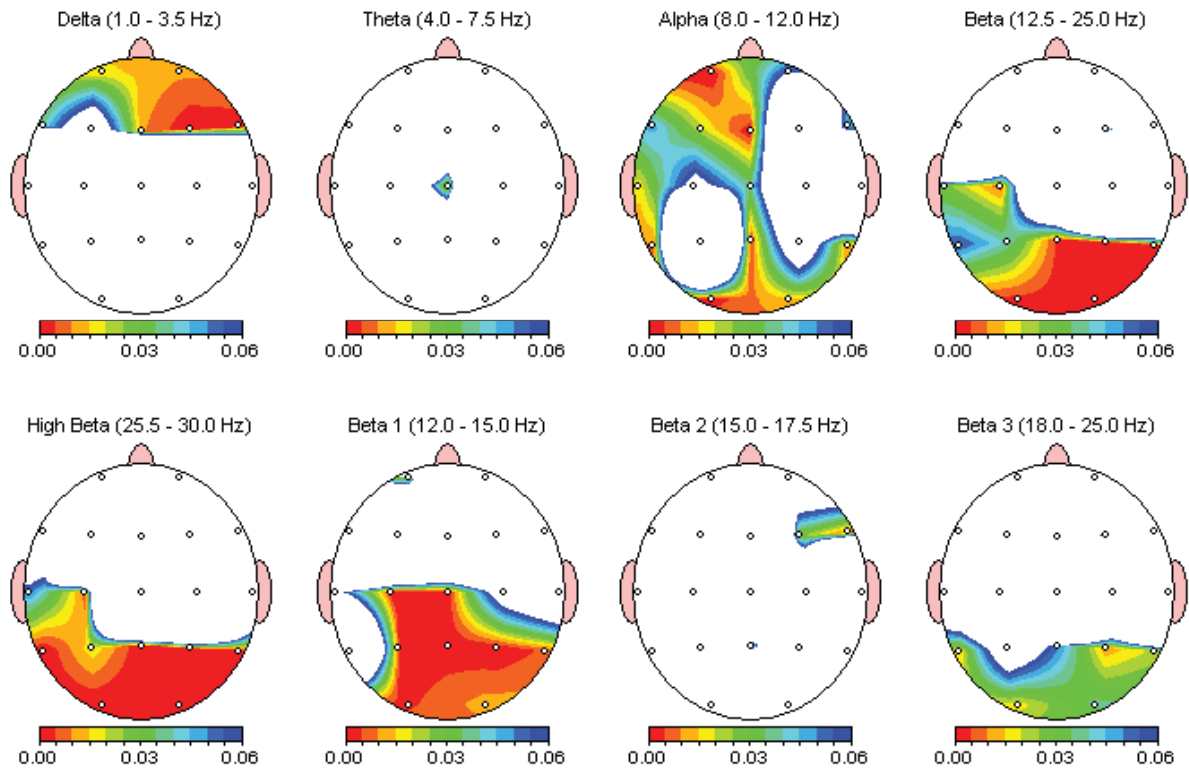


Figure D 11. Relative power topographic map for the 100 Hz CES Laplacian reference montage.

Montage: Laplacian

FFT Relative Power Group Paired t-Test (P-Value)

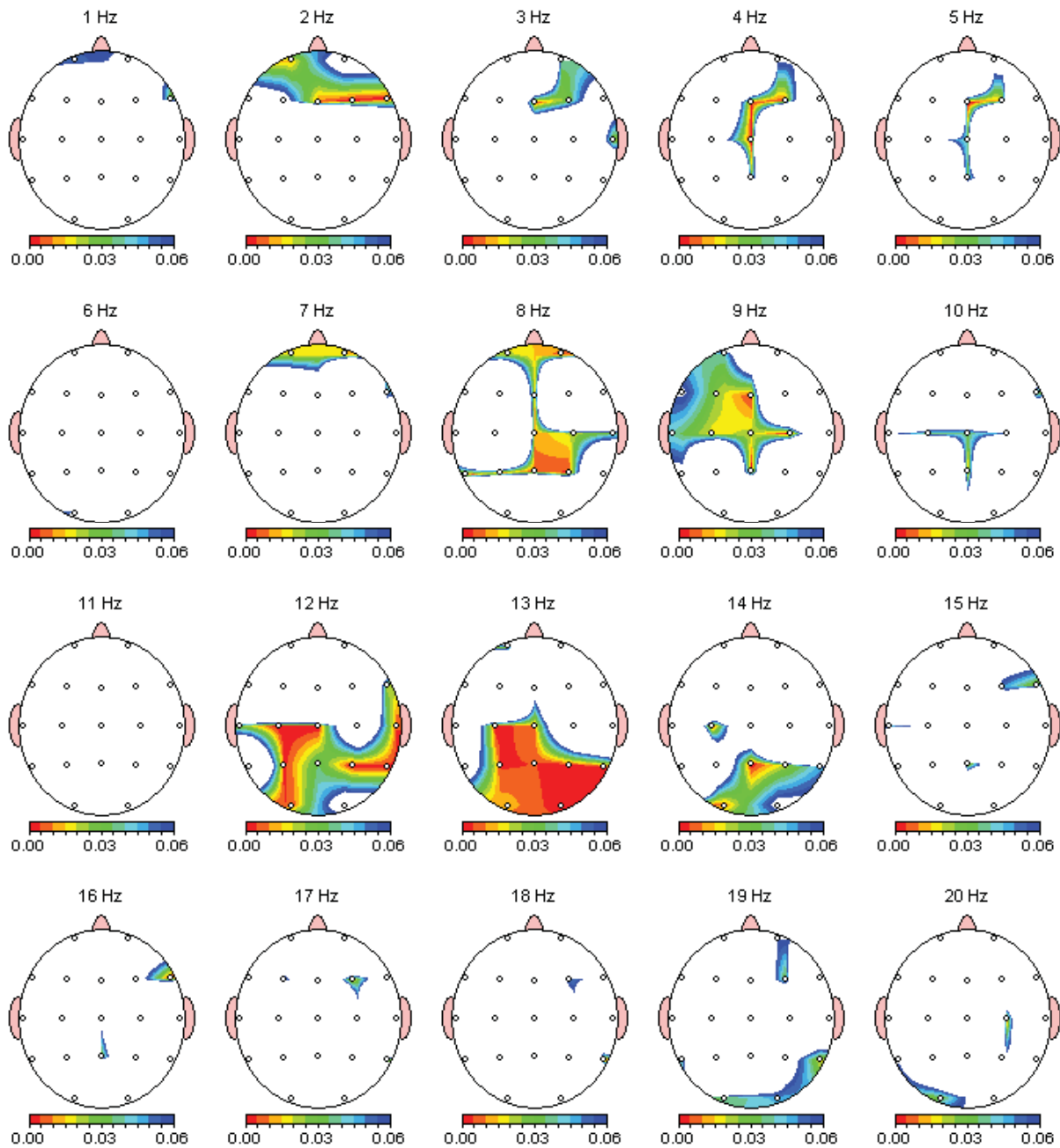


Figure D 12. Relative power topographic map for the 100 Hz CES Laplacian reference montage.

Montage: Laplacian

FFT Relative Power Group Paired t-Test (P-Value)

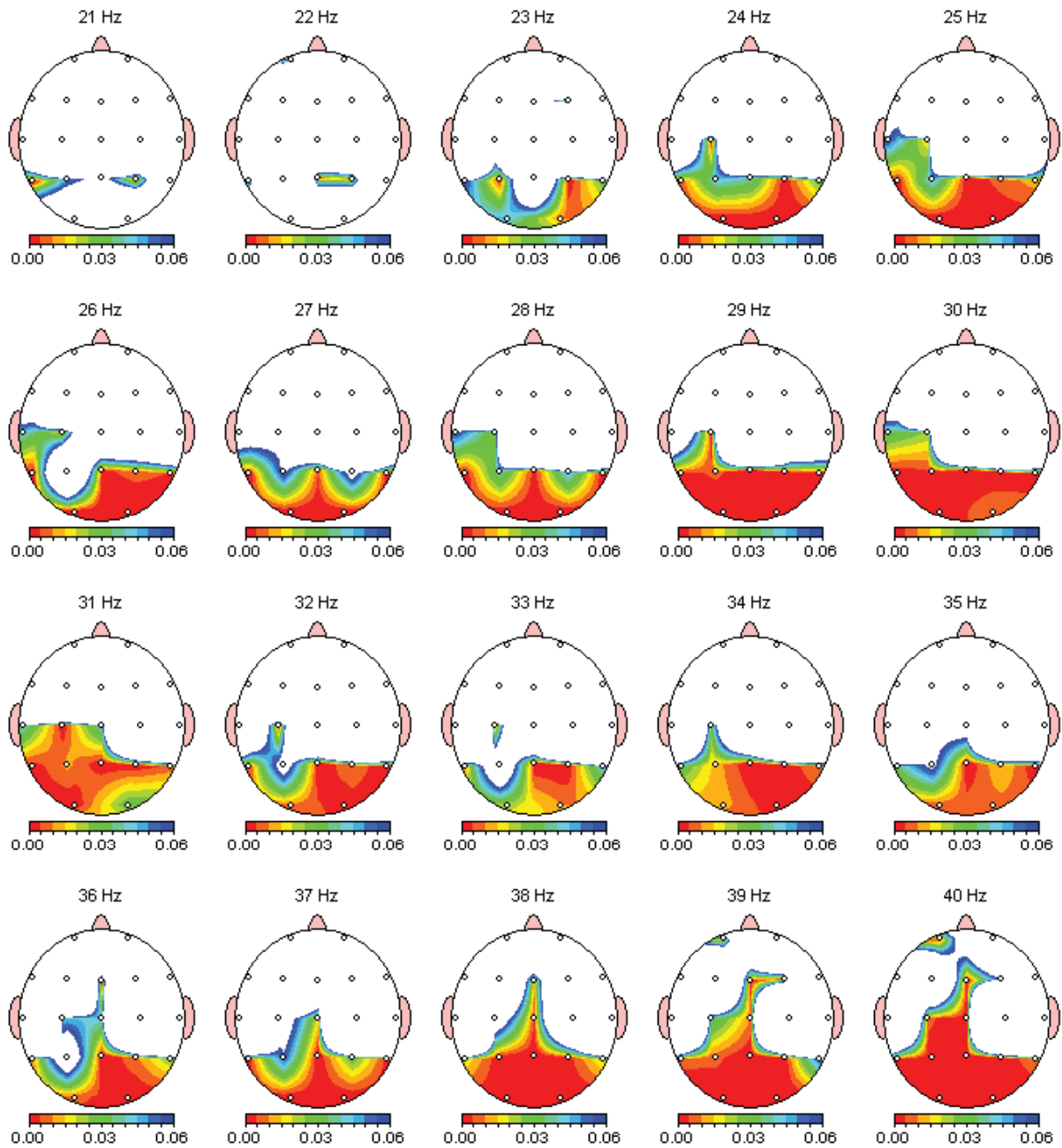


Figure D 13. Relative power topographic map for the 100 Hz CES Laplacian reference montage.

Montage: Laplacian

FFT Coherence Group Paired t-Test (P-Value)

Intrahemispheric: LEFT

	DELTA	THETA	ALPHA	BETA
FP1 F3	0.096	0.822	0.541	0.708
FP1 C3	0.018	0.055	0.072	0.416
FP1 P3	0.046	0.440	0.124	0.819
FP1 O1	0.845	0.345	0.132	0.947
FP1 F7	0.750	0.040	0.092	0.679
FP1 T3	0.048	0.778	0.174	0.467
FP1 T5	0.761	0.219	0.494	0.918
F3 C3	0.932	0.140	0.235	0.289
F3 P3	0.643	0.086	0.248	0.088
F3 O1	0.473	0.718	0.134	0.711
F3 F7	0.466	0.933	0.225	0.625
F3 T3	0.604	0.406	0.418	0.430
F3 T5	0.007	0.074	0.562	0.473
C3 P3	0.434	0.188	0.304	0.764
C3 O1	0.057	0.017	0.452	0.239
C3 F7	0.171	0.019	0.580	0.783
C3 T3	0.562	0.208	0.243	0.024
C3 T5	0.079	0.804	0.257	0.574
P3 O1	0.236	0.126	0.602	0.216
P3 F7	0.133	0.635	0.380	0.845
P3 T3	0.987	0.496	0.743	0.171
P3 T5	0.089	0.604	0.043	0.719
O1 F7	0.311	0.631	0.325	0.497
O1 T3	0.136	0.809	0.957	0.697
O1 T5	0.851	0.122	0.374	0.215
F7 T3	0.526	0.891	0.631	0.758
F7 T5	0.070	0.168	0.913	0.930
T3 T5	0.755	0.291	0.592	0.128

Intrahemispheric: RIGHT

	DELTA	THETA	ALPHA	BETA
FP2 F4	0.697	0.005	0.350	0.121
FP2 C4	0.019	0.617	0.675	0.458
FP2 P4	0.768	0.055	0.800	0.038
FP2 O2	0.775	0.391	0.965	0.305
FP2 F8	0.094	0.529	0.006	0.060
FP2 T4	0.295	0.696	0.849	0.488
FP2 T6	0.068	0.002	0.000	0.900
F4 C4	0.284	0.276	0.944	0.046
F4 P4	0.251	0.760	0.435	0.931
F4 O2	0.081	0.525	0.677	0.978
F4 F8	0.617	0.692	0.901	0.824
F4 T4	0.413	0.894	0.456	0.414
F4 T6	0.321	0.400	0.216	0.969
C4 P4	0.142	0.378	0.008	0.343
C4 O2	0.197	0.643	0.518	1.000
C4 F8	0.689	0.655	0.936	0.467
C4 T4	0.260	0.662	0.802	0.622
C4 T6	0.961	0.357	0.240	0.164
P4 O2	0.015	0.048	0.490	0.632
P4 F8	0.516	0.022	0.034	0.467
P4 T4	0.754	0.267	0.174	0.920
P4 T6	0.176	0.084	0.068	0.251
O2 F8	0.665	0.005	0.891	0.970
O2 T4	0.594	0.086	0.711	0.006
O2 T6	0.343	0.075	0.084	0.693
F8 T4	0.442	0.429	0.825	0.394
F8 T6	0.007	0.655	0.020	0.407
T4 T6	0.275	0.597	0.027	0.287

Interhemispheric: HOMOLOGOUS PAIRS

	DELTA	THETA	ALPHA	BETA
FP1 FP2	0.406	0.018	0.153	0.815
C3 C4	0.448	0.476	0.708	0.093
O1 O2	0.487	0.846	0.309	0.916
T3 T4	0.452	0.716	0.958	0.053

	DELTA	THETA	ALPHA	BETA
F3 F4	0.065	0.321	0.419	0.513
P3 P4	0.036	0.031	0.014	0.016
F7 F8	0.685	0.001	0.018	0.081
T5 T6	0.029	0.376	0.406	0.145

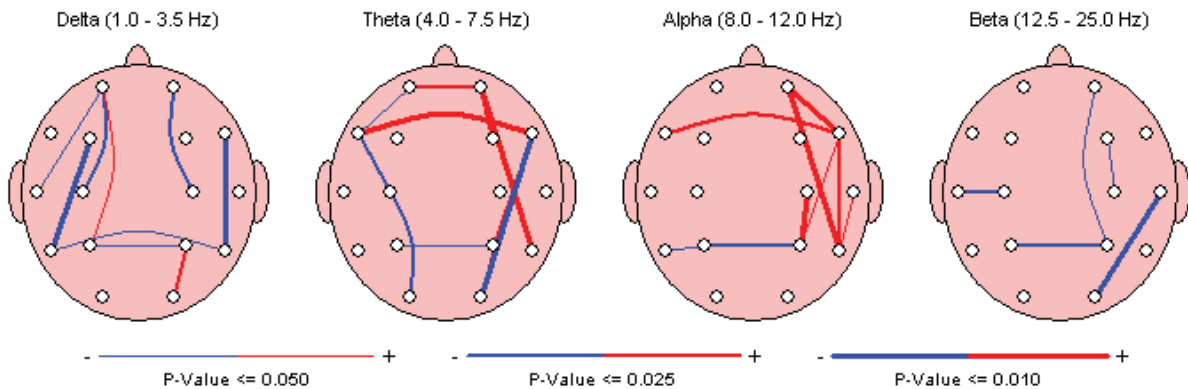


Figure D 14. Coherence for the 100 Hz CES Laplacian reference montage.

Montage: Laplacian

FFT Amplitude Asymmetry Group Paired t-Test (P-Value)

Intrahemispheric: LEFT

	DELTA	THETA	ALPHA	BETA
FP1 F3	0.986	0.178	0.121	0.531
FP1 C3	0.001	0.220	0.463	0.221
FP1 P3	0.002	0.031	0.955	0.252
FP1 O1	0.334	0.817	0.122	0.928
FP1 F7	0.297	0.745	0.914	0.173
FP1 T3	0.058	0.486	0.662	0.606
FP1 T5	0.007	0.076	0.077	0.213
F3 C3	0.002	0.007	0.004	0.546
F3 P3	0.018	0.024	0.179	0.657
F3 O1	0.553	0.541	0.094	0.879
F3 F7	0.199	0.428	0.102	0.949
F3 T3	0.009	0.041	0.127	0.263
F3 T5	0.004	0.004	0.008	0.783
C3 P3	0.333	0.220	0.759	0.791
C3 O1	0.338	0.362	0.949	0.413
C3 F7	0.012	0.243	0.459	0.671
C3 T3	0.092	0.685	0.455	0.097
C3 T5	0.608	0.211	0.716	0.787
P3 O1	0.012	0.034	0.184	0.171
P3 F7	0.006	0.076	0.725	0.801
P3 T3	0.109	0.235	0.575	0.169
P3 T5	0.128	0.725	0.178	0.824
O1 F7	0.972	0.925	0.125	0.475
O1 T3	0.580	0.405	0.235	0.599
O1 T5	0.146	0.017	0.924	0.147
F7 T3	0.124	0.292	0.617	0.088
F7 T5	0.015	0.073	0.060	0.597
T3 T5	0.298	0.117	0.102	0.078

Intrahemispheric: RIGHT

	DELTA	THETA	ALPHA	BETA
FP2 F4	0.675	0.180	0.068	0.127
FP2 C4	0.832	0.911	0.382	0.482
FP2 P4	0.122	0.206	0.213	0.959
FP2 O2	0.008	0.050	0.672	0.438
FP2 F8	0.796	0.533	0.323	0.531
FP2 T4	0.092	0.390	0.709	0.731
FP2 T6	0.015	0.007	0.233	0.365
F4 C4	0.932	0.276	0.966	0.028
F4 P4	0.225	0.047	0.015	0.129
F4 O2	0.085	0.022	0.158	0.276
F4 F8	0.455	0.044	0.104	0.352
F4 T4	0.290	0.060	0.499	0.645
F4 T6	0.041	0.003	0.003	0.761
C4 P4	0.490	0.163	0.273	0.620
C4 O2	0.041	0.245	0.647	0.996
C4 F8	0.630	0.933	0.653	0.254
C4 T4	0.442	0.486	0.755	0.360
C4 T6	0.142	0.047	0.037	0.141
P4 O2	0.308	0.688	0.607	0.855
P4 F8	0.143	0.240	0.067	0.475
P4 T4	0.623	0.126	0.121	0.506
P4 T6	0.028	0.007	0.267	0.068
O2 F8	0.032	0.219	0.364	0.680
O2 T4	0.111	0.609	0.765	0.573
O2 T6	0.513	0.057	0.041	0.229
F8 T4	0.094	0.447	0.910	0.938
F8 T6	0.033	0.015	0.010	0.403
T4 T6	0.022	0.003	0.019	0.311

Interhemispheric: HOMOLOGOUS PAIRS

	DELTA	THETA	ALPHA	BETA
FP1 FP2	0.674	0.659	0.522	0.030
C3 C4	0.101	0.524	0.236	0.455
O1 O2	0.002	0.028	0.550	0.147
T3 T4	0.988	0.638	0.685	0.023

	DELTA	THETA	ALPHA	BETA
F3 F4	0.282	0.829	0.641	0.061
P3 P4	0.211	0.835	0.233	0.997
F7 F8	0.218	0.361	0.571	0.242
T5 T6	0.300	0.137	0.142	0.211

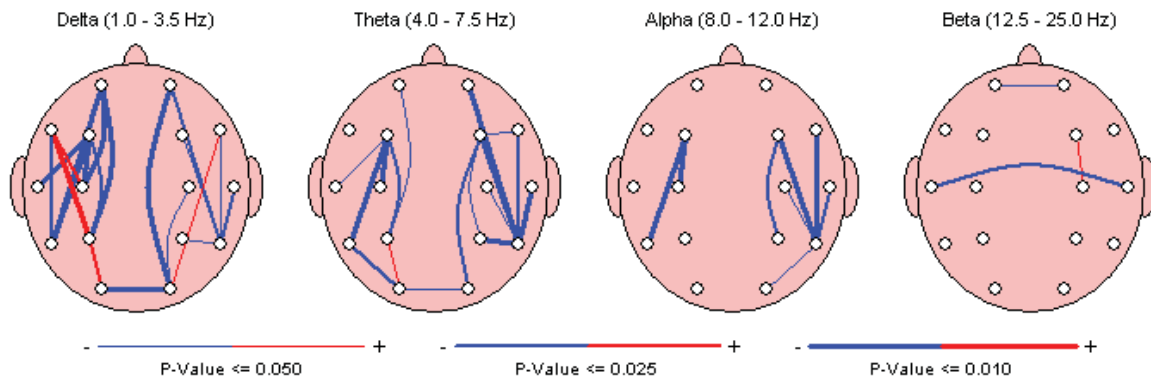


Figure D 15. Amplitude asymmetry for the 100 Hz CES Laplacian reference montage.

Montage: Laplacian

FFT Phase Lag Group Paired t-Test (P-Value)

Intrahemispheric: LEFT

	DELTA	THETA	ALPHA	BETA
FP1 F3	0.127	0.167	0.356	0.894
FP1 C3	0.146	0.363	0.703	0.066
FP1 P3	0.014	0.842	0.089	0.407
FP1 O1	0.088	0.991	0.210	0.396
FP1 F7	0.270	0.435	0.138	0.902
FP1 T3	0.834	0.828	0.952	0.065
FP1 T5	0.895	0.214	0.100	0.387
F3 C3	0.786	0.702	0.481	0.097
F3 P3	0.404	0.921	0.520	0.311
F3 O1	0.633	0.158	0.395	0.295
F3 F7	0.594	0.365	0.840	0.974
F3 T3	0.905	0.389	0.400	0.314
F3 T5	0.165	0.101	0.688	0.486
C3 P3	0.958	0.807	0.792	0.211
C3 O1	0.585	0.347	0.035	0.491
C3 F7	0.956	0.006	0.046	0.081
C3 T3	0.804	0.290	0.371	0.053
C3 T5	0.000	0.346	0.029	0.267
P3 O1	0.096	0.640	0.468	0.081
P3 F7	0.985	0.600	0.303	0.488
P3 T3	0.112	0.165	0.825	0.102
P3 T5	0.980	0.874	0.410	0.100
O1 F7	0.053	0.593	0.736	0.558
O1 T3	0.085	0.402	0.035	0.235
O1 T5	0.411	0.461	0.107	0.775
F7 T3	0.942	0.428	0.070	0.255
F7 T5	0.124	0.601	0.861	0.023
T3 T5	0.954	0.576	0.232	0.292

Intrahemispheric: RIGHT

	DELTA	THETA	ALPHA	BETA
FP2 F4	0.161	0.023	0.308	0.337
FP2 C4	0.621	0.063	0.418	0.475
FP2 P4	0.212	0.653	0.559	0.448
FP2 O2	0.400	0.742	0.930	0.092
FP2 F8	0.840	0.149	0.668	0.073
FP2 T4	0.150	0.658	0.672	0.555
FP2 T6	0.861	0.989	0.284	0.614
F4 C4	0.730	0.356	0.663	0.084
F4 P4	0.178	0.304	0.278	0.207
F4 O2	0.245	0.680	0.837	0.993
F4 F8	0.802	0.472	0.142	0.107
F4 T4	0.346	0.122	0.884	0.266
F4 T6	0.112	0.989	0.104	0.123
C4 P4	0.196	0.952	0.104	0.605
C4 O2	0.462	0.156	0.749	1.000
C4 F8	0.201	0.882	0.733	0.180
C4 T4	0.462	0.244	0.010	0.173
C4 T6	0.119	0.725	0.383	0.108
P4 O2	0.024	0.792	0.948	0.510
P4 F8	0.399	0.521	0.377	0.062
P4 T4	0.514	0.724	0.650	0.581
P4 T6	0.823	0.914	0.826	0.056
O2 F8	0.189	0.800	0.314	0.448
O2 T4	0.433	0.498	0.758	0.364
O2 T6	0.729	0.224	0.883	0.580
F8 T4	0.263	0.444	0.553	0.735
F8 T6	0.728	0.578	0.037	0.787
T4 T6	0.386	0.136	0.763	0.588

Interhemispheric: HOMOLOGOUS PAIRS

	DELTA	THETA	ALPHA	BETA
FP1 FP2	0.840	0.414	0.582	0.371
C3 C4	0.002	0.717	0.309	0.992
O1 O2	0.818	0.782	0.044	0.409
T3 T4	0.924	0.290	0.953	0.746

	DELTA	THETA	ALPHA	BETA
F3 F4	0.086	0.644	0.761	0.238
P3 P4	0.195	0.328	0.110	0.057
F7 F8	0.998	0.090	0.793	0.637
T5 T6	0.187	0.742	0.855	0.462

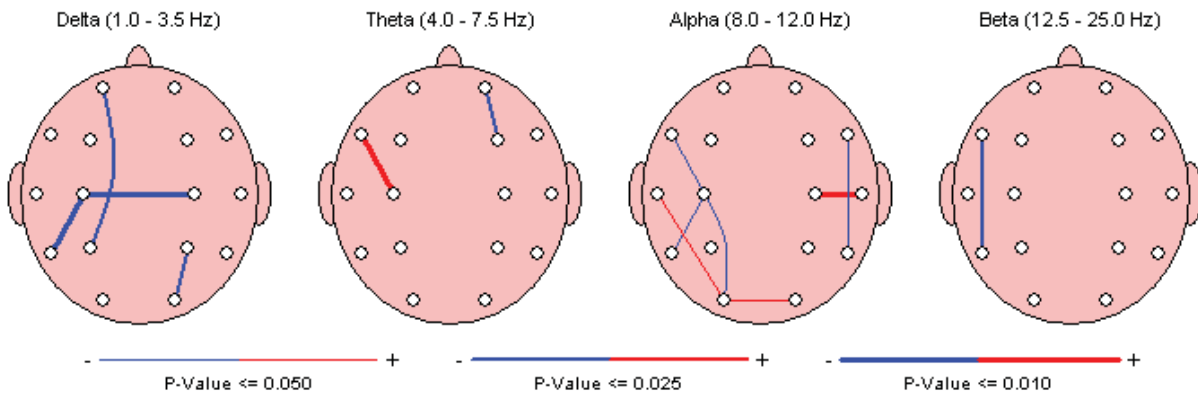


Figure D 16. Phase lag for the 100 Hz CES Laplacian reference montage.

Montage: Laplacian

FFT Power Ratio Group Paired t-Test (P-Value)

Intrahemispheric: LEFT

	D/T	D/A	D/B	D/G	T/A	T/B	T/G	A/B	A/G	B/G
FP1 - CSD	0.015	0.000	0.274	0.535	0.032	0.277	0.299	0.006	0.018	0.642
F3 - CSD	0.042	0.020	0.117	0.427	0.247	0.622	0.721	0.587	0.141	0.151
C3 - CSD	0.614	0.356	0.360	0.137	0.042	0.332	0.065	0.005	0.007	0.205
P3 - CSD	0.471	0.476	0.116	0.046	0.687	0.026	0.010	0.062	0.022	0.282
O1 - CSD	0.471	0.073	0.834	0.421	0.042	0.610	0.006	0.001	0.000	0.007
F7 - CSD	0.274	0.012	0.316	0.967	0.098	0.961	0.407	0.112	0.037	0.136
T3 - CSD	0.436	0.072	0.339	0.182	0.133	0.051	0.054	0.013	0.008	0.403
T5 - CSD	0.180	0.085	0.703	0.031	0.167	0.248	0.002	0.013	0.000	0.018

Intrahemispheric: RIGHT

	D/T	D/A	D/B	D/G	T/A	T/B	T/G	A/B	A/G	B/G
FP2 - CSD	0.005	0.011	0.033	0.189	0.127	0.885	0.771	0.215	0.222	0.616
F4 - CSD	0.243	0.000	0.001	0.034	0.027	0.017	0.321	0.301	0.669	0.045
C4 - CSD	0.129	0.273	0.494	0.783	0.811	0.682	0.295	0.501	0.307	0.291
P4 - CSD	0.288	0.272	0.742	0.433	0.420	0.052	0.008	0.006	0.005	0.194
O2 - CSD	0.819	0.651	0.373	0.124	0.316	0.198	0.009	0.002	0.000	0.027
F8 - CSD	0.001	0.001	0.008	0.046	0.231	0.782	0.637	0.396	0.160	0.249
T4 - CSD	0.253	0.197	0.559	0.884	0.461	0.665	0.297	0.349	0.182	0.185
T6 - CSD	0.483	0.362	0.374	0.124	0.651	0.044	0.009	0.001	0.000	0.028

Intrahemispheric: CENTER

	D/T	D/A	D/B	D/G	T/A	T/B	T/G	A/B	A/G	B/G
Fz - CSD	0.266	0.001	0.021	0.041	0.002	0.298	0.329	0.032	0.025	0.870
Cz - CSD	0.192	0.285	0.671	0.763	0.010	0.394	0.052	0.025	0.171	0.279
Pz - CSD	0.305	0.017	0.516	0.983	0.034	0.942	0.425	0.001	0.000	0.101

Figure D 17. Power ratios for the 100 Hz CES Laplacian reference montage.

Montage: Laplacian

FFT Power Ratio Group Paired t-Test (P-Value)

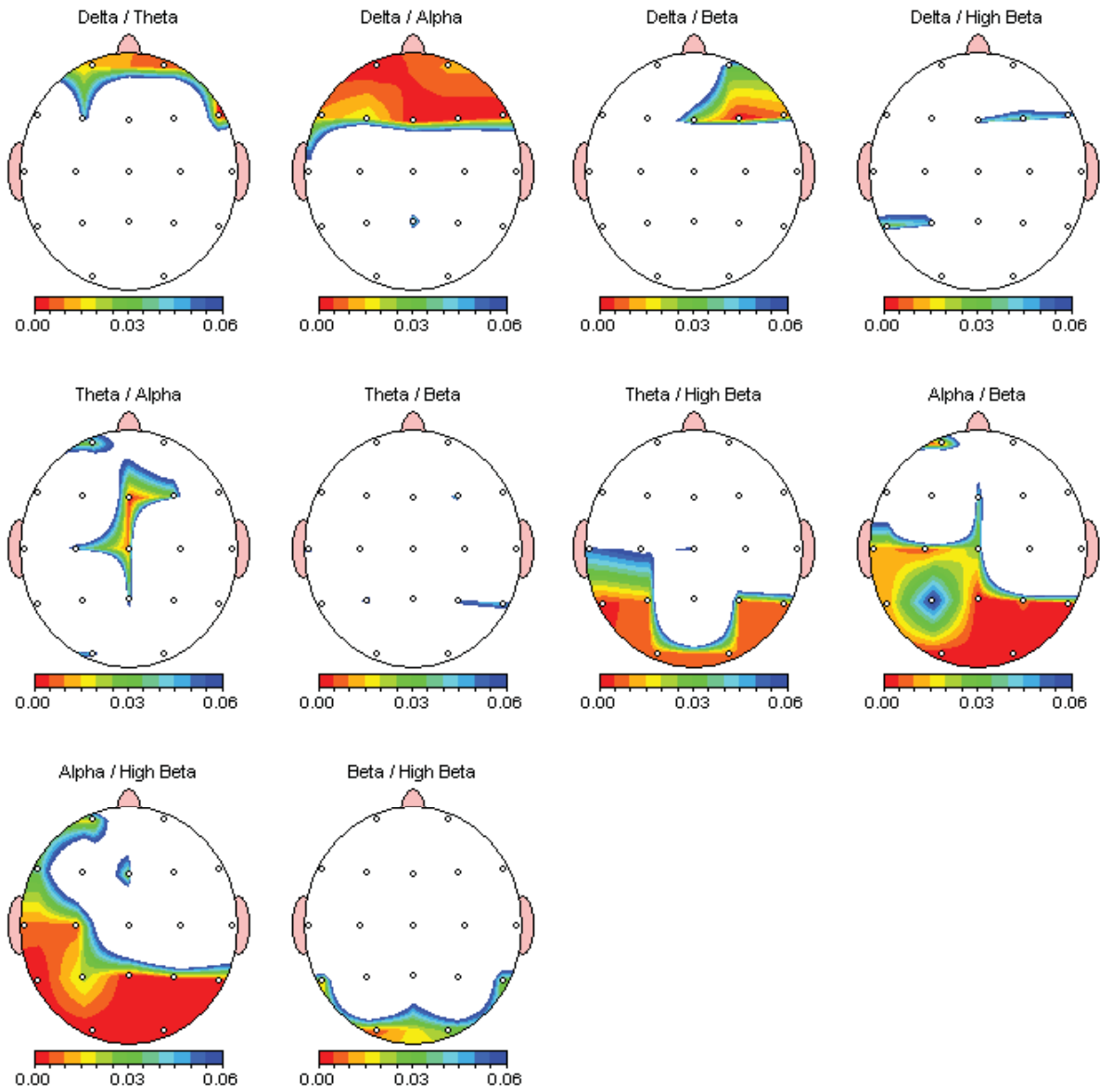


Figure D 18. Power ratio topographical maps for the 100 Hz CES Laplacian reference montage.

REFERENCES

- Allen, J., Urry, H., Hitt, S., Coan, J. (2004). The stability of resting frontal electroencephalographic asymmetry in depression. *Psychophysiology*, *41*, 269-280.
- Anderer, P., Saletu, B., Pascual-Marqui, R. D. (2000). Effect of the 5-HT_{1a} partial agonist buspirone on regional brain electrical activity in man: a functional neuroimaging study using low-resolution electromagnetic tomography (LORETA). *Psychiatry Research-Neuroimaging*, *100*, 81-96.
- Arnoult, M. (1972). *Fundamentals of scientific method in psychology*. Dubuque, Iowa: W. M. C. Brown Company Publishers.
- Baillet, S., Riera, J., Marin, G., Mangin, J., Aubert, J. Garnero, L. (2001). Evaluation of inverse methods & head models for EEG source localization using a human skull phantom. *Physics in Medicine & Biology*, *46*(1), 77-96.
- Berger, H. (1929). Über das elektrenkephalogramm des menschen *Archiv für Psychiatrie*, *87*, 527-570. [On the electroencephalogram of man].
- Bijal, T. (2006). Electrify your mind – literally. *New Scientist Magazine*, *2547*, 34.
- Bloom, J., and Anneveldt, M., (1982). An electrode cap tested. *Electroencephalography and Clinical Neurophysiology*, *54*, 591-594.
- Braverman, E., Smith, R., Smayda, R., & Blum, K. (1990). Modification of P300 amplitude and other electrophysiological parameters of drug abuse by cranial electrical stimulation. *Current Therapeutic Research*, *48*, 586-596.
- Braverman, E., Swartz, J., Blum, K., & Moss, B. (1992). Electrotherapy for addictions. *Addiction and Recovery*, *3*, 34-36.
- Briones, D., Rosenthal, S. (1973). Changes in urinary free catecholamine and 17-ketosteriods with cerebral electrotherapy (electrosleep). *Diseases of the Nervous System*, *34*, 57-58.
- Cameron, M., Lonergan, E., Lee, H. (2003). Transcutaneous electrical nerve stimulation (TENS) for dementia. *Cochrane Database of Systematic Reviews*, *3*, CD004032.
- Cantor, D. (1999). An overview of quantitative EEG and its application to neurofeedback. In J. R. Evans & A. Abarbanel (Eds.) *Introduction to quantitative EEG and neurofeedback*. San Diego, Ca: Academic Press.
- Carretie, L., Manuel, T., Mercado, F., Albert, J., Lopez-Martin, S., and de la Serna, J. (2004). Voltage-based versus factor score-based source localization analysis of electrophysiological brain activity: A comparison. *Brain Topography*, *17*(2), 109-115.

- Coan, J. A., & Allen J. B. (2003). The state and trait nature of frontal EEG asymmetry in emotion. In K. Hugdahl & R. J. Davidson (Eds.), *The asymmetrical brain* (2nd ed.). Cambridge, MA: MIT Press.
- Congedo, M. (2005). NTE Pack (EureKa!, MHyT3!, and NTE Map Insight) [Computer software]. Knoxville, TN: Nova Tech EEG, Inc.
- Congedo, M. (2005). Wave Generator (Marco's Tools v1.3) [Computer software]. Knoxville, TN: Nova Tech EEG, Inc.
- Collins, L., Holmes, C., Peters, T., and Evans, A. (1995). Automatic 3-D model-based neuroanatomical segmentation. *Human Brain Mapping*, 3(3), 190-208.
- Cox, A., & Heath, R. (1975). Neurotone therapy: A preliminary report of its effect on electrical activation of forebrain structures. *Diseases of the Nervous System*, 36(5), 245-247.
- Childs, A. (1993). Fifteen cycle cranial electrotherapy stimulation for spasticity. *Brain Injury*, 7(2), 179-181.
- Childs, A. & Crismon, M. C. (1998). The use of cranial electrotherapy stimulation in post-traumatic amnesia: A report of two cases. *Brain Injury*, 2, 243-247.
- Clark, M. S., Silverston, L. M., Lindenmuth, J., Hicks, M. J., Averbach, R. E. & Kleier, D. J. (1987). An evaluation of the clinical analgesia/anesthesia efficacy on acute pain using the high frequency neural modulator in various dental settings. *Oral Surgery, Oral Medicine, Oral Pathology*, 63(4), 501-505.
- Davidson, R., Jackson, D., Larson, C. (2000). Human electroencephalography. In J. T. Cacioppo, L. G. Tassinary & G. G Berntson (Eds.), *Handbook of psychophysiology*. Cambridge, UK: Cambridge University Press.
- Dierks, T., Jelic. V., Pascual-Marqui, R. D., Wahlund, L. O., Julin, P., Linden, D., Maurer, K., Winblad, B., Nordberg, A. (2000). Spatial pattern of cerebral glucose metabolism (PET) correlates with localization of intracerebral EEG-generators in Alzheimer's disease. *Clinical Neurophysiology*, 111, 1817-1824.
- Dougherty, P., Dong, W., Faillace, L., & Dafny, N. (1990). Transcranial electrical stimulation attenuates abrupt morphine withdrawal in rats assayed by remote computerized quantification of multiple motor behavior indices. *European Journal of Pharmacology*, 175, 187-195.
- Driscoll, D. & Rush, S. (1971). Influence of cerebral spinal fluid on current flow in the brain. In D. V. Reynolds and A. E. Sjöberg (Eds.), *Neuroelectric research*. Springfield, Illinois: Thomas.
- Duffy, F. H., Hughes, J. R., Miranda, F., Bernad, P., Cook, P. (1994). Status of quantitative EEG (QEEG) in clinical practice. *Clinical EEG (Electroencepalography)*, 25(4), vi-xxii.

- Empson, J. (1973). Does electrosleep induce natural sleep? *Electroencephalography and Clinical Neurophysiology*, 35(6), 663-664.
- Enoch, M. A., White, K. V., Harris, C. R., Rohrbaugh, J. W., Goldman, D. (2002). The relationship between two intermediate phenotypes for alcoholism: Low voltage alpha EEG and low P300 ERP amplitude. *Journal of Studies on Alcohol*, 63, 2002.
- Collins, D., Zijdenbos, A., Kollokian, V., Sled, J., Kabani, N., Holmes, C., and Evans, A. (1998). Design and construction of a realistic digital brain phantom. *IEEE Transactions on Medical Imaging*, 17(3), 463--468.
- Evans, A., Collins, D., Mills, S., Brown, E., Kelly, R., and Peters, T. (1993). 3D statistical neuroanatomical models from 305 MRI volumes. *Proceedings of the IEEE-Nuclear Science Symposium and Medical Imaging Conference*, 1813-1817.
- Evans, A., Collins, D., and Milner, B. (1992). An MRI-based stereotactic atlas from 250 young normal subjects. *Journal of Social Neuroscience*, 18, 408.
- Feighner, J. P., Brown, S. L., & Oliver, J. E. (1973). Electrosleep therapy: A controlled double blind study. *Journal of Nervous and Mental Diseases*, 157(2), 121-128.
- Ferdjallah, M., Bostock, F. X., & Barr, R. E. (1996) Potential and current density distributions of cranial electrotherapy stimulation (CES) in a four-concentric-spheres model. *IEEE Trans. Biomed. Eng.* 43, 939-943.
- Fink, M. (1999). *Electroshock: Restoring the mind*. New York: Oxford University Press.
- Flemenbaum, A. (1974). Cerebral electrotherapy (electrosleep): An open clinical study with a six month follow-up. *Psychosomatics*, 15(1), 20-24.
- Forester, S., Shapiro, A., Fine, L., Feldman, H., Berner, H., & Goldberg, M. (1967). Electrotherapeutic sleep and electroanaesthesia. In Wageneder, F., & St. Schuy (Eds.), *International congress series*, 136, 169-171. Amsterdam: Excerpta Medica Foundation.
- Forster, S., Post, B., & Benton, J. (1963). Preliminary observations on electrosleep. *Archives of Physical Medicine and Rehabilitation*. 44, 481-489.
- Frankel, B., Buchbinder, R., & Snyder, F. (1973). Ineffectiveness of electrosleep in chronic primary insomnia. *Archives of General Psychiatry*, 29, 563-568.
- Frei, E., Gamma, A., Pascual-Marqui, R., Lehmann, D., Hell, D., Vollenweider, F., (2001). Localization of MDMA-induced brain activity in healthy volunteers using low resolution brain electromagnetic tomography (LORETA). *Human Brain Mapping*, 14, 152-165.
- Fries, D. S. (2002). Opioid analgesics. In D. A. Williams & T. L. Lemke (Eds.) *Foye's principles of medicinal chemistry* (5 ed.). Philadelphia, PA: Lippincott Williams & Wilkins.

- Gibson, T., & O'Hair, D. (1983). Cranial application of low level transcranial electrotherapy vs. relaxation instruction in anxious patients. *American Journal of Electromedicine*, 4(1), 81-21.
- Giginshvili, G., Dombrovskaia, I., Orekhova, E., Radzievski, S. (1995). The differential use of electrosleep for restoring the work capacity of athletes [Abstract]. *Vopr Kurortol Fizioter Lech Fiz Kult*, 31-34.
- Gold, M. S., Pottash, A. L., Sternback, H., Barbaban, J., & Annitto, W. (1982). Anti-withdrawal effects of alpha methyl dopa and cranial electrotherapy. *Society for Neuroscience 12th Annual Meeting Abstracts*.
- Gomez, E., & Mikhail, A. (1974). Treatment of methadone withdrawal with cerebral electrotherapy (electrosleep). *British Journal of Psychiatry*, 134, 111-113.
- Gomez, J., F., Thatcher, R., W. (2001). Frequency domain equivalence between potentials and currents using LORETA. *International Journal of Neuroscience*, 107, 161-171.
- Grosse, P., Cassidy, M., and Brown, P. (2002). EEG–EMG, MEG–EMG and EMG–EMG frequency analysis: physiological principles and clinical applications. *Clinical Neurophysiology*; 113(10), 1523-1531.
- Guyton, A. C., & Hall, J. E. (1996). *Textbook of medical physiology* (9th ed.). Philadelphia: W. B. Saunders Company.
- Hearst, E., Cloninger, C., & Cadoret, R. (1974). Electrosleep therapy: A double-blind trial. *Archives of General Psychiatry*, 30, 463-466.
- Hayes, W. (1973). *Statistics for the social sciences*. New York: Holt, Rhinehart and Winston.
- Heffernan, M. (1996). The effect of a single cranial electrotherapy stimulation on multiple stress measures. *The Townsend Letter for Doctors and Patients*, 147, 60-64.
- Henriques, J. B., & Davidson, R. J. (1990). Regional brain electrical asymmetries discriminate between previously depressed and healthy control subjects. *Journal of Abnormal Psychology*, 99(1), 22-31.
- Henriques, J. B., & Davidson, R. J. (1991). Left frontal hypoactivation in depression. *Journal of Abnormal Psychology*, 100, 535-545.
- Himrich, B., Thornley, S. (1995). *Electrifying medicine*. Minneapolis: Lerner Publication Company.
- Hochman, R. (1988). Neurotransmitter modulation (TENS) for control of dental operative pain. *Journal of the American Dental Association*, 116(2), 208-212.

- Hozumi, S., Hori, H., Okawa, M., Hishikawa, Y., & Sato, K. (1996). Favorable effect of transcranial electrostimulation on behavior disorders in elderly patients with dementia: A double blind study. *International Journal of Neuroscience*, 88, 1-10.
- Hudspeth, W. (2003). NeuroRep QEEG Analysis and Report System (Version 4.0) [Computer software]. Los Osos, CA: Grey Matter, Inc.
- Itil, T., Gannon, P., Akpinar, S., & Hsu, W. (1971). Quantitative EEG analysis of electrosleep using frequency analyzer and digital Computer Methods. *Electroencephalography and Clinical Neurophysiology*, 31, 294.
- Jacobs, G., Friedman, R. (2004). EEG spectral analysis of relaxation techniques. *Applied Psychophysiology and Biofeedback*, 29(4), 245-254.
- Jarzembki, W., Sances, A., Larson, S. (1970). Evaluation of specific cerebral impedance and cerebral current density. *Annals of New York Academy of Science*, 170(2), 476-490.
- Jarzembki, W., Larson, S., Sances, A. (1972). Cerebral current density measurements during application of electrical currents through surface electrodes. *Physiological applications of impedance plethsmography* (R. D. Allison, ed.). Pittsburg, Pennsylvania: ISA.
- Jasper, H. (1958). The ten-twenty electrode system of the international federation. *Electroencephalography in Clinical Neurophysiology*, 2, 211-214.
- Jemelka, R. (1975). *Cerebral electrotherapy and anxiety reduction*. Unpublished master's thesis, Austin State University, Austin, Texas.
- Johns, E. (1999). *NxLink* (The Neurometric Analysis System) [Computer software]. New York, NY: Department of Psychiatry, Neurometric Evaluation, NYU Medical Center.
- Kaiser, D. (2000). QEEG: State of the art, or state of confusion. *Journal of Neurotherapy*, 4(2), 57-75.
- Katznelson, R. (1981). EEG recording, electrode placement, and aspects of generator localization. In P.L. Nunez (Ed.), *Electrical fields of the brain*. New York: Oxford University Press.
- Keren, G., & Lewis, C. (1993). *A handbook for data analysis in the behavioral sciences, methodological issues*. Hillside, NJ: Lawrence Erlbaum Associates, Publishers.
- Kiebel, S., Tallon-Baudry, C., Friston, K. (2005). Parametric analysis of oscillatory activity as measured with EEG/MEG. *Human Brain Mapping*, 26, 170-177.
- Keil, A., Stolarova, M., Heim, S., Gruber, T., Müller, M. (2003). Temporal stability of high-frequency brain oscillations in the human EEG. *Brain Topography*, 16(2), 101-110.
- Kirsch, D. L. (1996). Cranial electricotherapy stimulation, a safe and effective treatment for anxiety: A review of the literature. *Medical Scope Monthly*, 3, 1-16.

- Kirsch, D. L. (2002). *The science behind CES*. Edmonton, Alberta: Medical Scope Publishing Corp.
- Klawansky, S., Yeung, A., Berkey, C., Shah, N., Phan, H. & Chalmer, T. (1995). Meta-analysis of randomized controlled trials of cranial electrostimulation: Efficacy in treating selected psychological and physiological conditions. *Journal of Nervous and Mental Disease*, 183, 478-485.
- Kolb, B., & Whishaw, I. Q. (2000). *Fundamentals of human neuropsychology* (4th ed.). University of Lethbridge: W. H. Freeman and Company, Worth Publishers.
- Koles, Z., Kasmia, A., Paranjape, R., & McLean, D. (1989). Computed radial-current topography of the brain: Patterns associated with the normal and abnormal EEG. *Electroencephalography and Clinical Neurophysiology*, 72(1), 41-47.
- Kotter, G., Henschel, E., Hogan, W., & Kalbfleisch, J. (1975). Inhibition of gastric acid secretion in man by the transcranial application of low intensity pulsed current. *Gastroenterology*, 69, 359-363.
- Krupisky, E., Katznelson, Y., Lebedev, V., Flood, N., Patterson, M., Lipton, J., & Kozlowski, G. (1991). Transcranial electrostimulation (TENS) of brain opioid structures (BOS): experimental treatment of alcohol withdrawal syndrome (AWS) and clinical application. Presented at the Society for Neuroscience Annual Meeting, New Orleans.
- Krupisky, E., Burakov, A., Karandashova, G., Katsnelson, J., Lebedev, V., Grinenko, A., & Borodkin, J. (1991). The administration of transcranial electric treatment for affective disturbances therapy in alcoholic patients. *Drug and Alcohol Dependence*, 27, 1-6.
- Lang, J., Sances, A., Larson, S. (1969). Determination of specific cerebral impedance and cerebral current density during the application of diffuse electrical currents. *Medical Biological Engineering*, 7(5), 517-526.
- Levitt, E., James, N., Flavell, P. (1975). A clinical trial of electrosleep therapy with a psychiatric inpatient sample. *Australian and New Zealand Journal of Psychiatry*, 9, 287-290.
- Lichtbroun, A., Raicer, M., & Smith, R. (2001). The treatment of fibromyalgia with cranial electrotherapy stimulation. *Journal of Clinical Rheumatology*, 7(2) 72-78.
- Lipsey, M. W. (1990). *Design sensitivity, statistical power for experimental research*. London: Sage Publications.
- Magora, F. B., Aladjemoff, L., Magora, A., & Tannenbaum, J. (1965). Observations on electrically induced sleep in man. *British Journal of Anaesthesiology*, 37, 480-491.
- Magora, F., Beller, A., Assael, M., & Askenazi, A. (1967). Some aspects of electrical sleep and its therapeutic value. In F. Wagender, & St. Schuy (Eds). *Electrotherapeutic sleep and electroanesthesia*. Amsterdam: Excerpta Medica Foundation, International Congress Series No. 136.

- Malden, J. W., & Charash, L. I. (1985). Transcranial stimulation for the inhibition of primitive reflexes in children with cerebral palsy. *Neurology Report*, 9, 33-38.
- Malin, D. H., Lakea, J. R., Hamilton, R. F. and Skolnick, M. H. (1990). Augmented analgesic effects of L-tryptophan combined with low current transcranial electrostimulation. *Life Sciences*, 47(4), 263-267.
- Marshall, L., Mölle, M., Hallschmid, M., & Born, J. (2004). Transcranial direct current stimulation during sleep improves declarative memory. *Journal of Neuroscience*, 24, 985-9992.
- Matteson, M., & Ivancevich, J. (1986). An exploratory investigation of CES as an employee stress management technique. *Journal of Health and Human Resources Administration*, 9, 93-109.
- McKenzie, R., Costello, R., & Buck, D. (1976). Electrosleep (electrical transcranial stimulation) in the treatment of anxiety, depression and sleep disturbance in chronic alcoholics. *Journal of Altered States of Consciousness*, 2(2), 185-196.
- McKenzie, R., Rosenthal, S., & Driessner, J. (1976). Some psycho-physiologic effects of electrical transcranial stimulation (electrosleep). In Wulfsohn & Sances (Eds.), *The nervous system and electric current*. New York: Plenum.
- Melzack, R. and Wall, P. (1965). Pain mechanisms: A new theory. *Science*, 150: 971-979.
- Miller, G. (1991). The linked-reference issue in EEG and ERP recording. *Journal of Psychophysiology*, 5, 273-276.
- Moore, J., Mellor, C., Standage, K., & Strong, H. (1975). A double-blind study of electrosleep for anxiety and insomnia. *Biological Psychiatry*, 10(1), 59-63.
- Morgan, M., Witte, E., Cook, I., Leuchter, A., Abrams, M., Siegman, B. (2005). Influence of age, gender, health status, and depression on quantitative EEG. *Neuropsychobiology*, 52, 71-76.
- National Research Council, Division of Medical Science (1974). An evaluation of electroanesthesia and electrosleep. FDA Contract 70-22, Task Order No. 20, NTIS PB 241305, pp 1-54.
- Nidekker, I., and Antonov, A. (2003). Spectral analysis of long electroencephalographic records. *Human Physiology*, 29(3), 377-383.
- Nunez, P., Srinivasan, R., Westdorp, A., Wijesinghe, R., Tucker, D., Silberstein, R., Cadusch, P. (1997). EEG coherency I: Statistics, reference electrode, volume conduction, Laplacians, cortical imaging, and interpretation at multiple scales. *Electroencephalography and Clinical Neurophysiology*, 103, 499-515.

- O'Connor, M. E., Bianco, F., & Nicolson, R. (1991). Meta-analysis of cranial electro-stimulation (CES) in relation to the primary and secondary symptoms of substance withdrawal. Paper presented at the 12th Annual Meeting of the Bioelectromagnetics Society.
- Okoye, R., & Malden, J. W. (1986). Use of neurotransmitter modulation to facilitate sensory integration. *Neurology Report*, *10*(4), 67-72.
- Omura, Y. (1975). Electro-acupuncture for drug addiction withdrawal syndrome, particularly methadone, & individualized acupuncture treatments for the withdrawal syndromes of drug addictions and compulsive habits of excessive eating, drinking and smoking. *The International Journal of Acupuncture & Electro-Therapeutics Research*, *1*, 231-233.
- Overcash, S., (1999). A retrospective study to determine the efficacy of cranial electrotherapy stimulation (CES) on patients suffering from anxiety disorders. *American Journal of Electromedicine*, *16*(1), 49-51.
- Overcash, S., & Siebenthal, A. (1989). The effects of cranial electrotherapy stimulation and multisensory cognitive therapy on the personality and anxiety levels of substance abuse patients. *American Journal of Electromedicine*, *6*(2), 105-111.
- Padjen, A., Dongier, M., Malec, T. (1995). Effects of cerebral electrical stimulation of alcoholism: a pilot study. *Alcoholism, Clinical and Experimental Research*, *19*(4), 1004-1010.
- Pascual-Marqui, R. (2003). LORETA-KEY [Computer software]. Zurich, Switzerland: The KEY Institute for Brain-Mind Research, University Hospital of Psychiatry.
- Pascual-Marqui, R. (2002). Standardized low resolution brain electromagnetic tomography (sLORETA): technical details. *Methods & Findings in Experimental & Clinical Pharmacology*, *24*(D), 5-12.
- Pascual-Marqui, R., Esslen, M., Kochi, K., Lehmann, D. (2002). Functional imaging with low resolution brain electromagnetic tomography (LORETA): Review, new comparisons, and new validation. *Japanese Journal of Clinical Neurophysiology*, *30*, 81-94.
- Pascual-Marqui, R. (1999). Review of methods for solving the EEG inverse problem. *International Journal of Bioelectromagnetism*, *1*, 75-86.
- Pascual-Marqui, R., Lehmann, D., Koenig, T., Kochi, K., Merlo, M., Hell, D., Koukkou, M. (1999). Low resolution brain electromagnetic tomography (LORETA) functional imaging in acute, neuroleptic-naive, first-episode, productive schizophrenia. *Psychiatry Research-Neuroimaging*, *90*, 169-179.
- Pascual-Marqui RD, Michel CM, Lehmann D. (1994). Low resolution electromagnetic tomography: A new method for localizing electrical activity in the brain. *International Journal of Psychophysiology*, *18*, 49-65.

- Patterson, M. A., Firth, J., & Gardiner, R., (1984). Treatment of drug, alcohol and nicotine addiction by neuroelectric therapy: analysis of results over 7 years. *Journal of Bioelectricity*, 3, 193-221.
- Passini, F., Watson, C., & Herder, J. (1976). The effect of cerebral electric therapy (electrosleep) on anxiety, depression, and hostility in psychiatric patients. *Journal of Nervous and Mental Disease*, 163, 263-266
- Pavlov, I. V. (1928). *Lectures on conditioned reflexes*. New York: International Publishers.
- Philip, P., Demontes-Mainard, J., Bourgeois, M. & Vincent, J. D. (1991). Efficiency of transcranial electrostimulation on anxiety and insomnia symptoms during a washout period in depressed patients; a double-blind study. *Biological Psychiatry*, 29, 451-456.
- Pizzagalli, D., Pascual-Marqui, R. D., Nitschke, J. B., Oakes, T. R., Larson, C. L., Abercrombie, H. C., Schaefer, S. M., Koger, J. V., Benca, R. M., Davidson, R. J. (2001). Anterior cingulate activity as a predictor of degree of treatment response in major depression: evidence from brain electrical tomography analysis. *American Journal of Psychiatry*, 158, 405-415.
- Pozos, R. S., Richardson, A. W., & Kaplan, H. M. (1971). Electroanesthesia: a proposed physiologic mechanism. In D.V. Reynolds, & S. Anita (Eds.) *Neuroelectric Research*, Springfield Illinois: Charles Thomas.
- Purves, D. (1988). *Brain and body: A trophic theory of neural connections*. Cambridge, MA: Harvard University Press.
- Reid, S. (2003, October). Case reports of CES with an acute inpatient forensic psychiatric population, Vernon State Hospital. Presentation at the annual meeting of the Biofeedback Society of Texas, Arlington, Texas.
- Romano, T. J. (1993). The usefulness of cranial electrotherapy in the treatment of headache in fibromyalgia patients. *American Journal of Pain Management*, 3, 15-19.
- Rowan, J., Tolunsky, E. (2003). *Primer of EEG, with a mini-atlas*. Philadelphia, Pennsylvania: Elsevier Science.
- Rosenthal, R., & Rosnow, R. L. (1991). *Essentials of behavioral research methods and data analysis*. New York: McGraw-Hill, Inc.
- Rosenthal, S. & Wulfsohn, N. (1970). Studies of electrosleep with active and simulated treatment. *Current Therapeutic Research*, 12(3), 126-130.
- Rosenthal, S. (1972). Electrosleep: a double-blind clinical study. *Biological Psychiatry*, 4(2), 179-185.
- Rosenthal, S. (1973). Alterations in serum thyroxine with cerebral electrotherapy (electrosleep). *Archives of General Psychiatry*, 28(1), 28-29.

- Rush, S. & Driscoll, D. (1968). Current distribution in the brain from surface electrodes. *Analogues of Anesthesia*, 47, 717.
- Ryan, J., & Souheaver, G. (1976). Effects of transcerebral electrotherapy (electrosleep) on state anxiety according to suggestibility levels. *Biological Psychiatry*, 11(2), 233-237.
- Ryan, J., & Souheaver, G. (1977). The role of sleep in electrosleep therapy for anxiety. *Diseases of the Nervous System*, 38(7), 515-517.
- Sances, A., Larson, S., (1975). *Electroanesthesia: Biomedical and biophysical studies*. New York: Academic Press.
- Schroeder, M. J. (1999). *Acquisition and quantitative analyses of EEG during CES and concurrent use of CES and neurofeedback*. Doctoral dissertation, University of Texas at Austin, Austin, Texas.
- Schmitt, R., Capo, T., Frazier, H., & Boren, D. (1984). Cranial electrotherapy stimulation treatment of cognitive brain dysfunction in chemical dependence. *Journal of Clinical Psychiatry*, 45(2), 60-63.
- Schmitt, R., Capo, T., & Boyd, E. (1986). Cranial electrotherapy stimulation as a treatment for anxiety in chemically dependent persons. *Alcoholism: Clinical and Experimental Research*, 10(2), 158-160.
- Senulis, J., Davidson, R. (1989). The effect of linking the ears on the hemispheric asymmetry of EEG. *Psychophysiology*, 26, 555.
- Shealy, C. N., Cady, R. K., Wilkie, R. G., Cox, R., Liss, S., & Clossen, W. (1989). Depression: a diagnostic, neurochemical profile and therapy with cranial electrical stimulation (CES). *Journal of Neurological and Orthopaedic Medicine and Surgery*, 10(4), 319-321.
- Shealy, C., Norman, C., Roger, K., Wilkie, R., Cox, R., Liss, S., & Clossen, W. (1989). Depression: a diagnostic, neurochemical profile and therapy with cranial electrical stimulation (CES). *Journal of Neurological and Orthopaedic Medicine and Surgery*, 10(4), 319-321.
- Shealy, C., Norman, C., Roger, K., Culver-Veehoff, D., Cox, R., & Liss, S. (1998). Cerebralspinal fluid and plasma neurochemicals: Response to cranial electrical stimulation. *Journal of Neurological and Orthopaedic Medicine and Surgery*, 18(2), 94-97.
- Sing, B., Chhina, G. S., Anand, B. K., Bopari, M. S., & Neki, J. S. (1971). Sleep and consciousness mechanisms with special reference to electrosleep. *Armed Forces Medical Journal India*, 27(3), 292-297.
- Smith, R. (1982). Confirming evidence of an effective treatment for brain dysfunction in alcoholic patients. *Journal of Nervous and Mental Disease*, 170(5), 275-278.

- Smith, R., & Day, E. (1977). The effects of cerebral electrotherapy on short-term memory impairment in alcoholic patients. *International Journal of the Addictions*, 12(4), 575-562.
- Smith, R., & O'Neill, L. (1975). Electrosleep in the management of alcoholism. *Biological Psychiatry*, 10(6), 675-680.
- Smith, R. (2002). Introduction: *The science behind CES*. Edmonton, Alberta: Medical Scope Publishing Corp.
- Smith, R., Tiberi, A., Marshall, J. (1994). The use of cranial electrotherapy stimulation in the treatment of closed-head-injured patients. *Brain Injury*, 8, 357-361.
- Smith, R. (1999). Cranial electrotherapy stimulation in the treatment of stress related cognitive dysfunction, with an eighteen month follow up. *Journal of Cognitive Rehabilitation*, 17(6), 14-18.
- Smith, R., & Tyson, R. (2002). The use of transcranial electrical stimulation in the treatment of cocaine and/or polysubstance abuse. [Abstract] In *The science behind CES*. Edmonton, Alberta: Medical Scope Publishing Corp.
- Solomon, S., Elkind, A., Freitag, F., Gallagher, R. M., Moore, K., Swerdow, B., & Malkin, S. (1989). Safety and effectiveness of cranial electrotherapy in the treatment of tension headache. *Headache*, 29, 445-450.
- Stainbrook, E. (1948). The use of electricity in psychiatric treatment during the nineteenth century. *Bulletin of the History of Medicine*, 22, 156-177.
- Stanley, T., Cazalaa, J., Atinault, A., Coeytaux, R., Limoge, A., & Louville, Y. (1982). Transcutaneous cranial electrical stimulation decreases narcotic requirements during neuroleptic anesthesia and operation in man. *Anesthesia and Analgesia*, 61, 863-866.
- Stanley, T., Cazalaa, J., Limoge, A., & Louville, Y. (1982). Transcutaneous cranial electrical stimulation increases the potency of nitrous oxide in humans. *Anesthesiology*, 57, 293-297.
- Straus, B., & Bodian, C. (1964). Electrical induction of sleep. *The American Journal of the Medical Sciences*, 248, 514-520.
- Stevens, J. (1996). *Applied multivariate statistics for the social sciences* (3rd ed.). Hillside, New Jersey: Lawrence Erlbaum Associates.
- Sterman, M., B., & Kaiser, D., A. (2000). *SKIL QEEG analysis software* (Version 2.05) [Computer software]. Bel Air, CA: Sterman-Kaiser Imaging Laboratory.
- Taylor, D., (1995). Clinical and experimental evaluation of cranial tens in the US: A review. *Acupuncture and Electro-Therapeutics Research*, 20(2), 117-133.

- Taylor, J. R., Tompkins, R., Demers, R., Anderson, D. (1982). Electroconvulsive therapy and memory dysfunction: Is there evidence for prolonged defects? *Biological Psychiatry* 17, 1169-1193.
- Thakor, N., and Tong, S. (2004). Advances in quantitative electroencephalogram analysis methods. *Annual Review of Biomedical Engineering*, 6, 453-495.
- Thatcher, R. (2006). *Neuroguide* (2.2.6) [Computer software]. Bay Pines, FL: Applied Neuroscience, Inc.
- Thatcher, R., North, D., Biver, C. (2005). Parametric vs. non-parametric statistics of low resolution electromagnetic tomography (LORETA). *Clinical EEG and Neuroscience*, 36(1), 1-8.
- Thatcher, R., North, D., Biver, C. (2005). Evaluation and validity of a LORETA normative EEG database. *Clinical EEG and Neuroscience*, 36(2), 116-122.
- Thatcher, R., Walker, R., Biver, C., North, D., and Curtin, R. (2003). Quantitative EEG normative databases: Validation and clinical correlation. *Journal of Neurotherapy*, 7(3), 87-121.
- Thatcher, R. (1999). EEG database-guided neurotherapy. In J. R. Evans & A. Abarbanel (Eds.), *Introduction to quantitative EEG and neurofeedback*. San Diego, Ca: Academic Press.
- Thompson, M., & Thompson, L. (2003). *The neurofeedback book*. Wheat Ridge, Colorado: The Association for Applied Psychophysiology and Biofeedback.
- Tomarken, A., Davidson, R., Wheeler, R., Kinney, L. (1992). Psychometric properties of resting anterior EEG asymmetry: Temporal stability and internal consistency. *Psychophysiology*, 29, 576-592.
- Tomaszek, D. E., & Morehead, K. (2002). The use of CES in reducing pain in spinal pain patients. [Abstract] in *The science behind CES*, 2002, Edmonton, Alberta: Medical Scope Publishing Corp.
- Tomsovic, M., & Edwards, R. (1973). Cerebral electrotherapy for tension-related symptoms in alcoholics. *Quarterly Journal of Studies on Alcohol*, 34, 1352-1355.
- United States of America Code of Federal Regulations, Title 21 Food and Drugs, Chapter 1 Food and Drug Administration Department of Health and Human Services, subchapter H Medical Devices, Volume 8, Part 882 Neurological Devices, section Sec. 882.580 (Revised as of April 1, 2005); [44 FR 51730-51778, Sept. 4, 1979, as amended at 52 FR 17740, May 11, 1987; 60 FR 43969, Aug. 24, 1995; 62 FR 30457, June 4, 1997]
- Von Richtofen, C., Mellor, C. (1980). Electrosleep therapy: A controlled study of its effects in anxiety neurosis. *Canadian Journal of Psychiatry*, 25, 213-229.

- Voris, M. (1995). An investigation of the effectiveness of cranial electrotherapy stimulation in the treatment of anxiety disorders among outpatient psychiatric patients, impulse control parolees and pedophiles. [Abstract] in *The science behind CES*, 2002, p. 73, Edmonton, Alberta: Medical Scope Publishing Corp.
- Voris, M., Good, S. (1996). Treating sexual offenders using cranial electrotherapy stimulation. *Medical Scope Monthly*, 3(11), 14-18.
- Vitacco, D., Brandeis, D., Pascual-Marqui, R.D. and Martin, E. (2002). Correspondence of event-related potential tomography and functional magnetic resonance imaging during language processing. *Human Brain Mapping*, 17, 4-12.
- Vuga, M., Fox, N. A., Cohn, J. F., George, C. J., Levenstein, R. M., Kovacs, M. (2006). Long-term stability of frontal electroencephalographic asymmetry in adults with a history of depression and controls. *International Journal of Psychophysiology*, 59(2), 107-15.
- Wageneder, F. M., & Schuy, S. (1967). Electrotherapeutic sleep and electroanesthesia, (Vol. I). Proceedings of the first international symposium, Graz, Austria. New York: Excerpta Medica.
- Wageneder, F. M., & Schuy, S. (1970). Electrotherapeutic sleep and electroanesthesia, (Vol. II). Proceedings of the first international symposium, Graz, Austria. New York: Excerpta Medica.
- Weingarten, E. (1981). The effect of cerebral electrostimulation on the frontalis electromyogram. *Biological Psychiatry*, 16(1), 61-63.
- Weiss, M. F. (1973). The treatment of insomnia through use of electrosleep: An EEG study. *Journal of Nervous and Mental Disease*, 157(2), 108-120.
- Winick, R. (1999). Cranial electrotherapy stimulation (CES): a safe and effective low cost means of anxiety control in a dental practice. *General Dentistry*, 47(1), 50-55.
- Zhao M, Song B, Pu J, Wada T, Reid B, Tai G, Wang F, Guo A, Walczysko P, Gu Y, Sasaki T, Suzuki A, Forrester JV, Bourne HR, Devreotes PN, McCaig CD & Penninger JM (2006). Electrical signals control wound healing through phosphatidylinositol-3-OH kinase-gamma and PTEN. *Nature*, 27(442), 457-460.